Pediatr Radiol (2013) 43 (Suppl 2):S205–S458
DOI 10.1007/s00247-013-2638-9

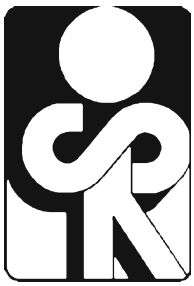

The logo for The Society for Pediatric Radiology was designed by Tamar Kahane Oestreich of Cincinnati, Ohio in 1985.

Founded in 1959
The Society for Pediatric Radiology
56th Annual Meeting & Postgraduate Course

Presented by
The Society for Pediatric Radiology

Hyatt Regency Hill Country Resort & Spa
San Antonio, Texas

Postgraduate Course
May 14-15, 2013

Annual Meeting
May 15-18, 2013

Jointly sponsored by the American College of Radiology

This supplement was not sponsored by outside commercial interests; it was funded entirely by the society's own resources.

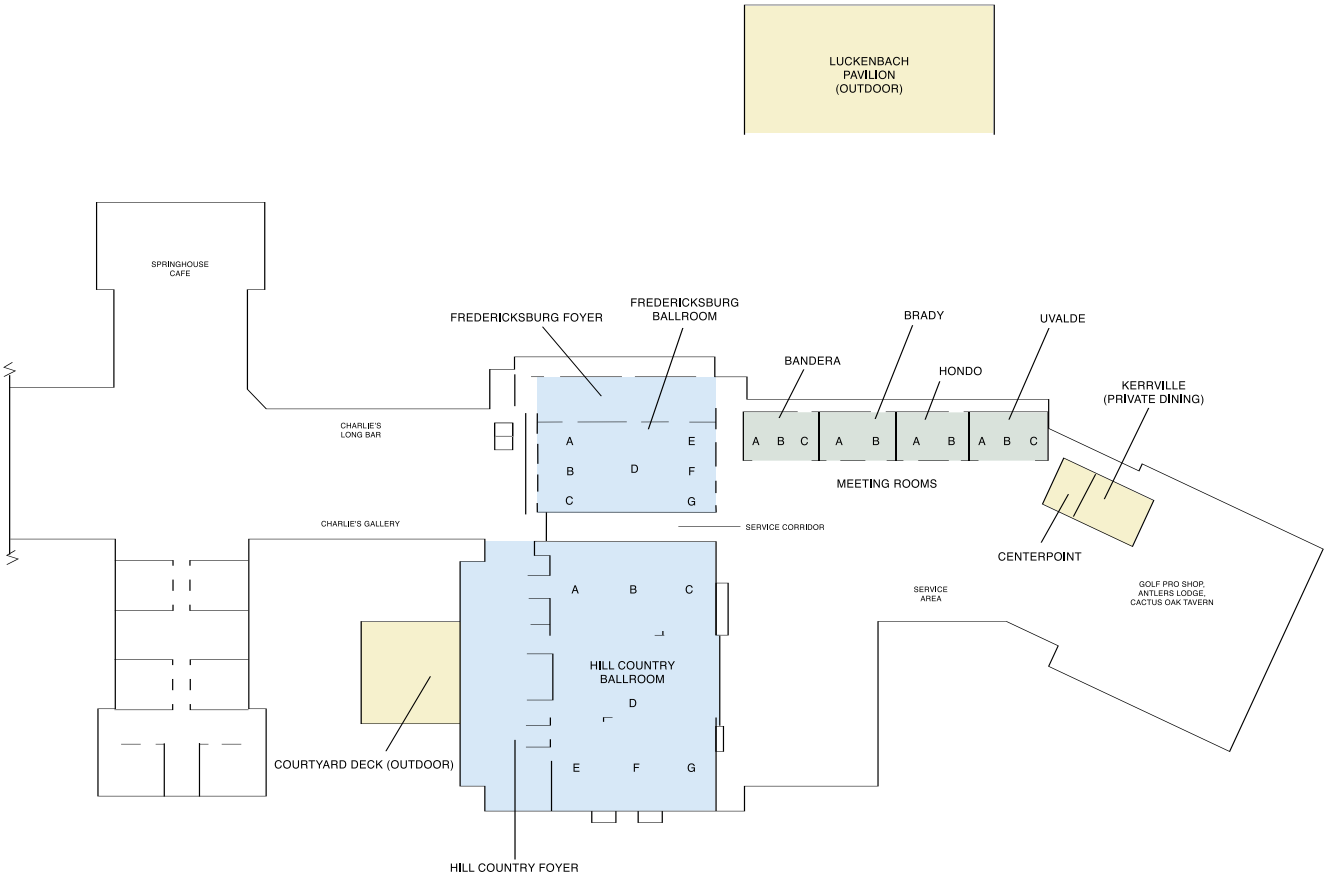
LUCKENBACH
PAVILION
(OUTDOOR)
SPRINGHOUSE
CAFE
FREDERICKSBURG FOYER
FREDERICKSBURG
BALLROOM
BRADY
UVALDE
BANDERA
HONDO
KERRVILLE
(PRIVATE DINING)
CHARLIE'S
LONG BAR
A
B
C
D
E
F
G
A B C
A B
A B
A B C
MEETING ROOMS
CHARLIE'S GALLERY
SERVICE CORRIDOR
CENTERPOINT
SERVICE
AREA
GOLF PRO SHOP,
ANTLERS LODGE,
CACTUS OAK TAVERN
HILL COUNTRY
BALLROOM
COURTYARD DECK (OUTDOOR)
HILL COUNTRY FOYER

The Society for Pediatric Radiology - San Antonio, Texas
May 14-18, 2013

	Postgraduate Course May 14-15			Annual Meeting May 15-18		
	Monday, May 13	**Tuesday, May 14**	**Wednesday, May 15**	**Thursday, May 16**	**Friday, May 17**	**Saturday, May 18**
7:00 AM		Continental Breakfast (7-8 am)	Continental Breakfast (7-8 am)	Continental Breakfast 6:45 - 8 AM		Continental Breakfast (7-8 am)
7:30				Sunrise Sessions-MSK, Thoracic, Onc, QI; Body MR Protocol (7-8:20 am)	Sunrise Sessions-Abd, Neuro, CEUS, Molecular; Neuro MR Protocol (7-8:20 am)	
8:00		Postgraduate Course CHEST	Postgraduate Course MSK			Concurrent Sessions Cardiac IR Neuro Nuclear Education (8 am-12 pm)
8:30				Concurrent Sessions III Neuro/Cardio (8:30-10:50 am)	Concurrent Sessions VII IR/Fetal (8:30-10:50 am)	
9:00						
9:30						
10:00		Break (9:55-10:15 am)	Break (9:55-10:20 am)			
10:30		Postgraduate Course NEURO	Postgraduate Course ONC	Break (10:50-11:00)	Break (10:50-11:00)	
11:00				Concurrent Sessions IV Policy/GU (11 am-12 pm)	Concurrent Sessions VIII Policy/Fetal (11 am-12:30 pm)	
11:30						
12:00 PM		Lunch Break (11:50-1:10 pm)	Lunch On Own OR 3D RWE & US Protocol (11:55-1:15 pm)	jSPR lunch, AAWR, CBPR CT Protocol Session 12-1:30 pm		
12:30					Business Meeting/Lunch (12:30-1:45)	
1:00	Board Mtg					
1:30		Postgraduate Course GI	Welcome	Concurrent Sessions V (1:30-3:40 pm)	Concurrent Sessions IX MSK/Onc-Nuc (1:45-3:55 pm)	
2:00			**Neuhauser Lecture**			
2:30			Session I - Onc/Nuc (2:30-3:30 pm)			
3:00	Registration	Break (2:45-3:15 pm)				
3:30		Postgraduate Course GU	Break (3:30-3:50)	Break (3:40-4:00)		
4:00			Session II - GI (3:50-5:10 pm)	Concurrent Sessions VI Neuro/GU (4-5:30 pm)	Break (3:55-4:20)	
4:30					Concurrent Sessions X MSK/IR (4:20-5:30 pm)	
5:00			**Awards Ceremony** 5:15 - 6:15 pm			
5:30						
6:00		Riverwalk Night Out 6:00-11:00 pm		Riverwalk Night Out 6:00 - 11:00 pm		
6:30			Welcome Reception 6:15-7:30 pm		Reception and Annual Banquet (6:30-11 pm)	
7:00						
7:30						

TABLE OF CONTENTS

WELCOME ADDRESS

Dear Colleagues,

The dedication of pediatric radiologists to the care of children has made pediatric imaging essential to modern pediatric healthcare. Thus, it is with great pride, that I welcome you to the 56th Annual Meeting of the Society for Pediatric Radiology! It has been more than 20 years since our meeting was last held in San Antonio! So much has changed in the world during that time but one thing that has remained constant (besides the Alamo) is the commitment, talent and vision of SPR members. It is through the active volunteerism of many members that this meeting advances education and provides a forum for networking and for both making new and renewing old friendships. We sincerely hope you find this great city and great meeting to be conducive to each of those goals.

These are interesting times. We find ourselves in an ever-evolving sphere of patient care, increasing governmental oversight, diminishing research funding and rapidly advancing technology. Compounded upon these variables, is a new era of molecular imaging, disease-specific targeted therapy and incorporation of genomic profile for diagnosis, treatment and monitoring disease. Certainly, imaging technology, frequency, methods and findings will be impacted by the incorporation of novel and targeted treatment agents into the clinical arena. Leading the Pediatric Genome Project is this year's Neuhauser lecturer, Dr. James Downing, Executive Vice President, Scientific Director, Deputy Director St. Jude Children's Research Hospital who will provide insight into the impact of genomic profiles on the diagnosis and treatment of pediatric cancers and the impact of this factor on clinical medicine.

The 2013 program builds upon the creativity and innovative spirit of prior years. Thanks to the tremendous efforts of the Program Committee Members, you will find that the Postgraduate Course (Drs. Cynthia Rigsby and Geetika Khanna, Co-Chairs) offers a diverse and robust agenda for which SAM credit may be obtained. Eight sunrise sessions (Drs. George Taylor and Michael Callahan, Co-Chairs) provide additional educational opportunities to start the day. In addition, the protocol sessions have been expanded to include ultrasound in addition to the popular body and neuro CT and MR sessions, five special half-day sessions Saturday morning with SAM credit available for each session, and a multi-vendor session providing hands-on workstation exposure in 3D **R**ead **W**ith the **E**xperts.

We welcome international participants and guests, without whom the World Federation of Pediatric Imaging would not be possible. Educational and social interactions between attendees from around the world should globally enhance pediatric imaging care and provides anopportunity to discuss diverse perspectives on pediatric diseases, challenges, imaging paradigms and answers.

Pediatric radiologists are not just 'imagers' but have sincere interest in caring and nurturing children in general. New this year, we are incorporating a community service project into the activities of the meeting. In giving-back to the local community, we are offering an outlet for the generosity of the membership through voluntary donations of books and DVDs to the pediatric ward at Children's Hospital of San Antonio. Thanks goes to Dr. Maria-Gisela Mercado-Deane for serving as liaison between the SPR and the hospital.

Many SPR members and guests have talents not readily apparent in the day-to-day practice environment. The Hooshang Taybi Art show will provide the opportunity for sharing hidden talents while contributing to the Research and Education Foundation! Donated items will be auctioned silently to the highest bidder with proceeds donated to the SPR REF!

Too often we fail to acknowledge individuals who have made a difference in our professional career or personal life. Take the opportunity to personally recognize and thank a mentor or colleague by adding a note or card to the Mentor Board. New this year, we are providing you with the opportunity to do so by supplying stationery and a board on which to leave your addressed message. Notes left at the end of the meeting will be forwarded to the addressee if they are unable to retrieve it in San Antonio.

This exciting, thoughtful and stimulating program would not be possible without the generous commitment of dozens of members, non-members, and vendors willing to support the SPR by sharing their expertise, time and resources. I hope you find the venue and networking, research and educational opportunities inspirational and fun.

So jump in with boots on and kick up some dust! The Board, Committee members and program planners are glad you are here!

Sue C. Kaste, DO

President, The Society for Pediatric Radiology

SPR 2013 ORGANIZATION

2013 MEETING CURRICULUM COMMITTEE

Sue C. Kaste, DO, Chair
Dianna M.E. Bardo, MD (Neuro MR Protocol Session)
Dorothy I. Bulas, MD (Education Session)
Michael J. Callahan, MD (Sunrise Sessions)
Laura Z. Fenton, MD (US Protocol Session)
Marilyn J. Goske, MD (Education Session)
Jeffrey C. Hellinger, MD (3D Sessions)
Geetika Khanna, MD (Postgraduate Course)
Rajesh Krishnamurthy, MD (Cardiovascular Course)
Edward Y. Lee, MD, MPH (CT Protocol Session)
Marguerite T. Parisi, MD, MS Ed (Nuclear Medicine Session)
Caroline D. Robson, MBChB (Neuroradiology Session)
Cynthia K. Rigsby, MD (Postgraduate Course)
Derek J. Roebuck, FRANZCR (Interventional Session)
George A. Taylor, MD (Sunrise Sessions)
Shreyas S. Vasanawala, MD, PhD (Body MR Protocol Session)

ABSTRACT REVIEW COMMITTEE – PAPERS

Sue C. Kaste, DO, Chair
Richard A. Barth, MD
Dorothy I. Bulas, MD
Christopher I. Cassady, MD, FRANZCR
Brian D. Coley, MD
James S. Donaldson, MD
Caroline L. Hollingsworth, MD, MPH
Diego Jaramillo, MD, MPH
Beth M. Kline-Fath, MD
Rajesh Krishnamurthy, MD
Marguerite T. Parisi, MD, MS Ed
Daniel J. Podberesky, MD
Derek J. Roebuck, FRANZCR
Laureen M. Sena, MD
Thomas L. Slovis, MD
Lisa J. States, MD
Keith J. Strauss, MS, FACR
Peter J. Strouse, MD
Alexander J. Towbin, MD
Stephan D. Voss, MD, PhD
Valerie L. Ward, MD
Tina Young Poussaint, MD

ABSTRACT REVIEW COMMITTEE – SCIENTIFIC EXHIBITS/POSTERS

M. Beth McCarville, MD, Chair
Michael J. Callahan, MD

Maria A. Calvo-Garcia, MD
Michael P. D'Alessandro, MD
Kassa Darge, MD, PhD
Steven Don, MD
R. Paul Guillerman, MD
Frederic A. Hoffer, MD
Thierry A.G. M. Huisman, MD
Douglas H. Jamieson, MD
Blaise V. Jones, MD
Nadja Kadom, MD
J. Herman Kan, MD
Geetika Khanna, MD
Maria Ladino Torres, MD
Craig S. Mitchell, DO
Helen R. Nadel, MD
Daniel J. Podberesky, MD
Janet R. Reid, MD
Douglas C. Rivard, DO
Ashley J. Robinson, MBChB
Susan E. Sharp, MD
Manrita K. Sidhu, MD
Stephen F. Simoneaux, MD
Alexander J. Towbin, MD

CASE OF THE DAY

Debra L. Pennington, MD, Chair, Community Hospital Based Pediatric Radiologists Committee

jSPR

Ryan W. Arnold, MD and Adrienne Bean, MD

CONTINUING MEDICAL EDUCATION

Accreditation Statement

This activity has been planned and implemented in accordance with the Essential Areas and Policies of the Accreditation Council for Continuing Medical Education through the joint sponsorship of the American College of Radiology and The Society for Pediatric Radiology. The American College of Radiology is accredited by the Accreditation Council for Continuing Medical Education to provide continuing medical education for physicians.

Designation Statement (Postgraduate Course)

The American College of Radiology designates this live activity for a maximum of 11.75 *AMA PRA Category 1 Credits*™. Physicians should claim only the credit commensurate with the extent of their participation in the activity.

Designation Statement (Annual Meeting)

The American College of Radiology designates this live activity for a maximum of 23.75 *AMA PRA Category 1 Credits*™. Physicians should claim only the credit commensurate with the extent of their participation in the activity.

Technologists

The American College of Radiology is approved by the American Registry of Radiologic Technologists (ARRT) as a Recognized Continuing Education Evaluation Mechanism (RCEEM) to sponsor and/or review Continuing Medical Educational programs for Radiologic Technologists and Radiation Therapists.

The American College of Radiology designates this educational activity as meeting the criteria for up to 39.25 Category A credit hours of the ARRT.

MAINTENANCE OF CERTIFICATION

The Postgraduate Course as well as the Saturday Cardiac, Education, Interventional, Neuroradiology and Nuclear Medicine sessions have been submitted to be qualified by the American Board of Radiology in meeting the criteria for self-assessment (SAM) toward the purpose of fulfilling requirements in the ABR Maintenance of Certification Program. Final information on the status of these applications will be provided at the meeting.

OBJECTIVES

The Society for Pediatric Radiology Annual Meeting and Postgraduate Course will provide attendees with an opportunity to:

1. Summarize the most current information on state-of-the-art pediatric imaging and the practice of pediatric radiology.
2. Describe and apply new technologies for pediatric imaging.
3. Discuss common challenges facing pediatric radiologists, and possible solutions.
4. Evaluate and apply means of minimizing radiation exposure during diagnostic imaging and image-guided therapy.

At the conclusion of the experience, participants should have an improved understanding of the technologies discussed, increasing awareness of the costs and benefits of diagnostic imaging in children and of ways to minimize risks, and an improved general knowledge of pediatric radiology, especially as it interfaces with clinical decision making.

DISCLOSURE

In compliance with ACCME requirements and guidelines, the ACR has developed a policy for review and disclosure of potential conflicts of interest, and a method of resolution if a conflict does exist. The ACR maintains a tradition of scientific integrity and objectivity in its educational activities. In order to preserve this integrity and objectivity, all individuals participating as planners, presenters, moderators and evaluators in an ACR educational activity or an activity jointly sponsored by the ACR must appropriately disclose any financial relationship with a commercial organization that may have an interest in the content of the educational activity.

The following planners, presenters, and evaluators have disclosed no financial interests, arrangements or affiliations in the context of this activity:

Presenters

Prachi P. Agarwal MD
Ahmad I. Alomari MD
João G. Amaral MD
Savvas Andronikou FRCR, PhD
Sudha A. Anupindi MD
D. Gregory Bates MD
Jane E. Benson MD
Sadaf T. Bhutta MD, MBBS
Deepa R. Biyyam MBBS
Timothy N. Booth MD
Alan S. Brody MD
Lorna P. Browne MBBS
Timothy M. Cain MBBS
Marguerite M. Caré MD
Christopher I. Cassady MD, FRANZCR
Nancy A. Chauvin MD
Ronald A. Cohen MD
Jamie L. Coleman MD
Jesse Courtier MD
Heike E. Daldrup-Link MD, PhD
Michael P. D'Alessandro MD
Kassa Darge MD, PhD
Molly E. Dempsey MD
Jonathan R. Dillman MD
James S. Donaldson MD
Lane F. Donnelly MD
James R. Downing MD
Hedieh Eslamy MD
Frederic Fahey PhD
Kate A. Feinstein MD, FACR
Laura Z. Fenton MD
Celia Ferrari MD
Robert J. Fleck MD
Lynn A. Fordham MD, FACR
Michael J. Gelfand MD
Maryam Ghadimi-Mahani MD
Hyun Woo Goo MD, PhD
Meaghan P. Granger MD
J. Damien Grattan-Smith MBBS
R. Paul Guillerman MD
Julie H. Harreld MD
Jeffrey C. Hellinger MD
Marta Hernanz-Schulman MD, FACR
Thierry A.G.M. Huisman MD
Charles A. James MD, FACR
Delma Y. Jarrett MD
Susan D. John MD
J. Herman Kan MD
S. Pinar Karakas MD
Boaz Karmazyn MD
Sue C. Kaste DO
Marc S. Keller MD
Teresa G. Kelly MD
Beth M. Kline-Fath MD
Matthew J. Krasin MD
Ganesh Krishnamurthy MD
Tal Laor MD
Bernard F. Laya DO
Edward Y. Lee MD, MPH
Leann E. Linam MD
David J.E. Lord MD, FRANZCR
Lisa H. Lowe MD, FAAP
Robert D. MacDougall MSc
Richard I. Markowitz MD
Prakash M. Masand MD
Shiraz A. Maskatia MD
M. Beth McCarville MD
Clare A. McLaren DCRR
Kieran McHugh MD
Adeka D. McIntosh MD
Yusuf Menda MD
M. Gisela Mercado-Deane MD
Sarah S. Milla MD
D. Andrew Mong MD
Shaine A. Morris MD
Marvin D. Nelson, Jr. MD
Kirsten K. Ness PhD
Beverley Newman MD, FACR
Jennifer L. Nicholas MD
Rutger A.J. Nievelstein MD
Darren B. Orbach MD, PhD
Harriet J. Paltiel MD
Ashok Panigrahy MD
Jeannette Perez-Rossello MD
Daniel J. Podberesky MD
Sanjay P. Prabhu MBBS, FRCR
Sumit Pruthi MD
Mantosh S. Rattan MD
Janet R. Reid MD, FRCPC
Allyson A. Richards MD
Rafael Rivera MD
Richard L. Robertson, Jr. MD
Noah Sabin MD, JD
Yutaka Sato MD, PhD
Mike Seed MBBS
Laureen M. Sena MD
Susan E. Sharp MD
William E. Shiels, DO
V. Michelle Silvera MD
Stephanie E. Spottswood MD
Lisa J. States MD
Jennifer Stimec MD
Sam Stuart FRCR
Mahesh M. Thapa MD
S. Ted Treves MD
Unni K. Udayasankar MD
Shreyas S. Vasanawala MD, PhD
Teresa Victoria MD
Frank M. Volberg MD
Stephan D. Voss MD, PhD
Steven G. Waguespack MD
Simon K. Warfield PhD
Dayna M. Weinert MD
Jennifer L. Williams MD
Beverly P. Wood MD, MS, Ed, PhD
Mary B. Wyers MD
Shi-Joon Yoo MD

Planning Committee/Presenter

Michael J. Callahan MD
Marilyn J. Goske MD
Rajesh Krishnamurthy MD
Geetika Khanna MD
Marguerite T. Parisi MD, MSEd
Cynthia K. Rigsby MD
Derek J. Roebuck FRANZCR
Alexander J. Towbin MD

Planning Committee

Caroline Carrico, MD – Content reviewer
Sue C. Kaste, DO
Karen S. Schmitt, CMP

The presenters and content reviewer listed below have disclosed the following relevant financial relationships. Potential conflicts have been resolved.

Name	Disclosure
Richard G. Barr MD, PhD	Bracco Diagnostics Inc., Research grant
Dianna M. E. Bardo MD	Koninklijke Philips Electronics NV, Consultant, Speakers bureau, honoraria received
Dorothy I. Bulas MD	Philips US, Consultant no fees received
Taylor Chung MD	Philips, Honoraria
J.A. Gordon Culham MD	Medvoxel, Shareholder
Andrea S. Doria MD	Bayer
Laura M. Fayad MD	Siemens
Neil D. Johnson MBBS	Philips
Harry K.W. Kim MD, MS, FRCSC	Roche and Pfizer, Grant funding
Rosewinter Kodzwa BSRS, RT (R) (MR)	Community Radiology Associates, Salary received
Raja Muthupillai, PhD	Philips Healthcare, Research support
Randolph K. Otto MD	Siemens, Speaker's bureau
Amol Pednekar PhD	Philips, Salaried Employee
John M. Racadio MD	Philips
Stephanie Wilson MD, FRCPC	Lantheus Medical Imaging – Consultant, Research grant received

The scientific presenters at the 2013 Annual Meeting have indicated their applicable disclosures at the end of their abstracts. No statement indicates that the authors have nothing to disclose.

ACKNOWLEDGEMENTS

The Society for Pediatric Radiology gratefully acknowledges the support of the following companies in presenting the 56th Annual Meeting and Postgraduate Course:

Platinum

GE Healthcare
Philips Healthcare
Siemens Healthcare
Toshiba America Medical Systems

Silver

Sidra Medical & Research Center

Exhibitors

Agfa Healthcare
Bayer HealthCare Pharmaceuticals
BioMarin
Elsevier
Hitachi Medical Systems America
Kubtec
Lippincott Williams & Wilkins
LMT Lammers Medical Technology
Medis Medical Imaging Systems
Mindways CT
PRA, a division of Aris
SREE Medical Systems

As of January 14, 2013

PROGRAM SCHEDULE

The Society for Pediatric Radiology
Postgraduate Course 2013
Sue C. Kaste, DO, Program Director
Geetika Khanna, MD and Cynthia K. Rigsby, MD, Course Directors
Supported in part by an educational grant from Bayer HealthCare Pharmaceuticals, Inc.

Tuesday, May 14, 2013

7:00–8:00 a.m.	**Continental Breakfast**
7:00 a.m.–5:00 p.m.	**Registration**
7:50–8:00 a.m.	**Welcome and Introduction** Geetika Khanna, MD and Cynthia K. Rigsby, MD
8:00–9:55 a.m.	**CHEST** R. Paul Guillerman, MD and Beverley Newman, MD, FACR, Moderators
8:00–8:20 a.m.	Digital Radiography Robert MacDougall, MSc
8:20–8:40 a.m.	Functional Chest MR Imaging Hyun Woo Goo, MD, PhD
8:40–9:00 a.m.	PE Evaluation in Children: What is New? Edward Y. Lee, MD, MPH
9:00–9:20 a.m.	Imaging of Acquired Thoracic Cardiovascular Diseases Beverley Newman, MD, FACR
9:20–9:45 a.m.	Interesting Cases R. Paul Guillerman, MD
9:45–9:55 a.m.	**Question and Answer**
9:55–10:15 a.m.	**Break**
10:15–11:50 a.m.	**NEURORADIOLOGY** Ashok Panigrahy, MD and Yutaka Sato, MD, PhD, Moderators
10:15–10:35 a.m.	Optimizing Head US Imaging Lisa H. Lowe, MD, FAAP
10:35–10:55 a.m.	Seizure Imaging Unni K. Udayasankar, MD
10:55–11:15 a.m.	Advances in Brain Tumor Imaging Ashok Panigrahy, MD

11:15–11:40 a.m.	Interesting Cases Yutaka Sato, MD, PhD
11:40–11:50 a.m.	**Question and Answer**
11:50 a.m.–1:10 p.m.	**Lunch Break**
1:10–2:45 p.m.	**GASTROINTESTINAL** Marta Hernanz-Schulman, MD, FACR and Shreyas S. Vasanawala, MD, PhD, Moderators
1:10–1:30 p.m.	Abdominal Applications of DWI Rutger A.J. Nievelstein, MD
1:30–1:50 p.m.	Update on MR Contrast Agents and Applications Shreyas S. Vasanawala, MD, PhD
1:50–2:10 p.m.	Rex Shunt Interventions James S. Donaldson, MD
2:10–2:35 p.m.	Interesting Cases Marta Hernanz-Schulman, MD, FACR
2:35–2:45 p.m.	Question and Answer
2:45–3:15 p.m.	**Break**
3:15–5:00 p.m.	**GENITOURINARY** Kassa Darge, MD, PhD and Jonathan R. Dillman, MD, Moderators
3:15–3:35 p.m.	Update on Contrast Material Use in Children Jonathan R. Dillman, MD
3:35–3:50 p.m.	Update on UTI Imaging Assessment: ACR and AAP Guidelines Boaz Karmazyn, MD
3:50–4:05 p.m.	Advances in Pediatric Urosonography Kassa Darge, MD, PhD
4:05–4:25 p.m.	Imaging of Mullerian Anomalies S. Pinar Karakas, MD
4:25–4:50 p.m.	Interesting Cases D. Gregory Bates, MD
4:50–5:00 p.m.	Question and Answer
6:00–11:00 p.m.	**San Antonio Riverwalk Night Out**

Wednesday, May 15, 2013

7:00–8:00 a.m.	**Continental Breakfast**
7:00 a.m.–5:00 p.m.	**Registration**
7:50–8:00 a.m.	**Welcome and Announcements** Geetika Khanna, MD and Cynthia K. Rigsby, MD
8:00–9:55 a.m.	**MUSCULOSKELETAL** Jeannette Perez-Rossello, MD and Tal Laor, MD, Moderators
8:00–8:20 a.m.	Advanced Imaging of Arthritis Andrea S. Doria, MD
8:20–8:40 a.m.	Imaging of Osteochondral Lesions J. Herman Kan, MD
8:40–9:00 a.m.	Update on Child Abuse Imaging Jeanette Perez-Rossello, MD
9:00–9:20 a.m.	Imaging of Myopathies Tal Laor, MD
9:20–9:45 a.m.	Interesting Cases Mary B. Wyers, MD
9:45–9:55 a.m.	**Question and Answer**
9:55–10:20 a.m.	**Break**
10:20–11:55 a.m.	**ONCOLOGY IMAGING** Jamie L. Coleman, MD and Geetika Khanna, MD, Moderators
10:20–10:45 a.m.	Late Effects of Cancer Treatment Kirsten K. Ness, PhD
10:45–11:10 a.m.	Pre and Post-operative Imaging of Limb Salvage Therapy Laura M. Fayad, MD
11:10–11:30 a.m.	Detection of CNS Metastases Noah Sabin, MD, JD
11:30–11:45 a.m.	PET-MR: Radiation Reduction and More Geetika Khanna, MD
11:45–11:55 a.m.	**Question and Answer**

The Society for Pediatric Radiology

Annual Meeting Program 2013

Sue C. Kaste, DO, Program Director

Michael J. Callahan, MD and George A. Taylor, MD, Workshop Directors

Wednesday, May 15, 2013

11:55–1:15 p.m.		Lunch Break	
11:55–1:15 p.m.		**3D Read with the Experts Lunch** *(advance registration required; attendance is limited)* *Supported by Philips Healthcare, Siemens Healthcare, Vital*	
		Ultrasound Protocol Lunch Session *(advance registration required; attendance is limited)* *Supported by GE Healthcare, Philips Healthcare, Siemens Healthcare, Toshiba America Medical Systems*	
1:20 p.m.		**Welcome** Sue C. Kaste, DO	
1:30–2:30 p.m.		**Edward B. Neuhauser Lecture** The Pediatric Cancer Genome Project – Implications for Clinical Medicine James R. Downing, MD Executive Vice President Scientific Director, Deputy Director St. Jude Children's Research Hospital Memphis, Tennessee	
2:30–3:30 p.m.		**Scientific Session I - Oncology & Nuclear Medicine** Susan E. Sharp, MD and Shreyas S. Vasanawala, MD, PhD, Moderators	
2:30–2:50 p.m.		Whole Body MR Techniques for Tumor Staging Shreyas S. Vasanwala, MD, PhD	
2:50–3:30 p.m.		Scientific Papers - Oncology & Nuclear Medicine	
PA-001	2:50	Servaes	Comparison of Diagnostic Performance of CT and MRI for Abdominal Staging of Wilms Tumor: A Report from the Children's Oncology Group
PA-002	3:00	Schlesinger	Disease Spectrum and Imaging Findings in Perivascular Epithelioid Cell Tumor (Pecoma) in Pediatric Patients
PA-003	3:10	Gawande	MRI of Pediatric Abdominal Tumors: Are Contrast Enhanced Studies Necessary?
PA-004	3:20	Ecklund	DW-MRI Characterization of Fast and Slow Diffusion in Treated Pediatric Osteosarcoma
3:30–3:50 p.m.		**Break**	

3:50–5:10 p.m. **Scientific Session II - Gastrointestinal**
M. Gisela Mercado-Deane, MD and Daniel J. Podberesky, MD, Moderators

3:50–4:10 p.m. Liver MR Elastography
Daniel J. Podberesky, MD

4:10–5:10 p.m. Scientific Papers – Gastrointestinal

PA-005	4:10	Mollard	Intravenous Glucagon Use in Pediatric MR Enterography: Effect on Image Quality, Length of Examination, and Patient Tolerance
PA-006	4:20	Obara	Performance of MR Enterography in Assessing Crohn's Disease Activity in the Pediatric Population
PA-007	4:30	Ortiz-Neira	The T2 Ratio: A Tool to Differentiate Bowel Wall Inflammation from Fibrosis
PA-008	4:40	Taphey	Comparative Assessment of individual CT Enterographic and MR Enterographic Imaging Features of Active Crohn's Disease in Pediatric Patients
PA-009	4:50	Shenoy-Bhangle	Added Value of Diffusion Weighted Imaging in MR Enterographic Evaluation of Crohn's Disease in Pediatric Patients
PA-010	5:00	Alvi	Plain Radiograph Evaluation of Pediatric Constipation: A Critical Analysis

5:15–6:15 p.m. **Awards Ceremony**

- Gold Medalist – Stuart A. Royal, MS, MD
- Pioneer Honoree – Barry D. Fletcher, MD
- Presidential Recognition Award – Alan E. Schlesinger, MD
- Honorary Member - Savvas Andronikou, MBBCh, FCRad, FRCR, PhD
- Singleton-Taybi Award – Lisa H. Lowe, MD

6:15–7:30 p.m. **Welcome Reception**

Thursday, May 16, 2013

6:45–8:00 a.m. **Continental Breakfast**

6:30 a.m.–5:00 p.m. **Registration**

7:00–8:20 a.m. **Sunrise Sessions (concurrent)**

Musculoskeletal Ultrasound
Mahesh M. Thapa, MD, Moderator

Ultrasound for Glenohumeral Dysplasia
Mahesh M. Thapa, MD

Ultrasound-guided Intra-articular Steroid Injection: Tricks of the Trade
Janet R. Reid, MD, FRCPC

Troubleshooting Pediatric Musculoskeletal Trauma with Ultrasound
Delma Y. Jarrett, MD

Thoracic Imaging
Alan S. Brody, MD, Moderator

Cross-sectional Imaging of Chronic Respiratory Disease in Children
Alan S. Brody, MD

Diaphragmatic Hernias: More than Just a Defect
Dorothy I. Bulas, MD

Imaging of Acute Respiratory Distress in Infants and Children
Mantosh S. Rattan, MD

Complications of Oncologic Disease
Kieran McHugh, MD, Moderator

Imaging of CNS Complications
Teresa G. Kelly, MD

Acute and Long-term Musculoskeletal Complications
Jennifer Stimec, MD

Secondary Malignancies: Imaging Strategies?
Kieran McHugh, MD

From Good to Great: Improving Quality
Stephan D. Voss, MD, PhD, Moderator

QI Programs: How We do It
Stephan D. Voss, MD, PhD

Think Fast and Slow: Biases and Heuristics in Radiology
J. Damien Grattan-Smith, MBBS

Diagnostic Errors in Radiology
Lane F. Donnelly, MD

Body MR Protocol Session *(advance registration required; attendance is limited)*
Supported by GE Healthcare, Philips Healthcare, Siemens Healthcare, Toshiba America Medical Systems
Session Topics: Body MRA/MRV, Bone Tumors, Iron/Fat Quantification

8:30–10:50 a.m. **Scientific Session III-A – Neuroradiology (concurrent)**
Marvin D. Nelson, Jr., MD and Ashok Panigrahy, MD, Moderators

8:30–8:50 a.m. fMRI Prematurity/Cognitive Function
Ashok Panigrahy, MD

8:50–10:50 a.m. Scientific Papers - Neuroradiology

PA-011	8:50	Mazori	Prevalence of Subdural Collections in a Large Cohort of Pediatric Patients With Benign Enlargement of the Subarachnoid Spaces
PA-012	9:00	Choudhary	MRI Features of Spinal Subdural Hemorrhage in Abusive Head Trauma

PA-013	9:10	Martin	Time Resolved Steady State Free Precession MRI of the Cranio-Cervical Junction
PA-014	9:20	Jacob	Magnetic Resonance Imaging of the Cervical Spine in Non-Accidental Trauma: A Tertiary Institution Experience
PA-015	9:30	Parnell	Cervical Spine MRI and Polysomnography Correlation in Pediatric Patients With Achondroplasia
PA-016	9:40	Bosemani	Pitfalls in Susceptibility Weighted Imaging (SWI) of the Pediatric Brain
PA-017	9:50	Miller	Angulated Scan Plane Modification for Faster Acquisition of Multiple Nonadjacent Gray and White Matter Spectroscopy Voxels
PA-018	10:00	Yeom	Pediatric Brain DWI With Dual-Echo Echo Planar Imaging (EPI)
PA-019	10:10	MacKenzie	Initial Experience and Potential Indications for Blood Pool MRI Contrast Agents in Pediatric Patients
PA-020	10:20	Bhargava	Bannayan Riley Ruvalcaba Syndrome and the Gamut of White Matter Abnormalities With Cysts
PA-021	10:30	Tanifum	Blood–brain Barrier Permeability in Transgenic Amyloid Overproducing Models: Implications for Downs Syndrome

8:30–10:50 a.m. **Scientific Session III-B–Cardiovascular (concurrent)**
Taylor Chung, MD and Laureen M. Sena, MD, Moderators

8:30–8:50 a.m. Imaging of Cardiomyopathies
Laureen M. Sena, MD

8:50–10:50 a.m. Scientific Papers – Cardiovascular

PA-022	8:50	Nazario	Size and Flow Characteristics of Internal Jugular Veins (IJV) Vs. Subclavian Veins (SCV) in Infants
PA-023	9:00	Hegde	What Is the Normal Size of the Abdominal Aorta in Children?
PA-024	9:10	Alaref	Distance Between the Carina and Cavoatrial Junction Normalized To Vertebral Body Height in Children
PA-025	9:20	Doliner	T2 Quantification of Normal Pediatric Myocardium
PA-026	9:30	Smith	Renal Sonography With Doppler for Detecting Suspected Pediatric Renin-Mediated Hypertension – Is It Adequate?
PA-027	9:40	Atweh	Comparison of Free Breathing Respiratory Triggered Retrospectively Cardiac Gated Cine Steady-State Free Precession (RT-SSFP) With Breath-Held SSFP in Unsedated Patients With Congenital Heart Disease (CHD)
PA-028	9:50	Hellinger	Volumetric Time Resolved Low Dose Renal CT Angiography (CTA) With Image Domain 3D Workstation Iterative Reconstruction: Initial Technical and Clinical Experience
PA-029	10:00	Masand	CT Angiographic Imaging of Complications Associated With Blalock-Taussig Shunts in Pediatric Patients
PA-030	10:10	Krishnamurthy	Comparison of Differential Pulmonary Blood Flow (d-PBF) Using First-Pass Pulmonary Perfusion (FPP) and Phase Contrast Imaging (PCI) in Children With Repaired Tetralogy of Fallot (rTOF)
PA-031	10:20	Prasad	Dynamic Evaluation of the Ostium and Proximal Course of Anomalous Coronary Arteries by Retrospective EKG Gated CTA
PA-032	10:30	Jacob	Non-Cardiac Vascular Imaging With Gadofosveset Trisodium, A Blood Pool Contrast Agent: initial Experience At A Tertiary Pediatric Hospital

10:50–11:00 a.m.		**Break**	
11:00 a.m.–12:00 p.m.		**Scientific Session IV-A – Public Policy, Healthcare, Education, Technology (concurrent)**	
		Marta Hernanz-Schulman, MD and Rafael Rivera, MD, Moderators	
11:00–11:20 a.m.		ACR Update	
		Marta Hernanz-Schulman, MD	
11:20 a.m.–12:00 p.m.		Scientific Papers - Public Policy, Healthcare, Education, Technology	
PA-033	11:20	Hawkins	Improving the Clinical History Provided for Radiographs
PA-034	11:30	Trout	Updated ACGME Fellowship Requirements: A Guide To Constructing an Online Curriculum That Fulfills Educational and Documentation Requirements
PA-035	11:40	Strain	Smart Sets: Decision Support for MRI order Entry
PA-036	11:50	Koc	Improved Depiction of Vessel Anatomy With Model Based Versus Adaptive Statistical Iterative Reconstruction for Pediatric CT Angiography
11:00 a.m.–12:00 p.m.		**Scientific Session IV-B – Genitourinary (concurrent)**	
		Kassa Darge, MD, PhD and Jonathan R. Dillman, MD, Moderators	
11:00–11:20 a.m.		MR Urography	
		Kassa Darge, MD, PhD	
11:20 a.m.–12:00 p.m.		Scientific Papers - Genitourinary	
PA-037	11:20	Hwang	Pediatric Epididymitis: Review of Clinical and Sonographic Features, and Differentiation from Intermittent Testicular Torsion
PA-038	11:30	Baron	Hydrocele of the Spermatic Cord: Clinical Presentation, Sonographic Features and Outcomes
PA-039	11:40	Adeb	Morphologic and Functional MR Urography Features of Duplicated Renal Systems
PA-040	11:50	Delgado	Optimizing Functional MR Urography (FMRU) Exam: Prime Time for a 30-Minute or Less MRU
12:00–1:30 p.m.		**Lunch Break**	
		CT Protocol Lunch Session *(advance registration required; attendance is limited)*	
		Supported by GE Healthcare, Philips Healthcare, Siemens Healthcare, Toshiba America Medical Systems	
		Session Topics: Chest, Abdomen, Oncology	
		Community Based Pediatric Radiologists Lunch *(advance registration required)*	
		AAWR and jSPR Joint Lunch Program *(advance registration required)*	
		Lynn A. Fordham, MD and Sarah S. Milla, MD, Moderators	
		Networking 101 – Traditional and Internet-Based	
		Dorothy I. Bulas, MD and Sarah S. Milla, MD	
1:30–3:40 p.m.		**Scientific Session V-A – Gastrointestinal (concurrent)**	
		Sudha A. Anupindi, MD and Dayna M. Weinert, MD, Moderators	

1:30–1:50 p.m.		MR Enterography Sudha A. Anupindi, MD	
1:50–3:40 p.m.		Scientific Papers – Gastrointestinal	
PA-041	1:50	Trout	The Pediatric Appendix: What Is Normal With Respect To Size?
PA-042	2:00	Trout	Assessment of Factors influencing Identification of the Normal Pediatric Appendix
PA-043	2:10	Trout	The Impact of Technical and Interobserver Factors on Appendiceal Measurement in Children
PA-044	2:20	Tulin-Silver	The Challenging Ultrasound Diagnosis of Perforated Appendicitis in Children: Constellations of Sonographic Findings Improve Specificity
PA-045	2:30	Sheridan	Sonographic Identification of Pediatric Candidates for Non-Surgical Treatment of Acute Appendicitis
PA-046	2:40	Van Atta	Implementing an Ultrasound-Based Protocol for Diagnosing Appendicitis While Maintaining Diagnostic Accuracy
PA-047	2:50	Orth	Prospective Comparison of MRI and Ultrasound for the Diagnosis of Pediatric Appendicitis
PA-048	3:00	Vogelius	The Eye Sees Only What the Mind Knows. Accuracy of Abdominal Ultrasound in the Evaluation of Visceral and Vascular Manifestations of Heterotaxy When Compared To MRI/CT: A Practice Quality Improvement Study
PA-049	3:10	Deng	Comparison of Quantitative MRI for Hepatic Fat Content Measurement in Pediatric Patients With Non-Alcoholic Fatty Liver Disease
PA-050	3:20	Saxena	Role of Contrast Enema Study in Diagnosis of Hirschsprung's Disease
PA-051	3:30	Bales	Intussusception Reduction: Does a Retention Balloon Make a Difference?
1:30–3:40 p.m.		**Scientific Session V-B – Chest (concurrent)** Ronald A. Cohen, MD and D. Andrew Mong, MD, Moderators	
1:30–1:50 p.m.		Diffuse Lung Disease in Children: A New Way of Classification and Understanding D. Andrew Mong, MD	
1:50–3:40 p.m.		Scientific Papers – Chest	
PA-052	1:50	Vorona	A Comparison of Airway Fluoroscopy With Endoscopy in the Evaluation of Children With Stridor
PA-053	2:00	Masand	Protocol for Dynamic Airway Imaging With Volume CT Angiography in Pediatric Patients: Our Experience With 20 Children
PA-054	2:10	Langenderfer	Improving Consistency of Contrast Enhancement During CT Pulmonary Angiography: A Quality Improvement Study
PA-055	2:20	Lee	Proximal Pulmonary Vein Stenosis Detection in Pediatric Patients: Value of Multiplanar and 3D MDCT Imaging Evaluation
PA-056	2:30	Guillerman	Congenital Multilobar Pseudo-Emphysema: A Severe Progressive Lung Growth Disorder Associated With Filamin A Gene Mutations
PA-057	2:40	Tilak	Analysis of CT Findings in Community-Acquired Viral Respiratory Tract infection in Children

PA-058	2:50	Mahomed	Chest X-Ray Findings in HIV-Infected Children Starting HAART at a Tertiary Institution in South Africa
PA-059	3:00	Lynn	The Value of Portable Computed Tomography (CT) in the Pediatric ICU: Our Results and Experience in 320 Consecutive Cases Over 3 Years
PA-060	3:10	Nava	Radiopacity of Fish Bones from 10 Common Fish Species in the Philippines
PA-061	3:20	Smith	Comparison of Pediatric CT Radiation Dose and Image Quality Utilizing Model Based Iterative Reconstruction and Adaptive Statistical Iterative Reconstruction Algorithms
PA-062	3:30	Tulin-Silver	A Phantom Based Technique To Lower Dose and Maintain Image Quality in Pediatric Body Imaging for 128 Slice CT Scanners Using Iterative Reconstruction

3:40–4:00 p.m. **Break**

4:00–5:30 p.m. **Scientific Session VI-A – Neuroradiology (concurrent)**
Julie H. Harreld, MD and Richard L. Robertson, Jr., MD, Moderators

4:00–4:20 p.m. Effects of Anesthesia and Sedation on Pediatric Brain MR Imaging
Julie H. Harreld, MD

4:20–5:30 p.m. Scientific Papers - Neuroradiology

PA-063	4:20 PM	Patel	Chronic Recurrent Multifocal Osteomyelitis (CRMO) of Mandible in the Pediatric Population: Spectrum of Imaging Findings With Clinicopathological Correlation
PA-064	4:30 PM	Booth	High Resolution 3D T2 Weighted Imaging in the Diagnosis of Labyrinthitis Ossificans: Emphasis On Subtle Cochlear involvement
PA-065	4:40 PM	Rollins	Brainstem Infarcts in Children: Imaging Features and Clinical Outcomes
PA-066	4:50 PM	Ghaghada	CT Angiography in a Transgenic Mouse Model of Cerebrovascular Disease
PA-067	5:00 PM	Nawas	Increased Dural Venous Sinus Diameters in Pediatric Patients With Sickle Cell Disease: A Magnetic Resonance Venography (MRV) Study
PA-068	5:10 PM	Andronikou	Corpus Callosum Thickness on MRI as a Surrogate Marker of Brain Volume in Children With HIV and Its Correlation With Developmental Scores and Clinical Parameters
PA-069	5:20 PM	Koral	Does Diffusion Weighted Imaging Improve the Accuracy of Preoperative Diagnosis of Common Pediatric Cerebellar Tumors?

4:00–5:30 p.m. **Scientific Session VI-B – Genitourinary (concurrent)**
Lynn A. Fordham, MD and Kate A. Feinstein, MD, Moderators

4:00–4:20 p.m. Robotic and Laparoscopic Surgery: What the Radiologist Needs to Know
Kate A. Feinstein, MD

4:20–5:30 p.m. Scientific Papers – Genitourinary

PA-070	4:20	Domina	Prospective Evaluation of Pediatric VCUG At An Academic Children's Hospital: Is the Scout Image Necessary?
PA-071	4:30	Sood	Comparison of Quality of Voiding Cystourethrogram (VCUG) Reports
PA-072	4:40	Gurram	CT Cystography in Detecting Perforated Reconstructed Bladders
PA-073	4:50	Jaimes	Diffusion Tensor Imaging (DTI) and Tractography of the Kidney in Children: Feasibility and Preliminary Experience
PA-074	5:00	Ucar	Low Fat Milk as Low Attenuation Oral Contrast Agent for Abdominal MDCT in Children and Teenagers
PA-075	5:10	Caleel	Can the Choice of Nomogram Used to interpret Sonographic Renal Measurements in Children With Myelomeningocele Affect Clinical Management?
PA-076	5:20	Tawadros	Pediatric Solitary Renal Cysts Found On Ultrasound – What is the Risk of Malignancy?

6:00–11:00 p.m. **San Antonio Riverwalk Night Out**

Friday, May 17, 2013

6:45–8:00 a.m. **Continental Breakfast**

6:30 a.m.–5:00 p.m. **Registration**

7:00–8:20 a.m. **Sunrise Sessions (concurrent)**

Abdominal Imaging: Old Dilemmas, New Paradigms
Richard I. Markowitz, MD, Moderator

Imaging of Diffuse Liver Disease: A Pattern-based Approach
Prakash M. Masand, MD

The Adolescent Girl with Abdominal Pain: Great Mimickers
Jesse Courtier, MD

Back to Basics: Pitfalls in Abdominal Radiography
Richard I. Markowitz, MD

Neuroradiology: "Crossing the Chiasm" Body and Neuroradiology Topics
Sanjay P. Prabhu, MBBS, FRCR, Moderator

US vs. MRI for Neonatal Head and Spine Imaging
Sumit Pruthi, MD

CR vs. CT for Cervical Spine Trauma
Sarah S. Milla, MD

CR vs. CT vs. MRI for Shunt Imaging
Sanjay P. Prabhu, MBBS, FRCR

Panel Discussion

Contrast Enhanced Ultrasound
Frank M. Volberg, MD and Stephanie Wilson, MD, FRCPC, Moderators

Contrast Ultrasound: State of the Art
Stephanie Wilson, MD, FRCPC

Current Status of IV Contrast Use in Ultrasonography
Harriet J. Paltiel, MD

Current Status of Non-intravenous Use of Contrast-enhanced US
Kassa Darge, MD, PhD

Contrast Enhanced Ultrasound Safety and Potential Applications in Pediatric Oncology
M. Beth McCarville, MD

Off-Label Use and CPT Codes for Contrast Enhanced Ultrasound
Richard G. Barr, MD, PhD

Molecular Imaging and Nuclear Medicine
Heike E. Daldrup-Link, MD, PhD, Moderator

Pediatric Thyroid Imaging
Jennifer L. Williams, MD

Pediatric Molecular Imaging: How I Do It
Heike E. Daldrup-Link, MD, PhD

Image Processing for Nuclear Medicine and Molecular Imaging: Bridging the Gap Between Advanced Technology and Clinical Practice
Simon K. Warfield, PhD

Neuro MR Protocol Session *(advance registration required; attendance is limited)*
Supported by GE Healthcare, Philips Healthcare, Siemens Healthcare, Toshiba America Medical Systems
Session Topics: *Specialized protocols/techniques, avoiding/reducing artifacts, 3D post-processing*

8:30–10:50 a.m. **Scientific Session VII-A - IR (concurrent)**
Marc S. Keller, MD and Adeka D. McIntosh, MD, Moderators

8:30–8:50 a.m. Challenging Situations in Pediatric Central Venous Access
Marc S. Keller, MD and Adeka D. McIntosh, MD

8:50–10:50 a.m. Scientific Papers – IR

PA-077	8:50	McDaniel	CT-Guided Localization of Pulmonary Nodules in Pediatric Oncology Patients Prior To Video-Assisted Thoracoscopic Surgery (VATS) Resection
PA-078	9:00	McIntosh	Treatment of Chylous Effusions in Children Using Thoracic Duct Embolization (TDE)
PA-079	9:10	Clemens	Characterization of Central Conducting Lymphatic Anomalies

PA-080	9:20	Delgado	Sclerotherapy of Foot Venous Malformations: A 6-Year Single Center Experience
PA-081	9:30	Gaballah	Catheter Directed and Mechanical Thrombolysis for Management of Lower Extremity Iliofemoral Deep Venous Thrombosis: A Single Pediatric Institutional Experience
PA-082	9:40	Raver	Detergent Enhanced Ethanol Ablation of Venous Endothelial Cells: An in-Vitro Study
PA-083	9:50	Green	Interventional Radiology Management of Post-Transplant Biliary Strictures in Children
PA-084	10:00	Gaballah	Single-incision Tunneled Femoral Vein Access in Neonates and infants: A Single Institutional Experience
PA-085	10:10	Yilmaz	Clinical, Histopathological, and Radiological Features of Congenital Anomalies of the Portal Venous System and a Proposed Algorithm for Management
PA-086	10:20	Gaballah	Single-incision Technique for internal Jugular Vein Tunneled Vascular Access in the Pediatric Population
PA-087	10:30	Hawkins	Pediatric Percutaneous Nephrostomy: A Single Institution's 10 Year Retrospective Review
PA-088	10:40	McLaren	Medium-Term Outcomes of Renal Artery Stenting in Children

8:30–10:50 a.m. **Scientific Session VII-B - Fetal (concurrent)**

Christopher I. Cassady, MD, FRANZCR and Beth M. Kline-Fath, MD, Moderators

8:30–8:50 a.m. Exit Procedures: What a Fetal Imager Needs to Know

Beth M. Kline-Fath, MD

8:50–10:50 a.m. Scientific Papers – Fetal

PA-089	8:50	Victoria	Fetal MRI - Jumping from 1.5 To 3 Tesla MRI: Preliminary Experience
PA-090	9:00	Schmit	Pediatric Image Assisted Autopsy: Why Pediatric Radiologists Should Be Part of It?
PA-091	9:10	Robinson	Inferior Vermian Hypoplasia—Preconception, Misconception
PA-092	9:20	Williams	Ventriculomegaly Diagnosed on Fetal MRI and the Risk of Post-Natal Hydrocephalus
PA-093	9:30	Maloney	A Sheep in Wolf's Clothing? Radiologic-Pathologic Correlation and Clinical Outcome in Congenital Glioblastoma
PA-094	9:40	Dixon	Arachnoid Cysts Diagnosed Prenatal and in Young Children: Is there a High Requirement for Surgical intervention?
PA-095	9:50	Shakir	Normative CT Data for Fetal Bone Length: Is It Possible to Accrue a Useful Database?
PA-096	10:00	Bhavane	Near Infra Red (NIR) Liposome Probe for Detecting Necrotizing Enterocolitis (NEC) in Premature Piglets
PA-097	10:10	Karmazyn	Effect of Pediatric Body Size on Dose Reduction for Abdominal MDCT With Automated Tube Current

PA-098	10:20	Ngo	Precocious Development of Adenoid Tissue in infants: Possibly Related to increased Pollutants in the Air
PA-099	10:30	Boyer	Amniotic Fluid Sludge: An Independent Risk Factor for Early Preterm Delivery, Chorioamnionitis, Funisitis, and Increased Perinatal Morbidity and Mortality in Twin Pregnancies With a Second Trimester Short Cervical Length
PA-100	10:40	Shenoy-Bhangle	Pause and Pulse - Recording of Effective Dose from Common Pediatric Abdominal Fluoroscopy Studies as a Quality Improvement (QI) Tool: Baseline Data and Comparison With CT

10:50–11:00 a.m. **Break**

11:00 a.m.–12:30 p.m. **Scientific Session VIII-A - Public Policy, Healthcare, Education, Technology (concurrent)**

Alexander J. Towbin, MD, Moderator

11:00–11:20 a.m. Pediatric Informatics and Patient Registry

Alexander J. Towbin, MD

11:20 a.m.–12:30 p.m. Scientific Papers – Public Policy, Healthcare, Education, Technology

PA-101	11:20	Braswell	The Simulation Experience as an introduction to Pediatric Radiology
PA-102	11:30	Yu	Computed Tomography Radiation Exposure: Dose Reporting Implementation and Adherence in a Radiology Housestaff Quality Improvement Project
PA-103	11:40	Wien	The American Association of Physicists in Medicine Method for Measuring the Size Specific Dose Estimate in Pediatric CT: Does It Really Work?
PA-104	11:50	Buchmann	The Impact of Advanced Iterative Reconstruction on Radiation Exposure and Image Quality in Children
PA-105	12:00	Goske	The Relationship Between SSDE and Diagnostic Image Quality: How a Dose index Registry (DIR) Can Determine the Minimum Radiation Dose Needed to Achieve Acceptable Diagnostic Image Quality in Pediatric Abdominal CT
PA-106	12:10	Brady	Clinical Implementation of ASiR™ Reconstruction for Substantial Dose Reduction in Pediatric CT While Maintaining Pre-ASiR™ Noise Levels: 21st Century Alchemy
PA-107	12:20	Don	Psychometric Function: A Novel Statistical Analysis Approach to Optimize CT Dose

11:00 a.m.–12:30 p.m. **Scientific Session VIII-B - Fetal (concurrent)**

Leann E. Linam, MD and Teresa Victoria, MD, Moderators

11:00–11:20 a.m. CT Imaging of the Fetus

Teresa Victoria, MD

11:20 a.m.–12:30 p.m.		Scientific Papers – Fetal	
PA-108	11:20	Johnston	Congenital Lobar Overinflation: Prenatal MRI and US Findings and Outcomes
PA-109	11:30	Mehollin-Ray	Specificity of Single or Multiple Fetal MR Imaging Findings in Identifying a Hernia Sac in Fetuses With Congenital Diaphragmatic Hernia
PA-110	11:40	Son	Is Echocardiography Necessary in Fetuses With Chest Masses?
PA-111	11:50	Flanagan	Prenatal Imaging of Bronchopulmonary Malformations: Is there a Role for Late Third Trimester Fetal MRI?
PA-112	12:00	Flanagan	Fetal Suprarenal Masses- Assessing the Complementary Role of MRI and Ultrasound for Diagnosis
PA-113	12:10	Brandolini	MR-I Can Do It: A Pilot Program Aimed to Reduce Sedation Rates for Pediatric Magnetic Resonance Imaging (MRI)
PA-114	12:20	Tyson	Child Life Services in Pediatric Imaging Sciences: Assessing the Value and Recommendations for Implementation
12:30–1:45 p.m.		**SPR Members' Business Meeting & Lunch**	
1:45–3:55 p.m.		**Scientific Session IX-A – Musculoskeletal (concurrent)** Molly E. Dempsey, MD and Allyson A. Richards, MD, Moderators	
1:45–2:05 p.m.		Juvenile Femoral Head Osteonecrosis: LCPD vs. GLC-induced ON Harry K.W. Kim, MD, MS, FRCSC	
2:05–4:00 p.m.		Scientific Papers – Musculoskeletal	
PA-115	2:05	Marine	Is the New ACR-SPR Practice Guideline for Addition of Oblique Views of the Ribs to the Skeletal Survey for Child Abuse Justified?
PA-116	2:15	Fagen	Frequency of Skeletal injuries in Children With Inflicted Burns
PA-117	2:25	Swami	Reliability of Estimation of 3D ACL Attachment Locations from Routine Pediatric Knee MRI
PA-118	2:35	Kim	The Patellofemoral Joint: Do Age and Gender Affect the Osseous Morphology in Children During Skeletal Maturation?
PA-119	2:45	Kim	The Patellofemoral Joint: T2 Relaxation Times and Thickness of the Cartilage in Different Ages and Genders in Children
PA-120	2:55	Guenther	Patterns of Meniscal injury in the Pediatric ACL Deficient Knee
PA-121	3:05	Jaimes	Diffusion Tensor Imaging of the Growing Ends of the Bones: Demonstration of Columnar Structure in the Physes and Metaphyses of the Knee
PA-122	3:15	Javadi	Wrist and Ankle MRI of JIA Patients: Significance of Unsuspected Multicompartmental Tenosynovitis and Arthritis
PA-123	3:25	Vogelius	Radiographic Variants of the Inferior Patellar Pole Revisited: Normal or Within the Spectrum of Patellar Avulsive injuries?
PA-124	3:35	Ponrartana	Chemical-Shift Fat-Water Separation MRI and Diffusion Tensor Imaging As Quantitative Imaging Markers for Disease Progression in Duchenne Muscular Dystrophy: Preliminary Study

PA-125	3:45	Chauvin	Detection of Enthesitis in Children With Enthesitis-Related Arthritis: Physical Examination Compared to Ultrasonography

1:45–3:55 p.m. **Scientific Session IX-B – Oncology & Nuclear Medicine (concurrent)**

M. Beth McCarville, MD and Kieran McHugh, MD, Moderators

1:45–2:05 p.m. Diagnostic Imaging and Radiation Oncology: Contemporary Relationship in Caring for Children with Cancer

Matthew J. Krasin, MD

2:05–4:00 p.m. Scientific Papers – Oncology & Nuclear Medicine

PA-126	2:05	Voss	Growth Plate Abnormalities in Pediatric Cancer Patients Undergoing Phase 1 Anti-Angiogenic Therapy: A Report from the Children's Oncology Group Phase I Consortium
PA-127	2:15	Hryhorczuk	Imaging and Histopathologic Characteristics of Post-Transplant Neoplasms in Children With Multivisceral Transplants
PA-128	2:25	Jones	Imaging Characteristics, Clinical Course, and Neuropsychological Outcome in 9 Pure Pineal Germinomas
PA-129	2:35	Lindsay	Pediatric Posterior Fossa Ganglioglioma: Unique MRI Features and Correlation With BRAF V600E Mutation Status
PA-130	2:45	Almuslim	Comparison of Semi-Automated Segmentation, Manual Segmentation and Maximum Diameter Product in Measuring Chemotherapy Response of Pediatric Neuroblastoma
PA-131	2:55	Sharp	FDG PET/CT Appearance of Locally Recurrent Osteosarcoma After Limb Salvage Surgery
PA-132	3:05	Gauguet	Evaluation of the Utility of 99mTc-MDP Bone Scintigraphy vs. 131 I/123 I-MIBG Scintigraphy and Cross-Sectional Imaging for Staging Patients With Neuroblastoma
PA-133	3:15	Mody	Thyroid Carcinoma in Pediatric Patients: Effective I-131 Ablation Dose and Outcome
PA-134	3:25	States	18F-FDOPA PET/CT Imaging in Congenital Hyperinsulinism: Patterns of Uptake in Diffuse and Focal Disease
PA-135	3:35	Rojas	Relapse Surveillance in AFP-Positive Hepatoblastoma: Is there a Role for Imaging?
PA-136	3:45	Ghaghada	Interrogation of Tumor Vasculature in Mouse Models of Neuroblastoma Using a Nanoparticle Contrast Agent

3:55–4:20 p.m. **Break**

4:20–5:30 p.m. **Scientific Session X-A – Musculoskeletal (concurrent)**

Michael J. Callahan, MD and Nancy A. Chauvin, MD, Moderators

4:20–4:40 p.m. Ultrasound of Muscle Hernias

Michael J. Callahan, MD

4:40–5:30 p.m.		Scientific Papers – Musculoskeletal	
PA-137	4:40	Jamieson	Variation of Alpha Angle in Hip Ultrasound for Developmental Dysplasia Due to Variation in Probe Orientation: Patterns Revealed Using 3D Ultrasound
PA-138	4:50	Wang	Prediction of Residual Hip Dysplasia and the Need for Future Surgical Treatment from MRI Features Visible Post Spica Cast Placement
PA-139	5:00	Stuleanu	Color Doppler Ultrasound Predictors of Short-Term Unfavourable Clinical Outcome in Developmental Dysplasia of the Hip
PA-140	5:10	Fader	Maturation Pattern of the Capitellar Ossification Center: Does This Affect Radiographic Interpretation of the Elbow?
PA-141	5:20	Chauvin	Treatment of Traumatic Shoulder Dislocation Among Adolescents: Does Hill-Sachs Lesion Size Matter?

4:20–5:30 p.m. **Scientific Session X-B – Interventional (concurrent)**

João Amaral, MD and Charles A. James, MD, Moderators

4:20–4:40 p.m. Pediatric Advanced Life Support for the Pediatric IR Physician

Charles A. James, MD

4:40–5:30 p.m.		Scientific Papers - Interventional	
PA-142	4:40	Racadio	Assessment of Angiographic Image Quality from a Flat Panel X-Ray Detector Using Diluted Iodinated Contrast Material in an Animal Model
PA-143	4:50	Benali	MRI of Vascular Anomalies: Value of Diffusion Imaging
PA-144	5:00	Stuart	Keep Your Nerve. The incidence of Neuropathy Following STS Sclerotherapy of Pediatric Venous Malformations
PA-145	5:10	Pimpalwar	Verrucous Hemangioma: Role of Ultrasound Marking Prior to Surgical Excision
PA-146	5:20	Annam	Clinical, Imaging, Surgical and Pathological Correlation of Non-involuting Congenital Hemangioma (NICH) in Children

6:30–11:00 p.m. **Reception & Annual Banquet**

Saturday, May 18, 2013

7:00–8:00 a.m. **Continental Breakfast**

7:00 a.m.–12:00 p.m. **Registration**

Cardiac Session

Pediatric Cardiac MRI: The What, How, Why and Why Nots

Rajesh Krishnamurthy, MD, Moderator

What is It?

8:00–8:10 a.m. Black Blood Imaging

Taylor Chung, MD

8:10–8:20 a.m.	Dynamic Bright Blood Imaging Amol Pednekar
8:20–8:30 a.m.	Quantification of Blood Flow Using Phase Velocity Cine MRI Mike Seed, MBBS
8:30–8:40 a.m.	3D SSFP Raja Muthupillai, PhD

How Do I Do It?

8:40–8:50 a.m.	Assess Segmental Cardiac Anatomy Shi Joon Yoo, MD
8:50–9:00 a.m.	Assess Ventricular Systolic and Diastolic Function Robert J. Fleck, MD
9:00–9:10 a.m.	Evaluate Valvular Stenosis or Regurgitation Sadaf T. Bhutta, MD, MBBS
9:10–9:20 a.m.	Perform Qp:Qs Randolph K. Otto, MD
9:20–9:30 a.m.	How to Set Up a Contrast -Enhanced MRA Dianna M.E. Bardo, MD
9:30–9:40 a.m.	Question and answer
9:40–10:00 a.m.	Break
10:00–10:10 a.m.	Evaluate the Systemic and Pulmonary Veins Prakash M. Masand, MD
10:10–10:20 a.m.	Evaluate Pulmonary Blood Flow J. A. Gordon Culham, MD
10:20–10:30 a.m.	How to Evaluate LV Outflow Tract and Aortic Arch Obstruction Shreyas S. Vasanawala, MD, PhD
10:30–10:40 a.m.	Evaluate the Neonate with Heterotaxy Rajesh Krishnamurthy, MD

Why Do I Do It?

10:40–10:50 a.m.	s/p TOF repair Shiraz A. Maskatia, MD
10:50–11:00 a.m.	Why I Do CMR After Arterial Switch Operation for d-TGA Marc S. Keller, MD

11:00–11:10 a.m.	s/p Atrial Switch for d-TGA Jeffrey C. Hellinger, MD
11:10–11:20 a.m.	Pre-Glenn and Pre-Fontan Shaine A. Morris, MD
11:20–11:30 a.m.	Post-Fontan Cynthia K. Rigsby, MD
11:30–11:40 a.m.	Anomalous Coronaries Lorna P. Browne, MBBS
11:40–11:50 a.m.	Vascular Rings and Slings Prachi P. Agarwal, MD
11:50 a.m.–12:00 p.m.	Cardiac Tumors Maryam Ghadimi-Mahani, MD

6th Annual SPR Education Summit

Educational Issues Worldwide

Dorothy I. Bulas, MD and Marilyn J. Goske, MD, Moderators

8:00–8:05 a.m.	Introduction Dorothy I. Bulas, MD
8:05–9:00 a.m.	World Federation of Pediatric Imaging: International Educational Issues - Challenges and Benefits International Panel Savvas Andronikou, MBBCh, FCRad, FRCR, PhD (Africa), Timothy M.Cain, MBBS (Australia), Kassa Darge, MD, PhD (United States), Celia Ferrari, MD (South America), Bernard F. Laya, DO (Philippines), Kieran McHugh, MD (European Union)
9:00–9:30 a.m.	Unique Issues in Africa Savvas Andronikou, MBBCh, FCRad, FRCR, PhD and Kieran McHugh, MD
9:30–9:40 a.m.	ABR Updates Lane F. Donnelly, MD
9:40–9:50 a.m.	RRC Updates Susan D. John, MD
9:50–10:00 a.m.	Milestone Updates Dorothy I. Bulas, MD
10:00–10:15 a.m.	Question and Answer
10:15–10:30 a.m.	Break

Educational Innovations

10:30–10:50 a.m.	There's an App for That: Radiology Education on Tablets and Mobile Phones Michael P. D'Alessandro, MD
10:50–11:00 a.m.	Engaging Learners in the Era of the iPad Jennifer L. Nicholas, MD
11:00–11:30 a.m.	Program Directors' Latest and Greatest Educational Tools/Projects Jane E. Benson, MD
11:30–11:45 a.m.	Question and Answer
11:45 a.m.	Closing Marilyn J. Goske, MD

Interventional Session
Derek J. Roebuck, FRANZCR, Moderator

8:00–8:30 a.m.	Renal Artery Denervation for Hypertension Sam Stuart, FRCR
8:30–9:00 a.m.	Advances in Musculoskeletal Intervention Neil D. Johnson, MBBS and William E. Shiels, DO
9:00–9:30 a.m.	Intravascular Ultrasound and Optical Coherence Tomography Clare A. McLaren, DCR(R)
9:30–9:50 a.m.	Break
9:50–10:20 a.m.	Vein of Galen Malformations David J.E. Lord, MD, FRANZCR
10:20–10:50 a.m.	Vascular Malformation Syndromes Ahmad I. Alomari, MD
10:50 a.m.–12:00 p.m.	Interventional Case Club John M. Racadio, MD

Neuroradiology Session

Head Injury
Thierry A.G.M. Huisman, MD, Moderator

8:00–8:30 a.m.	Parturitional Brain Injury Thierry A.G.M. Huisman, MD

8:30–9:00 a.m.	Abusive Head Trauma V. Michelle Silvera, MD
9:00–9:30 a.m.	Abusive Head Injury or Not? Differential Diagnoses to Consider Marguerite M. Caré, MD
8:30–9:45 a.m.	Discussion
9:45–10:00 a.m.	Break

Emergency Department Neuroimaging
Timothy N. Booth, MD, Moderator

10:00–10:30 a.m.	Arterial Ischemic Stroke in Children: A Neurointerventionalist's Perspective Darren B. Orbach, MD, PhD
10:30–11:00 a.m.	Emergency Imaging of the Head and Neck Timothy N. Booth, MD
11:00–11:45 a.m.	Beyond Trauma: Pediatric Emergency Brain Imaging Pearls and Pitfalls Laura Z. Fenton, MD
11:45 a.m.–12:00 p.m.	Discussion

Nuclear Medicine Session

Therapeutic Procedures in Pediatric Nuclear Medicine: Why, When, How
Marguerite T. Parisi, MD, MS Ed, Stephanie E. Spottswood, MD and Lisa States, MD Moderators

8:00–8:15 a.m.	Updates from the Pediatric Nuclear Medicine Dose Reduction Working Group S. Ted Treves, MD
8:15–8:35 a.m.	Multimodality Imaging of Neuroblastoma Susan E. Sharp, MD
8:35–8:45 a.m.	Curie Scoring - Prognostic Implications: How to do It Marguerite T. Parisi, MD, MS Ed
8:45–9:30 a.m.	Advances in Neuroblastoma Therapy: The role of I-131 MIBG Meaghan P. Granger, MD
9:30–9:45 a.m.	Break
9:45–10:15 a.m.	Developing an Institutional I-131 MIBG Therapy Program: Key Issues Frederic Fahey, PhD

10:15–10:25 a.m.	Reducing Dose to Nuclear Medicine Personnel During I-131 MIBG Therapy Michael J. Gelfand, MD
10:25–10:45 a.m.	Radiolabeled Somatostatin Analogues for Treatment of Neuroendocrine Tumors Yusuf Menda, MD
10:45–10:55 a.m.	Imaging in Pediatric Thyroid diseases Deepa R. Biyyam, MBBS
10:55–11:05 a.m.	Fine Needle Biopsy in Children with Thyroid Nodules Ganesh Krishnamurthy, MD
11:05–11:35 a.m.	I-131 Radiotherapy of Pediatric Thyroid Cancer Steven G. Waguespack, MD
11:35–11:50 a.m.	Radioimmunotherapy of Lymphoma Hedieh Eslamy, MD
11:50 a.m.–12:00 p.m.	Question and Answer
	Adjourn

SCIENTIFIC EXHIBITS/POSTERS

Case Reports

CR-001	Dunnavant	When Fear of Radiation Leads to Delay in Diagnosis: A Case of Neck Infection Progressing to Florid Mediastinitis With Abscess
CR-002	Ghadimi Mahani	Imaging of Criss-Cross Pulmonary Arteries
CR-003	Ghadimi Mahani	Multimodality Imaging Appearance of an Incidentally Detected Intra-Thoracic Gossypiboma Following Fontan Operation
CR-004	Schubert	Congenital Absence of the Portal Vein Case Report and Review of the Embryology of Portal Vein Development
CR-005	Iskander	Dislodged Percutaneous Placed ASD/ PDA Closure Devices ? Plain Film Diagnosis
CR-006	Morgan	From Perforation to Calcification What You Need to Know About Meconium Peritonitis
CR-007	Brunt	Urorectal Septum Malformation Sequence: A Case Report
CR-008	Loo	MRI Evaluation of Fetal Spine anomalies
CR-009	Dillman	Combined 3D-Rotational Fluoroscopic-MRI Cloacagram Procedure for Comprehensive Evaluation of Cloacal and Other Complex Pelvic Malformations
CR-010	Iskander	Megacystis Microcolon Intestinal Hypoperistalsis Syndrome
CR-011	Jones	Megacystis Microcolon Intestinal Hypoperistalsis Syndrome: A Case Series Imaging Review
CR-012	Zahra	Intrauterine Inferior Vena Cava (IVC) Thrombosis: An Imaging Challenge

CR-013	Liszewski	Radiographic Evaluation of Long Gap Esophageal Atresia and the Foker Staged Lengthening Procedure: A Pictorial Review
CR-014	Bandarkar	Portal Venous Gas and Gastric Pneumatosis in an Infant With Pyloric Stenosis - A Rare Presentation of a Common Condition
CR-015	Smith	Acute Uncomplicated Diverticulitis in Two Adolescent Males
CR-016	Birkemeier	Achalasia In Megacystis Microcolon Intestinal Hypoperistalsis Syndrome: A Case Report
CR-017	Ortiz-Neira	Fast Magnetic Resonance Enterography (FMRE): A New Technique for Rapid Assessment of Pediatric Inflammatory Bowel Disease
CR-018	Kunam	MR Evaluation of Liver Lesions in Children With Transfusion Hemosiderosis
CR-019	Thacker	Ovarian Teratoma Associated NMDA Receptor Encephalitis: Two Cases With Rad-Path Correlation of a Potentially Treatable Paraneoplastic Neuropsychiatric Condition
CR-020	Powers	When Rare and Common Meet: An Unusual Case of Concurrent Adrenal Cortical Tumor and Bilateral Wilms Tumor in an Infant
CR-021	Munden	Immune Reconstitution Inflammatory Syndrome Causing Hypertension in a Child
CR-022	Ashton	Direct Thrombolytic therapy of Superior Mesenteric Artery in an Infant On ECMO
CR-023	Pimpalwar	Imaging and Endoscopy (Laparoscopy/Thoracoscopy) Guided Placement of Peritoneovenous and Pleurovenous (Denver) Shunts in Children
CR-024	Pimpalwar	Institution of Combined Surgical Endoscopic and Interventional Radiologic Approach to Management of Difficult Esophago-Bronchial Connections in Children
CR-025	Pimpalwar	Percutaneous Trans-Splenic Embolization of Roux Limb Varices in Children With Chronic Portal Vein Occlusion (PVO) Post Orthotopic Liver Transplant (OLT)
CR-026	Ramanathan	Pharmacomechanical Pulverization of Mycetoma in the Renal Collecting System
CR-027	Annam	Imaging of the Thoracic Duct Using C-Arm CT Lymphangiography (CTL) Following Ultrasound Guided Inguinal Nodal Injection in Children With Right to Left Shunts
CR-028	Hailey	Interventional Management of Ruptured Hepatoblastoma: Case Report of a Life Threatening Emergency
CR-029	Ramanathan	Radiofrequency Ablation of Multifocal Hepatoblastoma in a Child With Right to Left Intracardiac Shunt: Is there Risk of Microbubble Embolization?
CR-030	Aria	Treating Complex Vascular anomalies With Novel Techniques
CR-031		WITHDRAWN
CR-032	Pimpalwar	Trans-Splenic Recanalization and angioplasty of Anastomotic Portal Vein Occlusion Post OLT
CR-033	Aria	Radiofrequency Ablation: An Alternative Treatment for Large Venous Malformations
CR-034	Carr	The Posterior Femoral Fat Pad? A New Radiological Sign
CR-035	Rosenbaum	Peripheral Cholangiocarcinoma Associated With a Benign Cystic anomaly in an Adolescent
CR-036	Rotaru	Unusual Presentation of a Rare Case of Extramedullary Hematopoiesis Involving the Sino-Nasal Tract in an African American Patient With Sickle Cell Anemia

CR-037	Zammerilla	Histopathologic Diagnosis of Neurofibroma In Lesion With Imaging Features Resembling Vascular Anomalies
CR-038	Yamanari	Spectrum of Klippel-Trenaunay Presentation

Educational Exhibits

EDU-001	Hopkins	A Multi-Departmental Initiative to Reduce Cumulative Radiation From Pediatric Modified Barium Swallow Studies: Methods and Outcomes
EDU-002	Shroff	How Much Radiation Will My Child Get From This CT? How to Easily answer This Question in Your Daily Practice
EDU-003	Karmazyn	A Journey to Decrease Dose Level and Optimize Body CT Scans in Children
EDU-004		WITHDRAWN
EDU-005	Jacob	MR Imaging of Coronary Arteries in Children: Case Based Teaching File
EDU-006	Mitchell	Mom What's My "Itis?" A Clinical and Radiologic Review on Pediatric Vasculitides
EDU-007	Dydynski	Rapid Spiral Dual Source CT for Imaging Congenital Heart Disease With Technical Considerations
EDU-008	Popescu	Fontan Procedure: What Every Pediatric Radiologist Need to Know - A Pictorial Review
EDU-009	George	The Unlucky Seven: The Radiographic Appearance of Children With Congenital Heart Disease Part 1: Anatomy and Presurgical Appearance
EDU-010	George	The Lucky Seven: The Radiographic Appearance of Children With Congenital Cardiac Defects Part 2: Surgeries Post-Surgical Appearance and Complications
EDU-011	Deaver	Congenital Anomalies of the Hand
EDU-012	Sintim-Damoa	Prenatal Ultrasound and MRI Imaging Features of Trisomy 18
EDU-013	Lanier	Perinatal Imaging and Correlations of the Chest and Abdomen: A Case Based Approach
EDU-014	White	Meconium In Fetal and Perinatal Imaging: Associations and Clinical Significance
EDU-015	Gundogan	MR Imaging in Fetal Abdominal and Pelvic Pathologies: It Is NOT Just Pretty Images!
EDU-016	Dawson	Limitations and Advantages of Ultrasound in Evaluating Necrotizing Enterocolitis
EDU-017	Glazer	MR Enterography? Beyond Crohn Disease
EDU-018	Mehta	Plumbing Made Easy: Imaging Findings in Unusual Congenital Anomalies of the Colon
EDU-019	Ayyala	An Unforgettable Journey Through the Diseases of the "Forgotten Organ": The Spleen
EDU-020	Pugmire	MR Enterography of Crohn's Disease Related Abscesses in Young Patients: Pearls and Pitfalls
EDU-021	Fox	Focal Liver Lesions in the Pediatric Patient: A Multimodality Pictorial Review With Pathologic Correlation
EDU-022	Hammer	Crohn Disease of the Perineum - Review of MRI Findings
EDU-023	Jenkins	Gastrojejunostomy Tubes in the Pediatric Population: Risks and Common Complications
EDU-024	Braithwaite	Test Your Skills: Appendicitis or Not by Ultrasound
EDU-025	Assaad	A Practice Model for the Air Reduction of Intussusception

EDU-026	Ching	Multimodality Imaging of Gastrointestinal Pediatric Surgical Emergencies: What Residents Need to Know for Call
EDU-027	Kwon	Improving the Performance of Appendix Ultrasound Examinations: the Step-By-Step Process Undertaken At A Dedicated Pediatric Healthcare Facility
EDU-028	Saylors	Appearance and Follow-Up of Cystic Ovarian Lesions in the Post-Menarchal Teenager: What the Pediatric Radiologist Should Know
EDU-029	Pruthi	Beyond Wilms Tumor- Revisiting Pediatric Renal Masses: Radiologic-Pathologic Correlation
EDU-030	Tawadros	The Spectrum of Imaging and Pathology of Renal Cysts In Children
EDU-031	Machado	Additional Imaging of Upper Abdominal Organs on First Time Renal Sonograms. Is it of Value?
EDU-032	Gawande	Pediatric Renal Masses: Spectrum and Imaging
EDU-033	Otjen	The Twists and Turns of Pediatric Ovarian Torsion ? A Pictorial Review
EDU-034	Stuart	Neonatal Angiography - Little Difficulty
EDU-035	Patel	Push Pull and Buried Bumpers - Removing Pediatric Gastrostomies the Interventional Radiology Way
EDU-036	Subramanian	All Slow Flow Malformations are Not Created Equal: Simple Versus Complex Venous and Lymphatic Malformations: Imaging and Treatment Implications
EDU-037	Chauvin	Shoulder MR Arthrography: Tips for the General Pediatric Radiologist
EDU-038	Dunnavant	Magnetic Resonance Imaging of the Temporomandibular Joint in Juvenile Idiopathic Arthritis and Other Pediatric Rheumatologic Diseases
EDU-039	Chadalavada	Pictorial Review of Osteochondral Lesions of the Knee: To Drill or Not to Drill
EDU-040	Meyers	The Temporomandibular Joint in Juvenile Idiopathic Arthritis: Spectrum of MRI Findings
EDU-041	Meyers	Mandibular Distraction Osteogenesis in the Treatment of Micrognathia: Pre-Operative Imaging Post-Operative Imaging and Complications What the Craniofacial Surgeon Wants to Know
EDU-042	Gowdy	An Illustration of the Clinico-Radiological Findings in Children Presenting From Birth to Puberty With a Brachial Plexus Birth Injury
EDU-043	Shailam	Leg Length Discrepancy More Than Just Numbers: A Pictorial Review From the Perspective of Alignment and Etiology
EDU-044	Llanos	VEPTR? What You Need to Know as a Pediatric Radiologist
EDU-045	Alhammad	Congenital Foot Deformity: How Can I Describe It?
EDU-046	Jadhav	MR Imaging and Arthrographic Findings of Femoroacetabular Impingement (FAI) Based on the Stulberg Classification of Healed Perthes
EDU-047	Horsley	Restricted Diffusion on Brain MRI of the Pediatric Population: A Pictorial Review
EDU-048	Rollins	Diffusion Tensor Imaging of Brainstem Malformations
EDU-049	Linscott	A Slippery Slope: Imaging and Pathology of the Pediatric Clivus
EDU-050	Cakmakci Midia	MR Imaging of the Developing Pediatric Pineal Gland
EDU-051	Subramanian	Magnetic Resonance Imaging of Pediatric Brachial Plexus
EDU-052	Nakagawa	Cerebrospinal Image Findings of Mucopolysaccharidosis: A Pictorial Essay
EDU-053	Alhammad	Imaging Susceptibility in Intracranial Tumors
EDU-054		WITHDRAWN
EDU-055	Chandra	Pediatric Jaw Lesions
EDU-056	Khasawneh	Kinematic MRI: Application and Utility in Evaluation of Cervical Spine Instability in Children

EDU-057	Mody	Utility of Susceptibility Weighted Imaging in Pediatric Neurological Disorders
EDU-058		WITHDRAWN
EDU-059	Cornejo	Bone Scintigraphic Findings in MRSA Osteomyelitis
EDU-060	Gelfand	Avoidable Image Quality Problems in I-123-MIBG Imaging
EDU-061	Narayanan	New Onset Childhood Leukemia: Elusive Musculoskeletal Imaging Findings
EDU-062	Horsley	Pediatric Emphasis Diagnostic Radiology Alternative Pathway (PEDRAP): An Update
EDU-063	Fagen	Ergonomics in the Radiology Workspace
EDU-064	Bennett	Pediatric Vascular Support Device Placement: The Good Bad and Ugly
EDU-065	Goncalves	Radiology-Pathology Conferences of Children's Hospital of Michigan-A Live Teach File for the Apple iPad
EDU-066	Horsley	Abdominal Findings in Non-Accidental Trauma: A Pictorial Review
EDU-067	Malone	Lymphangiectasia With Radiologic-Pathologic Correlation
EDU-068	Coleman	Lumps and Bumps Referred From Pediatricians: What is Encountered on a Superficial Ultrasound?
EDU-069	Liszewski	MRI Evaluation of Lung Parenchyma Airways Vasculature Ventilation and Perfusion: Review of State of the Art Imaging Techniques With Pediatric Applications
EDU-070	Eutsler	Pulmonary Ground Glass Opacities: From the Cradle Through Puberty (and Beyond)
EDU-071	Kusmirek	Radiographic Presentation of Acute Lung Injury Due to Accidental Aspiration and Inhalation in Children
EDU-072	Chawla	The "Testy Testes": A Jeopardy style Quiz on Pediatric Scrotal Imaging

Scientific Exhibits

SCI-001	Harty	Adult-Based Imaging Facilities vs. a Children's Hospital: Comparison of CT Radiation Exposure With Outreach
SCI-002	Moriarity	Evaluating Radiologic Management and Treatment Outcomes of Suspected Pediatric Appendicitis in a Single Healthcare System
SCI-003	McLellan	Phantom Iterative Reconstruction Technique (PIRT)- A Quantitative ALARA Method to Test Iterative Reconstructions Effect On Image Quality and Dose in the Pediatric Population
SCI-004	Dawson	Retrospective Analysis of Weight Exposure Index and Deviation Index in Neonatal Chest Radiography
SCI-005	Lam	Systemic and Pulmonary Venous Connections in Heterotaxy Syndrome: A Review of 50 Cases Comparing MRI/CTA and Echocardiography (Echo)
SCI-006	Cheyne	Position of Umbilical Arterial Line (UAL) In Neonates With Left Congenital Diaphragmatic Hernia (CDH) as Predictor of ICU Length of Stay
SCI-007	Bixenmann	Prenatal and Postnatal Evaluation for Syringomyelia in Patients With Spinal Dysraphism
SCI-008	Bandarkar	Imaging Features of Atypical Intussusception in Children
SCI-009	Wang	Visualization of the Pediatric Appendix at 1.5 T
SCI-010	Nguyen	Intussusception Revisited: Is Immediate On-Site Surgeon Availability at the Time of Reduction Necessary?
SCI-011	Atweh	Radiologic-Pathologic Correlation of Unusual Pediatric Hepatic Tumors Based on MR Imaging Features

SCI-012	Imsande	Morbidity Associated With Delayed Treatment of Cholelithiasis in Pediatric Patients With Sickle Cell Disease
SCI-013	Saxena	Portal Vein Colour Doppler in the Prediction of Feed Intolerance in Neonates With Antenatally Detected Absent/Reversed End Diastolic Flow (AREDF) in Umbilical Artery
SCI-014	Bandarkar	Beware! Inguinolabial Hernia Containing Reproductive Organs in Female Children is Not as Rare as You Think
SCI-015	Abramovici	The Claw Sign: Can it Determine the Organ of Origin of a Retroperitoneal Mass?
SCI-016	Imsande	Renal Imaging Abnormalities as a Predictor of Sickle Cell Nephropathy
SCI-017	Viers	An Update on the Utility of Screening for Malignancy in Beckwith-Wiedemann Syndrome and Idiopathic Hemihypertrophy
SCI-018	Guo	Reduction of Dose Area Product in Pediatric Genitourinary Cases: An Effective and Sustained Departmental Initiative
SCI-019	Narayanan	Identifying Renal Imaging Biomarkers of Motor Inhibitor Therapy for Tuberous Sclerosis Complex
SCI-020	Patel	Percutaneous Management of Cervico-Mediastinal Lymphatic Malformations Associated With Airway Compromise
SCI-021	Annam	Imaging Findings of Central Conducting Lymphatics (CCL) Using Dynamic Magnetic Resonance Lymphangiography (MRL)
SCI-022	Aria	Greater Saphenous Venous Access as an Alternative in Young Children
SCI-023	Karbach	Minimal Incremental Value of Frogleg Lateral View of the Pelvis in Children With Suspected DDH
SCI-024	Karbach	Effectiveness of Screening DDH With and Without Acetabular Angle Measurements. Is Gestalt Diagnosis Adequate?
SCI-025	Munir	Evidence-Based Outcomes of Studies Addressing Diagnostic Accuracy of MRI of Juvenile Idiopathic Arthritis in the Axial Skeleton - A Systematic Review
SCI-026	Doria	Ultrasound and MRI of Growing Joints in Healthy Boys: Correlation With Ex-Vivo Phantom Measurements
SCI-027	Wang	Evidence-Based Outcomes on Diagnostic Accuracy of Quantitative Ultrasound for Assessment of Pediatric Osteoporosis
SCI-028	Narayanan	Fish Tail Deformity: Trochlear Osteonecrosis-A Delayed Complication of Distal Humeral Fractures
SCI-029	Lai	False Positive Shunt Discontinuity at Digital VP Shunt Survey Radiography
SCI-030	Nagaraj	Evaluation of Optic Pathway Gliomas in Patients With Neurofibromatosis Type I Under the Age of 4 Years
SCI-031	Lefebvre	Role of MRI in the Evaluation of Obstetrical Brachial Plexus Injury in Pediatric Patients
SCI-032	Jordaan	Chiari Type 1 Malformations in Adolescent Sportspersons- Size Isn't Everything!
SCI-033	Reavey	Appendiceal 18F-FDG Uptake in Children: What's Normal?
SCI-034	Tran	Fusion PET-MR: Correlation of Contrast Enhancement and 18-FDG-PET Activity for the Development of an Integrated Scanning Protocol
SCI-035	Weber	Clinical Presentation Imaging Characteristics and Management of Parotid Hemangiomas

GENERAL INFORMATION

MISSION STATEMENT

The Society for Pediatric Radiology is dedicated to fostering excellence in pediatric health care through imaging and image-guided care.

SITES OF PREVIOUS MEETINGS

1991 & IPR'91	Stockholm, Sweden
1992	Orlando, Florida
1993	Seattle, Washington
1994	Colorado Springs, Colorado
1995	Washington, D.C.
1996& IPR'96	Boston, Massachusetts
1997	St. Louis, Missouri
1998	Tucson, Arizona
1999	Vancouver, British Columbia
2000	Naples, Florida
2001 & IPR'01	Paris, France
2002	Philadelphia, Pennsylvania
2003	San Francisco, California
2004	Savannah, Georgia
2005	New Orleans, Louisiana
2006 & IPR '06	Montreal, Quebec, Canada
2007	Miami, Florida
2008	Scottsdale, Arizona
2009	Carlsbad, California
2010	Boston, Massachusetts
2011 & IPR '11	London, England
2012	San Francisco, California

FUTURE MEETINGS

2014	May 13–17, 2014	Washington, DC
2015	April 27-May 1, 2015	Seattle, Washington
2016 & IPR '16	May 16–20, 2016	Chicago, Illinois

OFFICERS, DIRECTORS AND COMMITTEES 2012–2013

Board of Directors

Donald P. Frush, MD, FACR, Chair
Sue C. Kaste, DO, President
Richard A. Barth, MD, President-Elect
Brian D. Coley, MD, 1st Vice President
James S. Donaldson, MD, FACR, 2nd Vice President
James S. Donaldson, MD, FACR, Secretary
Brent H. Adler, MD, Treasurer
Christopher I. Cassady, MD, Secretary-Elect
Molly E. Dempsey, MD, Treasurer-Elect
Peter J. Strouse, MD, FACR (SCORCH)
Lisa H. Lowe, MD
Heike E. Daldrup-Link, MD
Beverley Newman, MD, FACR
Rafael Rivera, MD
George S. Bisset III, MD, FACR
Dorothy I. Bulas, MD, FACR, Past President
Neil D. Johnson, MD, Past President
M. Ines Boechat, MD, FACR, Past President, WFPI President
Marilyn J. Goske, MD, Image Gently Liaison
Marta Hernanz-Schulman, MD, FACR, ACR Commission Liaison
Thomas L. Slovis, MD, Editor (to 12/2012)
Mary R. Board Wyers, MD, Website Editor

Bylaws

Donald P. Frush, MD, FACR, Chair
Heike E. Daldrup-Link, MD
Peter J. Strouse, MD, FACR

Cardiac Imaging Committee

Rajesh Krishnamurthy, MD, Chair
Dianna M. E. Bardo, MD
Sadaf T. Bhutta, MD, MBBS
Lorna P. Browne, MB BS
Maryam Ghadimi-Mahani, MD
S. Bruce Greenberg, MD
Jeffrey C. Hellinger, MD
Prakash M. Masand, MD
Randolph K. Otto, MD
Cynthia K. Rigsby, MD, FACR
Laureen M. Sena, MD
Shreyas S. Vasanawala, MD, PhD

Child Abuse Committee

Jeannette M. Perez-Rossello, MD, Chair
Leslie A. Bord, MD
Stephen D. Brown, MD
Judith A. Craychee, MD
Jerry R.l. Dwek, MD
P. Ellen Grant, MD, MSc
Laura L. Hayes, MD
Thaddeus W. Herliczek, MD, MS
Daniel M. Schwartz, MD
Sabah Servaes, MD
Andy Tsai, MD
Terry J. Vaccaro, MD
Consultants:
Ingrid Holm, MD
Carole Jenny, MD
Paul K. Kleinman, MD
Joelle Moreno

Clinical Practices Steering Committee
James S. Donaldson, MD, FACR, Chair
Judy A. Estroff, MD
Lynn A. Fordham, MD, FACR
Sue C. Kaste, DO
Beth M. Kline-Fath, MD
Rajesh Krishnamurthy, MD
Edward Y. Lee, MD, MPH
Marguerite Theresa Parisi, MD, MS
Jeannette M. Perez-Rossello, MD
Daniel J. Podberesky, MD
Tina Young Poussaint, MD
Dennis W Shaw, MD
Michael John Temple, MD
Shreyas S Vasanawala, MD, PhD
Sjirk Jan Westra, MD

Community Hospital-based Pediatric Radiologists
Debra J. Pennington, MD, Chair
Christopher E. Dory, MD
Maria-Gisela Mercado-Deane, MD
Michael D. Rubin, MD
Amaya Ormazabal, MD

Contrast-Enhanced Ultrasound Task Force
Frank M. Volberg, MD, Chair
Dorothy I. Bulas, MD, FACR
Kassa Darge, MD, PhD
Lynn A. Fordham, MD, FACR
M. Beth McCarville, MD
Harriet Joan Paltiel, MD

CT Committee
Sjirk Jan Westra, MD, Chair
Steven L. Blumer, MD
Jonathan R. Dillman, MD
Thaddeus W. Herliczek, MD, MS
Edward Y. Lee, MD, MPH
Grace S. Phillips, MD
Anil G. Rao, DMRD, DNB
Sabah Servaes, MD
Alexander J. Towbin, MD

Diagnostics
Daniel J. Podberesky, MD, Chair
Karen Blumberg, MD, FACR
Marcus M. Kessler, MD
Edward Y. Lee, MD, MPH
Arthur B. Meyers, MD
Shawn E. Parnell, MD
Ethan A. Smith, MD

Education – Curriculum
Peter J. Strouse, MD, FACR, Chair
Brent H. Adler, MD
Brian D. Coley, MD
Donald P. Frush, MD, FACR
Sue C. Kaste, DO
Sarah S. Milla, MD

Fellowship Program Directors
Jane E. Benson, MD, Chair

Fetal Imaging
Beth M. Kline-Fath, MD, Chair
Leslie A. Bord, MD
Dorothy I. Bulas, MD, FACR
Maria A. Calvo-Garcia, MD
Lucia Carpineta, MD, CM
Christopher I. Cassady, MD
Kimberly A. Dannull, MD
Judy A. Estroff, MD
Hollie A. Jackson, MD
Ashley J. Robinson, MBChB
Chetan C. Shah, MD
Teresa Victoria, MD

Finance
Molly E. Dempsey, MD, Chair
Brent H. Adler, MD
Richard A. Barth, MD
Brian D. Coley, MD
Sue C. Kaste, DO
Randheer Shailam, MD
Stephen F. Simoneaux, MD

Honors
M. Ines Boechat, MD, FACR, Chair
Dorothy I. Bulas, MD, FACR
Neil D. Johnson, MD

Informatics
Alexander J. Towbin, MD, Chair
R. Paul Guillerman, MD
James D. Ingram, MD
Neil D. Johnson, MD
Edward Y. Lee, MD, MPH
Janet R. Reid, MD
Mahesh M. Thapa, MD, BS
Keith S. White, MD

Innovation
Donald P. Frush, MD, FACR, MD, Chair

International Task Force
M. Ines Boechat, MD, FACR, Chair
Dorothy I. Bulas, MD, FACR
Ronald A Cohen, MD

James S. Donaldson, MD, FACR
Carmen Emery, MD
Charles A. Gooding, MD
Neil D. Johnson, MD
Stuart A. Royal, MS, MD, FACR
Rebecca Stein-Wexler, MD

Interventional
Michael J. Temple, MD, Chair
Mark A. Bittles, MD
G. Peter Feola, MD
Marc S. Keller, MD
Els Nijs, MD
Ashley J. Robinson, MBChB
Manrita K. Sidhu, MD
Charles A. James, MD, FACR, ex officio

Judiciary
Richard B. Gunderman, MD, FACR, Chair
Stephen D. Brown, MD
Neil D. Johnson, MD
Charles D. Williams, MD

MR Committee
Shreyas S. Vasanawala, MD, PhD, Chair
Adina L. Alazraki, MD
Sudha A. Anupindi, MD
Lauren W. Averill, MD
Kiery A. Braithwaite, MD
Govind B. Chavhan, MD DNB
Kassa Darge, MD, PhD
Ramesh S. Iyer, MD
S. Pinar Karakas, MD
Arzu Kovanlikaya, MD
Jeannie K. Kwon, MD
Edward Y. Lee, MD, MPH
Prakash M. Masand, MD
Anil G. Rao, DMRD, DNB
Mahesh M. Thapa, MD, BS
Neil Vachhani, MD

Neuroradiology
Tina Young Poussaint, MD, Chair
Thierry A.G.M. Huisman, MD
Nadja Kadom, MD
Paritosh C. Khanna, MD, DMRE
Arzu Kovanlikaya, MD
Sarah S. Milla, MD
Sumit Pruthi, MD
Gaurav Saigal, MD
Aylin Tekes, MD
Lynn M. Trautwein, MD
Unni K. Udayasankar, MD

Newborn
Judy A. Estroff, MD, Chair
Leslie A. Bord, MD
Christopher I. Cassady, MD
Teresa Chapman, MD MA
Monica Epelman, MD
Maria F. Ladino Torres, MD
Kathleen M. McCarten, MD, FACR
Ashok Panigrahy, MD
Eva I. Rubio, MD
Valerie L. Ward, MD
Consultant: Richard Parad, MD

Nominating
Donald P. Frush, MD, FACR, Chair
Kassa Darge, MD, PhD
Edward Y. Lee, MD, MPH
Beverley Newman, MD, FACR
Cynthia K. Rigsby, MD, FACR
Lisa J. States, MD
Raymond W. Sze, MD

Nuclear Medicine
Marguerite T. Parisi, MD, MS, Chair
Larry A. Binkovitz, MD
Elizabeth A. Hingsbergen, MD
Ruth Lim, MD, BS
Gerald A. Mandell, MD, FACR
Helen R. Nadel, MD, FRCPC
Marla BK Sammer, MD
Victor J. Seghers, MD, PhD
Susan E. Sharp, MD
Stephanie E. Spottswood, MD, MSPH
S. Ted Treves, MD
Pranav K. Vyas, MD
John B. Wyly, MD
Lisa J. States, MD

Oncology Committee
Sue C. Kaste, DO, Chair
Heike E. Daldrup-Link, MD
Michael J. Gelfand, MD
M. Beth McCarville, MD
Marguerite T. Parisi, MD, MS
Susan E Sharp, MD
Marilyn J. Siegel, MD, FACR
Thomas L. Slovis, MD
Alexander J. Towbin, MD
Shreyas S. Vasanawala, MD, PhD
Stephan D. Voss, MD, PHD
Consultants*:*
Peter C. Adamson, MD
Greg Reamon, MD

Physician Resources Committee
Ellen C. Benya, MD, Chair
Rebecca L. Hulett-Bowling, MD
Ramesh S. Iyer, MD
Vesna M. Kriss, MD
Sosamma T. Methratta, MD
Jason B. Mitchell, MD

Public Policy
Richard M. Benator, MD, FACR, Chair
Richard A. Barth, MD
Kate A. Feinstein, MD, FACR
Donald P. Frush, MD, FACR

Publications
Ashok Panigrahy, MD, Chair
Johan G. Blickman, MD, PHD, FACR
Dorothy I. Bulas, MD, FACR
Jonathan R. Dillman, MD
Charles M. Glasier, MD
Edward Y. Lee, MD, MPH
Ethan A. Smith, MD
Alexander J. Towbin, MD
Christopher I. Cassady, MD, ex officio
James S. Donaldson, MD, FACR, ex officio
Editors:
Brian D. Coley, MD
Cynthia K. Rigsby, MD, FACR
Thomas L. Slovis, MD
Peter J. Strouse, MD, FACR

Research and Education Foundation Board
Brian D. Coley, MD, President
Sue C. Kaste, DO, Vice President
James S. Donaldson, MD, FACR, Secretary
Brent H. Adler, MD, Treasurer
Christopher I. Cassady, MD, Secretary-Elect
Molly E. Dempsey, MD, Treasurer-Elect
Johan G. Blickman, MD, PHD, FACR
Kassa Darge, MD, PhD
Lisa H. Lowe, MD
William H. McAlister, MD, FACR
Richard L. Robertson, MD
Stuart A. Royal, MS, MD, FACR

Safety
Dennis W. Shaw, MD, Chair
Sudha A. Anupindi, MD
Einat Blumfield, MD
Thomas R. Goodman, MBBCh
Marilyn J. Goske, MD
Ramesh S. Iyer, MD
David B. Larson, MD
Grace S. Phillips, MD
Ramon Sanchez, MD
Consultant: Thomas L. Slovis, MD

Thoracic Imaging
Edward Y. Lee, MD, MPH, Chair
Alan S. Brody, MD
Maryam Ghadimi-Mahani, MD
R. Paul Guillerman, MD
Jeffrey C. Hellinger, MD
David A. Mong, MD
Beverley Newman, MD, FACR
Daniel J. Podberesky, MD
Sjirk Jan Westra, MD

Ultrasound
Lynn A. Fordham, MD, FACR, Chair
Jeanne S. Chow, MD
Ellen M. Chung, MD
Harris L. Cohen, MD, FACR
Jamie L. Coleman, MD
Monica Epelman, MD
Boaz Karmazyn, MD
Shailee Lala, MD
Leann E. Linam, MD
Martha M. Munden, MD
Els Nijs, MD
Sara M. O'Hara, MD
Henrietta K. Rosenberg, MD, FACR
Cicero T. Silva, MD
Andrew T. Trout, MD
Dayna M. Weinert, MD

Website Editorial Committee
Mary R. Board Wyers, MD, Chair
Benjamin H. Taragin, MD

Representatives
Kimberly E. Applegate, MD, MS, FACR, Liaison to ACR CSC
Richard Max Benator, MD, FACR, ACR Alternate Councilor
Dorothy I. Bulas, MD, FACR, Academy of Radiology Research
Christopher I. Cassady, MD, American Academy of Pediatrics
Brian D. Coley, MD, American Institute of Ultrasound in Medicine
Kate A. Feinstein, MD, FACR, ACR Councilor
Donald P. Frush, MD, FACR, American Board of Radiology
Susan D. John, MD, FACR, American Society of Emergency Radiology
Tina Young Poussaint, MD, American Society of Pediatric Neuroradiology

GOLD MEDALISTS

1988	Frederic N. Silverman, MD
1989	John L. Gwinn, MD
1990	John F. Holt, MD
1991	John A. Kirkpatrick, Jr., MD
1991	Bernard J. Reilly, MB, FRCP
1992	Edward B. Singleton, MD
1993	Hooshang Taybi, MD
1994	Walter E. Berdon, MD
1994	J. Scott Dunbar, MD
1995	Guido Currarino, MD
1995	Derek C. Harwood-Nash, MD, DSc
1996	Andrew K. Poznanski, MD
1996	Beverly P. Wood, MD
1997	N. Thorne Griscom, MD
1997	John F. O'Connor, MD
1998	William H. McAlister, MD
1999	E. Anthony Franken, MD
2000	Eric L. Effmann, MD
2001	Giulio J. D'Angio, MD
2002	David H. Baker, MD
2003	Brinton B. Gay, Jr., MD
2003	William H. Northway, Jr., MD
2004	Diane S. Babcock, MD
2004	Virgil R. Condon, MD
2005	Jerald P. Kuhn, MD
2005	Thomas L. Slovis, MD
2006	Robert L. Lebowitz, MD
2006	John C. Leonidas, MD
2007	Leonard E. Swischuk, MD
2008	Barry D. Fletcher, MD
2009	Charles A. Gooding, MD
2010	Janet L. Strife, MD
2011	Carol M. Rumack, MD
2012	Marilyn J. Goske, MD
2013	Stuart A. Royal, MS, MD

PIONEER HONOREES

1990	John Caffey, MD
1991	M.H. Wittenborg, MD
1992	Edward B. Singleton, MD
1993	Frederic N. Silverman, MD
1994	John P. Dorst, MD
1995	E.B.D. Neuhauser, MD
1996	Edmund A. Franken, MD
1996	Kazimierz Kozlowski, MD
1996	M. Arnold Lassrich, MD
1997	Arnold Shkolnik, MD
1998	Heidi B. Patriquin, MD
1998	William H. Northway, Jr., MD
2000	Jerald P. Kuhn, MD
2001	Diane S. Babcock
2001	Fred E. Avni, MD, PhD
2003	Walter E. Berdon, MD
2004	G.B. Clifton Harris, MD
2005	Rita L. Teele, MD
2006	Robert L. Lebowitz, MD
2007	Carol M. Rumack, MD
2008	Paul S. Babyn, MD
2009	Kenneth E. Fellows, MD
2010	David K. Yousefzadeh, MD
2011	Massoud Majd, MD
2012	George S. Bisset, III, MD
2013	Barry D. Fletcher, MD

PRESIDENTIAL RECOGNITION AWARDS

1999	David C. Kushner, MD
2000	Paul K. Kleinman, MD
2001	Neil Johnson, MD
2001	Christopher Johnson
2002	Jennifer K. Boylan
2002	Thomas L. Slovis, MD
2003	Danielle K.B. Boal, MD
2003	Marta Hernanz-Schulman, MD
2004	Kenneth L. Mendelson, MD
2005	Taylor Chung, MD
2005	J. A. Gordon Culham, MD
2005	Shi-Joon Yoo, MD
2006	L. Christopher Foley, MD
2007	Donald P. Frush, MD
2008	Mary K. Martel, PhD
2008	Connie L. Mitchell, MA, RT(R)(CT)
2008	Harvey L. Neiman, MD
2009	Karen S. Schmitt
2010	Richard A. Barth, MD
2011	Kimberly E. Applegate, MD, MS, FACR
2011	Keith Strauss, MS, FACR
2012	David C. Kushner, MD, FACR
2012	Stuart A. Royal, MS, MD
2013	Alan E. Schlesinger, MD

HONORARY MEMBERS

1985	Jacques Sauvegrain, MD
1987	Bryan J. Cremin, MD
1987	Ole A. Eklof, MD
1987	Clement C. Faure, MD
1987	Andres Giedion, MD
1987	Denis Lallemand, MD
1987	Arnold Lassrich, MD
1987	Ulf G. Rudhe, MD
1998	Frederic N. Silverman, MD
1989	John L. Gwinn, MD
1990	John F. Holt, MD
1990	Richard G. Lester, MD
1991	Gabriel L. Kalifa, MD
1991	Javier Lucaya, MD
1991	John P. Masel, MD
1991	Noemi Perlmutter-Cremer, MD
1991	Hans G. Ringertz, MD
1991	John A. Kirkpatrick, Jr., MD
1991	Bernard J. Reilly, MB, FRCP(C)
1992	Edward B. Singleton, MD
1992	Donald R. Kirks, MD
1992	Beverly P. Wood, MD
1993	Hooshang Taybi, MD
1992/94	Walter E. Berdon, MD
1994	Marie A. Capitanio, MD
1994	Edmund A. Franken, Jr., MD
1994	John C. Leonidas, MD
1994	William H. McAlister, MD
1994	Andrew K. Poznanski, MD
1994	J. Scott Dunbar, MD
1995	David H. Baker, MD
1992/95	Derek C. Harwood-Nash, MD, DSc
1995	N. Thorne Griscom, MD
1995	Guido Currarino, MD
1996	Francis O. Brunelle, MD
1996	Lloyd L. Morris, MD
1996	Heidi B. Patriquin, MD
1997	John F. O'Connor, MD
1997	Theodore E. Keats, MD
1998	Rita L. Teele, MD
1998	H. Ted Harcke, MD
1999	J. Bruce Beckwith, MD
2000	Joseph Volpe, MD
2001	Ulrich V. Willi, MD
2001	Henrique M. Lederman, MD
2001	Mutsuhisa Fujioka, MD
2002	Eric J. Hall, DSc, FACR, FRCR
2002	Walter Huda, PhD
2003	Michael R. Harrison, MD
2004	Lee F. Rogers, MD
2005	Carden Johnston, MD, FAAP, FRCP
2006	Alan B. Retik, MD
2007	Robert R. Hattery, MD
2008	Professor Hassen A. Gharbi
2009	Dolores Bustelo, MD
2009	Pedro A. Daltro, MD
2009	Cristian Garcia, MD
2009	Antônio Soares de Souza, MD
2010	Stephen Chapman, MD
2011	Catherine M. Owens, MBBS
2011	Madan M. Rehani, PhD
2012	Harvey L. Neiman, MD, FACR
2013	Savvas Andronikou, MBBCh, FCRad, FRCR, PhD

PAST PRESIDENTS

1958-59	Edward B. Neuhauser, MD*
1959-60	Frederic N. Silverman, MD*
1960-61	John F. Holt, MD*
1961-62	Arthur S. Tucker, MD*
1962-63	John W. Hope, MD*
1963-64	R. Parker Allen, MD
1964-65	Edward B. Singleton, MD
1965-66	J. Scott Dunbar, MD*
1966-67	Harvey White, MD*
1967-68	M.H. Wittenborg, MD*
1968-69	David H. Baker, MD
1969-70	John A. Kirkpatrick, Jr., MD*
1970-71	Norman M. Glazer, MD*
1971-72	Bertram R. Girdany, MD*
1972-73	Donald H. Altman, MD
1973-74	Hooshang Taybi, MD*
1974-75	John L. Gwinn, MD*
1975-76	Lawrence A. Davis, MD*
1976-77	Marie A. Capitanio, MD
1977-78	John P. Dorst, MD*
1978-79	Bernard J. Reilly, MB, FRCP (C)*
1979-80	Walter E. Berdon, MD
1980-81	Andrew K. Poznanski, MD
1981-82	N. Thorne Griscom, MD
1982-83	Virgil R. Condon, MD
1983-84	Jerald P. Kuhn, MD
1984-85	Lionel W. Young, MD
1985-86	John C. Leonidas, MD*
1986-87	Derek C. Harwood-Nash, MD, DSc*

IPR '87	Denis Lallemand, MD (ESPR)
1987-88	Beverly P. Wood, MD
1988-89	John F. O'Connor, MD*
1989–90	E.A. Franken, Jr., MD
1990–91	Donald R. Kirks, MD
IPR '91	Hans G. Ringertz, MD, PhD (ESPR)
1991-92	William H. McAlister, MD
1992-93	M. B. Ozonoff, MD
1993-94	Joanna J. Seibert, MD
1994-95	Eric L. Effmann, MD
1995–96	Kenneth E. Fellows, MD
IPR '96	Paul S. Thomas, MD (ESPR)
1996–97	Diane S. Babcock, MD
1997–98	Charles A. Gooding, MD
1998–99	Robert L. Lebowitz, MD
1999–00	Thomas L. Slovis, MD
2000–01	Janet L. Strife, MD
IPR '01	Francis Brunelle, MD (ESPR)
2001–02	Bruce R. Parker, MD
2002–03	Richard B. Towbin, MD
2003–04	David C. Kushner, MD
2004–05	Stuart A. Royal, MS, MD
2005–06	George A. Taylor, MD
IPR '06	Richard Fotter, MD (ESPR)
2006–07	Marilyn J. Goske, MD
2007–08	Marta Hernanz-Schulman, MD
2008–09	M. Ines Boechat, MD
2009–10	Neil D. Johnson, MBBS
2010–11	Dorothy I. Bulas, MD
IPR '11	Catherine M. Owens, MD
2011–12	Donald P. Frush, MD

*Deceased

SINGLETON-TAYBI AWARD

2006	Corning Benton, Jr., MD
2007	Michael P. D'Alessandro, MD
2007	Janet R. Reid, MD
2008	Dorothy I. Bulas, MD
2009	Lane F. Donnelly, MD
2010	Wilbur L. Smith, Jr., MD
2011	Ralph S. Lachman, MD, FACR
2012	Alan Daneman, MD
2013	Lisa H. Lowe, MD

JOHN A. KIRKPATRICK YOUNG INVESTIGATOR AWARD

This award is given to the author of the best paper presented by a Resident or Fellow at the SPR meeting. Beginning in 1995, the award became known as the John A. Kirkpatrick Young Investigator Award.

1993	Philipp K. Lang, MD
1993	Stephanie P. Ryan, MD
1994	Sara O'Hara, MD
1995	Philipp K. Lang, MD
1996	Fergus V. Coakley, MB, FRCR
1997	Ronald A. Alberico, MD
1998	Laura J. Varich, MD
1999	A. E. Ensley, BS
1999	R.W. Sze, MD
2000	S. H. Schneider, MD
2001	Valerie L. Ward, MD
2002	Ricardo Faingold, MD
2003	Andrea Doria, MD
2004	Nina M. Menezes, PhD
2005	Lena Naffaa, MD
2006	Courtney A. Coursey, MD
2007	Ashley J. Robinson, MBChB
2008	Hee Kyung Kim, MD
2009	Conor Bogue, MD
2010	Albert Hsiao, MD, PhD
2011	Ethan A. Smith, MD
2012	Saivivek Bogale, MD

WALTER E. BERDON AWARDS - 2011

Best Basic Science Paper

Castaneda RT, Boddington S, Henning TD, Wendland M, Mandrussow L, Liu S, Daldrup-Link H. Labeling Human Embryonic Stem-Cell-Derived Cardiomyocytes for Tracking With MR Imaging

Best Clinical Research Paper

Schachar JL, Zampolin RL, Miller TS, Farinhas JM, Freeman K, Taragin BH. External Validation of the New Orleans Criteria (NOC), the Canadian CT Head Rule (CCHR) and the National Emergency X-Radiography Utilization Study II (NEXUS II) for CT Scanning in Pediatric Patients With Minor Head Injury in a Non-Trauma Center

2012 recipients will be announced at the meeting. For a list of prior recipients, please visit the SPR website.

THE SPR RESEARCH AND EDUCATION FOUNDATION AWARDS

The SPR Research and Education Foundation is dedicated to promoting research and scholarship in pediatric radiology. The SPR Board of Directors has supported research through grants since 1990. The Foundation was established in 1994 with an initial donation from the Society's reserves.

The Jack O. Haller Award for Excellence in Teaching

2005 Alan Daneman, MD
2006 William R. Cranley, MD and John F. O'Connor, MD
2007 Cindy R. Miller, MD
2008 Sara J. Abramson-Squire, MD
2009 Michael A. DiPietro, MD
2010 George A. Taylor, MD
2011 Paul K. Kleinman, MD
2012 Richard I. Markowitz, MD
2013 Gary L. Hedlund, DO

The Heidi Patriquin International Fellowship

2005 Luy Lyda, MD, *Angkor Hospital for Children,* Siem Reap, Cambodia
2006 Hakima Al-Hashimi, MD *Salmaniya Medical Complex*, Manama, Bahrain
2006 Pannee Visrutaratna, MD, *Chiang Mai University,* Chiang Mai, Thailand
2006 Juana Maria Vallejo, MD, *Clinica del Country,* Bogota, Colombia
2007 Nathan David P. Concepcion, MD, *St. Luke's Medical Center*, Quezon City, Philippines
2008 Rolando Reyna Lopez, MD, *Hospital Santo Tomas*, Panama City, Panama
2009 Ahmed Mussa Jusabani, MD, *Kilimanjaro Christian Medical Centre*, Moshi Town, Tanzania
2010 Omolola Mojisola Atalabi, MD, *College of Medicine, University of Ibadan,* Nigeria
2011 Kushaljit Singh Sodhi, MD, *Postgraduate Institute of Medical Education and Research (PGIMER),* Chandigarh, India
2012 Wambani Sidika Jeska, MBchB, *Kenyatta National Hospital, Nairobi, Kenya*
2012 Yocabel Gorfu, MD, *Addis Ababa University, Addis Ababa, Ethiopia*
2013 Regina Nava, MD, *St. Luke's Medical Center, Quezon City, Philippines*
2013 Olubukola Abeni Omidiji, MBBS, University of Lagos, Lagos, Nigeria

Pilot Award

M. Ines Boechat, MD, FACR, Developing the framework of the global federation of pediatric radiologists, *David Geffen School of Medicine at UCLA on behalf of the WFPI Board of Directors*

Seed Grant

Bairbre Connolly, MD, Testing the use of the emerging γ-H2AX biomarker for quantifying DNA damage from pediatric interventional procedures involving ionizing radiation - the first step in assessing the use of DNA protective agents in children, *The Hospital for Sick Children, University of Toronto*

Fellow Awards

Bruno P. Soares, MD, Arterial Spin Labeling Brain Perfusion MR in the Evaluation of White Matter Injury of Prematurity, *University of California, San Francisco*; Mentor, Dr. James Barkovich

Skorn Ponrartana, MD, MPH, MR imaging for the assessment of Duchenne muscular dystrophy: diffusion tensor imaging and fat quantification as imaging markers of disease progression, *Children's Hospital Los Angeles*; Mentor: Dr. Vicente Gilsanz

For a list of prior grant recipients, please visit the SPR website.

SOCIAL EVENTS

SPR Fun Run
Benefiting the Research & Education Foundation
Wednesday, May 15th
6:00 a.m.
Join us for this 3-mile run through the resort's scenic property and get your day off to a great start! Runners and walkers are all welcome. Entrance fee - $25. See the Registration Desk for details.

Welcome Reception
Wednesday, May 15
6:15–7:30 p.m.
Hyatt Regency Hill Country Resort
Hors d'oeuvres and Refreshments
Resort Casual Attire (this will be an outdoor event)

Reception and Annual Banquet
Friday, May 17
6:30–11:00 p.m.
Hyatt Regency Hill Country Resort
Reception, Dinner and Dancing
Diamonds and Denim Attire

Riverwalk Night Out
Tuesday, May 14 & Thursday, May 16
6:00–11:00 p.m.
The San Antonio Riverwalk is a scenic pathway that winds along the banks of the San Antonio River offering restaurants, shops, river cruises and much more. The SPR will provide motorcoach transportation to the Riverwalk, departing the Hyatt at 6:00 p.m., with buses returning from the Riverwalk at 10:30 p.m. Anticipated arrival time back at the Hyatt is 11:00 p.m. Please make sure you have registered in advance to confirm your transportation.

SPR 2013 Gold Medalist

The Gold Medal of The Society for Pediatric Radiology is our most distinguished honor. The SPR Medal is awarded to pediatric radiologists who have contributed greatly to the SPR and our subspecialty of pediatric radiology as a scientist, teacher, personal mentor and leader.

Stuart A. Royal, MS, MD, FACR

The Society for Pediatric Radiology Gold Medal is our most distinguished honor. It is awarded to pediatric radiologists who have contributed greatly to the SPR and to our specialty as a scientist, teacher, leader, and mentor. The 2013 SPR Gold Medal is awarded to Dr. Stuart Royal, who is most deserving of this recognition. His career has been characterized by a deeply committed lifetime of outstanding academic leadership, seminal research contributions, significant national and international accomplishments in medical education, as well as astute guidance in the business aspects of the SPR as well as his medical center. His keen mind, boundless enthusiastic energy, and warm heart make him a precious colleague. He epitomizes the type of person we should all try to be.

Dr. Royal considers his greatest contribution to pediatric radiology to be the reorganization of the SPR business function. This represented an extremely important milestone in the history of the SPR. It brought the SPR under the auspices of the ACR for society and meeting management and it will have an enduring impact. Furthermore, Stuart led the visualization, development, and implementation of a fundraising process for the SPR Research and Education Foundation, named the SPR Campaign for Children. This included a method for obtaining corporate support for the SPR. Also, the ACR provided Stuart with an outlet for his altruistic characteristic of improving worldwide healthcare by working with the ACR International Outreach Committee to assist in the reconstruction of the Children's Hospital in Port-au-Prince, Haiti and helping to improve medical imaging in Sri Lanka. His work with the World Federation of Pediatric Imaging also broadens his impact on children's health worldwide.

One of the several research projects of which he is most proud was his participation in an NIH funded project while he was a resident at UCSF. He and his colleagues developed an animal model, involving pancreatectomy, which produced hepatic fatty infiltration. Comparing hepatic computed tomographic findings with histological correlates was a seminal contribution. Albert Szent-Gyorgyi has said: "Discovery consists of seeing what everybody has seen and thinking what nobody has thought." That characterizes Stuart! Stuart has been an NIH co-investigator on a University of Alabama (UAB) program for study of congenital anomalies of the kidney and urinary tract and co-investigator of a study aimed at detecting a gene target for intracranial intraventricular hemorrhage.

Stuart attended Rice University for only 3 years before being accepted into medical school at UAB where he received his M.S. degree in immunology and M.D. degree, magna cum laude, and had half a dozen other awards conferred upon him. He had his pediatric internship at UCSF and then segued into the UCSF radiology residency where he was also an NIH research fellow. This was followed by a pediatric radiology fellowship at Boston Children's Hospital. He returned to Birmingham and quickly ascended the UAB academic ranks so that he is now Radiologist-in-Chief at Children's of Alabama, recipient of the Henry M. Burns endowed chair, and Clinical Professor of Radiology and Pediatrics at UAB. He has been president of the medical staff at UAB Children's Hospital, has served as a member of the Board of Trustees of Children's of Alabama Health System, and a member of the Joint Operating Committee for UAB. This latter group coordinates pediatric care across service lines in the medical center and has recently overseen a four hundred million dollar hospital expansion.

Numerous honors have been bestowed upon Dr. Royal, including AOA medical school honor society, UAB Best Teacher Award, UAB Excellence in Radiology Education awards, RSNA cum laude awards, Fellowship in the ACR, and he is listed in several editions of "Best Doctors in America". He has received the Physician Recognition Award from the AMA and from the Medical Association of Alabama. In 2012, he received the SPR Presidential Recognition Award.

Stuart has served on multiple important SPR committees and as president of the SPR, he presided over the very successful 2005 meeting in New Orleans. This was followed by being Chairman of the SPR Board of Directors. He has been president of the Society of Chairman of Radiology in Children's Hospitals (SCORCH) and has been president of the Southern

Pediatric Radiology Society. Stuart has been an invited lecturer and visiting professor at numerous institutions and he serves on the Siemens Advisory Board. He has published seventy scientific articles and is a reviewer for seven journals. He is a contributor to the widely used book "Congenital Anomalies of the Urinary Tract", published by Saunders.

Dr. Royal was born in Birmingham to his father, a pediatrician, and his mother, a community volunteer. He has three sisters and a twin brother who is an oral surgeon. When Stuart first met his wife, Barbara, Stuart says "It was love at first sight!" Barbara is an immensely talented and successful individual in her own right. She merged a Children's Museum Discovery Place with the Birmingham City Museum to form the McWane Science Center which is now an integral part of Birmingham. Stuart and Barbara have lived in Birmingham for 33 years and they have two children, Rachael McDonald (married to Matt) who is a bond rater for Moody's in Manhattan and Jeremy Royal, an academic radiologist at Emory University (married to Dayna, who has been a law professor). Stuart and Barbara have four adorable grandchildren.

Nobel Peace Prize laureate, Mother Teresa, has said "A life not lived for others is not a fit life." Stuart has lived a life for others, as a physician, scientist, professor, leader, and mentor. Because of all that he has accomplished in his illustrious career, the SPR is proud to bestow its 2013 Gold Medal upon Dr. Stuart Royal.

Charles A. Gooding, MD, FACR, FRCR

SPR 2013 Pioneer Honoree

Pioneer Honorees were first acknowledged in 1990 as a means to honor certain physicians who made special contributions to the early development of our specialty.

Barry Davis Fletcher, MD, CM

Each year, the Society for Pediatric Radiology bestows the Pioneer Award upon one of its distinguished members who has contributed to the advancement of diagnostic imaging for the care of children and in pioneering techniques for use in their care. Dr. Barry D. Fletcher embodies the commitment, creative thinking and professional attributes deserving of this award. He has been nationally and internationally recognized for his imaging innovations and academic prowess. In the words of Dr. Arthur Neinhuis, Director of St. Jude during the period when Barry was Chairman, "Dr. Fletcher was an outstanding diagnostician and built a strong

department. He was very dedicated to providing the best possible care for our patients."

Dr. Fletcher was raised in a medical environment in a small southern Ontario community where his father was a general practitioner who made house calls and his mother was a nurse. Interestingly, Barry's father also had an interest in radiology. Barry graduated from McGill University medical school and served his internship and radiology residency at the Royal Victoria Hospital, Montreal. His next 4 years were spent at Johns Hopkins Hospital as chief resident, fellow and junior faculty member.

Neonatal lung disease was Barry's first research focus, pursued during his time at the Montreal Children's Hospital. His 1970's papers were the first to document such topics as pulmonary interstitial emphysema, transient tachypnea of the newborn, hyaline membrane disease and renal abnormalities associated with extraventilatory air in newborns. He was a coauthor of Dr. Mary Ellen Avery's book, *The Lung and its Disorders in the Newborn Infant.*

It was at Rainbow Babies and Children's Hospital in Cleveland (1976–1987) where Dr. Fletcher developed an interest in imaging congenital heart disease. He was a key resource for pediatricians and cardiovascular surgeons in caring for these children, spending long hours reviewing miles of cine clips in the basement of the department. With the arrival of one of the first superconducting MRI systems, Barry explored its potential in understanding the anatomy of these complex cardiac abnormalities. He published some of the first MRI papers and a book on congenital heart disease with cardiologist, Dr. Mark Jacobstein. He also delved into the use of MRI for detecting neuroblastoma metastases and was among the first to describe osteomyelitis using this modality.

With his move from Cleveland to St. Jude Children's Research Hospital in Memphis in 1987, Dr. Fletcher embarked on building an outstanding academic oncologic imaging department that, to this day, continues to 'push the envelope' of technology for the benefit of children and young adults worldwide. His commitment to imaging research flourished in Memphis, culminating in his being awarded an endowed Chair in 1996. He is especially proud of the collaborative environment he helped create among biomedical scientists and radiologists. Barry published extensively while at St. Jude, describing characteristics of unusual tumors and probing the utility of MRI for tumor staging and monitoring treatment response. He left an indelible mark on MRI imaging of musculoskeletal tumors, including development of dynamic contrast-enhanced sequences to monitor treatment response of osteosarcoma. Other investigations during that period delineated MRI characteristics of bone marrow in patients receiving granulocyte cell stimulating factor (GCSF), skeletal abnormalities associated with radiation and bone marrow transplantation and the optimization of MR sequences for tumor assessment.

Dr. Fletcher's commitment to and expertise in imaging research is further exemplified by his receipt of six extramural grants as Principal Investigator and four as Co-Investigator, considerable achievements for a clinical pediatric radiologist. Always a proponent of education and intellectual exploration, he advised investigators on research initiatives covering a broad range of topics. Most importantly, he established the role of imaging research as a major component of clinical trials through his leadership in the Pediatric Oncology Group (POG). Equally important, he guided career development for two generations of pediatric radiologists, trainees and junior faculty working under his unique guidance in Montreal, Cleveland and Memphis.

Certified by the American Board of Radiology and the Royal College of Physicians and Surgeons of Canada, he was an examiner for the American Board of Radiology and was one of the first examiners of candidates for added qualifications in pediatric radiology. He is a fellow of the American College of Radiology.

Barry has served on the SPR Board of Directors and multiple committees: Judiciary, Cooperative Research, Added Qualifications in Pediatric Radiology, CT/MRI, and the Research and Education Foundation. He was awarded the Society's gold medal in 2008.

In retirement, Barry has continued to consult and occasionally returned to work at St. Jude. He has enjoyed reviewing submissions to *Pediatric Radiology* and was editor of the musculoskeletal section of the 10th edition of *Caffey's Pediatric Diagnostic Imaging*. Barry has always been generous in sharing his knowledge and expertise with colleagues around the world. He is proud of his former voluntary consulting association with Project Hope, China at Shanghai Children's Medical Center**.** He remains an avid volunteer in his home city of Asheville, North Carolina.

In summary, Dr. Fletcher is one of the early pioneers in developing and exploiting medical imaging for children and particularly, influencing its use in caring for children with catastrophic diseases. His "eye" for identifying imaging patterns and his ability to assimilate these findings with clinical information, has provided insight into a wide range of diagnoses. His career has been devoted to developing imaging techniques – particularly MR – to benefit pediatric patients, generously sharing his expertise worldwide and promoting the careers of the next generation of researchers and pediatric imagers.

Sue C. Kaste, DO

SPR 2013 Presidential Recognition Award

The Society bestows Presidential Recognition Awards on members or other individuals whose energy and creativity have made a significant impact on the work of the Society and its service to its members.

Alan E. Schlesinger, MD

It comes as no surprise to those in the Society for Pediatric Radiology that Dr. Alan Schlesinger has been named the 2013 Recipient for the Society for Pediatric Radiology President's Award in recognition of his many years of dedication to the Society.

Born in New Jersey in 1954, Dr. Schlesinger received his undergraduate degree at the University of California at Los Angeles where he graduated Summa Cum Laude with Departmental Honors and was named to the Phi Beta Kappa Honorary Society. Alan graduated from Yale Medical School where he met his lovely wife Paula, a future outstanding pediatrician, who agreed to marry him. During his Radiology residency at Boston City Hospital, Alan's leadership skills and affable personal style resulted in his being named Chief Resident. It was there that he met Pediatric Radiologist and SPR Luminary Dr. Jack O'Connor. Jack became Alan's mentor, and the O'Connor and Schlesinger families became life-long friends. Following a Fellowship in Pediatric Radiology under Dr. Andy Poznanski and colleagues at Children's Memorial Hospital in Chicago, Alan fulfilled a military service obligation at the Wilford Hall Medical Center, Lackland Air Force Base, Texas as Chief of the Pediatric Radiology section, assuming a great responsibility immediately out of Fellowship. This was followed soon by his being named Director of the Residency Training Program, another acknowledgement of Alan's exceptional interest and skill in educating young trainees.

Upon Honorable Discharge from the Air Force, Alan began four academically productive years as Assistant Professor of Radiology at University of Michigan's CS Mott Children's Hospital with Dr. Ramiro Hernandez and colleagues. Paula then received an attractive offer from a pediatric practice in St. Louis. Although Alan liked Ann Arbor and had become very popular with the Radiology and Pediatric faculty, residents (Radiology Teacher of the Year 1991) and staff, Alan decided that Paula had followed him for several moves and that it was now time for her career to take priority. Michigan's loss was Washington University's gain. Once again Alan's intelligence, enthusiasm, and spirit of team play led to the next stage of his academic career. While at St. Louis Children's Hospital Alan especially enjoyed working with Dr. Gary Shackelford.

In the mid 1990s, Dr. Bruce Parker assumed Chair of Radiology at Texas Children's Hospital after Dr. Ed Singleton's decades of holding that position. Bruce was recruiting new faculty and in 1995 he convinced Alan to join his department as Associate Professor of Radiology, Baylor College of Medicine. Alan, Paula, and their three children went to Houston where Paula joined a Pediatric practice. Alan's career continued to flourish at Texas Children's, where he has been Professor of Radiology since 2001. Alan has presented over 40 scientific presentations, 18 exhibits, and many invited lectureships. His teaching method is straightforward, highly interactive, and well received by audiences. Al has written over 27 book chapters and has participated in numerous editions of *Caffey's Pediatric X-ray Diagnosis*.

The SPR's President's Award recognizes service to the Society, and it is in this regard that Alan's career has special significance. He is an avid photographer. It is perhaps Alan's eye and attention to clarity and framing of the image delivering a clear direct message which has led him to produce many fine exhibits and lectures. Dr. Gary Shackelford shares this avocation and discusses Al's passion for photography. He discusses their companionship while photographing side by side and their review and critique of each

others' images. Alan continues a relationship of comparing and critiquing photographs from a distance with Gary and more recently, directly with Texas Children's Radiology colleague and photographer, Dr. Jim Crowe. Whether it is regarding radiology or photography, Al maintains a similar open style and invites and provides commentary on his and colleagues' work in a non-defensive manner. Alan is a great collaborator. He demonstrates optimism and enthusiasm in balance with some healthy skepticism, honesty, and humor. This is part of what has made Alan such an esteemed and liked colleague in many departments and in the SPR.

He took a leadership role in the SPR as photographic historian for the Society which included creation of the digital archive and the video for the SPR's 50th anniversary. This was no simple task. It involved coordinating a videographer at the RSNA meeting in 2006, inviting recollections and remembrances of colleagues, and eliciting reflections on the importance of the Society. Alan took the considerable footage from that meeting and spliced in selected footage and photos from prior meetings. This was incredibly time consuming, but for Alan it was also a labor of love! Those who work with him have described Alan as "having a great attitude", being fun to work with, in short, being the perfect colleague. He is willing and eager to take on responsibility. Alan takes his work seriously without taking himself too seriously and the result is he is always enjoying himself. This old Educators' trick is one Alan knows well: if work has some aspect of fun and exploration, people will forget they are working! Alan exemplifies that spirit, and it spreads to those around him.

Alan is extremely humble and is very deserving of this award. He is a great role model for younger SPR members as to what exemplifies a fine inquisitive pediatric radiologist, a fine teacher, and a fine professional colleague and a friend to many.

The Society for Pediatric Radiology is grateful for Dr. Alan Schlesinger's significant contributions to the Society, as a former member of the Board of Directors, as an academic contributor and as the Society's historian.

Marilyn J. Goske, MD, Michael A. DiPietro, MD and Gary D. Shackelford, MD

SPR 2013 Honorary Member

The Society extends Honorary membership to individuals outside of pediatric radiology who have made outstanding contributions to the care of children.

Savvas Andronikou, MBBCh, FCRad, FRCR, PhD

It is indeed a very uplifting act to witness an African – in particular an African pediatric radiologist – being elevated by our Society of Pediatric Radiology to an honorary member. Prof. Andronikou is currently the most senior and renowned South African pediatric radiologist with a stellar academic background and intensive commitment to advance pediatric radiology in Africa. He was born in 1968 and is of Greek origin.

Prof. Andronikou was trained in Witwatersrand Medical School, Germiston General Hospital (House Officer), Hilbrow Hospital (Senior House Officer), Whittington Hospital London (Specialist Registrar, radiology) and Great Ormond Street Hospital London (Specialist registrar, radiology). He is a full professor currently working as a visiting professor at the University of Witwatersrand, the University of Pretoria and the University of Limpopo. Formerly, he was the Head of the Department of Pediatric Radiology, Red Cross Hospital, University of Cape Town Medical School and later Chair Professor and head of Department, at the Tygerberg Hospital, University of Stellenbosch in the Western Cape. Prof. Andronikou is currently President of the College of Radiologists of South Africa and also Chairman of the South African Society of Pediatric Imaging. His achievements include an MBBCh (Witwatersrand, 1991), FCRad (Diagnostic, South Africa, 1998), FRCR (London, 2000) and a PhD (University of Cape Town, 2005).

He is a very active researcher with over 200 publications, nine books and book chapters and over 50 published abstracts. He is currently number 4 on the list of highest number of publications in our journal "Pediatric Radiology". Prof. Andronikou has given over 165 invited talks nationally and internationally. He is not only a reviewer for a number of scientific journals but also sits on the editorial boards of some, including our "Pediatric Radiology" journal. He was Chief Editor of the South African Journal of Radiology from 2005 to 2008. He has organized a number of diagnostic radiology and in particular pediatric radiology refresher courses and meetings in South Africa over the years.

Prof. Andronikou has received a number of nominations and awards including the following ones: Derek Harwood-Nash Scholarship Toronto Hospital for Sick Children 2001, Maurice Weinbren Award of the College of Radiology 2001 and 2002, RSNA Derek Harwood Nash Fellow 2007, Rector's award for Outstanding Research at the University of Stellenbosch 2007 and the Dean's award for research at the University of the Witwatersrand in 2012.

He is a very active member of the European Society of Pediatric Radiology (ESPR) coming with several presentations at every annual meeting and engaging in a number of committee activities. He is currently making outstanding contributions to pediatric radiology through his participation in the World Federation of Pediatric Imaging (WFPI). He is the Chairman of the Outreach Committee of the WFPI. Prof. Andronikou has worked relentlessly to establish connections with institutions in the African continent, both to create an African Pediatric Radiology Society under the auspices of the African Society of Radiology and to provide care via teleradiology and training. He is a member of Medecens Sans Frontier (MSF) and is working on different national and international projects including teleradiology. He is collaborating with the Children's Hospital of Philadelphia, Department of Radiology International Pediatric Outreach Program in Ethiopia as an external board examiner and faculty in the pediatric radiology continuing medical examination course.

His accomplishments are not only as an excellent diagnostician, but also as a fully committed academician and researcher with a very long list of past and current research mentees. He is presently mentor of researchers of various types and levels from residents to researchers in master's programs at multiple South African universities. He has a very wide spectrum of research interests and projects with some neuroimaging and tuberculosis and HIV imaging focuses. The research commitment needs to be regarded with highest respect coming from a part of the world with limited resources and least priority for radiology research, especially pediatric radiology research, in the presence of seemingly insurmountable public health challenges.

Prof. Andronikou is a brilliant teacher giving lectures that fully engage the audience from start to end. His mix of real life anecdotes with facts and humour coupled with self-criticism bring him very close to his mesmerized audience during the presentations. His Greek origin with a relatively long hair mixed with grey strands adds a picture of further depth of a mix of experience and wisdom to the whole affair.

In conclusion, awarding an honorary membership to Prof. Savvas Andronikou from South Africa by our Society of Pediatric Radiology is a commendable act. This gesture will not only emphasize the international outreach of our Society, but also recognize the contributions of a colleague to a continent dominated by a pediatric population, but confronted with a severe shortage of pediatric radiologists.

Kassa Darge, MD, PhD

SPR 2013 Singleton-Taybi Award

The Singleton-Taybi Award is given in honor of Edward Singleton and Hooshang Taybi, in recognition of their personal commitment to the educational goals of the SPR. Initiated in 2006, the Award is presented annually to a senior member of the SPR whose professional lifetime dedication to the education of medical students, residents, fellows, and colleagues has brought honor to him/her and to the discipline of pediatric radiology.

Lisa H. Lowe, MD

"Of those who start taekwondo training, only about 5% stick with it until they achieve the Black Belt Rank." (Duk Sung Son)

It is not surprising that Lisa Lowe, a recommended black belt in Taekwondo, is this year's recipient of the Singleton/Taybi Award. Her dedication to pediatric radiology, passion for educational initiatives, indomitable skills and strong work ethic make her the perfect recipient of this honor.

Lisa Lowe overcame many challenges in her younger years by being resourceful, hard working and determined. Growing up in an unstable environment, Lisa had to mature quickly, helping care for her sister and mother. She knew she wanted to make a difference in the world and would have to depend on herself to succeed. She got through college initially just dedicating herself to being an outstanding student. Always interested in teaching, Lisa thrived in the academic environment of inquiry, discovery and education. By her second year at the University of Tennessee, she realized not only that she could graduate and support herself, but that she could aim much higher for an exciting future making a difference in the world. She decided to go into medicine, yet always knew education would be an important part of her future. It turns out Lisa comes from a long line of teachers. Her great grand-father, a train engineer during the depression, pushed all his children, both boys and girls, to get a college education. Her father and step mother both have degrees in education. Education and teaching are clearly in her blood!

Lisa thrived in college and medical school graduating from the Meharry Medical College in 1991. Honors included Phi Kappa Phi honor society, Alpha Omega Alpha (AOA) in her junior year and becoming president of the AOA her senior year. On the Deans list all semesters, she was awarded several scholarships including the George Alden academic scholarship, Dewitt Wallace academic scholarship, McGraw Hill publication academic scholarship, Helena Rubinstein Foundation academic award and the World Peace "all around" award.

Dr. Lowe completed a diagnostic radiology residency at Wake Forest University and then came to Children's National Medical Center to complete a pediatric radiology fellowship under the leadership of Dr. David Kushner. Her first professional job was as assistant professor at the University of Texas-Southwestern Children's Medical Center of Dallas. She then spent 2 years at Vanderbilt as assistant professor of radiology and pediatrics under the leadership of Marta Hernanz-Schulman, MD. During her time at Vanderbilt, Lisa participated in the Marconi-American University Radiology Academic career development program.

Dr. Lowe then moved to Children's Mercy Hospital and the University of Missouri-Kansas City (UMKC) where she initially was promoted to Associate Professor. She quickly became a leader in radiology education becoming associate residency program director of the diagnostic radiology residency in 2005 and program director in 2007. She also started and was the pediatric radiology fellowship program director at Children's Mercy Hospitals and UMKC from 2006 to 2008. Dr. Lowe has participated in numerous leadership development programs including the Society for Chairs of Academic radiology Department (SCARD), APDR/A3CR3 certificate Teaching Program from the AUR, Clinician Educator development program ARRS, and AUR AGFA Radiology in Management program. For her efforts, she received one of the first two Academy of Radiology Leadership and Management certificates awarded through the Radiological Society of North America (RSNA) in 2012.

Because of her leadership skills, unwavering support of her residents, and indomitable spirit, Dr. Lowe was appointed the Academic Chair of the Department of Radiology at UMKC in 2007. The residents clearly value her efforts honoring her with instructor of the year in 2003, Resident Advocate of the year in 2011 and the Resident Certificate of Appreciation in 2012. She has volunteered to be a panel member on student career and research days, serves as a speaker for questions regarding match day, and has been a mentor for numerous trainees.

Dr. Lowe is well known for her beautiful poster presentations. She has mentored medical students, residents and fellows on these projects throughout her career. She has received numerous awards for her work from the IPR, SPR, ARRS, ASNR and RSNA, many of which have been accepted for CME credit. She was awarded the first place poster Caffey award from the SPR on "Neuroimaging of nonaccidental trauma" in 2007, and "Sensorinerual hearing loss in children: radiologic evaluation" in 1997.

Dr. Lowe is an active member in numerous societies including the AUR, SCARD, APDR, AAP, ASPNR, SPR, ACR, AAWR, ARRS and RSNA. She has been extremely supportive of SPR initiatives and has been a member of the awards, program and neuroradiology committees. She helped chair the poster committee for 4 years. Due to her interest in education, she was appointed chair of the work task force committee at a time when few fellows were entering our specialty. She currently is on the SPR nominating and judiciary committees and on the Board of the RE foundation and Board of Directors.

Her leadership skills and passion for education made her the obvious choice to chair the Pediatric Certifying Exam Committee for the American Board of Radiology (ABR). She has been an examiner for the oral boards and reviewer of the ABR self assessment modules. She is a member of the neuroradiology program subcommittee for the RSNA. Lisa has also been on the committee for accreditation of CME for the ACR, and the ACR commission on pediatric guidelines.

Her love of education is demonstrated by her work as a course director/panel member for seven national courses and an invited speaker for over 30 national meetings and 17 regional meetings. She has been a visiting professor at 17 centers. She has given over 42 national oral presentations

Dr. Lowe has authored over 64 peer reviewed articles, 48 abstracts, 74 posters. She is a chapter contributor for the last two Caffey editions, Resident Review Series, as well as authored numerous other chapters. She serves on the editorial board of the AJR, US Radiology Journal, and helps review for Pediatric Radiology, AJNR and JCAT.

"Black belt is nothing more than a belt that goes around your waist. Being a black belt is a state of mind and attitude," says Rick English.

Lisa is clearly a force of nature and her work does not end in the hospital. Married to Wes, a loyal, tolerant and loving companion whom she has known since age 14. Wes sacrificed his own career plans for hers and has mostly raised their two boys, Jake and Josh. Jake is a 13-year old who loves travel, architecture and science, whereas Josh is 10 years and loves dancing, sports and math. Her family and faith keep her grounded, and allow her to enjoy other passions, including Harry Potter, alternative/indie music, and reading, particularly science fiction, fantasy and historical fiction. The support of her family, especially her sister Julie, friends and mentors have kept life fun and exciting.

Lisa states, "When I was a medical student applying to radiology, I recall sitting with my grandmother who showed me a scrapbook of letters and follow up she had received from her elementary students over the years. I remember thinking if only I could be that lucky. I can't image any job where I did not get to teach. The success of my students is the most gratifying thing in my career".

It is clear that Lisa is a dedicated teacher, great physician and generous mentor. The SPR is thrilled to bestow the 2013 **Singleton/Taybi Award** on Dr. Lisa Lowe for her tireless devotion to pediatric radiology education.

Dorothy I. Bulas, MD

John Caffey, MD 1895–1978

Dr. Caffey was regarded throughout the world as the father of pediatric radiology. His classic textbook, "Pediatric X-Ray Diagnosis", which was first published in 1945, has become the recognized bible and authority in its field. The seventh edition of this book was completed several months before his death in 1978. It has been among the most successful books of its kind in the medical field.

Dr. Caffey was born in Castle Gate, Utah on March 30, 1895. It is interesting that he was born in the same year that Roentgen discovered the x-ray. Dr. Caffey was graduated from University of Michigan Medical School in 1919, following which he served an internship in internal medicine at Barnes Hospital in St. Louis. He spent 3 years in Eastern Europe with the American Red

Cross and the American Relief Administration, and returned to the United States for additional training in medicine and in pediatrics at the Universities of Michigan and Columbia, respectively.

While in the private practice of pediatrics in New York City at the old Babies Hospital of Columbia University College of Physicians and Surgeons, he become interested in radiology and was charged with developing a department of pediatric radiology in 1929. He frequently expressed appreciation and admiration for the late Ross Golden, Chairman of Radiology at Columbia Presbyterian Hospital, who allowed him to develop a separate department of diagnostic radiology without undue interference, and who was always available to help and advise him.

Dr. Caffey's keen intelligence and inquiring mind quickly established him as the leader in the fields of pediatric x-ray diagnosis, which recognition became worldwide almost instantaneously with the publication of his book in 1945.

Dr. Caffey received many awards in recognition of his achievements. Outstanding among these were the Mackenzie Davidson Medical of the British Institute of Radiology in 1956, the Distinguished Service Award of the Columbia Presbyterian Medical Center in 1962, the Outstanding Achievement Award of the University of Michigan in 1965, the Howland Award of the American Pediatric Society in 1967, the Jacobi Award of the American Medical Association in 1972, and the Gold Medal Award of the American College of Radiology in 1975. He had been a member of the American Journal of Roentgenology. He was a counselor of The Society for Pediatric Radiology and was an honorary member of the European Society of Pediatric Radiology.

Dr. Caffey's contributions to the pediatric radiologic literature were many. He was instrumental in directing attention to the fact that a prominent thymic shadow was a sign of good health and not of disease, an observation that literally spelled the end to the practice of thymic irradiation in infancy. Infantile cortical hyperostosis was described by him and is called "Caffey's Disease". Dr. Caffey in 1946 first recognized the telltale radiographic changes that characterize the battered child, and his students helped disseminate his teachings about these findings. It was Dr. Caffey who first recognized and descried the characteristic bony changes in vitamin A poisoning. He recognized and described the findings associated with prenatal bowing of the skeleton.

In 1963, 3 years after his retirement from Babies Hospital, he joined the staff of the Children's Hospital of Pittsburgh as associate radiologist and as Visiting Professor of Radiology and Pediatrics at the University of Pittsburgh School of Medicine. Although Dr. Caffey came to Children's Hospital and the University of Pittsburgh in an emeritus position, he worked daily and on weekends throughout the years he was there. In Pittsburgh, he made four major new contributions to the medical literature. He described the entity, "idiopathic familial hyperphosphatasemia". He recognized and described the earliest radiological changes in Perthes' Disease. He called attention to the potentially serious effects of shaking children, and used this as a subject of his Jacobi Award lecture. He described, with the late Dr. Kenny, a hitherto unrecognized form of dwarfism which is now known as the Caffey-Kenny dwarf.

The John Caffey Society, which includes as its members pediatric radiologists who have been intimately associated with Dr. Caffey, or who have been trained by his students, was established in 1961. This society is now among the most prestigious in the field of radiology. His book and the society named in his honor will live on as important memorials to this great man.

His greatness was obvious to all who worked with him. He was warm, kind, stimulating, argumentative, and above all, honest in his approach to medicine and to x-ray diagnoses. His dedication to the truth was expressed in his abiding interest in the limitations of x-ray signs in pediatric diagnosis and in his interest in normal variation in the growing skeleton. He was concerned with the written and spoken word and was a skilled semanticist. His book and his articles are masterpieces of language and construction. He stimulated and was stimulated and loved by all who had the privilege of working with him. Radiology and Pediatrics have lost a great man, but they shall ever have been enriched by his presence.

Bertram R. Girdany, MD

Caffey Award for Best Basic Science Research Paper

2005 Quantitative Measurement of Microbubble Ultrasound Contrast Agent Flow to Assess the Efficacy of Angiogenesis Inhibitors In Vivo. McCarville B, Streck C, Li CS, Davidoff A

2006 ^{64}Cu-Immuno-PET Imaging of Neuroblastoma with Bioengineered Anti-GD2 Antibodies. Voss SD, Smith SV, DiBartolo NM, McIntosh LJ, Cyr EM, Bonab AA, et. al

2007 MR Imaging of Adenocarcinomas with Folate-Receptor Targeted Contrast Agents. Daldrup-Link HE, Wang ZJ, Meier R, Corot C

2008 Evaluation of Quality Assurance Quality Control Phantom for Digital Neonatal Chest Projection Imaging. Don S.

2009 Faster Pediatric MRI Via Compressed Sensing. Vasanawala S, Alley M, Barth R, Hargreaves B, Pauly J, Lustig M

2010 Clinical Evaluation of Readout-Segmented-EPI for Diffusion-Weighted Imaging. Bammer R, Holdsworth S, Skare S, Yeom K, Barnes P

2010 High-Resolution Motion-Corrected Diffusion-Tensor Imaging (DTI) in Infants. Skare S, Holdsworth S; Yeom K; Barnes P, Bammer R

2010 3D SAP-EPI in Motion-Corrected Fast Susceptibility Weighted Imaging (SWI). Bammer R, Holdsworth S, Skare S, Yeom K, Barnes P

2010 T1-Weighted 3D SAP-EPI for Use in Pediatric Imaging. Bammer R, Holdsworth S, Skare S, Yeom K, Barnes P

2011 An MR System for Imaging Neonates in the NICU. Tkach J, Giaquinto R, Loew W, Pratt R, Daniels B, Jones B, Donnelly L, Dumoulin C

2012 Advantages of a Nanoparticle Blood Pool Contrast Agent Over Conventional Intravascular Glomerular-Filtered Contrast Agents for Pulmonary Vascular Imaging. Annapragada A, Guillerman RP, Hoffman E, Kaczka D, Ghaghada K, Badea C

Caffey Award for Best Clinical Research or Education Paper

2005 Evaluation of High Resolution Cervical Spine CT in 529 Cases of Pediatric Trauma: Value Versus Radiation Exposure. Shiran D, Jimenez R, Altman D, DuBose M, Lorenzo R

2006 Alterations in Regional O_2 Saturation (StO_2) and Capillary Blood Volume (HbT) with Brain Injuries and ECMO. Grant PE, Themelis G, Arvin K, Thaker S, Krishnamoorthy KK, Franceschini MA

2007 Evaluation of Single Functioning Kidneys Using MR Urography. Grattan-Smith D, Jones R, Little S, Kirsch A, Alazraki A

2008 Evaluating the Effects of Childhood Lead Exposure with Proton MR Spectroscopy & Diffusion Tensor Imaging Neuroradiology. Cecil KM

2009 Improving Patient Safety: Effects of a Safety Program on Performance and Culture in a Department of Radiology at a Children's Hospital. Donnelly L, Dickerson J, Goodfriend M, Muething S

2010 Juvenile Osteochondritis Dissecans (JOCD): Is It a Growth Disturbance of the Secondary Physis of the Epiphysis? Laor T, Wall E; Zbojniewicz A

2011 Quantitative Assessment of Blood Flow with 4D Phase-Contrast MRI and Autocalibrating Parallel Imaging Compressed Sensing. Hsiao A, Lustig M, Alley M, Murphy M, Vasanawala S

2012 Multidetector CT Pulmonary Angiography in Children with Suspected Pulmonary Embolism: Thromboembolic Risk Factors and Implications for Appropriate Use. Lee EY, Tse SK, Zurakowski D, Johnson VM, Donald TA, Boiselle PM

CAFFEY AWARD FOR POSTERS

2005 3D MRI and CT in the Evaluation of Congenital Anomalies of the Aortic Arch. Dehkharghani S, Olson K, Richardson R

2006 Diffusion Weighted Imaging in Pediatric Neuroradiology: A Primer. Sagar P, Grant PE

2006 Imaging of Suprarenal Fossa in Children: Radiological Approach and Clinico-Pathological Correlation. Kukreja K, Restrepo R, D'Almeida M

2007 Neuroimaging of Nonaccidental Trauma: Pitfalls and Controversies. Lowe L, Obaldo RE, Fickenscher KA, Walsh I,

2008 Estimation of Cumulative Effective Doses from Diagnostic and Interventional Radiological Examinations in Pediatric Oncology Patients. Thomas KE, Ahmed BA, Shroff P, Connolly B, Chong AL, Gordon C

2009 *Case Report :* Multi-Modality Imaging Manifestations of the Meckel's Diverticulum in Pediatric Patients. Kotecha MK, Bellah RD, Pena AH, Mattei P

2009 *Educational:* MR Urography: Functional Analysis – Made Simple! Khrichenko D, Darge K

2009 *Scientific:* MRI Findings in the Term Infant with Neonatal Seizures. An Etiologic Approach. Rebollo Polo M, Hurteau-Miller J, Laffan E, Tabban H, Naser H, Koujok K

2010 *Scientific:* Dual Phase Intravenous Contrast Injection in Pediatric Body CT. Mann E, Alzahrani A, Padfield N, Farrell L, BenDavid G, Thomas K

2010 *Educational:* Hemangiomas Revisited: The Useful, the Unusual and the New. Restrepo R, Palani R, Matapathi U, Altman N, Cervantes L, Duarte AM, Amjad I

2010 *Case Report:* MRI of Congenital Urethroperineal Fistula. Mahani M, Dillman J, Pai D, Park J, DiPietro M, Ladino Torres M

2011 *Scientific:* Updated Estimated Radiation Dose for Pediatric Nuclear Medicine Studies. Grant F, Drubach L, Treves ST, Fahey F

2011 *Educational:* Button Battery Ingestion in Children: What the Radiologist Must Know. Kappil M, Rigsby C, Saker M, Boylan E

2011 *Case Report:* MR Imaging Features of Fetal Mediastinal and Intrapericardial Teratomas. Rubio E, Kline-Fath B, Calvo-Garcia M, Guimaraes C

2012 *Case Report:* Neuroimaging in Hemiplegic Migraine: Cases and Review of the Literature. Stence NV, Kedia S, Maloney JA, Armstrong-Wells J, Bernard T

2012 *Educational:* Primary and Secondary Amenorrhea in Pediatric Patients: From the Beginning to the End. Cortes C, Ramos Y, Restrepo R, Diaz A, Sequeira L, Lee EY

2012 *Scientific:* Prenatal Evaluation of Limb Body Wall Complex with Emphasis on MRI. Aguirre-Pascual E, Victoria T, Johnson A, Chauvin N, Coleman B, Epelman M

For a list of Caffey award papers and posters prior to 2005, please visit the SPR website.

2013 Edward B. Neuhauser Lecture

The Pediatric Cancer Genome Project – Implications for Clinical Medicine

James R. Downing, MD
Executive Vice President
Scientific Director, Deputy Director
St. Jude Children's Research Hospital
Memphis, Tennessee

Dr. Downing received a BS in Biochemistry in 1977 and an MD in 1981 from the University of Michigan. He then completed a residency in Anatomic Pathology at Washington University in St. Louis, and a fellowship in Hematopathology at the University of Florida in Gainesville. He joined the faculty of St. Jude Children's Research Hospital in 1984 and has risen through the ranks to become Chair of Pathology and now the Scientific Director and the deputy Director of the institution.

The work in his own laboratory is focused on the investigation of the fundamental regulatory mechanisms that control normal and leukemic hematopoiesis, and on cancer genomics and its application to the diagnosis and treatment of pediatric cancers. He is currently leading the St. Jude Pediatric Cancer Genome Project, a world recognized project to map the genome of major leukemias, brain tumors and solid tumors in children and adolescents; exciting contributions have already impacted our understanding of pediatric cancers.

Previous Neuhauser Lectures

1997 S. Steven Potter, PhD, Cincinnati, Ohio
"Homeobox Genes and Pattern Formation (Master Genes)"

1998 Roy A. Filly, MD, San Francisco, California
"Fetal Thoracic Surgery"

1999 Harold A Richman, PhD
"Child Abuse: From a Radiologist's Discovery to a Major Issue of Public Policy. What Have We Wrought?"

2000 William D. Lyman, PhD, Detroit, Michigan
"Prenatal Molecular Diagnosis and Fetal Therapy"

2001 Jerry R. Dwek, MD, Columbus, Ohio
"Médecins Sans Frontiéres/The Doctors Without Borders Experience – Afghanistan"

2002 Eric J. Hall, DSc, FACR, FRCR, New York, New York
"Lessons We Have Learned From Our Children: Cancer Risks From Diagnostic Radiology"

2003 Jeffrey A. Towbin, MD, Houston, Texas
"Molecular Cardiology: Laboratory to Bedside"

2004 Bruce R. Rosen, MD, PhD, Boston, Massachusetts
"New Advances in MRI: A Guide for the Practicing Pediatric Radiologist"

2005 Bruce R. Korf, MD, PhD, Birmingham, Alabama
"Pathobiology and Management of NF1 in the 'Genomic Era'"

2006 Richard M.J. Bohmer, MD, MPH
"Evolution, Innovation and the Changing Nature of Healthcare Delivery"

2007 Nogah Haramati, MD
"21st Century Radiology: Growth and Development of Our Workflows and Processes"

2008 Emanuel Kanal, MD, FACR, FISMRM, AANG
MR Technology: Where Are We, Where Are We Going?

2009 Roberta G. Williams, MD
"Cardiology and Radiology: Partners in Producing Healthy Adults with Congenital Heart Disease"

2010 Regina E. Herzlinger, PhD
"The Economic Basis of Change in Healthcare"

2011 Sanjiv Gambhir, MD, PhD
"Molecular Imaging"

2012 William R. Hendee, PhD
Past and Future Patient Benefits of Radiologist/Physicist Collaboration

For a list of Neuhauser Lecturers prior to 1997, please visit the SPR website.

POSTGRADUATE COURSE ABSTRACTS

Tuesday, May 14, 2013

CHEST

Digital Radiography

Robert MacDougall, MSc

The era of Digital Radiography (DR) has brought with it many benefits including: fast image transfer and display, more efficient image receptors and advanced image processing algorithms. Despite these advancements, converting from analog to DR presents a learning curve that has taken many imaging departments by surprise. The steps of image acquisition, processing and display have been decoupled in the digital era such that each component has a very complex relationship to the final quality of the radiographic image.

The wide dynamic range of DR detectors means that a wide range of detector exposures are capable of producing a diagnostic image. Often times, there is no QA technologist to approve films before an image is sent for interpretation. The result can be a loss of consistency with respect to technique as well as a gradual increase in patient exposure over time; a phenomenon known as "dose creep". As a result, the task of optimizing image quality and exposure poses a challenge to physicists and radiologists.
The goal of this session is to provide an understanding to the pediatric radiologist of the relationship between the many steps in the imaging chain that affect image quality and patient dose. The following topics will be covered:

- The effect of technique selection, image processing parameters and display settings on the final image display.
- Using exposure indicators to improve consistency in Digital Radiography.
- Methods for developing pediatric technique charts based on detector type, imaging task and noise tolerance.
- Advanced topics such as the effect of added filtration and methods for estimating patient absorbed dose.
- Common pitfalls and methods for troubleshooting image quality issues in DR will be presented. Examples cases are presented to demonstrate the most common image quality problems and solutions.

Functional Chest MR Imaging

Hyun Woo Goo, MD, PhD

The lungs and airways are the organs with fairly complex functions, including ventilation, perfusion, respiratory motion, and gas exchange. Along with the advantages of thoracic MR imaging including no use of ionizing radiation, excellent soft tissue contrast, high temporal resolution, and easier implementation of dynamic protocols, its limitations including low signal-to-noise ratio due to the low proton density of the lung, motion artifacts from respiratory motion and cardiac pulsation, long examination time, and susceptibility artifacts from multiple air- tissue interfaces should be recognized. Despite recent technical advancements in MR imaging, MR imaging evaluation of the pediatric thorax is still challenging at 1.5 T and even worse at 3.0 T. Regional lung perfusion can be assessed qualitatively or quantitatively with contrast-enhanced time-resolved MR angiography, phase contrast imaging, non-contrast arterial spin labeling techniques, and oxygen-enhanced MR imaging. Hyperpolarized gas MR imaging has been studied for the assessment of regional lung ventilation and perfusion in various lung diseases. Diffusion weighted imaging and dynamic contrast-enhanced imaging may be used for evaluating lung nodules and masses. Non-contrast-enhanced perfusion-weighted and ventilation-weighted imaging using Fourier decomposition MR imaging, real-time dynamic MR imaging, and MR elastography are promising techniques. Functional chest MR imaging has potential to detect early or mild change of lung diseases, to quantify altered lung function caused by lung diseases, to give insights into the pathophysiology of lung diseases, and to evaluate the effectiveness of established and new therapies. A majority of these imaging techniques can be applied to pediatric population.

PE Evaluation in Children: What is New?

Edward Y. Lee, MD, MPH

Pulmonary embolism (PE) is a potentially life-threatening condition that requires accurate diagnosis and timely management. In recent years, the awareness and understanding of PE in infants and children have been substantially increased due to evidence-based scientific investigations in this patient population. This presentation provides an updated review of the risk factors, clinical presentation, and management of PE in pediatric patients. In addition, current policies and practices regarding the evaluation of pediatric patients with PE are discussed. Furthermore, this presentation also highlights the current diagnostic tools and protocols used to optimally evaluate PE in pediatric patients.

Imaging of Acquired Thoracic Cardiovascular Diseases

Beverley Newman, MD, FACR

The line of separation between congenital and acquired cardiovascular disease is often quite blurred. When a condition is present at birth, it is usually considered congenital although some entities may be acquired prenatally associated with an adverse in utero environment. Examples include

cardiovascular abnormalities associated with gestational diabetes and fetal alcohol syndrome. Additionally a number of genetically inherited conditions may have little or no apparent abnormality at birth but predispose the individual to develop cardiovascular disease later in life. Prominent examples include Marfan syndrome, Turner syndrome, glycogen storage disease, familial hypertrophic cardiomyopathy, arrythmogenic right ventricular dysplasia and sickle cell disease.

This presentation will be confined to discussing conditions that are truly acquired postnatally with no major genetic predisposition. Etiologies include infectious, autoimmune, traumatic, iatrogenic and neoplastic causes. Examples will be shown and imaging recommendations illustrated in each of the following categories.

1. Endocardial, Myocardial and Valvular Disease
2. Pericardial Disease
3. Coronary and Great Vessel Disease
4. Cardiac Masses

NEURORADIOLOGY

Optimizing Head US Imaging

Lisa H. Lowe, MD, FAAP

Recent technological advances in ultrasound have allowed modern imaging to be an increasingly accurate and highly sensitive method for diagnosing pediatric cranial pathology. Ultrasound offers the benefits of being non-invasive (no sedation or radiation required) and portable, enabling examination of critically ill patients at the bedside. Ultrasound with Doppler allows for rapid characterization of many acute intracranial anomalies within these first days of life. This enables clinical determination as to whether lesions require urgent intervention or additional imaging with CT or MR imaging. However, in order to take full advantage of the benefits of modern sonography, one must be aware of updated cranial gray scale and Doppler sonography techniques and protocols. Familiarity with an array of normal variants that may occur is required, in order to avoid unnecessary clinical referral, imaging and worry. This presentation will review modern cranial sonographic protocols and anatomy, as well as common pitfalls and variants that may mimic pathology.

Seizure Imaging

Unni K. Udayasankar, MD

This talk will review the common causes of seizures in children with special emphasis on refractory seizures. Seizure is one of the most commonly encountered disorders in pediatric neurological practice. Recurrent seizures occur in approximately 1 to 2% of children with the highest incidence in the first year of life. An aggressive approach is recommended for diagnosis and management of refractory seizures to prevent adverse effect on early brain development, learning and memory. Neuroimaging plays a crucial role since structural abnormalities of the brain as noted on imaging studies have a higher correlation with medical intractability of seizures. Imaging techniques employed in diagnosis as well as preoperative surgical planning will also be discussed. MRI is the most commonly used and most sensitive imaging modality for evaluation of anatomical causes of intractable epilepsy. A spectrum of MR identifiable pathologies will be discussed including cortical malformation due to abnormalities of neuro-proliferation, abnormal neuronal migration, abnormal cortical organization, abnormal neuronal and glial proliferation or apoptosis, mesial temporal sclerosis, a variety of metabolic or genetic conditions, infections, trauma, and tumors. This talk will provide a broad overview of childhood seizure disorders with special focus on presentation and imaging findings related to the clinical workup of pediatric patients with pharmacologically resistant seizures. Relevant intracranial anatomy with imaging findings related to both common and rare seizure etiologies will be illustrated.

Advances in Brain Tumor Imaging

Ashok Panigrahy, MD

Pediatric astrocytomas are among the most common solid neoplasm in the pediatric population. Current neuroimaging biomarkers have limitations to meet the evolving needs in the treatment of pediatric astrocytoma. Combining targeted molecular imaging with multi-parametric MR imaging could result in earlier validation of an innovative therapy thus avoiding life threatening toxicities or re-direction of therapeutic efforts. The overall hypothesis of our research is that by combining innovative molecular imaging and MR techniques, we can improve our ability for initial characterization, risk assessment and treatment monitoring of pediatric brain tumors. We will: (a) demonstrate the use of advanced MR imaging techniques which can be integrated into routine clinical imaging of pediatric astrocytomas for initial assessment and differentiation from non-neoplastic lesions; (b) showcase the use of advanced post-processing techniques including quantitative short echo MR spectroscopy, diffusion weighted MR (functional diffusion mapping) and perfusion imaging (arterial spin labeling and dynamic contrast enhancement) in the evaluation of treatment of pediatric astrocytomas; and (c) compare advanced MR imaging biomarkers (including sodium MR) to routine conventional MRI in distinguishing between true progression and pseudo progression in pediatric astrocytomas being treated with innovative immunotherapy.

GASTROINTESTINAL

Abdominal Applications of DWI

Rutger A.J. Nievelstein, MD

Thanks to technological advances over the past few years (particularly the development of high-performance magnetic field gradients and parallel acquisition methods), diffusion-weighted imaging (DWI) can now routinely be performed in the abdomen. However, because the technique is rather susceptible to various factors that can degrade image quality (challenges include its inherently lower signal-to-noise ratio, fat suppression, the effects of respiratory and cardiac motion, etc.) and should be tailored to the clinical question(s) that need to be answered, optimization of the technique is required. In the first part of this lecture, some key concepts for DWI acquisition optimization will be addressed. Once optimized, DWI allows one to obtain additional biologic and diagnostic information that cannot be depicted with conventional MRI sequences. A variety of diseases can be evaluated with DWI, including cancer, inflammation, and infection, and the number of applications is rising. Most scientific evidence on the utility of DWI has been collected in the adult population. However, the use of DWI in the pediatric population is growing. In the second part of this lecture, some important established and emerging clinical applications of DWI in the (pediatric) abdomen will be discussed.

Update on MR Contrast Agents and Applications

Shreyas S. Vasanawala, MD, PhD

Various MRI contrast agents with unique properties are now available, requiring careful assessment of the clinical goals of each MRI exam to ensure optimal contrast agent selection. First, an overview of the classification of agents will be presented. In particular, MRI contrast agents may be classified as extracellular or non-extracellular, and as macrocyclics or linear agents. Macrocyclic agents have greater kinetic stability and hence are potentially safer in the setting of renal insufficiency. Then a strategy for selection of contrast agents in abdominal MRI will be presented. Briefly, most abdominal and pelvic applications are best served by extracellular agents. However, specific applications, such as biliary leaks, follow-up evaluation of known hepatic metastases, and evaluation of suspected focal nodular hyperplasia may be aided by gadoxetate. Conversely, evaluation of venous pathology may be facilitated with gadofosveset. Finally, iron oxide agents may be used in selected indications for diagnostic purposes.

Rex Shunt Interventions

James S. Donaldson, MD

A common cause of portal hypertension in children is extrahepatic occlusion of the portal vein (PV) often secondary to umbilical venous catheterization in infancy. This can lead to portal hypertension and its associated complications. In 1993 Ville de Goye from Belgium created a surgical shunt from the superior mesenteric vein to the left portal vein at the depth of the Rex recessus of the liver in a patient with extrahepatic PV occlusion. This surgical bypass using the internal jugular vein as graft has become an excellent shunt for these patients because instead of diverting blood to the systemic venous system blood from the gut is redirected back into the liver. This surgical bypass has become known as a Rex or Meso-Rex Shunt.

Pre-operatively the diagnosis of extrahepatic PV occlusion with patent intrahepatic PVs must be confirmed by imaging before a patient can be accepted as a candidate for the Rex Shunt. Although non-invasive imaging is often sufficient, a transjugular wedged hepatic vein portal venogram is sometimes needed to confirm patency of the intrahepatic portal veins. The technique of optimizing the visualization of the PV will be discussed.

Technically, the Rex Shunt is quite challenging for the liver surgeon primarily because the intrahepatic PV is very small. This leads to stenosis at the PV anastomosis in approximately 17% of patients. Rarely stenosis arises at the mesenteric vein end. Percutaneous transhepatic portal interventions including balloon angioplasty and occasional stent deployment can salvage 80% of patients with stenoses. Some patients require multiple interventions in order to maintain patency of the shunt. Technical details of the transhepatic interventions and patient follow-up will be discussed.
Interventional radiology is vital to the success of a surgical Rex shunt program. The interventional radiologist can help the surgeons select proper candidates for surgery and also provide essential interventions to keep the shunts patent and functioning properly.

GENITOURINARY

Update on Contrast Material Use in Children

Jonathan R. Dillman, MD

Intravascular contrast materials are commonly employed in children and adolescents, most often in the settings of contrast-enhanced computed tomography and magnetic resonance imaging. While modern intravascular contrast agents are generally quite safe in patients of all ages, mild and severe as well as immediate and delayed adverse events following

their administration can occur. Immediate adverse events to intravascular iodinated and gadolinium-based contrast material injections include physiologic and allergic-like (anaphylactoid) reactions. Delayed adverse events related to iodinated contrast materials include acute kidney injury (contrast-induced nephrotoxicity, or CIN) and hypersensitivity-like (most often cutaneous) reactions. While also rare in children, nephrogenic systemic fibrosis (NSF) is a delayed adverse reaction to gadolinium-based contrast material administered in the setting of acute or chronic kidney injury that can be associated with substantial morbidity. I will present an up-to-date review of key issues pertaining to intravascular contrast material use in the pediatric population, including discussions of allergic-like reactions, CIN, and NSF.

Update on UTI Imaging Assessment: ACR and AAP Guidelines

Boaz Karmazyn, MD

There is no consensus on optimal imaging of children with urinary tract infection (UTI). Pyelonephritis typically presents with fever and may result in renal scarring. Currently there is limited medical evidence to support imaging in children with the first episode of febrile UTI. Prospective studies did not demonstrate that prophylactic antibiotics decrease risk for renal scarring and surgical correction of vescicoureteral reflux (VUR) was not found to improve outcome. In addition, with the increased use of prenatal US it was found that most renal atrophies and dysplasia are congenital and are not the sequelae of pyelonephritis. Pyelonephritis rarely leads to chronic renal failure or hypertension.

Both the AAP and the ACR appropriateness criteria recommend imaging with renal ultrasound (US) for the first episode of UTI with fever in children older than 2 months and younger than 2 years of age. Voiding cystourethrography (VCUG) is not recommended for the routine evaluation of the first episode of febrile UTI. VCUG is mainly performed for the detection of VUR. It is mainly indicated in children with recurrent UTIs or atypical UTI (poor response to antibiotics within 48 h, sepsis, urinary retention, poor urine stream, raised creatinine, or non-E. coli UTI). Renal cortical scintigraphy (Tc-99 m DMSA) performed 4 to 6 months after the acute episode of UTI is the most sensitive imaging to detect renal scarring. There are studies suggesting that Tc-99 m DMSA may decrease the need for VCUG studies. However, compared to VCUG, it is less widely available and delivers more radiation.

Advances in Pediatric Urosonography

Kassa Darge, MD, PhD

Ultrasound (US) plays a central role in the diagnostic imaging of the urinary tract in children. Innovations in US technology and US contrast agents have major positive impact on pediatric urosonography. High resolution US with high frequency transducer delivers US images approaching macro-histology specimen. Harmonic imaging produces artifact-free images with high resolution. It has been shown to be superior to fundamental mode in many urosonographic applications. Panorama imaging allows improved documentation of longer than the transducer structures including markedly enlarged kidneys or renal tumors. It also allows presentation options comparable to MR and CT scans. Curved measurement is possible with panorama scan. Color Doppler is an established imaging modality, but its use for diagnosis of stones in the urinary tract, especially in children, is relatively new. The so-called twinkling sign, a color Doppler artifact at the site where one normally expects the acoustic shadow to be, enhances the conspicuity of the small stones. A further development is three-dimensional (3D) US. It offers better volume measurement of the bladder and kidneys than 2D US. Contrast enhanced voiding urosonography (ceVUS) has already proven to be a valuable alternative in the diagnosis of vesicoureteral reflux. It is not only free of radiation but has much higher vesicoureteric reflux detection rate when compared to the conventional modalities. The routine use of advanced urosonographic modalities in children will promote the use of the widespread, safe and less costly method of US.

Imaging of Mullerian Anomalies

S. Pinar Karakas, MD

This talk will review the embryology, classification, imaging pearls and pitfalls of Mullerian anomalies (MAs). MAs form a rare but important group of entities and accurate diagnosis and treatment requires a skilled team approach. MAs result from a defective sequence during Mullerian duct organogenesis, fusion or septal resorption, while an ideal progression would form the fallopian tubes, uterus, cervix and the upper two-thirds of the vagina. Clinical presentation of MAs would depend on the type of anomaly and can range from being asymptomatic to presenting with pelvic mass, primary amenorrhea or dysmenorrhea in adolescence, or infertility and recurrent spontaneous abortions in young adulthood. The American Society of Reproductive Medicine classification system is the most widely accepted system and it delineates the accurate treatment path. This system should only be used as a framework, however, rather than a requisite since some of the anomalies are very complex and defy the classification system. In such complex cases, it is important to describe and communicate the key imaging findings rather than trying to force fit the anomaly into the classification system. Ultrasound is invariably the initial imaging modality in MAs but the emphasis of this talk will be on the technique and interpretation of MRI due to its indispensible role in evaluation of the MAs. In imaging, it is imperative to accurately identify the

morphology of the uterine fundus, anatomy of the cervix and vagina, and presence of functional endometrium in case of an isolated unicornuate uterus. In addition, associated anomalies and obstructive outflow tract disorders of the vagina will also be discussed.

Wednesday, May 15, 2013

MUSCULOSKELETAL

Advanced Imaging of Arthritis

Andrea S. Doria, MD

Imaging often plays a key role in establishing the presence of arthritis, determining its extent or defining the specific diagnosis. There has been a tremendous increase in the quantity and quality of imaging technology available for early diagnosis of arthritis in recent years. Previously, conventional radiography was the principal method used to evaluate and follow bone damage in patients with inflammatory arthritis. More recently the use of magnetic resonance imaging (MRI) and ultrasonography (US) has gained wider acceptance due to their ability of multiplanar techniques and use of contrast agents. MRI is a very accurate technique for diagnosis of macroscopic soft tissue (joint effusion/hemarthrosis, synovial hyperplasia, hemosiderin deposition) and osteochondral (cartilage loss, subchondral cysts) changes. US holds the potential for being an adjunct tool to MRI in the assessment of soft tissue changes, which typically precede osteochondral changes, and peripheral cartilage abnormalities.

In the near future, the implementation of currently available imaging techniques for assessment of arthritis should certainly improve diagnostic imaging accuracy. These techniques include quantitative MRI methods for data analysis of cartilage and definition of US and MRI standard criteria for quantification of normal cartilage in children of different age groups which are currently under way in ongoing clinical trials, and data acquisition using fusion ultrasound–MRI which still requires engineering development of hardware and further validation in clinical trials before translation into clinical practice.

Looking ahead further, functional and molecular imaging techniques may be able to demonstrate microscopic soft tissue and osteochondral abnormalities that will help us to understand the biological basis of early physiological events in arthritis. Within the soft tissues, imaging techniques such as dynamic contrast-enhanced MRI with intravenous administration of ultrasmall paramagnetic iron-oxide (USPIO) particles, MR spectroscopy, diffusion tensor imaging, blood oxygen level-dependent (BOLD) imaging, positron emission tomography (PET) may be of value for assessment of minimal changes in joints. Within the osteochondral tissues, T1 and T2 mapping may be used for quantification of biochemical and histological changes in the cartilage prior to the detection of macroscopic joint changes which are identifiable with the currently available imaging arsenal. Microcomputed tomography (microCT) may enable identification of very early bone loss. This new functional-microscopic information on the status of arthritic joints at a given timepoint will certainly have a major impact on the way pediatric radiology will stand in clinical practice and research.

Imaging of Osteochondral Lesions

J. Herman Kan, MD

An osteochondral lesion is a broad term that includes normal osteoarticular ossification variants and osteochondritis dissecans. To add to the challenge, sometimes normal osteoarticular ossification variants may become symptomatic and are difficult to clinically or radiologically differentiate from osteochondritis dissecans. The knee, ankle, and elbow are most frequently affected. Clinical and radiologic challenges are frequent particularly in children in the first decade because location and imaging findings may overlap between normal ossification variants and osteochondritis dissecans.

In this session, we will examine the most common locations for osteochondral lesions by radiography and cross sectional imaging. We will cover and compare asymptomatic and symptomatic osteoarticular ossification variants and show how these lesions are similar and different from osteochondritis dissecans. We will cover imaging criteria that the orthopaedist needs to know to help determine treatment for osteochondritis dissecans.

Update on Child Abuse Imaging

Jeanette Perez-Rossello, MD

The detection of skeletal injuries depends on the technical quality and thoroughness of the skeletal survey. Failure to perform an adequate skeletal survey may result in the return of a child to a potentially dangerous environment. The 2011 ACR-SPR guidelines added oblique images of the ribs to increase detection of rib fractures. Concern about the number of images and radiation burden to infants undergoing the skeletal survey has led pediatric radiologists to evaluate protocols to decrease the number radiographs in the initial and follow-up skeletal surveys. This discussion will include a review of rare injuries seen in abuse, namely vertebral, hands and feet, and pelvic fractures.

Imaging of Myopathies

Tal Laor, MD

The spectrum of pediatric myopathies is broad, ranging from congenital and infantile myopathies of neurologic origin, to non-congenital muscular dystrophies and inflammatory myopathies such as dermatomyositis. Imaging of the muscles, with particular emphasis on MR imaging, can be used to optimize a site for biopsy as well as to provide both clinical and research endpoints for therapy. Although several disorders have a variable distribution of affected muscles, certain conditions may result in a specific pattern of involvement on MR imaging. Recognition of these patterns can be helpful to suggest a diagnosis when not yet determined. In some cases, MR imaging can replace the need for muscle biopsy.

Muscle abnormalities include changes in muscle size (both diminished and increased) and in signal intensity. Fatty atrophy and infiltration as well as edema-like signal are hallmarks of various disorders, and can help to determine the acuteness or chronicity of a disorder. In this session, we will examine the more common pathologies that affect muscles in children and review both qualitative MR imaging methods (such as T1-, T2- and inversion recovery-weighted sequences) as well as quantitative imaging analyses, such as T2 mapping, that can be used to diagnosis and monitor children with various myopathies.

ONCOLOGY IMAGING

Late Effects of Cancer Treatment

Kirsten K. Ness, PhD

Sophisticated radiation therapy techniques, multiple agent chemotherapy regimens, advanced surgical procedures and improved hospital care have increased 5 year survival to over 80% among children diagnosed with cancer. There are over 260,000 survivors of childhood cancer in the United States today. One in 680 of individuals 20 to 50 years old is a childhood cancer survivor. Unfortunately, cure is not without consequences. Adult survivors of childhood cancer are at risk for chronic conditions, many of which are related to their previous radiation exposure. This session will summarize data from the literature and two large cohort studies, the Childhood Cancer Survivor Study and the St. Jude Lifetime Cohort Study, to describe medical late effects and their potential association with radiation exposure. Second neoplasms, thyroid dysfunction, cardiac health, pulmonary impairment, neurocognitive disorders, metabolic deficits, and problems with bone health will be described in the context of radiation exposure history. The symposium will also discuss the Children's Oncology Group recommended guidelines for medical, laboratory and imaging based surveillance for radiation associated chronic conditions, and report the increased disease yield realized when screening guidelines are applied to reveal asymptomatic or subclinical disease. This discussion will conclude with a focus on the importance of utilizing risk-based screening/surveillance guidelines to screen for disease where, like breast cancer or coronary artery disease, when it is detected and treated early, may result in less morbidity and mortality for this vulnerable young population.

Pre and Post-operative Imaging of Limb Salvage Therapy

Laura M. Fayad, MD

Limb salvage surgery represents a variety of surgical techniques that are designed for resection of a limb sarcoma and subsequent reconstruction of the limb, such that an optimal oncologic, cosmetic and functional outcome occurs. Imaging, especially with MRI, has been established as an accurate method for the preoperative determination of the extent of disease. Following resection, serial radiographs are employed to monitor healing and to detect complications, although radiography is limited in its inability to provide cross-sectional information need to identify subtle complications. MRI is usually the ideal modality for the assessment of local recurrence after tumor resection, but MRI sequences suffer in the presence of metal hardware. Hence, CT imaging, with 3D CT reconstructions, can be valuable for the assessment of suspected postoperative complications following limb salvage surgery, or for the evaluation of cases in which complex reconstructions have occurred. We will review imaging techniques that can be used for treatment planning prior to surgery, describe the various surgical techniques of limb salvage surgery, and illustrate the appearance of a normal postoperative course and potential complications of limb salvage surgery with imaging.

Detection of CNS Metastases

Noah D. Sabin, MD, JD, Julie H. Harreld, MD, Kathleen J. Helton, MD, Zoltan Patay, MD, PhD

Accurate detection of metastases is critical for staging malignant neoplasms and establishing prognoses in children. At our institution, we have used a variety of imaging techniques to optimize detection of metastatic disease in the central nervous system. These include post gadolinium FLAIR imaging for detection of intracranial leptomeningeal metastases and diffusion weighted imaging for intracranial leptomeningeal disease and brain parenchymal ingrowth. Thin section images allow for better visualization of metastatic disease intracranially and

within the spine. Subtraction of precontrast T1-weighted images from post contrast T1-weighted images allows for improved detection of subtle enhancing metastatic lesions. Interleaving of sagittal images facilitates accurate identification of spinal leptomeningeal metastases. 3D imaging sequences with multiplanar reformations may be helpful for clarifying ambiguous findings intracranially and in the spine. Improved metastasis detection can be achieved using greater imaging efficiency as some of our MRI protocols take less time than those used at other institutions. This talk will present some of the techniques found to be useful for detection of leptomeningeal CNS metastases at St. Jude Children's Research Hospital and how they may be incorporated at other institutions.

PET-MR: Radiation Reduction and More

Geetika Khanna, MD

The success of PET-CT in clinical practice has stimulated research for development of hybrid imaging techniques such as PET-MRI. The first PET-MRI hybrid imaging systems were based on spatially separate PET and MR scanners that were connected by a moving patient table. However, these sequential scanners were limited by long scan times. The development of MR compatible PET detectors, MR based methods of attenuation correction, and MR surface coils that do not attenuate gamma rays, has led to the development of PET-MR scanners that allow for truly simultaneous acquisition of PET and MR data. In the simultaneous PET-MR scanner, the PET detectors are located inside the MR gantry, allowing for simultaneous whole body PET and 3Tesla MR imaging. Unlike PET-CT, which uses the CT data for attenuation correction, the primary method of attenuation correction in PET-MR uses 2-point Dixon sequence that can separate the four main tissues (fat, soft tissues, lung, air/background). Preliminary data suggests that there is good correlation between standardized uptake values (SUV) estimated by PET-CT and PET-MR. PET-MR is an exciting new imaging modality that can combine the anatomic and functional abilities of MR with the molecular abilities of PET. Other advantages include better soft tissue contrast, better co-registration, and less radiation dose than PET-CT systems. Imaging with PET-MR though has its challenges including the need to adjust the MR protocols to match the multiplanar abilities of PET, SAR (specific absorption rate) issues and artifacts inherent to scanning at 3 Tesla.

This talk will discuss the opportunities and challenges associated with PET-MR imaging. Potential applications in the pediatric population will be discussed with case-based examples.

SCIENTIFIC PAPERS

Authors are listed in the order provided. An author listed in bold identifies the presenting author.

Paper #: PA-001

Comparison of Diagnostic Performance of CT and MRI for Abdominal Staging of Wilms Tumor: a Report from the Children's Oncology Group

Sabah Servaes, *CHOP, Philadelphia, PA, servaes@email.chop.edu;* Geetika Khanna, Arlene Naranjo, Eric Gratias, James Geller, Peter Ehrlich

Purpose or Case Report: To compare the diagnostic performance of CT and MRI for local staging of Wilms tumor.

Methods & Materials: The study population was drawn from the renal tumors classification, biology and banking study of the Children's Oncology Group- a HIPAA compliant and IRB approved study. Between March 2006 and March 2012, baseline abdominal imaging performed with both CT and MRI, within 30 days of surgery, was available for retrospective review in 82 Wilms tumor (WT) cases. Two pediatric radiologists consecutively reviewed all CTs followed by all MRIs, blinded to all patient information. Each case was evaluated for the presence/absence of the following: capsular penetration, lymph node (LN) metastasis, tumor thrombus, tumor rupture, and synchronous lesions. The surgical/pathologic findings at central review were considered the reference standard.

The sensitivity and specificity with confidence intervals were computed according to the continuity-corrected efficient-score method from Newcombe. McNemar's two-sided test was used on the CT/MRI paired data for each patient to test the null hypothesis of equality of the sensitivity and specificity of CT and MRI

Results: The age range for the cohort was 31 days-19.4 years (median: 3.94 years), and 47/82 subjects were female. The stage distribution was: stage I: 19, stage II: 17, stage III: 24, stage IV: 16, stage V: 1, 5 missing.

The sensitivity of CT and MRI for detecting capsular penetration was 68.6% and 62.9% (P: 0.73), while specificity was 86.5% and 83.8% (P: 1.0). The sensitivity of CT and MRI for detecting LN metastasis was 76.5% and 52.9% (P: 0.22), and specificity was 90.4% and 92.3% (P: 1.0). Venous extension was present in four subjects (3 renal vein, 1 IVC) and was correctly classified by CT in 85.4% (70/82) and by MR in 89.0% (73/82). Tumor rupture was present in only two subjects and was correctly classified in 85.4% (70/82) by CT and in 91.5% (75/82) by MR. Additional synchronous lesions were identified by CT in eight cases and by MR in 12 cases.

Conclusions: Both CT and MRI have high specificity but relatively low sensitivity in detecting LN metastasis and capsular penetration. Though CT had higher sensitivity in detecting LN metastasis, and MR detected more synchronous lesions, these differences were not statistically significant. The choice of imaging modality for initial staging of WT should be based on institutional expertise with consideration of radiation exposure and need for sedation.

Paper #: PA-002

Disease Spectrum and Imaging Findings in Perivascular Epithelioid Cell Tumor (PEComa) in Pediatric Patients

Alan Schlesinger, MD, *Department of Pediatric Radiology, Texas Children's Hospital, Houston, TX, alanschlesinger@mac.com;* John Hicks, R. Paul Guillerman

Purpose or Case Report: The purpose of our study was to review the disease spectrum and the imaging appearance in eight patients with surgically-proven perivascular epithelioid cell tumors (PEComas). PEComas are a diverse group of tumors that contain perivascular epithelioid cells and include angiomyolipoma (AML) and its variants, clear-cell "sugar" tumor, lymphagngioleiomyomatosis (LAM), clear-cell myomelanocytic tumor of the falciform ligament/ligamentum teres, and other rare clear-cell tumors.

Methods & Materials: The pathology department database at a single children's hospital was searched for patients diagnosed with tumors in the PEComa spectrum who underwent surgical excision of their tumors between 1994 and 2012. The imaging studies and pathology reports were retrospectively reviewed.

Results: The eight patients (5 female, 3 male) with PEComas ranged in age from 5 to 19 years at the time of surgery (mean= 13 years). Five of the eight patients had tuberous sclerosis (TS). All eight patients had renal AMLs. Four had renal AMLs alone (2 of which were the epithelioid variant) while the other four had additional lesions involving other sites including liver (4), uterus (1), and lung (2). Seven patients had preoperative imaging including US in 6, CT in 7, and MRI in 3. Renal lesions were multiple in four patients and single in 4. They were hyperechoic on US in all cases. CT showed nonfatty renal lesions in three patients and confirmed fat in the renal lesions in the remaining four patients (purely fatty in 1, mixed fatty and nonfatty in 3). MRI showed both fatty and nonfatty renal lesions in two patients and only nonfatty renal lesions in 1. The renal lesions in the two patients shown to have the epithelioid variant of AML at histology did not contain fat on imaging. Imaging revealed evidence of fat in the hepatic lesions but not in the lesions in the remaining extrarenal sites.

Conclusions: Radiologists should be aware of the recently described spectrum of related tumors (PEComas) that are defined by the presence of a unique cell type: the perivascular epithelioid cell. These tumors are often seen in patients with TS. When evaluating patients with TS, in addition to evaluating for renal AML, it is important to evaluate for masses in other reported extrarenal sites of involvement. Furthermore, the absence of fat in a renal lesion in these patients should raise concern for the potentially more aggressive epithelioid varient of AML.

Paper #: PA-003

MRI of pediatric abdominal tumors: Are contrast enhanced studies necessary?

Rakhee Gawande, M.D, *Radiology, Stanford University School of Medicine, Stanford, CA, rakheegawande@yahoo.com;* Kevin Chi, Matthew Schmitz, MD, Jennifer Trinh, Bo Yoon Ha, Heike Daldrup-Link

Purpose or Case Report: Advances in MR imaging along with the risk of nephrogenic sclerosis associated with gadolinium chelates have led to eliminations of contrast enhanced sequences for many MRI applications. The purpose of our study was to evaluate, if contrast enhanced MRI sequences provide additional information compared to unenhanced sequences for staging and restaging of pediatric abdominal tumors.

Methods & Materials: MRI scans of 87 pediatric patients with 43 (49.4%) malignant and 44 (50.6%) benign abdominal tumors were retrospectively analyzed after institutional review board approval. The MRI protocol included: (1) Precontrast sequences: Axial/coronal fat suppressed T2 2000–11000 ms/67–82 ms (TR/TE), pre-contrast axial/coronal T1-LAVA 12–15°/3.8–7.2 ms/1.9–7.2 ms (flip angle/TR/TE) and DWI 5250–7500/54–64 ms sequences (TR/TE, b=0, 500) with ADC maps; and (2) axial/coronal T1-LAVA after Gd-BOPTA injection. Pre- and postcontrast MRI scans were independently evaluated regarding image quality, lesion characteristics and final diagnosis. The histopathology report was considered as the standard of reference.

Results: The image quality was rated satisfactory in 31.4% and excellent in 68.6% cases. The sensitivity for detecting primary tumors was not significantly different between

precontrast sequences (78.1%) and postcontrast sequences (79.5%, $p>0.05$). The final diagnosis between pre and post contrast sequence matched on 80.7% cases. The presence of central necrosis was detected on 18.3% of precontrast scans and 27.5% postcontrast scans; vascular encasement 10.3% precontrast scans and 20.6% postcontrast scans; tumor thrombosis 5.7% precontrast scans and 4.5% postcontrast scans; liver metastases 9.2% precontrast scans and 5.7% postcontrast scans; bone metastases 2.3% precontrast scans and 4.5% postcontrast; lymph node metastases on 19.5% precontrast scans and 10.3% postcontrast scans (Figure 1). On going statistical analysis will compare data of different reviewers to determine inter-observer reliability scores.

Conclusions: In the majority of cases, contrast enhanced MRI sequences did not provide additional information compared to unenhanced sequences for staging and restaging of pediatric abdominal tumors.

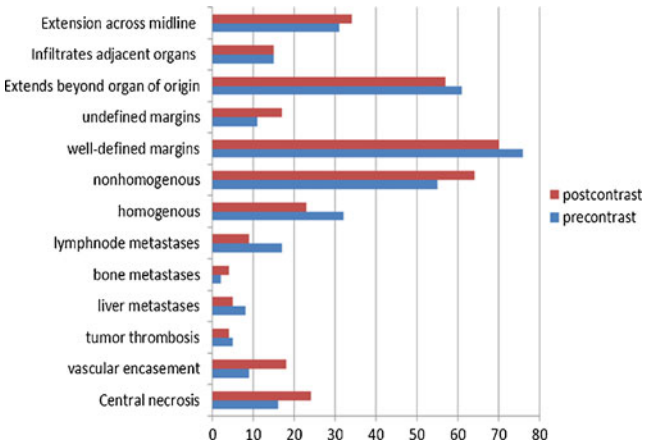

Figure 1: Lesion characteristic evaluated on precontrast and contrast enhanced scans. (n=numbered of patients)

Paper #: PA-004

DW-MRI Characterization of Fast and Slow Diffusion in Ttreated Pediatric Osteosarcoma

Kirsten Ecklund, MD, *Radiology, Boston Children's Hospital, Boston, MA, kirsten.ecklund@Children's.harvard.edu;* Moti Freiman, Simon Warfield

Purpose or Case Report: Response to therapy assessment in children with osteosarcoma may be complicated by increased tumor size due to hemorrhage, necrosis, ossification or tumor growth. Diffusion-weighted MRI (DW-MRI) has been used assess overall diffusivity as measured by apparent diffusion coefficient (ADC) analysis, with increased ADC value suggesting tumor necrosis and enhanced extra-cellular space. Increased ADC, however, may also result from fast diffusion related to increased perfusion, as occurs with tumor progression. The goal of this study was to utilize Intra-Voxel Incoherent Motion (IVIM) analysis to characterize fast and slow diffusion variations from DW-MRI data of osteosarcoma tumors following chemotherapy.

Methods & Materials: We reviewed MRI studies of five patients (4 males, 1 female) with osteosarcoma undergoing adjuvant chemotherapy. Average age was 12.6 years (range 7–17). MR sequences included coronal T1, IR, fat suppressed axial T2, post contrast fat suppressed axial and coronal T1, and axial DW-MRI with multiple b-values ranging from 0 to 800 s/mm2. Based upon review of all images, three regions of differential diffusivity were selected in each tumor on the DW-MRI, b-value= 500 s/mm2, and designated as good response (high ADC, low contrast enhancement), poor response (low ADC, high enhancement), or indeterminate (intermediate ADC, enhancement). Within each tumor, poor and good response regions were quantitatively compared by Apparent Diffusion Coefficient (ADC) and by Intra-Voxel Incoherent Motion (IVIM) with slow-diffusion (D) and fast-diffusion fraction (f) parameters. Average parameter values were calculated for the annotated regions.

Results: Fifteen tumor regions in five patients: seven regions classified as poor response, five as good response and three as indeterminate (which were eliminated from analysis). Each tumor had both good and poor response regions. In 5/7 (71%) poor response regions, the fast-diffusion component (f) was >25% higher than f in the good response regions in the same tumor, but ADC and D were only mildly lower, <20%, or even higher in these same poor response regions.

Conclusions: IVIM analysis differentiates the fast and slow diffusion components of DW-MRI signal decay observed in osteosarcoma. Increased ADC regions in these tumors must be interpreted carefully as they may reflect perfusion-related fast diffusion rather than tumor necrosis associated slow

diffusion. IVIM DW-MRI is a promising new technique which may prove useful for therapy response assessment in patients with osteosarcoma.

Paper #: PA-005

Intravenous Glucagon Use in Pediatric MR Enterography: Effect on Image Quality, Length of Examination, and Patient Tolerance

Brett Mollard, MD, *University of Michigan Health System, Ann Arbor, MI, bmollard@med.umich.edu;* Jonathan Dillman, Ethan Smith, Peter Strouse

Purpose or Case Report: To evaluate the use of intravenous (IV) glucagon in pediatric patients undergoing MR enterography (MRE).

Methods & Materials: Institutional review board approval was obtained. Forty-seven patients underwent clinical MRE examinations containing identical breath-held T1-weighted 3D gradient recalled echo fat-saturated pulse sequences before and after IV glucagon administration. Images were reviewed in a blinded manner by two pediatric radiologists to determine the effect of glucagon on small and large bowel visualization. Image timestamps were documented separately to determine how this adjunctive medication affects examination length. A separate cohort of 50 patients was evaluated for glucagon-related symptoms, including nausea and emesis.

Results: Glucagon improved overall bowel visualization in 40/47 (85%) examinations for reader #1 (p=<0.0001) and 36/47 (77%) for reader #2 (p=0.0001). There was improved visualization of the terminal ileum following glucagon administration in 29/47 (62%) examinations for both readers (p=0.03). Glucagon improved visualization of the small bowel for reader #1 (3.3±1.0 vs. 2.2±0.7; p<0.0001) and reader #2 (3.4±1.1 vs. 2.5±0.9; p<0.0001), using a 5-point Likert-like scale. Glucagon also improved large bowel visualization for reader #1 (3.3±0.9 vs. 3.0±0.8; p=0.005) and reader #2 (3.4±1.1 vs. 3.0±1.0; p=0.002). On average, the use of glucagon added 13.7 min to examination length. Twenty-four of 50 (48%) patients self-reported glucagon-related nausea, while four (8%) patients experienced emesis.

Conclusions: IV glucagon improves bowel visualization at pediatric MRE, increases examination length, and commonly causes nausea. Less than 10% of patients experience glucagon-related emesis in our practice.

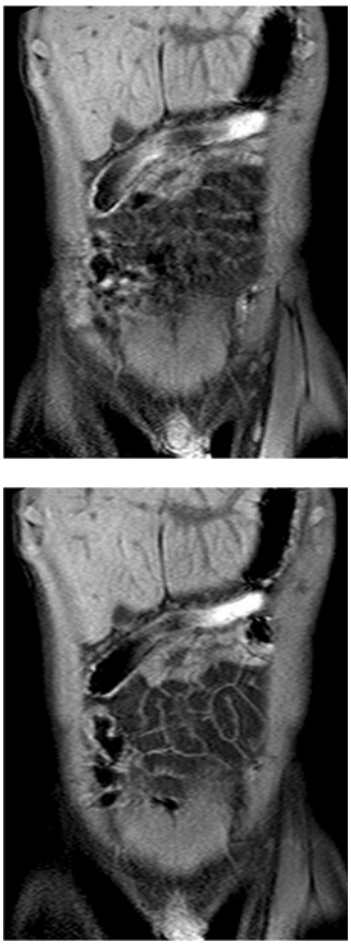

Paper #: PA-006

Performance of MR Enterography in Assessing Crohn's Disease Activity in the Pediatric Population

Piotr Obara, MD, *Radiology, University of Chicago, Chicago, IL, probara@gmail.com;* Seng Ong, Mario Zaritzky, Kate Feinstein, MD

Purpose or Case Report: Evaluate performance of MR enterography (MRE) in assessing Crohn's disease activity in the pediatric population.

Methods & Materials: We retrospectively reviewed reports of MRE exams performed during a 5-year study period for patients with known Crohn's disease who were age 18 years old or younger. Findings indicative of active bowel inflammation were recorded, including location and any complications related to inflammation. Medical records were subsequently reviewed and pathology findings from either colonoscopy sampling or surgical specimens were recorded, if available. Only patients with pathology results within a 90 day period of the MR exam were included. The study was performed under approval of the institutional review board.

Results: Thirty-six patients matched inclusion criteria (9 males, 27 females; mean age: 14.5 years, range: 6–18 years). Pathology samples were obtained from colonoscopy in 25 cases and surgical specimen in 11 cases. Compared to pathology results, MRE had an accuracy of 81% (80% [24/30] sensitivity; 83% [5/6] specificity) in detecting active inflammation (p=0.0062). All cases of moderate to severe inflammation of the terminal ileum (TI) were detected. Pathology for the six false negative cases revealed mild to moderate colitis without TI involvement in four cases, and mild TI activity in two cases. For the one false positive case, only minimal, short segment wall thickening of the TI was noted on MR, however, pathology did not reveal any active inflammation. MR findings of active disease in true positive cases (n=24) included wall thickening (n=22), wall enhancement (n=18), restricted diffusion on DWI sequences (n=7), and decreased peristalsis (n=2).

Conclusions: MR enterography showed excellent performance in assessing moderate to severe inflammation of the terminal ileum. In our experience, MRE was less sensitive in detecting mild inflammation of the terminal ileum and mild to moderate colitis.

Paper #: PA-007

The T2 ratio: a tool to differentiate bowel wall inflammation from fibrosis

Cheryl Zvaigzne, David Patton, Seemab Haider, Amy Davis, Weiming Yu, **Clara Ortiz-Neira, MD,** *Alberta Children's Hospital, Calgary, AB, Canada, claraneira@shaw.ca*

Purpose or Case Report: Treatment for inflammatory bowel disease (IBD) includes pharmacological therapy for inflammation and surgical resection of fibrotic segments, but it remains a challenge to differentiate between these characteristics. Bowel thickening and qualitative T2 hyperintensity on magnetic resonance imaging (MRI) are known predictors of inflammation. We propose that a quantitative ratio of bowel wall T2 SI to that of nearby skeletal muscle provides an objective parameter differentiating inflammation from fibrosis.

Methods & Materials: Retrospective review was performed of MRIs of pediatric Crohn's disease patients who either A) responded to medical therapy or B) had surgical resection of a bowel segment after failure to respond to therapy. Axial T2 HASTE images were reviewed for the presence of thickened (> 3 mm) small bowel segments. On T2 HASTE Fat Saturation images, a region of interest (ROI) was drawn in the bowel wall in an area of maximal thickness having the greatest SI. A second ROI was traced in the iliopsoas muscle (Fig. 1). T2 ratios of mean SI in the bowel to iliopsoas muscle were compared between groups A and B. In group B, scores of 0 (normal) to 3 (severe) were assigned according to the presence of inflammation and fibrosis on histology. A ratio of inflammation to fibrosis scores was calculated for each patient and compared to the T2 ratio. Finally, trends in T2 ratio over time were compared with trends in ESR, CRP, clinical symptoms, and bowel thickness.

Results: Twenty-one patients (10 female, mean age 14.7 ±2.7 years) were studied. T2 ratios were significantly different between groups A (5.35±1.88; n=8), and B (3.73±1.01; n=13) (Fig. 2; unpaired t-test, p=0.004). In eight patients who had multiple bowel MRIs, a decrease in T2 ratio over time tended to correspond to reduced inflammatory markers, bowel wall thinning, and subjective clinical improvement of symptoms. Histological inflammation to fibrosis ratio had a weak positive correlation with T2 ratio (R=0.12).

Conclusions: Quantitative T2 ratios provide a possible means of differentiating fibrotic and inflamed bowel without use of intravenous contrast in pediatric IBD patients, and may provide a rapid tool to assess response to medical therapy. Pediatric MRI assessment of IBD is technically challenging, requiring further

standardization. A prospective study correlating trends in T2 ratio, clinical disease score, inflammatory markers, and outcome would be valuable.

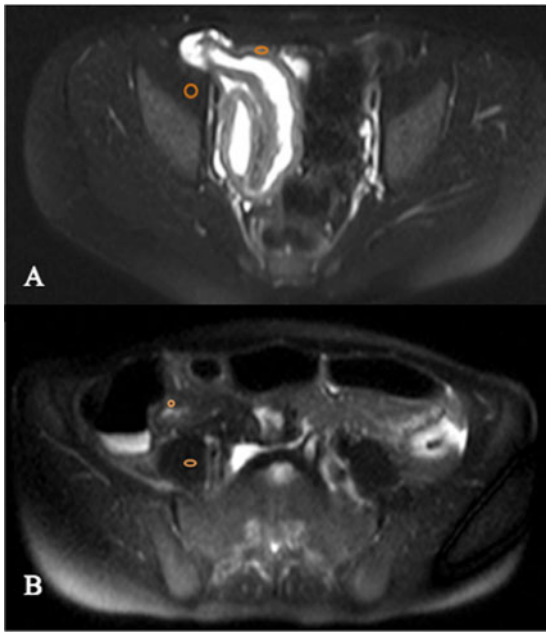

Figure 1. T2 HASTE FS Images with ROIs drawn in bowel and iliopsoas in patients who (A) respond to medical theraphy (T2 ratio=5.05), and (B) underwent surgical resection (T2 ration=1.89).

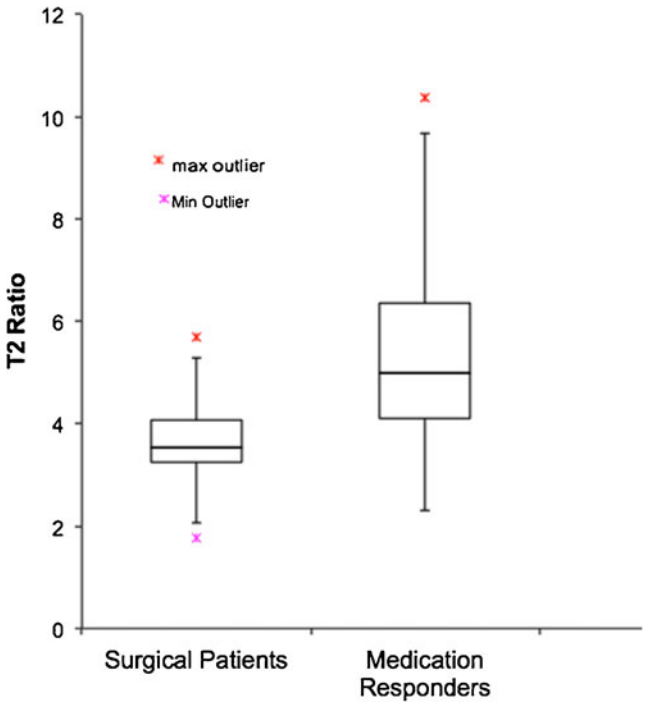

Figure 2. Box and Whisker Plot comparing T2 ratios

Paper #: PA-008

Comparative assessment of individual CT enterographic and MR enterographic imaging features of active Crohn's disease in pediatric patients

Mayureewan Taphey, *Pediatric Radiology, MGH, Boston, MA;* Debra Gervais, Michael Gee

Purpose or Case Report: Diagnosis of active Crohn's disease (CD) on CT enterography (CTE) and MR enterography (MRE) typically involves identification of multiple characteristic imaging features, all of which often are not present. It would be helpful to know which imaging feature is the best biomarker of active disease and, in addition, whether the optimal imaging biomarker varies between the two imaging modalities. In this study, we compare the performance of several established imaging biomarkers of active CD on CTE and MRE in pediatric patients, compared with histologic reference.

Methods & Materials: In this IRB-approved, HIPAA-compliant retrospective study, an imaging database query identified patients <20 years old who underwent either CTE or MRE from 2005 to 2011. Electronic medical records then identified all pediatric patients with known CD who underwent either CTE or MRE with recent colonoscopic biopsy. All CTE and MRE exams were performed according to standard protocol using high volume neutral (CT) or biphasic (MR) oral contrast and intravenous contrast. All studies were reviewed by a radiologist blinded to the histologic results. For each study, the bowel was divided into seven segments (from terminal ileum to anus) and each segment was scored for the presence/absence of the following imaging features: 1) wall thickening >3 mm, 2) mucosal hyperenhancement, 3) mesenteric inflammatory changes, 4) mesenteric hypervascularity, 5) fibrofatty proliferation, 6) lymphadenopathy >10 mm short axis. Test performance characteristics of each imaging feature were calculated based on endoscopic mucosal biopsy results.

Results: Three hundred sixty-two bowel segments (65 CTE, 297 MRE) were evaluated from 63 patients (mean age 16.3 years) with available histologic reference (mean time to endoscopy 9.3 days). Among the imaging features evaluated, bowel wall thickening >3 mm (85% accuracy/85% sensitivity/84% specificity CTE; 84%/79%/88% MRE) and mucosal hyperenhancement (79%/60%/87% CTE; 75%/50%/94% MRE) were the best features for detecting active Crohn's disease, both on CTE and MRE. The other features were significantly less accurate on both imaging modalities.

Conclusions: Bowel wall thickening >3 mm and mucosal hyperenhancement are the two imaging features on both CTE and MRE that demonstrate best performance as imaging biomarkers of active Crohn's disease in pediatric

patients. Pediatric radiologists interpreting these studies should emphasize the presence or absence of these two imaging features when performing imaging assessment of disease activity.

Paper #: PA-009

Added value of Diffusion Weighted Imaging in MR enterographic evaluation of Crohn's disease in pediatric patients

Anuradha Shenoy-Bhangle, MD, *Abdominal and Interventional Radiology, Massachusetts General Hospital, Boston, MA, anuradhabhangle93@gmail.com;* Katherine Nimkin, Michael Gee

Purpose or Case Report: MR enterography (MRE) is increasingly utilized for imaging evaluation of disease activity in pediatric patients with Crohn's disease, which has important implications on clinical management. Diffusion weighted imaging (DWI) is a rapid imaging technique that measures molecular diffusion of water and is sensitive to the inflammatory process. The purpose of this paper is to determine whether addition of DWI to MRE is helpful in evaluating Crohn's disease activity in pediatric patients compared with histological reference.

Methods & Materials: In this single institution, IRB-approved retrospective study, an imaging database query identified pediatric patients <20 years of age who had MRE studies performed between 2000 and 2011. Electronic medical records were searched and relevant data recorded. DWI was performed according to standard department protocol using a breath-hold echo planar imaging fat-suppressed DWI sequence with B-values of 0 and 600–800 centered in the terminal ileum in the axial plane with a coverage of 10 cm. All scans were performed on either a 1.5 T (GE) or 3 T (Siemens) clinical MR scanner with phased array torso coil configuration. Apparent diffusion coefficient (ADC) maps were generated automatically. For each segment of bowel evaluated by DWI (terminal ileum, ascending and descending colon), average ADC value was determined by the average of three voxels within the bowel wall based on anatomic localization from B=0 images. Restricted diffusion was defined as average ADC value $<2.0\times10$–3 mm2/s. Conventional MR enterographic assessment of disease activity was determined in the same segments at a separate readout session, with standard criteria for active disease. Both DWI and MRE evaluation of CD activity were performed by a radiologist who was blinded to the histology results.

Results: A total of 78 bowel segments from 27 patients with known CD and recent colonoscopy were included in the study. Thirty-three segments were found to have active disease based on endoscopy and histopathology results. Table 1 denotes our calculated results.

Conclusions: Although DWI alone does not perform as well as conventional MRE for detection of active CD, the combination of DWI plus MRE increases the sensitivity as well as accuracy in determining CD activity compared with either technique alone. These results suggest that DWI should be included in MRE protocols for CD evaluation in pediatric patients.

	Accuracy (%)	Sensitivity (%)	Specificity (%)
MRE	54/78: 69.2	18/32: 56.3	36/45: 80.0
DWI	50/78: 64.1	26/33: 76.5	24/45: 53.3
MRE + DWI	60/78: 76.9	40/45: 88.9	20/33: 60.6

Paper #: PA-010

Plain Radiograph Evaluation of Pediatric Constipation: A Critical Analysis

Fozail Alvi, MD, *Radiology, Geisinger Medical Center, Danville, PA, fialvi@geisinger.edu;* Faruq Mahmud

Purpose or Case Report: Chronic constipation continues to be one of the most common causes of angst for children, parents, and clinicians. Despite recent literature advocating limited intra-reader validity and poor diagnostic accuracy, it is still common practice to obtain plain radiographs of the abdomen in children with constipation to assess the extent and amount of stool burden. The purpose of this study is to find if there is any significant difference on plain radiographs between constipated and non-constipated children.

Methods & Materials: A large database of abdominal radiographs was obtained from our institution from children ranging from ages 3 to 12 years over a 12 month period (July 2010 to June of 2011). There were a total of 904 cases which were labeled as "constipated group", and a total of 812 cases which were labeled as "non-constipated group" based on provided clinical history. A total of 508 radiographs were then randomly selected from both groups and examined by an experienced pediatric radiologist. For the purpose of assessment and quantification of stool burden, criteria established in multiple prior studies was employed in dividing the colon into four segments.

Results: The results showed that the majority of the patients (231/255) with constipation fall into the middle categories (91%). Similarly, majority of the patients with no history of constipation fell into the middle categories (84%). No significant difference was noted between the two groups. Only at the two ends of our spectrum, that is no stool or large burden, was any significant difference noted between the constipated and non-constipated groups. Our study shows that mild or moderate or moderately large stool burden may be

prevalent equally in constipated and non-constipated children, and may be a sign of constipation or a normal finding. Only in children suspected to have a very large stool burden did abdomen radiography show justification. However, only a small percentage (4%) in our sample of constipated children belongs to this category.

Conclusions: We believe plain radiographs of the abdomen for diagnosis of constipation and assessment of stool burden are overdone and overused, and in majority of constipated children can be avoided. We believe constipation is a symptom and not a radiographic sign, and clinical assessment should take precedence over radiographs.

Paper #: PA-011

Prevalence of Subdural Collections in a Large Cohort of Pediatric Patients with Benign Enlargement of the Subarachnoid Spaces

Daniel Mazori, *NYU Langone Medical Center, New York, NY, daniel.mazori@med.nyu.edu;* Jennifer Vaughn, Nancy Fefferman, MD, Sarah Milla

Purpose or Case Report: Benign enlargement of the subarachnoid spaces (BESS) has been suggested to be a risk factor for incidental subdural collections. The proportion of pediatric patients with BESS who develop this complication is unknown. Our purpose was to calculate the prevalence of subdural collections in pediatric patients with BESS, and to compare the neuroimaging features and demographics of patients with and without subdural collections in this population.

Methods & Materials: We performed an IRB-approved retrospective review of all pediatric outpatients evaluated with sonography for macrocephaly and related indications at a private urban hospital over a 5-year period. Data were collected on patient age at presentation, sex, and indication for sonography. The following parameters were measured: sinocortical distance visualized on coronal images obtained with a high-resolution linear probe; size of the lateral ventricles at the frontal horns in the coronal plane; and width of the subdural collection when present. Furthermore, when a subdural collection was present, the patient's clinical history and follow-up imaging, when available, were reviewed. BESS was defined as a sinocortical distance of at least 4 mm.

Results: During the study period, 256 patients with macrocephaly met the inclusion criteria and 198 of them were found to have BESS. Of the patients with BESS, 7 (3.5%) had subdural collections. Four of these seven patients were evaluated by the child protection team. MRI in all four patients did not show additional findings concerning for child abuse. Skeletal surveys were performed in two patients and did not show abnormalities. Thus, child abuse was not suspected in any of the seven cases. Patients with BESS and subdural collections were younger (4.7 vs. 6.3 months), more commonly male (86% vs. 62%), and had significantly ($p<0.0001$) greater sinocortical distance (9.7±2.5 vs. 6.0±2.0 mm) and ventricular size (9.0±2.6 vs. 4.8±1.9 mm), compared to patients with BESS without subdural collections.

Conclusions: This study is the first to report the prevalence of subdural collections in pediatric patients with BESS, and to compare these patients with their counterparts who do not develop subdural collections. With a prevalence of 3.5%, subdural collections should be recognized as a known incidental finding in pediatric outpatients who are evaluated for macrocephaly and found to have BESS. This prevalence raises the question of how and whether these patients should be further imaged and evaluated for potential child abuse.

Paper #: PA-012

MRI Features of Spinal Subdural Hemorrhage in Abusive Head Trauma

Arabinda Choudhary, MD, MRCP, FRCR, *Hershey medical center, Hershey, PA, achoudhary@hmc.psu.edu;* Danielle Boal, Mark Dias

Purpose or Case Report: Spinal subdural hemorrhage in abusive head trauma (AHT) has been recently identified as an important finding in >60% of abusive head trauma. It is an important finding which is rarely seen in accidental trauma and therefore holds potential to become a cardinal feature of AHT. However not much is known about the distribution or appearance of spinal subdural hemorrhage. We also wanted to assess if spinal subdural hemorrhage can be seen in the absence of posterior fossa hemorrhage.

Methods & Materials: We identified all cases of AHT managed at our institute between 2001–2012 who also had spinal subdural hemorrhage identified on MRI. We reviewed the age, gender, MRI brain and spine for the distribution and appearance of subdural hemorrhage on T1 and T2 sequences.

Results: We had 29 AHT cases with spinal subdural hemorrhage identified on MRI. There were 19 males and 10 females. The age ranged from 1 to 59 months with a median age of 5 months. In 18/29 cases the entire spine was imaged. In 11/29 cases only the cervical spine was imaged with some visualization of upper thoracic spine on some of these studies. The proximal extent of hemorrhage varied from C1-T10. 14/29 cases had hemorrhage extending from the cervical spine region with 10/29 cases starting from C1. So if only the cervical spine is imaged in these cases we will miss the hemorrhage in 15/29. In cases where the entire spine was imaged the lower extent of the hemorrhage extended to the lower extent of the thecal sac in 15/18 cases. The spinal subdural hemorrhage was T1 bright in 26/29 cases with three cases being isointense to the spinal cord. The appearance of spinal subdural on T2 was

predominantly hyperintense in 12/29 cases, hypointense in 15/29 cases. 2/29 cases had no T2 imaging available to review. All the cases also had posterior fossa hemorrhage.

Conclusions: 1. If only the cervical spine is imaged in AHT, we will miss spinal subdural hemorrhage in 15/29 (51%) of cases.
2. All the cases had posterior fossa hemorrhage.
3. So complete evaluation of spine is recommended in AHT with posterior fossa hemorrhage.
4. Spinal subdural was predominantly T1 hyperintense in 26/29 (89%). However this may reflect the fact that T1 bright subdural hemorrhage is easier to identify and we are probably missing isointense or hypointense spinal subdural hemorrhage.
5. The spinal subdural hemorrhage was predominantly T2 hypointnese 15/29 (51%) likely reflecting the early subacute nature of the hemorrhage.

Paper #: PA-013

Time Resolved Steady State Free Precession MRI of the Cranio-Cervical Junction

Kenneth Martin, MD, *Diagnostic Imaging, Children's Hospital and Research Center Oakland, Oakland, CA;* Taylor Chung, MD

Purpose or Case Report: Ordinary two and three dimensional MR imaging techniques suffer from motion artifacts. In certain circumstances, it is desirable to minimize motion artifact or accurately depict objects in motion. It is possible to cardiac gate MRI sequences and create movies of objects whose motion is coupled to the cardiac cycle. This method was used to diagnose a mobile obstructive membrane which was causing symptomatic cervico-thoracic syringohydromyelia. All other MR imaging sequences attempted failed to accurately establish the correct diagnosis.

Methods & Materials: Philips Intera 1.5 T, Best, Netherlands. Multi-slice and single-slice, cardiac gated, steady state free precession two dimensional imaging sequences (b-TFE) were modified from existing cardiac imaging protocols. FOV 200×150 mm, voxel 1×1.5×5 mm, 3 NSA, 20 cardiac gated partitions, TR 4.3, TE 2.1, imaging time 40 s. The single-slice method was subsequently improved to 1x1x2 mm resolution and thickness requiring 1 min 55 s.

Results: Both the multi-slice and single-slice methods performed well as written. Constrained by limitations of time, the single-slice method was designed to have superior spatial and temporal resolution to the multi-slice method. The localization of the single-slice image was based upon initial results from the multi-slice technique. A mobile web was identified obstructing the dorsal spinal canal which inverted and everted rhythmically with each cardiac cycle and its resulting cerebrospinal fluid pulsation. The motion of the web presumably prevented its detection due to both flow and blur artifacts. The addition of cardiac gating allowed for sufficient temporal resolution to "freeze" the mobile obstructive membrane, thus allowing for its recognition on both static and cinegraphic review. The presence of the web has been confirmed by direct visualization during surgery. This cine b-TFE method has subsequently been used to study a variety of conditions affecting the cranio-cervical junction.

Conclusions: Cardiac gated steady state free precession imaging techniques have been successfully adapted to imaging of the cranio-cervical junction. In our first application of this method, an accurate diagnosis was made possible by this sequence alone. How this time resolved imaging technique might aid in understanding and diagnosing pathology elsewhere in the central nervous system remains to be investi-gated.

Paper #: PA-014

Magnetic Resonance Imaging of the Cervical Spine in Non-Accidental Trauma: A Tertiary Institution Experience

Roy Jacob, MD, *Children's Medical center, Dallas, TX, Roy.Jacob@utsouthwestern.edu;* Bradley Weprin, Matthew Cox, Korgun Koral, Timothy Booth, MD

Purpose or Case Report: To examine the incidence and spectrum of cervical ligamentous and spinal cord injury (SCI) diagnosed by MR in children in the setting of non-accidental trauma (NAT).

Methods & Materials: Using a trauma service clinical data base, a retrospective review of medical records of children diagnosed with NAT in a tertiary referral pediatric hospital for the last 10 years was performed. Children less than 5 years of age with a diagnosis of NAT and had MR of cervical spine performed within 1 week of presentation were included in the study. CT of the brain, cervical X-ray and skeletal survey were also evaluated to identify any predictors for spinal injuries. CT head was evaluated for subdural hematoma (SDH) and parenchymal injury. MR evaluation included the presence or absence of cord, ligamentous, joint capsule, hemorrhage and osseous injury. MR sequences for cervical spine imaging included: Sagittal T1, STIR; Axial T2 and GRE sequences. The images were reviewed by two experienced Pediatric Neuroradiologists by consensus evaluation.

Results: Twenty-eight patients with NAT who had imaging of the cervical spine satisfied inclusion criteria. The mean age at imaging was 10 months, M: F ratio=0.86:1. MR demonstrated findings suggestive of cervical spine injury (CSI) in 64% including; osseous injury in 3.5%, ligamentous injury in 57%, capsule injury at occiput-cervical junction in 43% and cord injury in 17%. The partially imaged thoracic spine showed injury in 11%.

CT head showed SDH in 82%, focal parenchymal injury in 21% and global injury in 36% and skull fractures in 32%. 87% of children with parenchymal injury (focal and global) had cervical injury. 55% of children with skull fractures and 68% without skull fractures had spinal injury. C spine X-rays were normal in all patients; however were suboptimal in 21%. Skeletal survey showed high specificity fractures in 39% and no fractures in 39%.

Conclusions: Children evaluated with cervical MR for NAT have a high incidence of CSI. Ligamentous injury was most common with the interspinous ligaments most commonly involved. The presence of which may suggest a hyperflexion mechanism in this population. Children with CT evidence of parenchymal injury have an increased incidence of CSI diagnosed using MR. MR may be helpful in diagnosing clinically unsuspected CSI, especially in the presence of parenchymal injury. C spine radiographs are commonly sub optimal and have low sensitivity in evaluating children with NAT for CSI.

Paper #: PA-015

Cervical Spine MRI and Polysomnography Correlation in Pediatric Patients with Achondroplasia

Shawn Parnell, MD, *Seattle Children's Hospital, Dept. of Radiology, Seattle, WA, shawn.parnell@seattleChildren's.org;* Klane White, Yemiserach Kifle, Marcella Blackledge, Viviana Bompadre

Purpose or Case Report: Children with achondroplasia have a small foramen magnum, midface hypoplasia, frontal bossing, spinal stenosis, and rhizomelia. Central sleep apnea, with potential resultant sudden death, is thought to be related to compression of the spinal cord at the cervicomedullary junction in these patients. Screening polysomnography and cervical spine MRI are performed for infants with achondroplasia at many institutions. Decompressive suboccipital craniectomy has been performed in selected cases. We aim to better delineate the relationship between polysomnography and cervical spine MRI in achondroplasia.

Methods & Materials: Retrospective review of all children with achondroplasia in our IRB-approved skeletal dysplasia registry who had received at least one screening polysomnography and one cervical spine MRI examination. Electronic medical records were reviewed. Spearman correlations of polysomnography and MRI parameters were performed.

Results: Twenty-five patients with both polysomnography and an MRI of the cervical spine were identified. Six patients were excluded due to inadequate sleep study or MRI data. The average age was 5.5 years, including ten patients under 1 year of age. An abnormal apnea -hypopnea index was found in 18/19 patients, with central sleep apnea found in 4/19 (all four were under 18 months of age). One of these four had mild cord compression, and none required surgical decompression. Four other patients required foramen magnum decompression, all demonstrating significant cord compression on MRI, two demonstrating cord signal change on T2 sequences, and one demonstrating the presence of a syrinx. None of these four demonstrated central sleep apnea. Counter intuitively, obstructive sleep apnea was associated with greater foramen magnum diameter (r=0.81) and anterior CSF space (r=0.62). Overall apnea-hypopnea index was negatively correlated with the presence of abnormal T2 cord signal change on MRI. We found no statistically significant correlation between central sleep apnea and abnormal MRI findings suggestive of foramen magnum stenosis.

Conclusions: Sleep disordered breathing is common in pediatric patients with achondroplasia and can include both obstructive and central sleep apnea. Screening polysomnography is an important tool but does not appear to correlate with MRI findings of foramen magnum stenosis. Cord compression, with either associated T2 cord signal abnormality or clinical findings of clonus, was most common in those receiving subsequent surgical decompression.

Paper #: PA-016

Pitfalls in Susceptibility Weighted Imaging (SWI) of the Pediatric brain

Thangamadhan Bosemani, MD, *Division of Pediatric Radiology, Johns Hopkins University- School of Medicine, Baltimore, MD, tbosema1@jhmi.edu;* Sylvia Verschuuren, Andrea Poretti, Thierry A.G.M. Huisman

Purpose or Case Report: Susceptibility weighted imaging (SWI) is a recently developed 3D gradient echo MRI technique which accentuates the magnetic properties of various substances such as blood, blood products, non-heme iron, and calcifications. Based on these properties, SWI has proven to be useful in the evaluation of several pediatric neurological disorders such as vascular malformations, hemorrhage, and traumatic brain injury. For every new technique, it is important to know not only the indication and advantages, but also possible pitfalls which may lead to a wrong diagnosis. We present various potentially misleading pitfalls, with discussion of several cases.

Methods & Materials: Our protocol includes an axial dataset of a magnitude image, filtered phase map, combined SWI processed image and a minimum intensity projection (mIP) of the processed image. We reviewed our pediatric MRI database searching for SWI studies with possible pitfalls. For the pitfall cases, we present the SWI images, discuss the initial diagnosis and the factors leading to the initial wrong evaluation, and also point out how to detect them.

Results: We were able to include up to six pitfall cases in this report. We classify the pitfall cases into four categories: 1) Dependency of the venous signal from blood oxygenation:

deoxygenated hemoglobin in veins is typically hypo intense on SWI imaging; however, the signal characteristics can vary from differing oxygen and carbon dioxide levels, and hence impede tissue characterization; 2) Dependency of the venous signal from the field strength: high field strength (3 T) improves significantly signal-noise and has also the potential for signal drop-outs accentuated due to air tissue geometry adjacent to bony surfaces; 3) Postprocessing misregistration: SWI processed mIP images are invaluable in demonstrating the vessel or venous channel connectivity over a number of sections, however with the distinct possibility of misregistration depending on the thickness of the reconstructed mIP images, causing false representations of lesions, particularly in neonates; 4) Mimickers: the presence of true findings, i.e., presence of gas, blood or calcium in local tissue can be a mimic of other findings or behave as pseudo lesions.

Conclusions: SWI has facilitated the diagnosis of various pediatric neurological disorders and is increasingly used in pediatric neuroradiology. The illustration of these potential diagnostic pitfalls in SWI should provide further familiarity to this technique and prevent misdiagnosis.

Paper #: PA-017

Angulated Scan Plane Modification for Faster Acquisition of Multiple Nonadjacent Gray and White Matter Spectroscopy Voxels

Jeffrey Miller, MD, *Radiology, Phoenix Children's Hospital, Phoenix, AZ, jhmiller@phoenixChildren's.com;* Amber Pokorney, Padmaja Naidu

Purpose or Case Report: To validate angulated scan plane modification of standard 3D MR multivoxel spectroscopy imaging in patients requiring multiple nonadjacent regions of interest. Comparison of the imaging time of the angulated scan plan technique compared to single gray and white matter voxels acquisition

Methods & Materials: Twenty patients undergoing MR spectroscopy were included. Ten were evaluated for neonatal encephalopathy, five for developmental delay and five for metabolic disease. Standard protocol multiple single voxel intermediate TE was performed at 3 T for each patient. Single voxels were placed unilaterally within the basal ganglia and the posterior white matter several slices cranially at or above the centrum semiovale. Each patient also underwent 3D multivoxel spectroscopy. A fast single shot TSE planning sequence was initially performed with an approximately 20° declined plane of scanning compared to standard canthomeatal orientation. The plane of the slab included the basal ganglia and the posterior cerebral white matter at or just above the centrum semi ovale. Following the multivoxel acquisition, spectra from voxels located within the same regions as the single voxel scan were selected. The spectrums from the single voxel technique were compared to the spectrums from the correlating voxels chosen from the 3D spectroscopy. Two neuroradiologists reviewed each patient's two sets of spectroscopy data. For each patient, the single and multivoxel techniques were classified as equivalent if the major peak ratios (choline, creatine and NAA) and lactate presence or absence were similar between each technique. Any patient with variable major peak ratios or variable lactate peak presence or absence was classified as not equivalent.

Results: The spectra from all patient's (20/20) single and multivoxel spectroscopic acquisitions were equivalent by the independent review of two neuroradiologists. Lactate peaks seen in five patients (8 total peaks) were equivalent using both techniques. The average scan time of each single voxel acquisition was approximately 5 min (10 min/patient). The average scan time for each patient's single multivoxel acquisition was 4 min.

Conclusions: In patients requiring evaluation of multiple nonadjacent regions of interest, the performance of 3D multivoxel spectroscopy, with the above described simple declined angulation scan plane modification, yielded equivalent results (20/20) in less total scan time (4 vs 10 min) as compared to multiple single voxel technique.

Paper #: PA-018

Pediatric Brain DWI with Dual-echo Echo Planar Imaging (EPI)

Kristen Yeom, MD, *Stanford University, Palo Alto, CA, kyeom@stanford.edu;* Stefan Skare, Roland Bammer, Samantha Holdsworth

Purpose or Case Report: We propose the use of a parallel-imaging enhanced dual-echo DWI technique as an alternative approach to conventional DWI in evaluating ischemic injury in pediatric brain.

Methods & Materials: We devised a parallel-imaging-enhanced dual echo DWI sequence consisting of two EPI trajectories (or Echoes) for one diffusion-preparation period. Echo 1 and Echo 2 were acquired at echo times (TE) of 46 ms/79 ms, respectively - both with an acceleration factor, R=3. ADC maps were computed for both echoes. Another set of Echo 1 and 2 images were computed by estimating and removing the signal intensity variation (coil sensitivity and proton density) using the echoes themselves. Data were acquired on a 4 day old infant presenting with embolic infarcts using a 1.5 T GE scanner and an 8-channel head coil. The routine vendor-supplied DWI was acquired as a reference (equivalent imaging parameters but with R=2, TE=70 ms).

Results: Both Echo 1 and Echo 2 DWIs presented higher image quality than the reference. Echo 2 had higher sensitivity to acute infarcts than Echo 1 (short arrows). The coil-sensitivity corrected Echo 2 image diminished bright artifacts in the

posterior brain regions (long arrow). Due to low SNR of Echo 2, Echo 1 was still important in creating high-fidelity ADC maps.

Conclusions: Dual-echo DWI may be a useful method for evaluating acute brain injury. Due to its longer TE, Echo 2 DWI exhibited superior sensitivity to brain lesions with reduced diffusion; Echo 1 provided high SNR ADC maps for specificity to acute injury. Furthermore, information from both echoes could be used to flatten-out the DWI echoes and thereby replace the need for additional coil calibration scan.

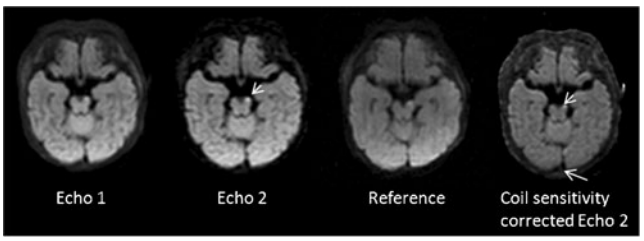

Paper #: PA-019

Initial experience and potential indications for blood pool MRI contrast agents in pediatric patients

Jane Kim, MD, Anand Patel, Jesse Courtier, MD, **John MacKenzie, MD,** *Department of Radiology, UCSF Medical Center, San Francisco, CA, john.mackenzie@ucsf.edu*

Purpose or Case Report: Blood pool (BP) MRI contrast agents are a relatively new and promising option in the imaging assessment of pediatric disease, but currently, the experience and published/recognized indications for the use of these agents are limited in the pediatric population. We review the imaging technique, advantages/disadvantages, and provide examples of cases where BP contrast MR imaging may provide new options for pediatric disease detection and monitoring.

Methods & Materials: We retrospectively reviewed all MRI studies performed at our institution in children (0–18 years-old) using Gadofoveset Trisodium (Ablavar) over the past 12 months. The patient demographic and clinical history, indication for the examination, MRI technique, and imaging findings as they pertained to dynamic MR angiographic (MRA) and BP imaging were recorded. Two pediatric radiologists assessed image quality (rated as 1=poor, 2=adequate, 3=excellent) and diagnostic confidence (1=low, 2=moderate, 3=high) for depicting blood vessels and disease.

Results: The most common indication for utilization of BP contrast agent in our population was for pediatric venography (n=9 of 22). Other indications included evaluation of liver vessel patency/anatomy (n=7), vasculitis (n=2), acute gastrointestinal bleeding (n=2), evaluation of vascular supply of an intra-abdominal mass (n=1), and evaluation for refractory hypertension (n=1). Image quality and diagnostic confidence were higher for extremity (3.00 ±0.00 and 3.00 ±0.00, respectively) vs. chest/abdominal imaging (1.70 ±0.68 and 1.80 ±0.71, respectively). Factors that led to low image quality/diagnostic confidence included respiratory and cardiac motion and a selection bias towards patients who were deemed a priori to be less likely to provide good early arterial/portal imaging e.g. difficulty holding still or non-sedated, and might benefit from added information obtained on delayed BP imaging.

Conclusions: Blood pool MRI contrast agents can be extremely useful in pediatric imaging for certain indications, particularly when a large area of venous anatomy must be covered at high resolution. Knowledge of the advantages and disadvantages and optimization of technique are fundamental to performing a diagnostic examination with excellent image quality that provides a high degree of diagnostic confidence.

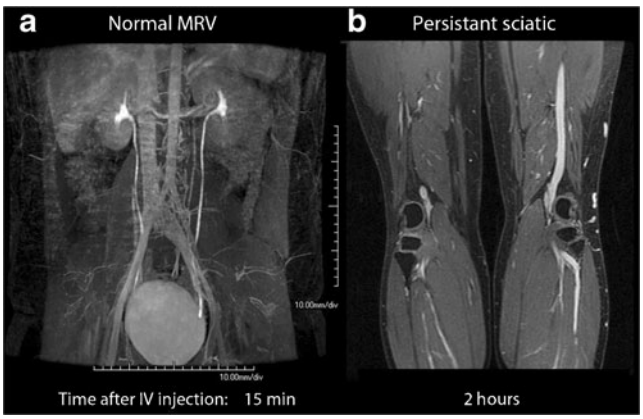

Paper #: PA-020

Bannayan Riley Ruvalcaba syndrome and the gamut of while matter abnormalities with cysts

Ravi Bhargava, *Radiology, Stollery Children's Hospital / University of Alberta, Edmonton, AB, Canada;* Kong Au-Yong, J-Stephen Bamforth, Norma Leonard

Purpose or Case Report: Bannayan Riley Ruvalcaba syndrome (BRRS), is a congenital disorder characterized by macrocephaly, intestinal hamartomatous polyposis, lipomas, and pigmented macules of the glans penis. The purpose of this study was to review the brain MRI findings in BRRS as well as to compare and contrast the findings with other brain disorders that also have brain cysts associated with white matter lesions.

Methods & Materials: The genetic disorder database at our children's hospital was searched for all cases of BRRS diagnosed since 1994. All available MR imaging studies were reviewed in patients with a diagnosis of BRRS, and representative images are provided with a description of the findings.

Results: Since 1994, nine patients (all males) have been diagnosed with BRRS at our institution, including seven evaluated with brain MRI. The average age of the patients at the time of

MRI was 3.7 years (8 months–7 years). PTEN analysis was performed in six of the seven patients. Two had the PTEN mutation, two had absence of the PTEN protein with molecular status unknown indicating an abnormality of PTEN, two had no detectable PTEN mutation and their protein status is unknown, and one has not been tested for molecular status or protein status. The imaging findings include CSF signal intensity white matter cysts in the parietal lobe (7/7), frontal lobe (2/7), and temporal lobe (1/7). These were associated with white matter T2 hyperintensities predominantly around the cysts (7/7) and macrocephaly (6/7). Additional findings in one patient included a cavum velum interpositum arachnoid cyst. A review of the literature indicates that white matter brain cysts are seen with Soto's syndrome, Lowe's syndrome, Mucopolysaccharidosis, and Van der Knaap syndrome. Ancillary imaging findings allow for diagnosis of these condition. The imaging findings are also distinct from the other PTEN mutation syndromes; Cowden syndrome, Proteus syndrome, and Proteus-like syndrome.

Conclusions: Although a rare syndrome, the cystic lesions seen on brain imaging findings in BRRS are quite prevalent. Knowledge of the differential diagnosis of brain cystic lesions in the setting of a white matter disorder and some of the distinguishing features can allow the radiologist to suggest a diagnosis of BRRS on brain MRI.

Paper #: PA-021

Blood–brain barrier permeability in transgenic amyloid overproducing models: implications for Downs Syndrome

Eric Tanifum, *Radiology, Texas Children's Hospital, Houston, TX, eatanifu@texasChildren's.org;* Stephanie Fowler, Joanna Jankowsky, Zbigniew Starosolski, Yifeng Jiang, Ananth Annapragada, PhD

Purpose or Case Report: While the deposition of extracellular amyloid-β (Aβ) protein constitutes one of the neuropathological hallmarks of Alzheimer's disease (AD), it is rarely recognized that it is equally significant in Down's syndrome (DS). While there is much speculation about the source of toxicity from Aβ, a marked effect of Aβ deposition is compromise of the blood–brain barrier (BBB). Sequelae of this leak include microbleeds, spontaneous (recurrent) intracerebral hemorrhages, hemorrhagic strokes and dementia. Cerebral amyloid angiopathy CAA has been reported in DS patients as early as 30 years old and stroke as early as 15. In this study we use the TetO-APPsw/ind transgenic mouse line as a model for Aβ pathologies in DS, and evaluate the extent of BBB compromise using a nanoparticle blood pool CT contrast agent.

Methods & Materials: Six TetO-APPsw/ind animals and six non-transgenic sibling controls were injected with a rhodamine labeled iodinated liposomal blood pool contrast agent and imaged up to 10 days post injection to allow for complete clearance of contrast within the blood pool. CT angiography was performed using a small animal micro-CT scanner with the following scan parameters: 70 kVp, 500 uA, 850 ms exposure, 1440 projections. Ultra-high resolution images at 19 um isotropic voxel size were reconstructed.

Results: Pre-contrast scans revealed extensive calcospheritic deposition in the amyloid positive mice. Acute phase post-contrast scans visualized the vasculature in exquisite detail, successfully visualizing vessels of 50 μ diameter. Segmentation of the major vessels in the Circle of Willis demonstrated that the amyloid positive mice had significantly narrower Circles of Willis, and reduced caliber and curvature of the right internal carotid artery. Delayed phase images showed extensive leak even in the major vessels of the Circle of Willis, and numerous locations throughout the cortex, both in association with blood vessels suggestive of hemorrhages due to CAA, and isolated points suggestive of bleeds around senile plaques.

Conclusions: These results represent the first report of a CT methodology with the ability to locate and quantify microbleeds and hemorrhages in a mouse model of amyloid deposition. The penetration of the BBB in this model represents a departure from the behavior of the normal BBB, implying that systemic drug and contrast agent use should consider the potential effects of significant extravasation in the brain.

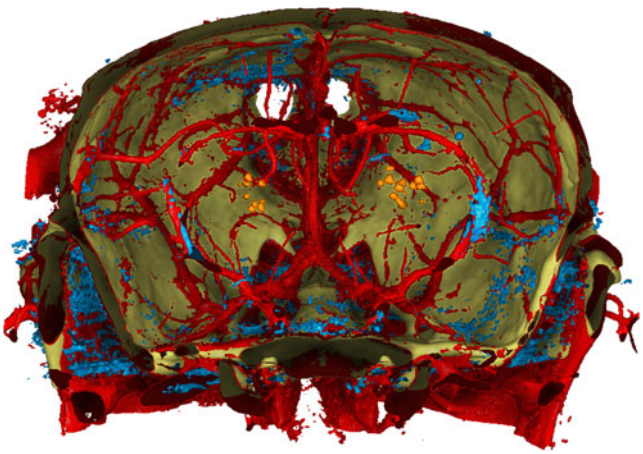

Figure 1. Axial view of amyloid positive mouse brain created by the overlay of three independent and co–registered CT scans. Contrast agent was a liposomal nanoparticle iodine. A precontrast scan visualized calcospheritic deposits (orange), an acute phase post–contrast scan visualized the blood vessels (red) and a delayed phase scan visualized the vascular leak (blue) (Extracranial blue spots are most likely to be artifacts due to the proximity of bony structures). The skull has been windowed to grey for clarity. Note the proximity of leaks to blood vessels, but not to the calcospheritic deposits.

Disclosure: Dr. Annapragada has indicated a relationship with Marval Biosciences as a Scientific Advisor and Stock Owner.

Paper #: PA-022

Size and Flow Characteristics of Internal Jugular Veins (IJV) vs Subclavian Veins (SCV) in Infants

Maricarmen Nazario, *Dept of Radiology, Children's Hospital of Philadelphia, Philadelphia, PA, nazariom@email.chop.edu;* Marc Keller, MD, Matthew Harris, Kevin Whitehead, Mark Fogel

Purpose or Case Report: Long term central venous access is frequently used in pediatric care. The use of upper extremity PICC is popular among clinical providers; yet, it carries a substantial incidence of SCV thromboses creating morbidity and potential loss of future access via this route. Use of the right IJV as the access point shows less tendency to thrombose, but remains a less popular choice among clinicians despite an excellent success and safety record among interventional radiologists using it. We decided to study the size and flow properties of these vessels in infants to provide objective data about their characteristics.

Methods & Materials: We shared a research database that included 36 infants with functional single ventricles, stage 1 palliation, who were imaged under general endotracheal anesthesia on room air with ECG gated static axial SSFP thin section chest imaging and phase contrast imaging of their IJVs and superior vena cavas (SVC). The infants averaged 5.7 +/− 3.5 months old (range 3–24 months) and average BSA was 0.31+/− 0.035 m2 (range: 0.25–0.41 m2). We used the formula:

(SVC flow) − (RIJV flow + LIJV flow) = Bilateral SCV flow and we assumed the SCV flows would be equal.

Measurements of the anteroposterior (AP) vein diameters were made from the SSFP images for the SCVs and from the magnitude images for the IJVs.

Results: The RIJVs averaged 0.54 +/− 0.12 cm in AP diameter, and the LIJVs averaged 0.52 +/− 0.14 cm in AP diameter.

Both the RSCVs and the LSCVs averaged 0.27 +/− 0.030 cm in AP diameter.

Measured flows in the RIJVs averaged 0.22 +/− 0.010 L/min, while the LIJV flows averaged 0.21 +/− 0.011 L/min.

Calculated SCV flows using the formula above averaged 0.093 +/− 0.056 L/min.

Average flow ratio of RIJV/SCV was 2.4

Average diameter ratio of RIJV/RSCV was 2.0

Conclusions: We studied the systemic venous returns of high flow veins in a group of infants who need periodic staged acute care owing to their heart disease and typify those who need intermittent long term central venous access. The RIJV is not only a shorter and straighter route to the central venous circulation, but our data shows that in this group, its diameter is twice that of the RSCV and that the flow in the RIJV averages 2.4 times greater than in the RSCV. Our results suggest that the clinical use of PICCs tunneled via the RIJV should lead to fewer thrombotic complications than the use of upper extremity PICCs in infants.

Paper #: PA-023

What is the normal size of the abdominal aorta in children?

Shilpa Hegde, *Arkansas Children Hospital, Little Rock, AR, shilpavhegde@gmail.com;* S Bruce Greenberg

Purpose or Case Report: Normal values for abdominal aorta size are established in adults, but not for children. The diagnosis of abdominal aorta hypoplasia or aneurysm in children is subjective. Our purpose was to determine the normal abdominal aorta diameter size ranges for children.

Methods & Materials: Fifty-three intravenous contrast enhanced abdomen and pelvis computed tomography examinations performed on children ranging in age from newborn to 18 years of age (mean age 9.1 years, SD 5.2) were evaluated on a workstation. Children with vascular abnormalities were excluded from the study. Double oblique 1 mm multiplanar reformations were created perpendicular to the abdominal aorta at three levels: superior abdominal aorta (superior to celiac axis), mid-abdominal aorta (level of renal artery origins) and lower abdominal aorta (superior to aorta bifurcation). The mean of AP and lateral diameter measurements of the aorta were measured and the average of the two recorded as the aorta diameter. The body surface area for each patient was determined from height and weight measurements recorded at the time of computed tomography. Correlation and linear regression were utilized to relate body surface area to aorta diameter at each level. Linear regression equations and standard errors were determined.

Results: Correlation coefficient values between body surface area and aorta diameter at the three abdominal aorta levels were: upper abdomen r=0.9, mid-abdominal aorta r= 0.9 and lower abdominal aorta r=0.9. The results show strong correlation between body surface area and aorta diameter. Linear regression equations and standard error were calculated:

Superior abdominal aorta diameter (mm) = 5.1 (BSA) + 5.5 (SE 0.4)

Mid-abdominal aorta diameter (mm) = 4.9 (BSA) + 3.9 (SE 0.4)
Lower abdominal aorta diameter (mm) = 3.2 (BSA) + 2.7 (SE 0.4)
As an example of the utility of the equations, a graph representation of the superior abdominal aorta equation with accompanying lines showing the range of normal is included.
Conclusions: Our study has generated linear regression equations that allow radiologists to determine the normal range of abdominal aorta diameters in children. Hypoplasia or aneurysm of the abdominal aorta can now be objectively determined.

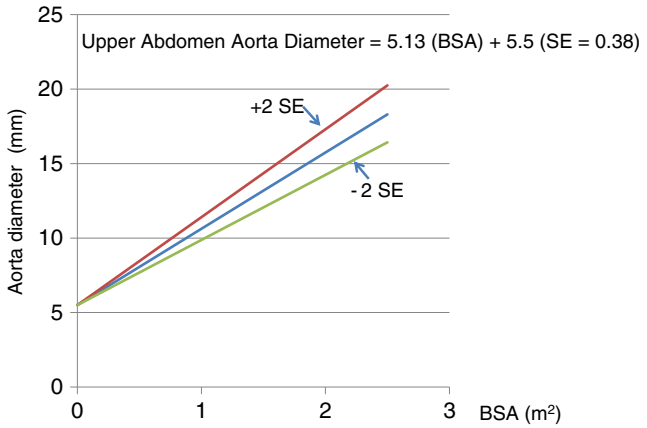

Paper #: PA-024

Distance Between the Carina and Cavoatrial Junction Normalized to Vertebral Body Height in Children.
Amer Alaref, *diagnostic imaging, Children hospital of eastern ontario, Ottawa, ON, Canada, ameraref@yahoo.com;* Juan Bass, Nishard Abdeen, MD
Purpose or Case Report: The goal of our study was to establish the true vertical distance between the carina and the inferior margin of the SVC (carina to cavoatrial junction distance CCD) in children, as a guide to accurate catheter placement. Radiographic landmarks (the junction of the right heart border and svc) are actually superior to the anatomic cavoatrial junction and may identify satisfactorily placed catheters as being in the right atrium. We hypothesized that the vertical distance between the carina and the true cavoatrial junction could be expressed in terms of vertebral body heights below the carina.
Methods & Materials: Contrast enhanced CT of the thorax in 18 children between the ages of 9 months and 14 years was reviewed. Age distribution was 0–1 years (n=5), 2–5 years (n=5), 5–10 years (n=4) and 10–14 years (n=4). Children with congenital heart disease or tracheal abnormalities were excluded. The distance between the inferior margin of the carina (coronal images) and the inferior border of the superior vena cava was measured on sagittal reformatted images. The cross reference line on our PACS system was used to indicate the level of the carina on the sagittal image.
The craniocaudal height of the T5 vertebra was chosen as a normalizing factor. This was measured from the superior endplate of T5 o the superior endplate of T6, on the coronal reformatted image through the center of the vertebra.
The normalized CCD was defined for each patient by dividing the CCD by the above vertebral height.
Results: Vertebral body heights ranged from 0.75 cm to 2.04 cm (mean 1.43 cm, SD 0.42 cm). The mean normalized CCD was 1.42 vertebral body heights (SD 0.34). The range was 0.85 to 1.98 vertebral body heights. A range of 0.8–1.8 vertebral body heights below the carina would include 17/18 or 94% of the patients.
Conclusions: The position of the anatomic cavoatrial junction varies between 0.8 and 1.8 vertebral body heights in the great majority of children. This criterion requires further validation with larger sample size, but may be a useful rule of thumb for acceptable central venous catheter tip positioning.

Paper #: PA-025

T2 Quantification of Normal Pediatric Myocardium
Marina Doliner, MD, *Ann & Robert H. Lurie Children's Hospital of Chicago, Chicago, IL, marina.doliner@gmail.com;* Cynthia Rigsby, Bruce Spottiswoode, Andrada Popescu, MD, Xiaoming Bi, Jie Deng
Purpose or Case Report: MRI is routinely being used for qualitative or semi-quantitative assessment of T2 myocardial signal intensity to assess for abnormalities including myocarditis, rejection in heart transplant patients, iron deposition, and infiltrative disorders. T2-weighted (T2W) fast-spin-echo sequences have suffered from problems including signal intensity variability, high subendocardial T2 signal from slow moving ventricular blood that mimics elevated T2 values, motion artifacts, and the subjective nature of qualitative T2W image interpretation. Recently, quantitative cardiac T2W techniques have been developed which may provide improved accuracy and reliability. However, normal T2 pediatric myocardial values have not been established. We aim to determine the normal T2 of pediatric myocardium.
Methods & Materials: Pediatric patients without underlying myocardial disease were scanned with a T2-prepared single shot steady-state free precession sequence yielding three basal, mid, and apical short axis images with T2 preparation times (TET2p) of 0, 24 and 55 ms. Pixel-by-

pixel T2 values were calculated by fitting the T2 signal decay equation: S=M0*exp(TET2p/T2) where S is the signal intensity at each TET2p and M0 is the equilibrium magnetization. The T2 values are displayed on color images (Figure 1). A region of interest (ROI) was manually drawn to include the LV midwall on each slice separately. T2 values within each ROI for each slice in each patient were averaged yielding the normal T2 value. T2 values between each individual slice in each patient and normal T2 values to T2 value in a patient with expected high T2 (clinically proven myocarditis) were compared using a two tailed, two-sample equal variance *t*-test. Relationship between age and T2 and heart rate and T2 was assessed using the Pearson correlation coefficient (r).

Results: Nineteen patients without myocardial disease (mean age 14.2 +/−5.2 years) underwent T2W imaging. Normal mean myocardial T2 was found to be 51.1±2.8 ms (range 47.0–56.3 ms). No significant difference in T2 values between slices was seen (all $p>0.6$). Weak negative correlation was found between age and T2 ($r=-0.23$) and weak positive correlation was found between heart rate and T2 ($r=0.27$). T2 in the patient with myocarditis was 62.6±3.2 ms showing a statistically significant difference from normal ($p<0.0001$).

Conclusions: Quantitative T2 mapping may address the problems associated with T2W cardiac imaging and offers potential for increased accuracy in detecting myocardial abnormalities.

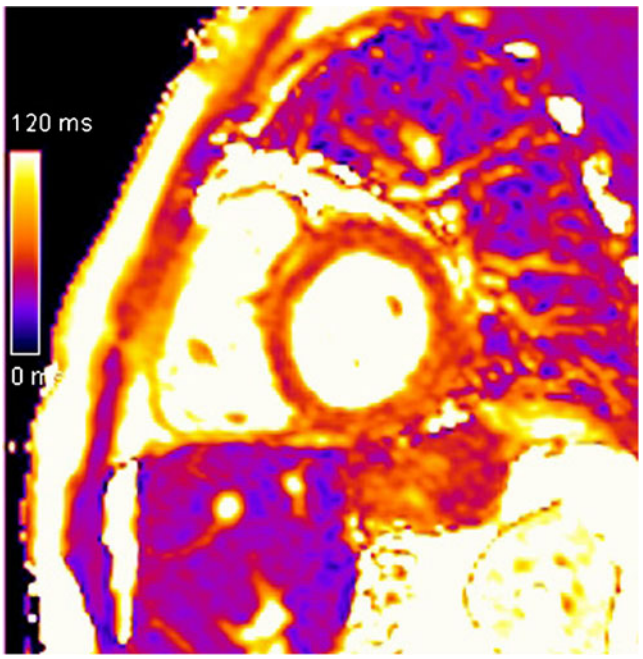

Paper #: PA-026

Renal Sonography with Doppler for Detecting Suspected Pediatric Renin-Mediated Hypertension – Is it Adequate?

Patricia Castelli, Jonathan Dillman, MD, David Kershaw, James Stanley, **Ethan Smith, MD,** *University of Michigan, Ann Arbor, MI, ethans@med.umich.edu*

Purpose or Case Report: Ultrasound is commonly used to evaluate for suspected vascular causes of hypertension in children although its diagnostic performance characteristics are unknown. The purpose of this study is to retrospectively assess the ability of renal Doppler sonography to detect vascular causes of hypertension in children with suspected aortic and/or renal artery narrowing.

Methods & Materials: Pediatric patients that underwent renal Doppler sonography for evaluation of hypertension between January 1995 and June 2010 were identified. Subjects without follow-up angiography [CT, MR, or catheter-based (IADSA)] were excluded. Ultrasound and angiographic imaging reports were retrospectively reviewed and findings were correlated. Secondary analyses were also performed analyzing the performance of renal sonography compared to only IADSA as the reference standard, as well as in patients with isolated renal artery stenosis and no aortic narrowing (using IADSA alone as well as using CTA, MRA, and/or IADSA as reference standards).

Results: Thirty-eight boys and 15 girls underwent renal Doppler sonography and subsequent angiography (mean age = 8.8 years). Twenty-four ultrasound examinations were negative, six were falsely negative, 16 were truly positive, and seven were falsely positive. Ultrasound had a sensitivity of 73% (95% CI, 50–89%), specificity of 77% (95% CI, 59–90%), positive predictive value of 70% (95% CI, 47–87%), and negative predictive value of 80% (95% CI, 61–92%). By secondary analysis using IADSA alone as the reference standard ($n=26$), ten renal sonography with Doppler examinations were truly positive, four were falsely positive, eight were truly negative, and four were falsely negative [sensitivity = 71% (95% CI, 42–92%); specificity = 67% (95% CI, 35–90%); positive predictive value = 71% (95% CI, 42–92); negative predictive value = 67% (95% CI, 35–90%)].

Conclusions: Renal Doppler sonography alone is inadequate for the evaluation of hypertensive pediatric patients with clinically suspected aortic or renal artery narrowing. In children with a high clinical suspicion for renin-mediated hypertension, angiographic imaging should be obtained regardless of the ultrasound findings.

Paper #: PA-027

Comparison of Free Breathing Respiratory Triggered Retrospectively Cardiac Gated Cine Steady-State Free Precession (RT-SSFP) with Breath-held SSFP in unsedated patients with congenital heart disease (CHD)

Lamya Atweh, MD, *Radiology, Texas Children's Hospital, Houston, TX, laatweh@texasChildren's.org;* Esben Vogelius, MD, Amol Pednekar, Wei Zhang, Raja Muthupillai, Rajesh Krishnamurthy, MD

Purpose or Case Report: Breath-held SSFP cine imaging (BH-SSFP) is the method of choice for the evaluation of ventricular function due to its superior blood-to-myocardial contrast, edge definition, and high intrinsic SNR. In this paper, we validate a free breathing respiratory triggered cine steady state free precession (RT-SSFP) sequence against the conventional breath held acquisition in unsedated patients with CHD.

Methods & Materials: After obtaining IRB approval, this prospective study was performed on 18 unsedated patients (age 23±14 years). Imaging was done on a commercial 1.5 T MR scanner (Achieva, Philips Healthcare). The cine SSFP sequence was modified to include respiratory triggering with the ability to have a user-prescribed minimum duration for start-up excitations before the cardiac gated acquisition. Identical imaging parameters were used for the BH-SSFP and RT-SSFP in the short-axis (SA) orientation covering both ventricles. Image quality scores (figure legend) and volumetric analysis was performed on the datasets by independent blinded users. One-sided Wilcoxon signed rank test was performed to compare the RT-SSFP clinical scores against BH-SSFP. Bland-Altman (BA) analysis was performed on LV and RV volumes.

Results: The clinical scores for RT-SSFP were consistently better than BH-SSFP except for the edge definition in unsedated patients (Table 1) who had irregular respiratory pattern. BA analysis (Table 2) for LV volumes indicates that variability between RT and BH acquisitions is comparable to inter and intra-observer variability reported in the literature [1]. In the unsedated population, ISA scores were significantly better for RT-SSFP than BH-SSFP. The BMC scores were identical, and EDef scores were not significantly different between RT-SSFP and BH-SSFP. Total score with equal weights to each clinical score category was significantly better for RT compared to BH. Total scan duration for SA stack using RT-SSFP (3.6±1.3 min) was slightly shorter than BH-SSFP (4.4±1 min) acquisitions as time for breath holding instructions was eliminated.

Conclusions: Releasing the constraint of breath holding for cardiac gated cine SSFP imaging allows clinically diagnostic images in unsedated patients without any penalty for contrast, spatio-temporal resolution, or total scan time. RT-SSFP may overcome problems related to inter-slice misalignment caused by inconsistency in the amplitude of breath-holding in young children.

References: 1. JMRI 28(39–50), 2008.

Table 1: RT vs. BH (n=18)

	BMC		EDef		ISA		Total Score	
	RT	BH	RT	BH	RT	BH	RT	BH
Mean	1.11	1.11	1.33	1.22	1.06	1.72	3.5	4.06
Median	1	1	1	1	1	2	3	4
P-value	0.5		0.375		0.0027		0.05	

Table 2: RT vs. BH (n=18)

	LV			RV		
	EDV ml	ESV ml	EF %	EDV ml	ESV ml	EF %
Bias	−1.7	2.1	−1.8	−0.5	2.3	−0.8
Limit of Agreement	14.7	12.6	8.5	28	20.9	9.6

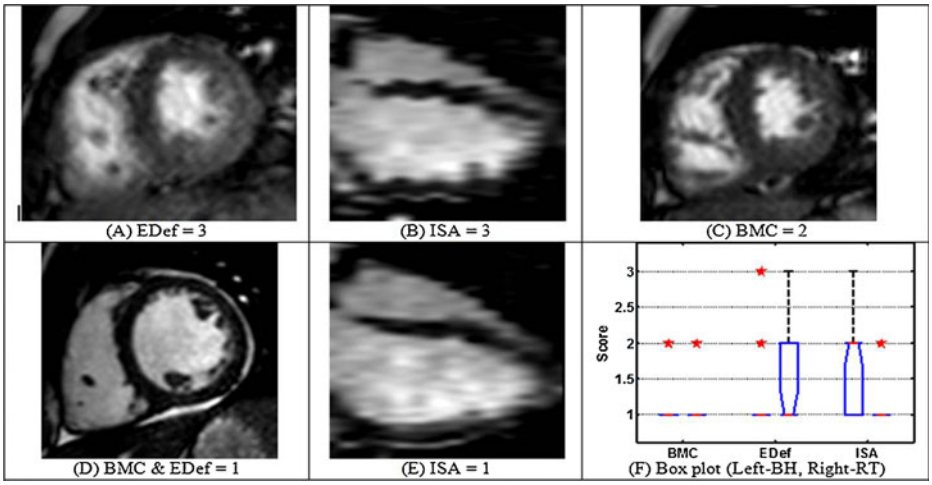

Figure 1: (A-E) Representative images for the clinical scores. The clinical scoring system was as follows: A. Blood-myocardial contrast (BMC): 1-like SSFP, 2-like turbo GRE, 3-worse than turbo GRE; B. Endocardial edge definition (EDef): 1-excellent, 2-good, 3-poor; C. Inter-slice Alignment (ISA): 1-Excellent alignment, 2- <2 slices misaligned, 3- >2 slices misaligned. BMC score reflects quality of the steady state, and EDef score indicates intra-slice motion blurring. ISA was determined by visualizing the SA stack as a volume. (F) Box plot for clinical scores depicts spread of the scores.

Paper #: PA-028

Volumetric Time Resolved Low Dose Renal CT Angiography (CTA) with Image Domain 3D Workstation Iterative Reconstruction: Initial Technical and Clinical Experience

Jeffrey Hellinger, MD, *New York Cardiovascular Institute, New York City, NY, jeffrey.hellinger@yahoo.com;* Blerim Arifi, Faton Bytyci, Zain Kassam, Gazmend Nura

Purpose or Case Report: Catheter angiography remains the "gold standard" for diagnostic evaluation of renovascular disease in pediatric patients for its ability to reliably generate high resolution arterial images to the intraparenchymal fifth order branches, while assessing global renal perfusion and regional flow. Low dose CTA has been shown to be a valuable alternative diagnostic modality in select patients. One limitation with renal CTA is the ability to resolve peripheral intraparenchymal renal arteries (IPRA) consistently with accurate detail. This is often related to early parenchymal and venous enhancement. We present our initial experience with low dose time resolved (TR) volumetric renal CTA, whereby individual arterial phases can be interrogated and multiple phases are evaluated in CINE mode to evaluate dynamic flow and perfusion.

Methods & Materials: To date we have performed 10 (5 male, 3 female; average 9 years old, 35 kg) TR renal CTAs for the evaluation of suspected or known renovascular hypertension. All exams were performed on a 320 multidetector-row CT with acquisition of four stationary phases, a section thickness of 0.5 mm, overlap of 0.4 mm, and a voltage of 80 or 100 kV. Tube current (15–40mAs) varied by body weight. Contrast (350mgI/ml) was power-injected at a rate of 4–6 ml/sec depending upon the accessed vein and body weight. Image domain 3D workstation iterative reconstruction was selectively applied in all cases by the interpreter to reduce background noise. Technical visualization to the 5th order branches and dynamic flow was evaluated independently by two readers using a five point scale.

Results: Six of the exams were normal, while one demonstrated segmental IPRA stenosis, and three revealed ostial stenosis. In all exams, early arterial phases could be isolated to depict IPRAs to the 5th order (score 4.25). In the case of IPRA segmental stenosis, asymmetric decreased flow was identified by both readers. Other patients demonstrated symmetrical IPRA flow and enhancement of high image quality (score 4.5). Individual phases had an average exposure of 0.4 mSv, yielding a total average exposure of 1.6 mSv. In all exams, additional catheter angiography was not required.

Conclusions: Time resolved low dose renal CTA with 3D workstation iterative reconstruction is a promising novel volumetric CTA application. Continued evaluation is required to further assess its utility and clinical performance as well as its impact on invasive catheter angiography in pediatric patients.

Paper #: PA-029

CT Angiographic Imaging of Complications Associated with Blalock-Taussig Shunts in Pediatric Patients

Prakash Masand, MD, *Pediatric Radiology, Texas Children's hospital, Houston, TX, drmasand@gmail.com;* Esben Vogelius, MD, Lamya Atweh, MD, Siddharth Jadhav, MD, Rajesh Krishnamurthy, MD

Purpose or Case Report: The modified Blalock Taussig shunt (BT shunt) is a graft placed between the subclavian and the ipsilateral pulmonary artery for palliative management of right heart obstruction in pulmonary stenosis or atresia, tricuspid atresia and hypoplastic ventricle as part of Stage 1 of Norwood procedure. The aim is to increase pulmonary blood flow and allow for growth of the pulmonary arteries while the pulmonary vascular resistance falls sufficiently for further repair. During this period the shunt is a lifeline for the child, and knowledge of shunt complications is essential since the patients present with sudden desaturations in the emergency setting.

Methods & Materials: After obtaining IRB approval we conducted a retrospective search of our database for patients imaged for potential complications related to BT shunts from 2010 to date. Fourteen pediatric patients ranging from 1 month to 3 years of age are included and CT angiographic data is reviewed in all. The complications associated with BT shunts include shunt stenosis, anastomotic narrowing, shunt thrombosis, occlusion, seroma around graft site, and left upper lobe bronchial compression in one patient. The iodinated contrast is injected via a lower extremity IV line with dose calculated at 1.5–2 ml/kg, and rate varying between 1.5 and 3.0 cc/sec. The contrast injection is followed by a saline bolus at the same rate. The scans are triggered using a Smart prep technique with timing based upon opacification of the descending thoracic aorta. The radiation doses varied between 1–3 mSv. Post processing is performed on a Vitrea workstation with generation of multiplanar reformats and volume rendered images.

Results: The cardiac CTA images delineated the complications in all our patients. These include shunt stenois (n=2), anastomotic narrowing (n=3), partial thrombosis (n=1), complete occlusion (n=5), stented BT shunt with occlusion (n=1), perigraft seroma (n=1), and left upper lobe bronchial compression (n=1). The patients were imaged with CTA after initial suspicion on transthoracic echocardiogram.

Conclusions: CTA is the modality of choice after initial echocardiographic evaluation when a BT shunt complication is suspected. The presence of stenosis, partial or complete thrombotic occlusion, anastomotic narrowing, stent occlusion, perigraft seroma,and bronchial compression were aptly depicted in all 14 patients.

Paper #: PA-030

Comparison of Differential Pulmonary Blood Flow (dPBF) Using First-pass Pulmonary Perfusion (FPP) and Phase Contrast Imaging (PCI) in Children with Repaired Tetralogy of Fallot (rTOF)

Rajesh Krishnamurthy, MD, *Radiology, Texas Children's Hospital, Houston, TX, rxkrishn@texasChildren's.org;* Wei Zhang, Shaine Morris, Shiraz Maskatia, Prakash Masand, David Chu

Purpose or Case Report: Branch pulmonary artery (BPA) stenosis is a common complication following TOF repair, and d-PBF measurement using PCI is an important part of the routine MR protocol for rTOF to determine the need for intervention. The accuracy of PCI for d-PBF is diminished in the setting of flow turbulence related to stenosis and regurgitation, or due to stents and coils. A FPP technique that can directly assess blood flow and regional perfusion at the parenchymal level will avoid the pitfalls, and is therefore desirable.

Methods & Materials: A FPP tchnique was developed with the following parameters: CEMRA sequence with 2×2 parallel imaging factor, 20% keyhole window, 3D coverage of lungs at 1.5–2 mm resolution, half-dose Gd, age-based power injection protocol, and temporal resolution of 0.8–1.5 s to obtain 20–30 time points over 20 s. Sixteen patients with repaired TOF were studied, four without BPA stenosis, four with mild BPA stenosis, and eight with moderate to severe BPA stenosis. PCI of the BPA was performed in all patients to assess d-PBF. FPP was followed by a high resolution diagnostic CEMRA using 1.5-dose Gd for morphologic assessment. FPP analysis comprised of qualitative and quantitative assessment of global and regional perfusion of the lungs

and differential PBF assessment using customized software. The RPA:LPA net flow ratio was calculated using FPP and PCI, and correlated using linear regression analysis.

Results: There was poor overall correlation between net flow ratio calculated by FPP and PCI (graph). Subset analysis revealed that there was good correlation of net flow ratio between the two techniques in patients with absent or mild BPA stenosis, and poor correlation in patients with moderate or severe stenosis. This is a preliminary analysis, with final results pending.

Conclusions: Preliminary results of a new technique for pediatric FPP in the setting of rTOF are described, offering an alternative means of assessment of dPBF and severity of BPA stenosis. There is poor correlation between dPBF assessments by FPP and PCI in the setting of moderate to severe BPA stenosis. This may be a result of PCI assessment being erroneous in the setting of severe turbulence related to stenosis and regurgitation. Since the FPP technique can directly assess blood flow and regional perfusion at the parenchymal level, it can avoid the pitfalls that affect PCI. Correlation of FPP results with nuclear perfusion scans and with pulmonary venous PCI may be helpful to clarify this finding.

Disclosure: Dr. Krishnamurthy has indicated a relationship with Philips MR as a Principal Investigator and Research Support; Vital Images, Scientific Advisory Board.

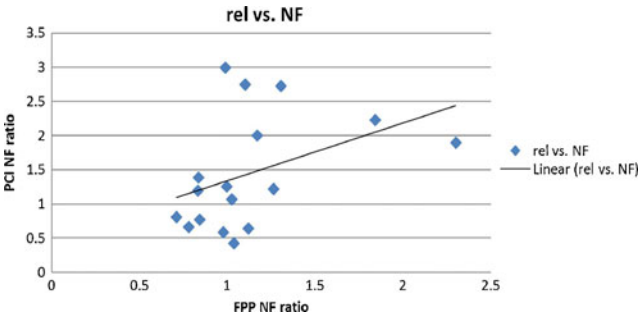

Paper #: PA-031

Dynamic Evaluation of the Ostium and Proximal Course of Anomalous Coronary Arteries by Retrospective EKG Gated CTA

Shashank Prasad, MBBS DMRD, *Pediatric Radiology, Texas Children's Hospital, Houston, TX, shashanksprasad@yahoo.com;* Esben Vogelius, MD, Carlos Mery, Prakash Masand, George Bisset, Rajesh Krishnamurthy, MD

Purpose or Case Report: Current imaging techniques, including echocardiography, CT, MRI or catheterization do not allow an accurate evaluation of the coronary ostium or an intramural segment. We describe a novel technique of reconstruction, which in conjunction with a new radiographic sign, may allow accurate diagnosis of the shape of the coronary ostium, and the length of the intramural segment. This could play an important role in defining the optimal management strategy for patients found incidentally to have anomalous coronary arteries by stratifying their risk of sudden cardiac death.

Methods & Materials: Patients with anomalous coronary arteries undergo retrospectively EKG-gated CT angiography as part of their clinical evaluation, with approximately 20–30 phases reconstructed across the cardiac cycle to provide dynamic information of the coronary arteries. An intermediate-dose dynamic volume technique is utilized along with adaptive iterative reconstruction with a maximal dose of 5 mSv. The data is loaded and studied on an independent 3D workstation and dynamic virtual endoscopic visualization of the coronary ostium is performed, allowing for recognition of the changes in ostial shape and caliber across the cardiac cycle. Segmentation of the pericoronary fat is utilized to distinguish intramural segment from the intra-mediastinal segment of the anomalous coronary artery. To date, four patients aged 8–16 years have been studied using this novel protocol.

Conclusions: We believe that this novel reconstruction protocol will provide important insights into the dynamic behavior of anomalous coronary arteries and guide the management of patients by a process of risk-stratification.

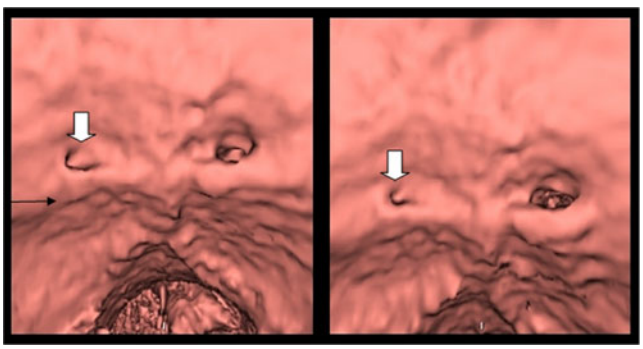

Virtual endoscopic reconstruction of the proximal aorta from above demonstrates a high origin of bilateral coronary arteries, just above the level of the sinotubular junction (horizontal arrow). There is a slit-like ostium (white arrow) of the right coronary artery (left image) which further narrows in systole (right image).

Paper #: PA-032

Non-cardiac vascular imaging with Gadofosveset trisodium, a blood pool contrast agent: Initial experience at a tertiary pediatric hospital

Roy Jacob, MD, *Children's Medical center, Dallas, TX, Roy.Jacob@utsouthwestern.edu;* Fara Naderi, Nancy Rollins, MD

Purpose or Case Report: 2D time of flight (TOF) MR venography (MRV) is traditionally used to delineate central venous anatomy but is time consuming, prone to motion artifacts, and provides no information about arterial structures. We report our initial experience with Gadofosveset trisodium (Ablavar) enhanced MRV in pediatric patients.

Methods & Materials: This was a retrospective review of 14 studies performed with Gadofosveset (0.03 mmol/kg) in children with normal renal function ages 9 months to 19 years. MR was acquired at 1.5 or 3 T using dynamic and steady state acquisitions with spoiled gradient 3D acquisition TR/TE: 2.9–3.7 msec/1.1–1.5 msec; Flip angle: 10–15°; Bandwidth: 200-850Hz/pixel; Voxel size varied from 1.0×2.0×2.0 mm to 1.5×1.5×3.0 mm; Matrix: 256×256 to 360×360 mm and a FOV of 200–420 mm. The dynamic acquisition provides arterial anatomy. Multi station imaging was performed when multiple regions were studied.

The dynamic phases of the sequences were evaluated for arterial findings; venous phases were reviewed for acquisition time and image quality and whether additional 2D-TOF sequences were requested by the radiologist. Image quality was graded with a five point system (1-Non diagnostic, 2-Poor quality; 3-Moderate; 4-Good and 5-excellent quality) based on sharpness of vessel border and blurring artifacts.

Results: Image quality was 4 or 5 for all studies; mean scan time was 10 min, in comparison to conventional MRV of central veins which requires 40–80 min of scan time. Three patients had post-contrast 2-D TOF MRV which did not change the initial interpretation. Findings included absent inferior vena cava, thrombus in internal jugular vein, portal vein thrombosis, aneurysmal dilation of internal jugular vein and an iliofemoral arteriovenous fistula. Arterial abnormalities included occluded iliac artery, aberrant subclavian artery and absent left hepatic artery. No patients experienced itching or vomiting related to the Ablavar.

Conclusions: Benefits of venous imaging with Gadofosveset are shorter imaging time, high quality studies, and ability to evaluate multiple territories using multi station imaging. Decreased scan times resulted in improved MR scanner utilization.

Paper #: PA-033

Improving the clinical history provided for radiographs

C Matthew Hawkins, MD, *Cincinnati Children's Hospital Medical Center, Cincinnati, OH, hawkcm@gmail.com;* Christopher Anton, Wendy Bankes, Michael Zeno, Rebecca Pryor, David Larson

Purpose or Case Report: The purpose of this quality initiative was to improve the consistency with which pediatric radiologists are provided with an adequate clinical history for radiographs obtained in the emergency department (ED) and outpatient settings.

Methods & Materials: Two pediatric staff radiologists and a radiology resident determined by consensus that criteria for an adequate clinical history accompanying outpatient and ED radiographs should be threefold: nature of the event or symptoms, duration of symptoms or date of event, and site of pain or abnormality, if applicable. This project was termed WHAT - WHEN - WHERE, based on these three elements. We asked our technologists to complete any incomplete histories provided by clinicians. A goal was established to achieve complete histories accompanying 95% of chest, abdomen, and extremity radiographs from the ED and outpatient settings. Interventions to improve performance included in-person educational sessions, weekly group performance reports (Figure 1), weekly learning points, and weekly individual performance feedback. These were facilitated by the development of an automated auditing and email notification system. Weekly audits of randomly selected clinical histories for 40 chest radiographs, 40 abdominal radiographs, and 120 extremity radiographs were performed throughout the change phase of the project (16 weeks).

Results: An initial audit revealed a baseline performance of 38% of adequate clinical histories. Performance gradually improved over the 16-week period, with 95% adequate histories by the end of the project (Figure 1). Improvement was most dramatic following the initial launch and following individual feedback of audit results.

Conclusions: With the help of radiography technologists, radiologists now receive an appropriate clinical history

95% of the time. To maintain these results, the automated auditing and feedback will be continued and performance has been incorporated into technologists' yearly evaluations, according to personal goals they have set.

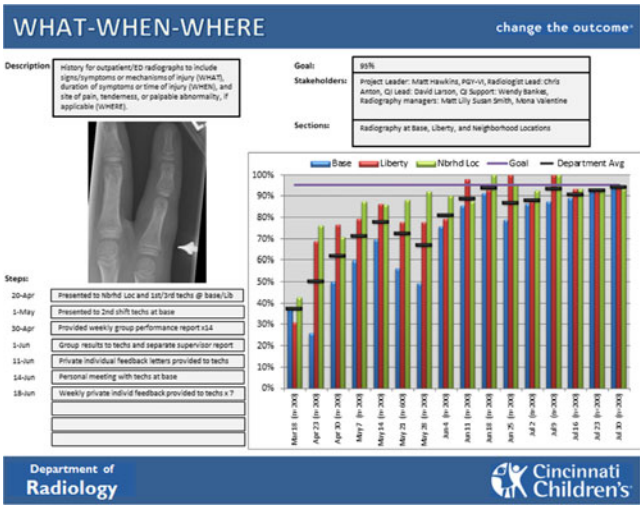

Paper #: PA-034

Updated ACGME Fellowship Requirements: A Guide to Constructing an Online Curriculum that Fulfills Educational and Documentation Requirements

Andrew Trout, *Cincinnati Children's Hospital Medical Center Department of Radiology, Cincinnati, OH, andrew.trout@cchmc.org;* Marilyn Goske, MD, Eric Crotty, Alexander Towbin, MD

Purpose or Case Report: Providing quality training while meeting ACGME documentation requirements is a challenge for residency and fellowship programs. We describe the development of a web-based resource that facilitates these tasks and can serve as a template for others developing online curricula.

Methods & Materials: An online training resource was created to deliver educational content organized according to the ACGME core competencies and to meet the documentation needs of our pediatric radiology fellowship. Resources already in place to address the practice based learning, communication skills and professionalism competencies were incorporated into the website with logging of these achievements through the institutional education management system (EMS). The medical knowledge component of the curriculum was divided into nine clinical subspecialties plus radiation safety and MR physics. Faculty from each subspecialty defined the learning objectives and provided related educational resources (articles, online lectures, books) for each topic. Website design and content were assessed with a survey of two classes of fellows. Website traffic was monitored using Google analytics.

Results: Goals and objectives for the fellowship in general and for each subspecialty rotation are provided with rotation specific educational milestones (basic, advanced) linked to specific and manageable learning resources (Figure 1). The integrated EMS allows documentation of duty hours, evaluations, scholarly activity, and completion of eight procedural competencies. Educational, journal club and quality improvement conference schedules are integrated into the website.

14 fellows reviewed the online resources. Using a 5-point Likert scale, 13/14 fellows rated the website as 4 or 5 at providing needed resources. All 14 fellows felt the medical knowledge materials were more manageable than a textbook and 13/14 were more likely to use the online resources than a textbook. Free text comments included: "clear and easy to use" (n=4), and "focuses learning" (n=3).

Between May 25 and September 30, 2012 there were 339 unique views of the main curriculum webpage with relatively steady traffic over time (mean 26 hits/wk, range: 5–63) with the bulk of traffic (62.5%) directed to the medical knowledge materials.

Conclusions: We describe the successful development of an online educational resource that provides a single site for organizing and documenting fellowship activities and ACGME requirements.Figure 1: Screen capture

from a representative medical knowledge page showing educational milestones (basic and Advance) and the related learning resources

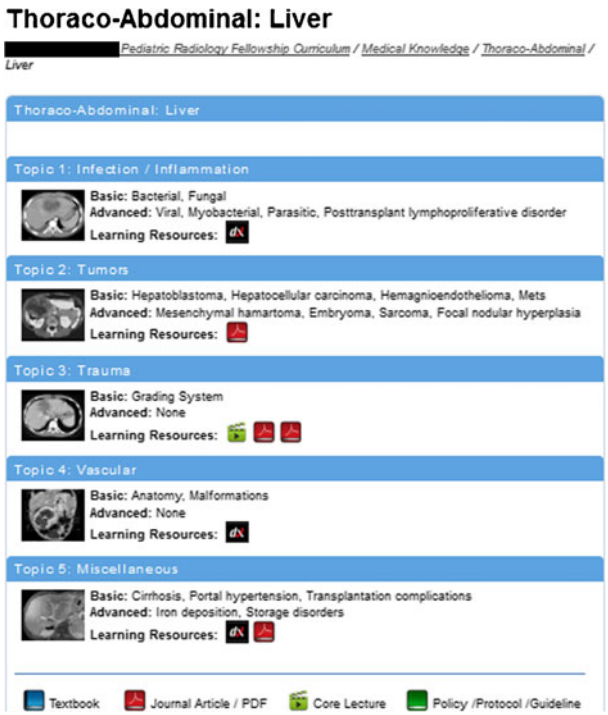

Paper #: PA-035

"Smart Sets": Decision Support for MRI Order Entry

John Strain, MD, *Children's Hospital Colorado, Greenwood Village, CO, John.Strain@Children'scolorado.org*

Purpose or Case Report: Radiology is well positioned to define, promote and optimize appropriate imaging. A Radiologist's review of orders for appropriateness based on indication can be time consuming, delays pre authorization and scheduling and is often met with resistance from providers. Pre authorization of incorrect orders wastes time and effort. Orders changed after authorization risks denial of payment. We sought to define a process by which indication driven order entry could assure consensus driven best practice based upon clinical indication and at the same time facilitate patient scheduling of MRI prior to patient discharge from clinic.

Methods & Materials: Multidisciplinary consensus was used to create nested indication driven order sets for common MR examinations requested by the department of orthopedics. These "Smart Sets" were embedded into the order entry window used by orthopedic providers in Epic. In practice the requesting provider was asked to tab through nested body parts and indications to derive the recommended MR order. For example: Selecting 1) Hand, 2) Infection, 3) Right from a series of nested choices would generate the order: "MRI Right Hand without and with Gd".

Orders generated by this process were accepted by a single click and would subsequently bypass the Radiologist order review queue for immediate scheduling.

Results: The "Smart Set" order entry process reduced the number of Orthopedic MRI orders requiring modification by 8%. Bypassing the order review queue eliminated the delay associated with Radiologists' review. Indication/Order compliance with most appropriate imaging eliminated waste related to authorization of inappropriate studies. Clinic personnel were able to schedule exams before the patient left the clinic. Following "Smart Set" implementation the only pre-authorized orders that required modification were those in which clarification of an unsuspected finding required an order change.

Conclusions: "Smart Set" indication driven order entry was well received when implemented in Orthopedics and Ophthalmology. The process worked easily into their current workflow. The process eliminated indication/order mismatch and allowed patient scheduling before the patient left the orthopedic clinic.

Paper #: PA-036

Improved Depiction of Vessel Anatomy with Model Based Versus Adaptive Statistical Iterative Reconstruction for Pediatric CT Angiography

Gonca Koc, MD, *Peds radiology, UCSF, San Francisco, CA, gonca.koc@ucsf.edu;* Jesse Courtier, MD, Andrew Phelps, John MacKenzie, MD

Purpose or Case Report: The purpose is to compare pure model based iterative reconstruction (MBIR) and hybrid adaptive statistical iterative reconstruction (ASIR) techniques for the depiction of vessels on pediatric CT examinations.

Methods & Materials: Fifteen patients (mean age 3.4 years [range 2 days to 13 years]; 5 girls; 10 boys) underwent enhanced MDCT examinations of the chest and abdomen (GE Healthcare - Discovery CT750 HD). Raw data were reconstructed with both MBIR and our current standard ASIR algorithm (soft tissue, 30% ASIR blended with 70% filtered back projection recon.) then maximum intensity projection images (3 mm sl thk, 2 mm sl interval) were created and subjectively evaluated by three blinded pediatric radiologists for vessel depiction, resolution of small anatomical structures, and qualitative image noise. Objective image noise as measured by assessing standard deviation (SD) for Hounsfield units (HU) from a region of interest (ROI) drawn in the descending thoracic aorta was evaluated by paired *t*-test. The number of branches and vessel lengths were measured for the apical segmental branch of the right upper lobe pulmonary artery (PA), right hepatic (HA), splenic (SA) and renal (RA) arteries and compared using Wilcoxon signed-rank test.

Results: On average the three readers preferred MBIR images in 89%, 75%, 95% of cases, for vessel definition, small structure resolution and noise, respectively. MBIR had significantly lower image noise in the aorta (mean SD of HU±SD=8.9±2.2) than ASIR images (11.4±5.2, $p<0.01$) while mean HU did not significantly differ ($p=0.16$). Vessel lengths were significantly increased in MBIR images vs. ASIR (mean lenghts± SD in mm for MBIR vs ASIR images: 32±11 vs. 29±11 [$p<0.001$], 31±16 vs. 29±16 [$p<0.008$], 20±4 vs.18 ±3 [$p<0.042$], 18±3, vs. 16±4 [$p<0.003$] for PA, HA, SA and RA, respectively). Although the number of small branches of HA, SA and RA were challenging to count due to obscuration by enhancement of the adjacent parenchyma, volume rendered images clearly showed better depiction of branch vessels (Figure 1). The numbers of branch vessels depicted in PAs were significantly different on MBIR (mean number of branch vessels ± SD=8.5±2) vs. ASIR (4.4±2, $p=0.004$).

Conclusions: Model based iterative reconstruction reconstructed images for pediatric CT angiography appear to provide a superior depiction of small vessels.

Fig-1:Renal artery volume rendering

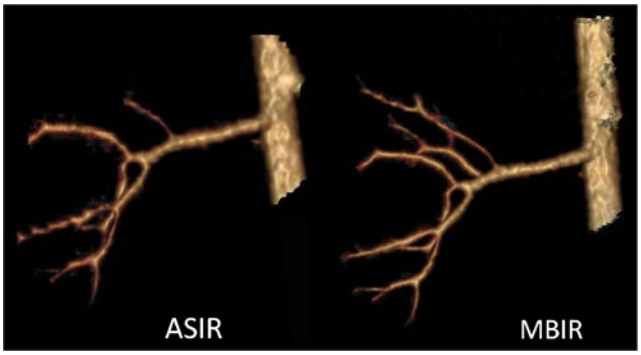

Vessel	**MBIR** mean ± SD (mm)	**ASIR** mean ± SD (mm)	**p value**
Pulmonary artery	32±11	29±11	<0.001
Hepatic artery	31±16	29±16	0.008
Splenic artery	20±4	18±3	0.042
Renal artery	18±3	16±4	0.003

Table: Vessel lengths for MBIR vs. ASIR.

Paper #: PA-037

Pediatric Epididymitis: Review of Clinical and Sonographic Features, and Differentiation from Intermittent Testicular Torsion

Becky Hwang, DO, *Texas Children's Hospital, Baylor College of Medicine, Houston, TX, bjhwang@texasChildren's.org;* Martha Munden, MD

Purpose or Case Report: Epididymitis is a less common cause of an acute scrotum in the pediatric population, with characteristic clinical and sonographic features. Differentiating epididymitis from intermittent testicular torsion (ITT) can be challenging due to overlapping features, such as an enlarged, hyperemic epididymis, as well as recurrent episodes of scrotal pain. Nevertheless, an accurate diagnosis is essential for appropriate management of patients medically or surgically. This retrospective review discusses the pathophysiology and sonographic appearance of pediatric epididymitis.

Methods & Materials: A retrospective search of the PACS data for pediatric patients with epididymitis diagnosed by ultrasound over a 1-year period was performed with IRB approval. Those with an obvious torsed appendage,

hematoma, or acute trauma were excluded. The sonographic findings, medical records for clinical presentation, surgical outcomes, and comorbidities relevant to epididymitis were reviewed.

Results: Twenty-four patients with an initial sonographic or clinical diagnosis of epididymitis were included. Twenty-one percent (n=5) were ultimately diagnosed with ITT; four were treated surgically. Of the 24 patients, 21% (n=5) had an appearance suggesting a pseudomass; of these 5, 60% (n=3) ended up with a diagnosis of ITT. Recurrent episodes were seen in 21% (n=5) of the 24 patients; only one of these five had a final diagnosis of epididymitis, and four were ultimately diagnosed with ITT. Two of the patients with repeat episodes had urological abnormalities (neurogenic bladder and urethral narrowing).

Conclusions: The characteristic sonographic features of acute epididymitis, an enlarged heterogeneous epididymis with increased vascular flow, are not specific for acute epididymitis. In our series of cases, 21% of patients initially diagnosed with epididymitis were ultimately diagnosed with ITT either by sonographic reevaluation or at surgery. Recurrent episodes, which can be seen with both entities, are more common with ITT in our series. The presence of a pseudomass strongly suggests ITT, but the vascularity within the cord should nevertheless be carefully scrutinized to identify twisting of the spermatic cord vasculature contributing to the pseudomass appearance. The presence of a straight yet hyperemic cord favors a diagnosis of epididymitis.

Paper #: PA-038

Hydrocele of the Spermatic Cord: Clinical Presentation, Sonographic Features and Outcomes

Lindsay Baron, MD, *Boston Children's Hospital, Boston, MA, lindsay.baron@Children's.harvard.edu;* Caleb Nelson, Judy Estroff, MD

Purpose or Case Report: Spermatic cord hydrocele is a sometimes-perplexing clinical entity that may be confused with other inguinal and scrotal conditions. We sought to define sonographic features of this condition, associated treatment and outcomes.

Methods & Materials: A retrospective review of medical records between 1999 and 2012 revealed 208 patients with a sonographic diagnosis of hydrocele of the spermatic cord. Forty-one of these patients did not have ultrasound images available at our institution and were excluded from consideration. Images and electronic medical records were reviewed. Imaging features, associated GU anomalies and patient management was recorded.

Results: Patients ranged in age from 3 weeks to 19 years. The most common patient presentation was scrotal/inguinal "bulge", "swelling", "mass" or "lump" (86%). Most hydroceles were right-sided (68%) and one case was bilateral. Most hydroceles were oval (49%) or tear-drop shaped (40%). Three hydroceles were thick-walled (1–2 mm) and 64 (38%) were complex, containing debris or septations. Cryptorchidism was seen in 6 (3.5%) patients: 1 bilateral, 4 ipsilateral, and 1 contralateral relative to the cord hydrocele. 15 (9%) patients had other genitourinary or systemic anomalies, including Beckwith-Wiedemann Syndrome, varicocele, hypospadias, and pelvic kidney. Ninety-six patients (57%) had surgery during the time between clinical presentation and our chart review, 85 (88.5%) of whom also underwent herniorrphaphy (78 (92%) ipsilateral to the cord hydrocele and 7 (8%) bilateral). 14 hydroceles (8%) resolved clinically and sonographically without treatment.

Conclusions: Hydrocele of the spermatic cord has a characteristic clinical presentation and sonographic appearance. There appears to be an association with ipsilateral inguinal hernia.

Paper #: PA-039

Morphologic and Functional MR Urography Features of Duplicated Renal Systems

Melkamu Adeb, MD, *Department of Radiology, The Children's Hospital of Philadelphia, Philadelphia, PA, melkdm @gmail.com;* Lesli LeCompte, Michael Carr, Dmitry Khrichenko, Kassa Darge, MD, PhD

Purpose or Case Report: To describe the morphological and functional findings of duplex renal systems in MR urography (MRU)

Methods & Materials: A retrospective review of the electronic medical records of 300 patients who had an MRU study from January 2006 to June 2010 was performed with institutional review board approval. All cases of duplex renal system were identified. Those with extravesical ectopic ureteral insertion were excluded from the study. A total of 28 patients were included in the study and a pediatric radiologist and fellow reviewed the MRU images in consensus. In those cases where consensus could not be reached the final decision was made together with a pediatric urologist. There were 16 female and 12 male patients with a mean age of 9.6 years (range,

0.5–19.2 year). Each moiety was evaluated separately for its morphology and function.

Results: There were 24 unilateral (Rt=11, Lt=13) and four bilateral duplex renal systems with a total of 64 moieties. Forty-two (65.6%) of the moieties had normal morphological features with normal functional results. The remaining 22 moieties (34.4%) had one or more pathologies including pelvicaliectasis, ureteropelvicaliectasis, and dysplastic moiety as shown in Table 1. The functional values for each moiety are also presented in the table for comparison. Eight patients had at least one urologic intervention prior to the MRU exam while 14 patients (50%) underwent urologic surgery for a primary abnormality noted on MRU.

Conclusions: MRU provides excellent anatomic detail for morphologic evaluation of duplex renal systems, including in cases of nonfunctioning or dysplastic moieties. The additional functional data obtained from fMRU is of importance in evaluating the contribution of each moiety to the total renal function.

Table 1: Morphological and functional parameters of upper and lower pole moieties in duplicated renal systems

			Upper pole moiety				Lower pole moiety			
			Normal n=23	UPJO† n=4	UVJO‡ n=4	Dysplstic n=7	Normal n=19	UPJO n=7	UVJO n=6	Dysplstic n=3
MORPHOLOGICAL FEATURES										
Grading of pelvicalyceal dilataion (1–5): median (range)*			1 (1–3)	3(2–5)	2(2–3)	1(0–3)	1 (1–2)	4 (3–5)	2(1–4)	3(3–5)
Mean intrarenal AP pelvic diameter (mm):			4.9	52.9	9.5	5.4	6.3	22.4	14.4	7.2
Corticomedullary Differentiation:	*Normal*		23	1	1	1	19	3	1	0
	Decreased		0	2	1	3	0	4	3	3
	Non-evaluable		0	1	2	3	0	0	3	0
Ureters	*Dilatation*		0	0	4	4	0	0	6	1
	Ureter visualization	*Precontrast*	23	3	4	7	19	6	6	3
		Early postcontrast	23	3	4	5	19	4	6	2
		Only on delayed	0	1	0	2	0	1	0	1
FUNCTIONAL PARAMETERS (mean)										
Calyceal Transit Time-CTT in sec			141.8	140	192	166.6	158.6	129	129.3	159.5
Renal Transit Time-RTT in sec			158.8	334	247	186.8	170.9	227	166.3	354.5
Time To Peak-TTP in sec			157.3	111	184	140.8	168.6	151.5	151.8	154.5
Volumetric Differential Renal Function-vDRF%			22.4	21.3	7.1	10.0	27.7	18.1	18.7	13.8
Patlak Differential Renal Function-PDRF%			30.1	29.6	23.2	26.0	25.2	35.8	33.7	35.6
Vol-Patlak Differential Renal Function-vpDRF%			18.8	19.4	6.6	9.2	23.0	19.5	17.9	14.7

*Pelvicaliceal dilatation grading based on Riccabona et al., † Ureteropelvic Junction Obstruction; ‡Ureterovesical junction obstruction

Paper #: PA-040

Optimizing Functional MR Urography (fMRU) Exam: Prime Time For A 30-Minute Or Less MRU

Jorge Delgado, *Radiology, Children's Hospital of Philadelphia, Philadelphia, PA, delgadoj@email.chop.edu;*
Melkamu Adeb, MD, Lesli LeCompte, Ann Johnson, Dmitry Khrichenko, Kassa Darge, MD, PhD

Purpose or Case Report: Current protocols for functional MR urography (fMRU) require long scan time. This limits widespread use in children. The aim of this study was to find ways to reduce the exam time without compromising the morphological and functional results.

Methods & Materials: A retrospective review of technical aspects of our fMRUs was carried out. The inclusion criterion was the presence of all our seven standard sequences: sagittal T2, axial T2 fs (high-resolution), coronal T1, coronal T2 fs, coronal 3D T2 fs, post-contrast T1fs dynamic (15 min) and sagittal 3D T1 fs. Each sequence was analyzed for its utility and factors that affect its duration.

Results: Eighty-one fMRU exams (m=31, f=50; mean age 8.3 years; pelivicaliectasis (PC) with/without ureterectasis), fulfilled the inclusion criterion. Mean exam durations were as

follows: 81/81 supine 64.5 min (40.5–173), 19/81 supine followed by prone 95.3 min (66–242), turning patient from supine to prone 10.5 min (6–17). Minimum actual scan time 36 min.
A] 3/8 sequences were categorized as essential as is:
1. sagittal T2: planning oblique coronal plane (100%).
2. axial T2 fs: grading of PC and measuring pelvic diameter (100%), best assessment of corticomedullary differentiation (22.2%=abnormal) and cortical thinning (43.2%=abnormal).
3. coronal 3D T2 fs: coronal plane of urinary tract plus 3D (100%) pre-contrast.
B] One sequence was categorized as essential but needs to be shortened: post-contrast T1 fs dynamic. For calculation of differential renal function only images prior to calyceal filling (Calyceal Transit Time, CTT) are required. Both CTTs were possible to calculate in 77/81 and both Renal Transit Times (RTT) in 62/81 fMRUs. In 80% of the cases calculated CTT <3 min and RTT<5.2. In 12/19 (63%) fMRUs scans in prone position, all ureters were contrasted. In supine position there was significant ($p<0.01$) positive correlation between RTT and PC dilatation grade and uretero-pelvic angle at the hilum on the axial plane in relation to a pre-vertebral horizontal line at the same level.
C] 3/8 sequences were categorized as non-essential: sagittal T1 fs did not provide additional information in (97.5%) and coronal T2 fs and post-contrast sagittal T1fs in (100%). The actual scan time of the essential sequences with the shortened post-contrast dynamic one add up to 18 min (80%), with potential further decrease in prone position.
Conclusions: Comprehensive fMRU can be done in less than 30 min with just four sequences and a short dynamic scan, optimally in prone position.

Paper #: PA-041

The Pediatric Appendix: What is Normal with Respect to Size?

Andrew Trout, *Cincinnati Children's Hospital Medical Center Department of Radiology, Cincinnati, OH, andrew.trout@cchmc.org;* Alexander Towbin, MD, Bin Zhang

Purpose or Case Report: Appendiceal diameter is used as a criterion to diagnose appendicitis by CT with multiple diameter cutoffs described in the literature. Yet, to date, there has been no large study systematically defining the diameter of the normal pediatric appendix. Without knowledge of normal, accurate assessment of the abnormal appendix is limited. The purpose of this study was to define the normal size of the pediatric appendix and identify non-imaging related factors that influence its diameter.
Methods & Materials: We sampled abdomen/pelvis CTs performed in our department in 2010 to identify 35 CTs from each calendar month for a total of 420 unique patients. Exams were included based on the following criteria: age <18 years, appendix identified by both reviewers, and absence of appendiceal pathology. If a patient had multiple exams, only the first was evaluated.
Two reviewers independently measured the greatest transverse diameter of the appendix along its short axis on axial images. Demographic data, appendiceal content and the presence of prominent abdominal lymph nodes were recorded. Statistical analysis was used to determine the effect of these variables on appendix diameter.
Results: Seven hundred ninety-two CTs were reviewed to identify 420 unique patients. Of these 420 patients, 51.4% were female and the mean age was 11.0±4.8 years (range: <0.1–18). Appendiceal diameter was relatively normally distributed in the population (Figure 1) with mean, median, mode, range and normal range (±2 standard deviations) detailed in Table 1.
Appendiceal diameter was not dependent on gender or time of year but was dependent on patient age ($p<0.0001$), the presence of prominent lymph nodes ($p\leq0.0007$) and appendiceal content ($p<0.0001$). Appendiceal diameter increased by 0.1 mm/yr and was ~0.5 mm larger in patients with prominent abdominal lymph nodes. Appendices containing stool, fluid or an appendicolith were larger in diameter than appendices with other contents.
Conclusions: Appendiceal diameter is relatively normally distributed in children with a mean diameter of 5.6–5.7 mm and a wide normal range extending above 8 mm. Diameter varies based on age (increasing by 0.1 mm/yr over the first 18 years of life) and is influenced by the presence of lymphatic stimulation (+0.5 mm) and appendix content. The broad range of normal appendiceal diameters and the multiple factors that influence diameter call into question the commonly described diameter cut-offs used to diagnose appendicitis.

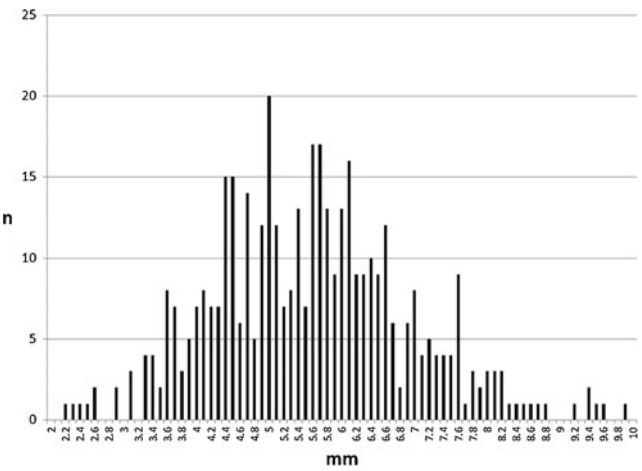

Figure 1: Histogram showing the distribution of appendiceal diameters in the population measured in the axial plane by reviewer 1

Table 1: Appendiceal diameter measurements in the axial plane

Reviewer	Mean (SD)	Median	Mode	Range	Normal Range (mean ±2 SD)
R1	5.57 mm (1.35 mm)	5.60 mm	5.00 mm	2.2–9.9 mm	2.87–8.27 mm
R2	5.68 mm (1.50 mm)	5.70 mm	6.30 mm	2.2–10.3 mm	2.68–8.68 mm

Paper #: PA-042

Assessment of Factors Influencing Identification of the Normal Pediatric Appendix

Andrew Trout, *Cincinnati Children's Hospital Medical Center Department of Radiology, Cincinnati, OH, andrew.trout@cchmc.org;* Alexander Towbin, MD, Bin Zhang

Purpose or Case Report: CT of the abdomen and pelvis can be used to exclude appendiceal pathology when ultrasound has failed to identify the appendix. In these cases, identification of a normal appendix is as important as identifying an inflamed appendix. The purpose of this project was to determine patient specific and technical factors that influence identification of the normal pediatric appendix in a large patient population.

Methods & Materials: A random sample of abdomen/pelvis CTs performed in our department on patients without appendicitis was reviewed. Each study was reviewed independently by two pediatric radiologists with a consensus session to review cases in which the appendix had been identified by only one reviewer. Each reviewer also reported if oral contrast had reached the cecum, described appendiceal content, and quantified the amount of pericecal fat. Univariate analysis was performed to identify factors that improve visualization of the appendix.

Results: Five hundred seventy-two CTs in 472 unique patients were reviewed. The normal appendix was identified in 88.6% of cases by reviewer 1 and 84.3% of cases by the reviewer 2 ($p<0.05$). Factors statistically significantly associated with identification of the normal appendix included: patient age ($p=0.001$), quantity of pericecal fat ($p<0.01$), use of IV contrast ($p=0.0004$), use of oral contrast ($p=0.0003$), and appendix size ($p<0.0001$). Patient gender and whether oral contrast had reached the cecum were not significantly related to identification of the appendix.

Conclusions: The normal pediatric appendix can be identified on CT in 84–89% of cases. Factors that influence identification of the appendix include patient specific factors such as age, quantity of pericecal fat and appendix size as well as technical factors such as the use of IV and oral contrast. While patient specific factors are largely out of our control, the identified technical factors can be exploited to maximize identification of the appendix.

Paper #: PA-043

The Impact of Technical and Interobserver Factors on Appendiceal Measurement in Children

Andrew Trout, *Cincinnati Children's Hospital Medical Center Department of Radiology, Cincinnati, OH, andrew.trout@cchmc.org;* Alexander Towbin, MD, Bin Zhang

Purpose or Case Report: Appendiceal diameter has been used as a diagnostic criterion for acute appendicitis yet little is known about measurement uncertainty due to factors such as the plane of image reconstruction, interobserver variability, and fluctuation of appendiceal diameter in a given patient. The aim of this study is to assess sources of measurement error in appendiceal diameter in a large population of pediatric patients.

Methods & Materials: A random sample of abdomen/pelvis CTs performed in our department was reviewed independently by two pediatric radiologists with a consensus session to review cases in which the appendix had been identified by only one reviewer. The reviewers identified the appendix and measured its greatest transverse dimension on both the axial and coronal reformatted images. Results from repeat CTs performed within 1 month in a single patient were compared to assess short term variability in appendix diameter. Both patients with and without appendicitis were included in this study as the primary aim was to assess measurement variability.

Results: Six hundred ninety-eight CTs were reviewed. The appendix was identified by each reviewer independently or after a consensus session in 631 (90.4%) CTs performed on 519 unique patients. Of these 519 patients, 456 had normal appendices and 63 had appendicitis. Mean patient age at scan was 10.9±4.9 years. While there was significant correlation between axial and coronal measurements for each observer ($\rho=0.84$ and 0.82 respectively, $p<0.0001$ for both), coronal measurements were significantly larger for both observers (mean + 0.4 mm, $p<0.0001$). Between reviewers there was significant correlation in measurements made in the axial ($\rho=0.74$, $p<0.0001$) and coronal planes ($\rho=0.76$, $p<0.0001$) with measurements for reviewer two significantly larger in both planes (axial: +0.15 mm, $p=0.003$; coronal: +0.14 mm, $p=0.007$). Among patients with repeat exams within 1 month, there was significant variance in measured appendix diameter (Table 1) over the short interval.

Conclusions: Multiple factors affect the measured appendiceal diameter including the plane of measurement (difference of 0.4 mm) and interobserver variability (difference of 0.15 mm) with the greatest variability relating to fluctuations in appendiceal diameter in patients with short interval follow-up imaging (difference of 0.3–0.75 mm over less than 1 month). The sources of measurement difference identified in this study introduce uncertainty into the use of diameter as a criterion for diagnosing acute appendicitis.

Table 1: Mean variance in appendix diameter within individual patients with multiple CTs performed within 30 days.

Reviewer	Plane	Estimated Variance Within Individuals	p-|value
1	Axial	0.46 mm	0.031
	Coronal	0.29 mm	0.065
2	Axial	0.67 mm	0.022
	Coronal	0.75 mm	0.02

Paper #: PA-044

The Challenging Ultrasound Diagnosis of Perforated Appendicitis in Children: Constellations of Sonographic Findings Improve Specificity

Sheryl Tulin-Silver, *New York University School of Medicine, New York, NY, sheryl.tulin-silver@nyumc.org;* Nancy Fefferman, MD, Lynne Pinkney, Naomi Strubel, Sarah Milla, Shailee Lala

Purpose or Case Report: Distinguishing perforated from non-perforated appendicitis in children, a known limitation of ultrasound, may alter surgical management. We evaluated the diagnostic utility of select groups of sonographic findings for diagnosis of perforated appendicitis.

Methods & Materials: With IRB approval, we retrospectively reviewed 116 abdominal ultrasound (US) exams obtained for evaluation of abdominal pain in children aged 2–18 years from 1/2008 to 9/2011 at a university hospital pediatric radiology department. The study group consisted of surgical and pathology proven acute appendicitis (n=51) and perforated appendicitis (n=22) US exams. Negative US exams for appendicitis (n=43) confirmed by follow up verbal communication comprised the control group. The de-identified US exams were independently reviewed on PACS workstations by four experienced pediatric radiologists blinded to diagnosis and clinical information. The radiologists recorded the presence of dilated bowel, right lower quadrant (RLQ) echogenic fat, increased hepatic periportal echogenicity, and intraperitoneal fluid, indicating quantity (number of abdominal quadrants) and quality of the fluid (simple or complex). Logistic regression for correlated data was used to evaluate the association of diagnosis with the presence versus absence of each US finding in addition to selected groups of US findings.

Results: The select groups of findings included increased hepatic periportal echogenicity, echogenic fat, and complex fluid yielding a specificity of 95.0% for perforated appendicitis; increased hepatic periportal echogenicity and 2+ quadrants of fluid yielding a specificity of 96.1%; increased hepatic periportal echogenicity and dilated bowel with a specificity of 98.0%; and dilated bowel, echogenic fat and complex fluid with a specificity of 99.5%. The above constellations of sonographic findings yielded higher specificities than that of each of the following individual findings in isolation: presence of complex fluid (92.8%), dilated bowel (95.7%), 2+ quadrants with fluid (88.3%), increased hepatic periportal echogenicity (79.2%), and RLQ echogenic fat (62.7%) for distinguishing perforated appendicitis from both acute appendicitis and control exams.

Conclusions: Our study demonstrates that select combinations of specific sonographic findings when visualized within individual patients increases the specificity for perforated appendicitis in children and therefore improves the diagnostic utility of ultrasound in this setting.

Paper #: PA-045

Sonographic Identification of Pediatric Candidates for Non-Surgical Treatment of Acute Appendicitis

Alison Sheridan, MD, *Yale School of Medicine, New Haven, CT, alisondsheridan@gmail.com;* Raffaella Morotti, Thomas Goodman

Purpose or Case Report: Management of acute appendicitis (AA) has classically been surgical. However, a growing body of evidence suggests non-surgical treatment (NST) with antibiotics has similar efficacy in a select group of patients who present early. Diagnosis of AA is increasingly being made on the basis of ultrasound (US) findings, wherein two distinct morphologic presentations are seen: a fluid filled lumen (FFL) or an appendix with wall thickening (WT) only. We hypothesize that patients presenting with WT represent lymphoid hyperplasia early in the disease process and may be candidates for NST. To this end, two cohorts of representative cases of FFL and WT were selected to assess for potential clinical, laboratory and pathological differences.

Methods & Materials: Two cohorts of ten patients (pts) each who had undergone surgical appendectomy were selected based on US findings of 1) a dilated (>6 mm), non-compressible, fluid filled appendix (FFL group), or 2) a dilated (>6 mm), appendix with wall thickening and no fluid (WT group). Demographic data including age, gender, and body temperature at presentation, as well as white blood cell (WBC) count with differential were collected. Pathological

samples were reviewed and graded as either lymphoid predominant (LP), mixed or suppurative predominate (SP).
Results: At presentation, pts in the CMS group in comparison to the WT group were significantly more likely to have a lower neutrophil count (20% vs. 80%, p=0.026) and more likely to have higher mean percent lymphocytes on differential (22% vs. 15%, p=0.049). WT pts also trended toward a lower likelihood of having an abnormally elevated WBC (30% vs. 80%, p=0.076) and lower mean percent neutrophils (68% vs. 76%, p=0.063). On pathologic evaluation, WT pts were significantly more likely to have a LP pattern (50% vs. 0%, p=0.010) and trended toward a lower likelihood of an SP pattern (40% vs. 80%, p=0.068). There was no significant difference in body temperature, age or gender between the two groups.
Conclusions: Presented here are the results of a pilot study for the development of a radiographic model for the identification of pediatric pts for NST of early AA. We have shown significant differences in laboratory data and pathologic features based on initial ultrasound findings. The next step in the development of our model will be a larger validation cohort analysis of all appendectomy cases over the past 3 years at our institution.

Paper #: PA-046

Implementing an Ultrasound-Based Protocol for Diagnosing Appendicitis While Maintaining Diagnostic Accuracy

Angie Van Atta, *University of Utah, Salt Lake City, UT;* David Dansie, MD, Michael Mundorff, Henry Baskin, Connie Maves

Purpose or Case Report: Diagnosing appendicitis in children with ultrasound (US) is well-documented but not universally employed. For institutions and radiologists, various obstacles exist to abandoning a successful and accurate computed tomography (CT)-based imaging protocol in favor of a US-based protocol. During the recent transition to an US-based protocol at our institution, we quantified how our ability to unequivocally visualize the appendix with US increased, our use of CT decreased, and the likelihood of a patient going to the OR based only on positive US findings increased. Overall diagnostic accuracy was unchanged. We also discuss how we overcame several barriers to implementing a US-based protocol.
Methods & Materials: A multidisciplinary team (pediatric surgery, pediatric emergency medicine, and pediatric radiology) approved an imaging protocol using US as the primary modality and CT as a secondary modality for equivocal cases. The protocol accounted for institutional limitations of physician and sonographer experience and availability. Clinical education consisting of didactic lectures and periodic formal case review commenced before implementing the protocol and continued throughout the study. US results were coded according to the likelihood of appendicitis, on a four-point scale ranging from unequivocally positive to unequivocally negative. Clinical notes, surgical reports, and pathology reports were reviewed to establish a final diagnosis of positive or negative for appendicitis. Diagnostic accuracy during the first 12 months and the last 12 months of the study period was calculated.
Results: Five hundred twelve patients were enrolled and underwent US for evaluation of appendicitis over a 30 month period. Accuracy for the diagnosis of appendicitis was stable during the study, unchanged from our prior protocol using CT only, and comparable with other published results for combined US/CT protocols. Comparing the first 12 month period to the last 12 month period of our study, the likelihood of achieving an unequivocal US result increased from 30.2% to 52.8% and the likelihood of going to the OR on the basis of positive US findings alone increased from 55% to 84%. Overall, 64% of patients avoided CT.
Conclusions: During the study period, our ability to visualize the appendix and our success in avoiding CT increased, but the diagnostic accuracy of the protocol did not change. Accuracy during the first 12 months and the last 12 months were comparable with other published studies.
Disclosure: Dr. Dansie has indicated a relationship with General Electric as an Advisory Committee Member; travel reimbursement received.

Paper #: PA-047

Prospective Comparison of MRI and Ultrasound for the Diagnosis of Pediatric Appendicitis

Robert Orth, MD, PhD, *Robert Chappell Orth, Texas Children's Hospital, Houston, TX, rcorth@texasChildren's.org;* R. Paul Guillerman, Prakash Masand, MD, Wei Zhang, George Bisset

Purpose or Case Report: Recent retrospective studies have shown the potential of MRI for diagnosing pediatric appendicitis. The purpose of this study is to prospectively compare the accuracy of non-contrast MRI and ultrasound (US) for the diagnosis of acute appendicitis in children.
Methods & Materials: Fifty-six patients (M:F=28:28, mean age=11.2 +/− 3.5 years, range=4–17 years) referred for limited right lower quadrant US were enrolled in this prospective study. Inclusion criteria were age of 4–17 years and clinical suspicion of acute appendicitis. Patients unable to undergo MRI (e.g., metallic device implants or unable to cooperate) were excluded. Prior to or immediately following the US examination, patients underwent a 15 min, non-contrast, non-sedated abdominopelvic MRI exam employing six sequences: DWIBS (B-value=40 and 400), coronal and axial fast-spin echo (FSE) T2, axial FSE T2 with fat-

saturation, and axial gradient echo T1. MRI exams were independently reviewed by two pediatric radiologists blinded to US results and clinical findings. Choices were 1) No appendicitis, 2) Equivocal, and 3) Acute Appendicitis. Discrepant interpretations were resolved by a third pediatric radiologist. Sensitivity and specificity of MRI and US (based on the clinical US report) were calculated and compared to a gold-standard of surgical pathology or clinical follow-up.

Results: Twenty-four of the 56 (42.9%) patients had pathologically proven acute appendicitis. When equivocal interpretations for MRI and US were considered positive, the sensitivity of MRI and US were 95.8% and 79.2%, respectively (p=0.188), and the specificity of MRI and US were 93.8% and 78.1%, respectively (p=0.148). When equivocal interpretations for MRI and US were considered negative, the sensitivity of MRI and US were 83.3% and 79.2%, respectively (p=1), and the specificity of MRI and US were 93.8% and 100%, respectively, (p=0.492). All equivocal MRI interpretations (n=3) were positive at surgery and all equivocal US interpretations (n=7) were negative by clinical follow-up. Inter-observer agreement was moderate, κ=0.596.

Conclusions: Non-contrast MRI without sedation may provide accuracy equivalent or superior to ultrasound for the diagnosis of acute appendicitis in children and may be a viable alternative to CT at institutions without the experience and personnel to perform ultrasound examinations on these patients. MRI should also be considered as an alternative to CT in patients with equivocal ultrasound examinations.

Disclosure: Dr. Orth has indicated that this research was supported by a grant from the Association for Medical Imaging Management and Toshiba. The grant paid for MR imaging time and research coordinator support; no direct financial benefit was received.

Paper #: PA-048

The Eye Sees Only What the Mind Knows. Accuracy of Abdominal Ultrasound in the Evaluation of Visceral and Vascular Manifestations of Heterotaxy When Compared to MRI/CT: A Practice Quality Improvement Study.

Esben Vogelius, MD, *Pediatric Radiology, Texas Children's Hospital, Houston, TX, esvogeli@texasChildren's.org;* Umakumaran Ponniah, Christopher Lam, MD, Prakash Masand, George Bisset, Rajesh Krishnamurthy, MD

Purpose or Case Report: The primary objective of our study was to determine the accuracy of ultrasound for detection of abdominal vascular and visceral manifestations of heterotaxy when compared to MRI or CT, highlight clinically relevant findings that are often missed by ultrasound, categorize the reasons for error, and suggest a standardized protocol to improve accuracy of ultrasound in this setting.

Methods & Materials: A retrospective study was performed on 39 patients (mean age 1.6 years at the time of the ultrasound, age range 1 day to 10 years, 46% male) with confirmed diagnosis of heterotaxy, who had both a complete abdominal ultrasound and CT or MRI of the chest and upper abdomen. The position and appearance of the solid abdominal organs, SMA/SMV relationship, and status of the IVC, and hepatic veins and were noted on the basis of the initial ultrasound report. The same images were retrospectively evaluated by an experienced pediatric radiologist blinded to the cross-sectional results. The sensitivity and accuracy of the initial ultrasound report and the re-interpretation was calculated, using the MRI/CT results as the gold standard.

Results: Of the 39 heterotaxy patients, 21 were of the asplenia type, 14 of the polysplenia type, four had situs ambiguous with a single spleen. The overall accuracy of the initial ultrasound report for characterization of situs was only 51% which improved to 79% with re-interpretation by the expert reader. Situs ambiguous with a single spleen necessarily leads to erroneous classification as situs solitus or situs inversus by abdominal ultrasound leading to four false negative results, and decreasing overall sensitivity. Other results are in Table 1. The poor performance regarding the status of the hepatic veins was secondary to inadequate demonstration of the upper IVC and hepatic venous entry into the atria.

Conclusions: The accuracy for characterization of situs and the sensitivity for sonographic diagnosis of the spectrum of visceral and vascular findings of heterotaxy by initial abdominal ultrasound report were poor. This was significantly improved by retrospective analysis of the same images by an expert reader. The largest improvements came in the detection of pancreatic configuration and abnormal SMA/SMV relationship. Many abdominal ultrasounds were limited by suboptimal technique rather that incorrect interpretation. These shortcomings could potentially be addressed by adopting our proposed ultrasound protocol in the setting of suspected heterotaxy.

Table 1: Sensitivity for detection of intra-abdominal abnormalities by ultrasound

Sensitivity for detection of:	Initial ultrasound report	Re-interpretation of ultrasound
Situs	51%	79%
Position and number of spleens	64%	83%
Position and configuration of liver	73%	92%
Position and configuration of pancreas	0%	67%
Relationship of SMA and SMV	17%	83%
Status of IVC	40%	68%
Status/insertions of the hepatic veins	0%	10%

Paper #: PA-049

Comparison of Quantitative MRI for Hepatic Fat Content Measurement in Pediatric Patients with Non-alcoholic Fatty Liver Disease

Jie Deng, PhD, *Medical Imaging, Ann & Robert Lurie Children's Hospital of Chicago, Chicago, IL, jdeng @lurieChildren's.org;* Cynthia Rigsby, James Donaldson, Mark Fishbein

Purpose or Case Report: Non-alcoholic fatty liver disease (NAFLD) is the most common liver disease in the United States. Gold standard for diagnosis is liver biopsy. Non-invasive imaging modalities such as ultrasound, CT and MRI are helpful to identify NAFLD. MRI is the only quantitative method, and allows for an absolute measurement of hepatic fat content. The methodology is particularly appealing to the pediatric population due to its rapidity and radiation-free imaging techniques. The objective of this study was to compare conventional 2-point Dixon in and opposed phase imaging, 3-point Dixon and LIPO-Quant (Liver Imaging of Phase-related signal Oscillation and Quantification) methods for liver fat fraction measurement.

Methods & Materials: Pediatric patients with suspected or identified NAFLD were scanned on a 1.5 T MRI scanner using a six-echo spoiled gradient echo sequence. Images on four center liver slices were acquired during breathold with the following parameters: TR=120 ms, TE=2.3, 4.6, 6.9, 9.2, 11.5 and 13.8 ms, matrix=115×192 and flip angle=10°. Fat fraction (FF) was calculated by using different methods described in Table 1, which included 2-point, 3-point Dixon and LIPO-QUANT methods. LIPO-QUANT separated water and fat signals by non-linear curve fitting of the signal oscillation, with fat spectrum modeling and T2* decay correction. Before patient studies, three methods were compared and calibrated on ex-vivo pork liver-fat homogenate phantom with fat fraction 3.5%–46%.

Results: In ex-vivo liver-fat homogenate phantom, LIPO-QUANT method with bi-exponential water and fat T2* correction and with all 1, 3, 5-peak fat spectral models provided similarly accurate FF measurements with linear regression of $FF_{1peak,\ 2T2*}=1.03xFF_{true}+1.1$, $FF_{3peak,\ 2T2*}=1.07xFF_{true}+1.2$ and $FF_{5peak,\ 2T2*}=0.98xFF_{true}+0.9$, respectively. In comparison, 2-point, 3-point Dixon methods and LIPO-QUANT with mono-exponential T2* correction methods underestimated FF. In 39 clinical patients, FF measured by 2-point, 3-point and calibrated LIPO-QUANT methods were 12±8.0 (%), 15.8±7.9 (%) and15.6±7.7 (%), respectively. Statistically significant differences were shown between each pair of three methods with $p<0.0001$ (paired *t*-test). However, 3-point FFs were alternative to calibrated LIPO-QUANT FFs.

Conclusions: Conventional 2-point Dixon method underestimated fat fraction in hepatic fat measurement. Methods that take account of T2* correction and fat spectrum models should be considered in clinical use to improve the measurement accuracy.

	2-point Dixon	3-point Dixon	LIPO-QUANT
TE (ms)	2.3, 4.6	2.3, 4.6, 9.2	2.3, 4.6, 6.9, 9.2, 11.5,13.8
T2* correction	NO	YES	YES mono-exponential T2* decay: $T2^*=T2^*_{water}=T2^*_{fat}$ bi-exponential T2* decay: $T2^*_{water}= T2^*_{fat}$
Fat Spectrum modeling	NO	NO	YES 1 fat peak (f_n =1.3 ppm) 3 fat peaks (f_n = 0.9, 1.3 and 2.1 ppm) 5 fat peaks (f_n = 0.9, 1.3, 2.1, 4.2, 5.3 ppm)
Fat Fraction (FF)	$FF(2\text{-point}) = (S_{TE4.6}-S_{TE2.3})/(2xS_{TE4.6})$	$T2^* = (9.2\text{-}4.6)/\log(S_{TE4.6}/S_{TE9.2})$ $corrected\_S_{TE4.6} = S_{TE4.6}\exp((4.6\text{-}2.3)/T2^*)$ $FF(3\text{-point}) = (corrected\_S_{TE4.6}-S_{TE2.3})/(2xcorrected\_S_{TE4.6})$	$S(TE)=\left\lvert\rho_w+\rho_f\sum_{n=1}^{3}c_n\exp(2\pi i f_n TE)\right\rvert\cdot\exp(-TE/T2^*)$ $S(TE)=\rho_{water}\cdot\exp(-TE/T2^*_{water})+\rho_{fat}\sum_{n=1}^{3}c_n\exp(2\pi i f_n TE)\cdot\exp(-TE/T2^*_{fat})$ $FF_{LIPO\text{-}QUANT}=\rho_{fat}/(\rho_{water}+\rho_{fat})$

Paper #: PA-050

Role of Contrast Enema Study in Diagnosis of Hirschsprung's Disease.

Akshay Saxena, MD, *Department of Radio Diagnosis, Post Graduate Institute of Medical Education and Research, Chandigarh, India, fatakshay@yahoo.com;* Madhan Murugan, Kushaljit Sodhi, Katragadda Rao, Kim Vaiphei, Niranjan Khandelwal

Purpose or Case Report: (i)To evaluate the performance of contrast enema (CE) study in management of clinically suspected Hirschsprung's disease (HD) (ii) To evaluate the concordance of radiologists in identification of radiographic transition zone (RTZ) (iii) To evaluate the concordance of RTZ and pathological transition zone (PTZ).

Methods & Materials: This prospective study was approved by our institute ethics committee. Contrast enema was performed in children suspected to have HD. Demonstration of RTZ and/or contrast retention in 24 h film was considered diagnostic for HD. All the studies were evaluated by two pediatric radiologists independently and differences resolved by consensus. Diagnostic performance of CE was evaluated using histopathological data (biopsy and/or laparotomy) alone as the gold standard as also using the combination of histopathological examination and clinical follow up as gold standard. Concordance rate between RTZ and PTZ was noted.
Results: CE was performed in 82 children while 24 h delayed film was done in 72 patients. Age of the patients was 3 days to 10 years (mean=22.25±26.835 months). The inter observer agreement for identification and localization of RTZ was in excellent agreement range with kappa value of 0.924 and 0.870 respectively. The sensitivity, specificity, positive predictive value and negative predictive value of CE for diagnosis of HD using HPE as gold standard was 95.23%, 36.36%, 58.82% and 88.89% respectively. The corresponding figures, with HPE and/or clinical follow up as gold standard, were 95.24%, 56.90%, 44.40%, 97.10% respectively. The concordance rate between RTZ and PTZ was 100% for short segment disease and 90.9% for overall population. Seven patients were operated based on clinical grounds despite negative CE study. None of these patients had negative laparotomy. In addition 14 patients, with CE positive for HD, were managed conservatively based on clinical grounds. 11/14 of these patients showed normalization of bowel habits and weight gain during follow up.
Conclusions: CE is a good screening test for HD as it has high sensitivity. However, specificity is low suggesting need for confirmatory follow up investigation like rectal biopsy. Interobserver agreement for identification and localization of RTZ is excellent. There is high rate of concordance between RTZ and PTZ for short segment HD. Clinical acumen has an important role in management of patients with suspected HD and reliance solely on radiological findings for decision making should be avoided.

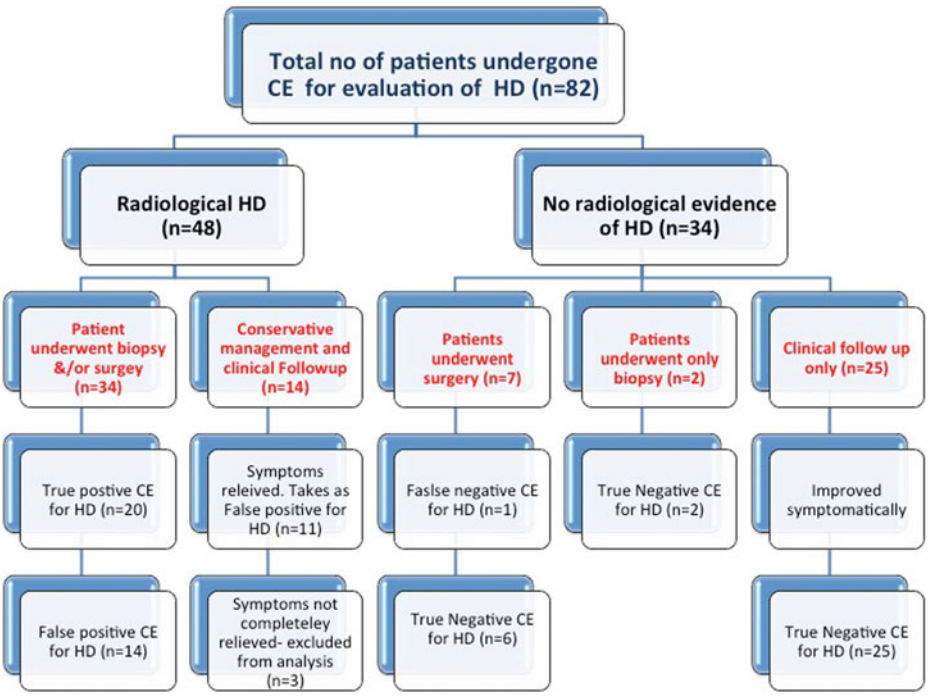

Paper #: PA-051

Intussusception Reduction: Does a Retention Balloon Make a Difference?

Christopher Cassady, Christi Herrejon, **Brandy Bales**, *Texas Children's Hospital, Houston, TX* ; Melissa Cano

Purpose or Case Report: To determine the efficacy of using a retention balloon during enema procedures for intussusception reduction in children.
Methods & Materials: We retrospectively reviewed hospital charts, radiology reports, and surgical notes of patients at a large children's hospital spanning a three and half year period (2008–7/2011) who underwent enema reduction for

intussusception. Data from 234 studies were sorted by contrast technique (positive, negative or combined) and by use or not of a retention balloon with the enema catheter. We calculated the success rates with and without balloon for each group, which were compared using the one-sided *t*-test and Fisher's Exact test as appropriate. P-values <0.1 were considered statistically significant.

Results: Overall, the success rates for complete reduction were 87.2% and 74.4%, with and without a balloon respectively (p-value 0.02). Success rates by category were as follows: 88.2% for air (negative contrast) enema with balloon; 78.5% for air enema without balloon; 92.3% for hydrostatic (positive contrast) enema with balloon; and 77.5% for hydrostatic enema without balloon. There were no anorectal complications with use of the balloon in any case. Two perforations occurred during pneumatic enema reductions, one with the use of a retention balloon and one without. No other perforations occurred, regardless of technique.

Conclusions: Intussusception reductions performed with the aid of a retention balloon are more successful than those performed without.

Paper #: PA-052

A Comparison of Airway Fluoroscopy with Endoscopy in the Evaluation of Children with Stridor

Gregory Vorona, MD, *The Children's Hospital of Philadelphia, Philadelphia, PA, gavorona@gmail.com;* Avrum Pollock

Purpose or Case Report: To evaluate the effectiveness of airway fluoroscopy in diagnosing airway lesions confirmed by direction visualization using laryngoscopy.

Methods & Materials: After obtaining IRB approval, a retrospective review was performed of patients who underwent airway fluoroscopy at our institution for the indication of "stridor" from 2007 to 2009. Patients who additionally underwent flexible laryngoscopy within 30 days, and/or direct laryngoscopy and bronchoscopy performed within 60 days, of airway fluoroscopy were included in our study. Airway fluoroscopy and laryngoscopy reports were compared for concordance of findings. The sensitivity, specificity, positive and negative predictive values of airway fluoroscopy in the diagnosis of laryngomalacia, airway stenosis, airway mass, and vocal cord paralysis were then determined using endoscopy as the "gold standard".

Results: Sixty-four patients (34 males, 30 females) were included in our study, with a mean age of 0.7 years (range= 0.0 to 2.5 years) at the time of their first endoscopic study. There was an average time interval of 7.1 days (range=0 to 27 days) between airway fluoroscopy and flexible fluoroscopy, and an average interval of 8.7 days (range=1 to 40 days) between airway fluoroscopy and direct laryngoscopy/bronchoscopy. The sensitivity of airway fluoroscopy in the diagnosis of laryngomalacia (n=26), airway stenosis (n=12), airway mass lesion (n=8), and vocal cord paralysis (n=3) was 0.08, 0.64, 0.63, and 0.0 respectively. The specificity of airway fluoroscopy for these same diagnoses was 0.94, 0.94, 1.0, and 0.94 respectively. The PPV was 0.67, 0.88, 1.0, and 0.0 respectively. The NPV was 0.39, 0.79, 0.83, and 0.88 respectively.

Conclusions: Airway fluoroscopy is both a minimally invasive and a highly specific diagnostic examination to characterize airway lesions which cause stridor in children. However, our findings suggest that it demonstrates only a moderate sensitivity in the detection of airway stenosis and airway mass lesions, and a poor sensitivity in the diagnosis of laryngomalacia and vocal cord paralysis. A negative airway fluoroscopy result in a symptomatic patient does not exclude significant underlying pathology, and if clinically indicated, further diagnostic evaluation is needed either via direct visualization or a tailored low-dose CT examination.

Paper #: PA-053

Protocol for Dynamic Airway Imaging with Volume CT Angiography in Pediatric Patients: our Experience with 20 Children

Prakash Masand, MD, *Pediatric Radiology, Texas Children's hospital, Houston, TX, drmasand@gmail.com;* Rajesh Krishnamurthy, MD

Purpose or Case Report: Dynamic imaging of the airway with simultaneous opacification of the heart and mediastinal vascular structures allows evaluation of intrinsic and extrinsic abnormalities responsible for airway narrowing in pediatric patients. To our knowledge, this protocol for dynamic imaging of the airway and the vasculature is unique and holds immense potential.

Methods & Materials: We obtained IRB approval for this project and reviewed the CT angiography images obtained on 20 patients using our imaging protocol. The scans are performed on a Volume CT (Toshiba) with prospective EKG gating and simultaneous acquisition of the datasets during contrast administration. This allows angiographic datasets to be acquired during the same time as the airway is evaluated with a low dose technique.There are 6–8 volumetric datasets

obtained in a continous or intermittent fashion, which is predecided based on the patients respiratory rate. The parameters are set at 80 kv and 30 mA which drastically cuts down the radiation dose, coupled with iterative reconstruction techniques to further lower the doses.

Results: The cohort of patients includes those diagnosed with intrinsic airway problems like tracheomalacia and bronchomalacia with or without extrinsic compressive pathologies. This includes vascular rings like double aortic arch, pulmonary artery sling, innominate artery compression syndrome, patients with complete cartilagenous rings, extrinsic compression due to persistent esophageal dilation, and significantly dilated pulmonary arteries. Two patients with tracheal stenosis were also included in the study. The main criterion for tracheobronchomalacia on dynamic imaging was airway collapse of greater than 50% cross sectional diameter. All these patients had bronchoscopy either prior to or after the CT angiograms, which correlated well with our findings. Nine patients underwent surgery with no discrepant findings.

Conclusions: The dynamic airway imaging protocol highlighted in our abstract holds promise to be a one stop shop for evaluating airway abnormalities, along with simultaneous depiction of the vascular and cardiac anatomy. More importantly coupled with an iterative reconstruction technique, we are able to achieve significantly low radiation doses.

Paper #: PA-054

Improving Consistency of Contrast Enhancement during CT Pulmonary Angiography: A Quality Improvement Study

Robert Fleck, MD, **Eric Langenderfer,** *Cincinnati Children's Hospital Medical Center, Cincinnati, OH, Langenea@mail.uc.edu;* Sara Smith

Purpose or Case Report: To increase the contrast-to-noise ratio of CT pulmonary angiography (CTPA) by increasing the percentage of studies with contrast density in the main pulmonary artery (MPA) of 250 Hounsfield units (HU) or greater.

Methods & Materials: Documentation of existing CTPA process and results was performed for the year prior to the initiative using the radiology information system. Contrast volume, injection rate, IV site and gauge, weight, main pulmonary artery HU, ascending aorta HU, technique utilized, patient movement, and report comments on quality were documented for each patient during the intervention period. Four protocol adjustments were made to improve consistency in results; each adjustment was treated as a separate trial.

Results: Baseline measurements revealed MPA density of ≧250 HU in 44% (15/34) of studies. Trial 1 emphasized the proper placement of the ROI using visual triggering if needed, resulting in 61% (52/20) of studies achieving ≧250HU. Trial 2 emphasized scanning 30 s after the initiation of contrast injection, resulting in 56% (40/72) of studies achieving ≧250 HU. Causes of 20 of the lowest HU cases included insufficient amount of contrast delivered (6/20), narrowing at the subclavian vein and/or possible overlap with Valsalva effect (10/20), insufficient IV caliber (3/20), and Valsalva effect alone (1/20). Trial 3 modified the injection rates, applied suspended breathing, and used a 6 ml/sec flush, resulting in≧250 HU in 72% (23/32) of studies. Causes of substandard HU cases included combined narrowing of SCV and Valsalva effect (5/9), slower injection than prescribed (2/9), subclavian narrowing alone (1/9), and unknown (1/9). Trial 4 moved the initiation of the CT back to 27 s, resulting in ≧250 HU in 92% (11/12) of studies.

Conclusions: Improvement in the outcome of CT angiography for pulmonary embolism can be achieved by using rapid cycle quality improvement methods resulting in a simplified CT protocol with fewer operator dependences.

MPA Contrast	Baseline Data		Trial 1		Trial 2		Trial 3		Trial 4	
	Number	Percent	Number	Percent	Number	Percent	Number	Percent	Number	Percent
	N=34		N=18		N=72		N=32		N=12	
HU>150	33	97.1%	16	88.9%	69	94.5%	32	100.0%	12	100.0%
HU>200	29	85.3%	15	83.3%	57	78.1%	27	84.4%	11	91.7%
HU>225	23	67.7%	12	66.7%	50	68.5%	25	78.1%	11	91.7%
HU>250	15	44.1%	11	61.1%	41	56.2%	23	71.9%	11	91.7%
HU>275	12	35.3%	7	38.9%	33	45.2%	19	59.4%	10	83.3%
HU>300	8	23.5%	5	27.8%	25	34.3%	17	53.1%	8	66.7%
Ave HU	259		268		275		304		335	

Paper #: PA-055

Proximal Pulmonary Vein Stenosis Detection in Pediatric Patients: Value of Multiplanar and 3D MDCT Imaging Evaluation

Edward Lee, MD, MPH, *Department of Radiology, Boston Children's Hospital and Harvard Medical School, Boston, MA, Edward.Lee@Children's.harvard.edu;* Kathy Jenkins, Muhammad Muneeb, Donald Tracy, David Zurakowski, Phillip Boiselle

Purpose or Case Report: To compare diagnostic accuracy and interpretation time of axial, multiplanar and 3D MDCT images for detection of proximal pulmonary vein stenosis in pediatric patients, and to assess the potential added diagnostic value of multiplanar and 3D MDCT images.

Methods & Materials: We identified all consecutive pediatric patients with proximal pulmonary vein stenosis (PVS) who had both a thoracic MDCT angiography study and a catheter-based conventional angiography within 2 months. Two pediatric radiologists independently reviewed each MDCT study for the presence of proximal PVS defined as≥50% of luminal narrowing on axial, multiplanar, and 3D MDCT images. Final diagnosis was confirmed by angiographic findings. Diagnostic accuracy was compared using the z-test. Confidence level of diagnosis, perceived added diagnostic value, and interpretation time of multiplanar or 3D MDCT images were compared using paired t-tests. Interobserver agreement was measured using the chance-corrected kappa coefficient.

Results: The final study population consisted of 28 children (15 M/13 F). Diagnostic accuracy based on 116 individual pulmonary veins for detection of proximal PVS was 72.4% (84/116) for axial MDCT images, 77.5% (90/116) for multiplanar MDCT images, and 93% (108/116) for 3D MDCT images with significantly higher accuracy with 3D MDCT compared to axial ($p<0.001$) and multiplanar ($p<0.001$) images. Confidence levels for detection of proximal PVS was significantly higher with 3D MDCT images (mean level=4.6) compared to axial MDCT images (mean level=1.7) and multiplanar MDCT images (mean level=2.0) ($p<0.001$). 3D MDCT images (mean added diagnostic value=4.7) was found to provide added diagnostic value for detecting proximal PVS ($p<0.001$); however, multiplanar MDCT images did not provide added value ($p=0.89$). Interpretation time was significantly longer and interobserver agreement was higher when using 3D MDCT images than using axial MDCT images or MPR MDCT images for diagnosing proximal PVS ($p<0.001$).

Conclusions: Use of 3D MDCT images in the diagnosis of proximal PVS in pediatric patients significantly increases accuracy, confidence level, added diagnostic value, and interobserver agreement. Thus, the routine use of this technique should be encouraged despite its increased interpretation time.

Paper #: PA-056

Congenital Multilobar Pseudo-Emphysema: A Severe Progressive Lung Growth Disorder Associated with Filamin A Gene Mutations

R. Paul Guillerman, *Department of Pediatric Radiology, Texas Children's Hospital, Houston, TX, rpguille @texasChildren's.org;* Zeyad Metwalli, Lindsay Burrage, Seema Lalani, Claire Langston, George Mallory

Purpose or Case Report: Filamin A (FLNA) is an X-linked gene encoding an actin-binding cytoskeletal protein involved in neuronal migration, cardiovascular development and connective tissue integrity. FLNA mutations have been associated with periventricular nodular heterotopia, cardiovascular anomalies, bowel pseudo-obstruction, skeletal dysplasia and Ehlers-Danlos variants. In this report, we describe the characteristic imaging features of a severe progressive lung growth disorder associated with FLNA mutations and respiratory failure in infancy.

Methods & Materials: A retrospective review was conducted of the clinical charts and imaging exams of all patients with both FLNA mutations and lung growth disorders diagnosed from 2005 to 2012 at a children's hospital.

Results: Four patients (all female; three full-term and one of 34-weeks gestational age) met the inclusion criteria. Two patients had an uncomplicated perinatal course, and two patients required oxygen supplementation for perinatal respiratory distress. Serial chest radiographs and chest CT exams obtained during infancy in all patients revealed severe progressive multilobar hyperinflation with hyperlucent lung parenchyma and attenuated peripheral pulmonary vasculature, especially in the upper lobes and right middle lobe, as well as parahilar and dependent atelectasis, and central pulmonary artery enlargement. Expiratory CT obtained in two patients showed air trapping and tracheobronchomalacia. Bronchoscopy in the other two patients showed tracheobronchomalacia. V/Q scintigraphy obtained in one patient showed matched ventilation-perfusion defects. All patients developed respiratory failure requiring lung transplantation at 5–15 months of age. Multilobar "emphysema" was noted on surgical and gross pathological inspection, and simplified enlarged alveoli and pulmonary hypertensive changes were noted on histopathology of all patients. Additional findings included a patent ductus arteriosus and periventricular nodular gray matter heterotopia in all patients, and ascending aorta dilation in three patients.

Conclusions: FLNA mutations are associated with a severe lung growth disorder characterized by simplified enlarged

alveolar air spaces and hyperinflation simulating emphysema, implying an important role of the filamin A actin-binding protein in alveolar modeling during lung growth. This lung growth disorder leads to respiratory failure during infancy, and recognition on imaging is important to guide genetic testing and referral for lung transplant evaluation.

Paper #: PA-057

Analysis of CT Findings in Community-Acquired Viral Respiratory Tract Infection in Children

Gauri Tilak, MD, PhD, MPH, *Radiology, The Children's Hospital of Philadelphia, Philadelphia, PA, gstilak@yahoo.com;* David Mong, Camilo Jaimes, MD, Richard Hodinka

Purpose or Case Report: Viral pneumonias account for up to 29% of patients with community-acquired pneumonia requiring hospital admission. Children, especially those affected by chronic illness or immunosuppressed, are at particularly high risk of serious illness from community-acquired respiratory infection. The literature describing the specific CT findings of viral lower respiratory tract infections (LRTI) has been recently described in adult populations. However, the immune response of children to infection is different from that of adults, and the technical challenges of CT imaging in younger patients are unique. The goal of this study is to determine the chest CT imaging features of documented viral LRTI in a pediatric population.

Methods & Materials: A retrospective analysis was performed on randomly selected chest CT scans performed within 6 days of pediatric patients presenting with symptoms suggesting lower respiratory tract infection who also tested positive for PCR-based assays of respiratory viral infection between 01/01/2006 to 01/01/2011. We report the prevalence of two characteristic patterns on chest CT: bronchiolitis [multifocal tree-in-bud opacities, peribronchial ground glass opacity, and/or widespread bronchial wall thickening] and pneumonia [multifocal consolidation or ground glass opacity without airway inflammation] as well as a normal study. Twenty-eight patients with viral respiratory tract infections were evaluated. The reviewer was blinded to virus type.

Results: Patients tested positive to the following viruses: influenza (n=5), RSV (n=4), metapneumovirus (n=4), rhinovirus (n=11), adenovirus (n=11), and parainfluenza virus (n=3). Five patients tested positive for more than one virus. Three patterns of the disease were seen with viral lower respiratory tract infection: (1) limited infection with normal imaging (14%), (2) bronchitis/bronchiolitis characterized by bronchial wall thickening and tree-in bud opacities (55%), and (3) pneumonia characterized by multifocal consolidation or ground-glass opacities without airway inflammation (31%).

Conclusions: CT scans of symptomatic pediatric patients with viral infections most commonly show two characteristic patterns: consolidation or bronchial wall thickening and tree-in-bud opacities. While historically taught that the former represents bacterial pneumonia and the latter a viral pattern, it is important that radiologists recognize the overlap of these findings when interpreting chest CTs for viral infection.

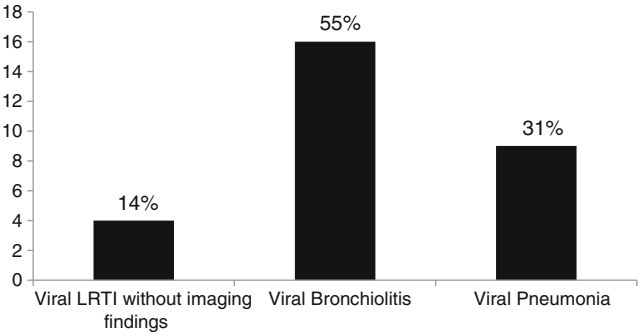

Paper #: PA-058

Chest X-Ray Findings In HIV-Infected Children Starting HAART at a Tertiary Instituition In South Africa

Nasreen Mahomed, MBBCh, FC Rad (Diag), *Radiology, University of Witwatersrand, Johannesburg, South Africa, nmneersan8@gmail.com;* Savvas Andronikou, Jayshree Naidoo, Mbaliso Mbakaza, Annelies Van Rie, Shobna Sawry

Purpose or Case Report: INTRODUCTION: Respiratory infections are common in HIV-infected children. There is limited information on the radiographic presentation of children eligible to start Highly Active Anti-retroviral Treatment (HAART) in resource-limited settings.

OBJECTIVES: To determine the radiographic patterns on pre-HAART chest X-rays in children, to compare the pre-HAART Chest X-Ray findings of immune suppressed vs. non immune suppressed children, to compare the percentage of children with radiographic features of pulmonary TB to the proportion of children on TB treatment and to assess the inter-observer variability between three paediatric radiologists.

Methods & Materials: METHODS: Children(0–8 years) participating in a cohort study of TB and BCG-IRIS who had an acceptable routine pre-HAART CXR were included. CXRs were independently assessed by three radiologists,

blinded from clinical data, using a standardized assessment form. All three readings were used to create a majority consensus finding.

Results: RESULTS: Amongst 161 children, the median age was 2.3 years(41/161 were <1 year), 54%(87/161) were on TB treatment and 62%(100/161) were immune-suppressed (CD4%<25% or CD4 count<350). The majority(71%) had an abnormal CXR finding, predominantly air space disease(42%) and parenchymal interstitial disease(20%). Of the 112(70%) CXRs that could also be assessed for lymphadenopathy (i.e. evaluable airways); 74(66%) had lymphadenopathy. Among the 112 children with a CXR that could be fully evaluated, 67%(75/112) had one or more abnormalities suggestive of TB (74 lymphadenopathy, 2 cavities, 18 milliary infiltration). The inter-observer variability was fair(k=0.22) for airspace disease, moderate(k=0.54) for parenchymal interstitial disease and slight(k=0.051) for lymphadenopathy.

Conclusions: CONCLUSIONS: Among children eligible to start HAART, most(71%) presented with abnormal CXR findings and the majority(67%) had one or more CXR signs suggestive of TB. Of concern was the high proportion of CXRs that were of insufficient quality to be assessed for lymphadenopathy and the relatively poor inter-reader agreement for radiological features of TB.

Paper #: PA-059

The Value of Portable Computed Tomography (CT) in the Pediatric ICU; Our results and experience in 320 consecutive cases over 3 years

Robert Lorenzo, MD, **Matthew Lynn,** *Egleston Children's Hospital, Atlanta, GA;* Toni Petrillo, James Fortenberry

Purpose or Case Report: Children in the Intensive care are often so ill they do not tolerate significant movement or travel. However, it is also these same patients who benefit from having CT imaging done to help elucidate plan of care or prognosis. In 2009 we purchased a portable CT scanner (Ceretom; Neurologica, Danvers, MA) to help facilitate imagining on these tenuous patients who were not amenable to cross-sectional imaging using our fixed CT scanner.

Methods & Materials: We evaluated 320 consecutive portable CT scans in a span of approximately 3 years including 41 patients on extracorporeal life support(ECMO) and newborns with complex chest and/or abdominal masses. Included in this population were several patients who would have been too unstable to be transported for traditional CT scan ie HFOV. Our smallest patient was 1.8 kg and our largest was 107.8 kg. Guidelines for indications and utilization were analyzed including numerous parameters such as time to scan, personnel utilization, change in patient management, complications and quality of images. All neurologic scans were interpreted by a pediatric neuroradiologist

Results: Image quality was reported as good in >90% of the scans and poor in < 1%. The time and personnel required to complete the scans was reduced when compared to a cohort of patients done prior to purchasing the portable CT. Thirty-five of portable CTs (73%) in the ECMO patients revealed significant lesions which potentially impacted decision making. No patient suffered significant complications during imaging. Time to complete the portable scans continued to improve with experience. Review of data on all imaged patients will be presented.

Conclusions: The use of a portable CT scanner helps facilitate care safely and efficiently in the critically ill pediatric patients, including newborn chest and abdominal scanning. This is done without significant sacrifice in image quality.

Paper #: PA-060

Radiopacity of Fish Bones From 10 Common Fish Species In the Philippines

Regina Nava, *St. Luke's Medical Center, Quezon City, Philippines, rcnavamd@yahoo.com;* Nathan David Concepcion

Purpose or Case Report: The use of radiography in fishbone ingestion is in question. This research aims to determine the relative radiopacity of fish bones from ten commonly consumed fish in the Philippines whether or not they are detected on a radiograph.

Methods & Materials: Fish ribs were cut into three lengths and inserted singly into a soft tissue phantom approximating the thickness of an average Filipino neck. Blinded observers were asked if the fish bones were radiopaque or not using a standard survey form. Radiopacity is presented as percentage of observers who judged them to be visible. Statistical significance was determined using the Wilcoxon rank test and Friedman test.

Results: There were 37 respondents. Fish bones measuring 2.5 cm were more radiopaque compared to those measuring 0.5 cm. The four species with the highest visibility percentages are namely bisugo (100%), dalagangbukid (97%), salaysalay (97%), and tilapia (95%). Statistical tests showed significant difference of fishbone visibility scores between X-rays containing bones and those of the control, and in the percentages among the three lengths used. Mean overall sensitivity is 34% while mean overall specificity is 95%.

Conclusions: Knowledge of the radiopacity of fish bones can be applied in the assessment of soft tissue lateral radiographs of the neck in patients suspected of fishbone ingestion. This study is limited by the assumption that all bones in a particular species are of the same radiodensity regardless of their thickness. It is thus recommended that future trials also factor in the thickness of the bones used.

Paper #: PA-061

Comparison of Pediatric CT Radiation Dose and Image Quality Utilizing Model Based Iterative Reconstruction and Adaptive Statistical Iterative Reconstruction Algorithms

Ethan Smith, MD, *Department of Radiology - Section of Pediatric Radiology, University of Michigan - C.S. Mott Children's Hospital, Ann Arbor, MI, ethans@med.umich.edu;* Jonathan Dillman, MD, Mitchell Goodsitt, Emmanuel Christodoulou, Peter Strouse

Purpose or Case Report: To compare image quality and radiation dose between a reduced dose CT protocol using model-based iterative reconstruction (MBIR) vs. our standard dose CT protocol using adaptive statistical iterative reconstruction (ASIR).

Methods & Materials: Consecutive clinical CT exams (Discovery CT750 HD; GE Healthcare) of the chest, abdomen and pelvis using a reduced dose protocol were performed on pediatric oncology patients. Reduced dose exams were performed using an automatic tube current modulation noise index (NI) of 47.7 and were reconstructed using two algorithms: MBIR and 100% ASIR. All subjects had standard dose comparison CT exam performed within the prior year (mean=3.9 months) using a similar kVp, NI of 33.6, and 30% ASIR. Reduced dose MBIR, reduced dose 100% ASIR, and standard dose 30% ASIR images were evaluated objectively for image noise. Two readers independently rated exams for overall image quality and lesion detectability. Modulation transfer function (MTF) was measured (Catphan® 600 phantom and ImageOWL Catphan® QA software) to assess spatial resolution. CTDIvol values were recorded as a measure of scanner radiation output.

Results: Twenty-five patients were imaged using our reduced dose CT protocol (mean age=11.7 years). The mean decrease in CTDIvol using our reduced dose protocol (vs. standard dose comparison CT) was 46% (range=19–65%). Reduced dose MBIR images had significantly less noise compared to reduced dose 100% ASIR ($p=0.004$) and standard dose 30% ASIR ($p<0.001$) images. At 80 kVp, spatial resolution (10% MTF value) was better for reduced dose MBIR (9.6 lp/cm) than for reduced dose 100% ASIR (7.07 lp/cm) and standard dose 30% ASIR (7.05 lp/cm). Similar MTF results were obtained at 100 and 120 kVp. Subjectively, both readers rated reduced dose MBIR images as equivalent to standard dose 30% ASIR images regarding appearance of the lungs and soft tissues. The appearance of the bones with MBIR was rated as inferior to standard dose 30% ASIR ($p=0.004$). Reduced dose 100% ASIR images were rated as inferior to standard dose 30% ASIR images ($p<0.002$ for soft tissues, lungs, and bones). All reduced dose CT exam lesions were seen either better (32/84 ratings) or the same (52/84 ratings) on MBIR compared to 100% ASIR images.

Conclusions: CT imaging using a reduced dose protocol and MBIR is feasible in the pediatric population with substantially decreased patient radiation dose and maintained diagnostic quality.

Paper #: PA-062

A phantom based technique to lower dose and maintain image quality in pediatric body imaging for 128 slice CT scanners using iterative reconstruction.

Nancy Fefferman, MD, Emilio Vega, **Sheryl Tulin-Silver,** *New York University School of Medicine, New York, NY, sheryl.tulin-silver@nyumc.org;* Mitya Barreto

Purpose or Case Report: With the advent of iterative reconstruction, the opportunity for decreasing radiation dose has become increasingly viable. The purpose of our study is to develop a method for optimizing existing adolescent pediatric body CT protocols with the goal of achieving lower dose without compromising image quality using raw data based iterative reconstruction.

Methods & Materials: A customized anthropomorphic abdominal CT phantom composed of "tissue-equivalent" material containing inserts simulating an enhancing renal lesion and non-enhancing renal cyst was scanned on three 128 slice CT scanners (Siemens Definition Edge, AS and FLASH). Scanning parameters included 120 kV and effective mAs from 20 to 140 by increments of 20. Each data set was reconstructed at a slice thickness of 4 mm with soft tissue algorithm (B40) and corresponding iterative reconstruction (SAFIRE, I40) with strengths 1 through 3. Attenuation and noise measurements were acquired at two contiguous slices for the non-enhancing cyst and enhancing lesion, at the same z-axis for all image sets. CTDIvol was recorded for each scan. Mean attenuation and noise values were compared between scanners and within each algorithm using ANOVA and *t*-test.

Results: No differences in mean attenuation of the enhancing lesion were observed between reconstruction algorithms (B40: 38.8±4.7, I40[1]: 38.6±4.6, I40[2]: 38.6±4.5, I40[3]: 38.4±4.5 HU) and scanner types (Edge: 38.1±2.9, AS: 37±6, FLASH: 40.6±3.3 HU). Mean noise for the enhancing lesion and cyst were not statistically different between the scanners. Noise was signficantly lower for both renal inserts with iterative reconstruction ($p<0.001$) for strength 1 (10%), strength 2 (20%) and strength 3 (30%) compared to B40. Average CTDIvol for the CT scanners (Siemens Definition Edge, AS, FLASH) were 4.3±2.0, 4.3±2.0 and 4.5±2.1,

respectively. Graphical representation of the data for each algorithm enabled identification of corresponding noise levels at decreasing effective mAs. For example, at an effective mAs of 100 (B40), the image noise level of 16.6 is similar to the noise of I40 strength 1 at 80 mAs or strength 3 at 42 mAs (Fig. 1).

Conclusions: Using measurements from an anthropomorphic body phantom, we demonstrated the consistency in noise reduction with iterative reconstruction on all three 128 slice scanners and how this can be potentially applied to clinical pediatric scanning protocols to achieve lower dose without compromising image quality.

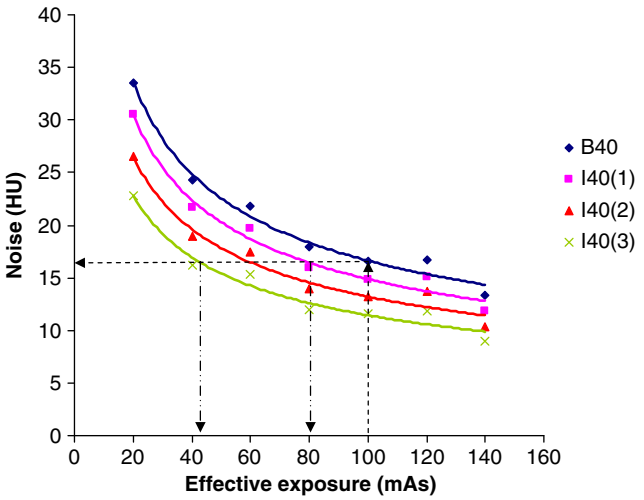

Figure 1. Plot of noise versus effective exposure using the Edge scanner with filter back projected (B40) and iterative reconstructed (I40) images for strengths 1, 2 and 3.

Paper #: PA-063

Chronic Recurrent Multifocal Osteomyelitis (CRMO) of mandible in the Pediatric Population: Spectrum of Imaging Findings with Clinicopathological Correlation

Rajan Patel, MD, *Department of Pediatric Radiology, Children's Medical Center, University of Texas Southwesten Medical Center, Dallas, TX, rajan_304@yahoo.com;* John McClay, Daniel Veltkamp, Timothy Booth, MD

Purpose or Case Report: CRMO has a predilection for involving the mandible and spine, can be unifocal in these regions. Diagnosis can be difficult; however, is critical to avoid multiple biopsies and unnecessary long term antibiotic therapy. The purpose of this study is to assess the potential diagnosis of CRMO in patients evaluated for radiological diagnosis of chronic osteomyelitis.

Methods & Materials: A retrospective search of PACS at Children's Medical Center, Dallas was performed using key words "chronic osteomyelitis" for a period of last 5 years. Cases with involvement of the mandible were included. The electronic medical records were reviewed for identifying age of patients, symptoms, laboratory tests, histopathology, treatment and follow up. On imaging, these cases were reviewed for their CT characteristics; including solid subperiosteal reaction, soft tissue involvement, associated fluid collection and dental involvement. Additional studies such as MR, skeletal survey and bone scan were reviewed if available.

Results: The PACS search revealed nine patients. Five cases satisfied imaging criteria with supporting clinical course and histopathological findings for a diagnosis of CRMO. Mean age at presentation was 9.5 years (range 3.5–12). Male:Female=4:1. All patients (n=5) were presented with mild pain and swelling. Three patients (n=3) had mild fever and mildly elevated sedimentation rate as well as C-reactive protein at presentation. CT findings demonstrated a mixed lytic sclerotic lesion involving the posterior half of the mandible with associated solid periosteal bone formation in all patients (n=5). Mild enlargement of the overlying masseter muscle was seen in three patients (n=3). No soft tissue abscess was seen. Three patients (n=3) had MRI, showing enhancement of the adjacent masseter muscle. Biopsy was performed in all cases (n=5) and revealed mild reactive inflammation and fibrosis in three patients (n=3). Remaining two patients (n=2) had negative biopsy result. One patient had skeletal survey and one patient had bone scan, neither revealed any additional lesion.

Conclusions: CRMO may be under-diagnosed and should be considered as an etiology when imaging findings suggest chronic osteomyelitis of the mandible. Radiologists can be the first to suggest this diagnosis given its characteristic radiological appearance and can prevent unnecessary repeated biopsies and prolonged antibiotic treatment. A trial of non-steroidal anti-inflammatory medication may be helpful in the appropriate clinical setting.

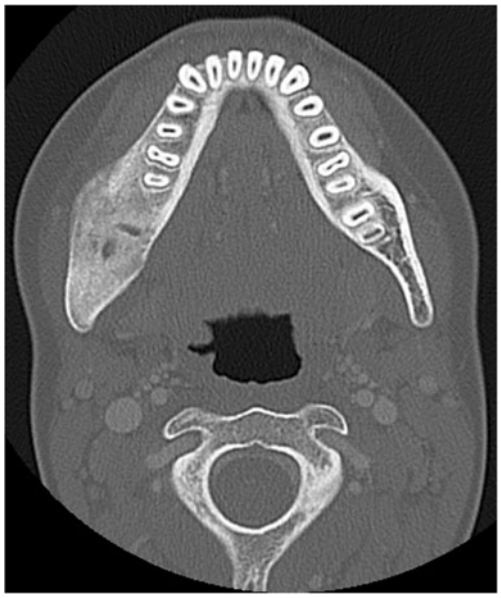

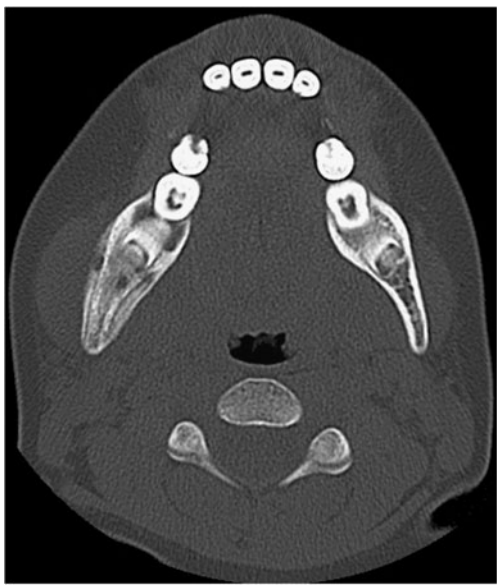

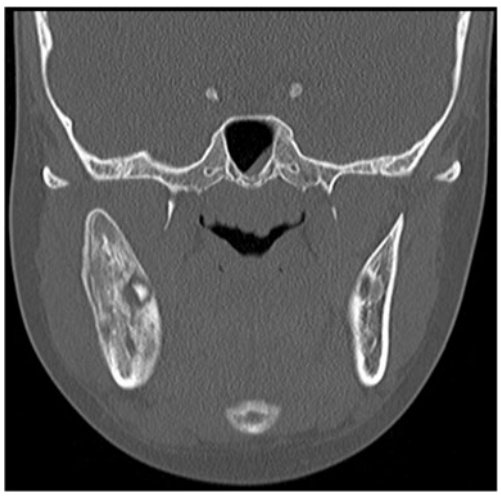

Paper #: PA-064

High resolution 3D T2 weighted imaging in the diagnosis of Labyrinthitis Ossificans: emphasis on subtle cochlear involvement

Timothy Booth, MD, *Children's Medical Center of Dallas, Dallas, TX, tim.booth@Children's.com;* Brandon Isaacson, Joe Kutz, Kenneth Lee, Peter Roland

Purpose or Case Report: Signal within the membranous labyrinth becomes low on T2 weighted imaging in the fibrous and ossifying stages of labyrinthitis ossificans (LO). The purpose of this study is to demonstrate the distribution and extent of involvement of the cochlea in children being evaluated for LO; using high resolution 3D T2 weighted imaging. One of the main objectives of this study was to evaluate subtle involvement of the scala tympani within the inferior basal turn of the cochlea.

Methods & Materials: A retrospective review from 2002 to 2012 was performed using a cochlear implant (CI) data base and PACS search. A PACS search function was used to access patients referred for or having imaging findings consistent with LO. Twenty-four patients were found to have MR findings consistent with LO (13 previously reported in Otolaryngol Head Neck Surg 2009; 140: 692). Axial 3D T2 weighted sequences were obtained in all patients and were reviewed for presence of abnormal decreased T2 signal within the scala tympani and vestibuli. Obstruction was graded; 1 - normal signal, 2 - abnormal signal in inferior basilar turn, 3 - involvement of ascending basal, middle and or apical turns, and 4 - near or complete obliteration of T2 signal. The medical record was reviewed for type of hearing loss, risk factors, and operative reports.

Results: Average age at imaging was 4.2 years. M:F ratio=5:1. 21/24 (88%) had bilateral SNHL and three had unilateral SNHL. The most common risk factor for LO was meningitis (19/24 (79%)). Seventeen patients had bacterial meningitis with pneumococcus the most common. Seven patients had other risk factors including; cholesteatoma, sickle cell, and ototoxic drug exposure. Average age of labyrinthitis was 1.2 year, time interval between insult and imaging was 2.2 year. 19/24 patients (79%) has CI. In a total of 48 ears, cochlear obstruction was documented in 40 (83%); 8 grade 1, 15 grade 2, 16 grade 3, 9 grade 4. In the patients with unilateral SNHL, no cochlear obstruction was shown in the normal hearing ears. Ears with grade 2 obstructions had disease limited to the scala tympani in all cases (Fig. 1). Asymmetric involvement of the cochlea was present in 11 patients.

Conclusions: Isolated involvement of the scala tympani within the inferior basal turn can be subtle and should be sought in all patients presenting for evaluation of SNHL. A history of meningitis is not always present in this group of patients. The extent of cochlear obstruction is important and may direct the side of implantation and type of electrode to be utilized.

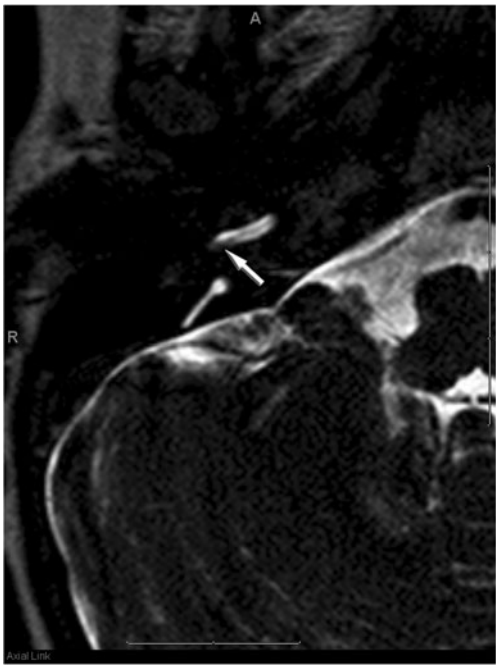

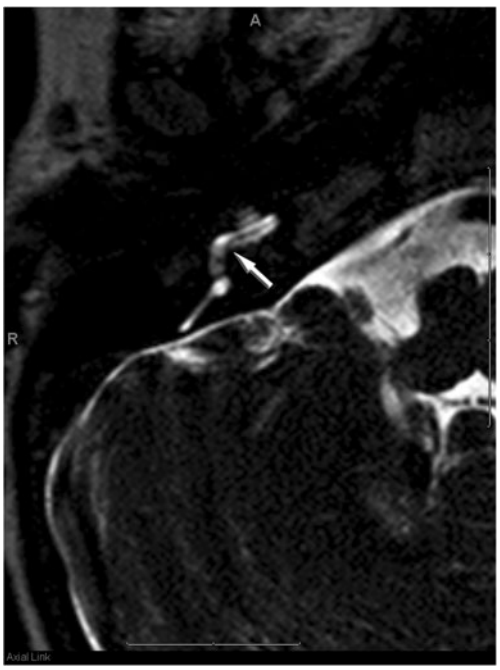

Paper #: PA-065

Brainstem Infarcts in Children: Imaging Features and Clinical Outcomes

Nancy Rollins, MD, *Children's Medical Center, Dallas, TX, nancy.rollins@Children's.com;* Lee Pride, Michael Dowling, Patricia Plumb

Purpose or Case Report: Brainstem infarcts in children differ from adults in terms of presentation, etiology, and outcome. We report a single institution series over 10 years.

Methods & Materials: An IRB-approved query of institutional database yielded 12 patients with brainstem infarcts from 2001 to 2012. Medical records were reviewed for presenting symptoms; assessment of stroke severity using the Pediatric NIH Stroke Scale (PedNIHSS); findings by MRI/A and catheter angiography; etiology, and outcomes using the Pediatric Stroke Outcome Measures (PSOM).

Results: There were 9 M/3 F; 9 mons-17 years. Six patients presented with involuntary rhythmic movements, four with hemiparesis, and three with altered mental status. MRI showed isolated pontine infarcts in three patients; and midbrain, pontomesencephalic, ponto-medullary in one each. Five had pontine infarcts with other posterior circulation infarcts; two had infarcts of different ages. MRA showed basilar artery (BA) occlusion in 5/9 patients without a vertebral artery (VA) dissection in 2; 1/5 had bilateral distal VA occlusion. Three patients had a VA dissection without BA thrombosis while MRA was normal in 2. Catheter angiography showed VA dissection in 4/9, hypoplasia of VA vertebral artery ipsilateral to a medullary infarct, and multiple peripheral posterior circulation emboli of unclear etiology in one patient each. Overall, five patients had VA dissection. Onset of symptoms was temporally related to sports in seven; most often football; five had no clear etiology. Management included initial early heparinization unless contraindicated, with conversion to long term anticoagulation or antiplatelet therapy based on results of vascular imaging, echocardiography, and coagulation profile; cardiac ECHO was normal in all patients. Maximum PedNIHSS ranged from 1 to 34 and was <10 in six patients; 10–20 in 2, and >20 in 4. NIHSS with BA occlusion ranged from 5 to 34; three patients progressed to locked-in state of which one died after withdrawal of support, one underwent successful clot extraction; and one survived. Of the 11 survivors, nine have been followed for >6 months; PSOM ranges from 0 to 4.5 on a scale of 1–10. In 8, PSOM is <2.5 and 6 are <1.0. The patient with the highest score also had sequellae of extreme prematurity

Conclusions: Prompt diagnosis of pediatric brainstem infarcts may be delayed by misleading symptoms and absence

of risk factors. Even with BA occlusion and high initial severity, outcome tends to be good with medical management

Paper #: PA-066

CT Angiography in a Transgenic Mouse Model of Cerebrovascular Disease

Ketan Ghaghada, *Radiology, Texas Children's Hospital, Houston, TX, kbghagha@texasChildren's.org;* Carlos Villamizar, Dianna Milewicz, Zbigniew Starosolski, Ananth Annapragada, PhD

Purpose or Case Report: It is now acknowledged that mutations in the smooth muscle-specific alpha-actin gene, ACTA2, lead to diffuse and diverse vascular diseases including Thoracic Aortic Aneurysms and Dissections (TAAD) and MoyaMoya disease (MMD). A transgenic mouse model expressing R258C (a mutation leading to 50% penetrance of either TAAD or MMD) has been engineered. Mice carrying the R258C transgene on a heterozygous background (Acta2+/− R258C TG) are stable, and following carotid ligation injury, show dramatic neointimal hyperplasia compared to heterozygous mice with no mutant transgene (Acta2+/−), and wild type mice. In this study, we used CT Imaging and a long circulating liposomal-iodinated blood pool contrast agent to investigate vascular anomalies in this genetically-engineered mouse model.

Methods & Materials: All in vivo procedures were approved by the Baylor College of Medicine IACUC. A novel liposomal CT contrast agent (~120 nm particle size, PEG surface coating, total iodine ~150 mg/ml, dose ~6 μL/g) was injected via tail vein into Test animals (Acta2+/− R258C TG) and controls (heterozygous and wild-type). CT angiography was performed using a small animal micro-CT scanner with the following scan parameters: 70 kVp, 500 uA, 850 ms exposure, 1440 projections. Ultra-high resolution images at 19 um isotropic voxel size were reconstructed. Diameter, tortuosity and vessel morphology were estimated for the carotids and intracranial vessels. Following imaging, the animals were sacrificed and their brains excised for histological evaluation.

Results: Excellent visualization of the neurovascular architecture, including the Circle of Willis (CoW), was demonstrated using the CTA technique. The Acta2+/−R258C TG mice exhibited highly variable cerebral vessel caliber compared to the control animals. Vessels in the The Circle of Willis in the Acta2+/−R258C TG mice showed significantly greater caliber variability when compared to control animals, and to the common carotid in any of the animals. Histological analysis of the brain tissue using a basal lamina (Collagen IV) stain confirmed the these vascular abnormalities. The characteristic contorted vasculature of Moyamoya disease was not visible, consistent with previous histological observations of this model.

Conclusions: CT angiography using a liposomal-iodinated contrast agent enabled non-invasive interrogation of vascular abnormalities in transgenic mouse model of Moya Moya disease.

Disclosure: Dr. Annapragada has indicated a relationship with Marval Biosciences as a Scientific Advisor and Stock Owner.

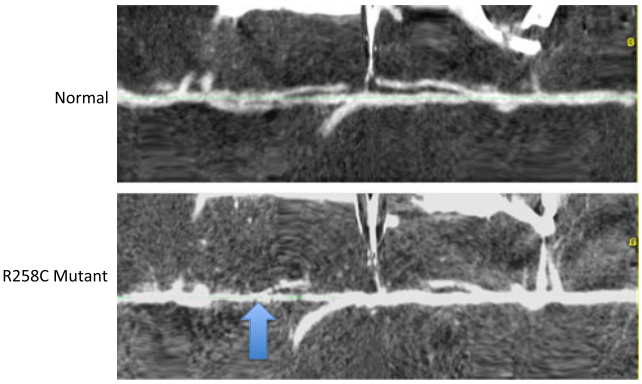

Paper #: PA-067

Increased Dural Venous Sinus Diameters in Pediatric Patients with Sickle Cell Disease: A Magnetic Resonance Venography (MRV) Study

Mariam Nawas, BA, *Children's Mercy Hospital-Pediatric Radiology, Kansas City, MO, mtn2m9@mail.umkc.edu;* Kalie Adler, Lisa Lowe, Simran Arora, Aaron Bonham, Ram Kalpatthi

Purpose or Case Report: By age 18, cerebral infarcts are evident on Magnetic Resonance Imaging (MRI) scans in one third of patients with Sickle Cell Disease (SCD). A recent study described increased cerebral blood flow transit time (CBFTT) on arterial spin-labeled perfusion MRI in SCD patients. If SCD patients are found to have abnormally large cranial venous drainage pathways, this could suggest a component of blood shunting through the brain that could contribute to an increased CBFTT and development of cognitive delay. The purpose of this study is to compare the diameters of dural venous sinuses in children with SCD with healthy controls, and to assess whether these results correlate with a history of cerebral infarct among SCD patients.

Methods & Materials: This is a retrospective review of MRVs, demographics, and past medical histories of children with SCD compared to controls. Imaging of the brain was performed with 1.5 T MR imaging with 2D time of flight venography. Dural sinuses were directly measured on MRV by an author who was blinded to presence or absence of SCD or history of cerebral infarct within the SCD group.

MRVs demonstrating stenosis or occlusion and patients with history of dural venous thrombosis were excluded. The target population includes all subjects with SCD who have undergone MRV between Dec 2004 - March 2011 and was identified using the PACS system. A control population from a similar timeframe was obtained. In order to determine whether there were any differences between SCD patients and controls, or among the SCD group, a series of one-way ANOVA's that controlled for age and sex as covariates were performed. A p-value of <0.05 determined significance.

Results: In total, there were 38 SCD patients and 38 control patients. SCD patients had significantly ($p<0.05$) larger dural venous sinus diameters than controls for all outcomes except the left internal jugular vein (IJV). The results of the comparisons are displayed in Table 1. Among SCD patients, the only outcome that differed between those with a history of stroke or silent infarct to those without was left IJV; those without a history had a 22% larger diameter ($p=0.043$).

Conclusions: Patients with SCD had larger dural venous sinus diameters than controls regardless of the former group's history of cerebral infarct. The reason for the anatomical difference of the sinuses is unknown; however, it may relate to blood shunting or the previously noted increased CBFTT in patients with SCD.

TABLE 1	Controls			SCD patients			% diff	p
Dural Sinus	n	Mean (mm)	SD	n	Mean (mm)	SD		
SSS pt. 1	38	7.0	1.3	38	8.9	1.4	27%	<0.001*
SSS pt. 2	38	6.1	1.2	38	7.3	1.4	20%	0.007*
ISS	23	1.7	0.4	23	2.5	0.3	47%	<0.001*
Straight	38	3.7	0.9	38	4.8	0.9	30%	0.001*
Galen	38	3.5	1.0	38	6.3	1.3	80%	<0.001*
R IC	38	1.9	0.4	38	2.3	0.3	21%	0.001*
L IC	38	1.9	0.4	38	2.3	0.3	21%	<0.001*
R Transverse	38	7.6	1.6	37	9.3	1.9	22%	0.003*
L Transverse	38	6.7	2.0	37	8.1	1.7	21%	0.004*
R Sigmoid	38	4.7	1.5	38	6.2	1.5	32%	0.003*
L Sigmoid	37	3.9	1.2	38	5.4	2.0	38%	<0.001*
R IJ	31	5.6	1.4	34	6.4	1.3	14%	0.015*
L IJ	28	4.7	1.4	34	5.4	1.3	–	0.105

*statistically significant ($p<0.05$)

SSS = superior sagittal sinus; ISS = inferior sagittal sinus; R IC = right internal cerebral vein; L IC = left internal cerebral vein; R IJ = right internal jugular vein; L IJ = left internal jugular vein; diff = difference

Paper #: PA-068

Corpus Callosum Thickness on MRI as a Surrogate Marker of Brain Volume in Children with HIV and its Correlation with Developmental Scores and Clinical Parameters

Savvas Andronikou, MBBCh, FCRad, FRCR, PhD, *Radiology, Faculty of Health Sciences, University of the Witwatersrand, Johannesburg, South Africa, DOCSAV@MWEB.CO.ZA*

Purpose or Case Report: To determine whether the overall and regional thickness of the CC may be used as a surrogate marker of brain volume in children with HIV and to correlate thickness with clinical and laboratory parameters.

Methods & Materials: Retrospective MRI analysis in children with HIV related neurology and controls. A custom tool divided the midline CC contour into 40 radial thickness segments and measured length.(see figure) Brain volume (total brain volume TBV; white matter volume WM; grey matter volume GM), was determined using MATLAB and Statistical Parametric Mapping software. Patients were compared to controls. Overall and segmental CC mean and maximum thickness as well as length was correlated against brain volume, Griffiths scoring tests, and laboratory tests.

Results: Thirty-three patients (16 m; 17 f) (mean 29; range 7–49 months) and 11controls (6 m 5 f) (mean 32; range 13–48 months) were evaluated. Overall and segmental CC

thickness was lower in patients than controls. TBV and WM volume was higher in patients.
Significant correlations:
Premotor CC (mean) with age [p=0.04]
Whole CC (mean) thickness with TBV [p<0.05]
Prefrontal CC (maximum) thickness and WM volume [p=0.02]
Premotor CC (mean) with TBV [p=0.04]; and with WM volume [p=0.02].
Premotor (maximum) and WM volume [p=0.03]
Sensory CC (mean) and TBV [p=0.02]
Motor CC (maximum) and general development score [p=0.02]
CC length with microcephaly [p=0.007] and with CD4 [p=0.04]
Conclusions: CC thickness decreases in HIV infected children and reflects brain volume through mean CC or segmental measurement at the prefrontal, premotor or sensory segments. The correlation of prefrontal and premotor maximum CC thickness with WM volume suggests that a clinical rule of thumb limit can be determined for thickness at these areas. Additional a clinical relevance limit can be inferred from the association of maximum motor CC thickness with general developmental score. Microcephaly and CD4 level of immunity is reflected by CC length.
The increase in brain volume of HIV patients however must be explained, as it is contrary to expectations.

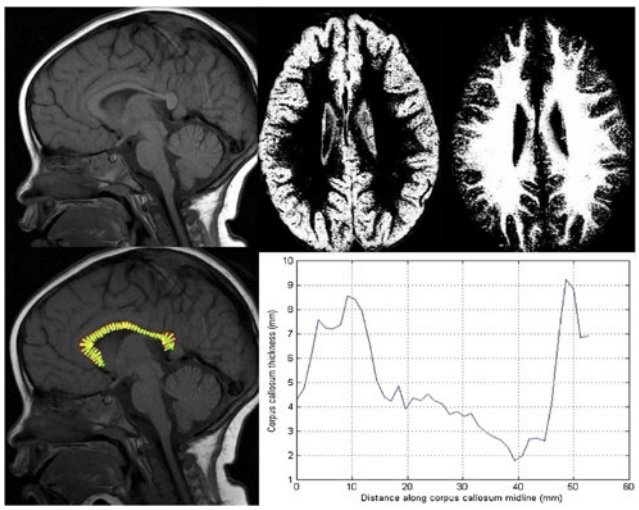

Paper #: PA-069

Does Diffusion Weighted Imaging Improve the Accuracy of Preoperative Diagnosis of Common Pediatric Cerebellar Tumors?
Korgun Koral, *Radiology, University of Texas Southwestern Medical Center and Children's Medical Center, Dallas, TX, korgun.koral@utsouthwestern.edu;* Nabila Choudhury, William Moore, Michael Seymour, Benjamin Garvey, Matthew Fiesta
Purpose or Case Report: To evaluate the impact of diffusion weighted imaging (DWI) on the preoperative diagnosis of common pediatric cerebellar tumors.
Methods & Materials: Review of neuro-oncology database yielded 96 patients (60 M) whose preoperative brain MRI included a DWI (diffusion weighted imaging) sequence - obtained with a b value of 1,000 s/mm2 - and an apparent diffusion coefficient (ADC) map. There were 38 pilocytic astrocytomas (PAs), 33 medulloblastomas, 17 ependymomas, and 8 atypical teratoid/rhabdoid tumors (AT/RTs). Six reviewers (4 third year radiology residents each with 32 months of residency training at the time of the study and two board certified radiologists with certificates of additional qualification in neuroradiology (with 3 and 8 years of post-fellowship experience) evaluated the examinations. None of the reviewers had seen the examinations previously. The studies were de-identified and randomly presented to the reviewers at PACS workstations. Two sessions (1–13 days apart) were conducted with each reviewer. On day 1, preoperative brain MRI studies without DWI data and on day 2 preoperative brain MRI studies including the DWI data were evaluated. Correct diagnoses were not revealed to the reviewers following completion of the sessions.
Results: There was no significant difference between the performances of the radiology residents and the neuroradiologists (p=0.80). There was a significant difference in the correct diagnoses made without and with the DWI data (p=0.02). The likelihood of rendering a correct diagnosis using the DWI data was 2.04 times (0.71–2.45, 95% confidence interval) greater than without the DWI data. The performances of the 5 out of 6 reviewers improved significantly with the addition of the DWI data (p=0.0003–0.0233). The performance of the remaining reviewer (a resident) also improved, but the difference did not attain statistical significance (p=0.1944)
Conclusions: DWI significantly improves the accuracy of reviewers with differing experience levels for diagnosing common pediatric cerebellar tumors preoperatively.

Paper #: PA-070

Prospective Evaluation of Pediatric VCUG at an Academic Children's Hospital: Is the Scout Image Necessary?
Jason Domina, MD, *Radiology, University of Michigan, Ann Arbor, MI, dominaj@med.umich.edu;* Ramon Sanchez, Maria Ladino-Torres, Indu Meesa
Purpose or Case Report: To comprehensively evaluate pediatric voiding cystourethrography (VCUG) at an academic children's hospital, with particular attention paid

to both scout image and total exam radiation dose estimates.

Methods & Materials: One hundred eighty-one pediatric (≤ 18 years-old) patients undergoing VCUG were prospectively evaluated during the first 6 months of the 2012 calendar year. There were 121 female and 60 male patients, with age breakdown into groups as follows: 0 years (56 patients), 1–5 years (66 patients), 6–10 years (43 patients), and 11–18 years (16 patients), with a mean patient age of 4.0 years. Of the 181 exams, 166 were performed on outpatients and 15 on inpatients. Regarding each patient's VCUG exam, patient demographics, exam clinical indication(s), scout image and total exam radiation dose estimates (measured in terms of dose-area product (DAP)), findings derived from the scout image, and overall exam findings/impression were evaluated.

Results: Vesicoureteral reflux (VUR) and urinary tract infection (UTI) were the most common clinical indications, mentioned in 40.9% and 37.0% of exams, respectively, while evaluation of a known or suspected genitourinary anatomic abnormality and hydronephrosis were each mentioned in 13.8% of exams. For the 181 patient cohort, total fluoroscopy time per study averaged 0.61 min, with the averages ranging from 0.58 to 0.66 min for all four age groups. In terms of DAP, the scout image dose accounted for an average of 68.1% of total exam dose, with the averages ranging from 66.5% to 71.7% for all four age groups. The scout image was reported as normal/unremarkable in 52.5% of studies. For the other 47.5%, findings regarding catheter location, bowel gas pattern, and/or osseous findings were mentioned; however, the vast majority of these findings were known from prior imaging or deemed to be of no clinical significance. The exam impression was considered normal in 44.2% of cases, while VUR was present in 41.4% of studies and an anatomic abnormality of the urinary tract present in 18.8%.

Conclusions: The VCUG scout image accounted for an average of 68.1% of total study DAP, while often providing minimal new or clinically relevant information. We feel that the scout image can likely be omitted if the patient has a prior abdominal radiograph, or alternatively a digital fluoroscopic image capture of the abdomen could be performed if necessary. These efforts would substantially reduce the radiation dose received from VCUG in pediatric patients.

Paper #: PA-071

Comparison of Quality of Voiding Cystourethrogram (VCUG) reports

Shreya Sood, MD, *Brigham and Women's, Boston, MA, ssood1@partners.org;* Caleb Nelson, Anthony Schaeffer, Ilina Rosoklija, Jeanne Chow

Purpose or Case Report: To compare the quality of VCUG reports across various groups, focusing on reports generated by board-certified pediatric radiologists to those generated by non-pediatric radiologists.

Methods & Materials: The study included patients evaluated for reflux in a pediatric urology clinic between 11/1/07–5/2/12 who had prior VCUG studies performed at various healthcare facilities. Outside VCUG reports were matched in a 1:2 ratio by age, gender, indication for procedure and presence of reflux to studies performed in a pediatric radiology department during the same time interval. A 26-item quality assessment tool was used to compare the two groups. The variables included demographic information (e.g. age), indication for study (e.g. pyelonephritis), technical data (e.g. radiation dose), anatomic findings (e.g. reflux grade), and functional information (e.g. bladder capacity). A report was defined as 'complete' if at least two-thirds of the parameters were included. Reports were compared based on whether they were generated by pediatric versus non-pediatric radiologists, created in facilities with a pediatric radiology department versus those without, or in academic versus non-academic settings.

Results: A total of 456 reports, 152 outside and 304 internal were included; 359 of which were generated by pediatric radiologists and 84 by non-pediatric radiologists. Reports generated by pediatric radiologists were more complete than those generated by non-pediatric radiologists: 73% vs. 2%, ($p<0.0001$). Reports from facilities with pediatric radiology departments were more complete than facilities without: 65% vs. 2%, ($p<0.0001$) and reports from academic hospitals were more complete than those from non-academic institutes: 74% vs. 3% ($p<0.0001$).

Conclusions: VCUG reports generated by pediatric radiologists are more complete, and thus higher in quality than those by non-pediatric radiologists. These findings suggest added benefit for both the patient and the healthcare provider to have VCUG studies performed and interpreted by pediatric radiologists. When such facilities are unavailable, dedicated pediatric radiology departments or academic hospitals may offer higher quality reports than those without.

Paper #: PA-072

CT cystography in detecting perforated reconstructed bladders

Sandeep Gurram, *Indiana University School Of Medicine, Indianapolis, IN, gurrams@indiana.edu;* Daniel Sova, Martin Kaefer, Boaz Karmazyn, MD

Purpose or Case Report: Perforation of reconstructed bladders (RB) is potentially a life-threatening complication. We

wanted to know the accuracy of CT cystography (CTc) in diagnosis of bladder perforation (BP).

Methods & Materials: A 9 year (1/2003 to 12/2011) retrospective study was performed. From the radiology information system we retrieved all patients with CT cystography. Only patients with RB were included. Medical records were reviewed for underlying diseases, type of bladder reconstructive surgery, symptoms and clinical findings. CTc was evaluated for presence of extraluminal contrast. The results of the CTs were compared to surgery, cystoscopy and clinical follow-up.

Results: The study group included 89 patients (48 males, age range of 4 to 18 years, average 11.5 years) who had 125 CTc (23 patients had more than one study). Abdominal pain was the most common indication (n=83; 93%) for the CTc. CTc diagnosed all of BPs in 14 (11%) patients, three (20%) of them had recurrent perforation. Overall 19 CTc demonstrated bladder perforation. Most (n=12; 86%) patients with BP had augmented bladder and the most common underlying etiologies included myelomeningocele (n=8; 57%), and bladder exstrophy (n=3; 21%). There was no case of false positive CTc.

Eight (57%) patients with BP reported decreased urine output. Only two (14%) patients presented with peritoneal signs. Only two (14%) patients had fever (>38.50 C) and six (43%) patients had leukocytosis (>12,000 cell/mL).

Conclusions: CT cystography is an accurate imaging for diagnosis of BP and should be considered in patients with reconstructed balder who present with abdominal pain. Clinical diagnosis of BP could be challenging as a third of the patients do not report a decrease of urine output, and most of them do not have peritoneal or systemic signs.

Paper #: PA-073

Diffusion Tensor Imaging (DTI) and Tractography of the Kidney in Children: Feasibility and Preliminary Experience

Camilo Jaimes, MD, *Radiology, The Children's Hospital of Philadelphia, Philadelphia, PA, camilojaimes12@gmail.com;* Kassa Darge, MD, PhD, D'mitry Khrichenko, Robert Carson, Jeffrey Berman, PhD

Purpose or Case Report: To evaluate the feasibility and utility of quantitatively assessing pediatric kidney structure with MR diffusion tensor imaging (DTI) and fiber tracking in the setting of functional MR Urography (MRU).

Methods & Materials: Nine children (6 boys, 3 girls) with a mean age of 4.3 years (0.5–14.8 years) were prospectively enrolled. All subjects were scanned at 3.0 T and DTI was acquired with an echo-planar sequence (TR/TE= 2300/69 msec), b=300 s/mm2, 12 non-collinear gradient directions, and three signal averages. All subjects had contrast-enhanced functional MRU. Fiber tracking was performed using a deterministic streamline tracking algorithm with a fractional anisotropy (FA) threshold of 0.1 and an angle threshold of 55°. Tractography was launched from a region of interest (ROI) placed within the entire renal parenchyma. Diffusion metrics were measured in ROIs drawn in the medulla and cortex. For analysis, the left and right kidneys as well as each moiety of a duplicated kidney was considered as a separate unit. MRU results were used to group the kidneys as normal or abnormal (presence of dilatation or abnormal function).

Results: A total of 19 renal units (kidneys/moieties) were analyzed (1=agenesis; 2=unilateral duplicated kidneys) with 13 normal and 6 abnormal units. In abnormal moieties there was insufficient corticomedullary differentiation to place separate ROIs. Fiber tracking of normal renal units showed numerous tracts with a radial arrangement and convergence into pyramids. Abnormal ones did not show these features and had tracts that were loosely arranged and left hollow spaces. Fiber track volume correlated with MRU parenchymal volume (normal: r2=0.93, p<0.01; abnormal: r2=0.93, p<0.05). Subject age also correlated with the fiber track volume (normal: r2=0.96, p<0.01; abnormal: r2=0.8, p< 0.01). In normal kidneys/moieties, the medulla had higher FA (0.401 +/−0.05) than the cortex (0.183 +/− 0.03) (p< 0.01); FA in these regions did not significantly change with age (cortex: r2=0.037, p>0.1; medulla: r2=0.018, p>0.1). There were no observed differences in ADC between the cortex and medulla (p>0.05). We observed a trend of increasing ADC with age in the cortex and medulla (cortex: r2=0.21, p>0.1; medulla: r2=0.135, p>0.1).

Conclusions: Renal DTI with tractography is feasible in children and may be combined with MRU. DTI and tractography provide additional information on tissue microstructure and architecture that is not demonstrated on conventional MRI sequences.

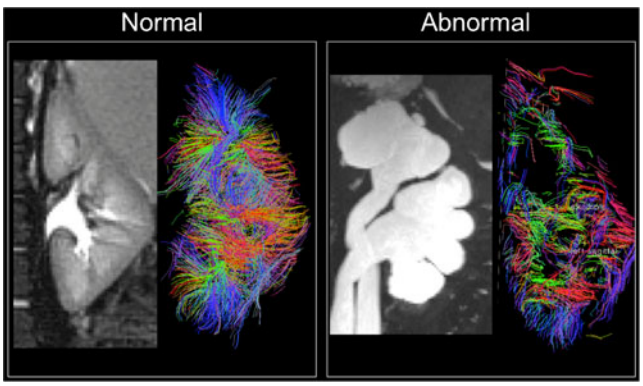

Paper #: PA-074

Low fat milk as low attenuation oral contrast agent for abdominal MDCT in children and teenagers

María Elena Ucar, *La Plata Children's Hospital, La Plata, Argentina, pepaucar@hotmail.com;* Celia Ferrari, Osvaldo Ibañez, Marcela Gatti, Cecilia Ripoll, Mariana Bepre

Purpose or Case Report: The aim of this presentation is to report the results obtained by using low attenuation oral contrast agent (low fat milk, 2%) to perform abdominal MDCT in children and teenagers.

Methods & Materials: From September 2011 to August 2012, low fat milk was administered as oral contrast to 37 patients who had to undergo abdominal MDCT with intravenous contrast agent ; in 29 cases the MDCT was a follow up study for oncology disease, and the remaining nine patients had other pathologies. The age range was 2–22 years old, 23 female and 14 males.

The oral contrast was ingested in a biphasic model and the volume was variable according to the age and weight of the patients (150–1000 ml).

The studies were reviewed by three pediatric radiologists, who analyzed: a) tolerance of patients (vomiting and discomfort), b) agreement of parents, c) duodenal-pancreatic area discrimination, stomach and intestinal wall characteristics, level reached by oral contrast, differentiation of bowel loop (jejunum-ileum and colon), artifacts and difficulties in interpretation.

Results: The low fat milk was well tolerated; no patient refused to drink the milk or present any vomiting; all parents agreed. There was interobserver agreement in 29 cases (78%). The wall of the stomach was well delimitated in 100% of the cases; discrimination of the duodenal-pancreatic area was possible in 35 cases (94%); in two cases with external artifacts the discrimination was not confident. Small bowel loops were well identified in 30 patients (81%). Discrimination between small bowel loops and colon was achieved in 36 cases (97%) based on the morphology and content of the guts, and only in one case by the presence of oral contrast agent in colon. In only one patient the level reached by the milk was the duodenum (low volume ingested), in another patient with pancreatitis, the low density contrast complicated the diagnosis of peripancreatic collection.

Conclusions: Low fat milk is a cheap alternative as low attenuation oral contrast agent to perform abdominal MDCT, and it is well tolerated by pediatric patients. The negative oral contrast agent facilitates an accurate and confident visualization of the gastrointestinal wall and discrimination of the duodenum-pancreatic area; but it should be avoided when intraperitoneal collections are suspected.

Paper #: PA-075

Can the choice of nomogram used to interpret sonographic renal measurements in children with myelomeningocele affect clinical management?

Ashley Caleel, DO, *Department of Medical Imaging, Ann & Robert H. Lurie Children's Hospital of Chicago, Chicago, IL, ashleycaleel@gmail.com;* Jennifer Nicholas

Purpose or Case Report: Several nomograms have been developed to evaluate sonographic kidney measurements in healthy children: Rosenbaum (1984), Babcock (1985), and Kadioglu (2010). At our institution, the Babcock nomogram is used to evaluate kidney lengths in all children, and measurements in patients with myelomeningocele (MM) often fall below the range of normal. Small kidney size and lack of kidney growth are used by pediatric urologists as markers of potential underlying renal disease, and length reported as below normal often prompts additional investigation. Acknowledging that kidney lengths in MM patients can be influenced by factors other than underlying kidney disease, Sutherland developed a renal length nomogram specifically for children with MM, with the hope of more accurately tracking renal length and growth in this patient population. The purpose of this study is to determine how often kidney lengths in children with MM are interpreted more favorably using the Sutherland nomogram, potentially influencing clinical management.

Methods & Materials: After IRB approval, we retrospectively reviewed serial renal ultrasounds performed for 20 children with MM who were scanned in our department between 1/1/1995 and 8/31/2012. At the time of their exams, the patients ranged in age from 1 to 18 years with an average of 7.5 scans per child (range: 4–11 scans). A total of 293 kidney lengths (147 right and 146 left) were plotted on the Babcock, Sutherland, and Rosenbaum nomograms. Kidney lengths plotted on the Sutherland nomogram that were closer to normal by at least one standard deviation when compared to the other nomograms were recorded as significant.

Results: When compared to the Babcock nomogram, kidney lengths in children with MM plotted on the Sutherland nomogram were interpreted as closer to normal by one standard deviation 22% of the time. When compared to the Rosenbaum nomogram, renal lengths plotted on the Sutherland nomogram were closer to normal by one standard deviation 58% of the time and by two or more standard deviations 8% of the time. Initial discussions with our pediatric urology colleagues indicate that the more favorable reports of kidney length may have prevented further clinical investigation.

Conclusions: Using the Sutherland nomogram to interpret and track kidney length in children with MM would produce more favorable results than using nomograms developed for

children without MM, likely positively influencing their clinical management.

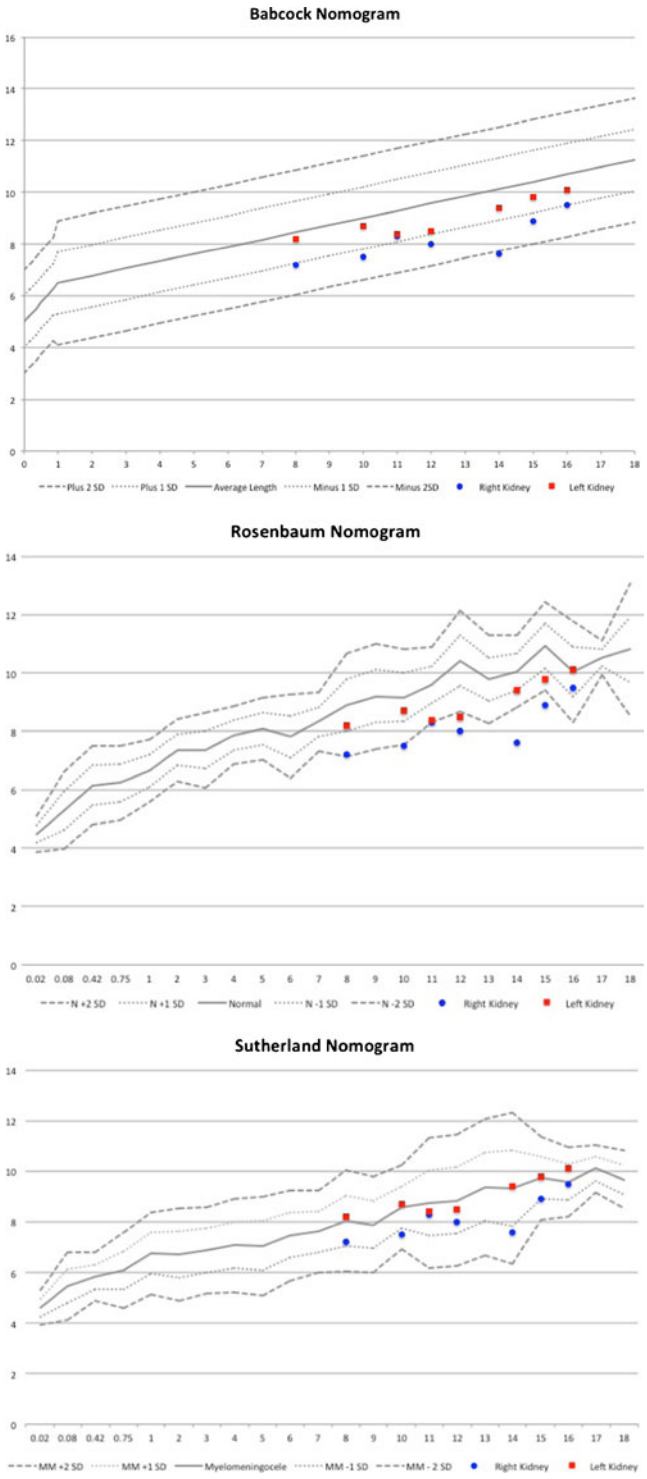

Figure 1: Sonographic renal length measurements were plotted for a child over seven exams on the Babcock, Rosenbaum, and Sutherland nomograms (above left, above right, and left, respectively).

Note the more favorable interpretation of the kidney lengths on the Sutherland nomogram, particularly the fifth measurement for the right kidney (blue circle) which fell more than two standard deviations below normal on the Babcock and Rosenbaum nomograms, but just more than one standard deviation below normal on the Sutherland nomogram.

Paper #: PA-076

Pediatric solitary renal cysts found on ultrasound – what is the risk of malignancy?

Alex Tawadros, *Indiana University School of Medicine, Indianapolis, IN, atawadro@iupui.edu;* Lisa Delaney, Rong Fan, Martin Kaefer, Boaz Karmazyn, MD

Purpose or Case Report: There are no guidelines on imaging and diagnostic workup of solitary renal cysts in children. We wanted to correlate ultrasound (US) characteristics of solitary renal cysts that had been evaluated with other imaging, surgery or pathology with definitive diagnoses to evaluate the risk of malignant cystic tumor.

Methods & Materials: From the radiology information system, we retrieved all ultrasound reports with diagnosis of a solitary renal cyst from 2003 to 2011. Medical charts were reviewed for demographic information, indication for the study, and other genitourinary and medical diagnoses. The renal cyst US characteristics were evaluated including shape, size, wall thickness, increased through transmission, and presence of septations, debris, and calcifications. If follow-up was performed, further imaging was characterized for change in the cyst's size and complexity.

Results: Two hundred ninety-three patients were diagnosed with solitary renal cysts. Only 23 (8%) patients (12 boys, age range 1 day to 17 years, 6 months, average 8 years) had definitive diagnosis of the renal cyst. The most common indications for the US were urinary tract infections (n=4) and ureteropelvic junction obstruction (n=4).

The diagnosis of caliceal diverticulum (n=13) was based on connection of the cyst with the collecting system. Other cysts (n=10) were diagnosed based on pathology: benign renal cysts (n=5), cystic renal dysplasia (n=3), and and multilocular cystic nephroma (MLCN, n=1). A nonrotated kidney with an extrarenal pelvis presented as a renal cyst mimic. There was no case of malignant tumor.

The cysts ranged from 0.5 to 11.2 cm (mean 2.7 cm). On US, 12 cases (52%) demonstrated complex elements. Only the MLCN had thickened septa and internal Doppler flow. 12 cases (52%) had followup imaging. Of these, three cysts increased in size (25%), two increased in complexity (17%), three increased in size and complexity (25%), and one increased in size and then decreased in size (8%).

Conclusions: Most solitary renal cysts will be followed by ultrasound and few will be definitively diagnosed by other imaging or biopsy. Only 8% of our patients' imaging and pathology resulted in a definitive diagnosis. All cysts were benign (the most common was caliceal diverticulum), and only one premalignant condition was seen (MLCN with typical US findings).

Paper #: PA-077

CT-guided localization of pulmonary nodules in pediatric oncology patients prior to Video-assisted thoracoscopic surgery (VATS) resection

Janice McDaniel, MD, *Radiology, Cincinnati Children's Hospital Medical Center, Cincinnati, OH, janicemcdanielmd@gmail.com;* Kamlesh Kukreja, Neil Johnson, Manish Patel, John Racadio, MD

Purpose or Case Report: Pulmonary nodules in pediatric oncology patients propose a management dilemma as these could represent metastatic disease or a benign process, often requiring tissue diagnosis. Some of the smaller sub-pleural nodules may not be visualized or palpated during Video-assisted thoracoscopic surgery (VATS), the preferred surgical technique over open thoracotomy for peripheral nodule resection. We present our experience at a large children's hospital using CT-guided pre-operative localization of pulmonary nodules.

Methods & Materials: After IRB approval, imaging and clinical database identified 35 pediatric oncology patients, who underwent pre-operative, CT-guided lung nodule localization for 40 nodules over a 15 year period (7/1999 to 1/2012). We performed a retrospective chart review to determine nodule size, localization technique, technical success and complications of our procedures. Corresponding surgical and pathology findings were also reviewed.

Results: Mean patient age was 12 years, (range: 8 months - 23 years) with 20 males (57%) and 15 females (43%). Patients had a variety of primary malignancies, most common being osteosarcoma (6), Ewing's sarcoma (5), hepatoblastoma (3), rhabdomyosarcoma (3), and synovial cell sarcoma (3). The nodules ranged in size from 1.4 mm to 15 mm (average: 4.3 mm). Of the 40 nodules, localization was performed by using Kopans biopsy wire in 12, methylene blue blood patch in 4, and both techniques were utilized in 24. All nodules were successfully localizes with CT-guidance. Three of 36 procedures that employed needle localization demonstrated pneumothorax (8%), which did not affect VATS localization. In 6 of the 36 nodule, the wire was dislodged (17%), however five of the nodules were localized by concomitant methylene blue injection while one was localized by the pulmonary hemorrhage at the site of wire insertion, thereby not affecting the localization procedure. There were no complications seen with the four nodules localized by methylene blue blood patch alone. A pathologic diagnosis was determined in 100% of nodules, with 8 of the 40 nodules showing metastatic disease (20%). The remaining nodules consisted of a variety of one or more benign etiologies, such as an inflammatory process (8), granuloma (6), normal lymph nodes (5), etc.

Conclusions: CT-guided lung nodule localization prior to VATS resection is safe, technically feasible, and highly successful in pediatric oncologic patients. In our experience, methylene blue blood patch is the most successful technique.

Paper #: PA-078

Treatment of Chylous Effusions in Children Using Thoracic Duct Embolization (TDE)

Adeka McIntosh, MD, *Children's Hospital of Philadelphia, Philadelphia, PA, adeka_mcintosh@yahoo.com;* Marc Keller, MD, Naim Maryam, Ganesh Krishnamurthy, Bird Geoffrey, Maxim Itkin

Purpose or Case Report: To desccribe our experience using diagnostic lymphangiography (LAG) and percutaneous TDE in children with persistent chylous effusions.

Methods & Materials: A retrospective review of 19 patients was conducted to assess technical and clinical success of the TDE for treatment of chylous effusion in children.

Initially pedal or intranodal LAG was performed to define thoracic duct (TD) anatomy and location of TD leak or occlusion. The TD was then accessed percutaneously in the upper abdomen and catheterized using a microcatheter. Injection of the TD was then performed to define the cause of the chylous leak. If indicated embolization of the TD was performed with glue and/or coils. Intravenous antibiotics were administered before the procedure.

Results: Twenty-two procedures in 18 children (11 male, 7 female) were performed. Average age was 1.9 years. Twelve patients had prior surgery, five had idiopathic chylothorax, and one had non-accidental blunt trauma. One patient presented with chylopericardium, 15 with chylothorax, and two with combination of chylothorax and chylopericardium. Average chylous drainage was 377 mL/day. Seven patients had previous attempted surgical ligation of the duct.

Ten intranodal LAGs were performed, 11 LAGs were done via cutdown, and one cutdown attempt was unsuccessful (95.5% success). The thoracic duct was successfully accessed and embolized in 13 cases. In one the duct was cannulated but not embolized due to a patent duct with no detectable leak. The thoracic duct could not be cannulated in seven cases (6 disruptions performed), and one procedure was only a diagnostic LAG.

Effusions resolved on average in 15 days in 13/18 patients (16 procedures) (72.2% success). In two of these patients TDE was performed twice.
6/18 patients continued with persistent effusions. Three of these had TDE, three could not be cannulated (2 had unsuccessful ductal disruptions, one had poor opacification of the TD, resulting in unsuccessful access).
Conclusions: TDE is a safe, effective alternative to surgical ligation of the thoracic duct in children with persistent large volume chylous chest effusions. Additionally, this procedure may be repeated for persistent leakage or performed after initial surgery fails to stop effusions.

Paper #: PA-079

Characterization of Central Conducting Lymphatic Anomalies

Robert Clemens, MD, *Interventional Radiology, Boston Children's Hospital, Boston, MA, robert.clemens@Children's.harvard.edu;* Tamara Kreindel, Anna Lillis, Ahmad Alomari

Purpose or Case Report: The central conducting lymphatic channels receive lymph return from the body and GI tract. Dysfunction leads to reflux and chylous leakage disorders. The purpose of this report is the characterization of central conducting lymphatic anomalies.
Methods & Materials: The medical records and imaging studies of patients with central conducting lymphatic anomalies were reviewed. Patients were divided in two major anatomical groups: thoracic and pelviabdominal.
Results: There were 41 patients (m=26, f=15) with an age range of 5 months to 52 years (mean=12.7 years). MR imaging was available for 32 patients and CT scans in 30. Clinical presentation varied depending on the anatomical involvement, including chylous pleural effusion (n=20), chylous ascites (n=17) and pericardial effusion (n=4). Abdominal involvement was found in 32 patients. Thoracic involvement was found in 32 patients, including lung involvement (n=14). One patient with lung involvement died of pulmonary failure. 32 patients had an involvement of both thoracic and pelviabdominal regions and only nine patients had a single region involved. Bone (n=11) and skin involvement (n=19) was also common. In addition to the chyle collections, typical imaging features include perivascular and peribronchial soft tissue thickening with loss of perivascular fat rim.
Conclusions: Central conducting lymphatic anomalies are characterized by chylous leakage from dysfunctional channels that are localized in the perivascular and peribronchial spaces. Combined clinical and imaging features may obviate the need for biopsy to establish the diagnosis.

Paper #: PA-080

Sclerotherapy of foot venous malformations: A 6-year single center experience

Jorge Delgado, *Children's Hospital of Philadelphia - Radiology, Philadelphia, PA, delgadoj@email.chop.edu;* David Low, Anne Marie Cahill

Purpose or Case Report: To evaluate a single institutional experience with percutaneous sclerotherapy of foot venous malformations (VM).
Methods & Materials: A 6-year retrospective descriptive review with IRB approval was performed of 16 patients (10 f, 6 m), mean age 14.67 years (range 6.07–27.8 years) that underwent 34 procedures for plantar (n=26) or dorsal foot (n=8) VM. Imaging and clinical records were reviewed. Sodium Tetradecyl foam was used in 33 procedures, mean dose of 9.53 ml (range 1–20 ml). One procedure was not performed due to deep venous flow from the VM. Double reader consensus was used to classify the VM's according to the Puig classification (Type 1–4) and to categorize imaging response to treatment comparing pre-treatment images to last follow-up image using a score for thrombosis volume: 1 (100–76%), 2 (75–51%), 3 (50–26%) and 4 (25–0%). VM to skin distance was measured on coronal C-arm CT. Spearman coefficient was use to seek correlation between skin to VM distance and complications.
Results: Technical success was 33/34 (97%). The mean number of sclerotherapy procedures/patient was 2.12 (range 1–5). VM classification was: Type 1 (1 patient), Type 2 (11) and Type 3 (4). The median fluoroscopic time was 5.3 min (range 2–10.3) and the median dose/area product was 32 microGy/m2 (range 1.4–411.4). Intra-procedural fluoroscopic and US images were obtained in all cases and C-arm CT in 19/33 (57.6%) cases. Clinical follow-up was available in 13/16 (81%) patients, median time 300 days (range 16–1545 days). Symptomatic improvement was seen in 24/29 (82%) of procedures. Complications: Intra-procedural blanching in 1/33 (3%), skin ulceration in 4 /29 (14%) and blistering 2/29 (7%). Mild post procedure pain was reported by 15/29 cases (51.7%) and moderate pain in 5/29 cases (17%). Follow-up US imaging post final procedure was available in 12/16 patients (75%). Thrombosis scores were as follows; 1 in 10 patients, 2 in 1 patient and 3 in 1 patient. All patients with imaging response scores 2–3 were classified with the Puig venous scale as Type 3.

VM to skin distance mean was 3.9 mm (range 0.5–12.9 mm). Shorter skin-VM distance was significantly correlated with a higher rate of skin complications ($p=0.027$).
Conclusions: Percutaneous sclerotherapy is an effective method to control symptoms in foot venous malformations. These lesions are especially challenging to treat due to the superficial nature, venous drainage and constant external pressure. VM to skin distance and skin complication are significantly correlated.

Paper #: PA-081

Catheter Directed and Mechanical Thrombolysis for Management of Lower Extremity Iliofemoral Deep Venous Thrombosis: a Single Pediatric Institutional Experience
Marian Gaballah, *Children's Hospital of Philadelphia, Philadelphia, PA, gaballma@umdnj.edu;* Chrystal Obi, Jillian Sola, Leslie Raffini, Marc Keller, MD, Anne Marie Cahill
Purpose or Case Report: The purpose of this study is to evaluate a single pediatric institutional experience with catheter directed (CDT) and mechanical thrombolysis (MT) for lower extremity iliofemoral DVT
Methods & Materials: A retrospective review was performed of 33 limbs (5 bilateral) in 28 patients, mean age 15.8 years (range 6.7–23.7) with lower extremity iliofemoral DVT treated over a 7-year period. Treatment consisted of either CDT alone or CDT in combination with MT. DVT diagnosis was performed with ultrasound in all patients. Two-reader consensus review of pre- and post-procedure venography was performed, and degree of patency was translated into a thrombus score for a total of seven venous segments. The lysis grade was calculated by comparing total segment thrombus scores. Post treatment venography was also evaluated for residual venous stenosis. The Modified Villalta scale was applied retrospectively to assess for Post-Thrombotic Syndrome (PTS).
Results: Technical success for 33 limbs was 32/33 (97%). The techniques used included; CDT with MT (19/33), CDT alone (14/33 limbs) and CDT with pharmacomechanical thrombolysis (5/33), angioplasty (27/33), and stent placement at time of thrombolysis (3/33). Mean thrombolysis duration was 46.9 h (range of 15.7–89.6). Mean duration of total therapy, including angioplasty was 51.6 h (range of 15.7–90.4). Post-therapeutic lysis grade was stage 4 (100% lysis) in 2/33, stage 3 (75–99%) in 18/33, stage 2 (50–74%) in 11/33 and stage 1 (<50%) in 2/33.
Residual venous stenosis was as follows: 0% (14), 1–25% (9), 26–50% (8), 51–75% (2), and 76–100% (0). Congenital venous abnormalities included May-Thurner Syndrome (13/28) and IVC anomaly (4/28).
Average time from completion of thrombolytic therapy to the most recent clinic follow-up was 26.8 months (range of 2.6–85.4). PTS Villalta scores at clinical follow-up were: 0 in 18/33 (55%) limbs, 1–2 (mild) in 14/33 (42%), and one patient was lost to follow-up. Thrombophilia screening was positive in 16/28 patients.
Conclusions: CDT and MT appear to be effective in treating extensive lower extremity DVT in children and young adults and may reduce the risk of developing PTS. Congenital venous anomalies and inherited thrombophilias are important in the development of lower extremity DVT in children and need to be considered.

Paper #: PA-082

Detergent Enhanced Ethanol Ablation of Venous Endothelial Cells: An In-vitro Study
Emma Raver, BA, William E. Shiels, DO, *Radiology, Nationwide Children's Hospital, Columbus, OH, emma.raver@nationwideChildren's.org;* Abigail Masunga
Purpose or Case Report: To evaluate potential synergistic action of combined sodium tetradecyl sulfate (STS) detergent and ethanol (ETOH) for sclerotherapy ablation of vascular endothelial cells.
Methods & Materials: Human umbilical vein endothelial cell (HUVEC) cultures were treated in-vitro with STS (dilutions: 3%, 0.75%, 0.188%, 0.047%, 0.0117%, 0.0029%, 0.0007%) and ETOH (dilutions: 100%, 25%, 6.25%, 1.56%, 0.39%, 0.098%, 0.024%) as sole agents each for 5 min contact time. HUVECs were then treated with both agents as a combined 5 min treatment using STS (0.0117%, 0.0029%, 0.0007%) each with varying dilutions of ETOH (6.25%, 1.56%, 0.39%, 0.098%, 0.024%). Following cell washing and 1 h post-treatment incubation, plates were assayed for cell survival using single wavelength 540-nm absorance.
Results: Cell survival with sole agents: ETOH dilutions (5 min) 100% and 25% with survival=0% and 7% respectively, and 6.25%, 1.56%, 0.39%, 0.098%, and 0.024% dilutions with 100% cell survival; STS dilutions (5 min) 3%, 0.75%, 0.188%, 0.047% with survival=0%, 0%, 2.9%, and 4% respectively; and 0.117%, 0.0029%, and 0.0007% with 100% survival.
When combined for 5 min treatment, non-lethal sole agent concentrations produced lethal synergy (representative data points: STS 0.0117%+ETOH 1.56%=19.8% survival; STS 0.0029%+ETOH 1.56%=17% survival; and STS 0.0007&+ETOH 1.56%=28.2% survival).
Conclusions: STS detergent and ETOH, when combined, produce synergistic cell death at concentrations where each agent solely is non-lethal. The proposed mechanism of action is cell poration (as a result of detergent release of lipoproteins and subsequent poration of cell membranes [increased cell membrane ETOH permeability]). This in-vitro synergistic effect is consistent with

clinical experience in both lymphatic (LM) and venous (VM) malformations.

Paper #: PA-083

Interventional Radiology Management of Post-Transplant Biliary Strictures in Children

Jared Green, MD, *Lurie Children's Hospital of Chicago, Chicago, IL, jared.green@alumni.duke.edu;* Stanley Kim, Bridget Whitehead, James Donaldson

Purpose or Case Report: To describe our institutional experience with percutaneous interventional radiology management of biliary strictures in children after liver transplant. Biliary strictures are a significant source of morbidity and mortality in the pediatric liver transplant population, affecting up to 30% of patients. We present our experience with percutaneous management of biliary strictures in pediatric patients post liver transplant.

Methods & Materials: An IRB approved retrospective analysis evaluated patients post transplant that were diagnosed with biliary stenosis and successfully stented, from August 1997 through August 2012. Records and imaging were reviewed for clinical management and outcomes. 72 patients (41 female, 31 male) were included. Median age at transplant was 16.5 months (range: 2–213 months). Median time from transplant to percutaneous intervention was 11.1 months (range: 0.3–187.4 months).

Results: The most frequent indications for initial transplant in our series included biliary atresia (n=35), metabolic deficiency (n=9), acute liver failure (n=9) and sclerosing cholangitis (n=5). Indications for percutaneous stenting included fever and suspected cholangitis, abnormal liver biopsy, elevated direct bilirubin and alkaline phosphatase levels. Strictures were managed with percutaneous transhepatic cholangiogram, balloon dilation of the stricture and placement of an internal-external plastic stent for 3 months (median: 93.5 days; range: 8–262 days). 28 patients (39%) experienced no recurrent stenosis after removal of the initial stent. 11 patients (15%) with recurrent stenosis were successfully managed by a second course of stenting. Two patients (3%) with recurrent stenosis after the second stent removal were successfully managed with a third course of stenting.

Conclusions: Percutaneous management of biliary stenosis after liver transplantation continues to be the standard of care, with a high rate of technical success and low incidence of complications. Percutaneous stenting may avoid the morbidity associated with surgical management of biliary stenosis; however, a multidisciplinary treatment approach is necessary, as evidenced by the patients requiring surgical revision after unsuccessful percutaneous stenting. Our series demonstrates that greater than one third of patients with post transplant biliary stenosis can be managed successfully with a single course of stenting. When considering repeat stenting, a percutaneous approach successfully managed more than half of these patients.

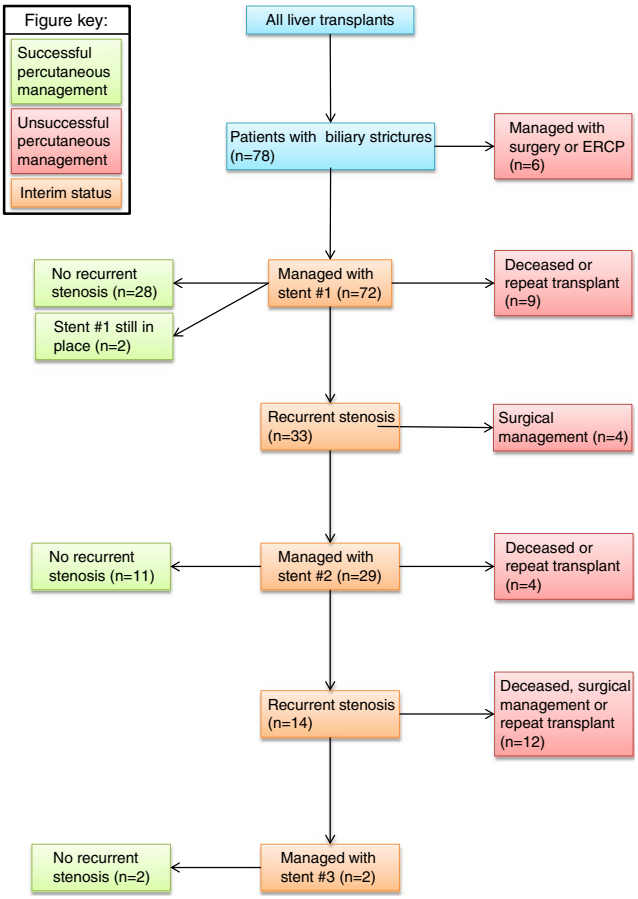

Paper #: PA-084

Single-incision Tunneled Femoral Vein Access in Neonates and Infants: A Single Institutional Experience

Marian Gaballah, *Children's Hospital of Philadelphia, Philadelphia, PA, gaballma@umdnj.edu;* Ganesh Krishnamurthy, Marc Keller, MD, Adeka McIntosh, MD, Tiffany Hwang, Anne Marie Cahill

Purpose or Case Report: To describe the technical success and outcomes of a single-incision technique for placement of tunneled femoral non-cuffed venous catheters in infants and neonates.

Methods & Materials: A 5-year retrospective review was performed of 203 children (116 m, 87 f) mean age 2.6 mths (range 1 day to 11 months), mean weight 3.5 kg (range 0.55 to 9.2), who underwent placement of a single-incision tunneled femoral venous catheter. A single incision was utilized

to create both the subcutaneous tunnel and the venous access site. Medical records were reviewed for technical success, mechanical and infectious complications. Indications for central access by SIR criteria included: IV medications/TPN (199) and antibiotic therapy (23).

Results: Two hundred twenty-two primary insertions were performed in 203 patients. Technical success was 100%. 188 patients received a single primary insertion at the femoral site; 15 received multiple (range 1–4). Catheter sizes included 1.9 F (9), 2.6 F (43), 3 F (66), 3.5 F (94), 4 F (9), and 5 F (1). Catheters were placed in IR/OR (176) or bedside (46). Procedural complications included oozing (9/222) and active bleeding (2/222). The mean fluoroscopy time was 1.4 min (range 0–11.4). 163/222 procedures were performed with IV sedation and 59/222 with general anesthesia. Total primary catheter days was 4482 days (mean 20.2, range 0 to 123.0). Overall total catheter days was 6285 (mean 28.3, range 0 to 220).

Mechanical complications occurred at a rate of 1.7 per 100 catheter days. Presumed/confirmed infectious complications, requiring IR salvage or removal, occurred at a rate of 0.42 per 100 catheter days. Management of mechanical complications included IR salvage, medical salvage, i.e. tpa or urokinase, and removal at a rate of 0.56, 0.67, and 0.45 per 100 catheter days respectively. Management of presumed/confirmed infections included IR salvage and removal at a rate of 0.05 and 0.37 per 100 catheter days respectively. Medical (50.6% of salvages) and IR salvages (49.4% of salvages) prolonged catheter days by an average of 21.7 (range 1 to 101).

The majority (>50%) of mechanical complications occurred in dual lumen catheters. However, salvages (73.3% of cases) were successful in more cases than required removal (26.7% of cases).

Conclusions: Tunneled single incision femoral vein access is technically feasible in neonates and infants and may be a desirable option for urgent bedside vascular access. Catheter lumen number may be an important consideration to reduce mechanical complications in this population.

Paper #: PA-085

Clinical, Histopathological, and Radiological Features of Congenital Anomalies of the Portal Venous System and a Proposed Algorithm for Management

Sabri Yilmaz, MD, *Children's Hospital of Pittsburgh of UPMC, Department of Radiology, Division of Interventional Radiology, Pittsburgh, PA, yilmazsdr@yahoo.com;* John Crowley, Charles Fitz, Fernando Escobar, Abhay Srinivasan, Jose Paredes, MD

Purpose or Case Report: The aim of this retrospective study was to describe the clinical, histopathological, and imaging features of congenital portosystemic shunts (PSSs) and to propose an algorithm for management of this rare entity.

Methods & Materials: The imaging and medical records for ten children with PSSs were retrieved and evaluated. The group included 5 girls and 5 boys, between 1 day and 11 years of age. Based on published series and our treatment outcomes, an algorithm was proposed for management of these rare but clinically significant vascular anomalies.

Results: Six children were diagnosed with intrahepatic PSSs and four were diagnosed with extrahepatic PSSs. Four patients presented with hypoxemia due to hepatopulmonary syndrome (HPS). One patient presented with epistaxis and clinical symptoms for hereditary hemorrhagic telangiectasia, one with failure to thrive, one with an unrelated heart failure secondary to a gastrointestinal hemangiomatosis, one with hyperammonemia and liver failure. One extrahepatic PSS was found incidentally in an asymptomatic patient who was evaluated for a ventricular septal defect. Four patients had liver biopsies. Hepatic US were available for all patients. Seven patients had abdominal CT, four patients had abdominal MRI, and five patients had conventional angiograms. Four patients were followed up for the shunts without any management. Two of these shunts involuted spontaneously and the other two remained asymptomatic. Four patients had transcatheter embolization of their shunts. One patient who had transcatheter embolization had no relief of his symptoms and received a liver transplant. A patient with an external PSS received a liver transplant with resolution of his HPS.

Conclusions: Asymptomatic patients who present with PSSs as newborns should be followed up for the first year of life with serial US to evaluate the shunt due to a high probability of spontaneous closure. In our experience, in symptomatic newborns and older symptomatic children endovascular approach should be attempted due to the high success and low complication rates. Liver transplant should be reserved for failed endovascular treatment.

Paper #: PA-086

Single-incision Technique for Internal Jugular Vein Tunneled Vascular Access in the Pediatric Population

Marian Gaballah, *Children's Hospital of Philadelphia, Philadelphia, PA, gaballma@umdnj.edu;* Ganesh Krishnamurthy, Marc Keller, MD, Adeka McIntosh, MD, Anne Marie Cahill

Purpose or Case Report: To describe the technical success and outcomes of a single incision technique for placement of internal jugular (IJV) tunneled vascular access devices in children.

Methods & Materials: A retrospective 4 year review was performed of 15 children (8 males, 7 females) who underwent placement of single incision IJV tunneled vascular

access catheters. The single incision technique was defined as utilizing one incision with an ultrasound-guided long needle tunneled venipuncture to create both the subcutaneous tunnel and the venous access.

Radiologic and medical records were reviewed for technical success, early and delayed mechanical and infectious complications. The mean age of the children was 11.0 years (range 1.00–18.7) and the mean weight was 44.2 kg (range 9.6–99.0). Indications for the vascular access as per SIR criteria included: TPN and medications (8), antibiotic therapy (5), chemotherapy (2), immunotherapy (1), and dialysis (1).

Results: Seventeen primary insertions were performed in 15 patients. Technical success was 100%. Catheter types included non cuffed central line (14), cuffed hemodialysis catheter (1), cuffed central line (1), and a port (1). One catheter was placed in 14 patients and three catheters in one patient. There were no procedure related complications. The mean fluoroscopy time was 5.3 mins (0.7–14.7). The total catheter days for initial insertions was 1265 catheter days (mean 74.4 days, range 3–502 days). Mechanical and infectious complications occurred at a rate of 0.29 and 0.14 per 100 total catheter days respectively. The rate of removal for mechanical and infectious complications was 0 and 0.07 per 100 total catheter days respectively. Non-IR salvages (tPa) (75% of salvages), and IR salvages (25% of salvages) prolonged catheter days by an average of 28.5 days (range 10–81 days). Three catheters were still in use at the end of this study.

Conclusions: The radiologically guided single-incision technique is a safe and technically feasible method for insertion of central venous access devices in pediatric patients. Placing them in children has appeal when the conventional double-incision technique may be challenging, such as in those with tracheostomy.

Paper #: PA-087

Pediatric percutaneous nephrostomy: A single institution's 10 year retrospective review

C Matthew Hawkins, MD, *Cincinnati Children's Hospital, Cincinnati, OH, hawkcm@gmail.com;* Kamlesh Kukreja, Neil Johnson, Manish Patel, Eugene Minevich, John Racadio, MD

Purpose or Case Report: The purpose of this retrospective review was to evaluate the common indications for percutaneous nephrostomy (PCN) as well as the most common complications encountered at a large tertiary care pediatric hospital. Additionally, ultrasound and cone beam CT guidance were separately evaluated in an effort to show which technique was most advantageous for non-dilated collecting systems.

Methods & Materials: Following IRB approval, an imaging and clinical database search for primary PCN access was performed for the time-period of July 2002 through July 2012. Data recorded included: clinical indication, presence of renal anomalies, presence or absence of a dilated collecting system, type of image-guidance used for access, accessed calyx, size of the nephrostomy catheter, duration of catheter, length of hospital stay, technical success, and presence of a complication directly attributable to nephrostomy placement.

Results: There were 138 PCNs performed on 101 different patients. (Mean age=9.3 years, range=2 days to 21 years) To our knowledge, this is the largest pediatric cohort in which this procedure has been studied. Whitaker tests that did not result in indwelling catheters and catheter exchanges were excluded from analysis. Indications for PCN access included urinary obstruction in 90 patients, lithotripsy access in 41 patients, and other indications such as stent retrieval or urinary leak in seven patients. The renal collecting system was dilated in 98 of 138 procedures (71%). PCN was technically successful in 96 of 98 dilated systems (98%) and 39 of 40 non-dilated systems (98%). Complications directly attributable to PCN were encountered in two cases (1.4%) including sepsis and pain at the insertion site requiring re-intervention. Ultrasound guidance was used in 127 cases and was successful in 124 procedures (98%). Cone beam CT guidance was 100% successful without any complications and used for 11 PCNs, ten of which were placed in non-dilated collecting systems.

Conclusions: Our study confirms that PCN is a safe procedure with high technical success and minimal complications in children. In our initial experience, cone beam CT guidance holds potential for safe and successful PCN access in difficult, non-dilated collecting systems in children.

Paper #: PA-088

Medium-term outcomes of renal artery stenting in children

Clare McLaren, DCR(R), *Department of Radiology, Great Ormond Street Hospital, London, United Kingdom, derek.roebuck@gosh.nhs.uk;* Kjell Tullus, George Hamilton, Derek Roebuck

Purpose or Case Report: Although there are numerous reports of renal artery stenting (RAS) in children, all describe the early results in small numbers of patients. The purpose of this paper is to review the outcomes of patients at 5 years after insertion of one or more renal artery stents.

Methods & Materials: Retrospective review of patients who underwent RAS by a single pediatric interventional radiology (IR) service between 2002 and 2008. Technical data were retrieved from a prospectively-maintained IR

database. Clinical follow-up was obtained from patient contact and electronic patient records.

Results: Over this interval RAS was performed in 13 children (9 male), aged between 30 months and 15 years (median 7.5 years) at the time of their first procedure. 22 balloon-expandable metal stents were placed in main renal arteries (16), polar arteries (2), or renal artery graft, gastroduodenal-renal arterial anastomosis, transplant or segmental arteries (1 each). One main renal artery received two overlapping stents at a single procedure. The indications for stenting in the 21 procedures were dissection (10), early recurrence of hypertension due to restenosis after successful angioplasty (8), recanalization of occluded artery (2) and pseudoaneurysm (1). Stent diameters used were 2.0 to 6.0 mm (median 4.0 mm).

The only immediate complications were two small groin hematomas and one stent migration.

In terms of hypertension, at last follow-up one patient (8%) was cured at 6.6 years and 12 (92%) were improved (at a median of 5.5 years). Four patients (31%) have undergone surgery since stent insertion. All 18 arteries treated are patent on imaging, at a median follow-up of 4.8 years (range 0 to 9.8), with primary patency of 28% and assisted primary patency of 83%.

Conclusions: RAS is acceptably safe in children. Patency of the stented artery is good, although most patients (72% in this series) require one or more endovascular and/or surgical procedures to maintain patency in the medium term (<5 years). Prospective studies should specifically assess the relationship between stent occlusion and stent diameter.

Paper #: PA-089

Fetal MRI - Jumping from 1.5 to 3 Tesla MRI: Preliminary Experience

Teresa Victoria, MD PhD, *Children's Hospital of Philadelphia, Philadelphia, PA, victoria@email.chop.edu;* Timothy Roberts, Ann Johnson, Arastoo Vossough, Erika Rubesova, Diego Jaramillo

Purpose or Case Report: Three Tesla MR imaging aims at improved image quality by increasing signal-to-noise ratio (SNR) and contrast-to-noise ratio (CNR). At our institution we have begun fetal imaging at 3 T after consulting safety guidelines. We sought to analyze our initial fetal imaging at 3 T compared to 1.5 T.

Methods & Materials: Following IRB approval, a database search for 3 T fetal MR studies showed five studies between July-September 2012, gestational ages (GA) 20, 26, 29, 30 and 34 weeks. Comparison: equal number of 1.5 T fetal MR studies done during the same time period for same GAs ($n=5$). Sequences evaluated: HASTE, TruFISP. Small fetal structures (spleen, adrenal glands, cartilage, airway, bone and kidney) were rated according to conspicuity (0=not visualized; 5=optimal visualization). Regions-of-interest (ROI) for signal intensity (SI) evaluated different tissues (bone, brain, cartilage, kidney, muscle, liver, lung, subcutaneous fat). Each SI was calculated 4–10 times per tissue. Noise measurements (10 data points per tissue) were calculated placing the ROI outside the maternal abdomen. SNR was calculated as mean SI divided by standard deviation of background noise.

Results: When scoring the subjective visualization of fine fetal structures at 3 T vs 1.5 T, the adrenal glands (4 vs 2), cartilage (5 vs 3) and airway (5 vs 2) were shown to be more conspicuous at 3 T than 1.5 T, particularly at increasing GAs. Grey/-white matter differentiation and small brain structures (deep grey nuclei, optic chiasm) were subjectively better visualized at 3 T. SNR did not have a statistically significant difference among the different tissues when comparing the different magnet strengths and across GAs. However, several technical variables (bandwidth, matrix, FOV and TE) differed among the sequences, limiting an adequate SNR comparison. Dielectric artifact was slightly more pronounced on TruFISP sequences without impeding imaging interpretation. Specific absorption rate (SAR) was always maintained below the 4 W/kg safety threshold implemented by the FDA and scanner vendor.

Conclusions: Preliminary evaluation of 3 T fetal MRI shows subjectively increased visual conspicuity and detail when evaluating fine fetal structures. Limitation of the study is the relatively low number of patients (total $n=10$). These preliminary findings are encouraging and may help us to better visualize and evaluate the fetus by MR imaging.

Paper #: PA-090

Pediatric Image Assisted Autopsy: Why Pediatric Radiologists Should be Part of it?

Pierre Schmit, MD, *IWK Health Centre, Dalhousie University, Halifax, NS, Canada, pierre.schmit@iwk.nshealth.ca;* Fergall Magee

Purpose or Case Report: To demonstrate through selected exemples why pediatric radiologists should get involved in post-mortem imaging.

Methods & Materials: Over the last 5 years, we have performed on pediatric patients: 27 skeletal surveys for death related to Medical Examiner investigation, they included plain fims and CT with multiplanar and 3D reformats of the whole patient; 480 skeletal surveys on fetuses ex-utero (plain films and whole fetus CT with multiplanar and 3D reformats) and eight MRI as part of a post-mortem or an ex-utero examination

Results: Skeletal maturation of the fetuses was similar on plain films and CT, anatomic detail of skeletal dysplasia or dysostosis were similarly displayed on both methods, but

were more easily apprehended on the 3D rendering. CT of fetuses did not provide information outside of the skeleton due to the absence of contrast and the lack of fat.
In ME's patients, no imaging findings were supportive of non accidental trauma, either on plain films or on CT, but CT provided definite confirmation of lesion related to intra osseous perfusion. In one case of pygopagus twins deceased of fulminans urinary tract infection, the bony connections were more easily apprehended on CT and 3D CT than on the plain films. In one patient with achondroplasia the death circumstances led to post-mortem imaging which found the skeletal changes related to the dysplasia.
The adjunction of MRI has provided additional information in fetuses with respect to the brain and spinal cord, upper mediastinum, great vessels, anatomy of the liver, adrenals, kidneys, spleen and main abdominal vessels, as well as bladder and uterus. This was also true for the pyopagus twins, post-mortem MRI. Epiphyseal morphology which could not be assessed by ex-utero CT can be by MRI.
Conclusions: Additional information is provided in a non-invasive manner as part of the fetopathology and autopsy examinations using plain films as well as CT and MRI. Gaining knowledge through patients with straightforward conditions will help for more complex cases and will help the pathologist to focus on complex cases or to limit their autopsy to areas not cleared by imaging.

Paper #: PA-091

Inferior Vermian Hypoplasia—Preconception, Misconception

Ashley Robinson, BSc MB ChB, *BC Children's Hospital, Vancouver, BC, Canada, ash@radiologist.net*

Purpose or Case Report: As a result of terminology such as "closure of the 4th ventricle", "craniocaudal growth of the vermis", "inferior vermian hypoplasia," and the numbering of the cerebellar lobules from superior to inferior, we are left with the preconception that the vermis grows from superior to inferior. There is then an incorrect assumption that partial agenesis or hypoplasia always involves the inferior lobules.
This paper proposes and provides the supporting evidence for an alternative concept regarding development of the cerebellum, and describes and dispels several misconceptions regarding both normal and abnormal cerebellar development, with specific reference to the cerebellar vermis.
Methods & Materials: Examples of cerebellar and vermian anatomy by both sonography and fetal MRI were retrospectively reviewed in both fetuses and in pre-term neonates between 8 and 40 weeks gestation. This was then correlated with already published knowledge of cerebellar embryology, phylogeny, somatotopic mapping and functional MRI.
Results: The evidence indicates that the cerebellar vermis probably does not develop in a cranio-caudal direction, but rather in a ventral to dorsal direction, and therefore the concept of inferior vermian hypoplasia is incorrect. There are actually three possible categories of abnormality; it may not NECESSARILY be the inferior vermis that is hypoplasitc, it may not ONLY be the inferior vermis that is hypoplastic or it may not be vermian hypoplasia AT ALL. Additionally the pattern of development suggests that in many cases it is the central lobules of the vermis rather than the inferior ones that are actually deficient.
Conclusions: The term "inferior vermian hypoplasia" is a preconception and a misconception. The term should only be used when it is actually the inferior vermis that is proven to be deficient. In cases where the more central lobules are deficient the term "neo-vermian hypoplasia" may be a more accurate description.

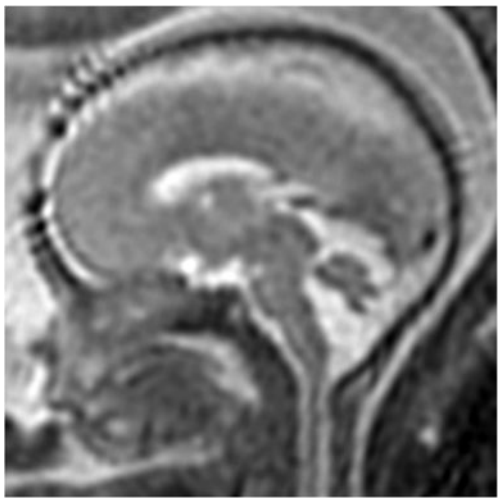

Paper #: PA-092

Ventriculomegaly Diagnosed on Fetal MRI and the Risk of Post-natal Hydrocephalus

Matthew Kole, **Jennifer Williams, MD,** *Baylor College of Medicine, Houston, TX, jennlynnwilliams@yahoo.com;* Angel Krueger, Debora Ybarra, William Whitehead, Christopher Cassady

Purpose or Case Report: Ventriculomegaly is among the most common anomalies diagnosed by fetal MRI. Limited data suggests severe ventriculomegaly is associated with a high risk of post-natal hydrocephalus, however the specific nature of this correlation remains unclear.
Methods & Materials: We performed a retrospective cohort analysis of 81 maternal-fetal dyads diagnosed with ventriculomegaly by fetal MRI over a ten-year period [2003–2012]. Patients were included if at least one lateral ventricle atrial diameter [AD] measured ≥10 mm (mean

15 mm) and ≥3 months of post-natal follow-up data was available (mean 26 months). We assessed the relationship between gestational age, fetal sex, AD for each lateral ventricle, the presence of other CNS anomalies, and post-natal hydrocephalus requiring surgical treatment.

Results: Mean gestational age at the time of fetal MRI was 27.3 weeks. 47 fetuses (58%) were male. In 34 cases (42%), no additional CNS anomalies were identified. Fifteen cases (19%) developed post-natal hydrocephalus. Mean AD was 23±7 mm in these cases, vs. 14±4 mm in fetuses who did not develop hydrocephalus ($p<0.001$). Excluding patients with myelomeningocele ($n=26$) and Dandy-Walker malformation ($n=2$), 3% (1/29) of patients with largest AD<15 mm underwent surgery for hydrocephalus, compared to 65% (11/17) with one AD≥ 20 mm and 86% (6/7) with one AD≥30 mm.

Conclusions: There is a strong association between severe ventriculomegaly on fetal MRI (one AD≥20 mm) and post-natal hydrocephalus. Conversely, in the absence of specific CNS anomalies, mild fetal ventriculomegaly (AD<15 mm) is not.

Paper #: PA-093

A Sheep in Wolf's Clothing? Radiologic-Pathologic Correlation and Clinical Outcome in Congenital Glioblastoma

John Maloney, MD, *Department of Radiology, Anschutz Medical Campus, University of Colorado Denver, Aurora, CO, john.maloney@ucdenver.edu;* Nicholas Stence, MD, Margaret Macy, B. Kleinschmidt-DeMasters, Laura Fenton, MD

Purpose or Case Report: Compared to glioblastomas in older children and adults, which are notoriously difficult to treat and have a poor prognosis, recent literature has shown congenital glioblastomas (cGBM) have better treatment outcomes even in the setting of incomplete surgical resection or biopsy and only moderate intensity chemotherapy.

Given the more favorable clinical course of cGBMs, we sought to evaluate these tumors for unique imaging and histological characteristics that may distinguish them from their counterparts in older children and adults, with the goal of facilitating future diagnosis and increasing awareness.

Methods & Materials: Following IRB approval, the neuro-oncology database at Children's Hospital Colorado was searched between 2002 and 2012 for infants diagnosed with glioblastoma. Patient demographics, presenting symptoms, imaging, pathology, treatment (including surgery and chemotherapy) and outcome were evaluated. Imaging studies were reviewed by two pediatric neuroradiologists and a pediatric radiology fellow, and histological samples were reviewed by a neuropathologist.

Results: Five patients with cGBM were identified (3 males and 2 females; mean age 43 days at first imaging). All five infants had a brain MRI, 4/5 had a brain CT, and 3/5 had an MRI of the spine. Tumors tended to be large (mean maximum diameter 6.0 cm), hemorrhagic, hyperdense on CT, and T1 iso- to hyperintense to gray matter on MRI. There were no calcifications. All five tumors were periventricular in location, with intraventricular extension in 3/5. One infant had spinal leptomeningeal metastases. One patient died during surgery from complications related to bleeding. The other four patients remain progression-free at a mean of 65 months from diagnosis following surgery (1 gross total resection and three subtotal resections or biopsies) and moderate intensity chemotherapy. Histologically, all five were glial tumors with moderate hypercellularity, relative cellular monotony, hemorrhage, necrosis, and brisk mitotic activity, and all met World Health Organization criteria for diagnosis of GBM. Although cGBMs have very similar gene expression profiles to pediatric and adult GBMs, distinguishing molecular characteristics include over-expression of genes regulating glucose metabolism and tissue hypoxia.

Conclusions: Congenital glioblastomas have a better prognosis than pediatric and adult GBMs, have unique molecular and genetic characteristics, and should be considered in a neonate with a large, hemorrhagic, periventricular brain mass.

Paper #: PA-094

Arachnoid Cysts Diagnosed Prenatal and in Young Children: Is there a High Requirement for Surgical Intervention?

Stephan Dixon, *University of Cincinnati, Cincinnati, OH, stephan.dixon@cchmc.org;* Beth Kline-Fath, MD, Maria Calvo-Garcia, Karin Bierbrauer

Purpose or Case Report: Arachnoid cysts (AC) are lesions filled with cerebral spinal fluid covered by arachnoid cells and collagen which tend to develop between the surface of the brain and calvarium or on an arachnoid membrane. The purpose of this study is to determine if fetal and early diagnosed (children < 6 months) isolated supratentorial AC have a high tendency for growth and thus require surgical intervention.

Methods & Materials: After IRB approval, a retrospective search of our data base was performed to identify those cases of AC diagnosed prenatal and in children less than 6 months of age. Imaging and charts were examined for prenatal, postnatal, clinical and surgical history.

Results: A review of 33 cases of AC identified prenatal and in infants less than 6 months of age was performed. Six cases were excluded as the cyst was not supratentorial (4 posterior fossa) or isolated (2 in the presence of agenesis of the corpus callosum). An additional five infants diagnosed with AC were found to have a ventricular or intraparenchymal cyst on sequential imaging. Six AC were studied by fetal magnetic resonance imaging (MRI) at a mean gestational age of 29 weeks. Three fetuses

with suprasellar AC had postnatal imaging but the remaining three were lost to follow-up. 16 infants at mean age of 65 days old were verified with isolated supratentorial AC. Therefore a total of 19 cases (3 prenatal and 16 postnatal) of supratentorial AC could be evaluated. Ten (52%) were present in the anterior middle cranial fossa (8) or anterior cranial fossa (2) and did not require intervention. Nine (47%) cases of AC grew causing significant mass effect thus requiring surgical fenestration and/or shunting. Location of these AC included suprasellar (4), perimesencephalic (2), quadrigeminal (1) and convexity with extension to lateral suprasellar cistern (2).

Conclusions: Isolated supratentorial AC less than 6 month of age requires a high rate of surgical intervention due to cyst growth. AC that were confined to the anterior and middle cranial fossa in our series did not undergo surgery. However, patients with isolated supratentorial AC in the midline, particularly suprasellar, as well as over the convexity tended to require surgical intervention. Our study suggests that young children with these AC would benefit from close clinical and imaging surveillance.

Paper #: PA-095

Normative CT data for fetal bone length: Is it possible to accrue a useful database?

Naseem Shakir, MD, *The Children's Hospital of Phiiladelphia, Philadelphia, PA, naseem.ukani@gmail.com;* Teresa Victoria, MD PhD, Pauline Germaine, Monica Epelman, Ann Johnson, Diego Jaramillo

Purpose or Case Report: Fetal CT is a novel method limited to evaluating fetuses with suspected severe skeletal dysplasia. Normative CT data for bone length at different gestational ages is not currently available. The purpose of the present study is to begin a CT bone length database of normal fetuses incidentally obtained from CT scans on gravid women presenting with an acute abdomen (acute appendicitis or post trauma). Associations between CT measures of long bone length, ultrasound standards, and gestational age are examined.

Methods & Materials: Following IRB approval, a retrospective review of a nearby hospital's adult emergency room radiology database revealed 17 CT examinations in 17 gravid patients. Five patients were excluded: three patients for lack of fetal visualization and two for lack of documented gestational ages. 3D images of the bones of the 12 remaining fetuses were reconstructed following editing of the maternal organs. The long bones (humerus, radius, ulna, femur, tibia, and fibula) of each fetus were measured bilaterally in true long axis. Other bony elements were also assessed.

Results: Gestational ages in the 12 fetuses ranged from 17 to 41 weeks (mean=28 weeks, SD=±8.1). Means and standard deviations are provided for each CT bone length measurement. Strong and significant associations between gestational age and CT bone length (Figure 1) are observed, with correlations ranging from 0.88 to 0.99 (all p values<0.001). Although a relatively small sample, comparison between the CT measurements and published ultrasound norms also show strong and significant associations (Figure 2), with correlations ranging from 0.95 to 0.99 (all p values<0.001).

Conclusions: Our findings show very strong associations of CT bone length measurements with gestational age as well as with ultrasound normative measurements (50th percentile) of bone length. Thus, our findings provide supportive evidence that CT measurements of bone length are reliable, and that a normative CT database can be created.

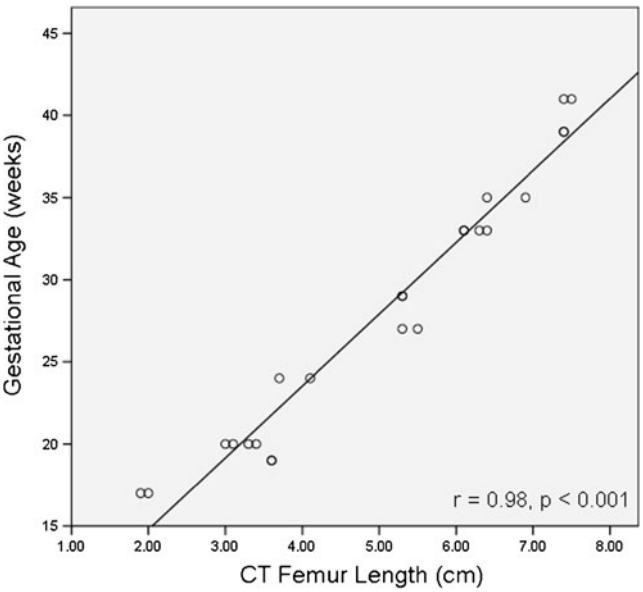

Figure 1: CT femur length (cm) vs. gestational age weeks, *n*=24

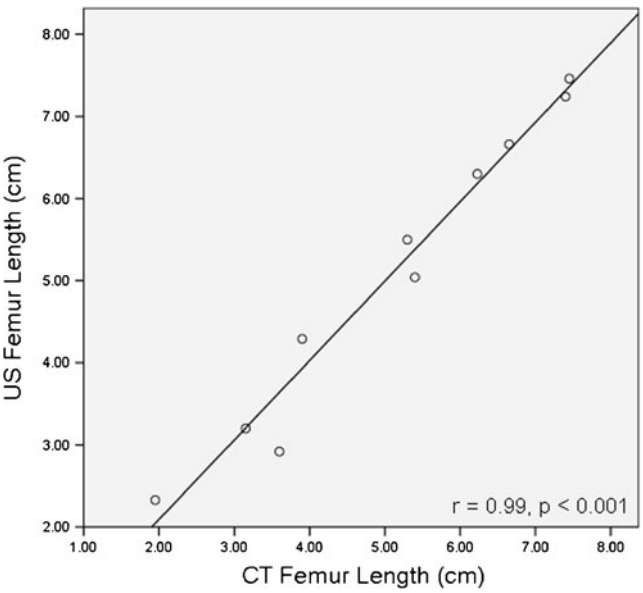

Figure 2: CT femur length (cm) vs. ultrasound femur lenght (cm)

Paper #: PA-096

Near Infra Red (NIR) liposome probe for detecting necrotizing enterocolitis (NEC) in premature piglets

Rohan Bhavane, *Radiology, Texas Children's Hospital, Houston, TX, rcbhavan@texasChildren's.org;* Barbara Stoll, Nada Ghoneim, Ketan Ghaghada, Douglas Burrin, Ananth Annapragada, PhD

Purpose or Case Report: Necrotizing enterocolitis (NEC) is an inflammatory bowel disease that strikes premature infants and exhibits high morbidity. It is currenty difficult to identify which premature infants will develop NEC, until they become symptomatic, by which time the prognosis is very poor. A non-invasive, early diagnostic for NEC would be of great value. In this study, we sought to target reporter nanoparticles to the inflammation that accompanies NEC in a newborn, premature pig model, and use imaging to identify particle localization into NEC lesions. We compared the results with a gold-standard pathology report.

Methods & Materials: Preterm piglets were split in two groups based on enteral feeding regimen as either; (1) Early Abrupt Feeding (EA): 2 days total parenteral nutrition (TPN), then fed formula orogastrically (50% of full intake), continue PN (50% of full intake), or (2) Late Abrupt Feeding (LA): 5 days TPN, then fed formula orogastrically (50% of full intake), continue PN (50% of full intake).

The animals were infused intravenously with liposomes containing a NIR dye, indocyanine green prior to being euthanized due to NEC onset or after 5 d enteral feeding. At the time of necropsy, liver, spleen and colon tissues were fixed in formalin and then imaged on a IVIS Lumina imaging system using the near infra red fluorescence settings.

Results: Visual observation of the fixed colon samples indicated that 7 out of 8 animals in the LA case, and 9 out of 10 animals in the EA case developed varying degrees of NEC. Colon samples from 5 of the 7 animals that developed NEC showed fluorescent signal due to presence of the liposomes in the LA case. Whereas, colon samples from three of the nine animals that developed NEC in the EA case showed signal. Results of fluorescent imaging are shown in figure 1.

The data was binarized as "NEC" or "No NEC". A similar binarization was applied to gross pathological evaluation of the tissues. The Kappa statistic was used to correlate the presence of fluorescence signal to the pathological identification of NEC. The LA protocol resulted in a Kappa value of 0.39, while the EA resulted in a value of −0.23, suggesting a fair to moderate correlation for the LA protocol, and a poor correlation (less than random chance) for the EA protocol.

Conclusions: These early results suggest that liposomes with a NIR dye could be used to detect development of NEC. We envision a handheld external Near IR fluorescence detector for early detection of NEC in vivo.

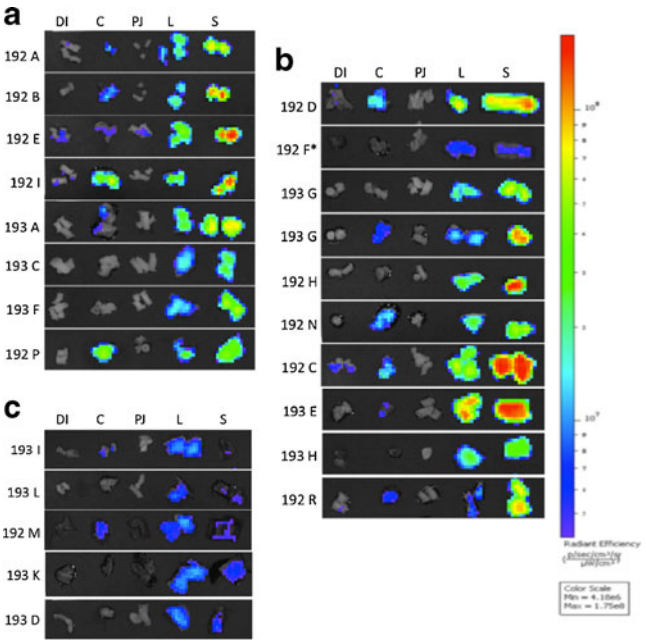

Figure1. Tissues from animals treated with NIR dye containing liposomes imaged on a NIR optical imaging system (a and b). (a) LA fed animals and (b) EA fed animals. (c) Tissues from animals not treated with the NIR liposomes. * Animal died 10 min after infusion of liposomes. DI–distal ileum, C–colon, PJ–proximal jejunum, L– liver, and S–spleen.

Paper #: PA-097

Effect of pediatric body size on dose reduction for abdominal MDCT with automated tube current

Boaz Karmazyn, MD, *Radiology, Riley Hospital for Children, Indianapolis, IN, bkarmazy@iupui.edu;* Yun Liang, Huisi Ai, Paul Klahr

Purpose or Case Report: The purpose of the study was to evaluate if dose reduction using tube current modulation depends on the patients body size in pediatric abdominal CT scans

Methods & Materials: This was a 9 month (2/2012–10/2012) retrospective evaluation of consecutive abdominal CT scans performed with Philips Brilliance iCT128. All studies were performed with longitudinal (Z-axis) tube current modulation. We included all children with body weight (BW) of less than 70 kg. Dose reduction from tube current modulation as reported in the dose page of every CT scan was recorded. ANOVA test was used to calculate difference between four groups of BW ≤20 kg, 21–40 kg, 41–60 kg, 61–80 kg.

Results: Three hundred eight abdominal CT scans were included in children with BW ranges from 3.5 kg to 70 kg (mean 32 kg). There was linear regression relationship between dose reduction and BW (R=0.7). There was significant (p<0.001) positive correlation between dose reduction and increased BW (ranged from 11% in BW ≤20 kg to 31% in BW range of 61–80 kg).
Conclusions: Dose reduction with automated tube modulation depends on BW and is less effective in small body size.

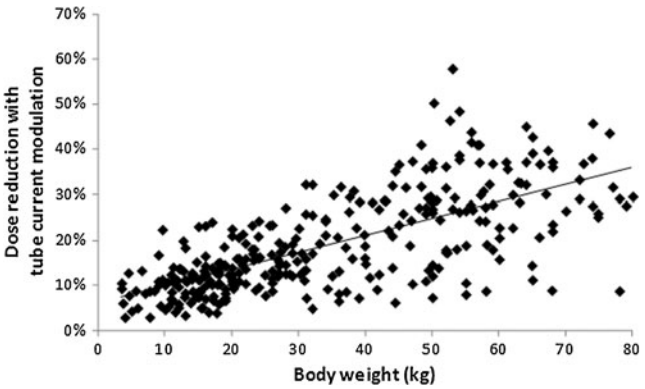

Paper #: PA-098

Precocious development of adenoid tissue in infants: Possibly related to increased pollutants in the air.

Thang Ngo, MD, *Radiology, Phoenix Children Hospital, Phoenix, AZ, tngo715@yahoo.com;* Gerald Mandell

Purpose or Case Report: To document that a significant change in size of adenoid tissue has occurred in the last few decades by measuring adenoidal thickness utilizing midline sagittal T1 weighted image on routine brain MR examinations in infants less than 6 months of age.

In1970 Drs. Capitanio and Kirkpatrick demonstrated that significant adenoidal lymphoid tissue on lateral neck radiographs could not be appreciated until 6 months of age in most infants. The presence of significant soft tissue in the nasopharynx in infants less than 6 months of age raises the possibility of a neoplastic process. Over the past few decades precocious development of adenoid tissue has been subjectively noted on lateral neck examinations in infants much younger than 6 months of age. In1999, Jaw TS et al. first demonstrated utilization of the midline sagittal T1-weighted image to determine adenoidal size. In their study of 53 patients less than 6 months of age, the mean adenoidal measurement for children less than 3 months of age was 0.8 mm +/− SD 1.9 mm; 3 months of age 5.1 mm +/− 2.1 mm and 6 months of age 7.5 mm +/− 2.4 mm.

Methods & Materials: One hundred one patients (41 F and 60 M), age ranging from1 day to 6 months underwent routine MR brain imaging for neurological indications at our institution. The adenoid thickness was measured using technique described by Jaw TS et al. It was measured from the point of maximal convexity of the adenoid, along the line perpendicular to a line parallel to the clival base. The midline sagittal T1-weighted image was used to measure adenoidal thickness. All MR brain examinations were included regardless of neurological indications. Children older than 6 months and those with signs and symptoms of infection, hematologic or immunologic disorders were excluded.

Results: In the group of 0–2 months of age (N=33), the measurement of adenoidal thickness ranges from 1 to 4.4 mm, mean 2.9 mm +/− SD 1.2 mm; 2–4 months of age (N=31) 2.3 to 7.4 mm, mean 4.8 mm +/− 1.7 mm and 4–6 months of age (N=37) 3.2–12 mm, mean 7.2 mm +/− 3.2 mm.

Conclusions: Our initial analysis of 101 patients demonstrates mean adenoidal measurements to be higher than reported in the past. The presence of a soft tissue mass in the nasopharynx is more likely due to precocious adenoid tissue rather than a tumor. Increase in adenoidal size, may potentially coincides with the increased incidences in asthma related illness in infants and children, is an effective way of developing immunologic adaptation to fight toxins and foreign matters by producing immunoglobulins.

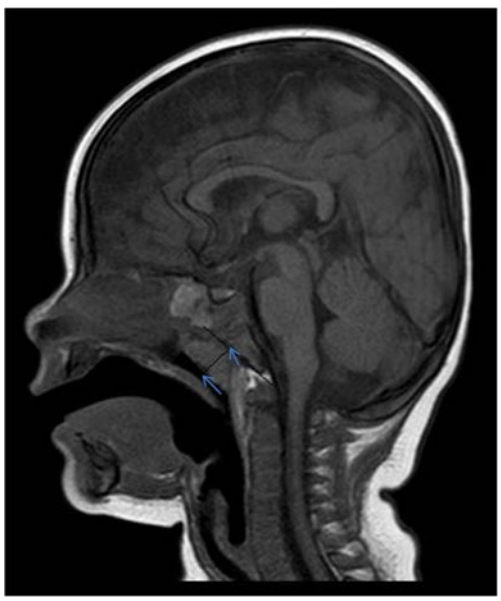

Distant between blue arrows denotes adenoid thickness on midline sagittal T1 weighted image

Paper #: PA-099

Amniotic fluid sludge: an independent risk factor for early preterm delivery, chorioamnionitis, funisitis, and increased perinatal morbidity and mortality in twin pregnancies with a second trimester short cervical length.

Ananda Boyer, MD, *Oakland University William Beaumont Hospital School of Mediciine - Department of Obstetrics and Gynecology - Division of Fetal Imaging, Royal Oalk, MI, ananda.boyer@beaumont.edu;* Lauren Cameron, Yolanda Munoz-Maldonado, Richard Bronsteen, Christine Comstock, Luis Goncalves, MD

Purpose or Case Report: To determine the clinical significance of amniotic fluid (AF) 'sludge' in twin pregnancies with a second trimester short cervical length.

Methods & Materials: Retrospective study including twin pregnancies referred to the Fetal Imaging Unit of William Beaumont Hospital between Jan 2004 and Feb 2011, and who had an ultrasonographic cervical length measurement≤25 mm between 16 and 24 weeks (n=78). Pregnancy outcomes in those with (n=27) vs. without (n=51) AF sludge were compared. Outcome variables included gestational age (GA) at delivery, premature rupture of membranes (PROM), clinical and histologic chorioamnionitis, funisitis, admission to the neonatal intensive care unit (NICU), composite neonatal morbidity, and perinatal death. For statistical analysis, each twin was studied as a separate outcome and a comparison between twins was performed. Outcomes were analyzed only for spontaneous deliveries (n=55).

Results: The prevalence of AF 'sludge' was 35% (27/78). The following observations were made when comparing pregnancies with vs. without AF sludge: 1) earlier GA at delivery (27.2±5.6 vs. 31.0±4.0 weeks, p <0.01); 2) higher frequency of PROM (63.3% vs. 36.7%, p=0.42); higher rate of spontaneous preterm delivery<26 weeks (70.6% vs. 29.4%, p <0.01); 3) higher rate of histological chorioamnionitis for twin A [twin A 66.7% vs. 33.3% (p<0.01), twin B 62.5% vs. 37.5% (p=0.13)]; 4) a trend towards a higher frequency of funisitis for twin A [75.0% (6/8) vs. 25.0% (2/8), p=0.06] but not for twin B [50% (2/4) vs. 50.0% (2/4), p=0.62]; 5) higher perinatal mortality [twin A 81.8% vs. 18.2%, p<0.001; twin B 72.7% vs. 27.3%, p=0.04]. Composite neonatal morbidity was similar regardless of the presence or absence of amniotic fluid sludge (twin A 48.0% vs. 52.0%, p=0.13; twin B 45.2% vs. 54.8%, p=0.22).

Conclusions: In twin pregnancies with a second trimester cervical length≤25 mm, the presence of amniotic fluid sludge identifies a subgroup of pregnancies at higher risk for early preterm delivery, histologic chorioamnionitis, and perinatal death.

Paper #: PA-100

Pause and Pulse - Recording of effective dose from common pediatric abdominal fluoroscopy studies as a quality improvement (QI) tool: baseline data and comparison with CT.

Anuradha Shenoy-Bhangle, MD, *Abdominal and Interventional Radiology, Massachusetts General Hospital, Boston, MA, anuradhabhangle93@gmail.com;* Sarabjeet Singh, MD, Kathryn Henault, Xinhua Li, Katherine Nimkin, Sjirk Westra

Purpose or Case Report: In order to develop Effective Dose (ED) from abdominal fluoroscopy as a QI tool, we collected baseline data ED from normal Upper Gastrointestinal (UGI) and Small Bowel Series (SBS) performed by different operators in the same outpatient imaging setting, and compared these with each other and with doses incurred by abdominal CT in an age-matched control group.

Methods & Materials: Over a 6 month time period, we identified 115 children (ages 1.5 months to 19 years) who underwent upper GI and SBS studies and who had normal results over a 6 month time interval, performed on a single pulsed fluoroscopy machine by five different experienced pediatric radiologists. We calculated effective doses from recorded dose area products of the entire studies (including overhead films), using published age-adjusted conversion factors. We also calculated CT effective doses in a control group who underwent abdominal CT at our facility in the past year, by multiplying dose-length product by published age-adjusted k-factors.

Results: Please refer to Figure 1: Tables.

Conclusions: The results of this study represent the typical dose range incurred. These may prove useful for pediatric radiologists to improve upon or recommend better techniques to further reduce radiation doses following individual feedback of results and educational intervention. When attention is paid to optimal dose reduction techniques, ED from fluoroscopy studies can be an order of magnitude lower than the corresponding CT doses. The results of our survey may be used as a reference for QI projects, and may add value to the discussion on which test to perform in patients evaluated for inflammatory bowel disease.

Fluoroscopy ED values, stratified by age, were:

Study/ Age range	N	ED (mSv) Mean+/−SD, (median)	ED range (mSv)
UGI:0mo–4mo	14	0.45+/−0.51 (0.31)	0.05–2.1
UGI : 4mo–<3y	41	0.02+/−0.13 (0.12)	0.01–0.51
UGI : 3–<8y	10	0.28+/−0.14 (0.27)	0.04–0.57
UGI : 8–<15y	4	0.32+/−0.27 (0.23)	0.08–0.70
UGI-SBS: 3–<8y	7	0.72+/−0.52 (0.67)	0.08–1.38
UGI-SBS: 8–<15y	18	1.32+/−0.90 (1.20)	0.37–3.68
UGI-SBS: >15y	21	1.14+/−0.66 (1.12)	0.34–3.17

ED values form abdominal CT in the control group were:

Age range	N	CTDI (mGy)	DLP (mGy.cm)	ED (mSv), range and (median)
4mo–<3y	6	2.3+/−0.2	54+/−5	4.0–4.3 (4.3)
3y–8y	21	4.7+/−0.7	162+/−49	3.0–8.7 (5.5)
8y–<15y	54	7.6+/−2.6	334+/−124	3.6–12.9 (7.4)
15–20y	42	8.1+/−2.1	375+/−114	3.4–9.7 (5.4)

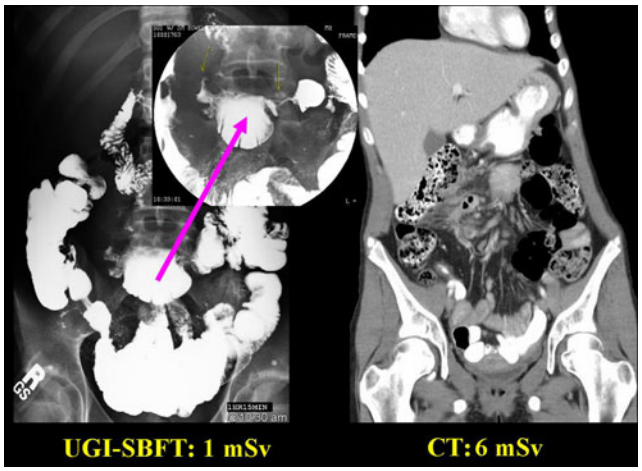

Paper #: PA-101

The Simulation Experience as an Introduction to Pediatric Radiology

Leah Braswell, *Arkansas Children's Hospital, Little Rock, AR, braswellleahe@uams.edu;* Carol Thrush, Linda Deloney, Mallik Rettiganti

Purpose or Case Report: Simulation in medical education has been shown to enhance traditional methods of learning by exposing learners to real-world situations in order to gain knowledge and experience. Pediatric radiology experience with simulation is lacking. The purpose of this IRB-approved study is to determine whether a simulation course in pediatric radiology is effective in order to prepare R1 and R2 radiology residents for competency in the diagnosis, management, and communication regarding common clinical scenarios.

Methods & Materials: This course included four simulation modules designed to enable residents to master common but challenging clinical scenarios: 1) Intussusception diagnosis, management plan, and parent consent; 2) Gastrojejunostomy tube dislodgement treatment plan and parent education; 3) Hip effusion consultation with emergency department physician and aspiration plan; 4) Contrast reaction simulation with mannequin. The principal investigator, a pediatric radiologist, debriefed the residents at course completion.

R1 (n=6) and R2 (n=6) residents attended the half-day course early in the academic year. Residents took 18-item pre- and post-surveys addressing self-perception of mastery. Resident anonymity was maintained by recording user-generated IDs on the paper surveys. Survey responses before and after the encounters were compared using the Wilcoxon Signed Rank test for paired data.

Competency was measured by scoring checklists for each learner at each station by video review. Number of tasks performed correctly for each segment was compared between R1 and R2 residents using Wilcoxon Rank Sum test for two independent groups.

Results: A two-sided Wilcoxon signed rank test comparing composite scores for Q1-Q10 between pre and post simulation training was statistically significant (p=<0.001); the median post simulation score was 3.80 while the median pre simulation score was 3.10. Similarly, the median composite score of 4 for Q15-Q18 post simulation was significantly higher than the mean score of three pre simulation (p=0.016). The outcomes from the checklist were compared between R1 and R2 residents using a two-sided rank sum test; median GJ tube score of 6 for R2 residents was significantly higher than the median score of 3.50 for R1 residents (p=0.002).

Conclusions: An introductory course using simulation scenarios is a feasible and effective method for teaching initial skills in pediatric radiology to first and second-year residents.

Table 1. Summary statistics for Survey Questions

Questions	N	Pre		Post		P
		Median	Mean (SD)	Median	Mean (SD)	
Q1	12	3	3.17 (0.94)	4	4.17 (0.94)	**0.001**
Q2	12	3	2.50 (1.24)	4	3.67 (0.49)	**0.008**
Q3	12	4	3.17 (1.19)	4	4.25 (0.87)	**0.004**
Q4	12	3.5	3.25 (1.22)	4	4.42 (0.51)	**0.004**
Q5	12	3	3.17 (0.94)	4	3.92 (1.08)	**0.016**
Q6	12	3	3.00 (0.85)	4	4.08 (0.90)	**0.002**
Q7	12	4	4.08 (0.90)	4	4.33 (0.65)	0.375
Q8	12	3	3.08 (1.00)	4	4.17 (0.58)	**0.004**
Q9	12	3	2.42 (0.79)	3	2.75 (0.97)	0.359
Q10	12	3	2.67 (1.30)	3	3.08 (1.08)	0.125
Q11	12	4	4.08 (1.08)	4	3.67 (1.07)	0.188
Q12	12	4	4.08 (0.79)	4	3.73 (0.90)	0.250
Q13	12	4	3.83 (1.11)	4	3.83 (0.94)	1.000
Q14	11	1	1.27 (0.65)	1.5	1.58 (0.67)	0.125
Composite - Q1 to Q10	12	3.10	3.05 (0.62)	3.80	3.88 (0.47)	**<0.001**
Composite - Q11 to Q14	12	3.50	3.38 (0.59)	3.29	3.19 (0.58)	0.375
Composite - Q15 to Q18	12	3.75	2.83 (1.11)	4.00	3.75 (0.45)	**0.016**

Table 2. Summary statistics of performance checklist by train ing level.

Outcome	R1			R2			P
	N	Median	Mean (SD)	N	Median	Mean (SD)	
Intussusception	4	4	4.25 (0.50)	6	5.5	5.50 (1.05)	0.105
GJ Tube	6	3.5	3.17 (0.98)	6	6	6.00 (0.89)	**0.002**
Hip Tap	4	3.5	4 (1.41)	6	3.5	3.67 (1.21)	0.782

Paper #: PA-102

Computed Tomography Radiation Exposure: Dose Reporting Implementation and Adherence in a Radiology Housestaff Quality Improvement Project

John-Paul Yu, MD, PhD, *Department of Radiology and Biomedical Imaging, University of California, San Francisco, San Francisco, CA, jp.yu@ucsf.edu;* Akash Kansagra, John Mackenzie

Purpose or Case Report: In light of the recent passage of California law SB 1237, which requies radiation dose reporting of all diagnostic CT examinations starting on July 1, 2012, we implemented a Radiology housestaff quality improvement project 1 year prior to the implementation of the law to track dose reporting among Housestaff with a goal of >80% of all finalized reports stating the dose received. The timing of the project also coincides with heightened awareness of the use of ionizing radiation in diagnostic imaging. With recent efforts by Society of Pediatric Radiology-sponsored ALARA conferences, ACR accreditation programs, and the American Society of Radiologic Technologists professional development course titled "Pediatric Body CT: Techniques and Tactics," this project not only helps develop a dose reporting system at our institution but also serves as a vehicle for educating Housestaff regarding appropriate radiation dose levels, proper study protocoling, and imaging issues specific to pediatric patients.

Methods & Materials: Consecutive reports from July 1, 2011 to June 30, 2012 of patients who underwent computed tomography examinations done at UCSF Medical Center, a 722-bed tertiary academic medical center in San Francisco, were retrospectively reviewed. Compliance of each study with the reporting requirement was assessed based on the presence or absence of a radiation dose statement within the finalized report

Results: A total of 36217 eligible consecutive computed tomography reports were identified within the review period for patients undergoing computed tomography examinations done at UCSF Medical Center. At total of 91.9% of eligible finalized studies reported the radiation dose for the examination.

Conclusions: We successfully implemented and completed a quality improvement dose reporting standard for CT examinations done at UCSF Medical Center with a final reporting rate of 91.9%, far above our target goal of 80%. Factors that contributed to a high adherence rate included establishing low barriers to compliance (standardized dictation templates, SmartText) and continuous resident and fellow education and feedback regarding radiation dose standards and reporting. Factors that contributed to noncompliance and low adherence to the reporting standard include dictations completed without template guidance and general unfamiliarity with dictation/template standards as residents rotate through multiple hospitals with different PACS/dictation systems.

Paper #: PA-103

The American Association of Physicists in Medicine Method for Measuring the Size Specific Dose Estimate in Pediatric CT: Does It Really Work?

Michael Wien, *Radiology, University Hospitals - Case Medical Center, Cleveland, OH, michaelwien@gmail.com;* Roshni Parikh, Paul Klahr, Ronald Novak, Leslie Ciancibello, Sheila Berlin, MD

Purpose or Case Report: Volume CT dose index (CTDIvol) and dose length product (DLP) are considered by many as the only two CT dose parameters that can be universally interpreted. However, because they do not incorporate a patient's dimensions, they cannot reflect individual patient dose. The size-specific dose estimate (SSDE) is a third parameter that includes a measurement of the scanned region of the body. The SSDE better approximates individual patient dose, allowing for a more precise approach to estimates of radiation risk from CT examinations. We compared two methods of calculating a patient SSDE: the manual method recommended by the American Association of Physicists in Medicine (AAPM) Task Group 204 report (Method M) and an automated method (Method A). We also compared the means of our calculated SSDEs (manual and automated) with the mean CTDIvol to affirm that CTDIvol grossly underestimates patient dose.

Methods & Materials: Thirty-nine CT examinations were retrospectively collected (8 Abdomen, 17 Abdomen/Pelvis, ten Chest/Abdomen/Pelvis). Method M involved calculating the sum of anteroposterior (AP) and lateral (LAT) dimensions at predetermined approximate maximum and minimum levels. These sums were then averaged. Based on this average, the AAPM report was used to determine the appropriate conversion factor (f_{size}), which was multiplied by the CTDIvol to determine the SSDE (SSDE=(f_{size})×CTDIvol). Method A measured the level-specific SSDE using the calculated equivalent circular diameter per slice. A mean SSDE was calculated by averaging data from all slice levels. Average SSDEs from

Method M and Method A were compared pairwise using the concordance correlation coefficient (ρ_c) and the paired sample t-tests. The SSDEs were also compared to CTDIvol.

Results: The ρ_c for Method M and Method A was 0.96, demonstrating substantial agreement. The mean SSDEs for Methods M and A were 6.68 mGy and 6.35 mGy, respectively. While statistically different, ($p<0.0001$), the absolute difference between the two groups is 4.98%, likely not a clinically significant difference. The mean CTDIvol was 4.02 mGy. When compared to Methods M and A, the absolute differences were 49.7% and 45.0%, respectively.

Conclusions: SSDE is a better metric for measuring pediatric CT dose compared to CTDIvol, which grossly underestimates dose. Given that Method M demonstrates substantial agreement with method A, we believe the AAPM's manual method to be a quick and practical option for measuring SSDE until dedicated software becomes widely available.

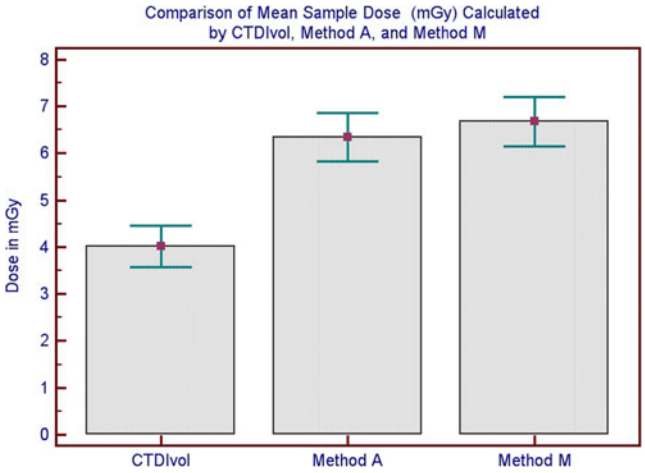

Paper #: PA-104

The Impact of Advanced Iterative Reconstruction on Radiation Exposure and Image Quality in Children

Robert Buchmann, DO, *Arkansas Children's Hospital, Little Rock, AR, buchmannrobert@uams.edu;* S Bruce Greenberg

Purpose or Case Report: Iterative reconstruction has the potential to reduce radiation exposure to children and reduce noise on computed tomography (CT) images. New forms of iterative reconstruction work in both image space and raw data space to improve image quality. Our purpose was to evaluate the impact of an advanced form of iterative reconstruction, Adaptive Iterative Dose Reduction (AIDR) 3D on image quality and radiation exposure on children undergoing computed tomography of the chest, abdomen and pelvis.

Methods & Materials: The standard CT reconstruction algorithm at a tertiary care pediatric hospital was changed from filtered back projection (FBP) to AIDR 3D in June, 2012. A retrospective study was performed analyzing 100 thorax, abdomen and pelvis examinations reconstructed using FBP and 101using AIDR 3D. Size-Specific Dose Estimates (SSDE) were calculated for each study. AP and lateral patient diameters were summed on the middle slice of each study to determine the conversion factor, which was multiplied by the scanner recorded CTDI volume to calculate the SSDE. Image noise was used as a proxy for image quality. Three 1.0 cm2 round regions of interest (ROI) were created, two in the right paraspinal muscles at the levels of the right pulmonary artery and the right kidney and one in the right gluteus maximus muscle. The standard deviation in each ROI constituted the measure of image noise. Unpaired t tests compared the age, SSDE, and image noise for each group.

Results: The results are summarized in the table. The children in each group ranged in age from 0 to 18 years. There was no significant difference in patient age between the two groups ($p=0.13$). The mean SSDE was 11.1 mGy in the FBP group and 8.4 mGy in the AIDR 3D group. The SSDE was reduced by 25% in the AIDR 3D group which was very significant ($p=0.0032$). No significant difference in image noise was present at any of the three ROIs (thorax ROI $p=0.71$, abdomen ROI $p=0.37$, pelvis ROI $p=0.53$).

Conclusions: AIDR 3D reduced the radiation exposure by 25% without any degradation in image quality. Advanced iterative reconstruction should be applied to all computed tomography examinations in children where possible.

Mean	Filtered Back Projection	Adaptive Iterative Dose Reduction 3D	Significance (p value)
Patients age (years)	8.5 (SD 5.7)	9.7 (SD 5.8)	0.1328
SSDE (mGy)	11.1 (SD 7.7)	8.4 (SD 5.1)	0.0032
Thorax ROI moise	20.3 (SD 5.5)	20.1 (SD 4.0)	0.7146
Abdomen ROI noise	18.6 (SD 4.2)	19.1 (SD 3.8)	0.3693
Pelvis ROI noise	23.0 (SD 7.0)	22.4 (SD 5.1)	0.5328

Paper #: PA-105

The Relationship between SSDE and Diagnostic Image Quality: How a Dose Index Registry (DIR) can Determine the Minimum Radiation Dose Needed to Achieve Acceptable Diagnostic Image Quality in Pediatric Abdominal CT

Marilyn Goske, MD, *Radiology, Cincinnati Children's Hospital Medical Center, Cincinnati, OH, marilyn.goske@cchmc.org;* Keith Strauss, Alexander Towbin, MD, Laura Coombs, David Larson, Consortium QuIRRC

Purpose or Case Report: Optimization in CT scans is a balance between patient risk (radiation dose) and benefit (study quality necessary for an accurate diagnosis). There are no national guidelines to determine minimum radiation dose needed to perform a diagnostic abdominal CT in

children. We describe the method used by a consortium within the ACR DIR to establish the relationship between Size Specific Dose Estimate (SSDE) and image quality.

Methods & Materials: This study was IRB approved. A retrospective review from six hospitals within the DIR was performed to evaluate the relationship between the radiation dose from an abdomen CT using SSDE and subjective image quality.

In order to define the minimum dose in SSDE required for diagnostic quality of abdomen CT in patients of different body widths (BW) we performed these steps: 1) obtain the radiation dose and patient's BW for a large number of abdominal CTs ; 2) identify the studies representing the median, lowest quartile and lowest overall SSDE for each BW; 3) determine number of studies to review; 4) create a bank of anonymized studies sampling images from scans performed at variable SSDE levels; 5) have six pediatric radiologists rate images for image quality and ability to make a diagnosis using a survey (Fig. 1); 6) use results to establish lower limit of SSDE for clinical applications. Image quality was rated using a 5-point RADLEX rating scale. Images were compared to a reference standard of five images where each image simulated the effect of cutting the dose in half as compared to the prior image (Fig. 2). Cases were assigned a non-diagnostic ranking if three or more of the six reviewers ranked them as such.

Results: The consortium rated 106/939 cases (11%) for diagnostic image quality. The reviewers ranked a total of 6/106 cases as non-diagnostic. Five of the non-diagnostic cases had SSDE less than the 25th percentile. The 25th percentile of SSDE was selected as the minimum radiation dose needed to achieve acceptable diagnostic image quality in pediatric abdominal CT within the consortium. The 25% SSDE in mGy was 5.8, 7.3, 7.6, 9.8, 13.1 for BW of <15, 15–19, 20–24, 25–29, >30 cm respectively.

Conclusions: The consortium developed a method to define the relationship between SSDE and image quality that takes advantage of the diversity of practice and large numbers of cases acquired through a DIR. This method provides radiologists a radiation dose estimate (SSDE) to use as a target range below which scans are non-diagnostic.

ACR NRDR QuiRCC Registry
Quality Improvement Registry in CT scans in Children
nrdr.acr.org

Image Quality Evaluation Form
v 1.1

1. *Facility ID Number	auto-filled
2. *Blind Image ID Number (1-80)	
3. *Objective Evaluation	
Indicate what scale was used	O Newborn to 1 year (N) O 1 year to 5 years (SC–small child) O 5 years to 10 years (MC–medium child) O 10 years to 15 years (OC-older child) O 15 years – 19 years (T-teen)
Compare this image to the reference scale and rate 1 through 10.	O 1-Non-diagnostic O 2 O 3 O 4 O 5-Exemplary
4. *Subjective Evaluation	
The gallbladder/liver interface is sharp	O 1-Not sharp O 2 O 3 O 4 O 5-Very sharp O N/A- Cholecystecomy, no GB
The liver/kidney or (kidney/spleen if no right kidney) interface is sharp	O 1-Not seen O 2-May be seen O 3-Probably seen O 4-Well seen O 5-Sharply seen
I am confident I could identify a low attenuation lesion the size of the aorta within the liver	O 1-Not confident O 2 O 3 O 4 O 5-Highly confident
Study is diagnostic	O No O Yes
5. *Name of site PI who did image evaluation	
First Name	
Last Name	
6. *Name of person who completed this form online	
First Name	auto-filled
Last Name	auto-filled
Submission Date	auto-filled

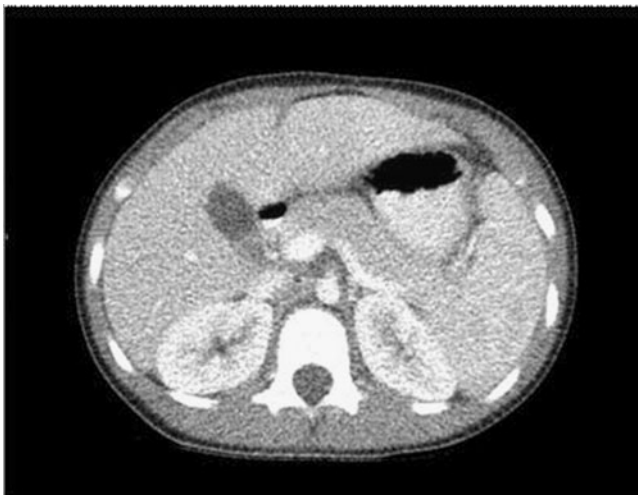

Referece scale image
Rank 5/5 on scale: exemplary

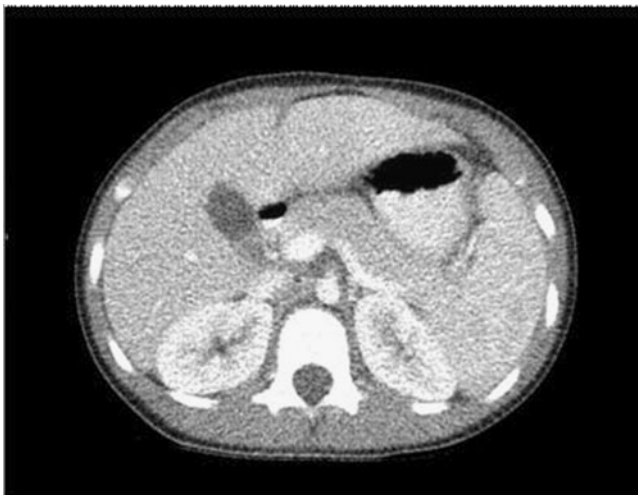

Referece scale image
Rank 1/5 on scale: non-diagnostic

Paper #: PA-106

Clinical implementation of ASiR™ reconstruction for substantial dose reduction in pediatric CT while maintaining pre-ASiR™ noise levels: 21st century alchemy

Samuel Brady, PhD, *Radiological Sciences, St Jude Children's Research Hospital, Memphis, TN, samuel.brady @stjude.org;* Bria Moore, Brian Yee, Robert Kaufman

Purpose or Case Report: This work represents a clinical implementation of 40% adaptive statistical iterative reconstruction (ASiR) combined with traditional filtered back projection (FBP) reconstruction for substantial dose reduction in pediatric CT imaging of the chest, abdomen, and pelvic regions while maintaining pre-ASiR image noise levels.

Methods & Materials: The IRB waived consent for this study. ASiR implementation was for dose reduction only. Target noise levels from images of the chest and abdomen/-pelvis were determined from 53 patients prior to implementing ASiR. Image noise was analyzed by placing multiple 100 mm^2 regions of interest in the aortic arch and surrounding soft tissue (for chest analysis), and throughout the liver and in the descending aorta at the level of the right portal vein in the liver (for abdomen analysis); no noise analysis was performed in the pelvis since the CT scan of the abdomen/pelvis utilizes the same noise target indices. The pre-ASiR target noise levels from the 53 patient analyses were used in conjunction with a recently published anthropomorphic phantom dose model study to establish new patient weight based tube current modulation (TCM) parameters. These parameters were used to maintain noise level in the reconstructed image using 40% ASiR, while reducing target tube current (mA). After 40% ASiR implementation, 389 consecutive patients were analyzed for image noise in similar fashion to the pre-ASiR analysis. Dose reduction was determined by comparing $CTDI_{vol}$ levels, modified according to patient size, between pre-and post-ASiR cohorts.

Results: Based on pre-ASiR patient analysis and the anthropomorphic phantom noise models, the TCM noise index levels for chest and abdomen/pelvis were increased by 33%, the minimum mA lowered by 20%, and 40% ASiR was implemented. Modification of the TCM parameters provided maximum dose reduction in the range of 55–70% across all weight categories (4.5–140 kg). Post-40% ASiR implementation analysis demonstrated noise levels in the chest and abdomen/pelvis similar in magnitude to pre-ASiR levels by an average of 1 HU, and contrast-to-noise ratio (CNR) levels increased by an average of 8% and 19%, respectively.

Conclusions: Implementation of 40% ASiR in conjunction with modified TCM parameters measured dose savings up to 70% with no significant change in image noise. The average difference over all weight categories for noise levels between pre- and post-ASiR exams of the chest and abdomen/pelvis was ~1 HU with a slight positive net increase in CNR.

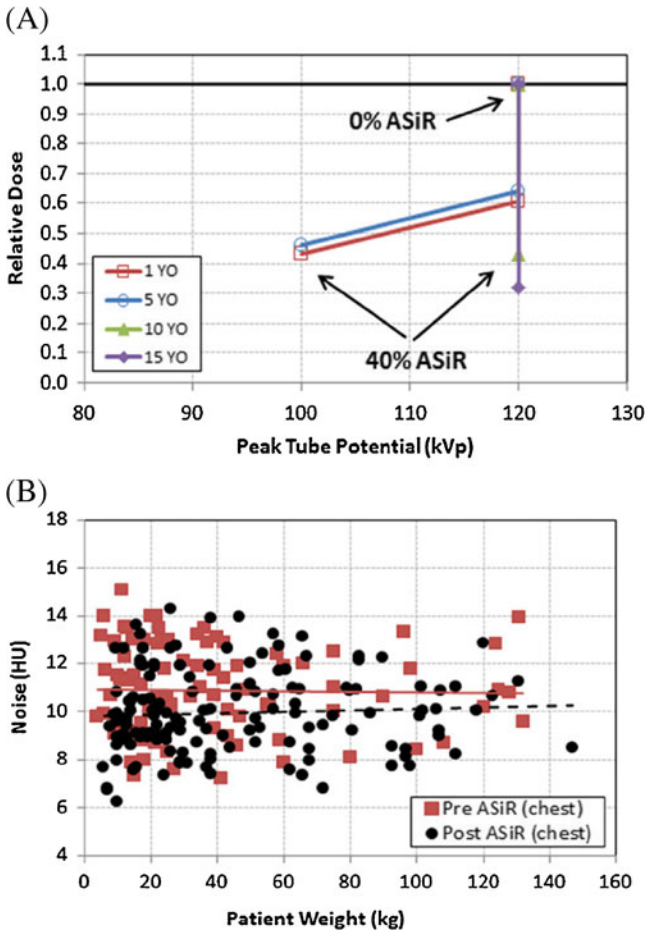

Fig. 1. (A) Relative dose reduction compared to pre-ASiR (0% ASiR) implementation. (B) Pre- and post-ASiR noise analysis of the chest demonstrates similar noise in the reconsructed image with and without ASiR implementation; similar scatter plot results are demonstrated for the abdomen/pelvis scan analysis.

Paper #: PA-107

Psychometric Function: A Novel Statistical Analysis Approach to Optimize CT Dose

Steven Don, MD, *Mallinckrodt Institute of Radiology, St. Louis, MO, dons@mir.wustl.edu;* Bruce Whiting, David Politte, Parinaz Massoumzadeh, Charles Hildebolt

Purpose or Case Report: To quantify radiologists' sensitivity to increased CT noise caused by simulated reduced radiation dose protocols.

Methods & Materials: Twenty radiologists participated in a noise reduction CT simulation study while attending the 2006 Montreal IPR. They were presented an image set consisting of ten abdominal CT images (5 normal, 3 non-perforated appendicitis, and 2 other abdomen lesions), each of which was simulated at ten increasing dose levels (1%, 10%, 15%, 20%, 30%, 40%, 50%, 60%, 70%, 85%) as well as the full dose examination (100%). Each observer localized the pathology and identified diagnostic confidence with a 5-point scale (no lesion to definite lesion). Weighted Kappa statistic quantified observer performance at each dose level, and dependence of performance as a function of relative noise was fit to a psychometric response function. The parameters of a Weibull cumulative function characterized noise threshold (noise level at midpoint agreement), width of noise transition (inverse of slope at midpoint), intra-observer variability, and guessing rate for individual observers. The parameters also allowed an objective measurement of the noise level at which performance begins to degrade (breakpoint on the shoulder of response curve). Using the psychometric function parameters, the variation in sensitivity for the observers was calculated. The number of cases and confidence intervals can be estimated for observer experiments.

Results: Plots for three representative observers are presented in Figure 1. The median midpoint noise level was 2.52 (1.8–3.12, 25% to 75% range) and the median slope value was 2.17 (1.27–3.56). The median relative noise tolerated at the shoulder breakpoint was 1.17 (0.17–1.90). Converting relative noise level to absolute dose reduction percentage, the median value was 27% (0%–77%). To achieve a confidence level of 5% at any given noise level would require between 400 and 3000 samples.

Conclusions: Parameterized psychometric functions are a convenient method to characterize the impact of CT noise on observer performance. Initial results indicate a wide variation in individual sensitivity to dose reduction. Individual observer experiments using conventional fixed noise level sampling require thousands of image samples, too many cases to reasonably assess an individual's sensitivity to noise. There is motivation to develop more efficient testing methodologies, such as adaptive testing where noise levels samples are determined by previous responses, rather than being predetermined.

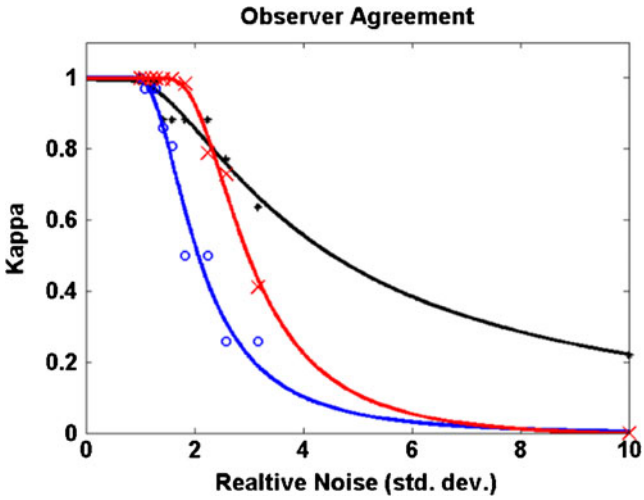

Figure 1. Pilot study of observer agreement as a function of noise level. At the International Pediatric Radiology Meeting in 2006, 20 volunteers participated in 30-minute sessions, and viewed ten abdominal images at 11 dose levels. The task was to determine if a lesion was present and to localize it. Samples were prepared by manually setting fixed noise levels (1%, 10%, 15%, 20%, 30%, 40%, 50%, 60%, 70%, 85%, and full dose [100%]), and observer agreement was characterized by Kappa statistics. Results from three typical observers are presented, with lines fitted to a Weibull function. The median threshold noise level (at Kappa=0.5) was 2.52.

Paper #: PA-108

Congenital Lobar Overinflation: Prenatal MRI and US Findings and Outcomes

Jennifer Johnston, MD, *Cincinnati Children's Hospital Medical Center, Cincinnati, OH, Jennifer.H.Johnston@uth.tmc.edu;* Beth Kline-Fath, MD, Constance Bitters, Maria Calvo-Garcia, Foong-Yen Lim

Purpose or Case Report: To identify fetal magnetic resonance imaging (MRI) and ultrasound (US) findings of congenital lobar overinflation (CLO) and assess the postnatal outcome.

Methods & Materials: Fetal MRI and prenatal US were reviewed in 25 fetuses diagnosed with CLO. Congenital pulmonary airway malformation (CPAM) volume ratio (CVR) was obtained by dividing the estimated volume of the lesion by head circumference. Charts were reviewed for indication, pregnancy outcome, postnatal imaging, interventions and pathologic results.

Results: Twenty-five fetuses at mean gestational age of 24 weeks were evaluated via fetal MRI based on US diagnosis of CPAM (16), lung lesion (8) and suspected CLO (1). On imaging when compared to normal lung, 24 (96%) were homogeneous increased echogenicity via US, and 23 (92%) homogeneous T2 hyperintensity on fetal MRI. The remaining, 2 MRI and 1 US, showed mild heterogeneity. There was absence of a systemic feeding vessel on US and MRI. Additional findings on fetal MRI included presence of a hilar T2 tubular cystic structure in 17 (68%) consistent with dilated bronchus and lack of pulmonary vascular distortion. Possible intralesional round cyst was noted on fetal MRI in two cases. Postnatally, one cyst was found to represent a bronchogenic cyst and the other a distal segmental bronchial atresia. Mediastinal shift was present in 12 (48%) and hydrops in 2 (8%). Mean CVR was 0.6 for asymptomatic and 4.7 for symptomatic fetuses. Most commonly involved lobes were the right and left lower lobes. The 2 (8%) hydropic fetuses that had high CVR and imaging findings resembling congenital high airway obstruction syndrome (CHAOS) were found to have central bronchial atresia. Both experienced fetal demise. One fetus (4%) with CLO developed respiratory distress due to extrinsic compression from a subcarinal bronchogenic cyst and required surgical intervention. 18 (72%) fetuses were asymptomatic. Two had normal chest radiographs and no further imaging. Postnatal CT in 16 confirmed CLO. Ten of these infants had verification via resection and/or bronchoscopy. The remaining eight infants were followed for a mean of 7 months without symptoms. Four fetuses were lost to follow-up.

Conclusions: Most CLO are asymptomatic, primarily in the lower lobes, and homogeneous on both US and MRI, thus aiding in differentiation from CPAM. On fetal MRI, a dilated bronchus is often observed. On US, a low CVR is supportive. High morbidity related to CLO is uncommon, occurring in fetuses with CHAOS-like lesions or CLO due to extrinsic compression.

Paper #: PA-109

Specificity of single or multiple fetal MR imaging findings in identifying a hernia sac in fetuses with congenital diaphragmatic hernia

Amy Mehollin-Ray, *Texas Children's Hospital, Houston, TX, armeholl@texasChildren's.org;* Irving Zamora, Christopher Cassady, Jennifer Williams, MD, Darrell Cass, Oluyinka Olutoye

Purpose or Case Report: Of fetuses with congenital diaphragmatic hernia (CDH), those with a hernia sac show improved mortality and reduced need for ECMO compared to those without a hernia sac. The goal of our study was to evaluate the sensitivity and specificity of various fetal MR

imaging findings, used singly and in combination, for identifying the presence of a hernia sac.

Methods & Materials: All fetal MR examinations performed for intrapleural congenital diaphragmatic hernia at a single institution over the past 10 year period were reviewed independently by two pediatric radiologists. The presence or absence of a hernia sac was defined at the time of repair and pathologic examination.

The MR studies were examined for four findings:

1. A meniscus of lung tissue posterior to the hernia contents on axial images or superior to the hernia contents on coronal or sagittal images;
2. Hernia contents appearing encapsulated, and exerting less than expected mass effect on the heart, mediastinum and contralateral lung;
3. The presence of pleural fluid outlining a sac from above;
4. The presence of ascites outlining a sac from below.

The two reviewers noted whether a hernia sac was thought to be present based on the presence of any of the four findings. Additionally they recorded how many total findings were present. Consensus was defined as agreement on positive diagnosis between the two observers.

Sensitivity and specificity were calculated for each finding independently and for the combination of any two or any three findings.

Results: Of 90 total patients, 21 had a confirmed hernia sac. For any single sac finding, the sensitivity and specificity for the presence of a hernia sac were 0.43 and 0.97, respectively. For a combination of two or three sac findings, the sensitivity and specificity for the presence of a sac were 0.38 and 0.97, respectively. Interobserver variability was moderate (Cohen's kappa: 0.46 for a single sac finding; 0.57 for any two or three findings).

Conclusions: On fetal MR imaging, the presence of a hernia sac in CDH can be suggested with very high specificity when a single finding is present. The specificity does not increase with the addition of multiple findings. The sensitivity is low, however, and decreases further when multiple findings are required for diagnosis.

Paper #: PA-110

Is Echocardiography Necessary in Fetuses with Chest Masses?

Jennifer Son, *Boston Children's Hospital, Boston, MA, jennifer.son@Children's.harvard.edu;* Alaina Kipps, Judy Estroff, MD

Purpose or Case Report: We assessed the added value of fetal echocardiography (echo) to diagnose cardiovascular malformations (CVM) in fetuses with chest masses on prenatal imaging.

Methods & Materials: We reviewed obstetric records and fetal imaging (US, MRI and fetal echo) for prenatally diagnosed chest masses from September 1999 to May 2008 at the Advanced Fetal Care Center, Boston Children's Hospital. Postnatal clinical records, imaging studies, surgical pathology and autopsy data were examined to determine perinatal/neonatal diagnosis and outcome. Patent ductus arteriosus, patent foramen ovale and abnormal cardiac position were excluded from the definition of CVM.

Results: Two hundred thirty-three cases of fetal chest masses were identified. 134 were congenital diaphragmatic hernias (CDH) and 98 were lung masses falling within the bronchial atresia spectrum, including 59 congenital pulmonary airway malformations (CPAM), 11 sequestrations, 21 hybrid lesions, five congenital lobar emphysema, and two bronchogenic cysts. There was one mediastinal lymphatic malformation. 119/134 fetuses (88.8%) with CDH had a fetal echo showing a CVM in 17/119 (14.3%). Postnatal echo was performed on 11 of the 15 patients who did not have a fetal echo; all were normal. Of the 102 cases with normal cardiac anatomy on fetal echo, 65 (63.7%) had a postnatal echo. Of these, 11 (16.9%) had new diagnoses of CVM; all were lesions known to be difficult to detect prenatally, including 4 VSDs, 4 ASDs, 2 coarctations, and one abnormal mitral valve. Of 99 fetuses diagnosed with non-CDH chest masses, 65 had fetal echo (65.7%). 2 (3.1%) [95%CI: 0.4%–10.7%] were found to have CVM: 1 TOF and 1 critical PS. 19/63 (30.2%) fetuses initially diagnosed with normal cardiac anatomy had normal postnatal echos.

Conclusions: In fetuses with non-CDH chest masses who had fetal echo, only two cases of CVM were diagnosed (3.1%), similar to the incidence of CVMs in the general population. Routine use of fetal echo in this group may not be warranted except for further evaluation of heart anomalies noted on the initial fetal survey or in cases with concern for hemodynamic compromise due to compression from the lung mass. In fetuses with CDH, routine use of fetal echo is advised due to the high incidence of concomitant CVM. Postnatal echo should be considered to search for CVMs not identified on initial fetal echo. These findings should be confirmed in a larger cohort.

Paper #: PA-111

Prenatal Imaging of Bronchopulmonary Malformations: Is There a Role for Late Third Trimester Fetal MRI?

Siobhan Flanagan, MD, *Pediatric Radiology, Stanford University/Lucile Packard Children' Hospital, Palo Alto, CA, CA;* Erika Rubesova, Susan Hintz, Claudia Mueller, Richard Barth, MD

Purpose or Case Report: To demonstrate the importance of late third trimester fetal MRI (>32 weeks of gestational age (GA)), for the evaluation of bronchopulmonary malformations (BPM) compared to early MR (20–26 weeks of GA) and its correlation with postnatal imaging.

Methods & Materials: Under institutional IRB, we conducted a retrospective review of a database of fetal pulmonary masses that underwent prenatal ultrasound, early MRI (late 2nd or early 3rd trimester MRI), late MRI (late third trimester fetal MRI), and postnatal (PN) imaging at our institution from 2005 to 2012. The size, location, presence of systemic feeding vessel, and characterization of BPMs into CLO, CPAM, hybrid lesion, sequestration, and bronchogenic cyst was determined by consensus of three radiologists. Correlation of MRI appearance and diagnosis compared with PN imaging was assessed.

Results: Twenty-six patients were identified. Early MRI was performed between 20 and 26 weeks GA and late MRI from 30 to 37 weeks GA. USs were performed the same day as the MRIs in all patients. Postnatal CT was performed in 25/26 patients between the ages of 5 days −16 months. One patient was sent to surgery without PN CT based on late MRI findings. Postnatal diagnoses were: nine CPAM, five sequestrations, six CLO, four hybrid lesions (CPAM and sequestration), two bronchogenic cysts.

Changes in the appearance of BPMs were noted between early and late MRI and included: decrease in signal intensity on T2WI (19/26), change in mediastinal shift (worsened in 2/26 and improved in 4/26), change in the area of lung involvement (16/26 late MR had better correlation with PN imaging than early MRI), and change in size (17/26 late MR had better correlation with PN imaging than early MRI). One case of a single large mass on early MRI appeared as two separate lesions on late MRI.

11/26 lesions were not detectable on the late ultrasound (same echogenicity as normal lung) but were all visible on late MRI. A systemic artery was detected in 9/9 early US, 7/9 late US, 6/9 early MRI, and 7/9 late MRI for ELS or hybrid lesions.

Characterization of the type of BPM was concordant with postnatal diagnosis in 19/26 cases with early MRI and in 22/26 cases with late MRI. Thus, late MRI compared to earlier MR provided the more correct diagnosis in 3/26 cases.

Conclusions: Late MRI adds information to that obtained from early MRI and correlates closely with postnatal imaging. Therefore, late MRI may improve patient counseling, prenatal clinical management and has the potential to delay or reduce postnatal imaging.

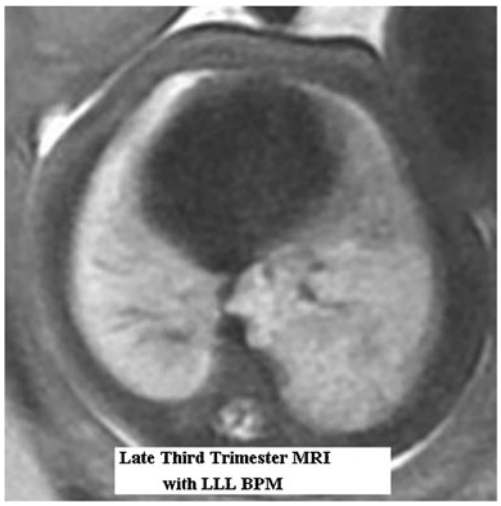

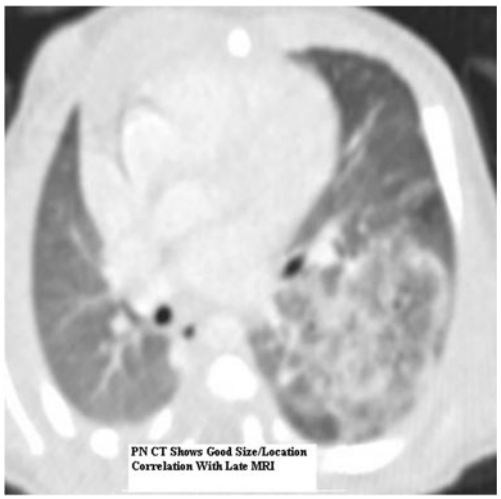

Paper #: PA-112

Fetal Suprarenal Masses- Assessing the Complementary Role of MRI and Ultrasound for Diagnosis

Siobhan Flanagan, MD, *Pediatric Radiology, Stanford University/Lucile Packard Children' Hospital, Palo Alto, CA, CA;* Erika Rubesova, Diego Jaramillo, Teresa Victoria, MD PhD, Richard Barth, MD

Purpose or Case Report: Purpose: To assess the value and complementary role of fetal MRI versus Ultrasound (US) for characterization and diagnosis of suprarenal region masses.

Methods & Materials: A multi-institutional retrospective database search for prenatally diagnosed suprarenal region masses from 4/1999 to 8/2012 was conducted. We evaluated

the role of prenatal US versus fetal MRI for characterization (predominantly cystic versus solid) and diagnosis, using postnatal diagnosis or surgical pathology as reference standard. On prenatal imaging, the masses were assessed for systemic arterial supply on Doppler US and for unique findings provided by each modality. MRI assessment of mass signal intensity was also performed to further characterize solid masses as high or intermediate signal intensity.

Results: Database search yielded 27 patients with fetuses with suprarenal region masses diagnosed between 20 and 37 weeks gestational age. 22 cases had prenatal US, 24 cases had MRI, 19 cases had both US and MRI. The postnatal diagnoses were: nine subdiaphragmatic extra-lobar sequestrations (ELS), seven adrenal hemorrhages, five neuroblastomas (NB)(4 metastatic), two lymphatic malformations, one mesenteric cyst, one duplex kidney with upper pole cystic dysplasia, one hemorrhagic ovarian cyst, and one adrenal hyperplasia. Final imaging diagnosis by US and MRI was concordant with the postnatal diagnosis in all cases. US was concordant with MRI for diagnosis in 14/19 cases. The five cases with discordant diagnoses between US and MRI were 3 NB and 2 adrenal hemorrhages. In 3 NB cases, US was equivocal for diagnosis and MRI was definitive for NB by demonstrating heterogeneous, intermediate signal solid masses and liver metastases. In 2/4 NB, Doppler US demonstrated a systemic artery suggesting initially ELS; however, MRI signal characteristics correctly diagnosed NB. In two cases of adrenal hemorrhage, US was equivocal, demonstrating a complex mass and the MRI was definitive with signal characteristics of hemorrhage. All cases of ELS were correctly diagnosed by US and MRI. Doppler US demonstrated a systemic artery in all cases of ELS. 8/9 ELS were hyperechoic on US and 9/9 demonstrated a high signal intensity solid mass on MRI.

Conclusions: US and MRI both accurately detect suprarenal masses. MRI complements US for equivocal diagnoses such as neuroblastoma and demonstrates additional findings such as liver metastases.

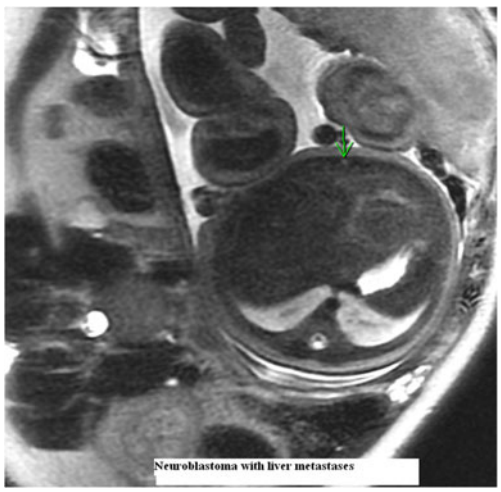

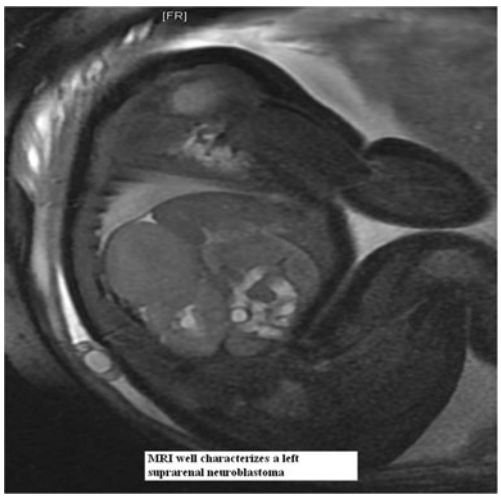

Paper #: PA-113

MR-I Can Do It: A Pilot Program aimed to reduce sedation rates for pediatric magnetic resonance imaging (MRI).

Kristen Brandolini, *Children's National Medical Center, Washington, DC, kbrandol@cnmc.org;* Tracy Sharbaugh, Erin Stanford, Laura Cronin, Nadja Kadom, Raymond Sze

Purpose or Case Report: The purpose of this study was to demonstrate the benefits of the MR-I Can Do It Program, (a program aimed at helping patients six and older complete their MRI without sedation), specifically cost and patient and family satisfaction.

Methods & Materials: In a 10 month period 147 patients and families were participants in the MR-I Can Do It Program. Data on the scan protocol, patient's medical history, age, time spent with certified child life specialist (CCLS), and if the patient completed the scan without sedation was collected. Additionally, patient satisfaction surveys were gathered. Data was collected regarding the average cost of anesthesia sedation per patient, and the amount of time the patient would spend in the MRI suite. From the data collected, we compared money and time saved by assisting the 147 patients complete their scan without sedation, as well as how the patient and family perceived the program and interaction with the CCLS.

Results: One hundred forty-seven participants ranging in age from 3 to 20 years old attempted the non-sedate program, and of the 147 total patients, 141 participants succeeded. The mean chronological age was 8.8 years; the mean amount of time spent with the CCLS on the scan day was 111 min, not including actual scan time. The average amount of time needed for a patient requiring sedation on the scan day was 135 min, again, not including actual scan time. However, for those patients requiring

sedation, they also required 1:1 nursing care which would be a total of 195 min on average.
The average cost of sedation per patient was calculated out to be approximately $1,644.00 which included the anesthesiologist and supplies. The average cost for the non-sedate program per patient was calculated out to be approximately $41.00, which included the CCLS's salary and supplies. This is a cost savings of $1,603.00, not including the 1:1 nursing care required for sedated patients.
The patient satisfaction surveys showed that the majority of families recommended the program to others, found the program to be helpful, and stated that the CCLS helped to ease both patient and parental anxiety.
Conclusions: The MR-I Can Do It Program helped lower the financial costs by reducing the need for anesthesia. Furthermore, the time a non-sedated spent in the MRI suite was significantly less than the time of sedated patients. Lastly, the patient satisfaction surveys showed that families found all aspects of the MR-I Can Do It program beneficial.

Paper #: PA-114

Child Life Services in Pediatric Imaging Sciences: Assessing the Value and Recommendations for Implementation

Mary Tyson, *Radiology, Golisano Children's Hospital, Rochester, NY, m_tyson@urmc.rochester.edu;* Chelsea Pino, Constance White, Stephanie Lemke, Lisa Snow, Johan Blickman, MD PhD

Purpose or Case Report: To assess the value of hiring a Certified Child Life Specialist (CCLS) in Pediatric Imaging Sciences in terms of financial impact, family/staff satisfaction as well as analyze how this Program should be structured to decrease costs and increase efficiency.
Methods & Materials: A controlled trial,stratified across procedure and age of the child, in the Pediatric Imaging Department assigned patients from 1 to 12 years old to a control or child life intervention group. Length of procedure, parent satisfaction, staff satisfaction, child satisfaction, parent perception of child distress, and staff perception of child distress were collected for both groups.
Benchmarking with national institutions was performed to analyze their use of child life and the impact on flow, patient satisfaction, and sedation rates. A cost-benefit analysis of employing a child life specialist was performed.
Results: Clear differences are present between the control and intervention group on all measures. Parent perception of child distress is 1.13 lower (all measures are on a 5 point scale) in the intervention group than the control group. Parents in the intervention group reported on average .74 higher than the control group that their child's emotional needs were met. Staff perception of family satisfaction is .63 higher with the child life intervention.
Benchmarking showed a national lack of statistical data to support their Child Life program. Anecdotally a decrease in sedation rates correlating to child life services was reported. At GCH the average reimbursement for an unsedated pediatric MR is $296. Avoiding sedation in just two MR patients a week would generate revenue of $26,702. Extrapolating these results for CT and conventional radiography would cover the cost of an experienced child life specialist in addition to added benefit of increased staff and parent satisfaction, marketing and brand benefits, and improved departmental work flow.
Conclusions: These results provide empirical support for the implementation of child life services in pediatric imaging departments to improve parent satisfaction, staff satisfaction, department flow, and hospital revenue stream.

Paper #: PA-115

Is the new ACR-SPR practice guideline for addition of oblique views of the ribs to the skeletal survey for child abuse justified?

Megan Marine, MD, *Pediatric Radiology, Indiana University School of Medicine, Indianapolis, IN, mbshelto @iupui.edu;* Boaz Karmazyn, Donald Corea, Scott Steenburg, Matthew Wanner, George Eckert

Purpose or Case Report: Evaluate if adding oblique bilateral rib radiographs to skeletal survey significantly changes detection of number of rib fractures.
Methods & Materials: We identified all patients less than 2 years of age who underwent skeletal survey for suspected child abuse (1/2003–7/2011) and age matched the same number of control patients. Two randomized series of radiographs of the ribs, two views (anteroposterior and lateral), and four views (added right and left obliques) were created. Three fellowship trained radiologists (2 pediatric and 1 trauma) blinded to original reports, independently evaluated the series using a Likert scale of 1 (no fracture) to 5 (definite fracture). Utilizing the readers' results, we analyzed the following: sensitivity and specificity of the two view series for detection of rib fractures using the four view series as gold standard, interobserver variability, and confidence level.
Results: The study group included 106 patients with at least one rib fracture and 106 age-matched controls with no rib fracture. The sensitivity and specificity of the two view series for detection of any rib fracture in a patient was on average 81% and 91%, respectively. Sensitivity and specificity for detection of posterior rib fractures was on average 74% and 92%, respectively.

There was good agreement between observers for detection of rib fractures in a patient in both series (average Kappa of 0.7 and 0.78 for two views and four views, respectively). Confidence significantly increased for four views.

Conclusions: Adding bilateral oblique rib radiographs to the skeletal survey results in increased rib fracture detection by an average of 19% and increased confidence of readers.

Two View Series	Patient	
	Any Rib Fracture	Posterior Rib Fracture Only
Sensitivity	74–85% (avg 81%)	67–82% (avg 74%)
Specificity	80–100% (avg 91%)	86–99% (avg 92%)

Paper #: PA-116

Frequency of skeletal injuries in children with inflicted burns

Kimberly Fagen, MD, *Walter Reed National Military Medical Center, Bethesda, MD, kimberly.fagen@med.navy.mil;* Eglal Shalaby-Rana

Purpose or Case Report: It is estimated that inflicted burn injuries in children occur with an incidence of approximately 10–12%. Little is known about the prevalence of skeletal injuries in children with intentional burns. We undertook this study to assess the prevalence of inflicted burns, as well as, the frequency of associated skeletal injuries, in a large children's hospital.

Methods & Materials: After IRB approval, we analyzed a data base of 654 children with suspected abuse who visited Children's National Medical Center from 1997 to 2009. 73 children with burn injuries were identified. All patients had undergone skeletal surveys as part of the diagnostic work-up. The final diagnosis of non-accidental (NAT), accidental and indeterminate (IND) was made by the child abuse pediatrician. In five patients, the final diagnosis was not known, so these children were excluded. One patient had a skin infection that mimicked a burn; this patient was also excluded. The different fractures seen on the skeletal surveys were recorded for each patient. If the patient had only the soft tissue abnormality from the burn seen on the skeletal survey, the result was recorded as a normal skeletal survey.

Results: There was a total of 67 reported cases. Thirty girls and 37 boys with ages ranging from 1 to 110 months, mean age of 18.4 months. Twenty-five(37%) were determined to be NAT, and 16 (24%) accidental and 26 (39%) were IND. The most common causative mediums were scald injuries and chemical burns. Most kids were under 2–3 years. No sex predilection was found.

Skeletal surveys were positive for fractures in 9/25 (36%) of the nonaccidental group; 0/16 (0%) in the accidental group and 4/26 (15%) of the indeterminate group. Fractures in the NAT group included healing rib fractures in six, healing shaft fractures in three, classic metaphyseal lesions in one and skull fracture in one patient. Fractures in the IND group included shaft fractures in three, one of which was healing, and spine fracture in one patient.

Conclusions: Regarding burn injuries in children, more than one third are intentionally inflicted, greater than what has been reported in the literature. In addition, over one third of these children with inflicted burns have associated skeletal injuries, most commonly healing rib fractures. Thus young children with non-accidental burns would benefit from undergoing a skeletal survey.

Paper #: PA-117

Reliability of estimation of 3D ACL attachment locations from routine pediatric knee MRI

Vimarsha Swami, *Department of Radiology and Diagnostic Imaging, University of Alberta, Edmonton, AB, Canada, vimarsha.swami@ualberta.ca;* June Cheng-Baron, Catherine Hui, Lucy Jamieson, Richard Thompson, Jacob Jaremko

Purpose or Case Report: Current techniques of anterior cruciate ligament (ACL) reconstruction in pediatric patients focus on placement of femoral and tibial tunnels at anatomic locations of ACL attachments, which can be difficult to identify intra-operatively. Many patients have pre-operative knee magnetic resonance imaging (MRI) available. We developed a computer technique where users identify points along the ACL attachments on routine clinical preoperative knee MRI. From these points, our computer algorithm calculates the centres of the ACL attachments in three-dimensional (3D) space, as estimates of the best locations for tibial and femoral tunnel placement. The purpose of this study was to determine whether the radiologic centre of ACL attachments can be reliably detected from routine MRI in patients with intact ACL, and whether the reliability of this technique changes if the ACL is torn.

Methods & Materials: Routine clinical 1.5-Tesla knee MRI of 37 pediatric patients (10–17 years) with ACL tears and 37 intact-ACL controls were examined. Two blinded observers identified ACL attachment sites on MRI slices. From the resulting cluster of user-identified attachment points, the location of the centre of each ACL attachment site and its area was calculated, and reliability assessed. User-identified attachments were also displayed on a 3D reconstruction model for intra-operative visualization.

Results: Inter-observer variation of the radiologic centres of ACL attachments for intact vs. torn ACLs was 1.7±0.9 vs. 1.8±1.1 mm (mean ± standard deviation, femoral attachment, $p>0.05$) and 1.4±0.9 vs. 1.7±1.0 mm (tibial attachment, $p>0.05$), with 99.9% power to detect a 1.5 mm difference between user-identified attachment centres. The 95% confidence interval for centre location was at most 4 mm. In all cases, intra-observer reliability was superior to inter-observer reliability.

Conclusions: The 3D locations of ACL tibial and femoral attachment centres were identified from routine clinical MRI with variability averaging <2 mm between two observers. Error was at most 4 mm, representing the thickness of one axial MRI slice, whether the ACL was intact or torn. Remnant tissue at attachments allows reliable assessment even of torn ACLs. This technique can reliably identify the centres of ACL attachments from routine clinical MRI in pediatric patients to allow improved tunnel placement in anatomic single-bundle ACL reconstruction.

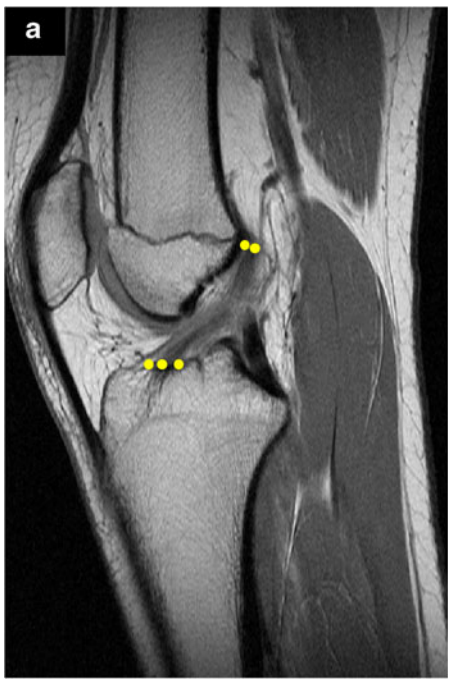

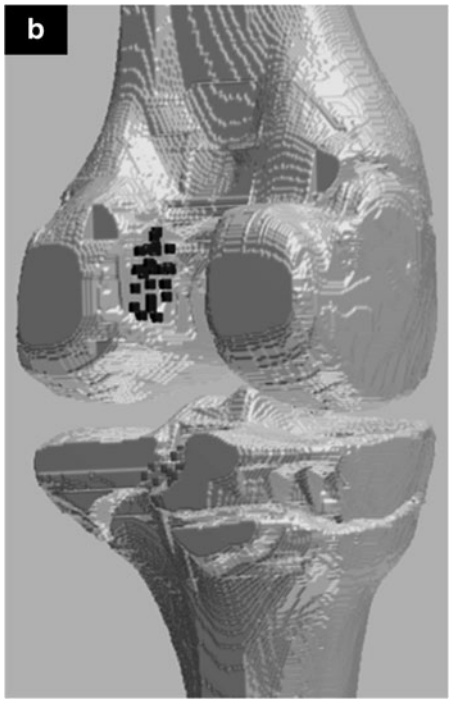

Figure 1: (a) ACL attachments to femur and tibia identified by one user on sagittal proton density MRI in a patient with complete ACL tear. Note that remnant tissue fibers at the bony attachments are clearly visualized. (b) 3D reconstruction showing bony surfaces and the 3D location of the femoral ACL attachment. This can be rotated freely into any orientation. Note that in this view the posterior cruciate ligament (PCL) tibial attachment is also visible.

Paper #: PA-118

The Patellofemoral Joint: Do Age and Gender Affect the Osseous Morphology in Children During Skeletal Maturation?

Hee Kyung Kim, *Radiology, CCHMC, Cincinnati, OH, Hee.-Kim@cchmc.org;* Sahar Shiraj, Christopher Anton, Paul Horn

Purpose or Case Report: To determine age and gender related differences in the osseous morphology of the patellofemoral joint in children during skeletal maturation.

Methods & Materials: This study was approved by the institutional review board and was HIPAA compliant. Ninety seven subjects (51 females and 46 males; mean age 14.3 years and 13.7 years respectively) without patellofemoral instability were included. 1.5-T knee semiquantitative MR exams were studied. The osseous

morphology of the patellofemoral joint (lateral trochlear inclination, trochlear facet asymmetry, trochlear depth, patellar height ratio, tibial tubercle-trochlear groove distance, and lateral patellofemoral angle) were measured for each MR exam. Measurements were compared to published values for patellofemoral instability. Physeal patency (open or closing/-closed) was determined on semiquantitative MR. The associations between MR osseous measurements, gender, age, and physeal patency were assessed using Wilcoxon Rank Sum Test and Least Square Means regression models.

Results: The osseous patellofemoral joint morphology measurements were all within a normal range. There were no significant correlations between MR osseous measurements and age, gender, or physeal patency.

Conclusions: During skeletal maturation, age and gender do not affect the osseous morphology or congruency of the patellofemoral joint.

Paper #: PA-119

The Patellofemoral Joint: T2 Relaxation Times and Thickness of the Cartilage in Different Ages and Genders in Children

Hee Kyung Kim, *Radiology, CCHMC, Cincinnati, OH, Hee.Kim@cchmc.org;* Sahar Shiraj, Christopher Anton, Paul Horn

Purpose or Case Report: To determine age and gender related differences in T2 relaxation time mapping and thickness of the patellar cartilage in children during skeletal maturation.

Methods & Materials: This study was approved by the institutional review board and was HIPAA compliant. Ninety seven subjects (51 females and 46 males; mean age 14.3 years and 13.7 years, respectively) without patellofemoral instability were included. 1.5-T knee MR imaging with T2 relaxation time mapping (T2 map) and semiquantitative images were studied.

Table 2. MR measurements of the osseous morphology

MR measurements	Open physis			Closing/Closed physis			Physis		
	Female	Male	P value*	Female	Male	P value*	Open	Closed	P value**
Lateral trochlear inclination (°)	20.3±4.1	19.4±5.1	0.414	18.8±4.2	18.0±4.0	0.682	19.8±4.6	18.5±4.1	0.108
Median	21.0	19.0		18.0	18.0		19.0	18.0	
95% CI	14.0–28.0	9.0–31.0		12.0–27.0	12.0–24.0		9.0–31.0	12.0–27.0	
Trochlear facet asymmetry (%)	71.5±8.8	72.3±8.9	0.591	68.8±13.0	68.7±12.3	0.854	72.0±8.8	68.8±12.6	0.171
Median	69.2	71.4		66.6	68.5		71.4	67.2	
95% CI	56.2–89.8	56.2–91.0		40.2–96.1	47.6–100.0		56.2–91.0	40.2–100.0	
Trochlear depth (mm)	5.2±1.6	4.9±1.7	0.343	5.0±1.0	5.3±0.8	0.309	5.1±1.7	5.1±0.9	0.822
Median	5.6	5.0		4.9	5.1		5.2	5.1	
95% CI	1.9–9.6	2.2–11.0		2.0–7.3	4.3–7.6		1.9–11.0	2.0–7.6	
Patellar height ratio	1.1±0.2	1.1±0.2	0.834	1.2±0.1	1.1±0.2	0.708	1.1±0.2	1.2±0.2	0.100
Median	1.1	1.1		1.2	1.2		1.1	1.2	
95% CI	0.8–1.4	0.7–1.3		0.9–1.4	0.8–1.4		0.7–1.4	0.8–1.4	
Tibial tubercle-trochlear groove distance (mm)	5.6±3.0	5.7±4.6	0.570	6.6±3.5	6.8±4.2	0.976	5.6±3.9	6.7±3.8	0.184
Median	4.6	4.7		6.8	7.1		4.6	7.1	
95% CI	1.4–11.8	0.8–17.1		0.8–12.0	1.7–15.6		0.8–17.1	0.8–15.6	
Lateral patellofemoral angle (°)	13.1±4.0	10.7±4.5	0.081	12.1±3.9	12.4±3.8	0.560	11.7±4.4	12.2±3.8	0.732
Median	13.0	10.0		12.0	13.0		11.5	13.0	
95% CI	3.0–20.0	0.0–18.0		5.0–20.0	2.0–18.0		0.0–20.0	2.0–20.0	

*P value determined from Wilcoxon Rank Sum test ** Gender-adjusted P value in ANOVA model

Mean T2 relaxation times and thickness of the patellar cartilage were obtained for each MR exam. Physeal patency (open or closed/closing) was determined on semiquantitative MR. The associations between T2 relaxation times, cartilage thickness, gender, age, and physeal patency were assessed using Wilcoxon Rank Sum Test and Least Square Means regression models.
Results: T2 relaxation times and thickness of the cartilage significantly decreased ($P<0.0001$) with increasing chronologic age. T2 relaxation times and cartilage thickness in the open physis group were greater than in the closed/closing physis group ($P<0.0001$). T2 relaxation times and cartilage thickness were greater in boys than in girls ($P<0.05$).
Conclusions: During skeletal maturation, T2 relaxation times and thickness of the patellar cartilage are age and gender dependent.

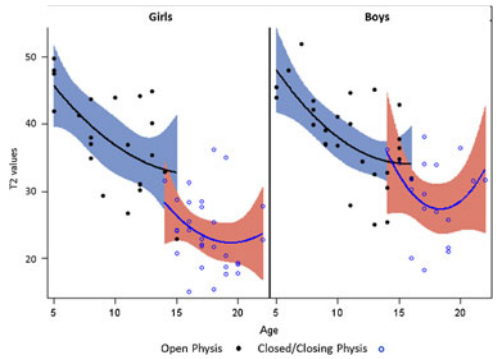

Paper #: PA-120

Patterns of meniscal injury in the pediatric ACL deficient knee

Zachary Guenther, BMedSc, *University of Alberta, Edmonton, AB, Canada, zguenthe@ualberta.ca;* Jacob Jaremko, Vimarsha Swami, Sukhvinder Dhillon

Purpose or Case Report: Anterior cruciate ligament (ACL) tears are common in the pediatric population and are frequently associated with meniscal injury. It has been shown previously that delay to surgery is associated with an increased rate of medial meniscal tears, but the prognosis of specific tear types has not been described. The purpose of this study is to use findings at Magnetic Resonance Imaging (MRI) and surgery to characterize the patterns of evolution of meniscal tears, in particular bucket-handle meniscal tears (BHMT), in adolescent patients with complete ACL tears.
Methods & Materials: Retrospective review of adolescents (10–16 years, average 15.4) who sustained ACL injuries followed by surgical repair from 2005 to 2011 ($n=112$) in a Canadian city. We compared dates of injury, MRI and surgery, and the findings at MRI and surgery.
Results: MRI was obtained in mean 77 days (range 1–377), and surgery in mean 342 days (range 42–1637). Meniscal injuries were present in 75% of patients at the time of MRI and 85% at the time of surgery. However, large or displaced tears were much more common at surgery (53%) than at MRI (19%). There was a significant increase in the rate of medial meniscal tears in patients operated >1 year (26/37) vs. <1 year (34/75) post-injury ($p=0.005$), while lateral meniscal tears remained stable over time. The development of BHMT's (Figure 1) was significantly more likely if surgery occurred >1 year after injury (17/37 vs. 21/75; $p=0.04$). The risk of meniscal tear progression between MRI and later surgery did not vary significantly with tear presence, type, or location.
Conclusions: Our study is the first to combine post-ACL injury MRI and intraoperative findings to describe patterns of evolution of meniscal tears in the pediatric ACL-deficient knee. Medial meniscal tears in general, and specifically BHMTs, increased steadily in frequency even after 1 year post-injury. The type of tear present at initial MRI is not a risk factor for tear progression, and

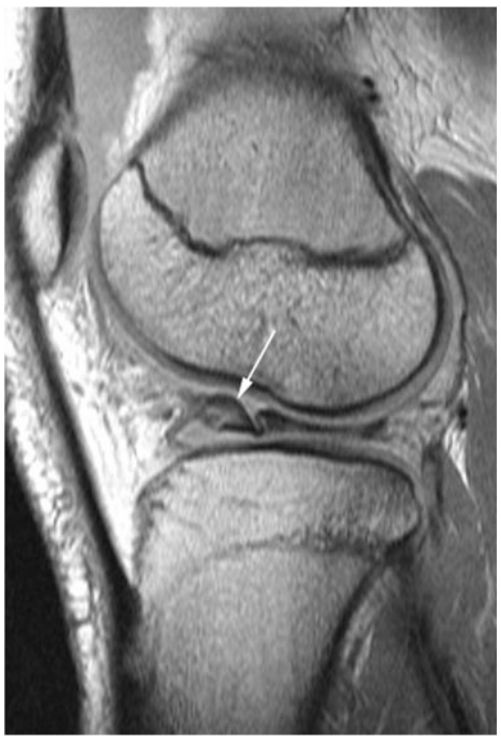

Figure 1 - Sagittal fat-saturated proton density MR image of a 16 year old with a bucket- handle tear of the lateral meniscus, demonstrating a folded displaced portion (arrow)

it is likely that all medial meniscal tears will worsen over time in a similar fashion due to ongoing knee instability.

Paper #: PA-121

Diffusion Tensor Imaging of the Growing Ends of the Bones: Demonstration of Columnar Structure in the Physes and Metaphyses of the Knee

Camilo Jaimes, MD, *Radiology, The Children's Hospital of Philadelphia, Philadelphia, PA, camilojaimes12@gmail.com;* Jeffrey Berman, PhD, Jorge Delgado, Victor Ho-Fung, Diego Jaramillo

Purpose or Case Report: To determine if diffusion tensor imaging (DTI) and tractography can demonstrate the columnar arrangement of the physis; and to examine changes related to rate of growth, location, and age.

Methods & Materials: We analyzed DTI of the knee in 40 subjects (26 girls; 14 boys), with a median age of 13.6 years (range: 4.8–18.6). Images were acquired at 3.0 T (n=30) and 1.5 T (n=10). We placed regions of interest (ROI) in the physis of the tibia and femur, and in the epiphyseal and articular cartilage of both bones. Tractography was performed using a fractional anisotropy (FA) threshold of 0.15 and an angle threshold of 40°. We recorded ROI- and tack-based apparent diffusion coefficient (ADC), FA, magnitude of main eigenvector (λ1) and track length. Bones were stratified into three groups based on skeletal maturity. In immature individuals we placed additional ROIs to compare the central and peripheral physis. Also, we compared ADC, FA, λ1 and tractography between epiphyseal cartilage and the physis.

Results: Fiber-tracking of immature bones (32 femurs; 27 tibias) demonstrated tracks that started in the physis and extended into the adjacent metaphysis. Femoral tracks (median length: 6.68 mm) were longer than tibial tracks (median length: 4.69 mm) (p<0.01); and tracks in the periphery of the physes were longer than in the center (p<0.01). Peak track length was observed between ages 12 and 14. In the physis of immature femurs and tibias there was an age-related decrease in ROI-based ADC, λ1, and transverse diffusion (p<0.05). Mature bones demonstrated short tracks with random arrangement. The ADC, FA and λ1 of epiphyseal cartilage were significantly different from those of the physis (p<0.01). Tractography in the epiphyseal cartilage showed a non-columnar organization of the tracks, which were shorter and did not have any definable structure.

Conclusions: DTI depicts the columnar microstructure of the physis and adjacent metaphysis and may provide further insights into normal and abnormal growth.

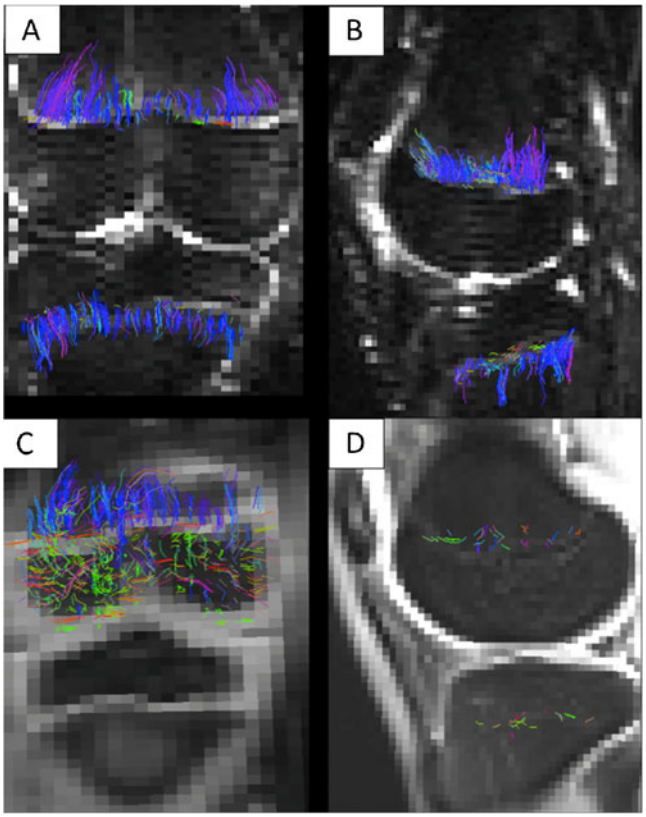

Paper #: PA-122

Wrist and ankle MRI of JIA patients: Significance of unsuspected multicompartmental tenosynovitis and arthritis

Sanaz Javadi, MD, *Baylor College of Medicine, Houston, TX;* J. Kan, MD, Marietta DeGuzman, Robert Orth

Purpose or Case Report: The purpose of this study was to characterize the extent of joint and tendon involvement in JIA patients referred for MRI of the ankle or wrist.

Methods & Materials: Forty-five patients (F:M=32:13; mean age=10 years; age range=1–19 years) with an established diagnosis of JIA were referred for MRI of the ankle or wrist between 1/2000 and 8/2012 (39 wrists, 33 ankles). All MRI exams and clinical notes were reviewed and individual joint and tendon involvement was recorded. Criteria for active joint inflammation were joint effusion, juxtasynovial edema, or marrow edema. The criterion for tenosynovitis was circumferential fluid surrounding the tendon.

Results: Fifty-six percent (25/45) of patients or 50% (36/72) of exams had tenosynovitis. Tenosynovitis was not documented in the clinical notes prior to MRI. When tenosynovitis was present, an average of two tendons were involved (range=1–12). In the wrist, 59% (23/39) had tenosynovitis. The most

commonly involved tendons were extensor digitorum 23% (9/39) and extensor digiti minimi 23% (9/39). In the ankle, 39% (13/33) had tenosynovitis. The most commonly involved tendons were tibialis posterior 33% (11/33) and peroneus complex 18% (6/33).

Eighty-seven percent (39/45) of patients or 81% (58/72) of exams had active joint inflammation. For the wrist, 90% (35/39) had active inflammation with an average of three joints involved (range=0–6). The most commonly involved joints were intercarpal 69% (27/33), radiocarpal 64% (25/39), and distal radioulnar 56% (22/39). For the ankle, 70% (23/33) had active inflammation with an average of two joints involved (range=0–5). The most commonly involved joints were tibiotalar 52% (17/33), talonavicular 36% (12/33), and subtalar 27% (9/33).

Conclusions: Tenosynovitis and multijoint involvement is very common in JIA patients referred for MRI of the wrist or ankle. Targeted steroid injections guided by clinical exam alone may lead to undertreatment of active disease. MRI identification of the involved compartments of the wrist or ankle may enhance efficacy of targeted steroid injections.

Paper #: PA-123

Radiographic variants of the inferior patellar pole revisited: normal or within the spectrum of patellar avulsive injuries?

Esben Vogelius, MD, *Pediatric Radiology, Texas Children's Hospital, Houston, TX, esvogeli@texasChildren's.org;* J. Kan, MD, Robert Orth

Purpose or Case Report: Irregular ossification at the inferior patella is a common finding on pediatric knee radiographs. Without associated anterior soft tissue swelling, patellar tendon thickening, or edema in Hoffa's fat, this finding if often dismissed as a normal variant. The purpose of this study was to determine whether irregular ossification at the inferior patellar pole is a true normal variant or represents patellar pathology.

Methods & Materials: A retrospective study was performed on 188 consecutive knee radiographs in 172 different patients between the ages of 5 and 10 from January 2000 to September 2012 (50.5% male, mean age 7.7 years). All patients had an MRI performed within 120 days of the knee radiographs (mean interval 16 days). Exclusion criteria were a history of tumor, infection, or prior surgery. Radiographs were reviewed by two radiologists. Irregular ossification at the inferior patella was identified in 31 knees (mean age 7.9 year, age range 5.5–9.5, 48% male) and classified by morphology into 1 of 5 categories: 1, rounded; 2, curvilinear contiguous; 3, curvilinear discontiguous; 4, rounded and curvilinear contiguous; 5, rounded and curvilinear and discontiguous. A 1:1 age and sex matched control group (N=31, mean age 7.9, age range 5.1–9.9, 48% male) was generated from the remaining 157 radiographs. The inferior patella was retrospectively assessed on MRI to evaluate for increased signal intensity on T2-weighted and STIR images. Clinical notes were reviewed for the presence of inferior patellar pain.

Results: 16.5% (31/188) of knee radiographs showed irregular ossification at the inferior patella. Of these 31 patients, 58% (18/31) had increased signal intensity on fluid-sensitive MRI sequences compared to 0% (0/157) for the radiographically normal controls (p<0.001). The incidence of increased inferior patellar pole signal intensity by category was 1: 45% (5/11), 2: 57% (8/14), 3: 67% (2/3), 4: 100% (2/2), and 5: 100% (1/1). Compared to the control group, patients with irregular ossification at the inferior patella had a significantly higher incidence of reported focal inferior patellar pain (26% vs. 3%, p=0.012).

Conclusions: Irregular ossification at the inferior patella is frequently associated with abnormal signal intensity on MRI and focal inferior patellar pole pain. Inferior patellar pole "variations" may represent unrecognized pathology within the spectrum of avulsive injury to the inferior patella.

Paper #: PA-124

Chemical-shift fat-water separation MRI and diffusion tensor imaging as quantitative imaging markers for disease progression in Duchenne Muscular Dystrophy: Preliminary Study

Skorn Ponrartana, MD, MPH, *Department of Radiology, Children's Hospital Los Angeles, Los Angeles, CA, sponrartana @chla.usc.edu;* Tishya Wren, Houchun Hu, Stefan Bluml, Leigh Ramos-Platt, Vicente Gilsanz

Purpose or Case Report: To investigate the potential of chemical shift fat-water separation MRI and diffusion tensor imaging (DTI) as quantitative imaging markers of disease severity in Duchenne muscular dystrophy (DMD) by correlating with clinical assessments. The development of objective and highly reproducible markers may be better than conventional clinical assessment in prediction of patterns of disease distribution, progression of disease, and therapeutic response.

Methods & Materials: Eight consecutive boys (mean age, 8.6 years±2.1 years) with DMD were evaluated using mDixon chemical shift water-fat separation and diffusion tensor imaging MRI sequences of the right lower extremity. A total of 19 muscles were individually evaluated. A pediatric neurologist who was blinded to the MRI findings performed clinical assessments (patient age, manual muscle tests, 10 m walk test, 6 min distance test, rise time from floor, and rise time from chair). Functional tests were compared with manual muscle testing,

muscle fat fraction (MFF) determined with mDixon MRI technique, and fractional anisotropy (FA) and apparent diffusion coefficient (ADC) determined by diffusion tensor imaging.

Results: MRI measures of muscle adiposity (MFF) and muscle structure (FA and ADC) had a stronger correlation with functional tests than did measurements obtained with manual muscle tests. Among the MRI measures, MFF was significantly correlated with mean ADC ($p<0.015$) and mean FA ($p<0.012$). However, MFF had a higher correlation with functional ability than did ADC or FA. Significant correlations were found between the mean MFF of all muscles and the patients' age ($p<0.01$) and Medical Research Council Score ($p<0.04$), with increased MMF positively correlated with age and negatively correlated with muscle strength. Mean FA was significantly negatively correlated with Medical Research Council Score ($p<0.024$), although there was no significant correlation with age. The pattern of disease distribution showed that there was significantly increased MFF ($p<0.01$), increased FA ($p<0.01$), and decreased ADC ($p<0.01$) in the muscles of the thigh and pelvis compared with leg.

Conclusions: MRI measures of muscle obtained with mDixon and DTI techniques are useful markers in assessment of disease severity in patients with DMD. Of these techniques, mDixon MRI measures of muscle fat fraction have the strongest correlation with manual muscle testing and functional assessment.

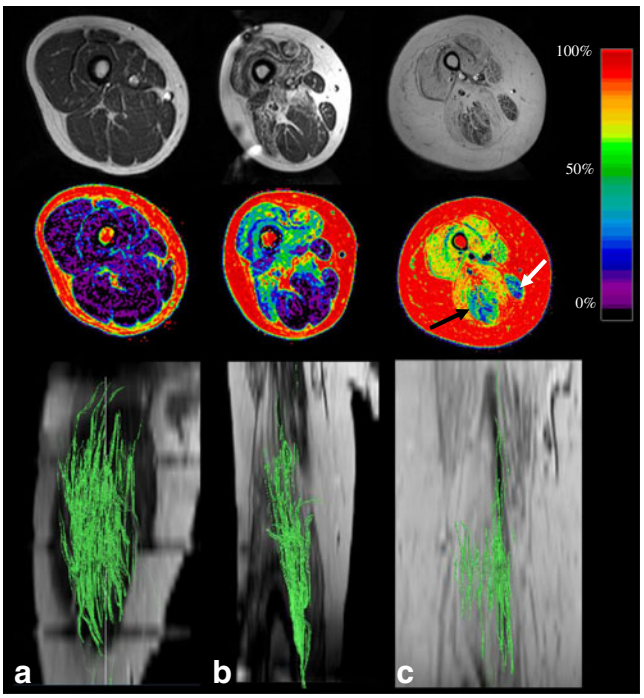

Figure 1. Axial T1-weighted of the right thigh (top), axial mDixon muscle fat fraction of the right thigh (middle), and coronal DTI tractography images of the right rectus femoris muscle. **(a)** 6-year old with DMD, early ambulatory stage, shows no significant intramuscular fatty infiltration and fibers that are large in number and organized in a superior-inferior distribution. **(b)** 8-year-old with DMD, late ambulatory stage, has up to 50% fatty infiltration in the quadriceps and adductor magnus muscles and decreasing number, length and organization of fiber tracks. **(c)** 12-year-old with DMD, early non-ambulatory stage, with >50% fatty infiltration in all muscles groups excluding the gracilis muscle (white arrow) and semitendinosus muscle (black arrow). There are scattered, short fiber tracks which are few in number.

Paper #: PA-125

Detection of enthesitis in children with Enthesitis-related arthritis: physical examination compared to ultrasonography

Nancy Chauvin, MD, *Department of Radiology, The Children's Hospital of Philadelphia, Philadelphia, PA, chauvinn@email.chop.edu;* Pamela Weiss, Andrew Klink, Diego Jaramillo

Purpose or Case Report: Enthesitis or inflammation at the sites where tendon or ligaments insert in the bone is a distinct pathologic feature of Enthesitis-related arthritis (ERA), a category of juvenile idiopathic arthritis (JIA). We wish to compare ultrasound with physical examination for the detection of enthesitis.

Methods & Materials: We performed a prospective cross-sectional study of 20 ERA subjects. The following insertion sites (bilateral) were assessed by physical examination using a standardized dolorimeter exam and by US with Power Doppler: common extensor tendons on medial humerus epicondyle, common flexor tendon on lateral humerus epicondyle, quadriceps at superior patella, patellar ligament at inferior patella, Achilles tendon and plantar fascia at the calcaneus. Physical examinations were performed by a pediatric rheumatologist and pain thresholds were recorded with the dolorimeter at each enthesis. US examinations were performed by a pediatric radiologist with experience in musculoskeletal imaging. Using sonography as the reference standard, the positive and negative predictive values (PPV and NPV) were calculated for dolorimeter exam pressures ranging from 1.5 to 4.5 kg, using US as the gold standard. The PPV and NPV of the dolorimeter exam at the quadriceps insertion at the superior patella are shown in the table.

Results: The ERA subjects had a median age of 14 years (IQR: 13,16). 65% were male and 60% were HLA-B27+. The sites with the most abnormal US findings (abnormal doppler signal intensity or tendon appearance) were the quadriceps insertion at the superior patella ($N=16/40$, 40%), the patellar ligament insertion at the inferior patella ($N=8/40$, 20%), the common extensor tendon insertion at

the lateral humerus epicondyle (*N*=6/40, 15%), and the Achilles tendon insertion (*N*=6/40, 15%). The most common tender entheses using 3.5 kg of pressure with the dolorimeter were the patellar ligament insertion at the inferior patella (*N*=31/40, 78%), the quadriceps insertion at the superior patella (*N*=29/40, 73%), and the common flexor tendon insertion on the medial humerus epicondyle (*N*=19/40, 48%).

Conclusions: Dolorimeter exam is not sensitive for detecting ultrasound confirmed enthesitis and thus cannot be used for screening purposes to detect early enthesitis. US may be needed for screening purposes, but it's ability to predict worsening disease and it's utility in guiding decisions to initiate therapy needs to be studied. Dolorimeter exam may be specific enough to rule out enthesitis at higher pressures.

Table. PPV and NPV of standardized dolorimeter exam using US as the gold standard

Pressure (kg)	Sensitivity (95% CI)	Specificity (95% CI)	PPV (95% CI)	NPV (95% CI)
1.5	0.19 (0.07, 0.31)	0.58 (0.43, 0.74)	0.23 (0.10, 0.36)	0.52 (0.36, 0.67)
2.0	0.44 (0.28, 0.59)	0.33 (0.19, 0.48)	0.30 (0.16, 0.45)	0.47 (0.32, 0.63)
2.5	0.56 (0.41, 0.72)	0.29 (0.15, 0.43)	0.35 (0.20, 0.49)	0.50 (0.35, 0.65)
3.0	0.63 (0.48, 0.78)	0.25 (0.12, 0.38)	0.36 (0.21, 0.51)	0.50 (0.35, 0.66)
3.5	0.69 (0.54, 0.83)	0.25 (0.12, 0.38)	0.38 (0.23, 0.53)	0.55 (0.39, 0.70)
4.0	0.75 (0.62, 0.88)	0.21 (0.08, 0.33)	0.39 (0.24, 0.54)	0.56 (0.40, 0.71)
4.5	0.75 (0.62, 0.88)	0.21 (0.08, 0.33)	0.39 (0.24, 0.54)	0.56 (0.40, 0.71)

Paper #: PA-126

Growth Plate Abnormalities in Pediatric Cancer Patients Undergoing Phase 1 Anti-Angiogenic Therapy: A Report from the Children's Oncology Group Phase I Consortium

Stephan Voss, *Radiology, Boston Children's Hospital, Boston, MA, stephan.voss@Children's.harvard.edu;* Julia Glade-Bender, Marvin Nelson, Brenda Weigel, Susan Blaney

Purpose or Case Report: Pre-clinical studies suggest that agents inhibiting angiogenic activity may be toxic to the developing growth plate by suppressing new blood vessel and trabecular bone formation along the zone of provisional calcification. We evaluated the incidence of growth plate abnormalities in children with refractory cancer receiving agents that are known to inhibit angiogenesis.

Methods & Materials: The cohort included 54 patients enrolled in eight different Children's Oncology Group phase 1 trials of tyrosine kinase inhibitors (*n*=35); monoclonal antibodies targeting VEGF (13) or IGF-1R (*n*=5); or a NOTCH1 inhibitor (*n*=1). Radiographs of the distal femur/proximal tibia were obtained at baseline in all study patients. In patients with open growth plates who did not experience disease progression, follow-up radiographs were obtained after completion of odd-numbered treatment cycles. Treating centers were instructed to obtain an MRI for further evaluation of patients with radiographic evidence of growth plate thickening or other physeal abnormality.

Results: Baseline and post therapy extremity radiographs were available in all 54 patients, 15 of whom received at least 5 cycles of therapy. All images were centrally reviewed by the same radiologist. Normal growth plates were observed in 50/54 patients. Three patients had growth plate widening that was apparent radiographically, but was not confirmed by MRI. In each case growth plate widening was observed on at least two successive radiographs. One patient had significant and progressive growth plate widening on therapy that was also confirmed by MRI, showing physeal cartilage thickening that corresponded to the radiographic findings. All growth plate abnormalities occurred in patients receiving a specific VEGF/VEGF-R blocking agent.

Conclusions: Growth plate abnormalities occur in a small, but relevant number of patients undergoing anti-angiogenic therapy. These results support the need for rigorous growth plate monitoring and more sensitive and specific methods to assess toxicity of these agents on the developing skeleton.

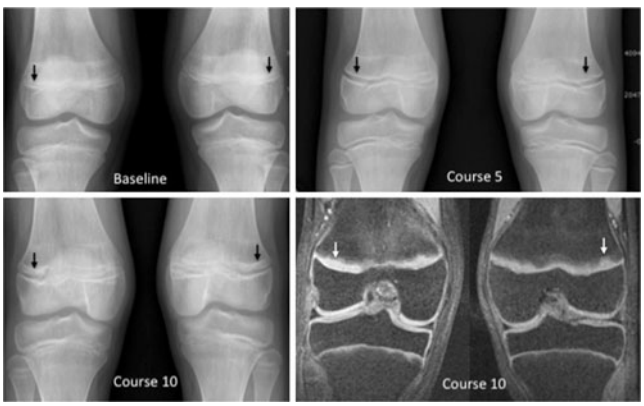

Paper #: PA-127

Imaging and Histopathologic Characteristics of Post-Transplant Neoplasms in Children with Multivisceral Transplants

Anastasia Hryhorczuk, *Radiology, Tufts Medical Center, Boston, MA, ahryhorczuk@tuftsmedicalcenter.org;* Heung Bae Kim, Sara Vargas, Edward Lee, MD, MPH

Purpose or Case Report: Solid organ transplantation carries a known risk of post-transplant neoplasm, often associated with Epstein Barr virus (EBV). While the clinical presentation and imaging findings of post-transplant neoplasms have been documented in children with single organ transplants, less is known about the radiological findings of post-transplant neoplasms in children undergoing multivisceral transplantation. The aim of this research is to analyze the clinical, imaging, and histopathological findings of post-transplant neoplasm among children following multivisceral transplantation.

Methods & Materials: IRB approval was obtained. From August 2004 to October 2011, 12 children were identified who received multivisceral transplants with at least 1 year of clinical and imaging follow-up. Two radiologists reviewed the clinical and imaging records for patients in the study population, and diagnosis of disease was made by consensus interpretation. Pathology specimens were also examined. Medical records of the patients were assessed to determine the exact nature of the transplant graft, pertinent clinical features of the post transplant course, treatment, and outcome.

Results: Seven boys and five girls comprised the 12 patients who received multivisceral transplants. The mean age at transplantation was 18.8 months (range: 3.5 months to 88.5 months). Of the 12 patients who received multivisceral transplants, three patients developed histologically confirmed post-transplant lymphoproliferative disorder (PTLD), a frequency of 25%. Two patients developed pathologically proven EBV-associated smooth muscle tumors (18%). As one patient developed both PTLD and an EBV-associated smooth muscle tumor, the overall frequency of post-transplant neoplasm was 33%. No patients developed recurrence of their post-transplant neoplasm. One patient died during treatment of his post-transplant neoplasm.

In this population, PTLD presented as tonsillar enlargement in one patient, gastric, pulmonary, and solid organ masses in a second patient, and multiple enlarged lymph nodes in a third patient. In both patients with EBV-associated smooth muscle tumors, tumors presented as hypointense solid masses on CT, with characteristic peripheral rim enhancement.

Conclusions: Post-transplant neoplasms are a significant source of morbidity and mortality in children receiving multivisceral transplants. Attention to the imaging characteristics of these neoplasms can aid in early diagnosis and treatment of these malignancies in this susceptible population.

Paper #: PA-128

Imaging characteristics, clinical course, and neuropsychological outcome in 9 pure pineal germinomas

Matthew Jones, MD, *University of Colorado, Aurora, CO, matt.jones@ucdenver.edu;* Laura Fenton, MD, Greta Wilkening, Sarah Rush, Nicholas Stence

Purpose or Case Report: Pure pineal germinomas have a strong male predominance and present between 10 and 30 years of age. Recently, significant cognitive deficits have been described; in particular, amnesia is a debilitating comorbidity. Our aim is to further investigate correlation between imaging characteristics, imaging response to therapy, and neuropsychological course in patients with pure pineal germinomas. Specifically, do pineal germinomas with cystic components fare worse long-term from a neurocognitive perspective?

Methods & Materials: A retrospective review of the Children's Hospital Colorado neuro-oncology database from 1995 to 2011 was performed. Patients with pathologically proven pure pineal germinomas, pretherapy and posttherapy magnetic resonance imaging, and cognitive testing were included. Charts were reviewed for demographics, neuropsychological assessments, therapy, and course. Imaging was evaluated for tumor size, solid and cystic characteristics, local extension, and presence of metastases.

Results: Seventy-eight patients were diagnosed with intracranial germ cell tumors over the 16 year period. Nine met inclusion criteria. Mean age at presentation was 16.3 years. All patients were male. Average duration of imaging followup was 3.8 years. 56% had tumors with cystic components by MRI. 33% had intracranial metastases at presentation. All patients were treated with neoadjuvant

chemotherapy and radiation. All but one patient had clinical remission following therapy. Seventy-eight percent of patients presented with amnesia, only one patient improved following therapy. Tumor extension to the red nuclei was the only imaging finding correlating with amnesia.

Conclusions: Although previously believed to be rare, 56% of the tumors in our series had cystic components. Prior studies have suggested that the presence of cystic components has negative prognostic significance; we found no such correlation. No clear explanation for memory disruption by pineal region tumors has previously been offered. We did note an association between memory disorder and extension of the tumor inferiorly to the level of the red nuclei. This area does not have known associations with memory function, and this finding may therefore be a surrogate for tumor aggressiveness rather than involvement of particular anatomic structures. Additionally, tumor extension into adjacent structures (i.e. medial thalami) may be present to a greater degree than is perceptible by imaging.

Paper #: PA-129

Pediatric Posterior Fossa Ganglioglioma: Unique MRI Features and Correlation with BRAF V600E Mutation Status

Aaron Lindsay, MD, *Department of Radiology, Children's Hospital Colorado, University of Colorado Denver, Aurora, CO, aaron.lindsay@ucdenver.edu;* Sarah Rush, Laura Fenton, MD

Purpose or Case Report: Ganglioglioma (GG) is a rare pediatric brain tumor (1–4% of all) with neoplastic glial and neuronal cells. Most GGs are supratentorial (ST), occur in the temporal lobe, present with seizure, and are well circumscribed and usually amenable to gross total resection (GTR). Posterior fossa (PF) GGs occur less frequently. Detection of the BRAF V600E gene mutation has been reported in 18% of supratentorial GGs, and is helpful for diagnosis as well as development of targeted therapies. We compare the presenting symptoms, MR imaging, BRAF V600E mutation status and treatment in children with ST and PF GGs.

Methods & Materials: Following IRB approval, the neuro-oncology database at a tertiary care Children's Hospital was retrospectively reviewed for patients with ST and PF GG from 1995 to 2010. Molecular testing results with BRAF mutation status were recorded. Symptoms, imaging, and treatment (including targeted BRAF inhibitors) were reviewed.

Results: Eleven patients with PF GGs and 20 patients with ST GGs were identified. PF GG patients ranged in age from 1 day to 23 years (5 of 11 male; median age 4 years) and ST GG from 10 months to 19 years (12 of 20 male; median age 8.5 years). Presenting symptoms differed: patients with PF GGs had ataxia (7), weakness (5), soft voice (4), sensory changes (4), speech delay (3), and dysphagia (3) whereas patients with ST GGs had seizure (17), headache (2) and weakness (1). Imaging differed: PF GGs were infiltrative and expansile (8 of 11), infrequently cystic (2 of 11), and had dorsal predominant "paintbrush" type enhancement (6 of 11) whereas ST GGs were solid (9 of 20), mixed cystic and solid (10 of 20) with homogeneous (5 of 20), heterogeneous (10 of 20), or no (3 of 20) enhancement of the solid portion. No PF GG was amenable to GTR compared to 16 of 20 ST GGs that were. 55% (6 of 11) of PF GGs and 67% (6 of 9 tested) of ST GGs expressed the BRAF V600E mutation. There was no difference in imaging of ST or PF GGs with or without the BRAF V600E mutation. One BRAF V600E mutation positive PF GG patient failed traditional therapy but had a dramatic response following treatment with Vemurafenib (BRAF inhibitor).

Conclusions: Unlike ST GGs, PF GGs are expansile, infiltrative, show dorsal predominant "paintbrush" enhancement and are not amenable to GTR. ST GGs are more likely to express the BRAF V600E mutation than PF GGs. No imaging features unique to BRAF V600E mutation positive PF or ST GGs were identified.

Paper #: PA-130

Comparison of Semi-automated Segmentation, Manual segmentation and Maximum Diameter Product in Measuring Chemotherapy Response of Pediatric Neuroblastoma

Ahmed Almuslim, MBBS, FRCR, *Children's Hospital of Eastern Ontario, University of Ottawa, Ottawa, ON, Canada, binmuslim@gmail.com;* Nishard Abdeen, MD, Elka Miller

Purpose or Case Report: The purpose of this study is to compare the correlation of semi-automated segmented measurement, manual segmentation, and the product of maximum

diameters in assessing the post-chemotherapy volume change of pediatric neuroblastoma on MR imaging. We hypothesized that due to the complex shape of these tumors, segmentation would be more accurate than the product of diameters.

Methods & Materials: Fourteen MR studies between January 1, 2009 to June 30, 2012 of 7 children (5 girls; ages 5–48 months, average 22 months) with neuroblastoma (abdominal (n=6) thoracic (n=1); before and post chemotherapy were included. Manual and semi-automated segmentation volume calculations were carried out on a General Electric Advantage workstation. Two radiologists independently measure the tumor. The two readers were blinded to the original report and they used the axial fat saturated T2-weighted images for the segmentation. The tumor volume was also calculated with the formula 0.5×length×width×height using measurements from the original report. The percent reduction in tumor volume was calculated as initial tumor volume minus final tumor volume divided by initial tumor volume x100%.

Results: There was excellent agreement between the automatic segmentation and manual segmentation of tumor volumes. The percent reduction in tumor volume ranged from 42 to 93% for manual segmentation and from 36 to 100% for semi automated segmentation. The difference between the two methods in percent reduction for each tumor ranged from 2% to 7%. The correlation coefficient R2 was 0.965. Average time for manual segmentation per exam was 93 s, while the average manual segmentation was significantly longer at approximately 14 min. The ellipsoid formula yielded reductions in tumor volumes of 37 to 96%. Agreement between the ellipsoid volume formula and the semiautomatic segmentation and manual segmentation was also good, although less than the correlation between the segmented volume methods, with correlation coefficients of 0.839 and 0.896 respectively.

Conclusions: Calculation of semi-automated segmentation is more rapid than manual segmentation and leads to similar results. It is more accurate than the product of maximum diameters, and merits further evaluation as a measure of treatment response in neuroblastoma.

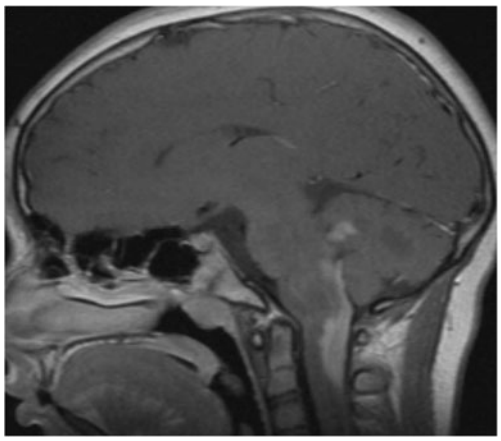

Figure 1: 13 year old girl with dorsal predominant “paintbrush” type enhancement, typical of that seen in 6 of 11 posterior fossa gangliogliomas.

Paper #: PA-131

FDG PET/CT Appearance of Locally Recurrent Osteosarcoma after Limb Salvage Surgery

Susan Sharp, *Radiology, Cincinnati Children's Hospital Medical Center, Cincinnati, OH, susan.sharp@cchmc.org;* Barry Shulkin, Michael Gelfand, MD, Beth McCarville, MD

Purpose or Case Report: Current surgical treatment of osteosarcoma most often involves limb salvage surgery rather than amputation. Metallic hardware placed at limb salvage causes MR and CT artifacts which limit evaluation for local recurrence. FDG PET can be used for detection of local recurrences, as well as distant metastases. We describe the FDG PET/CT appearance of locally recurrent osteosarcoma after limb salvage surgery.

Methods & Materials: Retrospective review of eight osteosarcoma patients (age at initial diagnosis 8–16 years, median 13 years) imaged with FDG PET/CT after limb salvage with histologically proven local recurrences.

Results: All eight local recurrences were seen in the periprosthetic soft tissues. On PET 5 local recurrences demonstrated solid FDG uptake, while three demonstrated peripheral nodular FDG uptake. Maximum SUVs ranged from 3.0 to 15.7 with a median of 6.7. Localization CT demonstrated soft tissue masses in 5 with 1 mass also demonstrating abnormal calcifications.

For four patients with distal femoral primary tumors, local recurrence occurred adjacent to the distal femoral hardware in 2, proximal femoral hardware in 1, and proximal tibial hardware in 1. For three patients with proximal tibial primary tumors, local recurrence occurred adjacent to the proximal tibial hardware in two with one patient demonstrating a large mass involving portions of the thigh and leg. For one patient with a proximal humeral primary tumor, local recurrence occurred adjacent to the mid humeral hardware. At the time of local recurrence, four patients also had lung metastases.

Time from limb salvage surgery to PET/CT demonstrating local recurrence ranged from 6 to 44 months with a median of 11 months.

Conclusions: After limb salvage surgery, local osteosarcoma recurrences were well demonstrated by FDG PET/CT. Recurrences occurred in the periprosthetic soft tissues, demonstrating either solid or peripheral nodular FDG uptake. The range of observed maximum SUVs was wide (3.0–15.7).

Paper #: PA-132

Evaluation of the Utility of ^{99m}Tc-MDP Bone Scintigraphy vs ^{131}I/^{123}I-MIBG Scintigraphy and Cross-sectional Imaging for Staging Patients with Neuroblastoma

Jean-Marc Gauguet, *Radiology, Boston Children's Hospital, Boston, MA, jean-marc.gauguet@Children's.harvard.edu;* Tamara Pace-Emerson, Frederick Grant, Suzanne Shusterman, Lindsay Frazier, Stephan Voss

Purpose or Case Report: The purpose of this study was to examine the relative contribution of ^{99m}Tc-MDP bone scintigraphy (bone scan) versus ^{131}I/^{123}I-MIBG scintigraphy (MIBG scan) for staging of neuroblastoma.

Methods & Materials: An IRB-approved search identified patients (pts) diagnosed with neuroblastoma between 1993 and 2012 who had undergone both bone and MIBG scans for disease staging. At least one cross sectional imaging modality (ultrasound, CT, or MRI) was used in each case to further establish disease burden and corroborate scintigraphy results. Clinical records were utilized to correlate imaging findings with clinical staging and patient management.

Results: One hundred seven pts (ages 1 week–15 years) were identified who underwent both bone scan and MIBG scan (103 ^{123}I and 4 ^{131}I) at the time of diagnosis. INSS staging revealed eight stage 1 (7.3%), 7 stage 2B (6.4%), 20 stage 3 (18.2%), 69 stage 4 (62.7%) and 3 stage 4S (2.7%) pts.

All stage 1, 2B, and 4S pts had MIBG uptake in the primary tumor, with negative bone scan and negative skeletal MIBG uptake.

For pts with stage 3 disease, skeletal uptake was reported on bone scans in 10/20 cases (50%), but determined to be false positive, based on lack of corroborating cross-sectional imaging or clinical findings. 1/20 (5%) of pts had false positive skeletal uptake reported on both MIBG and bone scan. The remaining 9 pts had MIBG uptake in the primary tumor, but no sites of skeletal disease.

For pts with stage 4 disease, bone scan and MIBG were positive in 53/69 (77%) of the cases. 50/53 bone scan-positive cases had corresponding MIBG positivity. In stage 4 pts, 6 of 69 bone scans (9%) and 4 of 69 MIBG studies (6%) were false negative based on positive marrow aspirates. Only 3 pts with positive uptake on bone scan had MIBG scans that were negative for skeletal involvement:

1) One pt's primary tumor was not MIBG-avid; bone marrow biopsy established stage 4 disease.

2) One pt's stage 4 disease was based on the presence of pulmonary nodules; bone marrow biopsy was negative and bone scintigraphy was considered false positive.

3) One pt had widespread MIBG uptake both at the primary site and in the mediastinum, establishing stage 4 disease independent of the bone scan results.

Conclusions: These results suggest the majority of the lesions identified by ^{99m}Tc-MDP bone scintigraphy are also detected by MIBG scan and/or cross-sectional imaging, and that bone scintigraphy does not identify unique sites of disease that affect disease stage or clinical management.

Paper #: PA-133

Thyroid Carcinoma in Pediatric Patients: Effective I-131 Ablation Dose and Outcome

Tejal Mody, MD, *Pediatric Radiology, Texas Children's Hospital, Houston, TX, tejal.mody@yahoo.com;* Jennifer Williams, MD, Nadia Mahmood, MD, Wei Zhang, Robert Orth

Purpose or Case Report: Differentiated thyroid carcinoma (DTC) in children is rare with an incidence of 0.5 per 100,000 children. However, the incidence has been increasing at a rate of 1.1% per year. DTC in pediatric patients is typically treated with total thyroidectomy followed by I-131 radio-ablation. However, I-131 dose determination remains highly variable in the pediatric population. The purpose of this study was to determine if there was a statistical difference in I-131 doses between pediatric patients with recurrent and non-recurrent differentiated thyroid carcinoma.

Methods & Materials: A retrospective review of all children receiving radioiodine ablation for thyroid carcinoma at a large children's hospital was performed. Twelve years (1999–2011) of PACS and electronic medical record data were reviewed. Patients were categorized into recurrent and non-recurrent groups. Ablative I-131 radiation doses, thyroglobulin levels, pathology results, and radiology reports were reviewed. Average radiation doses received by patients who recurred versus those who did not recur were compared using Wilcoxon rank test. The chi-square test was employed to evaluate for a statistical difference in recurrence rates between children receiving greater than 100 mCi versus those receiving less than 100 mCi.

Results: Therapeutic I-131 was administered to 27 children during the study period; 89% (24/27) had papillary carcinoma and 11% (3/27) had follicular variant. Recurrent disease after an initial therapeutic dose of I-131 occurred in 48% (13/27) of patients. Of patients with recurrent disease, 9/13 (69%) were treated with less than 100 mCi whereas only 3/14 (21%) patients without recurrence were treated with less than 100 mCi I131. Chi square test indicated a statistical difference in dose between these patient groups (p=0.03). The average dose for patients with recurrent disease was 89 mCi (std : 33, range 39–144) versus 105 mCi (std: 15, range 79.9–132) in patients without recurrence. The Wilcoxon rank test suggested a difference in average I-131 doses between these patient groups (p=0.10).

Conclusions: Pediatric thyroid cancer patients treated with initial I-131 doses below 100 mCi are more likely to recur than those treated with higher doses. Multi-institutional studies are needed to establish the optimal initial treatment dose.

Paper #: PA-134

18F-FDOPA PET/CT imaging in Congenital Hyperinsulinism: Patterns of uptake in diffuse and focal disease.

Lisa States, MD, *Radiology, CHOP, Philadelphia, PA, states@email.chop.edu;* Susan Becker, Andrew Palladino, N. Scott Adzick, Charles Stanley, Hongming Zhuang

Purpose or Case Report: The purpose of this study is to evaluate the patterns 18F-FDOPA uptake in the pancreas on attenuation corrected three dimensional Maximum Intensity Projection (3D MIP) images in focal and diffuse disease in patients with congenital hyperinsulinism.

Methods & Materials: From January of 2008 to January of 2012, at the Children's Hospital of Philadelphia,100 infants and neonates with medically unresponsive congenital hyperinsulinism underwent 18F-FDOPA PET imaging for the diagnosis of a focal lesion of beta cell adenomatosis. 86 cases were evaluable. Retrospective review of (3D MIP) images was performed by a single radiologist to determine the frequency of the various patterns of pancreatic uptake encountered on 18F-FDOPA PET/CT scans. All cases underwent surgery and histopathology analysis. The diagnostic categories were focal disease and diffuse disease. The focal lesions were evaluated and placed in the following descriptive categories: 1) focal, which was easily recognized as a single focus of increased activity; 2) dual head and body/ tail, which had mild increased uptake in the head associated with a hotter lesion in the body or tail; 3) heterogeneous; or 4) faint uptake in a single focus. The diffuse lesions were evaluated and placed in the following descriptive categories: 1) homogeneous, which was easy to recognize; 2) mild increased uptake in head and homogeneous throughout the rest of the pancreas; or 3) heterogeneous with patches of increased uptake in the head, body and tail.

Results: As detailed in Table 1., 59 of 86 (69%) cases were easily diagnosed as diffuse or focal disease on 3-D MIP images. 74% of focal lesions were easily diagnosed as a single lesion of increased uptake. 31% of cases required further evaluation using fused PET/CT images in axial, coronal or sagittal planes with or without SUV analysis. In this series, the sensitivity of diagnosis of a focal lesion was 85%. Failure to detect a focal lesion may be related to lesion size, shape or location.

Conclusions: 1. Recognition of the various patterns of uptake is essential for interpretation of 18F-FDOPA PET/CT scans.

2. The 3-D MIP is a useful tool in the diagnosis of focal congenital hyperinsulinism.

TABLE 1.

Patterns on 3D MIP images of 18F-FDOPA PET/CT in 86 cases

DIFFUSE DISEASE	***N*=33 (38%)**	**FOCAL DISEASE**	***N*=53 (62%)**
Homogeneous(easy)	*N*=20 (61%)	Focal(easy)	*N*=39 (74%)
Mild head uptake	*N*=5 (15%)	Dual H/body or tail	*N*=3 (6%)
Heterogeneous	*N*=8 (24%)	Heterogeneous	*N*=4 (7%)
		Faint uptake	*N*=7 (13%)

Paper #: PA-135

Relapse Surveillance in AFP-Positive Hepatoblastoma: Is There a Role for Imaging?

Yesenia Rojas, MD, *Pediatric Surgery Division, Michael E. DeBakey Department of Surgery, Texas Children's Hospital, Baylor College of Medicine, Houston, TX, yrojas@bcm.edu;* R. Guillerman, Wei Zhang, Sanjeev Vasudevan, Jed Nuchtern, Patrick Thompson

Purpose or Case Report: Hepatoblastoma (HB) is the most common primary liver malignancy in children, accounting for approximately 65% of all pediatric primary liver malignancies. In the past several decades, improvements in diagnostic modalities, chemotherapy, and operative treatment have led to overall improved survival and longer lifespan. The focus has shifted to minimizing adverse effects from diagnosis, treatment, and surveillance. Children with HB routinely undergo repetitive surveillance computer tomography (CT) scans for several years after therapy increasing the risk of radiation-induced cancer. The purpose of this study was to determine the cumulative radiation dose and the efficacy of surveillance CT scans compared to serum AFP levels for the detection of HB recurrence.

Methods & Materials: This retrospective study included patients diagnosed with HB from 2001 to 2011 at a single institution. Patients without serum AFP elevation at diagnosis were excluded from the study. The AFP levels and imaging exams performed following completion of therapy were recorded for all patients. Cumulative radiation dose and frequency of recurrence detection by these tests were determined.

Results: Twenty-six patients with HB were identified with a mean age at diagnosis of 2 years 4 months (range 3 months–11 years). Mean AFP level at diagnosis was 129,176 ng/mL (range 172.8–572,613 ng/mL). Five of the 26 patients had recurrent HB, with one recurring twice. The sites of recurrence included the lungs in five cases, and the liver resection margin in one case. A total of 140 imaging exams were performed following completion of therapy, consisting of 109 (78%) CT, 17 (12%) US, 9 (6%) MRI, and 5 (4%) PET/CT exams. A total of 503 AFP levels were drawn, with a mean of 19 per patient. The AFP level was elevated in all recurrences prior to detection by imaging. One false positive imaging exam occurred among patients without HB recurrence. The mean radiation effective dose per patient during surveillance was 35.1 mSv (range 0–104 mSv).

Conclusions: All patients with recurrent HB demonstrated an elevation in serum AFP level before detection of recurrent tumor by imaging. Given the high cost of repetitive imaging and the risk of secondary malignancy from cumulative ionizing radiation exposure, we recommend the use of serial serum AFP levels as the preferred method of surveillance for recurrent HB, with imaging reserved for determining the anatomic site of suspected recurrence.

Paper #: PA-136

Interrogation of Tumor Vasculature in Mouse Models of Neuroblastoma using a nanoparticle contrast agent

Ketan Ghaghada, *Radiology, Texas Children's Hospital, Houston, TX, kbghagha@texasChildren's.org;* Anna Lakoma, Caterina Kaffes, Jason Shohet, Eugene Kim, Ananth Annapragada, PhD

Purpose or Case Report: High-risk neuroblastoma (NB) is an aggressive embryonal malignancy arising in the peripheral nerves of young children which can rapidly metastasize to liver, bone and bone marrow. This cancer initially responds to therapy but chemotherapy-resistant disease relapse accounts for the majority of deaths. Advanced imaging techniques that would permit non-invasive therapeutic monitoring could have important implications in patient management. In this study, we sought to investigate the utility of a novel liposomal CT contrast agent for functional assessment of tumor vasculature in a mouse model with orthotopic neuroblastoma.

Methods & Materials: SY5Y and NGP, both MYCN-amplified human neuroblastoma cell lines, were intrarenally implanted into female nude mice and allowed to establish for 1–3 weeks. A liposomal CT contrast agent (~140 nm particle size, PEG surface coating, total iodine ~110 mg/ml, dose ~20μL/g) was injected via tail vein. Imaging was performed using a small animal micro-CT scanner with the following scan parameters: 60 kVp, 500 uA, 400 ms exposure, 540 projections. Quantitative analysis of tumor CT signal, tumor-associated vessel diameter and tumor size was performed. Following the final CT imaging session, the animals were sacrificed and the tumors excised for histological evaluation.

Results: The liposomal contrast agent enabled visualization of renal and tumor vasculature. Dynamic CT imaging demonstrated significant differences in nanoparticle contrast agent uptake as a function of tumor size. Uptake was generally low during the first week post implantation, but accelerated beginning in the 2nd

week. A high degree of variability in tumor CT signal and heterogeneity in tumor signal enhancement pattern was observed from animal to animal. A peripheral rim of signal enhancement was observed in most of the tumors, consistent with the highly permeable peripheral tumor vasculature. Histological analysis of the tumor tissue confirmed the heterogeneity of tumor vasculature seen in the CT images.

Conclusions: CT imaging using a liposomal-iodinated contrast agent enabled non-invasive interrogation of tumor vasculature in a mouse model of neuroblastoma. The heterogeneity of uptake implies that individual tumors will have dramatically different drug uptake, if drug were delivered using a nanoparticle carrier. Liposomal contrast agent based imaging could enable prognostication and monitoring of the effect of nanoparticle-based therapy.

Disclosure: Dr. Annapragada has indicated a relationship with Marval Biosciences as a Scientific Advisor and Stock Owner.

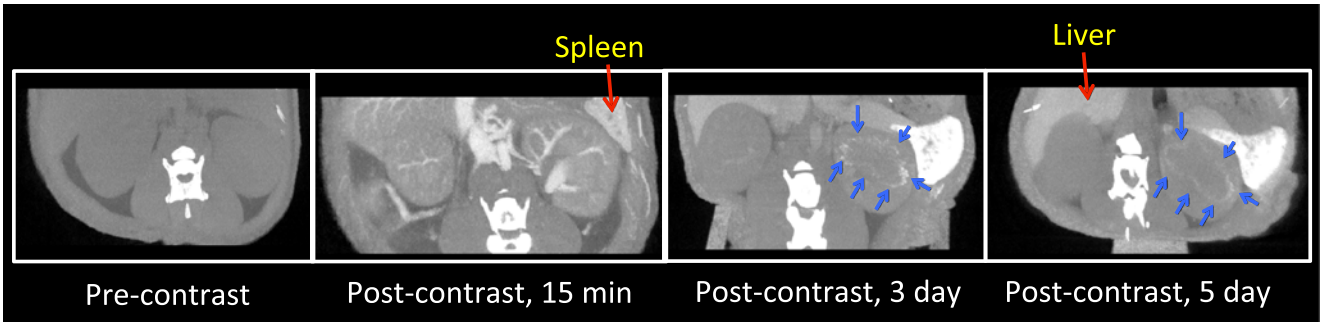

Coronal thick slab maximum intensity projection (MIP) abdominal CT images in a mouse with NGP tumor cells implanted in the renal capsule. Excellent visualization of renal vasculature in seen in the post–contrast 15 min image. Post–contrast images acquired at day 3 and day 5 demonstrate extravasation and accumulation of the liposomal contrast in the tumor (blue arrows). Signal enhancement is also seen in the liver and spleen (red arrows) due to the reticulo–endothelial system (RES) clearance of the liposomal agent.

Paper #: PA-137

Variation of alpha angle in hip ultrasound for developmental dysplasia due to variation in probe orientation: patterns revealed using 3D ultrasound.

Myles Mabee, Vimarsha Swami, **Lucy Jamieson, MD, FRCPC,** *Department of Radiology and Diagnostic Imaging, University of Alberta, Edmonton, AB, Canada, lucyjamieson88@gmail.com;* Kelvin Chow, Richard Thompson, Jacob Jaremko

Purpose or Case Report: The main ultrasound index classifying infant hip dysplasia is the acetabular alpha angle. Alpha angles >60° are considered normal, 50–59° indicates mild dysplasia, 43–49° moderate dysplasia. The alpha angle has a wide range of inter-observer variation in measurement, partly because the "standard plane" image on which it is measured can be produced across a range of different ultrasound probe orientations. With improving technology, it is becoming feasible to perform 3D hip ultrasound in clinical practice. Here, we tested the effect of changes in probe orientation on measured alpha angles by extracting different 2D scan planes from 3D ultrasound images of infant hips.

Methods & Materials: A 3D ultrasound scan (Philips IU22 scanner, 13VL5 probe) was performed in infants age <6 months referred for assessment of hip dysplasia. Using a custom computer algorithm in MATLAB, we resliced 3D ultrasound volumes in a direction approximating the ideal "standard plane" for alpha angle measurement, using landmarks including acetabular edges and the os ischium. We then extracted 2D ultrasound images at planes tilted from this orientation by 5° increments in two perpendicular axes, axis one representing antero-posterior probe tilt and axis two representing cranio-caudal tilt, as if a 2D ultrasound probe had been placed at these positions, until the 2D images no longer met criteria for the "standard plane". In each 2D image that did meet criteria, two observers measured the alpha angle.

Results: In 15 hips of eight patients, the alpha angle averaged 58.6+7.8° (mean+standard deviation). Variation in alpha angles was substantial, averaging 11.3°+6.0° for probe tilt in axis one and 11.3+5.1° in axis 2 (Figure 1). Variation was greater in axis 1 in 8 hips and in axis 2 in 7. The range of probe orientations producing interpretable "standard plane" images was 29+10°.

Conclusions: We used 3D ultrasound to show that the alpha angle traditionally used to measure hip dysplasia varies by an average of 11° (average 95% confidence interval 22–24°) simply by varying the angle at which the probe is held during 2D ultrasound scan. This range represents up to two 10° Graf diagnostic categories, so that the same hip could potentially be labeled normal or moderately dysplastic on two ultrasound scans performed the same day. 3D

ultrasound is less affected by probe tilt and may offer more reproducible assessment of hip dysplasia in future.

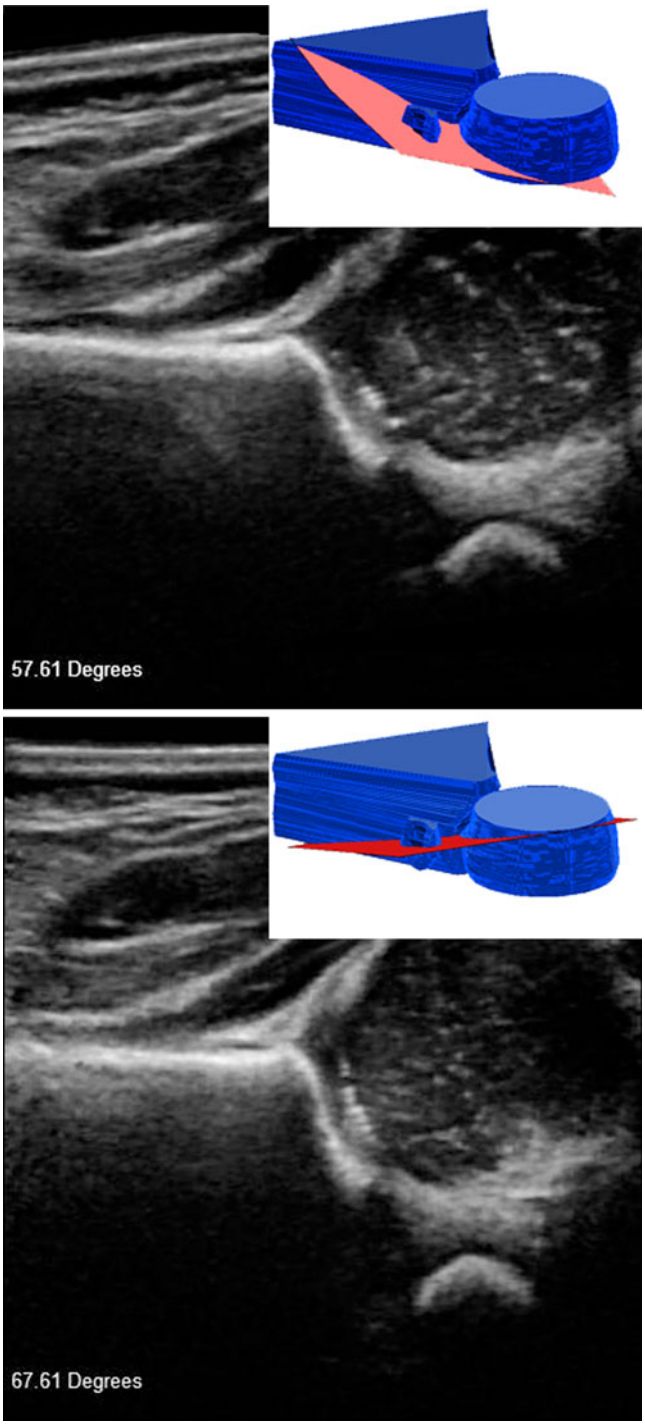

Figure 1: Two extracted 2D images from a single 3D ultrasound scan of an infant hip, taken at the orientations shown on the models at the top right of each frame, representing two different probe positions in axis 1 (antero-posterior). Note the typical 10° difference in the measured alpha angles between images.

Paper #: PA-138

Prediction of residual hip dysplasia and the need for future surgical treatment from MRI features visible post spica cast placement.

Charles Cong Wang, *Department of Radiology and Diagnostic Imaging, University of Alberta, Edmonton, AB, Canada, ;* Sukhdeep Dulai, Lucy Jamieson, Jacob Jaremko

Purpose or Case Report: Many infants whose hips are dysplastic enough to warrant placement of a hard spica cast are successfully treated by this, but in some, dysplasia persists. If these high-risk patients can be accurately identified early, more definitive treatment could be offered directly, and the risk of avascular necrosis in cast could be avoided. We tested whether measurements on MRI the day of spica casting could predict two clinical outcomes.

Methods & Materials: We reviewed patients aged 0–2 years who had MRI at time of first hip reduction & spica cast placement, and at >1 year of clinical follow-up. We recorded 28 indices of femur position and acetabular geometry for each hip, and two clinical outcomes: (1) presence/absence (1/0) of a later open hip reduction after initial casting, and (2) degree of hip dysplasia at clinical follow-up, collapsed for analysis into categories 0=stable/subluxable, and 1=subluxed/dislocated. Correlations between indices and logistic regression modeling were performed using SPSS.

Results: We had 52 hips in 26 patients (23 female), average age 10.6 months (range: 3.5–23.3 mo.) at MRI. Open reduction was later required for nine hips (17%) in seven patients. At last follow-up, 26/52 (50%) hips were subluxed or dislocated (5 dislocated). Variables correlating significantly ($p<0.05$) to clinical outcome were femoral head anterior displacement, pulvinar fat pad thickness, presence of low-signal structure blocking reduction, severity of acetabular dysplasia, coronal acetabular angle, and thickening of transverse ligament (see Figure). For outcome 1, a logistic regression model using the first four indices detected 7/9 cases requiring future open reduction, with three false positives FP and two false negatives FN, for sensitivity SN 78%, specificity SP 93%. For outcome 2, a model combined the acetabular angle and fat pad thickness to detect 24/26 subluxed/dislocated hips, with FP=6, FN=2, SP 77%, SN 92%.

Conclusions:

MRI indices of femoral position and acetabular shape at start of spica cast treatment in hip dysplasia were combined to give highly specific predictions of the need for later surgical procedure, and highly sensitive predictions of whether a hip would remain subluxed or dislocated

after treatment. MRI has potential to accurately identify patients at high risk of failure of spica casting, allowing early triage toward more effective therapy.

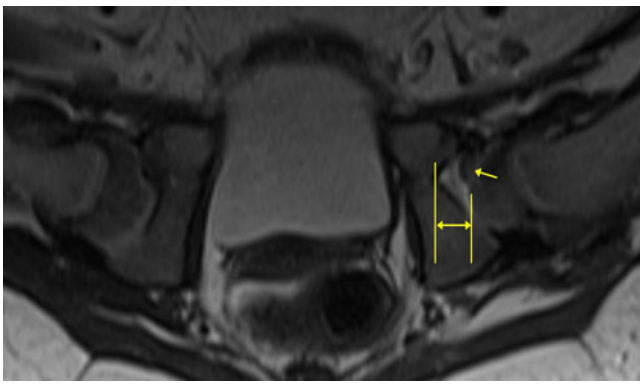

Figure: Transverse T2-weighted MR image of hips in a 5 month old girl with dysplastic left hip, following closed reduction. Note the wide fat pad (horizontal arrow) and the low-signal barrier to reduction (arrow: inverted labrum and thickened transverse ligament). This hip failed initial spica casting and required subsequent open reduction.

Paper #: PA-139

Color Doppler Ultrasound Predictors of Short-Term Unfavourable Clinical Outcome in Developmental Dysplasia of the Hip

Tommy Stuleanu, H.B.Sc., *The Hospital for Sick Children, Toronto, ON, Canada, t.stuleanu@alum.utoronto.ca;* Arun Mohanta, Carina Man, John Wedge, Clara Ortiz-Neira, MD, Andrea Doria

Purpose or Case Report: Background:

Vascular hemodynamic changes to the neonatal hip measured by color Doppler Ultrasound (CDU) may be related to impaired acetabular growth and lead to persistent hip morphologic abnormalities during the first months of life. CDU may be a non-invasive indicator of poor prognosis to conventional therapy of developmental dysplasia of the hip (DDH) having a direct impact on management decision-making, reducing costs of multiple imaging examinations, and improving efficiency of personalized therapy.

Objective:

To determine color Doppler ultrasound (CDU) predictors of an unfavourable clinical outcome in neonates with DDH.

Methods & Materials: A prospective cohort study of 50 (36 [72%] females) neonates with clinically suspected DDH was conducted: 100 hips of neonates with a mean [range] age of 41 [5–117] days of life at the baseline US study were evaluated by gray-scale and spectral CDU at rest and under stress maneuveurs (if not on harness) by a single sonographer. Vessels along the acetabular labrum, proximal femoral neck, within the epiphysis and ligamentum teres region (Fig.) were scanned longitudinally and tranversally at baseline and at 8–12 weeks after baseline, as clinically indicated, regardless of the use or not of harness. Predictors were resistive index (RI) and peak systolic velocities (PSV) of hip vessels. The outcome measure was unfavourable clinical outcome described as an alpha angle <60° representing persistent hip immaturity within the first 6 months of life (mean [range] age of 84 [44–176] days at follow-up stud). Logistic regression data analysis was performed based on hip units.

Results: At the follow-up study 14/50 (28%) patients were on harness, and 13/100 (13%) hips had alpha angle <60°. There was a difference in frequency of an unfavourable outcome between groups of patients with presence vs absence of fat pulvinar (P=0.0002) and subluxed hips under stress (P=0.007) at baseline (Chi-square test). By increasing hip vessels' RI the odds (odds ratio=0.06) for experiencing an unfavourable outcome decreased (P=0.005). Mean (SD) RIs in the favourable vs unfavourable outcome groups were 0.48 (0.27) vs 0.21 (0.33), respectively. No associations with an unfavourable outcome were noted between groups of patients according to biphasic flow PSV (P=0.12), gender (P=0.67) or age (P=0.06).

Conclusions: Spectral CDU holds potential as a predictor of an unfavourable clinical outcome in DDH.

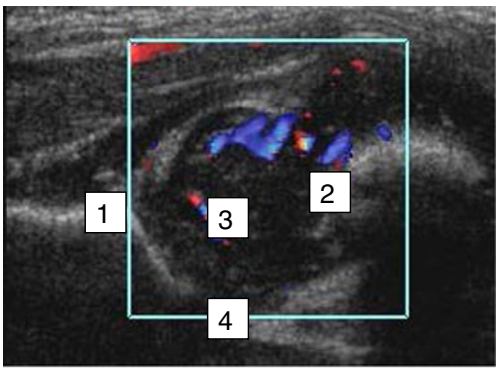

Fig. : Color Doppler scan of a 3-day old neonate hip. Regions-of-interest: 1. Acetabular labrum artery; 2. Lateral ascending cervical artery (3 branches); 3. Epiphyseal vessels; 4. Region of the ligamentum teres artery.

Paper #: PA-140

Maturation Pattern of the Capitellar Ossification Center: Does this Affect Radiographic Interpretation of the Elbow?

Lauren Fader, *Cincinnati Children's Hospital, Department of Orthopedic Surgery, Cincinnati, OH;* Tal Laor, Emily Eismann, Roger Cornwall, Kevin Little

Purpose or Case Report: The capitellar ossification center is used routinely to evaluate elbow alignment on conventional radiography. However, it is unknown if the capitellum ossifies in a centrifugal fashion to support this practice. Therefore, the purpose of our study is to determine the pattern of capitellar ossification at different patient ages.

Methods & Materials: Eighty-one children ages 1–13 years who underwent elbow MRI exams were identified through a radiology record search. At least three boys and three girls were included in each integer age group. Using PACS software, we determined the center point of the entire cartilaginous capitellum and the capitellar ossific nucleus on sagittal and coronal images. The percentage offset of the ossification center from the true center of the entire capitellum was calculated in three planes. Diameter and location (using percent offset) of the capitellar ossification center was compared across age groups and genders to determine normal progression during development. Linear regressions were used to ascertain effect of age on percent offset for all patients together and for each gender.

Results: Capitellar ossification begins eccentrically within the cartilaginous anlage, with anterior and proximal offset in the sagittal plane and medial and proximal offset in the coronal plane. With age, ossification proceeds distally, posteriorly, and laterally. Percent offset of the ossific nucleus gradually diminishes with age, such that the ossification center is located centrally within the capitellum by 12 years of age in the sagittal plane (Table 1). Coronally however, the capitellum ossifies medially beyond the proximal radioulnar joint into the emerging trochlear ossification center. This decreases the relative rate of lateral progression of the ossific nucleus (Fig 1). Capitellar ossification in boys lags behind girls in the anteroposterior and proximal-distal dimensions.

Conclusions: The capitellum ossifies in an eccentric rather than concentric pattern with a lag in development in boys behind girls. With increasing age, the ossification center progresses centrally and reaches the center of the capitellum by approximately 12 years, except in the coronal plane.

Significance: As the capitellum is used as a landmark to evaluate for normal elbow articulation, understanding that the ossification pattern begins eccentrically will allow for more accurate assessment of elbow malalignment, especially in children under 12 years of age.

	N	Percent Offset of Ossific Nucleus from Center of Capitellum		
		Anterior-Posterior	Proximal-Distal	Medial-Lateral
Age				
1	6	10.15±4.16%	13.10±2.45%	18.25±5.08%
2	6	11.76±2.84%	10.80±5.93%	14.63±3.40%
3	8	9.52±3.98%	8.21±1.38%	12.35±5.72%
4	8	6.29±3.82%	8.51±3.79%	12.72±2.53%
5	6	3.97±3.33%	3.22±2.96%	9.57±3.00%
6	8	4.28±2.52%	5.11±3.79%	11.35±3.35%
7	8	3.32±1.36%	6.02±3.27%	8.82±3.14%
8	7	2.76±2.76%	2.79±2.87%	14.25±2.76%
9	6	3.78±3.43%	2.69±2.56%	11.98±5.67%
10	6	1.66±1.45%	2.38±1.72%	9.02±5.23%
11	6	2.38±0.91%	3.75±3.35%	13.20±3.65%
12	6	0.85±1.36%	1.92±2.56%	13.28±4.51%
	81	% offset= 11.28–0.90**age*, $r=-0.70$, $p<0.001$*	% offset= 12.02–0.91**age*, $r=-0.67$, $p<0.001$*	% offset= 14.45–0.31**age*, $r=-0.23$, $p=0.044$*

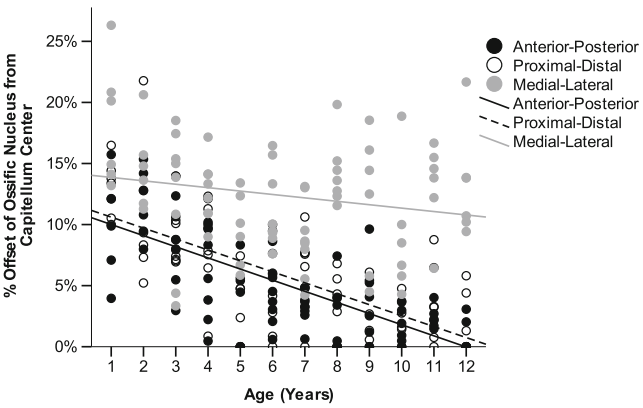

Paper #: PA-141

Treatment of Traumatic Shoulder Dislocation Among Adolescents: Does Hill-Sachs Lesion Size Matter?

Nancy Chauvin, MD, *Department of Radiology, The Children's Hospital of Philadelphia, Philadelphia, PA, chauvinn@email.chop.edu;* Tomás Díaz, Stuart Kinsella, Diego Jaramillo, Lawrence Wells

Purpose or Case Report: Recurrent shoulder instability is a common complication after traumatic anterior shoulder dislocation in adolescents. Treatment for shoulder dislocation in teenagers has traditionally involved immobilization

followed by a rehabilitation program. Some orthopedic surgeons advocate for a surgical approach in the management of acute traumatic first-time anterior shoulder dislocation in the adolescent population due to risk of recurrence, as utilized in adult patients. Our purpose is to measure the volumetric size of Hill-Sachs lesions in known traumatic dislocators and correlate lesion size with number of dislocations in order to demonstrate the relationship between Hill-Sachs lesion size and rates of recurrent shoulder dislocation in adolescents. In addition, we evaluate treatment algorithms for shoulder instability to determine if early surgical intervention might be warranted in patients with large Hill-Sachs lesions.

Methods & Materials: We retrospectively analyzed 28 adolescent patients with Hill-Sachs lesion visible on magnetic resonance arthrography. The humeral head was examined on T1-weighted, fat-saturated images in the axial plane using a radiologic technique to measure the volume of each defect. Lesion area was measured on each slice using a freehand region of interest measuring tool and the volume of the defect was calculated. Concurrently, the electronic medical records for dislocation history were reviewed. A Spearman correlation analysis was performed with the data.

Results: Increased average lesion volume was associated with an increasing number of shoulder dislocations (regression coefficient=0.0724, p=0.012).

Conclusions: Primary surgical repair, namely Hill-Sachs remplissage, has been proposed for young adult patients who have experienced first-time traumatic anterior shoulder dislocation. Our results suggest that similar surgical intervention might also benefit adolescent patients.

Number of Dislocations	Average Lesion Volume (cm^3)
0	0.0111
1	0.1240
2	0.1667
≥3	0.2420

Paper #: PA-142

Assessment of Angiographic Image Quality from a Flat Panel X-ray Detector using Diluted Iodinated Contrast Material in an Animal Model

Soumya Kashinkunti, **John Racadio, MD,** *University of Cincinnati, Cincinnati, OH, john.racadio@cchmc.org;* Rami Nachabe, Judy Racadio, Mary Beth Privitera, Todd Abruzzo

Purpose or Case Report: Some patients develop contrast-induced nephropathy after administration of iodinated contrast material, which may be dose-dependent. In an effort to reduce dose, we assessed the maximum dilution for commercially available iodine based contrast agent that would produce diagnostic images during fluoroscopy and digital subtraction angiography (DSA) on a current state of the art digital flat panel detector.

Methods & Materials: Fluoroscopy and DSA of the aorta, carotid, and renal arteries were performed on an anesthetized rabbit using each of the following dilutions of iodinated contrast (Optiray 350, Covidien, Hazelwood, MO) in normal saline: 100%; 80%; 50%; 33%; 20%. Eight pediatric radiologists evaluated the images and assigned a diagnostic quality score: 0 - non-diagnostic; 1 - poor quality that only enables diagnostic evaluation of 1st order branches; 2 - intermediate quality that enables evaluation of 2nd order branches; and 3 - high quality that enables evaluation of 3rd order branches. A one-way repeated measurement analysis of variance on ranks followed by Tukey's post hoc test was applied to investigate the difference in image quality scores for the various dilutions for each imaging modality.

Results: There was no significant difference between the DSA image quality scores for images produced with 100% and those produced with 80% dilution (Fig 1), with nearly all images being scored a "3". There was also no significant difference between the scores for images produced with 50% and 33% dilutions; however, the scores from the 50% and 33% dilutions were significantly lower than those from 100% and 80% dilutions. Similarly, there was no significant difference between the fluoroscopy image quality scores for images produced with 100% and 80% dilutions, and no significant difference between the images produced with 50% and 33% dilutions. Using 50% and 33% dilutions, the DSA scores for the aorta were greater than those for the carotid (Fig 2). The fluoroscopy image quality scores were all significantly higher for the renal artery than for the aorta or carotid artery.

Conclusions: This study indicates that, in a small animal model, iodinated contrast can be diluted to achieve a lower total dose and still produce meaningful images. The optimal dilution level will vary according to the clinical indication (e.g., there may be times when evaluating a 1st or 2nd order stenosis that an image quality score of 2 is acceptable) and anatomic location (i.e., vessel size and presence of bone).

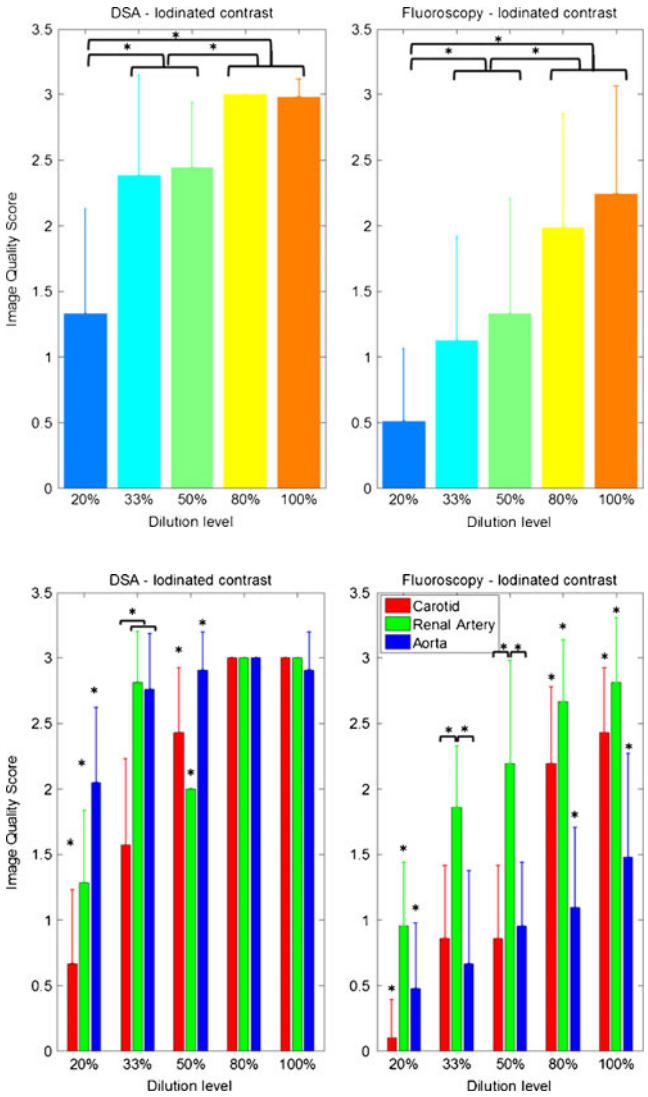

Paper #: PA-143

MRI of vascular anomalies: value of diffusion imaging

Sébastien Benali, *University of Montreal, Department of Radiology, Montreal, QC, Canada;* Josée Dubois, MD, MSc., Françoise Rypens, Chantale Lapierre, Gilles Soulez

Purpose or Case Report: MRI diffusion-weighted imaging (DWI) is a new method to evaluate the diffusion of intra and extracellular water. This method is presently used to depict areas of diffusion restriction (intracellular water) in ischemic stroke or malignant tumor. The goal of this study was to characterize diffusion imaging parameters in vascular anomalies.

Methods & Materials: Forty-one patients undergoing a baseline MRI for symptomatic vascular anomalies (venous malformations (VM)=17, lymphatic malformations (LM)=17, infantile hemangiomas=4, non-involuting common hemangiomas (NICH)=3) had a diffusion-weighted imaging using a fat-suppressed single-shot echo-planar diffusion-weighted technique in the axial plane with three diffusion b-factors (b values=0.500, 1000 s/mm2) and generation of apparent diffusion coefficient (ADC) maps. ADC values were calculated between B500 and B1000 to avoid confounding perfusion effect at low B values. Finally, ADC and signal enhancement after contrast injection (VIBE acquisition at baseline and 10 min after gadolinium injection) were correlated.

Results: The mean ADC values at B were estimated at 3.05±0.08, 3.25±0.12 and 3.07±0.14 respectively for VM, LM and hemangiomas. ADC values were significantly higher for LM as compared to VM (p=0.0001) and hemangiomas (p=0.02). However, no significant difference could be demonstrated between ADC values of VM and hemangiomas (p=0.89). A negative correlation between contrast enhancement and ADC values was observed (r=−0.578).

Conclusions: Vascular anomalies presented high ADC values. In case of LM, higher values were observed because most of the water is extracellular. Thus, DWI could be a useful tool to discriminate vascular anomalies from malignant lesions (typically shown with low ADC values below 1.5)

Paper #: PA-144

Keep your nerve. The incidence of neuropathy following STS sclerotherapy of pediatric venous malformations

Sam Stuart, *Great Ormond Street Hospital for Children, London, United Kingdom, sstuart@doctors.org.uk;* Premal Patel, Derek Roebuck, Samantha Chippington, Alex Barnacle

Purpose or Case Report: Sclerotherapy is advocated as the treatment of choice for venous malformations (VMs). Of the several sclerotherapy agents used a range of risk factors are associated with their use. Neuropathy resulting from sodium tetradecyl sulfate (STS) sclerotherapy is almost not reported in the published literature despite it being recognized as a potential complication. We report our experience of neuropathy as a complication of STS sclerotherapy when treating VMs in children.

Methods & Materials: All sclerotherapy procedures performed for VMs in children from 1999 to 2012 were reviewed. A standard technique was used with foamed STS (a 1:1:2 mixture of iohexol contrast, air & 3% STS). Technical & clinical details were recorded on a proforma at the time of treatment, including needle size & insertion technique, number, location & classification of treated

lesions, the volume and nature of sclerosant used & whether steroids or antibiotics were given. Routine follow-up included post-operative assessment, post discharge telephone call & outpatient clinic appointments. All nerve lesions were recorded and followed up for treatment and outcome.

Results: Motor &/or sensory nerve lesions occurred after 10 (1.2%) of a total 847 procedures. Neuropathy was seen following treatment of 5 Puig type II lesions, 5 type III & a single type I lesion. 7/10 cases were in patients that had undergone at least one previous sclerotherapy procedure. Nerve lesions were managed according to clinical need including surgical consultant with a peripheral nerve specialist, physiotherapy & nerve conduction studies. Neuropathy improved in all cases with complete resolution in 7 and partial resolution in three of whom two required surgery

Conclusions: When deciding to treat VMs the rare but potential complication of nerve injury must be considered. The literature to date doesn't report neuropathy with STS but our series demonstrates that nerve injury can occur. A degree of recovery was seen in most patients, but may be incomplete. We advocate active management of neuropathy with physiotherapy, nerve conduction studies and surgical consultation. Long-term follow up is recommended. The authors advocate sharing of clinical information about sclerotherapy complications, to enable prognostication of lesions, prevention, appropriate management of the complications.

Paper #: PA-145

Verrucous hemangioma: Role of ultrasound marking prior to surgical excision

Sheena Pimpalwar, MD, *Texas Children's Hospital- Interventional radiology, Houston, TX, ashwinsheena@hotmail.com;* Norma Quintanilla, Debra Kearney, Ashwin Pimpalwar

Purpose or Case Report: Verrucous hemangioma (VH) is an uncommon capillary-venous malformation in the dermis and subcutaneous (SC) tissue associated with reactive epidermal changes of hyperkeratosis, acanthosis and papillomatosis. Location in the lower extremity is typical and recurrence rate is high with inadequate surgical excision. We describe the role of preoperative skin marking under ultrasound to allow complete surgical excision of this uncommon vascular anomaly

Methods & Materials: Charts of two boys aged 2 and 7 years with surgical excision of VH over the last year were reviewed

Results: Clinical: Both boys presented with a well circumscribed dark red plaque (2x1cm) with a rough irregular surface over the mid tibial shin. The lesions were noticed at birth, grew slowly and had recurrent bleeding. Initial diagnosis in both cases was infantile hemangioma.

Ultrasound: Geographic homogenous hyperechoeic areas with no internal vascularity within the SC fat deep to the cutaneous plaque (CP) as well as extending into a large circumferential area (10x8cm) around it. Sharp demarcation from the surrounding hypoechoeic fat allowed skin marking at the boundary

MRI: Sharply marginated CP hypointense on T1, hyperintense on STIR with homogenous enhancement. Cloud like foci of STIR hyperintensity with minimal enhancement within the SC fat less extensive than on ultrasound with a satellite nodule in one patient.

Surgery: Preoperative skin marking to delineate the SC extent of the lesion using ultrasound revealed the total area of the involvement to be 3–4 times larger than the CP. The CP and its underlying SC fat were completely excised down to the fascia. The SC fat around the CP was shaved off from under the skin and removed followed by complete skin closure.

Histopathology: Pandermal lesion composed of small vessels in the dermis and subcutis and larger, dilated, thin-walled, ectatic vessels in the papillary dermis. The epidermis showed papillomatosis, acanthosis and hyperkeratosis and the upper dermis showed fibrosis and hemosiderin. Clear surgical margins were demonstrated in the majority of the specimen

Conclusions: The dark red CP of VH may be clinically mistaken for infantile hemangioma and diagnosis delayed until it fails to involute. The sonographic findings are striking and demonstrate the much larger SC extent of the malformation. MRI underestimates the SC extent but may show satellite lesions. Preoperative skin marking is a useful technique to achieve complete surgical excision with clear margins and thus reduce recurrence

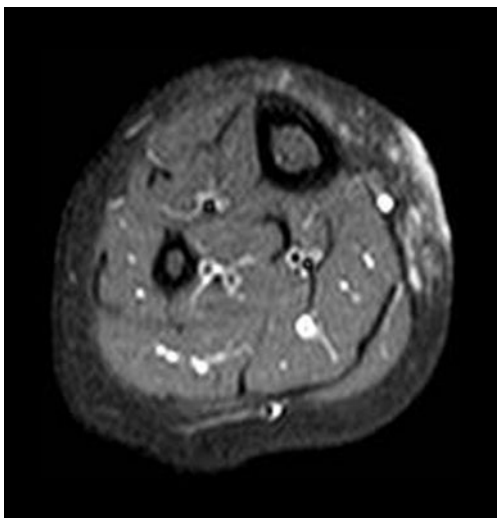

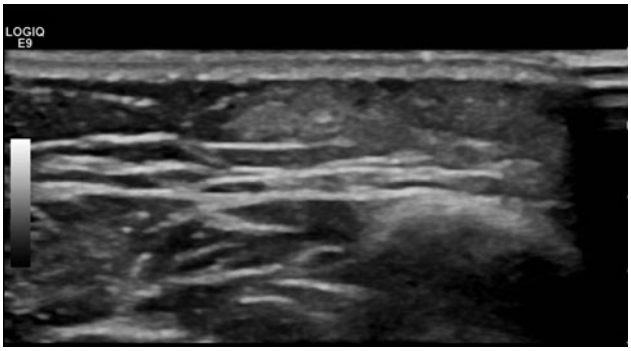

Paper #: PA-146

Clinical, imaging, surgical and pathological correlation of non-involuting congenital hemangioma (NICH) in children

Sheena Pimpalwar, MD, *Texas Children's Hospital- Interventional radiology, Houston, TX, ashwinsheena@hotmail.com;* Aparna Annam, Deborah Schady, Karen Eldin, Larry Hollier, Ashwin Pimpalwar

Purpose or Case Report: Retrospectively review the clinical exam, ultrasound, MRI,angiography and preoperative embolization findings of histologically proven NICH.

Methods & Materials: Charts of three patients diagnosed with NICH over the last year were reviewed.

Results: Three boys 5,6 and 13 year old presented with a painless lump in the right periareolar,anterior neck and right forearm. The lesions were present since birth, slow growing, plaque like or hemispherical and did not regress. The skin was bluish with interspersed telangiectasia, peripheral pale halo and prominent surface and peripheral subcutaneous veins. They were mildly warm, non tender and rubbery to palpation.
Ultrasound:Sharply demarcated hypoechoeic subcutaneous mass with a subtle lobular pattern and prominent compressible veins.
Doppler:Plethora of small arteries with low resistance waveform.
MRI:Well demarcated mass homogeneously isointense on T1, hyperintense on T2, intense uniform enhancement and interspersed fine linear flow voids from small arteries
Angiography:
Arterial phase:Multiple hypertrophied arterial feeders each supply a small tumor compartment via dichotomous branching with each terminal branch leading to a tumor nodule.
Capillary phase:Dense tumor blush contains an aggregate of 1 mm nodules separated by rims of non-enhancing tissue.
Venous phase:Multiple large veins drain into enlarged adjacent veins with no arteriovenous shunts.
Embolization:PVA particles,<20% residual vascularity
Venogram(1child):multiple dilated refluxing veins
Postembolization surgery:incisions designed around visible skin lesions minimizing skin excision,tumor completely and widely resected down to the fascia using bipolar and monopolar diathermy,marginal arteries and veins ligated,good skin closure achieved in all cases, minimal intraoperative blood loss.
Histopathology:Lobular architecture with each lobule composed of a conglomerate of endothelial lined channels (GLUT-1negative) with a central arteriole. Lobules were separated by fibrous septa containing dilated dysplastic veins.
Postoperative: All children did well and were discharged on the same day.4 week follow-up revealed well healed wounds.

Conclusions: The clinically apparent lesion of NICH looks much smaller than its true extent which is delineated by imaging. It has typical clinical characteristics and imaging correlates with a lobular architecture at pathology and well demarcated tumor margins at surgery. Surgical excision is facilitated by preoperative embolization

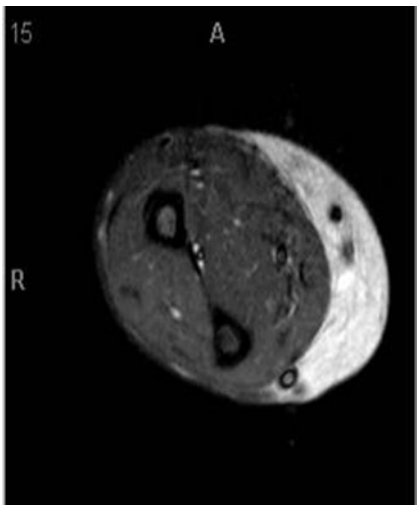

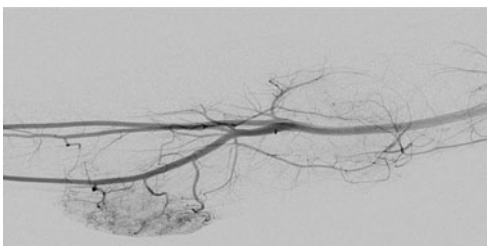

ALTERNATE PAPERS

Normative Shape Analysis of the Developing Piglet Femur in Forming a Metric for Characterizing Femoral Head Deformation Following Experimentally Induced AVN

Andy Tsai, *Department of Radiology, Boston Children's Hospital, Boston, MA*; Susan A. Connolly, Arthur Nedder, Frederic Shapiro

Purpose or Case Report: Childhood idiopathic AVN of the hip (Legg-Calve-Perthes disease) results in considerable morbidity. To simulate this disease for laboratory study, we used an AVN model in a skeletally immature

piglet hip created by placement of a tight silk ligature around the base of the femoral neck and sectioning of the ligamentum teres, rendering the femoral head completely avascular. The temporal characterization of this piglet's deforming femur, based on the metric established from a normative shape database we derived from a population of normal piglet femurs, forms the basis for this paper.

Methods & Materials: Normative piglet femur developmental data was generated via serial CT images of bilateral femurs from three normal piglets at regular time intervals. We applied a shape analysis technique to this data set—using level set method as the shape descriptor and principal component analysis as the feature selector—in deriving a shape subspace that compactly describes the normal development of the piglet femur. This parametric subspace efficiently captures the major temporal changes of the femurs, and can be used as an effective metric in quantifying how much a query femur deviates from the norm. We applied this shape metric to the experimental femur data generated via serial CT images of a piglet following experimental unilateral induction of femoral head AVN. The contralateral femur served as the control.

Results: The application of this shape metric to the experimental data traces out a deformation trajectory over time of the diseased femur that progressively differs from the trajectory of the same piglet's contralateral normal femur. Hence, this computational framework can objectively indicate the time point when the shape of the femur starts to deviate from the norm, and the amount of deviation. As a by-product, this technique's intuitive 3D visualization of the shape changes (via variations of selected eigenmodes and surface distance-difference colormaps) reveals patterns of changes in the normal and abnormal development of the femur that solidifies widely-accepted clinical observations.

Conclusions: The clinical application of this analysis tool is expected to play an important tool in (1) assessing disease progression; (2) directing clinical intervention; and (3) gauging the effectiveness of treatment.

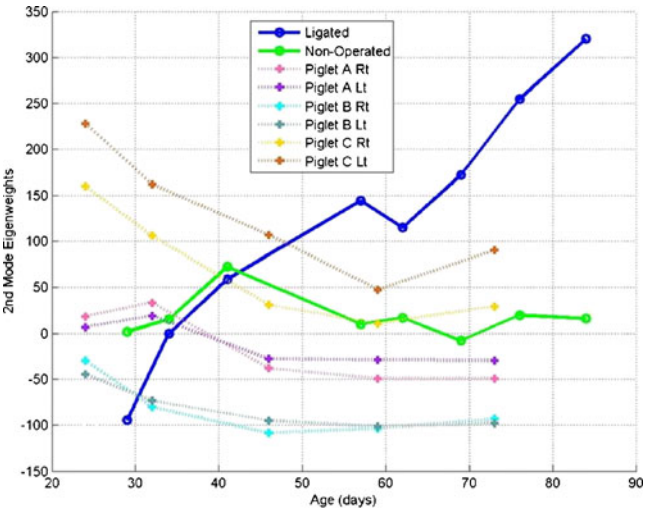

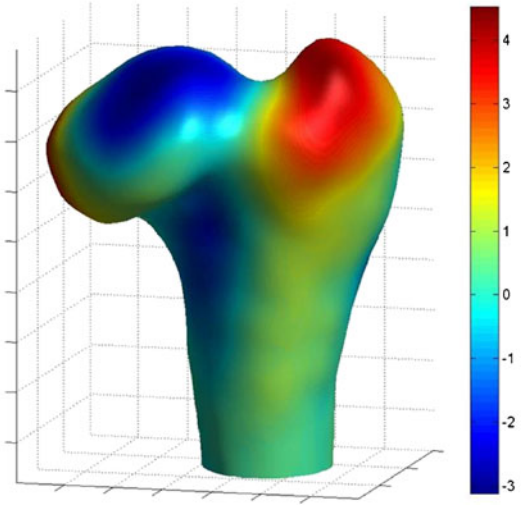

Left Side Image: Temporal trend of the 2nd eigenweights. Over time, the control eigenweights (green solid line) are in-line with the 2nd eigenweights of the normative data (dashed lines), while the AVN model eigenweights (blue solid line) diverge from the normative data and the control.

Right Side Image: 3D surface colormap demonstrates the surface distance differences between the femoral head with the AVN relative to the normative data at 84 days of age. Two eigenmodes were used for the normative data reconstruction. Red = outward distance (expansion), green = zero distance, and blue = inward distance (shrinkage).

Distinguishing Osteomyelitis from Ewing Sarcoma on Radiography and Magnetic Resonance Imaging

Beth McCarville, MD, *St. Jude Children's Research Hospital, Memphis, TN;* Jamie Coleman, Yimei Li, Robert Kaufman

Purpose or Case Report: The imaging features of osteomyelitis (OM) and Ewing sarcoma (EWS) overlap and biopsy can sometimes be non-diagnostic. We sought to identify features on radiographs and magnetic resonance imaging (MRI) that reliably distinguish these disease processes and might direct management when biopsy is inconclusive.

Methods & Materials: After IRB approval a panel of three radiologists blindly and retrospectively reviewed x-rays and MRIs of 32 subjects with EWS and 38 with OM. Based on the presence of specific imaging parameters and professional experience, reviewers independently predicted the diagnosis or judged the findings as indeterminate. Discrepancies in predictions were resolved by consensus. The consensus correct and incorrect classification rates were determined and frequency tables were produced for the true disease status for each parameter. Fisher's exact test or the Chi-square test were used to determine significant differences in the presence of parameters between EWS and OM. Demographic data were obtained and compared.

Results: Of 32 subjects with EWS, two were African-American in contrast to 19 of 38 with OM (p=0.00003). Radiologists were more likely to misdiagnose OM as EWS than vice versa. Among 30 patients with EWS examined by x-ray, 25 (25/30, 83%) were classified correctly, 1 (1/30, 3%) incorrectly and 4 (4/30, 13%) were indeterminate. Among 29 patients with EWS examined by MRI, 23 (23/29, 79%) were classified correctly, 1 (1/29, 3%) incorrectly and 5 (5/29, 17%) were indeterminate. Among 32 patients with OM examined by x-ray, 12 (12/32, 38%) were correctly classified, 10 (10/32, 31%) incorrectly and 10 (10/32, 31%) were indeterminate. Among 28 patients with OM examined by MRI, 19 (19/28, 68%) were correctly classified and 9 (9/28, 32%) incorrectly. There was better agreement on the diagnosis of EWS than OM. Frequency and significance of various imaging parameters are shown in Table 1.

Conclusions: Radiologists are more likely to misdiagnose OM as EWS than vice versa. African Americans are significantly more likely to have OM than EWS. Although many imaging parameters were useful, a single-layer periosteal reaction on x-ray or MRI (more common in OM), and a soft-tissue mass on MRI (more common in EWS) were the most significant parameters for distinguishing OM from EWS. In the future we will determine if there is a combination of imaging and clinical findings that can improve our ability to distinguish these entities.

	Soft Tissue Mass			
	MRI	**p-value**	**X-ray**	**p-value**
EWS	22/29	<0.001	16/30	0.0065
OM	07/28/13		05/01/32	
	Single-layer Periosteal Reaction			
EWS	8/29	<0.001	11/30	<0.0001
OM	09/28/13		12/01/32	
	Multi-layered Periosteal Reaction			
EWS	11/29	0.17	14/30	0.0051
OM	10/28/13		04/01/32	
	Spiculated Periosteal Reaction			
EWS	22/29	0.12	24/30	0.059
OM	18/28		18/32	
	Wide Transition Zone			
EWS	21/29	0.20	27/30	0.057
OM	25/28		23/32	
	Metaphyseal Involvement			
EWS	24/29	0.79	22/30	0.15
OM	21/28		16/32	
	Cortical Involvement			
EWS	28/29	0.013	29/30	0.0066
OM	20/28		21/32	
	Superficial or Deep Soft Tissue Edema			
EWS	24/29	0.11	12/30	0.14
OM	27/28		19/32	
	Codman Triangle			
EWS	2/29	0.0019	8/30	0.011
OM	0/28		01/01/32	

SCIENTIFIC EXHIBITS/POSTERS

Authors are listed in the order provided. An author listed in bold identifies the presenting author.

Poster #: CR-001

When Fear of Radiation Leads to Delay in Diagnosis: A Case of Neck Infection Progressing to Florid Mediastinitis with Abscess

Floyd Dunnavant, MD, *Radiology, The University of Alabama at Birmingham, Birmingham, AL, fdunnavant@uabmc.edu;* Nicholas CaJacob, Yoginder Vaid, Stuart Royal

Purpose or Case Report: Over the course of the last decade there has been extensive media scrutiny of reports concerning radiation exposure due to diagnostic x-ray examinations, particularly computed tomography. Many of these reports have suggested hypothetical risks of diagnostic radiation exposure based on extrapolation from data on populations receiving extremely high radiation doses, such as the survivors of the Hiroshima and Nagasaki explosions. The pediatric imaging community has responded with multiple initiatives to minimize radiation exposure in children, including ALARA and the Image Gently campaign. Pediatric CT protocols have been optimized to minimize patient radiation dose. Nonetheless, many of these reports have been sensationalized in the media, and parents are more aware than ever of the potential effects of radiation. While a more educated population of patients and parents is clearly a welcome change, there is a risk that parents will refuse diagnostic imaging procedures due to radiation concerns, while ignoring the substantial, and often overwhelming, potential benefits. We describe the case of an 11 month old male who presented to the emergency department with fever, neck swelling, and grunting with agitation. Lateral neck radiographs in the emergency department demonstrated borderline retropharyngeal soft tissue swelling, and neck CT was recommended for suspicion of retropharyngeal abscess. Due to concerns regarding radiation exposure, the child's parents refused the examination. An ultrasound of the neck demonstrated only adenopathy, with poor visualization of the retropharyngeal soft tissues and no identifiable abscess. He was admitted and treated with intravenous antibiotics, with initial improvement in respiratory symptoms, but persisting fevers. Over the next several days, the parents declined CT on multiple occasions. On hospital day four, a contrast enhanced MRI was performed despite risks associated with general anesthesia, as the parents continued to refuse CT. MRI demonstrated an abscess in the left neck, with extension into the mediastinum along the carotid sheath. Extensive mediastinitis was demonstrated with the entire anterior mediastinum infiltrated by a large multiloculated abscess. Sternotomy was performed, with abscess drainage and removal of the entire thymus. Cultures from the abscess grew methicillin sensitive Staph. aureus. Fortunately, the patient did well clinically following his operation, and was discharged on hospital day nine.

Poster #: CR-002

Imaging of criss-cross pulmonary arteries

Maryam Ghadimi Mahani, MD, *University of Michigan health system. Radiology Department, Ann Arbor, MI, maryamg@med.umich.edu;* Jimmy Lu, Adam Dorfman, Glenn Green, Prachi Agarwal

Purpose or Case Report: The purpose of this case report is to review the cross sectional imaging features of criss-cross pulmonary arteries and relevant literature. A 3 month old boy with respiratory failure secondary to left mainstem bronchus compression from a possible vascular abnormality was transferred to our institute for surgical correction and further care. Outside cardiac magnetic resonance images and high resolution computed tomography (HRCT) images revealed criss-cross branch pulmonary arteries with the left pulmonary artery arising from the pulmonary trunk to the right and above the origin of the right pulmonary artery. There was also moderate hypoplasia of the proximal right branch pulmonary artery and severe narrowing of the left main stem bronchus. Computed tomography of the chest with intravenous contrast agent for complete evaluation of the airways and pulmonary arteries and aorta was performed for further evaluation prior to surgical treatment. The CT images confirmed the criss-cross pulmonary arteries with a close relationship of the aorta and left branch pulmonary artery to the proximal left main stem bronchus and no evidence of vascular ring, tracheobronchomalacia and air trapping in expiratory images, close relationship of the aorta and left branch pulmonary artery to the proximal left main stem bronchus which was significantly narrowed and collapsed on expiratory images.

The patient underwent surgery to address the narrowing of the left main stem bronchus, severe bronchomalacia and hypoplastic right branch pulmonary artery. The patient improved clinically and subsequent imaging studies revealed improved aeration of the lungs with decreased air trapping and patent reconstructed right branch pulmonary artery.

Criss-cross pulmonary arteries is a very rare congenital abnormality that can be seen in association with other congenital heart disease or extracardiac abnormalities. Familiarity with the imaging features of this rare abnormality will help radiologists to diagnose this abnormality and facilitate management.

Poster #: CR-003

Multimodality imaging appearance of an incidentally detected intra-thoracic gossypiboma following Fontan operation

Maryam Ghadimi Mahani, MD, *University of Michigan. Department of Radiology. Section of Pediatric Radiology, Ann Arbor, MI, maryamg@med.umich.edu;* Jonathan Dillman, Sarah Gelehrter, Amer Heider, George Mychaliska, Jimmy Lu

Purpose or Case Report: A 3 year-old boy adopted from outside of the United States with D-looped transposition of the great arteries and valvar pulmonary stenosis, status post Fontan operation, was referred for cardiac magnetic resonance imaging (MRI). The cardiac MRI exam revealed a

well-defined, inhomogeneous, peripherally-enhancing mass-like abnormality in the right inferior hemithorax, along the posterior chest wall. MRI features were deemed nonspecific, and organized hematoma, infectious fluid collection (empyema), and neoplasm were suggested as possible etiologies. Review of a prior chest radiograph from 3 months earlier showed a round opacity projecting over the lower right hemithorax, suggestive of pneumonia, although the patient had no symptoms of a respiratory infection. Ultrasonography revealed a circumscribed, mixed echogenicity, shadowing mass-like abnormality located within the inferior right posterior pleural space with mass-effect upon the adjacent lung. The differential diagnosis again included hematoma, empyema, and neoplasm. Clinically, the patient was asymptomatic, and retained foreign body was also considered. Next, the patient underwent contrast-enhanced computed tomography (CT) imaging of the chest to further characterize the lesion. At CT, the abnormality appeared as a peripherally-enhancing fluid collection within the pleural space. No significant central enhancement was appreciated. Under ultrasound guidance a biopsy was performed. String-like material was obtained on several passes, and frozen section confirmed the presence of birefringent foreign material within the lesion. The lesion was surgically removed, and pathology confirmed a retained surgical sponge in the right pleural space.

Conclusion: Although relatively uncommon, important non-cardiovascular findings may be detected during cardiac MRI studies which require further evaluation and management. In patients that have undergone prior cardiac surgery, gossypiboma should be considered in the differential diagnosis for intra-thoracic mass-like lesions.

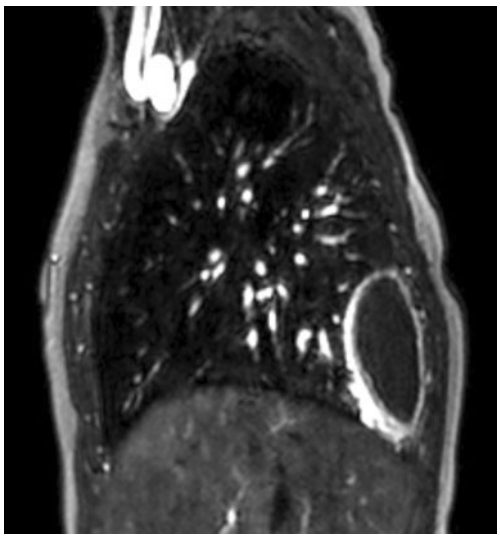

Poster #: CR-004

Congenital absence of the portal vein, case report and review of the embryology of portal vein development

Johanna Schubert, MD, *Creighton University Medical Center, Omaha, NE;* Megan Hora, Adam Stibbe, Homeira Zahiri

Purpose or Case Report: Introduction: Congenital absence of the portal vein (or Abernethy malformation) is a rare anomaly of the mesenteric vessels, where the portal blood is shunted into the systemic circulation bypassing the liver. To our knowledge, 84 of these cases have been reported in the english literature since 1793. Our case represents one of the more rare variants where the entire portal system is drained through the IMV and pelvic varices into the systemic circulation.

Case report: 4 year old girl presented with 2 year history or intermittent vaginal and rectal bleeding, and multiple inconclusive physical exams.

CT of the abdomen revealed complete absence of the main and inrahepatic portal veins, and a markedly enlarged IMV draining the portal blood into the internal iliac vein directly, and through innumerable pelvic varices into the systemic circulation. No findings of a secondary portal venous thrombosis such as gastric and splenic varices, cavernous transformation of the portal vein, splenomagealy or ascites were seen, proving our suspicion of a congenital abnormality. The single blood supply to the liver was the prominent hepatic artery. The patient had normal liver function, and US and MRI showed otherwise normal liver architecture.

Conclusion: Through this unique case we discuss the embryology of the portal venous system, and the various types of congenital extrahepatic portosystemic shunts with review of the literature.

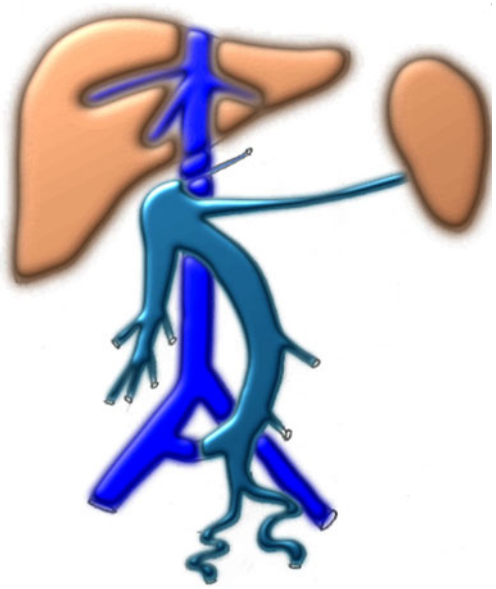

Poster #: CR-005

Dislodged percutaneously placed ASD/ PDA closure devices – Plain Film Diagnosis

Paul Iskander, MD, *Radiology, UCLA, Los Angeles, CA, piskander@mednet.ucla.edu;* Claire Isidro, Ines Boechat, MD

Purpose or Case Report: Percutaneous closure devices have become the mainstay of treatment for secundum type atrial septal defects and patent ductus arteriosus, with a lower overall complication rate when compared to surgery. The rate of immediate post procedure device embolization was as low as 0.5% in one study. Most complications occur immediately post procedure and are usually noted at the conclusion of the angiographic procedure. Delayed embolization is a much more rare complication and may be recognized on routine imaging studies.

We present three cases where post deployment angiographic images demonstrated the closure devices in proper position, while radiographs obtained either prior to or after discharge demonstrated migration of the closure devices. Recognition of abnormal position of these devices is important for the prompt management of patients. Currently, in addition to a frontal chest radiograph, a lateral chest and, if needed, abdominal radiographs are obtained to assist in the detection of closure device embolization after the angiographic procedure.

Poster #: CR-006

From Perforation To Calcification What You Need To Know About Meconium Peritonitis

Rustain Morgan, MD, *Radiology, University of Kansas Medical Center, Kansas City, KS;* Mallory Martinez, Brandy Conner, Kirk Miller

Purpose or Case Report: Utilize a case of meconium peritonitis to review pathophysiology, radiographic findings and associated disease processes.

Methods & Materials: After a thorough literature review we outline the causes of meconium peritonitis and their associated imaging findings with an additional focus on reviewing diseases which can result in meconium peritonitis.

Results: The diagnosis of meconium peritonitis is possible on prenatal ultrasound, with associated findings of intra-abdominal calcifications, ascites, intra-abdominal masses, bowel dilatation and polyhydramnios. Neonatal findings include, intra-abdominal calcifications on abdominal x-ray, failure to pass meconium, scrotal mass and bilious emesis. The overall mortality rate associated with meconium peritonitis has been reported as high as 60%. While there are multiple prognostic factors, accurate antenatal diagnosis allows for transfer of the mother to a tertiary center for delivery and management, which has been reported to improve overall outcomes.

Conclusions: Meconium peritonitis is a rare cause of intra-abdominal calcifications, which results from an intestinal perforation with spilling of meconium into the peritoneum. It is associated with meconium ileus, meconium plug, volvulus, small bowel atresia, intussusception, and Hirschsprung's disease. Accurate diagnosis is important to ensure timely and appropriate treatment.

Poster #: CR-007

Urorectal Septum Malformation Sequence: A Case Report

Amy Brunt, MD, *University of Arkansas for Medical Sciences, Little Rock, AR, BruntAmyL@uams.edu;* Leann Linam, Ashley Ross, Paul Wendel

Purpose or Case Report: ABSTRACT: Urorectal septum malformation sequence (URSMS) is a rare genetic anomaly characterized by severe abnormalities of the urorectal septum and the urogenital organs. URSMS is a sporadic condition, in which a deficiency in caudal mesoderm appears to be the primary cause of the malformation of the urorectal septum and other pelvic structures. A review of the literature reveals several clinical reports which discuss prenatal ultrasound findings. We highlight a case of URSMS that presented with ruptured bladder with abdominal ascites and oligohydramnios on prenatal ultrasounds. Fetal MRI was able to further delineate the findings associated of URSMS along with prune belly syndrome in a female fetus. We will discuss the prenatal findings on ultrasound and how MRI can assist with diagnosis of URSMS.

Poster #: CR-008

MRI evaluation of fetal spine anomalies

Jon Loo, MD, *University of Minnesota, Minneapolis, MN;* Tara Holm

Purpose or Case Report: Early prenatal diagnosis of fetal spine anomalies can significantly impact pre- and postnatal management and subsequent outcomes. Fetal MRI provides detailed anatomy of the fetal spine and is a powerful tool in the assessment of suspected spinal abnormalities. MRI is complimentary to ultrasound and allows for more accurate

prenatal diagnosis and proper patient care planning. This pictorial review will present various fetal spine anomalies and discuss their MRI findings.

Anomalies to be reviewed include caudal regression syndrome, sacrococcygeal teratoma, myelomeningocele, body stalk anomaly, positional hyperextension of the cervical spine, and akinesia sequence with marked spinal hyperlordosis. Fetuses with these anomalies were diagnosed with MRI during their second or third trimester. Fetal MRI images, as well as pertinent prenatal ultrasound and postnatal MRI images were chosen to illustrate key concepts of the above mentioned malformations.

Poster #: CR-009

Combined 3D-Rotational Fluoroscopic-MRI Cloacagram Procedure for Comprehensive Evaluation of Cloacal and Other Complex Pelvic Malformations

Jonathan Dillman, MD, *Department of Radiology, Section of Pediatric Radiology, University of Michigan C.S. Mott Children's Hospital, Ann Arbor, MI, jonadill@med.umich.edu;* Marcus Jarboe, Ranjith Vellody, Daniel Teitelbaum

Purpose or Case Report: Cloacal malformations occur when the urogenital sinus anomalously develops and fails to separate from the anorectal complex with a resultant common channel draining the lower urinary, genital, and gastrointestinal tracts. While these malformations have been traditionally characterized using a combination of physical examination, endoscopy, and 2D fluoroscopic genitography, 3D-rotational fluoroscopy recently has shown promise. However, this approach is often inadequate as obstructed lumens as well as associated anomalies of the uterus, kidneys, urinary tract, and spinal cord may go undetected. We have recently employed a novel combined 3D-rotational fluoroscopic-MRI cloacagram procedure, where dilute gadolinium-based contrast material is mixed with the injected low-osmolality iodinated contrast material. Immediately following 3D-rotational fluoroscopy in the interventional radiology suite, high-resolution 2D and 3D MR imaging is performed at a field strength of 3 T with catheters and retention balloons in place. This combined technique provides excellent depiction of both nonobstructed and obstructed lumens as well as associated abdominopelvic congenital anomalies, and it allows for high-quality 3D reconstructed images (volume-rendered and maximum intensity projection). We will present a cases series documenting our experience with this innovative imaging technique in the setting of cloacal and other complex pelvic malformations.

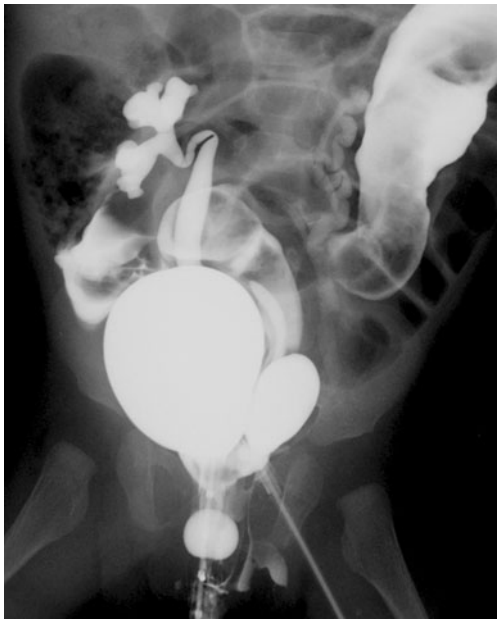

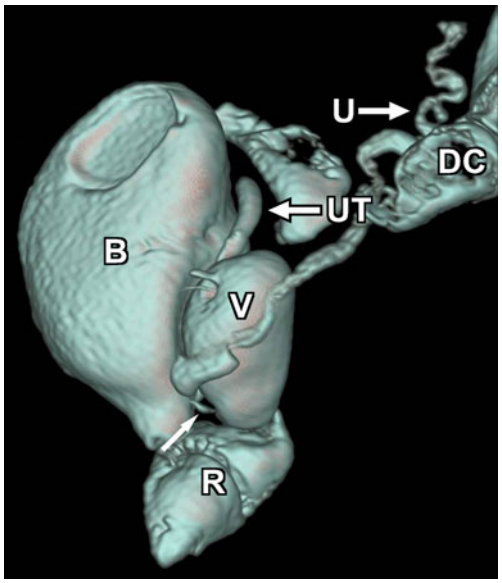

Poster #: CR-010

Megacystis Microcolon Intestinal Hypoperistalsis Syndrome

Paul Iskander, MD, *Radiology, UCLA, Los Angeles, CA, piskander@mednet.ucla.edu;* Shahnaz Ghahremani, M.D, Ines Boechat, MD

Purpose or Case Report: A 37 week female gestation was transferred from an outside institution at one day of life with a working diagnosis of megabladder, hydronephrosis, and concern for intestinal obstruction.
A renal ultrasound performed at our institution demonstrates a massively dilated bladder and bilateral hydronephrosis. A gastrografin enema was performed which demonstrates a malrotated microcolon. An upper GI series demonstrates no contrast passing beyond the duodenal bulb. The diagnosis of megacystis microcolon intestinal hypoperistalsis syndrome was made based on the constellation of imaging findings.
The patient subsequently went to surgery where a distended bladder, malrotated microcolon and an atretic second portion of the duodenum was noted. The patient underwent duodenotomy and ileostomy at that time. Colonic biopsy demonstrated the presence of ganglion cells.
A postoperative MRI provides a cross sectional illustration of the spectrum of imaging findings in this disease, including persistent bilateral hydronephrosis and a distended bladder. A dilated esophagus and microcolon are also noted. The patient expired by 6 months of life.
Megacystis microcolon intestinal hypoperistalsis syndrome has been previously characterized as the combination of a large dilated bladder, microcolon, and intestinal dysmotility. Associated findings include malrotation, hydronephrosis, and vesicoureteral reflux. The disease has a strong female predominance and most patients previously described in the literature have died by 1 year of age, which is also the case in our patient. We present one case diagnosed at our institution which we feel is representative of the typical multimodality imaging findings of this disease, with concordant findings noted at the time of surgery.

Poster #: CR-011

Megacystis Microcolon Intestinal Hypoperistalsis Syndrome: A Case Series Imaging Review

Stephen Jones, *McLane Children's Hospital, Scott and White, Temple, TX, ;* Krista Birkemeier, MD, Sara O'Hara, Jason Lee, Radiologist Assistant

Purpose or Case Report: Megacystis Microcolon Intestinal Hypoperistalsis Syndrome (MMIHS) is a very rare, and often lethal, syndrome presenting in the newborn with characteristic imaging findings secondary to poor visceral motility. It results in functional gastrointestinal and urinary obstruction. These patients are born with abdominal distention from a dilated hypotonic bladder and variable upper urinary tract dilation. They also have a microcolon and hypomotile gastrointestinal system with variable small bowel and esophageal dilation. Malrotation is common. This case series depicts the classic neonatal fluoroscopic imaging diagnostic of this rare syndrome, and the corresponding prenatal and postnatal sonography. The goal of this poster is to familiarize radiologists with the imaging findings in these patients so that they may prenatally suggest the diagnosis and postnatally confirm the diagnosis.
Disclosure: Dr. O'Hara has indicated that she is an author and shareholder in Amerisys, Inc. and on Toshiba's speaker's bureau.

Poster #: CR-012

Intrauterine inferior vena cava (IVC) thrombosis: an imaging challenge

Mahmoud Zahra, M,D, FRCR, *Radiology, women and children's hospital at Buffalo, Amherst, NY, mahmoudzahra867 @yahoo.com;* Puneet Gupta, Richard Thomas, Jan Najdzionek

Purpose or Case Report: The purpose of this presentation is to illustrate that IVC thrombosis should be listed among the differential diagnoses for unexplained intrauterine renal enlargement.
Methods & Materials: Intrauterine inferior vena cava (IVC) thrombosis is rare occurrence. Neonatal calcified thrombus has been reported and has been hypothesized to result from in-utero thrombosis. Renal vein involvement is a recognized co-morbidity. Although the etiology of intrauterine IVC thrombosis is uncertain, there are several associations. Maternal and fetal influences have each been implicated. Maternal factors include the presence of pregnancy-related hypertension, diabetes mellitus, placental abruption and either antinuclear or anti-cardiolipin antibodies. Fetal factors span multiple systems: the CNS (hydrocephalus), the GI tract (Hirschsprungs disease, imperforate anus), the urinary tract (congenital renal cell carcinoma), and systemic disorders (sepsis, TORCH infection, hydrops fetalis, intrauterine growth retardation).
Results: We report a case of presumed fetal IVC thrombosis in a diabetic 21 year female G 3 P1203, who presented with polyhydramnios. Antenatal US demonstrated enlargement of the fetal left kidney. Subsequent fetal MRI showed enlargement of the left kidney with heterogeneous signal intensity. Thrombus was not appreciated within the IVC. Based on MRI findings, the impression was mesoblastic nephroma or other congenital renal tumor. Post-natal Doppler Ultrasound demonstrated a thrombus in the IVC extending into the left renal vein, associated with decreased renal perfusion. No renal mass was present.

Conclusions: In the absence of calcification, antenatal diagnosis of IVC thrombosis, either with MRI or US, is difficult. If in utero IVC thrombosis remains suspect but unproven, the modality of choice is post-natal Doppler US. Abdominal MRI may be a helpful adjunct, particularly to confirm the absence of a renal mass, but is less sensitive and specific for vascular thrombus. The treatment of neonatal IVC thrombosis is typically conservative, relying on hydration and anticoagulation. The role of mechanical thrombectomy remains unconfirmed

Poster #: CR-013

Radiographic Evaluation of Long Gap Esophageal Atresia and the Foker Staged Lengthening Procedure: A Pictorial Review

Mark Liszewski, MD, *Radiology, Boston Children's Hospital, Boston, MA, mark.liszewski@Children's.harvard.edu;* Carlo Buonomo, Russell Jennings, George Taylor

Purpose or Case Report: Long gap esophageal atresia (LGEA) is characterized by esophageal segments that are too far apart for primary anastomosis. Though surgical repair utilizing interposition grafts or gastric transposition are often employed, there is general consensus among pediatric surgeons that every effort should be made to conserve the native esophagus. The Foker staged lengthening procedure is an alternative surgical method that employs continuous external traction on the esophagus to induce esophageal growth and allow for primary anastomosis, thus preserving the native esophagus. 40 cases of LGEA repair using the Foker procedure were reviewed. The step-by-step radiographic evaluation of the three-stage Foker procedure and the radiographic findings in the most commonly encountered complications are presented in this pictorial review.

Poster #: CR-014

Portal Venous Gas and Gastric Pneumatosis in an infant with Pyloric Stenosis - a rare presentation of a common condition

Anjum Bandarkar, MD, *Radiology, Children's National Medical Center, Washington DC, DC, anjumnb@gmail.com;* Eglal Shalaby-Rana, Nabile Safdar, Raymond Sze

Purpose or Case Report: Introduction: Infantile pyloric stenosis is a common condition affecting young infants and is a form of gastric outlet obstruction. Hitherto only three case reports have described the rare occurrence of pyloric stenosis with gastric pneumatosis and portal venous gas.

Case Report: A 4 week old previously healthy male infant presented with 2 week history of sweating with feeds, post-feed perioral cyanosis and frequent non bilious vomiting. The reason for his emergency visit was an apparent life threatening event when he vomited after a feed and began turning purple with slow breathing. He responded to suctioning of the nose and mouth. He had been gaining weight and did not have fever or any other illness. Initial differential considerations included severe gastroesophageal reflux, cardiac etiology, anatomic causes like tracheoesophageal fistula and pyloric stenosis (though this was considered unlikely given the presence of cyanosis).

On physical exam, the child was fussy, dehydrated and appeared very sick. Due to the paucity of physical findings, plain radiographs of the chest and abdomen were obtained as a road map. The chest was clear but the abdomen showed massive gastric distension with bubbly mottled appearance of the stomach suggesting gastric pneumatosis and linear, branching lucencies overlying the liver consistent with portal venous gas, both of which are considered ominous in gastrointestinal disease. At this point, his condition was very worrisome for underlying embolic event for which a complete abdominal sonogram was ordered. Blood tests showed hypochloremic metabolic alkalosis which is the characteristic biochemical disturbance in pyloric stenosis. Sonography confirmed hypertrophic pyloric stenosis. Pyloric muscle was thickened (4 mm) and channel was elongated (20 mm). Gastric wall was thickened with scattered echogenic specks confirming gastric pneumatosis. Portal venous gas was not appreciated on the sonogram, not unusual because of the dynamic nature of the movement of air in the wall of the GI tract and the portal venous system

The patient underwent laparoscopic pyloromyotomy, without complication.

Discussion: With gastric outlet obstruction, increased intraluminal pressure forces gas through the intact gastric mucosa from where gas enters the venules, then veins eventually draining into the portal venous system. This is a benign condition that resolves with pyloromyotomy. We aim to familiarize the readers with this rare association.

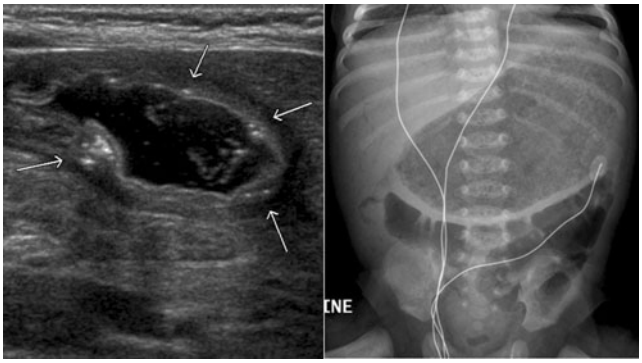

Poster #: CR-015

Acute Uncomplicated Diverticulitis in Two Adolescent Males

Ethan Smith, MD, *Department of Radiology - Section of Pediatric Radiology, University of Michigan - C.S. Mott Children's Hospital, Ann Arbor, MI, ethans@med.umich.edu;* Jonathan Dillman, MD, Christopher Anton, Daniel Podberesky

Purpose or Case Report: Colonic diverticular disease, including acute diverticulitis, is only very rarely encountered in pediatric patients. Diverticular disease in children has been described in association with underlying abnormalities, such as connective tissue disorders and Williams syndrome. This report describes the clinical and radiological findings two adolescent patients that presented to the emergency department with acute onset of abdominal pain and were both found to have acute colonic diverticulitis. Neither patient had any known predisposing medical condition other than obesity. Although unusual, these cases serve as a reminder that in the proper clinical setting and with suggestive imaging findings, a diagnosis of acute colonic diverticulitis should be considered, even in an adolescent.

Poster #: CR-016

Achalasia in Megacystis Microcolon Intestinal Hypoperistalsis Syndrome: A Case Report

Krista Birkemeier, MD, *Radiology, McLane Children's Hospital, Scott and White, Temple, TX, kbirkemeier@sw.org*

Purpose or Case Report: This case report describes a 7 year old Megacystis Microcolon Intestinal Hypoperistalsis Syndrome (MMIHS) patient who developed achalasia. MMIHS is a very rare disorder of gastrointestinal and urinary system hypomotility which had historically been considered lethal. The prognosis for MMIHS is improved due to parenteral nutrition support and multivisceral transplant, and we are beginning to see new radiographic findings in survivors. Some MMIHS patients lack the normal esophageal peristalsis necessary to open the lower esophageal sphincter (LES), and over time this may result in chronically increased LES tone, and failure of the LES similar to achalasia. This patient's initial newborn esophagram via refluxed contrast demonstrates a mildly dilated esophagus with a normal caliber gastroesophageal junction and no esophageal peristalsis. Radiographs at 4 years demonstrate megaesophagus with air contrast. At 7 years of age she began regurgitating undigested food and a barium esophagram demonstrates new narrowing of the gastroesophageal junction with the typical "bird's beak" appearance described with achalasia, with passage of only small amounts of barium assisted by gravity. Achalasia may develop in survivors with MMIHS and should be considered if the patient develops new symptoms of esophageal obstruction.

Poster #: CR-017

Fast Magnetic Resonance Enterography (FMRE): A New Technique for Rapid Assessment of Pediatric Inflammatory Bowel Disease

Clara Ortiz-Neira, MD, *Alberta Children's Hospital, Calgary, AB, Canada, claraneira@shaw.ca;* Cheryl Zvaigzne, David Patton, Martin Sheriff, Chris Waterhouse, Steven Martin

Purpose or Case Report: Magnetic Resonance Enterography (MRE) is widely used for evaluation of patients with inflammatory bowel disease (IBD), but it is an examination which can last up to 45 min in pediatric patients and requires intravenous gadolinium contrast and antiperistaltics. In order to overcome these limitations, we have developed a standardised fast MRE technique (FMRE) technique employing shorter sequences without contrast or antiperistaltic agents. The aim of this study was to evaluate the performance of FMRE in pediatric IBD patients who have undergone a full baseline MRE, and to determine if FMRE can evaluate response to therapy.

Methods & Materials: The FMRE protocol consists of the following sequences: Trufisp images to evaluate extraintestinal disease, HASTE images to evaluate bowel wall thickness, HASTE fat saturation images to determine T2 tissue characterization and to evaluate the presence of deep ulcerations, and diffusion weighted imaging to determine restricted diffusion in the bowel wall. The above images were obtained in both axial and coronal views. Prior to the FMRE, polyethylene glycol (PEG) oral contrast was administered (minimum of 10 mL/kg). Patients who had suspicion of a fistulous tract were excluded from this study as intravenous contrast is considered essential to their proper evaluation.

Results: Thirteen pediatic patients have undergone FMRE examinations at varying time periods following an initial full baseline MRE study. The range of scanning time for FMRE was 8 to 10 min. All FRME studies were of good quality. Jejunal and ileal disease could be assessed all 13 studies by FMRE (100%), along with determination of bowel wall thickness and T2 signal intensity. Changes in bowel wall thickness and T2 signal on FMRE HASTE fat saturation images compared to the initial full baseline MRE were noted, suggesting that these parameters could potentially be used to monitor response to medical therapy (Figure 1).

Conclusions: Fast magnetic resonance enterography (FMRE) is a rapid and potentially useful diagnostic modality that may allow clinicians to assess response to therapy in pediatric IBD, though this has yet to be evaluated in a prospective manner. FMRE avoids use of intravenous contrast or antiperistaltic agents and allows visualization of the entire bowel. Prospective performance of FMRE will be the basis of future studies.

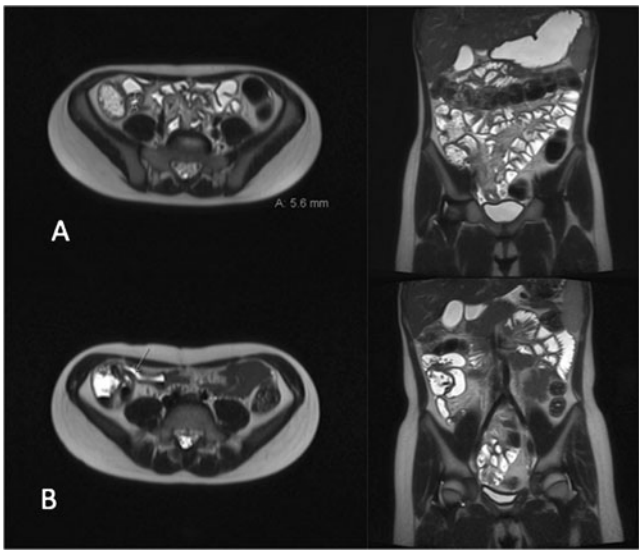

Fig 1: 10 year-old with chronic diarrhea, weight loss and abdominal pain. Axial and coronal HASTE fat saturation MRE images (A) at presentation and (B) following 4 months of azathioprine theraphy, demonstrating improvement in bowel wall thickness

Poster #: CR-018

MR evaluation of liver lesions in children with transfusion hemosiderosis

Vamsi Kunam, MBBS, MD, *Cleveland clinic, Cleveland, OH, vamsikunam@gmail.com;* Ellen Park, Neil Vachhani, Unni Udayasankar

Purpose or Case Report: Hepatic iron deposition is increasingly seen in pediatric population secondary to repeated blood transfusions for anemia following aggressive chemotherapy for pediatric malignancies in addition to primary hemochromatosis and anemia secondary to disorders of erythropoiesis. Chronic iron deposition predisposes these patients to cirrhosis of liver, regenerative nodules, dysplastic nodules and eventually increased risk of hepatocellular carcinoma. MR is an excellent tool for evaluation and quantification of iron deposition, however, characterization of focal liver lesions in the background of hepatic iron deposition can be challenging due to altered signal characteristics. The purpose of this exhibit is to illustrate our experience in MR evaluation of focal liver lesions in patients with hepatic iron deposition.

Methods & Materials: This case series will illustrate three patients with post transfusion hemosiderosis secondary to neuroblastoma (n=2), and surgically treated embryonal cell sarcoma of the liver (n=1). Routine follow-up abdominal MRI showed liver lesions with indeterminate characteristics. Ultrasound guided biopsy demonstrated benign liver lesions; regenerative nodule (n=1), FNH (n=2). US, CT and MRI characteristics of these lesions will be discussed with emphasis on MR imaging. We discuss optimal MRI protocol in this subset of patients, the MRI physics behind altered MRI signal in hepatic iron deposition, and algorithmic/systematic approach for delineation of focal liver lesions in patients with hepatic iron deposition. The signal characteristics as well as enhancement pattern of these focal liver lesions are substantially altered due to underlying parenchymal liver signal abnormality. The challenges, advantages and limitations of MRI in the setting of hepatic iron deposition will be described.

Conclusions: Signal intensity and enhancement characteristics of focal liver lesions are altered in the setting of hepatic parenchymal iron deposition. Although most lesions are benign, MR could be useful tool in distinguishing the benign from primary or metastatic malignant lesions. Additionally MR is a robust technique to identify and quantify the extent of liver iron deposition.

Poster #: CR-019

Ovarian teratoma associated NMDA receptor encephalitis: Two Cases with Rad-Path correlation of a potentially treatable paraneoplastic neuropsychiatric condition

Paul Thacker, MD, *Radiology and Radiological Sciences, Medical University of South Carolina, Charleston, SC, thackerp@musc.edu;* Jeannie Hill

Purpose or Case Report: Anti-N-methyl-D-aspartate receptor (NMDAR) limbic encephalitis is an extremely rare autoimmune disorder recently recognized as occurring in the pediatric population. Associated with neuropsychiatric symptoms, particularly seizures and dyskinesia, NMDAR encephalitis can be the result of an underlying teratoma, sometimes preceding teratoma detection by years. The authors describe two cases of ovarian teratoma mediated NMDAR encephalitis presenting to our institution within a 6 month period. Both patients underwent surgical resection with associated symptomatic improvement. Knowledge of this rare but treatable paraneoplastic syndrome may help the pediatric radiologist and their clinical colleagues in the assessment of acute onset, unexplained neuropsychiatric and/or seizure disorders.

Poster #: CR-020

When rare and common meet: an unusual case of concurrent adrenal cortical tumor and bilateral Wilms tumor in an infant

Andria Powers, MD, *Radiology, Fletcher Allen Health Care/ University of Vermont, Burlington, VT, andria.powers @vtmednet.org;* Timothy Higgins

Purpose or Case Report: Adrenal Cortical Tumors (ACT) are extremely rare in children, making up 0.2% of pediatric tumors. Although two cases in the literature describe development of a small ACT in a patient who previously had Wilms tumor and vice versa, there is no report of simultaneous occurrence of Wilms and ACT. We present an extremely rare case of an infant who presented with palpable abdominal masses and Cushingoid appearance to a pediatric neurologist. Abdominal ultrasound was performed which revealed multiple hypoechoic, solid renal masses in both kidneys. A large mass at the superior aspect of or superior to the left kidney contained linear hyperechoic regions thought to represent calcification. Subsequent contrast enhanced CT showed multiple round, noncystic, fairly homogeneous hypoenhancing lesions in both kidneys and a low attenuation round mass with central linear calcification abutting the superior pole of the left kidney. Biopsy of renal masses confirmed the diagnosis of Wilms tumor, and laboratory analysis revealed ACTH-independent Cushing's syndrome. The patient underwent debulking chemotherapy prior to surgical resection. A preoperative PET/CT showed dramatic interval decrease in renal tumor size with low residual FDG activity except for the left suprarenal mass which was unchanged in size and FDG avid. The patient went to surgery for bilateral partial nephrectomies and resection of the persistent left suprarenal/adrenal mass; pathology of the left adrenal mass revealed adrenal cortical tumor. The patient completed appropriate chemoradiation therapy with good response. Interestingly, though not hemihypertrophic at birth, the patient developed leg length discrepancy and asymmetry of thigh circumference over the year following cancer diagnosis, which was confounded by unilateral neurologic deficit since early infancy secondary to a right MCA territory infarct. Medical genetics evaluation was negative for Beckwith Wiedeman syndrome, but the patient was found to have a unusual maternally inherited microarray deletion of the short arm of chromosome 3, that is of unknown significance. We review imaging features of Wilms and ACT, and current literature regarding potential associations between the two.

Poster #: CR-021

Immune Reconstitution Inflammatory Syndrome Causing Hypertension in a Child

Martha Munden, MD, *Pediatric Radiology, Texas Children's Hospital, Houston, TX, mmmunden@texasChildren's.org;* Alyssa Riley, Arundhati Kale, Andre Cruz

Purpose or Case Report: Lymphadenopathy is the most common site for extrapulmonary tuberculous disease, with higher incidences in children and immunocompromised hosts. After initiating effective anti-tuberculosis medications, a patient occasionally may experience further lymph node enlargement, new lymphadenopathy, or pyrexia. This paradoxical worsening of symptoms is termed immune reconstitution inflammatory syndrome (IRIS).

We present a previously undescribed case of an immunocompetent child with cervical lymphadenopathy due to Mycobacterium tuberculosis who developed symptomatic hypertension after initiating anti-tuberculoisis therapy. Sonographic evaluation followed by CT angiography led to the discovery of renovascular compression from previously undiagnosed para-aortic lymphadenopathy. The

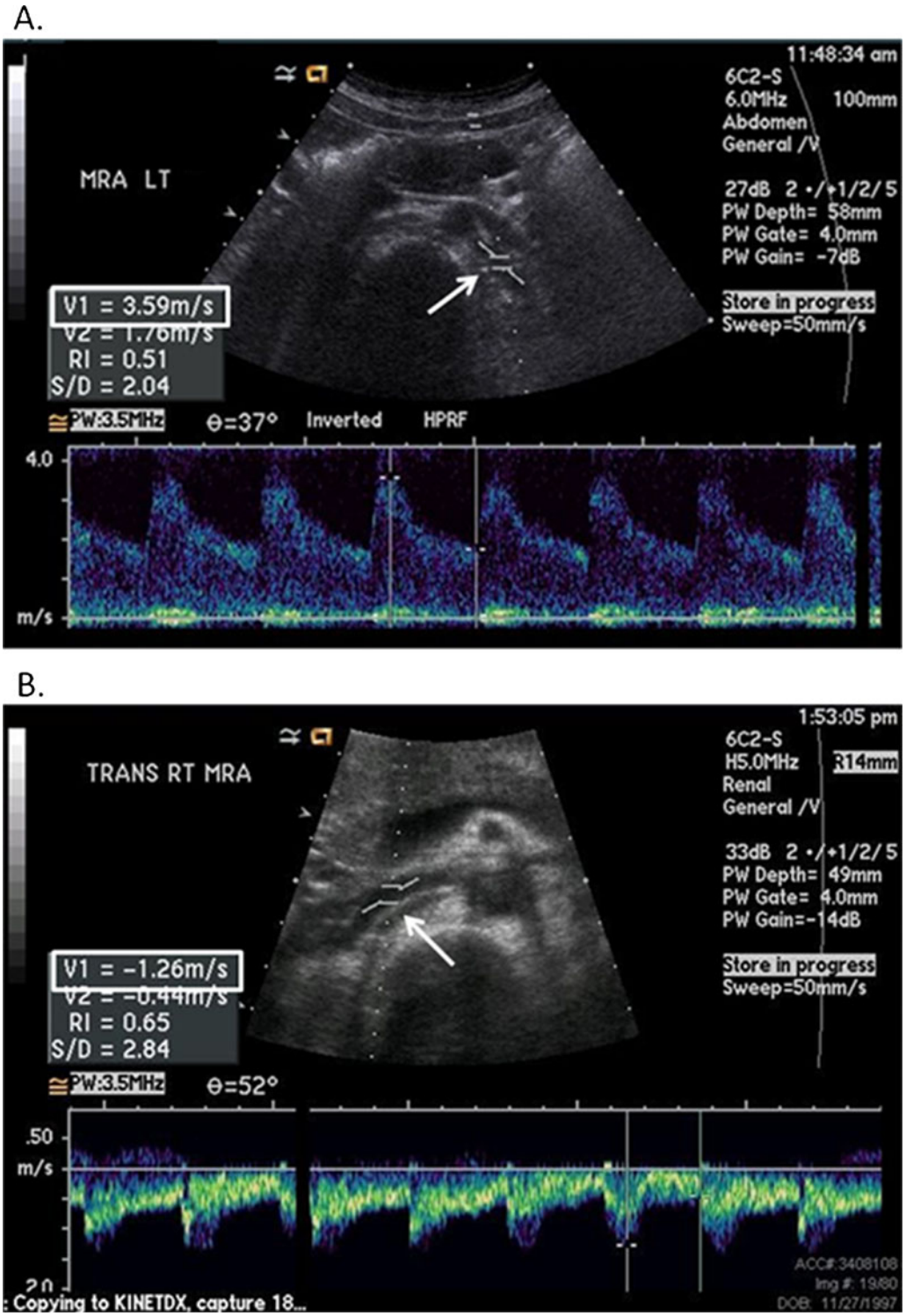

child's hypertension was treated with enalapril, and lymphadenopathy was treated with a 2-month course of oral steroids. 15 months following initial presentation, while the child still required anti-hypertensive therapy, serial renal Doppler ultrasounds demonstrated decreasing lymph node size.

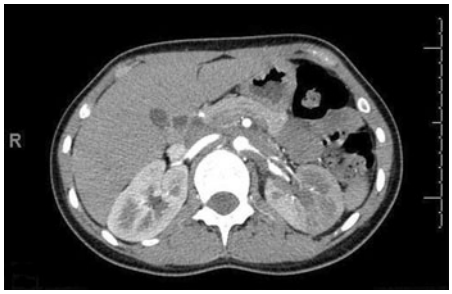

Poster #: CR-022

Direct thrombolytic therapy of superior mesenteric artery in an infant on ECMO

Daniel Ashton, MD, *Radiology, UT Southwestern Medical Center, Irving, TX, daniel.ashton@UTSouthwestern.edu;* Nancy Rollins, MD

Purpose or Case Report: : A 33 day old infant status post recent repair of aortic coarctation and PDA ligation on veno-arterial extracorporeal membrane oxygenation (ECMO) presented with lactic acidosis and elevated transaminases. Ultrasound revealed thrombus in the suprarenal abdominal aorta occluding the celiac axis and superior mesenteric artery (SMA). With the patient on ECMO, aortogram via right femoral artery using a 4 Fr catheter confirmed the sonographic findings. Thrombus was intentionally dislodged from the anterior wall of the proximal abdominal aorta. The SMA could not be directly catheterized, therefore the clot within the celiac axis was traversed using a 3 Fr Prowler Plus and a Gold-tip Glide wire and a total of 4 mg of TPA was infused into the superior pancreatico-duodenal arcade with recanalization of branches of the SMA and a replaced right hepatic artery. This was confirmed by Doppler during the procedure. The patient was maintained on systemic anticoagulation. The lactate dropped from 8.8 to 2.3. The clinical picture improved with resolution of the clot on ultrasound 1 week later. There was no perforation or recurrent sepsis. The patient was taken off of ECMO but subsequently developed a metabolic acidosis without elevation of serum lactate levels and abdominal distention. The parents declined surgical intervention and the patient expired the next day, DOL 42. Autopsy revealed diffuse ischemia of the bowel, splenic infarction, and hepatic congestion consistent with severe cardiopulmonary compromise.

Conclusions: Direct thrombolytic therapy of presumed embolic occlusion of the SMA in an infant on ECMO was technically feasible and not complicated by bowel perforation or sepsis.

Poster #: CR-023

Imaging and endoscopy (laparoscopy/thoracoscopy) guided placement of peritoneovenous and pleurovenous (Denver) shunts in children

Sheena Pimpalwar, MD, *Texas Children's Hospital- Interventional radiology, Houston, TX, ashwinsheena@hotmail.com;* Ashwin Pimpalwar

Purpose or Case Report: Denver shunts are used for palliation of refractory malignant or chylous peritoneal and pleural collections. We report our technique using ultrasound, fluoroscopic and laparoscopic/ thoracoscopic guidance.

Methods & Materials: Patient 1:

A 9 year old male presented with a large right lobe hepatocellular carcinoma extending into the inferior vena cava and right atrium making it unresectable at exploration. Postoperatively, he developed severe symptomatic refractory ascites, liver failure and severe coagulopathy. A denver shunt was requested to help transfer the patient to hospice care.

A 5-mm laparoscopic port was placed at the umbilicus to inspect the peritoneal contents, select the shunt path away from adhesions from previous surgery and allow direct visualization of the catheter into the peritoneal cavity. The shunt chamber was placed within a subcutaneous pocket and the venous catheter was tunneled and placed in the right internal jugular vein (IJV) using ultrasound and fluoroscopy.

Patient 2:

A 13 year old girl with mediastinal and left lower lobe lymphangiectasia, multiple left lower lobe AVM's and refractory chylopericardium and chylothorax occluded her chest tube.

A thoracoscopic port was placed in the midaxillary line to inspect the pleural space, remove the clogged in situ pigtail catheter and breakdown multiple adhesions. The pleural end of the shunt was placed in the posterior costophrenic sulcus under thoracoscopic guidance. The shunt chamber was placed within a subcutaneous pocket in the anterior axillary line just below the axillary crease. The venous catheter was advanced through a subcutaneous tunnel and placed in the left IJV using ultrasound and fluoroscopy.

Results: There were no intraoperative or postoperative complications. The first patient's follow up at 12 months

revealed a flat abdomen with a well-functioning shunt. The second patient has a well-functioning shunt at 1.5 months and is on a low fat oral diet at home.

Conclusions: Combined sonographic, fluoroscopic and endoscopic guidance for placement of a Denver shunt allows proper location of the shunt and is a safe and effective strategy for treatment of malignant/chylous refractory peritoneal and pleural collections in children.

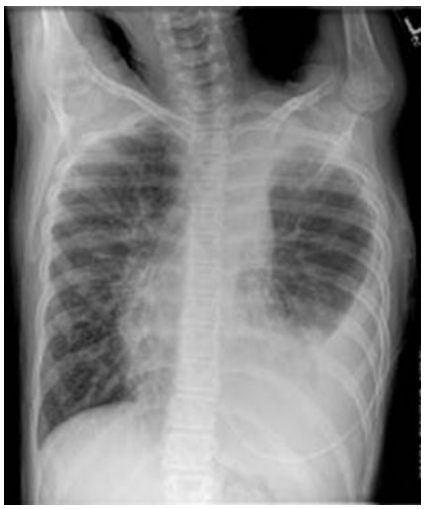

Poster #: CR-024

Institution of combined surgical endoscopic and interventional radiologic approach to management of difficult esophago-bronchial connections in children

Sheena Pimpalwar, MD, *Texas Children's Hospital- Interventional radiology, Houston, TX, ashwinsheena@hotmail.com;* Ashwin Pimpalwar

Purpose or Case Report: Esophago-bronchial fistula (EBF) after esophageal atresia (EA) with tracheo-esophageal fistula (TEF) repair is extremely rare. It is difficult to treat these fistulae with other minimally invasive techniques for repair of recurrent TEF. We describe a minimally invasive technique for the treatment of this extremely rare condition.

Methods & Materials: The case records of the child were retrospectively reviewed.

Case history:

A 2 year old boy who had undergone EA with TEF repair at an outside hospital at birth presented with choking and coughing after feeds and recurrent pneumonia. Esophagogram revealed EBF between the middle third of esophagus and a subsegmental bronchus of the posterior segment of right upper lobe. Rigid bronchoscopy did not reveal a TEF. The child was made NPO and a Laparo-endoscopic Gastrostomy tube was placed. Multiple attempts at fibrin glue injection under endoscopy failed to occlude the fistula.

First treatment attempt:

A pediatric esophagoscope was advanced into the middle third of the esophagus and the EBF was demonstrated. A 3FJB-1 catheter was advanced through the oral cavity under esophagoscopic and fluoroscopic guidance and the fistula was cannulated under direct vision provided by the esophagoscope. A fistulogram was performed followed by embolization using 0.5 ml 50% nBCA.

Second treatment attempt: 2 months after failed first attempt.

After cannulation of the fistula, a 2 mm×2 cm micro-Nester coil was deployed within the fistula followed by injection of nBCA opacified with tantalum powder and a drop of Ethiodol into the residual channel.

Results: The first embolization with glue alone failed with recanalization at 2 months. Repeat embolization was performed with coil and glue. At 12 months follow up after combined coil and glue approach, the child is doing well with no choking or coughing at feeds and complete occlusion of the fistula on esophagogram. He is on full oral diet and the gastrostomy has been removed.

Conclusions: A combined surgical endoscopic and interventional radiologic approach is useful to access and treat difficult EBF in children and may avoid major thoracotomy. The coil acts as a scaffold for glue polymerization and reduces recanalization.

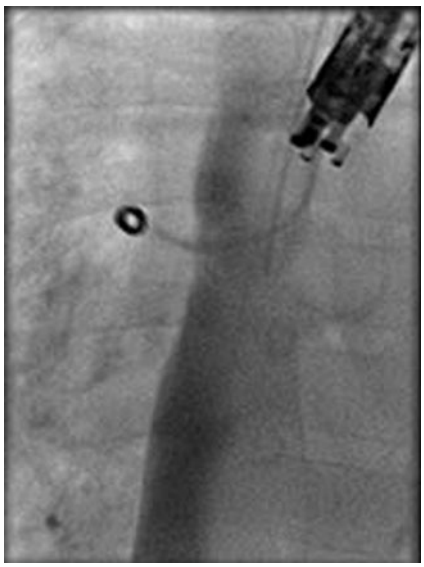

Poster #: CR-025

Percutaneous trans-splenic embolization of Roux limb varices in children with chronic portal vein occlusion (PVO) post orthotopic liver transplant (OLT)

Sheena Pimpalwar, MD, *Texas Children's Hospital- Interventional radiology, Houston, TX, ashwinsheena@hotmail.com;* Aparna Annam, Ponraj Chinnadurai, Alberto Hernandez

Purpose or Case Report: To report our technique of trans-splenic embolization for Roux limb variceal bleeding not amenable to endoscopic therapy in children.

Methods & Materials: Case history:

Patient 1

5 year old girl with chronic PVO post OLT for biliary atresia presented with chronic upper GI bleed and anemia requiring multiple transfusions despite adequate treatment of esophageal varices. MR and CT revealed heterotaxy, polysplenia with azygous vein connections and cavernous transformation of the portal vein. Enteroscopy could not detect these varices.

Patient 2

12 year girl with chronic PVO post OLT for biliary atresia presented with acute upper GI bleed. Upper GI endoscopy and enteroscopy were normal. CT abdomen showed varices within small bowel wall near the liver hilum.

Technique

C-arm CT (syngo DynaCT®, Siemens Medical Solutions USA Inc.) images were acquired using a 8-second DR body protocol with contrast injection into the superior mesenteric artery followed by delayed image acquisition during the venous phase to demonstrate the Roux limb varices with porto-portal collaterals through the liver capsule into the intrahepatic portal branches. A 4 F vascular sheath was placed within the splenic vein after accessing a peripheral splenic venous tributary using ultrasound. Superior mesenteric venography and selective venography of the Roux limb varices followed by embolization using microcoils, NBCA or Onyx was performed. Postembolization superior mesenteric venography and C-arm CT imaging in the venous phase were performed.

The splenic access tract was embolized using microfibrillar collagen slurry.

Results: Preembolization C-arm CT images were helpful in localization of the varices to the bowel wall and selection of varices for embolization. There was no intraperitoneal bleeding.

Patient 1 had successful initial resolution of GI bleed with recurrence at 4.5 months when further varices were embolized using the same technique. At 14 month follow up since the second procedure there has been no further bleed.

Patient 2 with acute GI bleed had cessation of bleeding and is stable at 2 month follow up.

Conclusions: A trans-splenic approach is a useful technique to embolize bleeding Roux limb varices which are beyond the reach of the endoscopist in the setting of portal vein occlusion in patents post OLT.

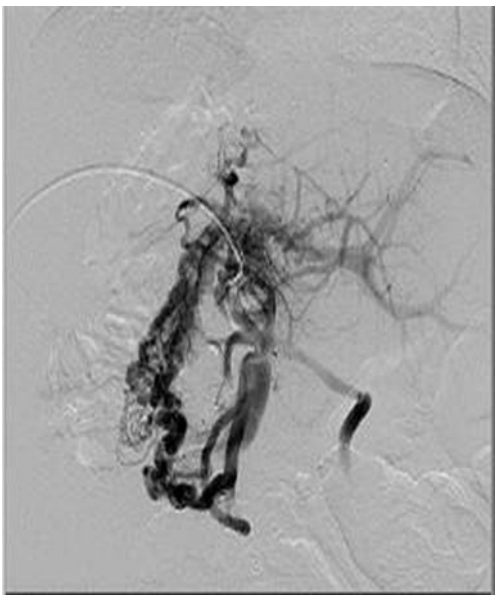

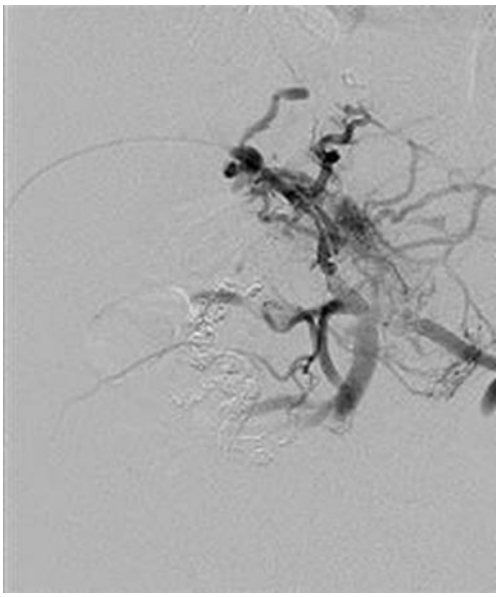

Poster #: CR-026

Pharmacomechanical pulverization of mycetoma in the renal collecting system

Rohit Ramanathan, *Baylor College of medicine, Houston, TX, rohit.ramanathan@gmail.com;* Sean Raj, MD, Sheena Pimpalwar, MD, Ewa Elenberg, Poyyapakkam Srivaths, Eileen Brewer, Alberto Hernandez

Purpose or Case Report: Renal mycetomas are rare manifestations of candidia infection in children, which if untreated may lead to urinary tract obstruction (UTO), renal failure and high mortality. We report successful use of a mechanical thrombectomy (AngioJet) device to pulverize an obstructing renal pelvis candida mycetoma resistent to conventional nephrostomy tube (NT) drainage in a small child with UTO and renal failure.

Methods & Materials: Case history:

A 2.5 year old, 10.5 kg, former 26 week premature girl was admitted with recurrent candida urinary tract infection and fungal balls within the right pelvicalyceal system leading to UTO, oliguria and renal failure (serum Cr 2.7 mg/dL). NT placement and administration of IV Amphotericin B (AmB) failed to improve urine output or renal failure. Ultrasound and antegrade pyelogram showed persistent dilatation of an obstructed right collecting system plugged with fungal balls.

Technique: The in situ 8.5 F NT catheter was exchanged for a vascular sheath through which a 6-French AngioJet Spiroflex catheter (AngioJet® Ultra thrombectomy system, Medrad International®) with a 15-mm active tip was advanced into the renal pelvis and calyces under ultrasound and fluroscopic monitoring. Fungal balls were drawn into the catheter,fragmented by saline pressure jets from the active tip and aspirated simultaneously. The saline in the AngioJet system was replaced with AmB solution and pharmacomechanical pulverization of the fungal balls was performed followed by upsizing of the NT to 10 F.

Results: After mycetoma pulverization, NT urine output improved from 0 to 490 mL in the first 12 hr, and serum Cr decreased to 1.65 within 24 hr. The patient had no complications from the AngioJet therapy. She completed a 21 day course of systemic and transcatheter AmB and NT was removed. At 2 week follow up, serum Cr was 0.6 mg/dL, and ultrasound and antegrade studies showed reduced hydronephrosis with no recurrence of fungal balls. At 12 month follow up, patient had no recurrence of candida infection, no imaging recurrence of mycetoma and serum Cr 0.5 mg/dL.

Conclusions: Pharmaco-mechanical pulverization using an AngioJet thrombectomy system is an effective treatment option for refractory renal collecting system mycetoma.

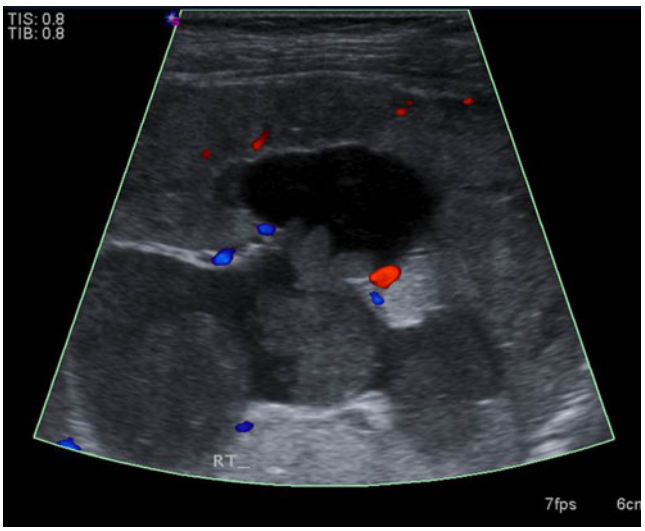

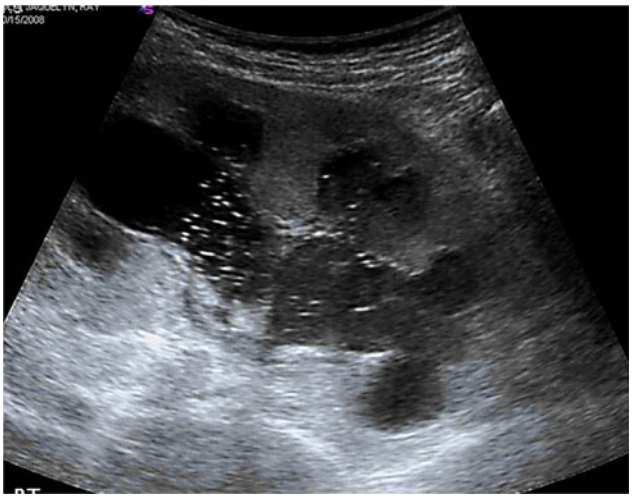

Poster #: CR-027

Imaging of the thoracic duct using C-arm CT lymphangiography (CTL) following ultrasound guided inguinal nodal injection in children with right to left shunts

Sheena Pimpalwar, MD, **Aparna Annam,** *Texas Children's Hospital- Interventional radiology, Houston, TX, axannam@texasChildren'shospital.org;* Ponraj Chinnadurai, Alberto Hernandez

Purpose or Case Report: Lipiodol cannot be used to perform traditional fluoroscopic lymphangiogram in children with right to left shunts due to the risk of systemic embolization. We describe the use of C-arm CTL following ultrasound guided inguinal lymph node injection of water soluble contrast media as an alternative imaging tool for the central conducting lymphatics in these children.

Methods & Materials: Case history:

Patient 1:

A 4 year old boy with complex congenital heart disease developed recurrent right sided chylothorax which resolved followed by left chylothorax requiring several chest tubes. A lymphangiogram was performed to look for thoracic duct leak.

Patient 2:

A 13 year old girl with multiple cutaneous epidermal nevi, simple renal and splenic cysts, multiple lytic bone lesions, bilateral interstitial lung disease, multiple left lower lobe pulmonary AVM's developed recurrent chylopericardium. This was managed with pericardial drainage and lymphangiogram was performed to look for leak.

Technique

Under ultrasound guidance bilateral inguinal nodes were accessed using 25 G needles followed by slow hand injection of Optiray 320. 2D-fluoroscopic visualization of the pelvic and lumbar lymphatics up to L2 level was possible beyond which dilution of contrast from leakage across the wall of the lymphatics precluded visualization. C-arm CT (syngo Dyna CT®, Siemens Medical Solutions USA Inc.) of the chest was performed using 8 s DR-body protocol and images were reconstructed.

Results: Patient 1

C-arm CTL showed a lobulated pseudoaneurysm of the thoracic duct at the level of T6 adjacent to a surgical clip with normal course and caliber of the rest of the duct to its insertion into the left subclavian vein and no leak.

Patient 2

C-arm CTL showed reflux of contrast into dilated lymphatics in the mediastinum, left hilum and left lower lobe suggestive of lymphangiectasia with uninterrupted course of the rest of the duct to the left subclavian vein. No leak into the pericardium was seen but the study was limited by artifacts from pericardial drainage catheter and nasogastric tube.

Conclusions: C-arm CTL can successfully demonstrate thoracic duct anatomy and pathology in combination with ultrasound guided inguinal nodal injection of water soluble contrast agent in children with contraindication for oily contrast media.

Poster #: CR-028

Interventional Management of Ruptured Hepatoblastoma: Case Report of a Life Threatening Emergency

Aparna Annam, DO, **Brian Hailey, MD,** *Texas Children's Hospital-Pediatric Interventional Radiology, Houston, TX, hailey@bcm.edu;* Alberto Hernandez, Patrick Thompson, Sheena Pimpalwar, MD

Purpose or Case Report: Hepatoblastoma is the most common primary pediatric hepatic malignancy. The clinical presentation is often indolent but in rare instances complications can develop including acute catastrophic tumor rupture with intraperitoneal hemorrhage. We present a case report of a ruptured hepatoblastoma successfully treated in the acute setting with embolization of actively extravasating tumor vessels. Special emphasis is made on angiography and choice of embolization agents.

Methods & Materials: A retrospective chart review of a 23 month old female with rutpured hepatoblastoma was performed.

Results: Case history: 23 month old female diagnosed by CT guided biopsy at an outside institution with PRETEXT IV multifocal hepatoblastoma, was referred to our institution for liver transplant evaluation. Post commencement of her first cycle of chemotherapy, she developed acute intraperitoneal bleeding requiring multiple blood transfusions and pressors.

Non-contrast CT abdomen demonstrated large volume hemoperitoneum and contour irregularity of the anterior inferior right liver lobe.

Selective hepatic angiography demonstrated neovascularity, hypetrophied and tortuous arterial feeders, arterial aneurysms, dense parencyhmal staining and venous lakes involving almost the entire liver. There was brisk intraperitoneal extravasation of contrast from a peripheral segment five branch.
Embolization: Subselection of the bleeding vessel was followed by combined particle and coil embolization. The injected particles infiltrated into the abnormal tumor bed containing leaky vessels. Particles were supplemented by additional coil embolization to reduce the arterial pressure head in the bleeding tumor bed. Use of coils as a single embolic agent would cause proximal embolization with immediate recruitment of collaterals by tumor vessels. Therefore, a combined particle and coil approach was utilized. The large volume hemoperitoneum, causing abdominal compartment syndrome, was managed with a peritoneal drain and 800 ml of hemorrhagic fluid was removed.
Post-embolization: The patient regained hemodynamic stability post embolization with gradual withdrawl of pressor support. Intermittent blood transfusions were required for 72 h. She had significant clinical improvement and successfully received an orthotopic liver transplant 2 weeks after her acute event.
Conclusions: Acute intraperitoneal rupture is an uncommon complication of hepatoblastoma. This life-threatening bleeding can be successfuly managed by transarterial embolization.

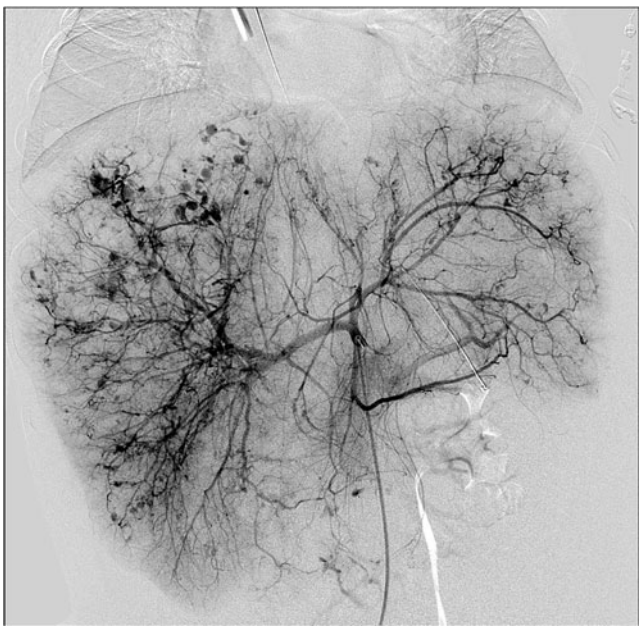

Poster #: CR-029

Radiofrequency ablation of multifocal hepatoblastoma in a child with right to left intracardiac shunt: is there risk of microbubble embolization?

Rohit Ramanathan, *Baylor College of medicine, Houston, TX, rohit.ramanathan@gmail.com;* Sean Raj, MD, Sheena Pimpalwar, MD, Patrick Thompson

Purpose or Case Report: Radiofrequency ablation (RFA) releases nitrogen micro-bubbles which could cause systemic embolization in patients with right to left shunts. Our purpose is to illustrate our experience with RFA of hepatoblastoma in a child with right to left intracardiac shunt.
Methods & Materials: Case history:
A 11 month old boy with Beckwith Wiedmann syndrome and right to left intracardiac shunt presented with non-resectable refractory recurrent multifocal hepatoblastoma with four lesions (all <5 mm) following chemotherapy. As a result of his cardiac disease he was not considered a candidate for liver transplantation. Consequently, he was referred for RFA.
Technique:
A 16 G Uniablate probe from AngioDynamics was utilized for ultrasound guided ablation and 100% oxygen was administered by the anesthesiologist during each ablation. Unlike routine RFA where liberation of nitrogen gas appears as diffuse echogenic bubbles that obscure the sonographic field, our ablation demonstrated an enlarging target appearance of the liver parenchyma at the distal end of probe with little to no micro-bubbles.
Results: No neurological complications were noted in the patient. His tumor maker, alpha feto protein (AFP), normalized following the procedure and follow up MRI revealed no recurrent disease at 8 months.
Conclusions: Radiofrequency ablation of hepatoblastoma in children with right to left intracardiac shunt using 100% oxygen helps in near- elimination of microbubbles reducing the risk of systemic embolization. For selected patients who are not candidates for surgery or transplant this RFA offers a potentially effective alternative for local control of their disease. Candidates for RFA should not be excluded based on the presence of a right to left intracardiac shunt.

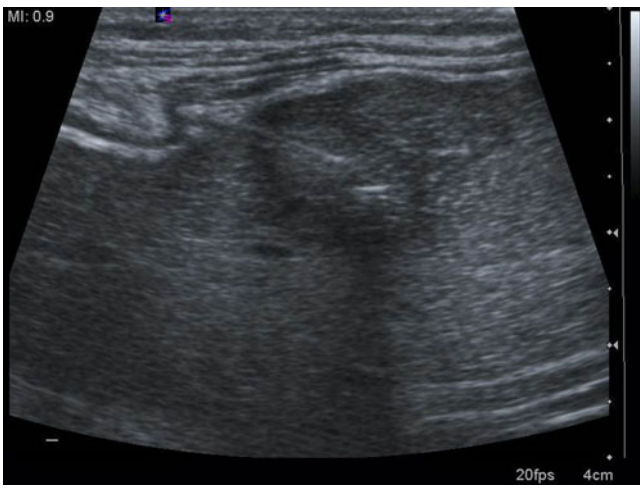

Poster #: CR-030

Treating Complex Vascular Anomalies with Novel Techniques

David Aria, MD, *Radiology, Phoenix Children's Hospital, Phoenix, AZ, daria@phoenixChildren's.com;* Richard Towbin, MD, Carrie Schaefer, Robin Kaye

Purpose or Case Report: An 8 year-old girl with a complex medical history including trisomy 21, multiple cardiac anomalies, and chronic anemia of mixed etiology, presented with gastrointestinal bleeding. Over the preceding year, she had become cyanotic and on physical examination, digital clubbing was noted. Laboratory evaluation revealed elevated serum ammonia levels. Abdominal ultrasound demonstrated a congenital portacaval shunt. Due to the large size of the shunt, traditional embolization agents such as coils could not safely be utilized. Although not generally used for this purpose, the decision was made to occlude the fistula with a 14-mm Amplatzer ASD occlusion [clamshell] device. The Amplatzer device was deployed at the inferior vena cava and portal vein communication without immediate complication. The patient's post-operative course was uneventful and the patient was discharged on post-operative day #2. Follow-up visits demonstrated resolution of the clinical signs and symptoms and imaging demonstrated closure of the shunt. This experience highlights the use of a novel technique for treatment of a large, symptomatic portacaval shunt.

Poster #: CR-031

Withdrawn

Poster #: CR-032

Trans-splenic recanalization and angioplasty of anastomotic portal vein occlusion post OLT

Sheena Pimpalwar, MD, *Texas Children's Hospital-Interventional radiology, Houston, TX, ashwinsheena@hotmail.com;* Aparna Annam, D.O., Henry Justino, Alberto Hernandez

Purpose or Case Report: Portal vein anastomotic stricture and occlusion is an uncommon late complication of OLT resulting in portal hypertension and its sequelae. We describe a percutaneous trans-splenic approach to image and treat this condition thus preventing surgical intervention.

Methods & Materials: Case history:

Patient 1

A 4 year old female 2.5 years post OLT for Alagille syndrome presented with multiple episodes of acute GI bleed. She had severe splenomegaly and esophageal varices that were banded. MRI abdomen showed an abrupt change in caliber at the porto-portal anastomosis without a flow jet to suggest stenosis.

Patient 2

A 5 year old male 4 years post OLT for Alagille syndrome presented with severe splenomegaly and platelet consumption. CT abdomen showed high grade celiac origin stenosis and a few portosystemic collaterals with normal appearing portal vein.

Technique

Wedged hepatic venography via a right femoral venous approach revealed normal portosystemic pressure gradient. Superior mesenteric arteriography revealed complete portal vein occlusion at the porto-portal anastomosis with portosystemic collaterals and delayed reconstitution of the intrahepatic portal venous branches.

A 4 F 45 cm vascular sheath was placed within the splenic vein after ultrasound guided access of a peripheral lower pole splenic vein tributary. The anastomotic portal venous occlusion was crossed and serially dilated from 6 mm to 10 mm. Post angioplasty splenic venogram showed rapid centripetal flow across a near normal caliber anatomosis into the liver with absence of collateral filling. The pressure gradient across the anastomosis reduced from 10 mm to 1 mm post angioplasty. The splenic access site was embolized using microfibrillar collagen slurry.

Results: Both patients did well with no post procedure intraperitoneal bleeding.

Patient 1

There was immediate cessation of acute GI bleed post embolization. At 12 months follow up, there has been no recurrence of GI bleed.

Patient 2

Improvement in platelet count was seen post embolization. Follow up imaging to monitor reduction in splenic size will be performed.

Conclusions: A trans-splenic approach to image and treat late portal venous complications post OLT is a safe and useful technique providing a minimally invasive alternative to surgical intervention. Anastomotic portal vein occlusion can be treated successfully using this technique.

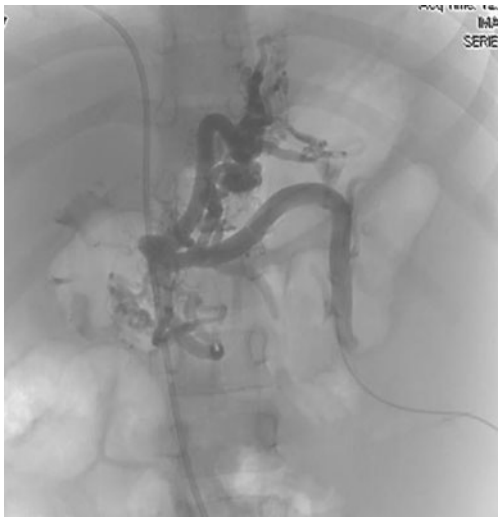

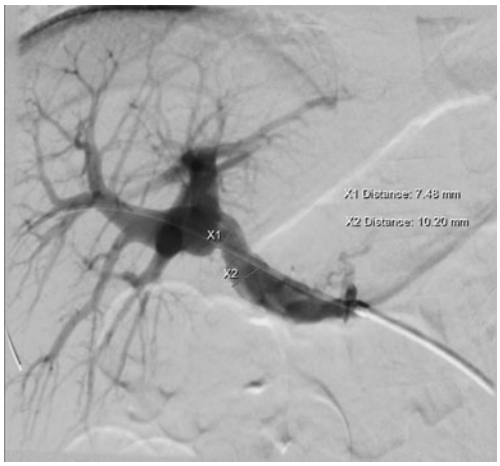

Poster #: CR-033

Radiofrequency Ablation: An Alternative Treatment for Large Venous Malformations

David Aria, MD, *Radiology, Phoenix Children's Hospital, Phoenix, AZ, daria@phoenixChildren's.com;* Richard Towbin, MD, Carrie Schaefer, Robin Kaye

Purpose or Case Report: A 12 year-old boy with a history of a large palpable right lower extremity venous malformation resulting in multiple pulmonary emboli presented with chest pain. The patient had undergone prior sclerotherapy procedures and was currently on anticoagulation. Doppler ultrasound of the right lower extremity demonstrated diffuse thrombus within the venous malformation, the largest component within an enlarged greater saphenous vein measuring 14 mm. Due to the large size of the greater saphenous vein and poor response to traditional sclerotherapy agents, such as Sotradecol and ethanol, an alternative approach was considered. Although not generally used for this purpose, the greater saphenous vein was sclerosed using radiofrequency ablation (RFA). There were no procedural complications and the patient's post-operative course was uneventful. Follow-up visits demonstrated resolution of the clinical signs and symptoms and imaging demonstrated occlusion of the right greater saphenous vein. This experience highlights the use of a novel technique for treatment of a large, symptomatic venous malformation.

Poster #: CR-034

The Posterior Femoral Fat Pad – A New Radiological Sign

Daniel Carr, *UMass Memorial Health Care, Worcester, MA;* Ellen Wallace, MD, Nancy Resteghini, Sjirk Westra

Purpose or Case Report: The purpose of this case series is to describe and name the fat pad posterior to the distal femoral diaphysis, and describe its utility in identifying underlying bone pathology.

On lateral radiographs, several fat pads around the knee are recognized, but we were unable to find a name for the normal fat pad that is located posterior to the distal femur. We suggest that it be named the "posterior femoral fat pad" (PFFP). Posterior displacement of this fat pad may be regarded as a positive posterior femoral fat pad sign.

In our experience, we have found that a positive PFFP sign is indicative of underlying bone pathology. We retrospectively identified six patients (3 male, 3 female; age range: 3–16 years); with a positive PFFP sign. Diagnoses were: subperiosteal abscess associated with osteomyelitis (N=3), subperiosteal hematoma due to fracture (N=2) and marrow infiltration due to leukemia (N=1). In addition to the positive PFFP sign, no other radiographic findings were seen in 2, subtle findings in 2, and positive findings in 2. MRI correlation was available for 5 of the 6 cases.

For comparison, we will demonstrate abnormal knee radiographs with a normal PFFP, with MRI and CT correlation. Therefore a normal PFFP does not exclude disease but a positive PFFP sign can expedite the diagnosis of unsuspected important underlying skeletal

disease processes, particularly those extending to and displacing the periosteum, which might otherwise be overlooked or delayed.

We believe that specific consideration of the posterior femoral fat pad during systematic review of knee radiographs will improve the diagnostic sensitivity of this test.

Poster #: CR-035

Peripheral cholangiocarcinoma associated with a benign cystic anomaly in an adolescent

Daniel Rosenbaum, MD, *NewYork-Presbyterian Hospital/Weill Cornell Medical Center, New York, NY, dgr2001@nyp.org;* Angela Bachmann, Debra Beneck, Michael Kluger, Nitsana Spigland, Paula Brill

Purpose or Case Report: A 16 year-old girl with no significant medical history presented to the emergency department complaining of 2 days crampy abdominal pain. On exam, the patient's abdomen was asymmetrically distended, with dullness to percussion throughout right hemiabdomen. Liver enzymes and serum bilirubin were normal. EBV and CMV titers, hepatitis serologies, and an HIV test were negative. CA-125, CEA, and CA 19–9 were elevated. An abdominal radiograph demonstrated density throughout the central abdomen with displacement of bowel loops. US showed a large multicystic abdominal mass of unclear origin. Further characterization with CT showed a multiloculated cystic and solid mass with variably calcified septations apparently arising from the right hepatic lobe, suspicious for a cystic neoplasm such as biliary cystadenoma or cystadenocarcinoma (Fig 1a). No associated biliary ductal dilatation was present. Exploratory laparotomy confirmed hepatic origin of the mass, and an extended right hepatectomy was performed. Pathology showed poorly differentiated adenocarcinoma of the intrahepatic bile ducts associated with a benign, multiloculated cyst lined by a single layer of bland, biliary-type epithelium (Fig 1b).

Cholangiocarcinoma is extremely rare in children, and typically arises in the setting of predisposing hepatobiliary pathology. The case presented here is atypical when compared to previously reported cases of pediatric cholangiocarcinoma (Table 1) in its peripheral location and association with a non-Todani type benign cystic anomaly of the liver. While the multiloculated cystic appearance of the mass initially suggested a mucin-secreting tumor, final pathology confirmed poorly differentiated ductal carcinoma, without evidence of papillary excrescences or mural nodules within the cysts (which were likely preexisting) to suggest cystadenocarcinoma. Congenital hepatic cysts may show an association with cholangiocarcinoma in adults, however to our knowledge, no such case has been reported in the pediatric population. Given the rarity of cholangiocarcinoma in this age group, interpreting radiologists should be aware of the particular settings in which these tumors may arise in order to facilitate prompt diagnosis and treatment.

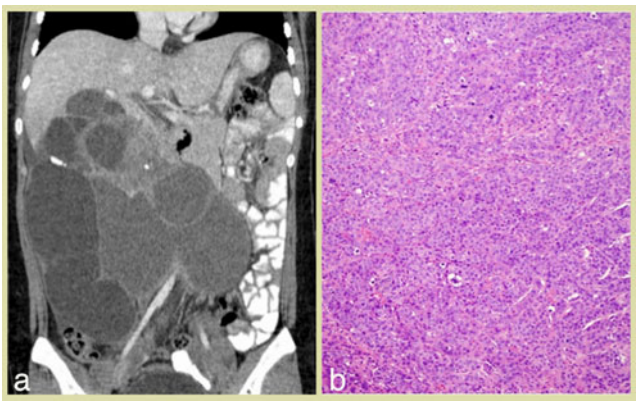

Figure 1. Peripheral cholangiocarcinoma associated with a benign cystic anomaly. **a)** Coronal CT shows a large multilocular cystic and solid mass with multiple septations extending inferiorly from the right hepatic lobe. **b)** H&E stain of the solid portion of the mass reveals sheets of malignant cells with nuclear pleomorphism and frequent mitoses.

Table 1: Previously reported cases of cholangiocarcinoma in the pediatric population

Author	Patient Age	Gender	Predisposing condition	Tumor location	Pathology
Lin (2012)	20	F	Perinatal HIV	Hilar	Poorly differentiated ductal adenocarcinoma
Deneau (2011)	17	M	Primary sclerosing cholangitis	Not specified	Ductal adenocarcinoma
Channabasappa (2010)	15	M	Orthotopic liver transplant at 14 months of age	Hilar	Papillary cholangiocarcinoma
Saikusa (2009)	3	M	Choledochal cyst (Todani type IA)	Hilar	Well-differentiated tubular adenocarcinoma
Mangeya (2008)	17	M	HIV (presumed perinatal)	Hilar	Well differentiated ductal adenocarcinoma
Nakamura (2008)	15	F	Choledochal cyst (Todani type IA)	Hilar	Papillary cholangiocarcinoma
Tanaka (2006)	11	M	Choledochal cyst (Todani type IVA)	Hilar	Tubular adenocarcinoma

Poster #: CR-036

Unusual presentation of a rare case of extramedullary hematopoiesis, involving the sino-nasal tract in an African American patient with sickle cell anemia

Carmen Rotaru, *Radiology, Children's Hospital of Eastern Ontario, Ottawa, ON, Canada, crotaru@cheo.on.ca;* Amer Alaref, David Grynspan, Matthew Bromwich

Purpose or Case Report: Sickle cell disease is a well known hematologic disorder related to abnormal hemoglobin structure, causing sickling of the red cells. In most of the cases the disease manifests with intravascular hemolysis, anemia and microvascular occlusion, the patients being prone to infections. The ensuing normocytic anemia and increased drive for compensatory red cell mass results in intra and extramedullary hematopoiesis (EMH). While there are many cases of EMH described in the head and neck as well as in other locations, most of them in liver, spleen or lymph nodes, EMH in the paranasal sinuses is very rare. We present a case of a young African American boy with sickle cell disease, who presented with new onset of headaches. The imaging demonstrated an expansile mass occupying the sphenoid. The biopsy confirmed EMH.

Poster #: CR-037

Histopathologic diagnosis of neurofibroma in lesion with imaging features resembling vascular anomalies

Sabri Yilmaz, MD, **Lauren Zammerilla,** *Children's Hospital of Pittsburgh of UPMC - Radiology, Pittsburgh, PA, LLZ3@pitt.edu;* Lorelei Grunwaldt, John Ozolek, Charles Fitz, John Crowley

Purpose or Case Report: Although rare, the initial clinical and imaging presentations of neurofibromas can mimic those of vascular anomalies, particularly if the characteristic clinical features of Neurofibromatosis are not present. In this communication, we discuss the diagnostic challenges encountered in patients with histopathological diagnosis of neurofibromas, which were initially misdiagnosed, followed up as vascular anomalies, and referred to our Vascular Anomalies Clinic for evaluation. We report the clinical, imaging, and pathologic features of five cases of neurofibromas, either plexiform or diffuse, resembling clinical and imaging characteristics of vascular anomalies, including infantile hemangiomas, venous malformations, and microcystic lymphatic malformations. The clinical and imaging differences between these entities are highlighted with the goal of preventing diagnostic pitfalls in the future.

Poster #: CR-038

Spectrum of Klippel-Trenaunay Presentation

Mauricio Yamanari, MD, *Instituto de Radiologia Hospital das Clinicas Universidade de Sao Paulo, Sao Paulo, Brazil, mauriciogustavo91@yahoo.com.br;* Lisa Suzuki, Fernanda Magalhaes, Silvia Rocha, Andrea Ferme, Luiz Oliveira

Purpose or Case Report: Klippel-Trenaunay syndrome is a congenital malformation characterized by the triad of cutaneous capillary malformations (port wine nevi), hypertrophy of soft tissue and / or bone of the limb or affected region and varicose veins / venous malformations.

Usually the findings are restricted to one limb, but cases with multiple extremities, visceral, half body and even the whole body involvement have been reported.

In this presentation we report cases with various forms of presentation of Klippel-Trenaunay syndrome evaluated by multiple methods including ultrasound, MRI and CT. Ultrasound is a noninvasive method suitable for initial evaluation of possible thrombosis and arteriovenous fistulae. We emphasize the importance of performing MRI or CT angiography to assess the extent of vascular malformation, thrombosis and arteriovenous fistulae in the limb and other organs.

- Case 1: Four months child with increased left leg and port wine nevi. MRI of this member presents massive vascular and lymphatic malformation extending from the retroperitoneal region posterior to the left kidney to the entire lower left leg and involvement of the pelvis (image attached).
- Case 2: Nine year old child with asymmetric members. MRI presents vascular malformations of the entire right lower limb, greatly increased compared with the contralateral limb.
- Case 3: Eighteen year old patient with increased abdominal size. Ultrasound and abdominal CT show a mass formed by a vascular structures ocuppying the entire pelvis. She also had an aneurysm of superior mesenteric vein with thrombus and splenic lymphangiomas.
- Case 4: Twenty-three year old patient with a history of increasing left lower limb. AngioCT presented varicose veins and increased bone and soft tissue in this limb with arteriovenous fistula in the popliteal region, featuring Klippel-Trenaunay-Weber syndrome or Parkes-Weber.
- Case 5: Fifteen year old patient with, slight increase of the left limb with varicose veins. Abdominal CT presented hypervascular hepatic nodules, agenesis / hypoplasia of the portal vein with portal hypertension. Portosystemic shunt with collateral vein originated from the splenic vein, forming a handle in the pelvic cavity and binding to the right common iliac vein was seen.

In the wide spectrum of presentation of Klippel-Trenaunay syndrome, the management of patients should be individualized and the prognosis depends on the severity and associated anomalies.

Poster #: EDU-001

A Multi-Departmental Initiative to Reduce Cumulative Radiation from Pediatric Modified Barium Swallow Studies: Methods and Outcomes

Nancy Sinden, Steven Gorsek, Janet Franco, Windy Stevenson, Daniel Kenron, **Katharine Hopkins, MD,** *Speech Language Pathology, Oregon Health & Science University, Portland, OR, hopkinsk@ohsu.edu*

Purpose or Case Report: In our university children's hospital radiology suite, modified barium swallow studies (MBSS) are the most frequently performed, most often repeated, and highest dose fluoroscopy procedures done. Moreover, they are commonly performed in our smallest patients who have complex medical issues, undergo multiple imaging studies, and have high cumulative radiation exposures. Although MBSS provide important diagnostic information, techniques with which they are performed are varied and endpoints are nebulous, sometimes resulting in unnecessary radiation. Standardization is made difficult by the number of personnel and departments involved in performance and usage of the procedure. This poster outlines our multi-departmental quality improvement initiative to reduce excess radiation from pediatric MBSS while maintaining diagnostic standards. We provide methods, results, and helpful problem solving tools for readers who wish to reproduce our process.

Methods & Materials: Representatives of Speech Language Pathology, Radiology, Pediatrics, and Quality Improvement were convened. Using A3 problem solving methodology (template to be provided), the issue of pediatric radiation exposure from MBSS was explored. Opportunities were identified to enhance the MBSS process to minimize patient radiation exposure, including: 1) pre-MBSS patient assessment and selection, 2) utilization of empiric feeding trials in lieu of MBSS, 3) timing of MBSS to maximize diagnostic impact and obviate unnecessary repetition, 4) consideration of cumulative exposure, and 5) attentiveness to exposure time. Steps were developed and implemented to achieve improvement goals, and outcome measures were monitored.

Results: While study quality was subjectively maintained, mean exposure time per study was reduced by 45%, from 170 s to 93 s. Variability in exposure time, number of studies done per week, number of studies scheduled without pre-procedural patient assessment, and number of studies repeated within a 6-month interval also declined.

Conclusions: Using a multi-departmental approach and established quality improvement methodology, we successfully reduced unnecessary radiation exposure associated with pediatric MBSS. Readers are encouraged to reproduce this Practice Quality Improvement (PQI) project at their own facilities, using the tools demonstrated.

Poster #: EDU-002

How much radiation will my child get from this CT? How to easily answer this question in your daily practice

Mona Shroff, MD, *Children's Hospital and Medical Center, Omaha, NE;* Sandra Allbery, Elizabeth Wipf, Nicole Hardin, Terri Love, Lisa Wheelock

Purpose or Case Report: Accurate pediatric radiation dose and risk from a CT examination are not easily interpreted from the vendor supplied CT dose profile. While a predetermined radiation Dose Length Product (DLP) is available from the patient profile even prior to scanning, it is not specific to the patient's size. A more accurate radiation dose can be easily obtained by applying a conversion factor specific to the patient's size to obtain Size Specific Dose Estimate (SSDE). A more accurate radiation risk can then be easily obtained by applying another conversion factor, the K factor, specific to the patient's age and type of exam. The radiation risk can then be explained in a meaningful way to the patient by comparing to common activities such as background radiation or airline flight.

Methods & Materials: We obtained patient profiles of single phase pediatric CT examinations (head, chest, and abdomen/pelvis) of 274 patients over 2 months with age range of 2 days to 20 years. We measured the patient's transverse diameter in centimeters directly from patient images. We then applied a conversion factor published by AAPM (American Association of Physicists in Medicine) Report No. 204 according to the phantom size used and patient diameter. To calculate the radiation risk, we applied a conversion fact, K factor, published by AAPM Report No. 96 according to patient's age and type of CT exam.

Results: SSDE averages were 24.2, 10.7, 15.6 mGy for head, chest, and abdomen/pelvis CTs respectively. Radiation risk averages were 2.3, 5.1, 9.5 mSv for head, chest, and abdomen/pelvis CTs respectively. To best communicate the degree of risk to our patients, referring physicians, radiologists, and staff, we created an educational chart showing comparable risk from common activities. This method was made readily available to key areas in the department to better answer patient queries and to improve patient satisfaction.

Conclusions: This educational exhibit will show how simple it is to obtain more meaningful estimates of dose and risk for patient's undergoing CT scans. With uncomplicated calculations, parameters available on the CT scanner are adjusted for patient size, age, and relative risk of each body part. The risks can be explained to the patient and referring physicians in a more meaningful way by giving a comparable radiation risk of a common activity such as background radiation or airline travel.

Poster #: EDU-003

A journey to decrease dose level and optimize body CT scans in children

Boaz Karmazyn, MD, *Radiology, Riley Hospital for Children, Indianapolis, IN, bkarmazy@iupui.edu;* Yun Liang, Erv Herman

Purpose or Case Report: To show how step-by-step changes in CT scan parameters resulted in decreased dose while maintaining quality.

Methods & Materials: Between October of 2010 and September of 2012 (approximately 2 years) we made the following changes (one at a time) to our pediatric body CT protocols: decrease of tube voltage, use of iterative reconstruction (iDose4), mAs modulation (ZDONE) and automated current selection (ACS).

Results: Tube voltage decreased from 120 to 80 kVp in children with body weight (BW) <20 kg, and 120 to 100 kVp in BW >20 kg with an average decreased in dose of 10%. Longitudinal mAs modulation decreased mean patient dose by 20%. iDose4 was optimized by BW (level 2 in BW <20 kg to level 4 in BW >60 kg) and resulted in improved image quality and decreased dose by 34%. Mean 32 cm phantom CTDIvol decreased from 7.2 to 4.1 mGy (43%) for the abdomen and from 6.7 to 2.1 mGy (67%) in the chest. Automated current selection resulted in a tailored dose with an excellent (R2=0.91) match of CTDIvol to BW.

Conclusions: Multiple imaging parameters can be changed to reduce dose while maintaining image quality; low kVp protocols, mAs modulation, and use of iterative reconstruction have the most impact

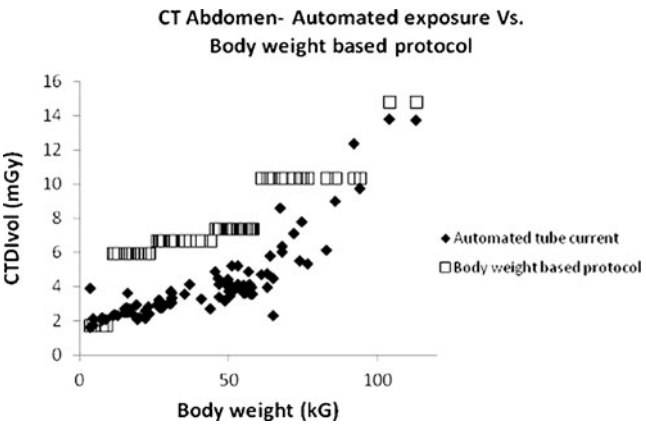

Poster #: EDU-004

Withdrawn

Poster #: EDU-005

MR imaging of coronary arteries in children: Case Based Teaching File

Roy Jacob, MD, *Children's Medical center, Dallas, TX, Roy.Jacob@utsouthwestern.edu;* Shannon Blalock, Jeanne Dillenbeck

Purpose or Case Report: Coronary artery imaging in children is performed for evaluation of congenital anomalies like anomalous origins, pre-surgical planning in congenital heart disease and in acquired conditions like Kawasaki's disease, which can predispose to formation of coronary artery aneurysms. Coronary artery imaging is traditionally performed with echocardiography which can have limitations, secondary to poor acoustic window. Cardiac CT and direct catheter angiography have excellent diagnostic capability, though their use in children is limited due to radiation concerns. Cardiac MR imaging has the advantage of being radiation free and the ability to perform multi planar imaging.

This electronic presentation outlines the following -

1. Review embryology and developmental anatomy of the coronary arteries.
2. Describe the MR techniques and protocols used for imaging coronary arteries.
3. Review the imaging features of common coronary artery anomalies seen in children.
4. Review the limitations of MR imaging of coronary arteries.

Methods & Materials: A retrospective search of PACS was performed on studies performed at the Children's Medical center Dallas for the last 5 years. Cardiac MR Studies for evaluation of coronary arteries were selected, that depicted relevant disease processes. All studies were de-identified prior to image export.

Results: Representative cases of the coronary artery anomalies detected by MR imaging including aneurysms and anomalous origins and courses of coronary arteries were selected for inclusion.

Conclusions: This educational exhibit provides a concise review of MR imaging of coronary arteries in children. The limitations of MR imaging of coronary arteries will also be discussed.

Poster #: EDU-006

Mom, what's my "itis?" A Clinical and Radiologic Review on Pediatric Vasculitides

Grace Mitchell, MD, MBA, *Radiology, Baystate Medical Center, Springfield, MA, grace.mitchell@alumni.tufts.edu;* Stanley Polansky, Tara Catanzano

Purpose or Case Report: - To review the different vasculitides that affect the pediatric population, with clinical and radiologic correlation

- Pathophysiology of small, medium and large-vessel vasculitides will be reviewed
- Clinical presentation and management will be reviewed
- Different imaging findings on various modalities will be reviewed

Methods & Materials: N/A

Results: N/A

Conclusions: Small, medium and large-vessel vasculitides exist in both the pediatric and adult populations. However, some entities are fairly unique to the former group, and an understanding of the pathophysiology, clinical presentation and multi modality imaging findings are essential for the radiologist to aid in optimal patient care.

Poster #: EDU-007

Rapid Spiral Dual Source CT for Imaging Congenital Heart Disease with Technical Considerations

Philip Dydynski, MD, *Kosair Children's Hospital, Louisville, KY, phildydynski@yahoo.com;* Marge Joyce, Sandeep Arora

Purpose or Case Report: The purpose of this presentation is to demonstrate the benefits of rapid spriral aquisition, dual source technique for imaging congenital heart disease (Siemens FLASH 256 slice CT). The reader of this presentation should have a better understanding of the techniques and benefits of dual source CT with regards to imaging congenital heart disease. The main benefits over earlier generation CT machines include decreased radiation dose and rapid scanning which decreases/eliminates the need for sedation in our youngest patients.

Methods & Materials: Multiple case examples will be presented including common indications such as vascular rings, coarctation, coronary artery anomalies, evaluating for branch pulmonary stenosis and evaluating Glenn and Fontan patency status post 3 stage correction. There will be emphasis on demonstrating 3D image reconstruction. Technical considerations needed for a successful study will be reviewed. Such considerations include timing of scanning, size of angiocatheter used depending on the size of the patient and contrast dose. All exams are prospectively gated.

Results: The effective dose (especially in infants) is often less than 1 mSv. The effective dose will be given for all case examples. Dual Source "FLASH" technique allows for rapid, low dose scanning. There is very little (if any) motion artifiact.

Conclusions: Improved image quality related to rapid image aquisition allows us to better help the referring cardiologists

and cardiothoracic surgeons. Basic understanding of the technical aspects is fundamental to a successful exam.

Poster #: EDU-008

Fontan Procedure: What Every Pediatric Radiologist Need to Know - A Pictorial Review

Andrada Popescu, MD, *Ann & Robert H Lurie Children's Hospital of Chicago, Medical Imaging Department, Chicago, IL, andrada.popescu@gmail.com;* Joshua Robinson, Kelly Jarvis, Andrew de Freitas, Carl Backer, Cynthia Rigsby

Purpose or Case Report: To review the imaging characteristics of the Fontan procedure, from initial development, through its numerous historical modifications, to more contemporary approaches and late complications.

Methods & Materials: The Fontan operation is a surgical procedure for complex single ventricle, congenital heart disease (CHD) which involves diverting systemic venous return to the pulmonary arteries, thereby unloading the single ventricle. Initially described in 1971 as a surgical treatment for tricuspid atresia, the Fontan procedure has undergone many variations. More recently it has been used in hypoplastic left heart syndrome and other complex CHD. There are many technical challenges to imaging the Fontan circulation. Pulmonary artery discontinuity, uneven and variable distribution of blood flow from the superior and inferior vena cavae to the pulmonary arteries, development of collateral circulation and presence of implanted devices present unique challenges for choice of imaging modality, method of contrast administration, and exam technique.

Results: We performed a single center, retrospective review of all patients who underwent Fontan palliation or conversion and who had imaging studies, including cardiac CT, MR and /or angiography. Current imaging indications, the staged surgical approach and Fontan complications are reviewed. Imaging challenges and protocols at our institution are presented.

Conclusions: The Fontan procedure is palliative, not curative, but in many cases may result in normal or near-normal growth and development, and good quality of life. As a result, many patients undergo serial imaging exams for operative planning, routine surveillance or clinical deterioration, each with unique technical challenges for the radiologist.

Poster #: EDU-009

The Unlucky Seven: The Radiographic Appearance of Children with Congenital Heart Disease Part 1: Anatomy and Presurgical Appearance

Michael George, MD, *Radiology, Baystate Health, Springfield, MA, mpg2001@gmail.com;* Tara Catanzano

Purpose or Case Report: Children with congenital heart disease (CHD) present a challenge to the pediatric radiologist as their appearance evolves through increasingly complex, multistep surgical procedures that alter anatomic form. Because the primary diagnosis of these anomalies is now often prenatal, the appearance of the post-surgical child may be doubly unfamiliar. This is the first of a two-part multimodal educational exhibit addressing pre- and post-surgical radiographic appearances of children with congenital heart disease. In this part, the "unlucky" seven most common congenital abnormalities with significant radiographic findings will be addressed in terms how their anatomy determines pre-surgical appearance. According to Hoffmann (JACC, 2002), these defects include Coarctation of the Aorta (CoA), Tetrology of Fallot (ToF), Transposition of the Great Arteries (TGA), Hypoplastic Left Heart (HLH), Truncus Arteriosus, Tricuspid Atresia, and Ebstein's Anomaly (EA).

CoA is a congenital stenosis of the aorta typically distal to the subclavian. CXR may demonstrate an abnormal aortic knob contour ("3" sign) and bilateral rib notching.

ToF is marked by four anomalies: VSD, pulmonary stenosis, RH hypertrophy, and overriding aorta. CXR shows pulmonary oligemia. PA concavity and elevated RV hypertrophy produce the classic "boot-shaped heart".

TGA is marked by anatomic switch of the PA and aorta. In dTGA there is ventriculoatrial (VA) discordance, whereas "congenitally corrected" TGA (cTGA) demonstrates both VA and AV discordance. Echo shows parallel great arteries.

HLH represents a spectrum of left heart malformation. CXR typically shows pulmonary edema, cardiomegaly, and thymic regression.

Truncus Arteriosus results in a conjoined aorta and PA. Findings include a right arch (33%), pulmonary edema, and VSD.

In Tricuspid Atresia there is malfunction of the tricuspid resulting in a hypoplastic RV and normal LV. The tricuspid is "platelike" on U/S and fatty on MR.

In EA, tricuspid adherence to the RV creates a "3 segment" right heart. Outflow obstruction and regurgitation leads to massive RA hypertrophy and pulmonary oligemia on CXR.

CHD presents a challenge to the radiologist both before and after surgery. The second part of this exhibit addresses the surgeries, post-surgical appearance, and complications facing these fascinating patients.

Poster #: EDU-010

The Lucky Seven: The Radiographic Appearance of Children with Congenital Cardiac Defects Part 2: Surgeries, Post-Surgical Appearance, and Complications

Michael George, MD, *Radiology, Baystate Health, Springfield, MA, mpg2001@gmail.com;* Tara Catanzano

Purpose or Case Report: Children with congenital heart disease (CHD) present a challenge to the pediatric radiologist as their appearance evolves through increasingly complex, multistep surgical procedures that alter anatomic form. This is the second of a two-part multimodal educational exhibit addressing the pre- and post-surgical radiographic appearances of children with CHD. In the first part, congenital anatomy and imaging was described for the seven most common forms of radiographically significant CHD. This second part will describe the surgeries, post-surgical appearance, and potential complications.

CoA repair may be performed in one of three ways: stenosis resection, subclavian flap, and synthetic patch. MR may identify post-operative aneurysm, restenosis, hematoma, or fistula.

ToF repair may be palliative or curative. Total repair involves VSD closure and RVOT cannulation. Palliative shunts, such as the Blalock-Taussig, are reserved for unstable infants. Complications of shunting include seroma and thrombosis.

Initially treated with a Mustard or Senning baffles, full anatomic repair with a Jatene is now typically performed for TGA. CXR shows dilatation of the neo-aortic root and widening of a previously narrow mediastinum.

HLH was previously a universally fatal condition now corrected with a multistage Norwood performed in conjunction with bidirectional cavopulmonary shunt and a modified Fontan. Complications include hepatomegaly, pleural and pericardial effusions.

Tricuspid Atresia is treated with a Birectional Glenn shunt in conjunction with either a lateral Fontan vs. extracardiac conduit Fontan. Complications include pulmonary AVM, right atrial overload, tunnel thrombosis, and anastomatic stenosis.

Truncus repair is performed with a modified Rastelli in which the PAs are seperated from the aorta and a valved homograft is placed from the right ventricle to the PA.

Ebstein's is now typically treated with valve reconstruction.

In conclusion, CHD presents a fascinating challenge to the pediatric radiologist both pre- and post-surgically. An appreciation of the initial anatomy, surgical alterations, and potential complications is critical to understanding this fascinating new population as it approaches adulthood.

Poster #: EDU-011

Congenital Anomalies of the Hand

Pamela Deaver, MD, *Brigham & Women's Hospital / Harvard Medical School, Boston, MA, pamela.deaver@gmail.com;* Judy Estroff

Purpose or Case Report: Congenital anomalies of the hand may be isolated or may occur as part of a syndrome. Recognizing these anomalies prenatally may have prognostic implications for expectant families and allows for advanced prenatal surgical planning when appropriate. Our purpose is to review syndromic and isolated examples of congenital hand anomalies with an emphasis on detection, nomenclature, associated prenatal radiological findings, and surgical treatment.

Methods & Materials: Approximately 5 years of cases of isolated and syndromic congenital hand anomalies from Boston Children's Hospital Advanced Fetal Care Center were reviewed. Representative examples with prenatal ultrasound and/or MRI were selected to illustrate the spectrum of prenatal findings in patients with congenital hand anomalies. Post-natal imaging for some patients was available, and radiographs before and after surgical correction of hand anomalies were obtained and reviewed.

Results: Congenital hand anomalies can be an important herald of fetal syndromes affecting the neonatal prognosis and surgical plan. Likewise, isolated anomalies may have a different etiology, prognosis, and treatment. Recognizing the radiological appearance of fetal hand anomalies as well as pre and postsurgical radiographic appearance of corrected hand anomalies is important for aiding our clinical colleagues with both diagnostic and prognostic information.

Conclusions: For many reasons, congenital hand anomalies are underdiagnosed prenatally, and improved understanding of both isolated and syndromic anomalies may positively affect the neonatal surgical plan.

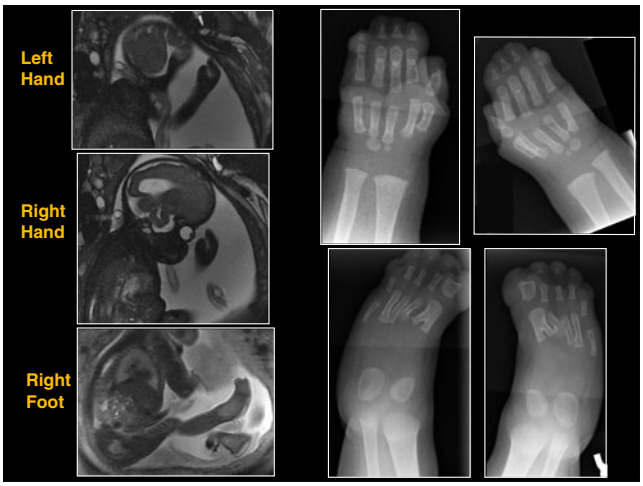

Poster #: EDU-012

Prenatal Ultrasound and MRI Imaging Features of Trisomy 18

Akosua Sintim-Damoa, MD, *Children's National Medical Center, Washington, D.C., DC, asdamoa@cnmc.org;* Eva Rubio, MD, Dorothy Bulas, Anna Blask, Rhonda Schonberg

Purpose or Case Report: To review sonographic and MRI prenatal findings and patterns in cases of Trisomy 18.

Methods & Materials: The imaging findings of seven fetuses with confirmed Trisomy 18 were reviewed. All seven had prenatal ultrasounds performed between 13 to 36 weeks 5 days gestation. Five also had fetal MRI performed on the same day (GA 19 weeks 5 days to 36 weeks 5 days) Anomalies were categorized into general, craniofacial, central nervous system, thoracic, cardiovascular, skeletal, gastrointestinal, and genitourinary defects.

Results: Table 1 lists findings made by US and MRI while Table 2 lists findings by organ system. Findings were variable, and several patients had multiple anomalies. The most common US findings included choroid plexus cyst (4/7), abnormal extremities (4/7) (club foot/wrist, rockerbottom foot, radial ray anomaly), polyhydramnios (3/7), IUGR (2/7). The most common MRI findings included CNS anomalies (4/5) (microcephaly, delayed opercular radiation, hypotelorism, pontocerebellar hypoplasia, posterior fossa cyst, cephalocele, low-lying spinal conus), abnormal extremities (3/5) (club foot, club wrist, radial ray anomaly, rockerbottom feet), and polyhydramnios (2/5). Choroid plexus cysts and cardiac anomalies were best seen by US. MRI was superior for the evaluation of CNS anomalies (pontocerebellar hypoplasia, small vermis, low lying conus). Extremity anomalies were visible both by US and MRI, although better seen by ultrasound.

Conclusions: Prenatal diagnosis of Trisomy 18 can be difficult due to manifold multisystemic abnormalities. A head to toe approach by US and MRI is important in analyzing the multiple potential anomalies that can be associated with Trisomy 18. Fetal MRI serves as an adjunct to US by providing increased detection and definition of CNS anomalies. Given an absence of clear patterns, the presence of 3 or more apparently unrelated anomalies in a fetus may prompt consideration of Trisomy 18.

Table 1 – US and MRI Findings (US *N*=7; MRI *N*=5)

	US	MRI
Polyhydramnios	3	2
Oligohydramnios	1	0
Symmetric IUGR	2	N/A
Single umbilical artery	1	0
Absent umbilical artery diastolic flow	1	N/A
Chorioamniotic separation	2	1
Abnormal calvarial contour	1	N/A
Micrognathia	1	1
Small nasal bone	1	N/A
Nuchal thickening	1	N/A
Microcephaly	N/A	1
Delayed opercular radiation	N/A	1
Prominent sylvian fissure	N/A	1
Pontocerebellar hypoplasia	N/A	1
Choroid plexus cyst	4	0
Hypotelorism	1	1
Posterior fossa cyst	1	1
Hypoplastic vermis	1	1
Mega cisterna magna	1	1
Cephalocele	1	1
Low-lying spinal cord conus	N/A	1
Tetrology of Fallot	1	N/A
AV Canal	1	N/A
DORV	1	N/A
VSD	1	N/A
Clubbed wrist	1	1
Radial ray anomaly	1	1
Rockerbottom feet	1	1
Clubfoot	2	2
Small stomach	2	2
Small abdominal circumference	2	N/A
Tracheoesophageal fistula	1	1
Omphalocele	1	1
Posterior urethral valves	1	1
Cystic kidneys	1	1

Table 2 – Findings by Organ System (US *N*=7; MRI *N*=5)

	Ultrasound	MRI
General	6	3
Craniofacial	4	2
Central Nervous System	4	4
Cardiac	3	1
Skeletal	4	3
Gastrointestinal	3	2
Genitourinary	1	1

Poster #: EDU-013

Perinatal Imaging and Correlations of the Chest and Abdomen. A Case Based Approach

Brandi Lanier, MD, *Baptist Memorial Hospital, Memphis, TN, brandilanier@gmail.com;* Anand Raju, Harris Cohen

Purpose or Case Report: Using a case based approach, we review various fetal abnormalities noted antenatally by Ultrasound (US) and Magnetic Resonance (MR) Imaging and their postnatal analyses using plain film, CT, US and MR. We sought to review the helpfulness of our imaging in providing adequate information for our surgeons, maternal fetal medicine clinicians and neonatologists. We sought to highlight how helpful the routine US and the addition of MR were in obtaining a correct perinatal diagnosis of congenital and acquired thoracic and abdominal abnormalities.

Methods & Materials: Cases will be shown of normal and abnormal anatomic findings in fetal chest and abdominal imaging. Key teaching points necessary for the diagnosis and differential diagnostic considerations of such anomalies as congenital diaphragmatic hernia, congenital cystic adenomatoid malformation, pulmonary sequestration, omphalocele, gastroschisis, ruptured omphalocele, duodenal atresia, jejunal atresia, bowel malrotation, multicystic dysplastic kidney, cystic renal dysplasia, recessive polycystic kidney disease, and posterior urethral valves will be discussed.
Results: US and MR have helped the antenatal identification of anomalies of the chest and abdomen proven postnatally.
Conclusions: Correlations across the life "border" of birth help both antenatal and postnatal analyses for maternal fetal medicine, neonatal clinicians and surgeons.

Poster #: EDU-014

Meconium in fetal and perinatal imaging: Associations and clinical significance

Amy White, MD, *Lucile Packard Children's Hospital, Palo Alto, CA, amywhite@stanford.edu;* Beverley Newman, Erika Rubesova

Purpose or Case Report: An abnormal location, distribution, volume or appearance of meconium is associated with a spectrum of bowel abnormalities including atresia, obstruction, perforation, fistula, aganglionosis, immaturity and absorptive dysfunction. This exhibit will review the fetal and perinatal imaging of these entities, their differential diagnoses, clinical significance and appropriate work-up.
Methods & Materials: Review of a series of infants with pre- and/or postnatal meconium abnormalities on imaging.
Results: Prenatal ultrasound (US) and MR imaging, and postnatal radiographs, US, contrast enema and occasionally CT or MR, all may have a role in evaluating an abnormal appearance or distribution of meconium along with other associated features such as abnormal bowel caliber, obstruction, atresia or calcifications. Water soluble contrast enema(s) frequently are also successful therapeutically for meconium ileus, small left colon and meconium plug syndrome. Visualization of prominent colonic meconium plugs on contrast enema is a nonspecific finding accompanying many conditions including meconium ileus, Hirschsprung's disease, small left colon syndrome, meconium plug syndrome and even small bowel atresia. Inspissated meconium in the distal small bowel with a "soap bubble" appearance and absent air fluid levels is a more specific finding suggestive of meconium ileus. Meconium peritonitis is associated with in utero bowel perforation. The resultant extravasated intraperitoneal meconium can calcify rapidly with an imaging appearance ranging from focal or widespread peritoneal surface calcifications to a loculated partially calcified meconium pseudocyst. Etiologies include bowel ischemia/necrosis and obstruction, with meconium ileus as the most common underlying cause. Calcified intraluminal meconium is an unusual entity with a distinctive appearance of rounded pebble-like concretions along the course of the colon. Recognition of this finding suggests the presence of imperforate anus in a male with a rectourethral fistula. Less common causes include Hirschprung's disease and bowel obstruction or atresia.
Conclusions: This exhibit provides a pictorial review of the spectrum of bowel anomalies associated with abnormal meconium. An understanding of the patterns of abnormality and significance of imaging findings helps generate the most likely differential diagnoses and guides appropriate imaging and clinical management.

Poster #: EDU-015

MR Imaging in Fetal abdominal and pelvic pathologies: It is NOT just pretty Images!

Munire Gundogan, *Radiology Dep, IWK Health Center, Halifax, NS, Canada, mgundogan04@hotmail.com*

Purpose or Case Report: MRI is becoming an increasingly important modality in the evaluation of sonographically complex or occult anomalies. Ultrasound is the primary imaging modality for fetal imaging. However it's small FOV, operator dependent nature, limited acoustic contrast by adipose tissue in large patients and poor visibility in the presence of oligo -hydroamnios makes MR imaging is more valuable in fetal assessment.
Methods & Materials: We will demonstrate a variety of abdominal and pelvic pathologies in this poster in a pictorial essay fashion to get radiologist to be more familiar with MR imaging characteristics in fetal abdominal and pelvic pathologies. We aim to demonstrate MR imaging features of cystic or solid intraabdominal and pelvic masses, congenital genitourinary and gastrointestinal anomalies, anterior abdominal wall defects, suspected fetal hematological and metabolic conditions in this poster.
Conclusions: MRI's role in fetal abdominal imaging includes confirming or excluding possible lesions, defining their full extent, aiding in their characterization, and demonstrating associated abnormalities. Prenatal awareness of an anomaly ensures better management of the pregnant patient, enables medical teams and parents to prepare for the delivery, and postnatal care. Therefore it is important to get familiar with the MR imaging findings.

Poster #: EDU-016

Limitations and Advantages of Ultrasound in Evaluating Necrotizing Enterocolitis

Fred Dawson, *Riley Hospital for Children, Indianapolis, IN, fdawson@iupui.edu;* Boaz Karmazyn, MD

Purpose or Case Report: Demonstrate by case series the normal ultrasound (US) anatomy of the bowel and various intra- and extra-intestinal pathologies that can be detected in necrotizing enterocolitis (NEC). We will also demonstrate advantages and limitations of US as compared to plain radiography.

Methods & Materials: From the radiology information system, we identified all patients examined by ultrasound for the evaluation of NEC. The medical records were then reviewed for treatment decisions (supportive versus surgical), clinical outcomes, and pathology reports when available.

Results: We selected representative cases showing normal US anatomy of the bowel, bowel wall thickening, increased bowel echogenicity, changes in vascularity, pneumatosis, portal venous gas, loculated peritoneal fluid, liver abscess and pneumoperitoneum. These were correlated with plain radiograph findings. US was most useful when there was a paucity or absence of bowel gas and was limited when there were multiple gas distended bowel loops. In three cases, US demonstrated pneumoperitoneum that was missed on lateral decubitus radiographs.

Conclusions: US has the advantage of direct visualization of the bowel wall and peritoneal fluid collections not seen on radiographs and has increased sensitivity for portal venous gas and minute pneumoperitoneum. Our experience shows that in selected cases, US has a role in evaluation for NEC and is most useful when there is a paucity or absence of bowel gas on plain radiographs.

Poster #: EDU-017

MR Enterography – Beyond Crohn Disease

Daniel Glazer, MD, *C.S. Mott Children's Hospital, University of Michigan, Department of Radiology, Section of Pediatric Radiology, Ann Arbor, MI, glazerd@med.umich.edu;* Jonathan Dillman, Ethan Smith

Purpose or Case Report: MR enterography (MRE) is increasingly used to diagnose and follow-up pediatric Crohn disease. We regularly encounter alternative diagnoses when interpreting these exams in the setting of suspected Crohn disease. Additionally, we commonly use MRE to diagnose and/or characterize a variety of non-Crohn disease conditions affecting the small and large bowel. The purpose of this educational exhibit is to illustrate the MRE appearances of numerous non-Crohn disease abnormalities affecting the bowel in children and adolescents.

Methods & Materials: Following institutional review board approval and in a HIPAA-compliant manner, we searched institutional Department of Radiology electronic medical records to identify all pediatric (≤18 years of age) MRE examinations. Imaging reports were then reviewed to identify abnormal studies with non-Crohn disease diagnoses. Important images from identified cases were then chosen, anonymized, and will be presented. Relevant electronic medical records were reviewed, with pertinent clinical data documented.

Results: We will present the pediatric MRE appearances of colitis (e.g., ulcerative and infectious), bowel obstruction (e.g., midgut volvulus and SMA syndrome), polyps/masses (e.g., Peutz-Jegher hamartomatous polyps, juvenile polyp of the colon, and adenocarcinoma of the colon), and other inflammatory abnormalities (e.g., omental infarction, Meckel diverticulitis, and appendicitis). Pertinent correlative clinical data, including surgical and histopathologic findings, will be presented when available.

Conclusions: Numerous non-Crohn disease conditions can be successfully diagnosed and/or characterized in a nonionizing manner using MRE in children and adolescents.

Poster #: EDU-018

Plumbing Made Easy: Imaging Findings in Unusual Congenital Anomalies of the Colon

Anita Mehta, MD, *Montefiore Medical Center, New York, NY, anita.mehta5@gmail.com;* Terry Levin, Seong Oh

Purpose or Case Report: The imaging findings in a variety of congenital anomalies of the colon are presented and the embryologic development of the colon is reviewed.

Methods & Materials: Clinical presentation, imaging and surgical findings in newborns with congenital colonic anomalies are retrospectively reviewed. Each entity is correlated with embryologic development of the colon.

Results: Radiographic and fluoroscopic imaging in five cases are discussed including colonic atresia, colonic duplication, total colonic aganglionosis, cloacal exstrophy, and megacystic microcolon. In all patients plain radiographs demonstrate functional or mechanical obstruction. Contrast enema further elucidates the diagnosis with subsequent surgical confirmation.

Conclusions: Congenital anomalies of the colon are uncommon. The complex embryologic development of the colon may lead to unusual anomalies. Characteristic findings on plain film and contrast enema lead to diagnosis and guide in surgical planning.

Poster #: EDU-019

An Unforgettable Journey through the diseases of the "Forgotten organ": The Spleen

Rama Ayyala, *Radiology, New York Presbyterian Hospital-Columbia, New York, NY, rsa9006@nyp.org;* Michael Gee, Manish Dhyani, Nancy Chauvin, MD, Victor Ho, Sudha Anupindi

Purpose or Case Report: The spleen is often referred to as the forgotten organ, despite its important role in the immune system. With exception of infection and metastases, solitary focal lesions of the spleen are rare, tend to be overlooked and are often found incidentally. Given the diverse pathologies that can involve the spleen, it can be challenging for radiologists to interpret imaging studies. The management of these lesions can pose a diagnostic dilemma and the potential complications related to splenic biopsy or splenectomy require the radiologist to provide a meaningful differential and appropriate pathway of work-up. The purpose of this exhibit is to illustrate the common and uncommon diseases of the spleen in children using a multi-modality approach with emphasis on US, MRI and PET-CT and propose a potential imaging algorithm for the work-up of these lesions in children.

Methods & Materials: A retrospective review of imaging studies was performed to identify non-traumatic splenic lesions in patients 2–25 years of age. We will discuss the normal development, variants and pathophysiology of the spleen. This will be followed by cases illustrating the diverse range of pathologies that can involve the spleen including: congenital, infectious, inflammatory, vascular, and malignant. In addition we will discuss the current role of MRI and PET imaging in the assessment of these diseases.

Results: Most common abnormality of the spleen is splenomegaly and the most common focal mass is the splenic cyst. Congenital lesions such as the wandering spleen are important to recognize early to avoid devastating consequences. We illustrate the imaging features of benign lesions ranging from hemangiomas, hamartomas, lymphangiomatosis, infections to more rare entities such as SANT (Sclerosing angiomatoid nodular transformation). Common malignancies such as lymphoma and less well known sarcomas and epithelioid hemangioendothelioma will be highlighted.

Conclusions: The discovery of incidental splenic lesions is a common occurrence and familiarity with the appearance of common and uncommon non-traumatic splenic lesions is essential to avoid unnecessary procedures. Because most of the lesions in our young population are benign, our proposed algorithm emphasizes the use of US and then contrast-enhanced MRI for definitive diagnosis and follow-up.

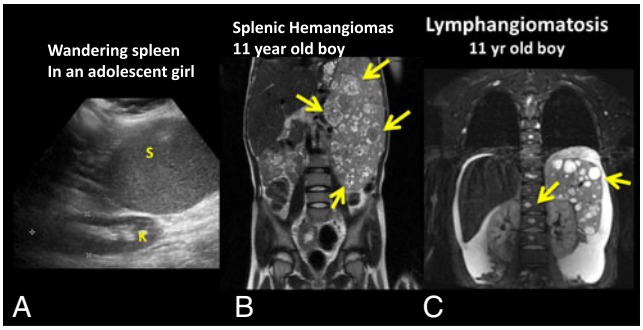

Poster #: EDU-020

MR Enterography of Crohn's disease related abscesses in young patients: pearls and pitfalls

Brian Pugmire, MD, *Radiology, Massachusetts General Hospital, Boston, MA, bpugmire@partners.org;* Katherine Nimkin, Michael Gee

Purpose or Case Report: Magnetic resonance enterography (MRE) is fast becoming a primary imaging modality in the evaluation of inflammatory bowel disease (IBD) given its lack of ionizing radiation and accuracy in the detection of IBD related pathology. Abscesses associated with Crohn's disease (CD) play an extremely important role in clinical management, as their presence typically is a contraindication to immunosuppressive or biologic therapy. Despite the excellent reported performance of MRE in imaging extraluminal CD pathology, CD related abscesses (CDRAs) can be very difficult to detect using this modality, especially in young patients. As more MRE examinations are performed for pediatric IBD, it is critical for radiologists to accurately detect and characterize CDRAs.

Methods & Materials: This exhibit will entail a focused review of the literature regarding extraluminal pathology in CD, specifically as it pertains to CDRAs and their characterization with MRE. It will also involve a review of illustrative clinical cases seen at our institution.

Results: In this exhibit, we will: 1. briefly discuss the role of MRE in evaluating patients with IBD with a particular emphasis on the clinical significance of CDRAs; 2. discuss the characteristic imaging findings of CDRAs on MRE; 3. describe the pitfalls that frequently make detection and assessment of CDRAs difficult including the location of the collection, the signal characteristics of the abscess fluid, similarities in appearance to adjacent inflamed bowel, and inability to appreciate foci of extraluminal air; 4. illustrate these points with instructive cases where such collections were and were not initially detected on MRE; 5. discuss

techniques to avoid missing CDRAs including which MRE sequences may best demonstrate CDRAs, suggestions for differentiating CDRAs from inflamed bowel, and other imaging signs that may suggest the presence of CDRAs; 6. discuss the use of other imaging modalities such as computed tomography with positive oral contrast or barium fluoroscopic examinations to assist in the diagnostic evaluation of difficult cases.

Conclusions: CDRAs are very important to identify on MRE, but are frequently difficult to detect and assess with this modality. Viewers of this exhibit will gain improved confidence in this essential aspect of MRE interpretation.

Poster #: EDU-021

Focal Liver Lesions in the Pediatric Patient: A Multimodality Pictorial Review with Pathologic Correlation

Lindsay Fox, *Baystate Medical Center, Springfield, MA, lindsay.fox83@gmail.com;* Jane An, Joseph Rozell, Tara Catanzano, David Gang, Stanley Polansky

Purpose or Case Report: 1. Review of the relevant liver anatomy.

2. Describe the CT, MR, and ultrasound characteristics of benign and malignant focal liver lesions in infants and children with pathology correlation.

3. Cases will be presented to illustrate imaging features of a broad array of disease entities including cystic cavernous hemangioma, focal nodular hyperplasia, hepatoblastoma, abscess and hydatid cyst. Relevant epidemiology, pathogenesis and clinical features will be discussed.

Methods & Materials: N/A

Results: N/A

Conclusions: A knowledge and understanding of the various focal liver diseases affecting the pediatric patient will aid the radiologist in making appropriate and timely diagnoses. At the end of this presentation, the viewer should be familiar with the characteristic clinical, imaging and pathologic features, epidemiology and pathogenesis of a variety of focal liver lesions in the pediatric population.

Poster #: EDU-022

Crohn Disease of the Perineum - Review of MRI Findings

Matthew Hammer, MD, *University of Michigan, Ann Arbor, MI, hammerm@med.umich.edu;* Jonathan Dillman, MD, Ethan Smith, MD, Peter Strouse

Purpose or Case Report: Crohn disease (CD) is a chronic granulomatous inflammatory condition affecting the gastrointestinal (GI) tract and on occasion extraintestinal structures. Up to 50% of pediatric patients experience perineal (including perianal) manifestations of CD, which sometimes precede GI tract symptoms. MR enterography and dedicated perineal MRI can be used to identify the presence and characterize the extent and complexity of perineal CD as well as guide medical and surgical management. The purpose of this educational exhibit is to illustrate the MRI appearances of common and uncommon manifestations of pediatric Crohn disease involving the perineum.

Methods & Materials: Following Institutional Review Board approval and in a HIPAA-compliant manner, we searched Department of Radiology electronic medical records to identify all pediatric (<20 years of age) MRI examinations of the perineum performed on patients with CD. MRI logbooks were also reviewed to identify pertinent imaging studies. Imaging reports and relevant electronic medical records then were reviewed by a single radiologist to identify abnormal MRI examinations. Anonymized images illustrating common and uncommon manifestations of pediatric CD involving the perineum (including perianal, vulvar, and scrotal regions) were collected and related clinical data were recorded.

Results: We will present an MRI-based review of the normal perineal anatomy. The MRI appearances of CD-related cutaneous involvement, perianal fistulae (including intersphincteric, transsphincteric, and suprasphincteric), and perianal abscesses will be illustrated. Fistula tracts and abscesses involving the perineal body, scrotum in boys, and vulva in girls will also be presented. Pertinent correlative clinical data, including physical exam and histopathologic findings, will be presented when available.

Conclusions: MRI of the perineum can clearly define numerous extraintestinal manifestations of Crohn disease as well as guide medical and surgical management in the pediatric population.

Poster #: EDU-023

Gastrojejunostomy Tubes in the Pediatric Population: Risks and Common Complications

Brad Jenkins, Radiologic Technologist, *Diagnostic Imaging and Radiology, Children's National Medical Center, Washington, DC, bjenkinsrtr@gmail.com;* Eva Rubio, MD, Raymond Sze

Purpose or Case Report: Gastrojejunostomy (GJ) tubes are an increasingly utilized device for nutritional support. Indications include severe reflux disease, neurologic impairment, cardiac disease, complex genetic syndromes, severe respiratory disease, and patients with complex medical or surgical GI disease. Advanced techniques for placement with improved safety profile have contributed to the

frequency of placement. The purpose of this study is to provide education on the imaging signs of common GJ tube complications.

Methods & Materials: IRB approval was obtained for review and compilation of selected radiographic, CT, and ultrasound studies. Search terms "gastrojejunostomy", "displaced", "coiled", "GJ", "complication", "perforation", "obstruction", "intussusception", and "volvulus" were used to identify individual cases. These cases were provided with a randomized study ID number so as to maintain patient confidentiality and the cases were viewed on PACS software via medical record number (MRN). The images and report were reviewed. Finally, in cases where the images appeared to depict a tube complication (operative or other), clinical notes were reviewed. Names, MRN, and other personal health infomation (PHI) of the cases were not retained after case number assignment. The information collected includes de-identified images, report descriptions, and clinical presentations and outcomes. All eligible cases were included regardless of race or gender. The randomized study ID number ("Case #") was not linked to any PHI.

Results: The risks and common complications of GJ tube placement include total migration of tube into the gastric lumen, migration of the tube into the esophagus, balloon encrustation by enteral feeds, balloon inflation within the duodenum or stoma tract, volvulus, small bowel intussusception, bowel tenting, perforation, placement of GJ instead of G-tube, and over-advancement of conventional GJ tube. Patients with GJ tube complications may present with increased fluid output on gastric venting, vomiting, abdominal pain, feeding intolerance, and abdominal distention.

Conclusions: Due to the potential risk for adverse patient conditions associated with GJ tube placement complications, it is vital that the spectrum of imaging presentations can be readily identified to prevent avoidable patient morbidity and mortality.

Poster #: EDU-024

Test Your Skills: Appendicitis or Not, By Ultrasound

Kiery Braithwaite, *Radiology, Emory University/Children's Healthcare of Atlanta, Atlanta, GA, kiery.braithwaite@choa.org;* Adina Alazraki, MD

Purpose or Case Report: There has been a recent resurgence in the use of ultrasound as a diagnostic tool in children presenting with abdominal pain. Sonography for the diagnosis or exclusion of appendicitis in children is a frequent request from many emergency departments. Although some cases are straight forward, others can be challenging. The purpose of this educational presentation is to test and enhance the interpreter's confidence in making the diagnosis of appendicitis in children utilizing ultrasound.

Methods & Materials: We briefly review the common sonographic features of appendicitis. A series of 20 illustrative examples will be presented in an unknown case format. Cases will include examples of acute appendicitis, subacute appendicitis, and normal appendices. Some equivocal cases will include subsequent computed tomography imaging. All cases include clinical history, including age and documented symptoms, as well as relevant laboratory results when available, including CRP and WBC.

Results: Twenty patients will be presented as unknowns for the viewer to test themselves. Cases of appendicitis were confirmed surgically and pathologically. The patients without pathologic confirmation improved symptomatically and did not return for treatment after discharge within a 2 week time period.

Conclusions: By reviewing these cases, the interpreter will improve their diagnostic acumen for appendicitis by ultrasound in an interactive format.

Poster #: EDU-025

A Practice Model for the Air Reduction of Intussusception

Peter Assaad, MD MPH, *Children's Hospital Los Angeles, Los Angeles, CA, peter.s.assaad@gmail.com;* Paul Iskander, MD

Purpose or Case Report: Intussusception reduction is a procedure that, while familiar to the pediatric radiologist, remains a cause for consternation for the average radiology resident. A recent survey of residency programs nationwide shows that 46.4% of radiology residents had no experience performing an intussusception reduction; an an additional 34% had only performed one or two reductions. The success rate of intussusception reduction is related to operator experience and the total number of prior cases performed by the radiologist or radiology resident. Residents in this survey expressed a desire for computer based simulation training as a way to help them prepare for this procedure.

We present a novel method of simulation training for intussusception reduction which involves an actual apparatus which can be visualized under fluoroscopy, similar to mannequins used by internal medicine and anesthesiology residents for the practice of procedures e.g. intubation and central venous catheter placement.

The practice model we have developed remains in its infancy. The model has a simulated rectum that residents can practice catheterizing using either a pediatric rectal tube or Foley catheter and balloon. Air reduction tubing and a manometer can then be connected and the model visualized under fluoroscopy. Trainees can then practice a simulated reduction of an intususception under video fluoroscopy as air pressure increases.

Future plans involve modifying the plastic tubing to appear more similar to colonic loops and fitting the apparatus into a child sized mannequin. Additional plans include the simulation of small bowel loops that fill with air once the intussusception has been reduced in order to provide accurate visual confirmation of a successful reduction.
Methods & Materials: Using readily available items from a local hardware store, a model for intussusception reduction was created utilizing bicycle tire tubing, a plastic container, metallic spray paint, spray adhesive, and various sized plastic and metallic occlusive balls.
Results: Air intussusception reduction was attempted under real time fluoroscopy utilizing different sized plastic and metallic balls to achieve adequate occlusion and simulate an intussusception.
Conclusions: A successful model was created enabling the user to practice air reduction via real time fluoroscopy.

Poster #: EDU-026

Multimodality imaging of gastrointestinal pediatric surgical emergencies: What residents need to know for call

Kevin Ching, MD, *University of Pittsburgh Medical Center, Pittsburgh, PA, chingk@upmc.edu;* Sameh Tadros

Purpose or Case Report: Abdominal pain in children leads to frequent visits to the emergency department and subsequent imaging studies. History and physical exam are often non-specific increasing the importance of a quick and accurate radiologic diagnosis. The aim of this educational exhibit is to review the imaging spectrum of non-traumatic pediatric surgical emergencies.
Methods & Materials: Cases from a busy tertiary care children's hospital were reviewed for image quality, modality, and presentation of radiographic findings. Electronic medical records were reviewed for operative findings and pathologic reports.
Results: Disease processes will include but are not limited to malrotation, volvulus, appendicitis, hypertrophic pyloric stenosis, intussusception, Meckel's diverticulum, inflammatory bowel disease, bowel obstruction, and intra-abdominal abscess. This exhibit will review the clinical presentation and pathophysiology of each diagnosis. Key examples will be shown on multiple imaging modalities including radiography, fluoroscopy, ultrasound, nuclear medicine, computed tomography, and magnetic resonance imaging.
Conclusions: Early recognition of pediatric abdominal emergencies is critical for all radiologists and especially junior residents beginning to take call. Following a brief multi-modality imaging review of pediatric abdominal pain, the reader will be better equipped to diagnose gastrointestinal surgical emergencies in the pediatric population.

Poster #: EDU-027

Improving the performance of appendix ultrasound examinations: The step-by-step process undertaken at a dedicated pediatric healthcare facility

Jeannie Kwon, MD, *University of Texas Southwestern Medical Center, Dallas, TX, kwonjk@gmail.com;* Li Ern Chen

Purpose or Case Report: This project was undertaken to improve the performance of appendix ultrasound, a highly operator-dependent examination with variable performance reported in the literature. This effort was done in conjunction with the development and implementation of an institution-wide Acute Appendicitis Clinical Pathway at our free-standing children's hospital. The pathway prescribes the clinical calculation of the Pediatric Appendicitis Score (PAS) to direct imaging work-up, with only patients of pre-test intermediate probability undergoing ultrasound as the first line-examination. This drives the need for better appendix ultrasound performance via standardization of technique. The improvement process addresses the multidimensional aspects of technologist performance, image interpretation, and radiologist reporting.
Methods & Materials: Input from institutional surgeons and emergency department physicians, as well as informal review of appendix ultrasound images and reports, were usedto identify specific areas for improvement. Published literature and the experience of seasoned radiologists and ultrasound technologists were used as resources for improving scan performance technique and image interpretation and reporting.
Results: A formal, directed imaging protocol, and an informal "how-to" document with practical tips for sonographers were created. Technologist education, consisting of classroom and hands-on training, over-scanning by a more senior technologist (and attending radiologist when feasible), completion of an exam findings worksheet and case log recording were implemented. A structured radiology report was developed to provide greater detail and uniformity in reporting and interpreting findings. Consistency in content and style of appendix ultrasound reports contribute to better informed decision-making by referring clinicians.
Conclusions: Multi-departmental and intra-departmental input led to specific interventions that improved the quality of performance, interpretation, and reporting of appendix ultrasound examinations.

Poster #: EDU-028

Appearance and follow-up of cystic ovarian lesions in the post-menarchal teenager: What the pediatric radiologist should know

Bradley Saylors, *Radiology and Radiological Sciences, Medical University of South Carolina, Charleston, SC, ;* Paul Thacker, MD

Purpose or Case Report: Cystic ovarian lesions are a relatively common finding in the post-menarchal teenager. However, little has been discussed in the pediatric radiology literature as pertaining to the classic sonographic appearance, size criteria, and follow-up of these lesions. This relative lack of discussion has led to confusion among pediatric radiologists about the underlying etiology of these lesions, the appropriate reporting terminology to be used, and what follow-up if any should be recommended. This confusion often translates into unnecessary or too frequent follow-up leading to increased patient and parental anxiety for their child's "ovarian cyst". The purpose of this educational exhibit is to provide the classic imaging characteristics of commonly found cystic ovarian lesions, size criteria for reporting, and suggestions for follow-up based on the Consensus Conference Statement from the Society of Radiologists in Ultrasound. The exhibit will include an interactive discussion of each lesion whereby the reviewer will be asked to select the most likely etiology as well as select the appropriate follow-up.

Poster #: EDU-029

Beyond Wilms tumor- Revisiting pediatric renal masses: radiologic-pathologic correlation

Beyond Wilms tumor- Revisiting pediatric renal masses: radiologic-pathologic correlation

Sumit Pruthi, *Monroe Carell Jr. Children's Hospital at Vanderbilt, Nashville, TN, sumit.pruthi@vanderbilt.edu;* Renee Bonetti, Mariana Cajaiba, Marta Schulman

Purpose or Case Report: Although Wilms tumor is most familiar to pediatric radiologists, pediatric renal masses present a spectrum that encompasses lesions with benign behavior as well as lesions that are highly malignant, with dismal prognosis. Despite the fact that many of these lesions are rare, they do occur and it is incumbent on the pediatric radiologist to be familiar with their clinical presentation, imaging findings, diagnostic approach, gross and microscopic pathologic correlates, and appropriate monitoring during therapy. This review will enhance the pediatric radiologist's understanding of these lesions and our ability to provide thoughtful and accurate diagnosis for our patients.

Methods & Materials: Describe the types of renal tumors that occur in the pediatric population, relating incidence, age at presentation, imaging characteristics and the role of emerging imaging technologies, such as MR Diffusion, Diffusion Tensor Imaging (DTI), MR Urography and FDG-PET, in the identifying key diagnostic features correlated to the anatomic, radiologic and histopathologic abnormalities.

The tumors described will include Wilms tumor, nephroblastomatosis, renal cell carcinoma, spectrum of mesoblastic nephroma, multilocular cystic renal tumor, clear cell sarcoma, rhabdoid tumor, angiomyolipoma, renal medullary carcinoma, ossifying renal tumor of infancy, metanephric adenoma, and infiltrative neoplasms of extrarenal origin, such as lymphoma and leukemia.

Conclusions: This education exhibit will identify differential diagnosis as well as diagnostic features of pediatric renal tumors, utility of emerging technologies and gross and histopathologic correlation with the imaging findings.

Poster #: EDU-030

The spectrum of imaging and pathology of renal cysts in children

Alex Tawadros, *Indiana University School of Medicine, Indianapolis, IN, atawadro@iupui.edu;* Lisa Delaney, Rong Fan, Martin Kaefer, Boaz Karmazyn, MD

Purpose or Case Report: To demonstrate the ultrasound (US) appearance of a variety of renal cysts in children with pathologic correlation.

Methods & Materials: From the radiology information system, we retrieved all reports of renal ultrasounds with solitary renal cystic lesions. The patients' charts were then reviewed for underlying medical conditions, clinical presentation, treatment, other imaging studies, and pathology when available.

Results: A solitary renal cyst can represent a variety of pathology including simple benign epithelial cyst, calyceal diverticulum, multilocular cystic nephroma, upper pole glomerulocystic renal disease, and renal abscess. Mimics of cystic renal lesions included urinoma, retroperitoneal lymphangioma, nephrogenic rest, and kidney malrotation with a large extrarenal pelvis. We did not have a case of renal malignancy presenting as a solitary renal cyst.

Conclusions: Solitary renal cystic lesions commonly represent benign cysts and calyceal diverticuli and uncommonly represent a variety of other pathologies, but malignancy is rare.

Poster #: EDU-031

Additional imaging of upper abdominal organs on first time renal sonograms. Is it of value?

Sandra Machado, *Loma Linda University Children's Hospital, Loma Linda, CA, smachado@llu.edu;* Beverly Wood

Purpose or Case Report: Renal sonography is one of the most commonly performed studies in children of all ages, for

many different reasons. Renal ultrasound protocol includes imaging of the kidneys and urinary bladder, however at our institution, imaging of the liver, gallbladder and spleen is included when the child is evaluated for the first time. The purpose of this study is to evaluate the worth of additional imaging by evaluating the rate and pertinence of abnormal findings in the additionally evaluated organs. Additional imaging is helpful in gaining experience for technologists examining the abdomen of infants and children.

Methods & Materials: Retrospective review and analysis of findings of randomly, chosen first-time renal ultrasounds performed from January to September of 2012.

Results: 200 renal ultrasounds were reviewed. (121) 60.5% of the children were males, and (79) 39.5% were female. Age ranged from 0 days to 17 years. Reasons for performing the renal ultrasound study varied, and the most common reasons were UTI (37%), hydroneprosis (19%) and evaluation for anomalies (9.5%). 180 (90%) of the ultrasounds had normal extra-renal, abdominal findings. The extra-renal findings for the remaining patients were, (some patients with more than one finding): gallbladder sludge=6, hepatomegaly=4, free fluid=4, splenomegaly=3, hepatosplenomegaly=2, cholelithiasis=2, fatty liver=2 and gallbladder polyp=1.

Conclusions: Only 10% of the reviewed ultrasounds demonstrated abnormal extra-renal findings, and none of them considered as requiring a change in management. We propose that it is not necessary to perform more detailed evaluation of the upper abdomen on first-time renal ultrasounds because the yield of abnormality is low, and most of the findings are considered incidental since none of them requered additional medical management. Further the practice will save time and decrease fatigue on ultrasound technologist.

Poster #: EDU-032

Pediatric Renal Masses – Spectrum and Imaging

Rakhee Gawande, M.D, *Radiology, Stanford University School of Medicine, Stanford, CA, rakheegawande@yahoo.com;* Beverley Newman

Purpose or Case Report: The purpose of this educational exhibit is to illustrate the spectrum of pediatric renal masses and their differential imaging features at the time of initial presentation. We will review the relative value of imaging modalities and emphasize important features in the performance and interpretation of plain film, ultrasound, CT and MR examinations.

Methods & Materials: Multiple pediatric patients with renal masses, ranging in age from 1 day to 20 years.

Results: Wilm's tumor represents approximately 95% of pediatric renal tumors with a peak incidence at age 2–4 years. This exhibit will illustrate the imaging spectrum of Wilm's tumor and its complications including tumor rupture, cystic/necrotic changes, tumor extension such as vascular and ureteral invasion and metastases; bilateral Wilm's tumor and syndromes predisposing to Wilm's tumor. Although they are collectively much less common than Wilms tumor, many other pediatric renal tumors occur and will be reviewed. These include more benign entities such as congenital mesoblastic nephroma, metanephric stromal tumor, nephroblastomatosis, multilocular cystic nephroma and angiomyolipoma as well as other malignant renal tumors including renal cell carcinoma, renal medullary carcinoma, clear cell sarcoma, rhabdoid tumor of the kidney and renal lymphoma.

This exhibit will also cover differential features of large contiguous extrarenal tumors such as neuroblastoma and other retroperitoneal neural tumors as well as retroperitoneal sarcoma and teratoma that may invade the kidney and be difficult to differentiate from a primary intrarenal tumor.

Additionally a number of nonneoplastic lesions that may be confused with a renal neoplasm will be illustrated. These include polycystic, multicystic and dysplastic kidneys as well as renal infection/abscess.

Conclusions: Wilms' tumor remains the most common renal tumor in children. A variety of less common benign and malignant entities are also included in the differential diagnosis, and these must be considered in the context of a renal/ abdominal mass.

Poster #: EDU-033

The twists and turns of pediatric ovarian torsion – a pictorial review

Jeffrey Otjen, MD, *University of Washington, Seattle, WA, jotjen@gmail.com;* Arta Luana Stanescu

Purpose or Case Report: The purpose of this educational exhibit is to:

1. Review classic imaging findings in pediatric ovarian torsion which can expedite diagnosis and guide definitive therapy.
2. Describe predisposing conditions that can lead to torsion correlated with patient's age (neonate to adolescents), reviewing the pathologic basis of the radiologic findings, with intraoperative images examples.
3. Identify common diagnostic pitfalls.

Methods & Materials: This pictorial review presents pertinent vascular and organ anatomy. A diagnostic imaging approach to this entity is discussed, along with classic findings and potential pitfalls. Cross sectional imaging (CT and

MRI) and their role in equivocal ultrasound examinations is reviewed, along with difficult cases and atypical presentations.
Sample cases include: in-utero ovarian torsion, neonatal ovarian cyst with torsion, simple ovarian cyst with torsion, ovarian tumors (including mucinous ovarian cystadenoma and ovarian teratoma) with torsion. Isolated fallopian tube torsion, and addition torsion of the uterus are presented as potential confounding cases.
Results: Major teaching points of this exhibit are:
1. The classic features of ovarian torsion on ultrasound and CT.
2. Understanding predisposing conditions for pediatric ovarian torsion, correlated with patient's age.
3. A description of potential pitfalls in imaging diagnosis of ovarian torsion.
Conclusions: Ovarian torsion is an important entity in pediatric emergency imaging, and complete knowledge of its imaging characteristics is important for the pediatric radiologist.

Poster #: EDU-034

Neonatal angiography - little difficulty
Premal Patel, *Great Ormond Street Hospital for Children, London, United Kingdom*, *premalpatel@doctors.org.uk*; Derek Roebuck, Samantha Chippington, Clare McLaren, DCR(R), Alex Barnacle**,** Sam Stuart
Purpose or Case Report: To explain indications for neonatal angiography
To describe the complications and risks from performing neonatal angiography
To describe the techniques, approaches and equipment available to overcome these obstacles
Methods & Materials: Catheter angiography is sometimes needed to be performed in neonates by interventional radiologists, often as a primary step in the endovascular management of conditions including Vein of Galen abnormalities and congenital haemangioma. Angiography in neonates is a daunting task due to the small size of the patient. Difficulties with vascular access, contrast and flush volume, differences in body surface area, risk of vascular thrombosis and the inherent differences in the neonatal vasculature are all present. Children are much more sensitive to radiation effects than adults and we must image gently. Great care and attention are needed to ensure complications are avoided. This poster describes how to successfully and safely perform angiography in the neonate with illustrated examples.
Results: We present a "how to guide" on performing angiography in the neonate emphasizing:
Crucial differences in performing angiography in a neonate compared to an older child or adult including ensuring coagulation, body temperature and positioning are optimized.
Tips and tricks for arterial access in the neonate including choices of access needles, wires and sheaths and equipment that is useful to make things easier
The importance of dose reduction and contrast volume sparing techniques
Doses of commonly used drugs in neonatal angiography
Access site complications, how to avoid them and how to manage them
Conclusions: The correct choice and application of technique, approach and equipment is imperative to ensure safe neonatal angiography can be performed. Difficulties with vascular access and patient size can be overcome to allow neonatal angiography to aid the diagnosis and provide endovascular treatment for the youngest patients in our care.

Poster #: EDU-035

Push, pull and buried bumpers - removing pediatric gastrostomies the interventional radiology way
Premal Patel, *Great Ormond Street Hospital for Children, London, United Kingdom, premalpatel@doctors.org.uk;* Alex Barnacle, Derek Roebuck, Samantha Chippington, Sam Stuart
Purpose or Case Report: How to remove a gastrostomy - IR techniques.
Explanation of the "Buried Bumper" syndrome
Removing a "stuck" gastrostomy - a pictorial illustration of different IR approaches to gastrostomy removal.
How to avoid complications associated with gastrostomy removal.
Methods & Materials: Percutaneous gastrostomy feeding tubes are required for an increasing number of children with long-term nutritional requirements. Antegradely placed gastrostomy tube have internal retention discs (bumpers) that oppose the stomach wall to keep the tube in situ. Buried bumper syndrome (BBS) occurs in 2–6% of percutaneous gastrostomy placements making removal difficult. Traditionally these "stuck" tubes were removed by surgical or endoscopic methods. Interventional radiology techniques have developed that allow removal of buried bumpers without the need for surgery or the use of an endoscope. We explain these methods with pictorial illustrations describing how to perform them.
Results: A description of different pediatric gastrostomy removal methods is given including
The cut and pass method and the inherent risks of this approach

Push removal over a wire floss
Balloon assisted removal with a pull technique
Removal with pull technique using antegrade snare placement
Conclusions: Successful and safe gastrostomy removal is important to prevent complications varying from pain to duodenal perforation and ileal obstruction. We describe methods that can be employed by intervnetional radiologists to remove a pediatric gastrostomy that can even be successful in cases of buried bumper. This variety of techniques can allow gastrostomy removal in children without need for surgery or endoscopic assistance and avoids the complications of tube remnants remaining in the GI tract.

Poster #: EDU-036

All slow flow malformations are not created equal: Simple versus complex venous and lymphatic malformations: Imaging and treatment implications
Subramanian Subramanian, MD, *Pediatric Radiology, Medical College Wisconsin, Milwaukee, Milwaukee, WI, drsubbusmc@yahoo.co.in;* David Moe, Patricia Burrows
Purpose or Case Report: The aim of this exhibit is to illustrate the imaging features of simple versus complex venous and lymphatic malformations with regard to treatment implications in pediatric patients. Malformation morphology, location, symptoms and extent dictate varied treatment strategies and goals.
Methods & Materials: We will present a review of imaging findings and treatment implications in simple and complex venous and lymphatic malformations. These malformations may be focal, diffuse and multifocal. Malformation morphology at a given site may vary from simple (unilocular and treatable by a single point of access) or complex (requiring treatment from multiple points of access). Malformations may reside in skin, subcutaneous tissue, muscle, viscera and bone, with treatment implications based on the tissues involved. Proximity to the airwayor a neurovascular bundle, involvement of a joint or orbit, and diffuse infiltration of a compartment in an extremity are some examples of situations requiring techniques that cause minimal swelling or neurotoxicity. Venous malformations that drain freely into large systemic veins should be managed with outflow occlusion to minimize nontarget administration of sclerosant that could result in DVT and pulmonary circulatory collapse. Potential toxicity of sclerosant due to systemic absorption must be taken into consideration, especially in infants. The goal of treatment in diffuse lesions might not be complete obliteration, but rather treating an area of maximum symptomatology.. Anticipating and preventing potential complications related to the location and angioarchitecture of the malformation is vital to a safe sclerotherapy procedure. Lymphatic malformations may be macrocystic, microcystic or combined. Small cysts can be treated with simple aspiration and injection of sclerosant whereas large cysts may require placement of a drainage catheter and injection of sclerosant in multiple settings. In addition, cutaneous involvement in the form of symptomatic vescicles is amenable to laser treatment. A variety of endovascular techniques (sclerotherapy, venous embolization, endovenous and cutaneous laser therapy) and sclerosant agents for treatment of the venous and lymphatic malformation will be discussed.
Conclusions: Knowledge of the varied presentations and subsequent treatment implications of venous and lymphatic malformations is necessary for the pediatric interventional radiologist to properly plan and safely execute treatment in these patients.

Poster #: EDU-037

Shoulder MR Arthography: Tips for the General Pediatric Radiologist
Hisham Dahmoush, Diego Jaramillo, Anne Marie Cahill, **Nancy Chauvin, MD,** *Children's Hospital of Philadelphia, Philadelphia, PA*
Purpose or Case Report: Shoulder dislocations are relatively common in adolescents, with 40% of all cases occurring in patients less than 22 years of age. Structural damage ensued can lead to significant pain and morbidity and predispose children to re-injury. When the static stabilizers of the shoulder are disrupted, patients will often experience recurrent dislocation. With surgical correction, young athletes are afforded the best opportunity to achieve long-term stability and return to play. MR arthrography (MRA) of the shoulder offers detailed joint anatomy; enabling depiction of ligament, tendon, bone and cartilage injury and is used to assist the orthopedic surgeons in surgical planning. This exhibit will serve to provide the general pediatric radiologist with a practical approach to shoulder MR arthrography from intraarticular injection to image interpretation.
Methods & Materials: Proper intraarticular injection technique will be demonstrated including the authors' experience using a posterior shoulder injection approach used because most abnormalities are found in the anterior labrum. Optimal MR patient positioning, sequence selection and imaging parameters will be described. The normal glenohumeral joint anatomy will be depicted as well as tips to depict normal variants (coracoid physis, sublabral recess, Buford complex and the bare spot) and image artifacts that should not be mistaken for pathology. Common pathologies involving the glenohumeral ligaments and anteroinferior glenoid will be explored

including hints to differentiate between cartilaginous Bankart injuries, Bony Bankart injuries, Perthes lesions and Anterior Labroligamentous Periosteal Sleeve Avlusions (ALPSA). In addition, strategies for accurate diagnosis of superior labral anteropeosterior (SLAP) tears will be highlighted.

Results: A good knowledge of the MR appearance of normal shoulder anatomy and anatomic variants is crucial in order to accurately evaluate for pathology. With proper intraarticular injection, MR acquisition and diagnostic experience; MRA is effective method for the detection of labroligamentous abnormalities, bone injuries and musculotendinous pathology.

Conclusions: When performed correctly, shoulder MRA is an important diagnostic modality that can aid with preoperative planning in the pediatric population.

Poster #: EDU-038

Magnetic Resonance Imaging of the Temporomandibular Joint in Juvenile Idiopathic Arthritis and Other Pediatric Rheumatologic Diseases

Floyd Dunnavant, MD, *Radiology, The University of Alabama at Birmingham, Birmingham, AL, fdunnavant@uabmc.edu;* Saurabh Guleria, Yoginder Vaid, Daniel Young, Stuart Royal, Randy Cron

Purpose or Case Report: Juvenile idiopathic arthritis (JIA, previously referred to as juvenile rheumatoid arthritis) is the most common cause of chronic arthritis in children, affecting about 1 in 1000 children worldwide. The temporomandibular joint (TMJ) is frequently involved in JIA, with multiple associated complications including pain, feeding issues, micrognathia, intubation problems and malocclusion. Although TMJ involvement has a reported prevalence as high as 75% at disease onset, the TMJ has been called the "forgotten joint" in JIA, and TMJ involvement remains one of the most underdiagnosed conditions in JIA. TMJ involvement can also be seen less frequently in Sjogren disease, dermatomyositis, sarcoidosis, and mixed connective tissue disease. MRI with contrast has been shown to be considerably more sensitive than physical exam or other imaging modalities in the diagnosis of TMJ involvement, and is now considered the gold standard for TMJ evaluation. The purpose of this exhibit is to show the spectrum of pathological changes by MRI of TMJ involvement in JIA and other rheumatologic diseases.

Methods & Materials: A large population of children with JIA and TMJ involvement are routinely imaged at our institution (approximately 1000 studies in the last 2 years). This exhibit will demonstrate typical examples of the pathologic findings of TMJ involvement in JIA, with varying degrees of severity, obtained at 3 T MRI of children at our institution. Images from normal patients will be provided for comparison, and CT correlations will be demonstrated where appropriate. TMJ involvement in other rheumatologic diseases will be shown for comparison. Our institution's TMJ imaging protocols will also be reviewed. A preliminary grading system will be demonstrated.

Results: Findings of TMJ involvement at MRI (including both acute and chronic changes) include synovial enhancement, joint effusion, pannus formation, deformed or displaced disc, bone marrow edema, and condylar head flattening, erosions, and destruction. Marked destructive changes can be demonstrated when unsuspected clinically.

Conclusions: Relatively little has been published about TMJ involvement in JIA, and imaging remains underutilized at many large pediatric centers. Routine MRI screening of the TMJ has been recommended for children with JIA. This presentation demonstrates the findings typical of TMJ involvement in JIA and other rheumatologic diseases so that a grading system can be developed for therapeutic and research purposes.

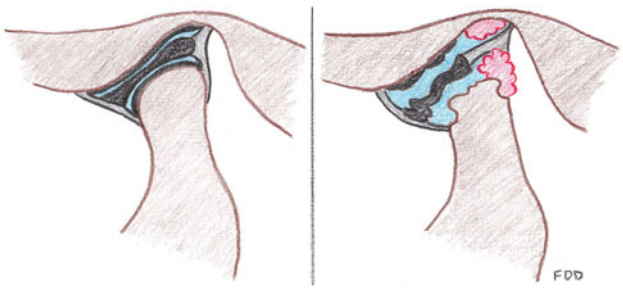

Poster #: EDU-039

Pictorial Review of Osteochondral Lesions of the Knee: To Drill or Not to Drill

Seetharam Chadalavada, MD, MS, *Hospital of University of Pennsylvania - Dept of Radiology, Philadelphia, PA;* Sabah Servaes, Diego Jaramillo, Lawrence Wells, Nancy Chauvin, MD

Purpose or Case Report: Osteochondritis dissecans (OCD) of the knee is a pathologic condition that results in destruction of the subchondral bone with secondary damage to the overlying articular cartilage. The etiology of OCD is still debated with trauma, ischemia, ossification defects and genetic causes suggested. OCDs are one of the most common causes of knee pain and dysfunction in teenagers, with the highest rates occurring in patients between 10 and 15 years of age. The natural history of OCD is not easily predicted

and treatment is determined by the stability of the fragment. MRI has been used successfully to evaluate the stability of the lesion and has proved useful in preoperative planning. This exhibit will review the pathogenesis of OCDs, appearance of common lesions and normal variant pitfalls, while highlighting typical MRI findings to accurately classify lesions. In addition, surgical approaches and post-operative imaging features will be discussed.

Methods & Materials: We will present a variety of cases that we have encountered at a large children's hospital. Included will be the normal MR appearance of the developing pediatric knee, variants in epiphyseal ossification that can mimic OCDs and characteristic MR findings to help distinguish stable versus unstable lesions. Indications for surgery and various operative techniques will be discussed along with correlative arthroscopic images to compliment the imaging findings. In addition, the post-operative MR appearance of treated lesions and the evaluation of healing response will be explored.

Results: Subchondral bone and cartilaginous defects of the distal femoral epiphyses need to be accurately characterized to avoid unnecessary follow up radiology studies as well as to allow for treatment planning; either with a conservative or surgical approach.

Conclusions: Familiarity with the MR appearance of the normal development of the pediatric knee and the ability to accurately diagnose and classify OCDs allows for prompt, optimal care for patients requiring orthopedic intervention.

Poster #: EDU-040

The Temporomandibular Joint in Juvenile Idiopathic Arthritis: Spectrum of MRI findings

Arthur Meyers, MD, *Radiology, Children's Hospital of Wisconsin, Milwaukee, WI, arthurbmeyers@yahoo.com;* Tal Laor, MD

Purpose or Case Report: For over a century it has been known that juvenile idiopathic arthritis (JIA) can involve the temporomandibular joint (TMJ). In more recent decades there has become an increased awareness of the variety of pathology that can affect the TMJ in patients with JIA. This pathology may lead to various symptoms ranging from decreased chewing ability, jaw/facial pain, headaches, and malocclusion, as well as craniofacial morphologic changes such as a retrognathic mandible. The purpose of this educational exhibit is to review the MRI appearance of the normal TMJ and the normal motion which occurs at this joint, and to demonstrate the spectrum of pathology that affect the TMJ in children with JIA.

Methods & Materials: We reviewed the magnetic resonance imaging (MRI) examinations of the TMJ which were performed at a large pediatric medical center. Relevant images from these studies were obtained to review the normal appearance and normal motion of the TMJ, and to demonstrate the spectrum of TMJ pathology in pediatric patients with JIA.

Results: MRI examinations obtained in children with JIA showed a variety of TMJ pathologies. These include abnormalities seen on static images such as: mandibular condylar erosions, condylar edema, synovitis, synovial cysts, and articular disc attenuation. Additionally, images comparing closed mouth and open mouth positions demonstrate dynamic abnormalities of condylar and intra-articular disc motion. Images showing the utility of TMJ MRI to monitor the treatment response in patients with JIA are also provided, as are incidental findings that can be seen when performing these studies.

Conclusions: TMJ pathology leading to symptoms and craniofacial morphologic abnormalities in patients with JIA are well demonstrated with MRI. This exhibit shows the normal appearance of the TMJ on MRI as well as pathology related to JIA in order to familiarize the radiologist who might be interpreting TMJ MRI examinations in these children.

Poster #: EDU-041

Mandibular distraction osteogenesis in the treatment of micrognathia: pre-operative imaging, post-operative imaging and complications, what the craniofacial surgeon wants to know

Justin Friske, **Arthur Meyers, MD,** *Medical College of Wisconsin, Milwaukee, WI, arthurbmeyers@yahoo.com;* Patrick Hettinger, Arlen Denny

Purpose or Case Report: Mandibular distraction osteogenesis techniques are mandibular lengthening procedures which are performed in infants and children with micrognathia to alleviate airway compromise and avoid the need for tracheostomy. These procedures have been performed at our institution for over 15 years with a high success rate and are becoming more widely performed at pediatric medical centers. The purpose of this educational exhibit is to demonstrate the information that the craniofacial surgeon wants to know on pre-operative imaging and to show the post-operative appearances of some of the various techniques and complications which are encountered following these procedures.

Methods & Materials: We reviewed the pre and postoperative imaging findings of patients who had mandibular distraction osteogenesis at a large pediatric medical center. Preoperative radiographs and computed tomography scans (CT) and postoperative radiographs and CT scans were

reviewed when available. Relevant images from these studies were obtained to pictorially demonstrate information of importance to the craniofacial surgeon.

Results: Preoperative radiographs and CT scans provide useful information about the mandible, particularly if the lengths of the mandibular rami are long enough to accommodate osteotomies and hardware associated with mandibular distractor devices. If preoperative CT scans are extended to the level of the carina they demonstrate the level(s) of airway obstruction; it is crucial to know preoperatively if there are additional areas of lower airway compromise which will not be corrected by alleviating the upper airway obstruction secondary to micrognathia. Postoperative radiographs show various types of external and internal hardware associated with mandibular distractor devices. Post operative radiographs and CTs also show complications which may occur after these procedures including delayed/nonunion at the osteotomy sites and hardware failure.

Conclusions: Mandibular distraction osteogenesis is becoming a more widely used technique for the treatment of airway compromise in patients with micrognathia. Therefore, radiologists need to be familiar with the preoperative and postoperative imaging features in these patients and what information the craniofacial surgeon wants to know.

Poster #: EDU-042

An illustration of the clinico-radiological findings in children presenting from birth to puberty with a brachial plexus birth injury

Susan Gowdy, BMBS, *Radiology, BC Children's Hospital, Vancouver, BC, Canada, scgowdy@doctors.org.uk;* Heather Bray, Cindy Verchere

Purpose or Case Report: Background: Brachial Plexus Birth Injury (BPBI) affects 1-3/1000 live born infants. The majority of injuries involve C5-7 and in 20-30% of cases the result is denervation of the rotator cuff muscles. Muscle imbalances allow the unopposed internal rotators to cause a shoulder deformity. There is a progressive and permanent developmental dysplasia of the glenohumeral joint associated with posterior subluxation of the humeral head and ensuing joint contractures. The early diagnosis of glenohumeral dysplasia is important to allow intervention and halt the progressive glenohumeral dysplasia. In our institution there is a strong multidisciplinary approach to such patients. An ultrasound examination with the arm held in neutral and external rotation shows any posterior subluxation and in conjunction with the clinical examination guides further management. An innovative method of splinting the shoulder joint has been developed and is applied early in the infant group. Dynamic ultrasound has been used to guide the placement of the cast and subsequently follow up the patient.

Objective: In this cohort of patients, many of whom have had both ultrasound and MRI examination, we present an illustration of the clinical and imaging findings in patients presenting from birth to puberty with a BPBI. We confirm the value of a dynamic ultrasound examination and propose this non-invasive test as the primary method for surveillance in such patients.

Methods & Materials: Method: This is an educational exhibit reviewing the aetiology and pathology of brachial plexus birth injury and it's sequelae affecting children from birth to puberty. The imaging characteristics of brachial plexus nerve damage are reviewed. The imaging findings and described methods of measuring the degree of glenoid dysplasia are illustrated using ultrasound and MRI. The method of dynamic ultrasound we use to identify glenoid dysplasia and glenohumeral joint congruity is described and displayed. The method of casting and splinting the shoulder to manage glenohumeral joint dysplasia is highlighted with images and a pictorial review of the clinical nature of brachial plexus injury in children is presented.

Results:.

Conclusions: Brachial plexus birth injury is relatively common. A spectrum of the sequelae of BPBI are presented in children of various ages. The imaging techniques are reviewed and dynamic ultrasound assessment described.

Poster #: EDU-043

Leg length discrepancy, more than just numbers: A pictorial review from the perspective of alignment and etiology

Randheer Shailam, MD, *Radiology, Massachusetts General Hospital, Boston, MA, rshailam@partners.org;* Vinitha Shenava, J. Kan, MD

Purpose or Case Report: To review causes of leg length discrepancies in a pictorial format with an emphasis on alignment disorders.

Methods & Materials: We reviewed leg length imaging studies of children from the newborn-18 years at a tertiary care children's hospital. Studies included leg-length radiographs, CT and MRI. Imaging findings and quantitative measurements including determination of mechanical axis, lateral distal femoral angle (LDFA), and medial proximal tibial angle (MPTA) were correlated with impact on operative technique.

Results: Alignment disorders with resulting leg length discrepancies have many causes. These include developmental and acquired extra-articular and intra-articular causes. Extra-articular causes can occur at the level of the diaphysis,

metaphysis, or physis. Intra-articular causes include epiphyseal dysplasias, epiphyseal overgrowth, or growth disturbance of the spherical growth plate, articular cartilage, or ligamentous injury. Determining mechanical axis, LDFA, and MPTA has important orthopaedic surgical implications and should be provided in every leg-length measurement report.

We will review normal patterns of physeal closure and etiologies for premature physeal closure including fractures involving the physis, juvenile idiopathic arthritis and osteomyelitis. Idiopathic cases such as Blount disease and Legg-Calve-Perthes will also be studied. Genetic and congenital causes including hereditary osteochondromatosis and proximal focal femoral deficiency and generalized overgrowth disorders such as Klippel Trenaunay malformation and Proteus syndrome are reviewed.

Conclusions: An understanding of the various causes of growth arrest and leg length discrepancies in children is important for accurate diagnosis and management. While providing measurements of the femur, tibia and total leg lengths is necessary, identifying the cause and detailing alignment abnormalities of the lower extremity are important to help with operative and non-operative management of these conditions.

Poster #: EDU-044

VEPTR–What you need to know as a pediatric radiologist

Robert Llanos, *Radiology, Children's National Medical Center, Washington, DC, rob.llanos@gmail.com;* Nabile Safdar, Laurel Blakemore

Purpose or Case Report: The purpose of this presentation is to:

1. Describe Vertical expandable prosthetic titanium rib (VEPTR) and its imaging appearances
2. Provide the indications and contraindications for its use.
3. Describe the imaging appearance of potential complications

Methods & Materials: All patients who had a VEPTR placement and/or lengthening and imaging over a four-year period were identified through a search of the radiology information system and a review of the electronic medical record. Indications, anatomic positioning, and complications were reviewed.

Results: Nine patients were identified with a VEPTR over a 4 year period. A total of 16 VEPTR prostheses were identified; there were a total of nine rib-to-rib, three rib to spine, and four rib to pelvis prostheses.

Indications were congenital scoliosis with fused ribs, Jeune's syndrome, Spondylocostal dysostosis (Jarcho-Levin), and myelodysplasia. One third of the patients were diagnosed with a thoracic insufficiency syndrome.

Potential complications include infection, migration or dislodgement of a portion of the prosthesis, and hardware failure due to loosening.

Conclusions: Vertical Expandable prosthetic titanium rib (VEPTR) (Synthes, Inc; West Chester, PA) is a prosthesis intended to mechanically stabilize and expand the thorax by rib distraction. The prosthesis can be connected from rib to rib, rib to vertebra, or rib to pelvis.

It has been approved by the FDA for the treatment of Thoracic insufficiency syndrome in skeletally immature patients and progressive thoracic scoliosis. The contraindications for use are: age less than 6 months and beyond skeletal maturity, absent proximal and distal ribs, weakened bones, absent diaphragmatic function, too little soft tissue for coverage of the prosthesis, local infection, and allergy to any component of the prosthesis.

Complications include infection, loss of fixation, pneumothorax, progression of the thoracic deformity and thoracic insufficiency syndrome, drift of rib attachments, chest wall scarring and hardware loosening. Although uncommon, VEPTR has been used in select patients to improve scoliosis and expand the thorax to improve clinical symptoms. As pediatric imagers, we need to be able to discern the normal postoperative appearance and be alert to any complications that arise in treatment, which includes hardware replacement and prosthesis lengthening.

Poster #: EDU-045

Congenital Foot Deformity, How can I describe it?

Abdullah Alhammad, *Children's Hospital of Eastern Ontario, Ottawa, ON, Canada, rad982@gmail.com;* Rita Putnins, Khaldoun Koujok

Purpose or Case Report: The purpose of this educational exhibit is to answer the following questions:

1. Is this child's foot anatomically normal: angles, alignment and articulation?
2. When can I say that this foot is deformed?
3. Where is the congenital deformity: forefoot, midfoot, hindfoot or mixed.
4. What is the terminology to describe the foot deformity?

After answering the previous questions we will provide examples of congenital foot deformities such as but not limited to clubfoot, hind foot valgus, metatarsus adductus, congenital vertical talus, skew foot and congenital coalition.

Methods & Materials: 1. Explain the normal ossification, alignment and angles of the foot.

2. The terminology used for description of foot deformity.

3. Provide examples of foot deformity using schematic drawings to illustrate the deformity.
4.At the end, showing some cases in quiz format.
Results: The aim of this exhibit is to answer the given questions regarding normal appearance, abnormality and the terminology used to describe the deformity. This will simplify the approach to deformed foot in children, mainly for the residents and fellows. Also, it might be possible to tailor the findings to one of the known congenital deformities.
Conclusions: The foot is one of the most important areas of weight bearing. When there is a foot abnormality, as a consequence, the ability to walk and weight bear will be affected. By knowing the normal, identifying the abnormal and utilizing the terminology in describing the abnormality will create a better communication with treating physician.

Poster #: EDU-046

MR imaging and arthrographic findings of femoroacetabular impingement (FAI) based on the Stulberg classification of healed Perthes
Siddharth Jadhav, MD, *Texas Children's Hospital, Department of Radiology, Houston, TX, spjadhav@texasChildren's.org;* J. Kan, MD, Scott Rosenfeld
Purpose or Case Report: To describe the use of MRI in pre-operative evaluation of FAI secondary to healed Perthes to complement the Stulberg classification and its impact on orthopaedic management.
Methods & Materials: Through case examples this exhibit will demonstrate various MRI findings that the orthopedic surgeon uses to plan surgery for femoro-acetabular impingement (FAI) in healed Perthes disease and how MRI may assist in management decisions based on the Stulberg classification.
Results: Legg-Calve-Perthes disease leads to hip deformity secondary to nonspherical femoral head, growth disturbance of the proximal femoral physis, overgrowth of the greater trochanter and secondary acetabular deformities. All of these individually and in conjunction can lead to abnormal hip mobility and femoroacetabular impingement (FAI). Intra and extra-articular impingement is more common with Perthes disease than normal hips and primary FAI. Orthopedic surgeons use the Stulberg classification, based on radiographic findings, as an estimate of femoral head sphericity in healed Perthes disease. This is useful for prognostication and management decisions. An aspherical femoral head may be treated by surgical dislocation of the hip or hip arthroscopy with re-shaping of aspherical portions. MRI may provide additional information about the exact location of the aspherical portion of the head, the size and location of a cam lesion, as well as the status of the labrum and articular cartilage. This may assist the surgeon in making treatment decisions and counseling the patient about the likelihood of success of hip preservation surgery. This exhibit will review how MRI may be able to optimally evaluate FAI in healed Perthes by providing information about femoral head shape, alpha angle measurement, trochanteric overgrowth, acetabular coverage, and labral and articular cartilage abnormalities.
Conclusions: MRI can provide a more global pre-operative assessment of the hip in healed Perthes disease in terms of precise evaluation of FAI, labral and cartilage abnormalities which are currently evaluated intra-operatively by surgical dislocation or arthroscopy. MRI should routinely be used to provide additional information to the Stulberg classification to facilitate orthopaedic management in patients with healed Perthes.

Poster #: EDU-047

Restricted Diffusion on Brain MRI of the Pediatric Population: A Pictorial Review
Erin Horsley, DO, *Hahnemann University Hospital, Philadelphia, PA;* Jacqueline Urbine, Eric Faerber
Purpose or Case Report: MRI of the pediatric brain is a useful tool for the diagnosis of many abnormalities. Diffusion weighted imaging has proven to be helpful in distinguishing between different etiologies of CNS lesions. A pictorial review of a wide spectrum of pediatric CNS lesions that restrict diffusion is demonstrated.
Methods & Materials: We retrospectively identified pediatric patients who demonstrated restricted diffusion on brain MRI. Medical records were reviewed and radiologic studies were correlated with clinical history and pathology results where indicated.
Results: A retrospective study over a 7 year period demonstrated restricted diffusion in multiple pediatric patients in the following categories: vascular, infectious/inflammatory, metabolic, neoplastic, traumatic, and iatrogenic. Within the vascular category, ischemia was the major etiology. The infectious/inflammatory category included: multiple sclerosis, abscess, and Gradenigo syndrome. Metabolic causes which demonstrated restricted diffusion were glutaric aciduria and Wernicke's encephalopathy. Patients with metastatic rhadomyosarcoma, epidermoid, and retinoblastoma also demonstrated restricted diffusion. A traumatic cause that showed restricted diffusion was diffuse axonal injury; an iatrogenic cause was hemorrhage in the postoperative brain.
Conclusions: Diffusion restriction on MRI of the brain in the pediatric patient is not restricted to ischemia but may be encountered in many diverse disorders.

Poster #: EDU-048

Diffusion Tensor Imaging of Brainstem Malformations

Nancy Rollins, MD, *Radiology, University Texas Southwestern Medical Center, Dallas, TX, nancy.rollins@Children's.com*

Purpose or Case Report: Diffusion tensor imaging provides information about white matter fibers not possible with conventional MRI (cMR). Malformations involving the mid-hindbrain (MHB) are rare and usually characterized using cMR. We describe patterns of alterations in white matter fibers in diverse MHB malformations which may aid in the further characterization of these uncommon malformations

Methods & Materials: An IRB-approved query of PACs at our institution for patients with a congenital brain malformation by cMR who also underwent DTI from 2005 to 2011. DTI was acquired with SS-EPI; (TR/TE) 7000–9000/72–84 msec; 128×128 matrix, 2 mm3 voxel; 2 mm slice thickness; n; 30 directions; b=700–1000-sec/mm2. Scan time for DTI ranged from 4 to 12 min. Tensor data was post-processed with EWS (Philips Healthcare Systems) to generate directionally encoded color maps used to assess corticospinal tracts (CST) and medial/lateral lemniscus (ML) complex at the level of the pons, decussation of the superior cerebellar peduncle (SCP) in the midbrain, and dorsal and ventral transverse pontine fibers (TPF). Tractography was done with FACT. Medical records were reviewed for neurologic status and genetic testing.

Results: Isolated MHB malformations included brainstem disconnection syndrome, inferior pontine segmentation anomalies, molar tooth deformity (MTS), and pontine tegmental cap dysplasia. DTI showed variable abnormalities of the TPF and the SCP with consistently preserved ML. When brainstem malformations were associated with diffuse anomalies, the malformations were most often lissencephaly or agyria/pachygria. More severe agryia/pachgyria was associated with hypoplasia or absence of the dorsal but not the ventral TPF. Holoprosencepahly was associated with small CST and ventral TPF. Brainstem DTI was usually normal in callosal agenesis/hypogenesis. Anomalies seen by DTI in ACC included absence of the TPF and midline fusion of the CST. The ML were consistently intact.

Patients old enough to undergo assessment of developmental status were consistently delayed. Isolated MHB malformation were usually associated with hearing loss. High-resolution chromosmal microarray (CMA) was normal in most patients.

Conclusions: Isolated malformations of the MHB readily identied with cMR were associated with more DTI abnormalities than MHB malformations occuring with cerebral malformations. With cerebral malformations, cMR findings did not predict the presence of DTI abnormalities in the MHB.

Poster #: EDU-049

A slippery slope: Imaging and pathology of the pediatric clivus

Luke Linscott, MD, *Radiology, Cincinnati Children's Hospital, Cincinnati, OH;* Arnold Merrow, MD, Blaise Jones, Bernadette Koch

Purpose or Case Report: Due to its proximity to the brain and spine, the clivus is one of the most frequent bones to undergo advanced cross-sectional imaging studies in pediatric patients. Yet the clivus receives relatively little attention in the pediatric musculoskeletal and neuroimaging literature. The purpose of our exhibit is to review the normal development and expected age-related imaging changes of the clivus with a subsequent discussion of clival abnormalities, including congenital, neoplastic, inflammatory, traumatic, and post-therapeutic processes.

Methods & Materials: Cases were collected from clinical encounters by the authors as well as through a search of radiology and pathology reports. Clinical information, including surgical pathology (when available), was subsequently reviewed using the main hospital electronic medical record.

Results: Abnormalities of the clivus may be related to a variety of local and systemic etiologies. Congenital and developmental skull base anomalies can be due to systemic metabolic disorders (such as rickets and osteogenesis imperfecta) and skeletal dysplasias (such as achondroplasia) or local influences on bone growth (as seen in Chiari 2 malformation). Similarly, tumors of the clivus can be relatively location specific (such as an intrinsic chordoma or invading parameningeal rhabdomyosarcoma), focal but not location-specific (e.g., fibrous dysplasia), or systemic with numerous sites of bony involvement (e.g., Langerhans cell histiocystosis, enchondromatosis, generalized lymphatic anomalies, and various marrow pathologies). Skull base trauma can result in relatively unique fracture patterns and associated soft tissue abnormalities in the pediatric patient, including diastasis of the spheno-occipital synchondrosis and retroclival epidural hematomas. Imaging abnormalities reflecting therapeutic effects, such as marrow changes after posterior fossa tumor radiation, may also be encountered. Adjacent inflammatory processes can involve the clivus as well.

Conclusions: Clival abnormalities, while relatively uncommon in children, cover a broad spectrum of pathologies. Given the frequency of clival imaging, intentional or not, a familiarity with characteristic normal and abnormal imaging patterns will guide the radiologist in diagnosing these important clinical entities.

Poster #: EDU-050

MR imaging of the developing pediatric pineal gland

Esin Cakmakci Midia, MD, *Children's Hospital of Wisconsin, Milwaukee, WI;* Teresa Gross Kelly, Saurabh Guleria, Tushar Chandra, Subramanian Subramanian, MD, Mohit Maheshwari

Purpose or Case Report: The aim of this educational exhibit is to depict MR imaging of the normally developing pineal gland and pediatric pineal gland lesions. The pineal gland is a curious, pea sized, pine cone shaped structure that was once believed to be the "seat of the soul" and was once also called the "third eye". When evaluating MRI scans of the pediatric patient we may see cysts, calcifications, mass lesions, or vascular abnormalities, within or around the pineal gland. The purpose of this poster is to review the embryology, microstructure, anatomy and pathology of the pediatric pineal gland.

Methods & Materials: This exhibit will review: (1) embryology, microstructure and anatomy of the pineal gland, (2) normal MRI appearance of the pineal gland of the infant, young child and adolescent, (3) pineal gland lesions and when possible, the corresponding histologic slides depicting pathology. Treatment for each type of pathology will also be touched upon.

Results: The developing pineal gland may contain cysts and calcifications. However, sometimes cysts and calcifications may be present in pineal gland lesions such as germ cell tumors, rhabdoid tumors, pineocytoma, pineoblastoma, teratoma, astrocytomas and others.

Conclusions: It is our hope that this review of the normal MRI appearance of the developing pineal gland and the pathological lesions that can affect it will facilitate detection and diagnosis of pineal gland abnormalities in the pediatric patient.

Poster #: EDU-051

Magnetic Resonance Imaging of pediatric brachial plexus

Subramanian Subramanian, MD, *Pediatric Radiology, Medical College Wisconsin, Milwaukee, Milwaukee, WI, drsubbusmc@yahoo.co.in;* Mohit Maheswari, Tushar Chandra, Teresa Kelly, Esin Cakmakci Midia, MD, Tejaswini Deshmukh

Purpose or Case Report: Brachial plexus pathology is relatively uncommon in pediatric patients and requires accurate imaging evaluation. MRI is the imaging modality of choice for evaluating brachial plexus in pediatric patients. The objective of this exhibit is to familiarize the radiologist with MRI protocol for brachial plexus imaging, normal MRI anatomy of brachial plexus and the spectrum of abnormalities in order to aid in accurate diagnosis and management of these cases.

Methods & Materials: We will present a succinct review of the normal brachial plexus anatomy. We will also discuss MRI protocol for evaluation of brachial plexus pathology including MR myelography and high resolution MR imaging techniques. The classic imaging features of post traumatic brachial plexus injury includes nerve root avulsion, pseudomeningocele, brachial plexus edema and scarring, spinal cord edema and shoulder joint abnormalities. In addition other causes of brachial plexus palsy like inflammatory pathology, neoplasm, plexiform neurofibroma and leukemic involvement of brachial plexus will be highlighted.

Conclusions: Imaging of pediatric brachial plexus is unique and technically challenging. MRI is the diagnostic modality of choice in pediatric patients. It is important that the radiologist is aware of these abnormalities and provide an accurate diagnosis.

Poster #: EDU-052

Cerebrospinal image findings of mucopolysaccharidosis: a pictorial essay

Motoo Nakagawa, *Radiology, National Center for Child Health and Development, Setagaya, Japan, lmloltlolol@gmail.com;* Shunsuke Nosaka, Osamu Miyazaki, Motomichi Kosuga, Yoshiyuki Tsutsumi, Mikiko Miyasaka

Purpose or Case Report: Mucopolysaccharidoses (MPS) are a group of rare genetic lysosomal storage disorders characterized by the deficiency or complete lack of necessary lysosomal enzymes required for the stepwise breakdown of glycosaminoglycans (GAGs). As a general rule, the impaired degradation of heparan sulfate is more closely associated with mental deficiency, and the impaired degradation of dermatan, chondroitin and keratan sulfate results in mesenchymal abnormalities.

The purpose of this educational exhibit is to demonstrate the cerebral and spinal image findings of various types of MPS. We also demonstrate key findings to distinguish from different type of MPS and other diseases.

Methods & Materials: MR and CT images of various types of MPS patients who treated at National Center for Child Health and Development during the past 7 years were reviewed retrospectively. MPS types contain Hurler, Hunter, Sanfilippo, Morquio and Maroteaux-Lamy syndrome (I, II, III, IV and VI respectively).

Results: In Hurler, Hunter and Sanfilippo syndrome (MPS type I, II and III), cerebral abnormality is prominent resulting from neuronal damage by the intralysosomal mucopolysaccharides. MRI in Hurler syndrome revealed the delayed myelination, atrophy, varying degrees of hydrocephalus and white matter changes. Typically, the perivascular spaces are dilated as the result of GAG accumulation which gives rise to a cribriform appearance in the periventricular white matter,

corpus callosum and basal ganglia on T1 and T2 weighted images. Although the symptoms in Hunter syndorme progress slower than those of Hurler syndrome, MRI findings resembles to those of Hurler syndrome. In Sanfillipo syndrome, cerebral atrophy and the white matter changes are more significant than the other type of MPS.

In Morquio and Maroteaux-Lamy syndrome (MPS type IV and VI), skeletal involvement dominates. Platyspondyly with central tongue-like projection and odontoid hypoplasia with instability is characteristic in Morquio syndrome. For thse characteristics, Morquio syndrome can be differentiated the other type of MPS. Because atlantoaxial instability with Morquio disease can cause tetraplegia and sudden death, imaging studies for cervical spine is important.

Conclusions: In this pictorial essay, we will try to provide key features of a variety of MPS seen on CT and MR images. Radiologists should be familiar with the imaging features of a variety of MPS to assist clinicians in diagnostic purpose as well as to monitor prognostic aspects.

Poster #: EDU-053

Imaging Susceptibility in Intracranial Tumors

Abdullah Alhammad, *Radiology, Children's Hospital of Eastern Ontario, OTTAWA, ON, Canada, rad982@gmail.com;* Nishard Abdeen, MD

Purpose or Case Report: Susceptibility weighted imaging (SWI) is a relatively new sequence based on phase differences induced by variation in local tissue susceptibility. Our goal is to review the utility of this sequence in the diagnosis and follow up of intracranial neoplasms.

Methods & Materials: At our institution, a tertiary care paediatric hospital, SWI is a component of all initial and follow up examinations. All patients with intracranial neoplasms who had undergone SWI between January 2010 and October 2012 were reviewed, and those with instructive findings on SWI were included in this pictorial essay. We focused on those findings which were useful for diagnosis of the initial tumour.

Results: A wide range of neoplasms were included including anaplastic astrocytoma, glioblastoma muliforme, meningioma, choroid plexus carcinoma, choroid plexus papilloma, germinoma, PNET medulloblastoma, ependymoma, atypical teratoid rhabdoid tumour.

The SWI findings in the above cases are presented in the context of the current literature. The physical basis of the SWI method as well as the image processing specific to SWI will be described, in order to facilitate understanding of its unique sensitivity to calcification, haemorrhage, and intratumoral vascularity.

Conclusions: SWI is sensitive to intratumoral vascularity, hemorrhage and calcification, and has an important role in the characterization of intracranial neoplasms.

Poster #: EDU-054

Withdrawn

Poster #: EDU-055

Pediatric Jaw Lesions

Tushar Chandra, MD, *Medical College of Wisconsin, Milwaukee, WI, drtusharchandra@gmail.com;* Mohit Maheshwari, Teresa Kelly, Bhawna Chandra, Tejaswini Deshmukh, Subramanian Subramanian, MD

Purpose or Case Report: Jaw lesions are not uncommon in pediatric population. They differ from adult counterparts in several aspects including spectrum of pathology, prevalence, imaging features, prognosis and therapy. The aim of this exhibit is to familiarize the radiologist with the spectrum and imaging features of various common and uncommon lesions of maxilla and mandible in children.

Methods & Materials: 1.We will briefly discuss the relevant anatomy of the pediatric jaw

2.We will categorize these lesions according to the imaging features

3.We will illustrate the imaging features of these lesions and pertinent specific pointers helpful in making the diagnosis.

4. Additionally, we will provide a succinct overview of the imaging algorithm for differential diagnosis of these lesions.

Results: Many common as well as uncommon lesions including, but not limited to rhabdomyosarcoma, ameloblastoma, radicular cyst, dentigerous cyst, odontogenic keratocyst, odontogenic myxoma, lymphoma, myofibroma will be discussed in the exhibit. Radiographs, CT and MRI images will be used to portray characteristic imaging appearances and key imaging signs of these conditions.

Conclusions: Pediatric jaw lesions are a diverse group with overlapping imaging characteristics. However, these diverse lesions have different surgical approaches and hence proper imaging evaluation is of utmost importance. Combining plain radiography with cross sectional imaging improves the characterization of these lesions. This exhibit will facilitate the radiologist in proper evaluation of these lesions.

Poster #: EDU-056

Kinematic MRI: Application and Utility in Evaluation of Cervical Spine Instability in Children

Raghu Ramakrishnaiah, MBBS.,FRCR, **Ruba Khasawneh, MD,** *Radiology, Arkansas Children's Hospital, Little Rock, AR, khasawneh_r@yahoo.com;* Gregory Albert, Chetan Shah, Danny Meek, Charles Glasier

Purpose or Case Report: Flexion and extension radiographs or fluoroscopy are the current standard medical practice for

assessing the stability of the cervical spine in patients with potential cervical spine instability. Radiographs are adequate in demonstrating the bone details but have limitation in assessing the biomechanical changes which occur in the soft tissues. The purpose of this exhibit is to demonstrate a novel kinematic MR technique for assessment of bony and soft tissue biomechanical changes that occur in the vertebral column, anterior and posterior longitudinal ligaments, intervertebral discs, spinal cord, thecal sac and the subarachnoid space during flexion and extension in patients with Down's syndrome, post traumatic ligamentous injury and congenital segmentation anomalies who may have potential cervical spine instability. To the best of our knowledge, this is the initial experience of kinematic MRI in children for cervical spine instability

Methods & Materials: A detailed description of the MRI technique for dynamic MRI study of the cervical spine for assessment of potential cervical spine instability will be presented under the following headings

a) Patient education
b) MRI sequence and parameters
c) Post-processing

The following objective measurements will be demonstrated

a) Segmental restriction in motion of the cervical spine.
b) Thecal sac compression
c) Spinal cord compression and flattening
d) Variation in the subarachnoid space dimensions
e) Space available for the cord and the degree of spinal canal stenosis

A comparison with the flexion and extension radiography will be made.

Advantages and limitation of kinematic MRI versus radiographic evaluation of cervical spine instability will be discussed

Results: Kinematic cine MRI evaluation of the cervical spine in patients with potential cervical spine instability is a dynamic, non invasive technique providing detailed evaluation of the cervical thecal sac, subarachnoid space, spinal cord, ligaments as well as segmental motion restriction of the cervical spine.

Conclusions: Further studies are required to objectively compare the routine flexion/extension radiographic series to kinematic MRI data.

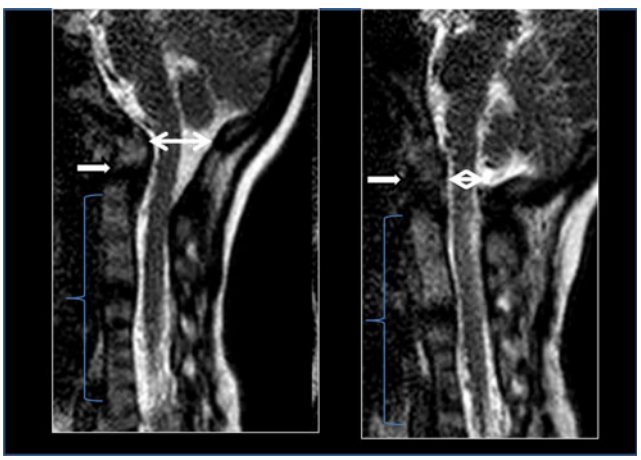

Flexion (Fig:1) and Extension (Fig:2) Images from a kinematic cine MRI sequence in a patient with Klippel-Feil syndrome. There is reduction of thecal sac dimension in extension (double arrow) and abnormal segmental mobility between the odontoid process Fused C2 and C3 vertebral body (arrow). Note the near complete lack of mobility from C2 through C7 (Left brace)

Poster #: EDU-057

Utility of Susceptibility Weighted Imaging in Pediatric Neurological Disorders

Swati Mody, MD, *Pediatric Imaging, Children's Hospital of Michigan, Detroit, MI, smody@dmc.org;* Aparna Joshi, MD

Purpose or Case Report: Susceptibility weighted imaging (SWI) is high resolution 3D gradient echo sequence that utilizes magnitude and filtered-phase with post processing to accentuate the paramagnetic properties of blood products. It is highly sensitive in the detection of intravascular venous deoxygenated blood as well as extravascular blood products. The sequence is also sensitive to iron and calcification, amd helps in differentiating between hemorrhagic products and calcification. SWI is being increasingly used clinically for pediatric neuroimaging. The purpose of exhibit is to review to the utility of SWI in pediatric neurological disorders.

Methods & Materials: A retrospective review of PACS was performed to identify MRI examinations of the brain where SWI was performed from 2008 to date at our institution. Multiple examples of characteristic imaging findings on SWI are presented in the exhibit with a review of the literature.

Results: SWI as an adjunct to conventional MRI sequences plays an important role in evaluation of multiple conditions such as 1) Traumatic brain injuries, in detection of microhemorrhages; 2) Vascular malformations, especially slow-flow malformations such as cavernous angiomas, capillary telangiectasia and developmental venous anomalies; 3) Stroke, in identification of hemorrhagic stroke, areas of decreased perfusion and acute thromboemboli in occluded vessels; 4) Hemiplegic migraine; 5) Phakomatoses, including Tuberous Sclerosis and Sturge-Weber Syndrome; 6) Infections, such as congenital cytomegalovirus and neurocysticercosis; 7) Brain tumors, in identification of calcification and hemorrhage; 8) Venous sinus thrombosis and venous stasis, in conditions such as hypoxic-ischemic injury; 9) Metabolic disorders with mineral deposition.

Conclusions: The findings on SWI in a variety pediatric neurologic disorders are often more striking and more specific than on conventional sequences. As such, SWI

provides useful additional diagnostic and prognostic information in evaluation of many pathologies.

Poster #: EDU-058

Withdrawn

Poster #: EDU-059

Bone Scintigraphic Findings in MRSA Osteomyelitis

Patricia Cornejo, MD, *Pediatric Radiology, Phoenix Children's Hospital, Phoenix, AZ, pcornejo@phoenixChildren's.com;* Gerald Mandell, MD

Purpose or Case Report: Staphylococcus aureus remains the most common etiologic agent of acute osteomyelitis in children. Recently, methicillin-resistant S. aureus (MRSA) has emerged as a major pathogen. MRSA leads to more aggressive cases of osteomyelitis. Abscesses and extraosseous involvement are commonly seen. Whole body bone scan shows a characteristic pattern of multifocal involvement which is important to recognize so that complete and proper medical and surgical medical therapy can be instituted. The acute lesions are frequently photopenic because of pressure on vascular supply by the purulent material and intraosseous abscess formation. MR imaging is very sensitive for extraosseous findings in MRSA osteomyelitis and should be perfomed to better define these processes.

Our purpose is to review bone scan findings indicative of MRSA and their correlation with MRI.

Methods & Materials: We performed retrospective analysis of a small group of patients with diagnosis of MRSA osteomyelitis, aged from 23 months to 14 years. The patients underwent three phase bone scan and Gadolinium-enhanced MRI.

Results: Bone scan showed long segment and multifocal involvement in 3 of 5 patients with areas of abnormal increased and decreased uptake. Patients with more localized disease also demonstrate a heterogeneous pattern of increased and decreased uptake within the area involved. Joint involvement was seen in four cases. Bone scan abnormalities correlated well with MRI findings of severe and extensive bone disease, abscess formation, muscle, joint and soft tissue involvement.

Conclusions: Community acquired MRSA osteomyelitis is a severe form of infection characterized by multifocal osseous involvement and abscess formation with increased frequency of extraosseous complications including pyomyosistis and septic arthritis. Bone scan findings in our patients correlate well with MRI and were useful for assessment of multifocal disease and follow-up treatment.

Poster #: EDU-060

Avoidable Image Quality Problems in I-123-MIBG Imaging

Michael Gelfand, MD, *Cincinnati Children's Hospital, Cincinnati, OH;* Susan Sharp, Brian Weiss

Purpose or Case Report: I-123-MIBG imaging is a standard part of neuroblastoma evaluation. Different techniques used for I-123-MIBG image acquisition and processing can cause wide variations in image quality. As a referral center for I-131-MIBG therapy, we receive many I-123-MIBG scans from referring hospitals, including other children's hospitals. The outside I-123-MIBG examinations frequently have image quality problems that limit the interpretation and utility of the examinations. Our purpose is to discuss ways in which image quality can be optimized.

Methods & Materials: Examples of I-123-MIBG studies with suboptimal image quality will be presented and solutions will be discussed.

Results: Image quality problems we address will include:

1. Inappropriate collimation for general diagnostic and pre-therapy I-123-MIBG imaging. In addition to the 159 keV (83% abundant) photon used for imaging, there are several low abundance high energy photons (<3%, 248–784 keV) that penetrate low energy high resolution collimator septae causing a non-linear "haze" of scattered photons, particularly in school age and adolescent patients. This problem disappears with use of a medium energy collimator.
2. Inappropriate collimation for post-I-131-MIBG therapy imaging with I-123-MIBG. Patients who receive MIBG therapy are re-studied 6 weeks after the I-131-MIBG therapy. Even minimal amounts of residual I-131 can cause severe image degradation unless there is appropriate collimation. High energy I-131 collimation may be required.
3. SPECT images are often presented as unnecessarily small secondary capture images that are difficult to interpret.

Conclusions: I-123-MIBG image quality can be optimized with appropriate techniques for image acquisition and processing.

Poster #: EDU-061

New Onset Childhood Leukemia: Elusive Muskuloskeletal Imaging Findings

Srikala Narayanan, MD, *Division of Pediatric Imaging, Massachusetts General Hospital, Boston, MA, snarayanan3@partners.org;* Katherine Nimkin

Purpose or Case Report: Childhood leukemia can have a variety of presentations with elusive and non-specific imaging findings. Our objective is to present cases of

childhood leukemia that were diagnostic challenges at presentation.

Methods & Materials: Retrospective review of interesting case folders and imaging database search engine from 2004 to 2012 of pathology proven cases of leukemia. Plain radiographs, CT and MRI of these cases will be presented.

Results: We had several challenging cases. One patient had diffuse marrow abnormality with acute medullary infarction. Erythroid hyperplasia was initially suspected. Two cases had joint effusion, synovitis and soft tissue edema suggesting septic arthritis and/or myositis. In one of these two cases, initial workup raised concerns for inflammatory arthritis and non-accidental trauma. One case had radiation changes to bone marrow from a previous malignancy, creating a diagnostic challenge in identifying subtle changes of leukemic infiltration of the marrow. One young child with compression fractures and osteopenia on radiographs was initially felt to have a metabolic bone disorder. Subtle diffuse bone marrow infiltration on MRI was initially overlooked in that case.

Conclusions: Acute leukemia represents more than one-third of pediatric malignancies. Clinical and imaging findings are often elusive at initial presentation. We review a variety of musculoskeletal imaging findings in this setting, including discussion of pediatric bone marrow pearls, patterns and pitfalls. Early diagnosis of acute leukemia in children is essential for prompt management. A review of diagnostically challenging cases should help to elucidate the range of imaging findings in this setting.

Poster #: EDU-062

Pediatric Emphasis Diagnostic Radiology Alternative Pathway (PEDRAP): An Update

Erin Horsley, DO, *Hahnemann University Hospital, Philadelphia, PA;* Raphael Yoo, Robert Koenigsberg, Eric Faerber

Purpose or Case Report: The Pediatric Emphasis Diagnostic Radiology Alternative Pathway was implemented by the American Board of Radiology in 2005 in response to the nationwide shortage of Pediatric Radiologists. Our program was accepted as a PEDRAP training site. Although the ABR discontinued this program, we have successfully continued the program, with a new program which allows radiology residents to focus on pediatric radiology during their residency years. The purpose of this poster is to share our experience with the program and discuss the curriculum's advantages and shortcomings.

Methods & Materials: The pediatric radiology tract is a separate NRMP position. The traditional PEDRAP candidates complete 28 four-week rotations at the parent institution and 24 four-week rotations at the affiliated children's hospital. Currently, there are two PEDRAP residents in our program. The pediatric radiology tract program is structured with the candidates completing 36 four-week rotations at the parent institution and 16 four-week rotations at the affiliated children's hospital.

Results: Our curriculum has proved to be successful. To date, all of the PEDRAP graduates have successful passed the radiology board examinations. The graduates have felt they have mastered the essentials of a fellowship trained Pediatric radiologist upon graduation from our program, fully supported by the pediatric radiology faculty.

Conclusions: We wish to draw attention to this alternative pathway which will attract many new recruits into the field of pediatric radiology. Our curriculum parallels the new approach to radiology education and allows residents with an affinity towards pediatric radiology to complete a fellowship during residency years. It would be encouraging for the PEDRAP residents and pediatric radiology tract residents to be eligible for the pediatric CAQ examination after completing a 1 year fellowship in any radiologic subspecialty or a 2 year faculty position as a pediatric radiologist at an ACGME approved institution, based on previous success on radiology board examinations and continued interest.

Poster #: EDU-063

Ergonomics in the Radiology Workspace

Kimberly Fagen, MD, *Walter Reed National Military Medical Center, Bethesda, MD, kimberly.fagen@med.navy.mil;* Ellen Chung

Purpose or Case Report: Modern technology has made Radiology a much more sedentary occupation, placing radiologists at risk for deleterious health effects. Ergonomics should be an important consideration in the way we design and use our workspaces. In addition to the known repetitive motion injuries for which radiologists are at risk, recent research highlights significant risk of morbidity and even shortened lifespan related to a sedentary lifestyle. For example, subjects who sit for 8 hours at work have a much lower level of cardiovascular health, even if they exercise for 30 min or more 5 days a week, than subjects who do not exercise but sit for only 3–4 h per day. Neck, back, and upper extremity pain are also known risks of prolonged sitting at a computer. Eye strain, leading to chronic headaches, may occur if the computer monitor and image screen position is not optimized (15–50° below eye level) and if periodic breaks are not taken.

These risks can be reduced with the use of ergonomically designed workstations, particularly those that allow standing and/or various positions. Treadmills can be placed in front of reading stations. Reading stations should be adjustable so that the position of the monitor can be tailored to the user. Purchase of ergonomic mouse, keyboard and foot supports would also help. Sitting while engaging the core to maintain balance is less risky that sitting in a standard chair. Adjustable chairs that require balancing on an exercise ball are available. Eye strain can be reduced by focusing on a distant object even for just 20 s every 20 min. Adjustable, indirect lighting fixtures reduce glare from computer monitors and may reduce eyestrain.

Educating staff and training radiologists in our departments about ergonomics as well as providing personalized analysis and instruction to radiologists at the workspace will help them design and integrate better ergonomic practices into their daily work routine. A survey of work habits before and after such interventions would make a useful Process Quality Improvement project. Awareness of the risks of a sedentary lifestyle along with use of ergonomic improvements in the work place may change radiologists' workplace behavior, decrease current and future symptoms related to poor ergonomic practices, and increase efficiency, accuracy and job satisfaction.

Poster #: EDU-064

Pediatric Vascular Support Device Placement: The Good, Bad and Ugly

Shelby Bennett, MD, *Dept of Radiology, University of Chicago, Chicago, IL, bennettshelbyj@gmail.com;* Barry Hansford, Seng Ong, Kate Feinstein, MD

Purpose or Case Report: 1. Demonstrate preferred positioning of pediatric vascular support devices including arterial and venous umbilical catheters, and peripherally inserted central catheters

2. Discuss relevant vascular anatomy, including normal anatomic variants, necessary for understanding the appropriate catheter course on radiographic examinations

3. Provide pictorial examples of malpositioned catheters, organized by catheter type, and discuss specific catheter associated position-based complications

Methods & Materials: Vascular support devices are commonly deployed in the care of pediatric patients. The radiologist is routinely tasked with confirming optimal placement of vascular support devices in an ever increasing number of patient encounters. It is important to have a sound understanding of the appropriate course and location for catheter tip termination since a malpositioned catheter may result in catastrophy.

Results: In the spirit of the classic American western, this exhibit divides the location of vascular catheters into the good, the bad and the ugly. For a catheter to merit classification as 'the good' the correct course must be followed and the tip is nothing short, or long, of optimal. The section describing 'good' catheter placement includes a discussion of key radiographic landmarks for appropriate catheter positioning as well as the relevant vascular anatomy, with examples of normal anatomic variations, that radiologists should know when evaluating vascular catheter placement.

Classified as 'the bad' are examples of catheters that, although likely effective, have suboptimal tip positioning or have been associated with higher rates of complications.

For a vascular catheter position to be 'the ugly', it is not only likely ineffective, but its location mandates immediate communication to the clinical service so that repositioning or removal is expedited in an effort to prevent potentially serious complications.

Radiographs of 'bad' and 'ugly' positions are divided by catheter type with a corresponding discussion of position-specific associated complications.

Conclusions: This educational exhibit will aid the radiologist's evaluation by providing a template for normal catheter placement followed with numerous examples of malpositioned catheters and a discussion of possible complications.

Poster #: EDU-065

Radiology-Pathology Conferences of Children's Hospital of Michigan - A Live Teaching File For The Apple iPad

Luis Goncalves, MD, *Detroit Medical Center - Children's Hospital of Michigan - Division of Pediatric Radiology, Detroit, MI, lgoncalv@med.wayne.edu;* Aparna Joshi, Janet Poulik, Thomas Slovis, Michael Zerin

Purpose or Case Report: Correlation between abnormal imaging and pathology findings is a tremendously rich teaching resource. At Children's Hospital of Michigan (CHM), Radiology-Pathology (RADPATH) conferences occur on a monthly basis, with 4–5 cases presented jointly by the Divisions of Pediatric Radiology and Pediatric Pathology. Although some of the most interesting and intriguing cases are presented monthly at RADPATH conferences, we are able to reach only a limited audience, composed of those who can be physically present in the conference room. Our goals are to record, peer-review, and disseminate the presentation content and discussions that occur monthly at the RADPATH conferences of CHM to a wide audience. We chose the Apple iBook format for this purpose because: 1) it allows seamless incorporation of static images, video clips,

and text into an electronic book format; 2) it allows easy creation of quizzes; 3) the software to produce an iBook (iBooks Author) is freely available; and 4) the iBook can be easily distributed to an audience that is as wide as we wish to reach.

Methods & Materials: The content of CHM RADPATH conferences presented from July 2011 to April 2013 will be recorded in iBook format. We will make the entire teaching file available free of charge to the Society of Pediatric Radiology members who attend the 2013 Annual meeting. The iBook layout format will be: 1) imaging studies initially presented as unknowns, 2) labeled imaging findings; 3) differential diagnosis; 4) pathology images; 5) discussion with review of the literature; and 6) quiz.

Results: The following conditions, among others, are included in the teaching file: bronchogenic carcinoid, skull base osteosarcoma, adrenal cortical carcinoma, invasive sinonasal mucormycosis, subcutaneous granuloma annulare, Rosai Dorfman disease, metastatic neonatal neuroblastoma, paratesticular ectomesenchymoma-rhabdomyosarcoma, pleomorphic adenoma of the submandibular gland, laryngeal inflammatory myofibroblastic tumor, and pleuropulmonary blastoma type Ir.

Conclusions: We present diagnostic imaging findings and pathology correlation of a wide spectrum of either interesting or rare pediatric conditions in a portable electronic format that is intended to reach an audience much wider than those who can normally attend the RADPATH conferences held monthly at Children's Hospital of Michigan.

Poster #: EDU-066

Abdominal Findings in Non-accidental Trauma: A pictorial review

Erin Horsley, DO, *Hahnemann University Hospital, Philadelphia, PA;* Mea Mallon, MD, Archana Malik

Purpose or Case Report: Typical osseous and intracranial findings in non-accidental trauma in children are well characterized. This presentation provides a review of visceral findings of non-accidental abdominal trauma in children.

Methods & Materials: We retrospectively identified pediatric patients from our imaging database with abdominal injuries resulting from non-accidental trauma. Medical records were reviewed and imaging studies were correlated with clinical history and child protective services where indicated.

Results: A retrospective study over a 2 year period demonstrated a variety of patterns of visceral injury related to non-accidental trauma. Examples include: Pancreatic laceration with associated pseudocyst, hepatic laceration, hepatic contusion, splenic laceration, adrenal gland hemorrhage, and shock bowel syndrome. A multi-modality review of these cases is presented with correlation to the clinical histories and patient demographics.

Conclusions: A radiologist must be aware of abdominal injuries that can occur with or without more typical findings of non-accidental trauma.

Poster #: EDU-067

Lymphangiectasia with Radiologic-Pathologic Correlation

LaDonna Malone, MD, *Diagnostic Radiology, Children's Hospital Colorado, Aurora, CO, ladonna.malone@Children'scolorado.org;* Jason Weinman, Laura Fenton, MD, Lorna Browne

Purpose or Case Report: Background: Lymphangiectasia is a rarely encountered lymphatic dysplasia characterized by lymphatic dilation without proliferation. While it can occur in any organ system, the most common locations are pulmonary, intestinal and osseous lymphatics. Typically presenting in neonates, it historically had a poor prognosis, however recent advances in care including surgical resection of intestinal involvement and substitution of long chain fatty acid with medium chain fatty acids have allowed survival beyond infancy in some.

Objective: To illustrate the imaging features of lymphangiectasia on cross-sectional imaging techniques (CT and MRI) and correlate with pathologic appearances.

Methods & Materials: A 5 year retrospective review of cases of lymphangiectasia was performed at a tertiary care pediatric hospital. Inclusion criteria were age less than 18 years, cross-sectional imaging demonstrating lymphangiectasia, and pathologic correlation.

Results: Twelve patients met inclusion criteria: pulmonary (n=6), intestinal (n=4) and diffuse lymphangiectasia (n=2). Age range was 1 day–16 years (median age=6 months).

The six cases of pulmonary lymphangiectasia presented in the neonatal period with smooth thickening of interlobular septa, scant ground glass opacities, and pleural effusions. Two-thirds of patients had complex congenital heart disease.

Two patterns of intestinal lymphangiectasia were recognized; widespread intestinal thickening presenting in infancy and focal thickening presenting in adolescence. Both patterns were associated with enlargement of the retroperitoneal lymphatics.

The two patients with diffuse disease manifested as widespread lymphatic dilation (see Figure 1) and multi-organ involvement with osseous involvement in one case. Pathological evaluation demonstrated dilated lymphatics in the intestinal villi, pleura and interlobular septae.

Conclusions: Lymphangiectasia is rarely encountered in the pediatric population and frequently poses a diagnostic dilemma, however recognition of the imaging manifestations can help confirm this diagnosis and enable appropriate therapies to be initiated.

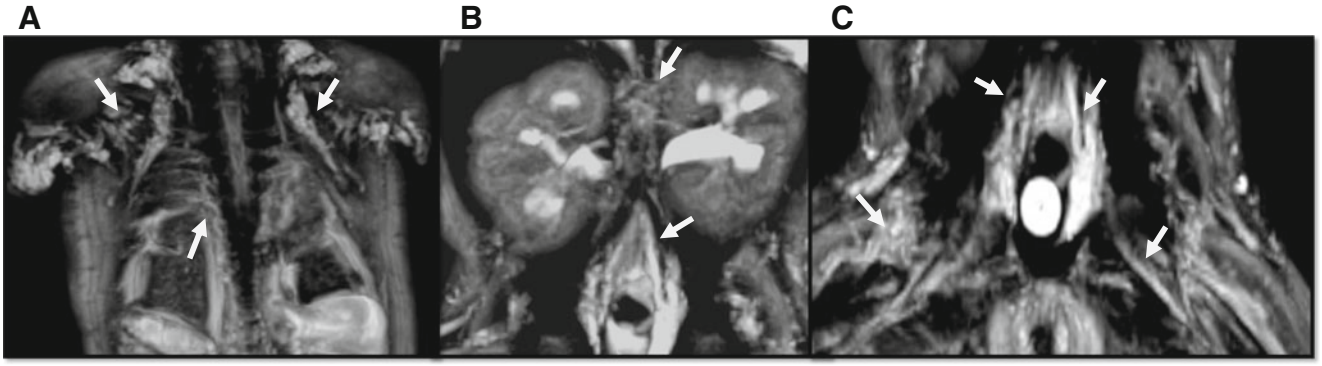

Figure 1:
6 week old male infant with recurrent chylothoraces and soft tissue swelling
Coronal MIP images from a Single Shot T2 weighted sequence with fat suppression of the chest (**A**), abdomen (**B**) and pelvis (C) demonstrating dilation of the upper extremity, thoracic and subcostal, retroperitoneal and pelvic lymphatics (arrows).

Poster #: EDU-068

"Lumps and Bumps" referred from Pediatricians: What is encountered on a superficial ultrasound?

Stephanie Coleman, MD, MPH, *Radiology, Boston Medical Center, Boston, MA, scoleman82@gmail.com;* Heather Imsande, MD, Powen Tu, Ilse Castro-Aragon, Bindu Setty, M.D

Purpose or Case Report: Pediatric patients are often referred to ultrasonography for palpable "Lumps and Bumps." The majority of these lesions are benign and discernable on physical exam, therefore not requiring imaging. However, when the clinical presentation is atypical and diagnosis uncertain, the patient is often referred for ultrasound, which can help to localize, evaluate extent, characterize, and determine the etiology of these lesions. Ultrasound serves as an excellent screening tool and helps determine the next best step in management, as well as helping to alleviate concerns of the patient, parent, and pediatrician.

Methods & Materials: In this educational exhibit, we discuss the sonographic characteristics of different superficial lesions encountered in pediatric patients, including features suggestive of malignancy. We will use multiple ultrasound images from our facility, as a pictorial guide, to aid in discussion and education.

Results: We will discuss a variety of such lesions seen from infancy through adolescence. Some of the infantile lesions include fat necrosis, neonatal mastitis, omphalitis, cephalhematoma, hemangioma, and fibromatosis coli. The most common cause of referral of "Lumps and Bumps" in different regions of the body are lymph nodes and lymphadenitis, which can have a varied appearance. Congenital lesions such as branchial cleft cysts and tumors such as pilomatrixoma and rhabdomyosarcoma will be discussed. Infection or inflammation of the submandibular or parotid glands can have atypical presentation and also commonly referred to ultrasound. Lesions occurring at any age and in any region of the body, from scalp to genitalia, will also be illustrated, including lipomas, hematomas, epidermal inclusion cysts, and abscesses. Lastly, we will illustrate normal anatomic variants such as asymmetric costochondral junctions, ovary in an inguinal hernia, axillary tail of the breast, all of which can present as a clinical challenge to pediatricians.

Conclusions: Ultrasound is non-invasive and does not expose patients to radiation. If used effectively and systematically, it can provide an insight to the etiology of " Lumps and Bumps" and enable the pediatrician to offer appropriate reassurance or to direct further work up if needed.

Poster #: EDU-069

MRI Evaluation of Lung Parenchyma, Airways, Vasculature, Ventilation and Perfusion: Review of State of the Art Imaging Techniques with Pediatric Applications

Mark Liszewski, MD, *Radiology, Boston Children's Hospital, Boston, MA, mark.liszewski@Children's.harvard.edu;* F. William Hersman, Talissa Altes, Yoshiharu Ohno, Simon Warfield, Edward Lee, MD, MPH

Purpose or Case Report: Given its lack of ionizing radiation, MRI is an attractive non-invasive imaging modality particularly for pediatric patients. However, many physical properties of lung parenchyma pose technical challenges to obtaining high quality MR images including inherent low signal-to-noise ratio, magnetic susceptibility differences at lung-air interfaces, and respiratory motion. The overarching goal of this educational exhibit is to present several newly developed MR imaging techniques which can overcome these challenges in the evaluation of various thoracic diseases and discuss their advantages and limitations in current clinical practice in children.

Methods & Materials: The current literature is reviewed. Up to date MR imaging techniques and protocols optimized for evaluation of lung parenchyma, airways, vasculature, ventilation and perfusion are presented with examples in both healthy and disease states in pediatric patients.

Results: MRI techniques and protocols optimized for the evaluation of the lung parenchyma, airways, vasculature, ventilation and perfusion are presented. Techniques including fast breath hold T1- and T2-weighted, respiration-triggered T2-weighted and contrast-enhanced fat-saturated three dimensional gradient echo (3D-GRE) sequences to evaluate lung nodules, masses, consolidations and airways are discussed. The use of steady-state free precession (SSFP) sequences and contrast enhanced MR angiography (MRA) in the evaluation of pulmonary vasculature in cases of pulmonary embolus and vascular anomalies is presented. Ventilation and perfusion MR imaging techniques utilizing hyperpolarized gas, dynamic contrast-enhancement (DCE), arterial spin labeling (ASL), two-compartment inversion recovery (TCIR) and Fourier decomposition (FD) are also reviewed.

Conclusions: New MR imaging techniques and protocols reviewed in this exhibit provide useful diagnostic tools in the evaluation of various thoracic diseases without the use of ionizing radiation, making them particularly attractive for pediatric patients.

Poster #: EDU-070

Pulmonary Ground Glass Opacities: From the Cradle Through Puberty (and beyond)

Eric Eutsler, *Radiology, Yale-New Haven Hospital, New Haven, CT, ;* Cindy Miller, MD

Purpose or Case Report: When reviewing images of the lungs, residents in radiology traditionally were first taught to distinguish between alveolar and interstitial disease. Currently beginning trainees are introduced to an additional term which has found a prominent place in the radiographic lexicon: ground glass opacity. This exhibit will review the term's definition and will demonstrate the wide range of pediatric pathology which can be characterized by the descriptor of ground glass opacity. It will also show how the differential diagnosis of ground glass opacity varies based on such features as gestational age at birth, chronologic age, symptoms, degree of immunocompetence, and extent of involvement of the lungs.

Methods & Materials: The radiologic file over the past 5 years of the Children's Hospital at our institution was reviewed with input from referring clinicians in order to select cases in which ground glass opacities represented the predominant pattern.

Results: In newborn premature infants, nearly every case of ground glass opacity represented surfactant B deficiency. In term infants such entities as neuroendocrince hyperplasia of infancy (NEHI) and surfactant ABCA3 deficiency, although uncommon, become more important considerations. In older children, disorders of surfactant dysfunction still need to be considered, but most cases of ground glass opacity were determined to represent diseases typically considered "adult diseases" including alveolar proteinosis, eosinophilic pneumonia, organizing pneumonia, Pneumocystis pneumonia, pulmonary veno-occlusive disease, and ARDS. In rare cases, diseases resembling surfactant ABCA3 deficiency are seen in older children and are determined via biopsy to represent such disorders as cellular interstitial pneumonitis and pulmonary interstitial glycogenosis.

Conclusions: 1. It is important to distinguish between ground glass opacity and consolidation when formulating a list of differential diagnoses. 2. There are several entities characterized by ground glass opacity which are strictly diseases of infants and children including some types of surfactant deficiency and NEHI. 3. Clinical features including degree, if any of prematurity; immune status; and assessment of response of radiographic findings to therapy; in combination with radiographic

features including distribution of disease (e.g. peripheral vs central); presence or absence of air trapping often allow a definitive diagnosis to be made without requiring tissue confirmation.

Poster #: EDU-071

Radiographic presentation of acute lung injury due to accidental aspiration and inhalation in children

Joanna Kusmirek, *UW Madison, Madison, WI, jkusmirek@uwhealth.org;* Kara Gill, Bradley Maxfield

Purpose or Case Report: Unintentional injuries are the leading cause of death and disability for children ≥1 year of age, adolescents, and young adults in the United States. Unintentional injuries resulting in lung damage occur as a result of drowning, poisoning, ingestion/aspiration or smoke exposure. Respiratory compromise heavily influences morbidity and may determine the patient's outcome.

Drowning is a leading cause of accidental death in children <5 years of age in states where swimming pools or beaches are more accessible. Relatively frequent cause of morbidity and mortality in kids are fire-related injuries. 70% of fire-related deaths are caused by inhalation of toxic gases and smoke, rather than thermal injury. Importantly, radiographic findings may be seen 2–3 h after injury and may precede clinical deterioration. Poisoning is another significant health issue for children with more than 1 million cases of chemical ingestion occurring among children younger than 6 years of age as reported to the American Association of Poison Control Centers. According to 27th (2009) Annual Report of the AAPCC National Poison Data System, the most common substances in pediatric exposure (age 0–5) are cosmetics/personal care products (13%) and cleaning substances (9%).

The goal of this poster presentation is familiarize the audience with different radiographic findings as well as causes and presentations of accidental aspiration and inhalational lung injury in the pediatric population.

Methods & Materials: University of Wisconsin in Madison is a level 1 burn and trauma center for all ages serving a large area in Wisconsin. Search of our imaging database was performed for representative cases of acute lung injury secondary to accidental aspiration or inhalation in children. Available images and clinical data for each patient were reviewed.

Results: Multiple cases fulfilling the search criteria were found, including lung injury related to caustic, gasoline, acetone and hydrocarbon ingestion/inhalation. Several cases of near drowning (water and manure) and smoke inhalation lung injury were identified. Representative images were chosen for presentation.

Conclusions: Unintentional injuries are the leading cause of death and disability for children. Acute lung injury due to accidental aspiration and inhalation represent a relatively common problem in pediatric population. Therefore, it is imperative for radiologists to recognize the imaging patterns and complications associated with aspiration and inhalational injuries.

Poster #:EDU-072

The "Testy Testes": A Jeopardy Style Quiz on Pediatric Scrotal Imaging

Yang Bia, Nina Woldenberg, **Soni C. Chawla**, *Olive View-UCLA Medical Center, Sylmar, CA*

Purpose or Case Report: The pediatric scrotum houses a wide spectrum of pathologies that can be roughly divided into four major groups—congenital, acquired conditions/infections, tumors/masses, and acute/painful disorders. The congenital pathologies include cryptorchidism, hernia, hydrocele, meconium peritonitis, etc. The acquired conditions/infections include epididymitis, orchitis, and microlithiasis. The acute/painful disorders include testicular torsion, torsion of the testicular appendage, obstructed or strangulated hernia and testicular trauma. Tumors/masses include germ cell, gonadal stromal cell and others. For most of these entities, high-resolution ultrasonography is the best screening and diagnostic tool, allowing for rapid evaluation with no radiation risks to the patient. This presentation showcases the characteristic radiographic findings of the various scrotal pathologies, from the benign, to the bizarre, through a series of cases collected at our institution since 2007. Familiarity of these characteristic findings is recommended to enable correct diagnosis and prompt management.

Poster #: SCI-001

Adult-Based Imaging Facilities vs. a Children's Hospital: Comparison of CT Radiation Exposure with Outreach

Mary Harty, MD, *Medical Imaging, Nemours Alfred I duPont Hospital for Children, Wilmington, DE, mharty@nemours.org;* Celia Foster, Heidi Kecskemethy, BS, Leslie Grissom, MD

Purpose or Case Report: To assess the mean radiation dose as measured by CT dose index (CTDI) in a group of children whose images were acquired at adult-based imaging facilities and compare them to the dose for similar patients imaged at our children's hospital. The goal is to offer information and instruction to the adult facilities to help them to employ Image Gently principles and reduce radiation exposure to children in our geographic region.

Methods & Materials: A retrospective review was conducted on all pediatric CT scans performed by other

imaging facilities and referred to our children's hospital between January 2011 and July 2012. Studies acquired at our children's hospital between January 2011 and July 2011 were randomly selected to serve as a comparison group, matched for age or weight based on body site being evaluated. Images from referring children's imaging centers, studies that did not include dose reports, images containing other body sites, and patients lacking weight information were excluded from the study. We examined the following body sites: Abdomen, Abdomen/Pelvis, Abdomen/Chest, Chest, Chest/Abdomen/Pelvis, Head, and Sinus. We report on mean CTDI of the two body sites with the greatest sample sizes and power: Head and Abdomen/Pelvis (A/P). Head CTs were divided by age groups and A/P were grouped by weight. Student t-tests were performed for significance.

Results: CT scans on 655 patients were performed by 57 adult imaging facilities. Complete information was available for 343 patients. Comparative CT scans acquired by our hospital on 379 patients were reviewed. Mean CTDI values for Head CT by age group were consistently higher in scans acquired by adult-based facilities (Table 1). Further, larger standard deviations were also noted by these adult facilities indicating a greater range of radiation exposure with more variability. Similar results were observed in the A/P CT scans from adult facilities, with consistently higher mean CTDI values by weight category and with larger standards of deviation. We are in the process of contacting the adult facilities from this study to provide our findings and suggestions for dose reduction.

Conclusions: Although the Image Gently campaign has been encouraging dose reduction to protect children from unnecessary radiation, adult-based imaging centers in our geographic region continue to expose children to higher than necessary radiation doses. Pediatric imaging centers can serve as a resource to help adult facilities improve imaging safety for children.

Table 1: Head CT CTDI Results

	Adult Facility Scans	Children's Hospital Scans					
Age Group (years	n	Mean age (years)	Mean CTDI (mGy) ± SD	n	Mean age (years)	Mean CTDI (mGy) ± SD	Mean CTDI p-value*
0–1	34	0.7	26.1±14.2	34	0.8	11.8±2.6	<0.0001
2–4	23	3.2	33.7±14.9	22	3.5	20.9±14.3	<0.0001
5–12	43	9.5	46.6±16.9	45	9.7	19.6±1.2	<0.0001
13+	55	15.7	61.5±18.5	55	15.9	19.3±3.1	<0.0001

*Student's *t*-test

Poster #: SCI-002

Evaluating radiologic management and treatment outcomes of suspected pediatric appendicitis in a single healthcare system

Andrew Moriarity, MD, *Henry Ford Hospital, Detroit, MI;* Safwan Halabi, Nour Baki

Purpose or Case Report: To present a single health system's experience with emergency radiologic management of pediatric patients with suspected appendicitis. Treatment pathways and outcomes for patients <18 years-old presenting to the emergency department and initially evaluated with transabdominal right lower quadrant ultrasound are examined.

Methods & Materials: After IRB approval, a database search for all appendix ultrasound (US) exams performed between January 2005 and June 2012 for patients <18 years-old was performed. 845 patients received dedicated transabdominal right lower quadrant US for evaluation of acute appendicitis. A chart review was performed to evaluate the US exam results and to determine patient outcomes. Patient outcome categories include: (1) No further workup, discharged home; (2)

Additional diagnostic imaging performed (e.g. CT abdomen and pelvis); (3) Admission to hospital for observation or surgery; (4) Transfer to local children's hospital for observation or surgery.

Results: Of initial US exams, 3.9% (n=33) were reported as positive for appendicitis, 36.4% (n=308) were negative and the appendix was identified. The appendix was not visualized in 59.6% (n=504) of cases. Dedicated CT of the abdomen and pelvis was recommended by the radiologist in 30.1% of cases (n=260). CT was ordered in 39.2% (n=102) of recommended cases and in an additional 112 patients (19% of CTs) when no recommendation was made. CT was positive in 15 cases performed after US recommendation, and in 13 cases performed without recommendation. Of the 88 patients admitted for observation, 22.9% had a positive US and 21.3% had a positive CT. Of the 136 were transferred to the local children's hospital, 15.4% had a positive US and 11.0% had a positive CT. Of the 44 admitted directly for surgery, 36.3% had a positive US and 25% had a positive CT.

Conclusions: Our health system is primarily serves adult patients, however pediatric patients make-up a significant volume of emergency department visits. The sensitivity, specificity and positive predictive value of transabdominal ultrasound are high in appropriately selected pediatric patient populations. The unnecessary use of CT in management of suspected pediatric appendicitis is on the rise nationally, and accounted for a significant portion of exams performed at our institution. Decision support tools, increased sonographer training and dedicated pediatric sonographers may all improve sonographic management of suspected pediatric appendicitis in adult-oriented centers.

Poster #: SCI-003

Phantom Iterative Reconstruction Technique (PIRT)- a quantitative ALARA method to test iterative reconstructions effect on image quality and dose in the pediatric population

Anne McLellan, Medical, *Radiology, Phoenix Children's Hospital, Phoenix, AZ, ayost@phoenixChildren's.com;* James Owen, John Egelhoff, John Curran, Jeffrey Miller, MD, Padmaja Naidu

Purpose or Case Report: Iterative reconstruction theoretically improves spatial resolution while decreasing CT dose/mAs. The purpose of our study was to demonstrate a replicable method, entitled Phantom Iterative Reconstruction Technique (PIRT), utilizing an ACR phantom, to test the effects of Iterative Reconstruction (IR) on image quality and dose in the pediatric population.

Methods & Materials: Utilizing an ACR phantom, PIRT was evaluated as a potential standardized method to assess image quality and dose between institutions and vendors. Image quality was evaluated for spatial resolution (SR), contrast resolution (CR), and homogeneity (H) per ACR criteria as mAs was decreased and levels of IR were increased.

Results: PIRT accurately measures data with ACR approved methods. As expected when mAs decreases, signal to noise (SNR) ratio and contrast to noise ratio (CNR) decrease while the standard deviation increases. Images become noisier as mAs is decreased. In contrast, as IR level increases, SNR and CNR increase and standard deviation decreases, so that an increased number of lower density lesions are visualized. At approximately the mid IR level (3–4) there is maximum benefit for spatial resolution, contrast resolution, homogeneity, and dose reduction. As IR is increased beyond this point, contrast resolution decreases so that lesions cannot be differentiated from background. At high IR levels, data becomes plasticized and subtle differences are lost. Preliminary results indicate there is 20%–30% dose reduction at an IR level of 2–4. There is less dose reduction savings with the pediatric population compared to adults as radiation doses are already decreased, with a narrower window for improvement in spatial resolution, contrast resolution and homogeneity.

Conclusions: The PIRT-Phantom Iterative Reconstruction Technique is a replicable low cost, ALARA method without patient radiation dose to evaluate Iterative Reconstruction's ability to improve dose reduction, spatial resolution, and contrast resolution. In the pediatric population, iterative reconstruction does demonstrate dose reduction and improved spatial resolution of 20–30%. However, because many pediatric doses are already low, the relative dose savings and improved resolution are not as great as in the adult population.

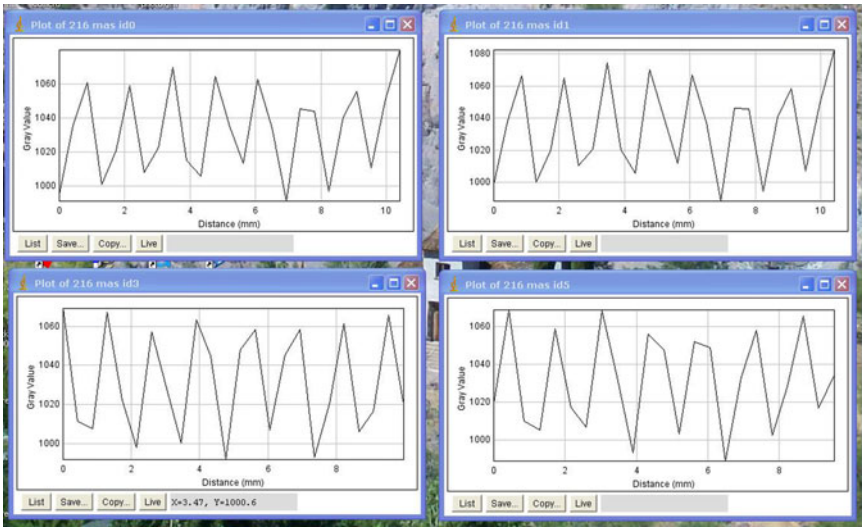
Plot of 216 mas id0
Plot of 216 mas id1
Plot of 216 mas id3
Plot of 216 mas id5
Gray Value
Distance (mm)
List
Save...
Copy...
Live
X=3.47, Y=1000.6

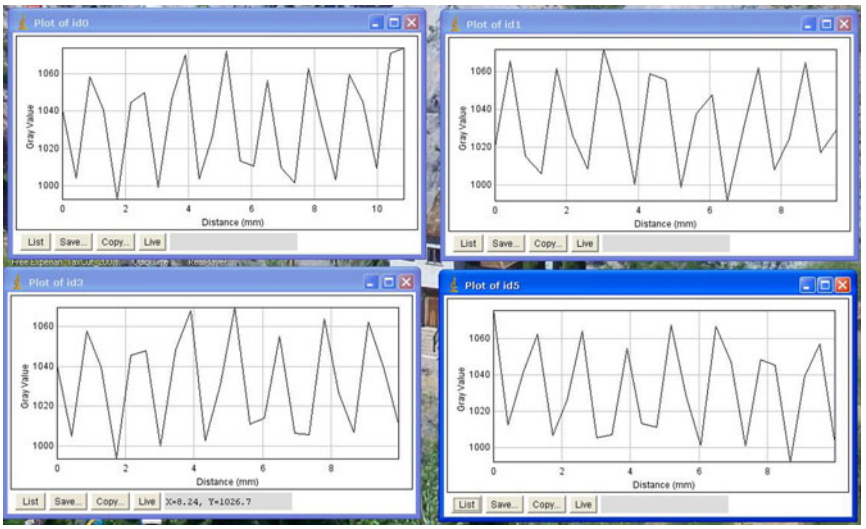
Plot of id0
Plot of id1
Plot of id3
Plot of id5
Gray Value
Distance (mm)
List
Save...
Copy...
Live
X=8.24, Y=1026.7

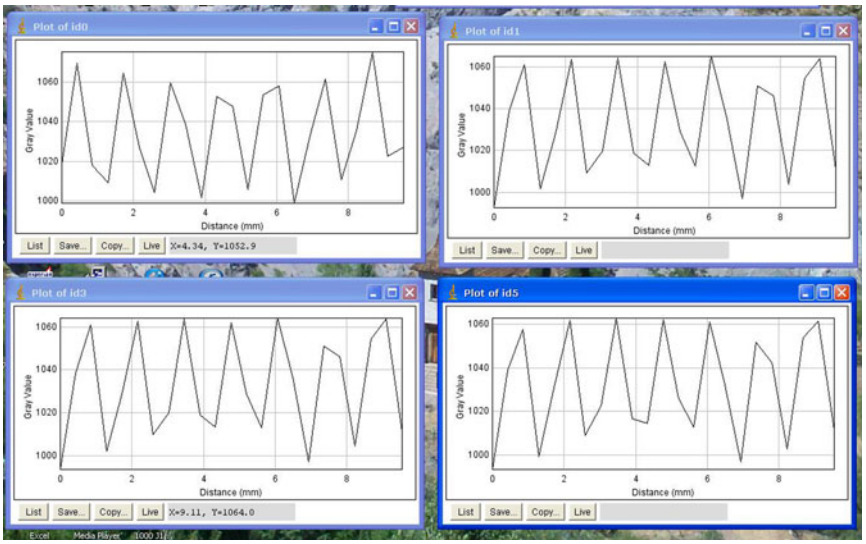
Plot of id0
Plot of id1
Plot of id3
Plot of id5
Gray Value
Distance (mm)
List
Save...
Copy...
Live
X=4.34, Y=1052.9
X=9.11, Y=1064.0

Poster #: SCI-004

Retrospective analysis of weight, exposure index and deviation index in neonatal chest radiography

Fred Dawson, *Riley Hospital for Children, Indianapolis, IN, fdawson@iupui.edu;* Mervyn Cohen, Bruce Apgar

Purpose or Case Report: Exposure index (EI), which measures the radiation exposure to the detector, and deviation index (DI), which measures variation from an ideal target EI value, are excellent quality assurance tools for monitoring exposure consistency and variability. While monitoring the EI and DI for all newborn portable chest x-rays, we noted that there is a broad bell-shaped distribution. Outliers, considered to be exams where the DI >+3 (exposure is more than twice the target) or<−3 (exposure is less than half the target exposure), should be minimized as it leads to excessive radiation exposure or noisy images. We postulated that patient size is an important factor governing the distribution of EI and DI. While seemingly intuitive, concretely demonstrating how patient weights relate to EI and DI may explain to what extent some outliers are the result of patients being at the extremes of weight ranges rather than technologist or equipment error.

Methods & Materials: Our exposure parameters for all neonatal chest radiographs are patient weight dependent. Peak voltage is held constant at 66 kVp for all exams. Technologists subjectively place patients into 1 of 4 weight categories assigned a specific mAs (0.64, 0.8, 1.0, and 1.25) and the exposure index and deviation index are calculated for every exam. For this study, the kVp and mAs were recorded for each exposure (n=507) and the medical record was investigated to obtain the patient's weight on the day of the exam.

Results: For each group where kVp and mAs were constant, linear regression model was used to explore the relationship between patient weight and DI. The slope was found to be negative for each relationship indicating that both EI and DI decreased as the weight of the patients increased. The coefficient of determination (R^2) for the 0.64 mAs group (n=167) was 0.01. The 0.8 mAs (n=131), 1.0 mAs (n=114) and 1.25 mAs (n=95) groups had R^2 values of 0.025, 0.14 and 0.197 respectively. In addition, the data in aggregate was normalized to simulate the same exposure technique for all neonates regardless of group and the EI and DI were recalculated for simulated exposure. The normalized data also demonstrated a decrease in EI and DI with an increase in weight with a R^2 of 0.292.

Conclusions: The exposure index and deviation index are related to neonatal weight. Any quality assurance program using EI and DI to monitor neonatal chest exposures must take into account the variations that will occur because of differing babies weights.

Poster #: SCI-005

Systemic and pulmonary venous connections in heterotaxy syndrome: A review of 50 cases comparing MRI/CTA and echocardiography (echo)

Christopher Lam, MD, *Diagnostic Radiology, University of Texas Health Sciences in Houston, Houston, TX, christopher.z.lam@uth.tmc.edu;* Umakumaran Ponniah, Prakash Masand, Shiraz Maskatia, Shaine Morris, Rajesh Krishnamurthy, MD

Purpose or Case Report: Heterotaxy syndrome is often associated with complex anomalous systemic and pulmonary venous return. Precise delineation of the extra cardiac vasculature is thus critical for planning single-ventricle or 2-ventricle surgical repair. While echo is an excellent first-line modality to assess the neonate, evaluation of the extracardiac anatomy is often limited. MRI/CTA have subsequently emerged as valuable complementary tools to image the heterotaxy patient. However, there are few papers that quantify the incremental role of MRI/CT on management. This study has two parts, 1) to compare MRI/CTA to echocardiography in the evaluation of venous connections in heterotaxy, and 2) to document the distribution of anomalous venous connections in the heterotaxy subtypes.

Methods & Materials: 61 cases of heterotaxy that had a MRI or CTA at Texas Children's Hospital between 1999 and 2012 were reviewed. 11 were discarded because imaging was performed following initial surgery that no longer preserved the original heart anatomy. The remaining 50 were analyzed to categorize the anatomy of the SVC, IVC, hepatic veins, and pulmonary veins. Of note, 31 of these 50 cases were performed in the neonatal period. All prior available echocardiography results were then compared for diagnostic discrepancies.

Results: Of the 50 heterotaxy cases, 27 were asplenia, 18 polysplenia, three single right-sided spleens, and two single left-sided spleens. The distribution of venous connections is presented (Table 1). When comparing imaging modalities, 35 (70%) of the MRI/CTAs had an anatomic discrepancy with echocardiography. The most common source of error was characterizing pulmonary veins, which echocardiography incorrectly or incompletely described in 24 cases (48%). The

hepatic veins were discrepant in 18 cases (36%), SVC in 13 cases (26%), and IVC in nine cases (18%). In addition, venous obstruction was noted by MRI/CTA in five cases (10%), which was not apparent on most recent echocardiogram.

Conclusions: MRI/CTA are important complementary modalities to echocardiography that offer valuable information regarding the extracardiac vasculature in heterotaxy patients. The high incidence of discrepancies on echo was partly related to the selected nature of this population which was referred to MRI/CT due to limitations on echo. However, it does illustrate inherent limitations of echo in dealing with the complex vascular anatomy often encountered in this population.

Systemic and pulmonary venousl connections in 50 cases of heterotaxy syndrome: Distribution in 27 cases of asplenia

Table 1a. Distribution in 18 cases of polysplenia. [a]This patient was status-post bilateral bidirectional glenn shunts limiting evaluation of the coronary sinus. [b]Presumed unroofed coronary sinus.

	N(18)	%
Superior vena cava anatomy		
Right-sided SVC	6	33.3%
Bilateral SVC without connecting vein and intact coronary sinus septum	4	22.2%
Bilateral SVC without connecting vein and unroofed coronary sinus	3	16.7%
Bilateral SVC without connecting vein[a]	1	5.6%
Bilateral SVC with connecting vein and intact coronary sinus septum	1	5.6%
Bilateral SVC with ipsilateral entry into common atrium[b]	1	5.6%
Left-sided SVC to intact coronary sinus	1	5.6%
Left-sided SVC to left-sided atrium[b]	1	5.6%
Inferior vena cava anatomy		
Interrupted IVC with azygous continuation	16	88.9%
Intact IVC	2	11.1%
Hepatic vein anatomy		
To unilateral atrium	11	61.1%
To left-side of common atrium via separate insertions	3	16.7%
To IVC and atrium	2	11.1%
To unilateral IVC	1	5.6%
To ipsilateral atria	1	5.6%
Pulmonary vein anatomy		
To morphologic LA	7	38.9%
To morphologic RA due to malposition of the atrial septum	5	27.8%
To ipsilateral atrium due to malposition of the atrial septum	3	16.7%
To common atrium	3	16.7%

Table 1b. Distribution in 27 cases of asplenia. [a/b]Distal extent of the left-sided SVC was diminuitive and difficult to assess. [c]4 left-sided to left-sided atrium, one left-sided to right-sided atrium, one right-sided to right-sided atrium, one right-sided to left-sided atrium.

	N(18)	%
Superior vena cava anatomy		
Right-sided SVC	9	33.3%
Bilateral SVC without connecting vein and intact coronary sinus septum	5	18.5%
Bilateral SVC without connecting vein and unroofed coronary sinus	4	14.8%
Left-sided SVC to left-sided atrium	3	11.1%
Left-sided SVC to unroofed coronary sinus	1	3.7%
Left-sided SVC to intact coronary sinus	1	3.7%
Bilateral SVC with connecting vein and intact coronary sinus septum	1	3.7%
Bilateral SVC with connecting vein and unroofed coronary sinus	1	3.7%
Bilateral SVC without connecting vein[a]	1	3.7%
Bilateral SVC with connecting vein[b]	1	3.7%
Inferior vena cava anatomy		
Normal IVC (right-sided IVC to right-sided atrium)	16	59.3%
IVC and aorta on same side[c]	7	25.9%
Interrupted IVC with azygous continuation	3	11.1%
Right-sided IVC to left-sided atrium	1	3.7%
Hepatic vein anatomy		
To unilateral IVC	14	51.9%
To IVC and atrium	6	22.2%
To unilateral atrium	4	14.8%
To ipsilateral atria	3	11.1%
Pulmonary vein anatomy		
Supradiaphragmatic TAPVR	10	37.0%
To morphologic RA due to TAPVR	5	18.5%
Infradiaphragmatic TAPVR	4	14.8%
To morphologic LA	3	11.1%
Mixed TAPVR	2	7.4%
To common atrium	2	7.4%
To morphologic RA due to malposition of the atrial septum	1	3.7%

Poster #: SCI-006

Position of Umbilical Arterial Line (UAL) in neonates with Left Congenital Diaphragmatic Hernia (CDH) as Predictor of ICU length of stay

Ian Cheyne, MD, *QEII Hospital, Dalhousie University, Halifax, NS, Canada, icheyne@outlook.com;* Pierre Schmit, Mike Giacomantonio

Purpose or Case Report: In neonates with left CDH, location of the stomach and liver have been inferred by the

position of the gastric tube and umbilical venous line, and established as a predictor of outcome. However little has been said regarding the position of the descending thoracic aorta based on the UAL position with respect to surgical difficulties and post operative course.

Methods & Materials: Retrospective review of the charts of patients with left CDH who underwent surgery at our institution and who had placement of UAL on day 1 of life. Correlation was made with the ICU length of stay.

Normal UAL positioning was established by analyzing 11 radiographs of neonates without CDH and with a UAL inserted on day 1. UAL deviation in 13 neonates with left CDH was determined by the horizontal distance in mm between the UAL and the left T8 pedicle. ICU length of stay commenced on day of surgery until patient discharge home or transfer out of ICU setting.

Results: From 2005 to 2011, there were 13 patients with left sided CDH fulfilling the inclusion criteria at our institution. Of these neonates, the descending aorta was in normal position in 0 patients, displaced slightly in one patient, moderately in four patients, and markedly in eight patients. Those patients with greater UAL deviations had longer postoperative stays in the ICU.

Statistical analysis yields a slope estimate of 22.55 with standard error of 14.8 and associated p-value of 0.156.

Although the slope correlating position of the descending thoracic aorta with the length of stay in the ICU appears to be clinically significant, statistical significance could not be achieved with the available sample size.

Additionally, there were four mortalities related to CDH. One in the moderately deviated UAL group, and three deaths in the markedly deviated UAL group. There were no deaths in neonates with slight UAL displacement.

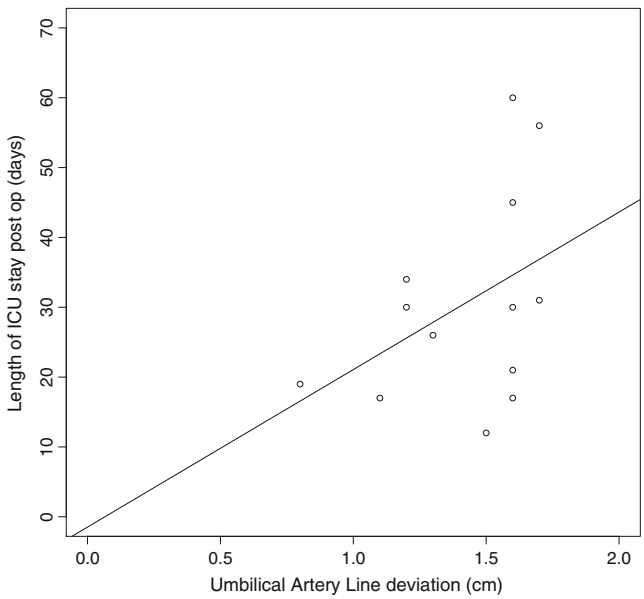

Conclusions: Displacement of the thoracic descending aorta is more frequent than previously reported and may serve as a predictor of extended ICU stay and overall outcome.

Poster #: SCI-007

Prenatal and Postnatal evaluation for syringomyelia in patients with spinal dysraphism

Benjamin Bixenmann, *Neurosurgery, University of Cincinnati, Cincinnati, OH;* Beth Kline-Fath, MD, Karin Bierbrauer, Danesh Bansal

Purpose or Case Report: Syringomyelia can be diagnosed in isolation but is more commonly found in the presence of craniocervical junction anomalies, spinal dysraphism or tethered cord. The etiology of syringomyelia has been hypothesized to be either congenital or acquired. The purpose of this study is to determine if a spinal cord syrinx is either a congenital or acquired condition that develops secondary to changes in cerebral spinal fluid flow dynamics.

Methods & Materials: We conducted an IRB approved, retrospective, non-randomized chart review of our data base for all patients between 3/2004-11/2011 who underwent a fetal MRI for evaluation of an intrauterine anomaly detected via prenatal ultrasound. Within this population, we selected those patients with a neural tube defect (NTD) and performed a chart review of all prenatal and postnatal imaging plus available clinical history.

Results: A total of 2,362 fetal MRI exams were performed. 109 of these were patients with a NTD. Of the 2,362 patient, five cases of syrinx were identified. All five cases were present in fetuses with a NTD. 3/5 were not a true syrinx but rather split cord syndrome. The other 2/5 showed fluid distention of the cord consistent with syrinx. Both fetal MRI exams were performed late in gestation at 31 and 38 weeks. This contrasts with the average gestational age of the fetal MRI exams (24 weeks/3 days). Therefore, syrinx was identified in the prenatal period in 2/2362 (0.08%) of our fetal MRI population or 2/109 (1%) of our NTD population.

63 patients with a NTD had both a prenatal and postnatal MRI. 29/63 (46%) had a syrinx identified during their follow up period. Of this group, 50 patients had an open NTD and 27/50 (54%) developed a syrinx. Closed NTD patients had a much lower rate of syrinx formation, 2/13 (15%). The initial identification of syrinx ranged from less than 30 days of birth up to 4 years of age (Figure 1).

Open NTD patients who developed syrinx had a greater rate of shunted hydrocephalus (93% vs. 65%), shunt revision procedures (1.44 vs. 1.13 shunt revisions/patient), Chiari decompression and tethered cord release surgeries when compared to those without syrinx (Table 1).

Conclusions: Our data suggests that syringomyelia is an acquired and not a congenital condition. Within the NTD population syrinx was not identified until late gestation or postnatal.

Also, syrinx patients were more likely to have abnormal cerebral spinal fluid flow due to hydrocephalus, shunt malfunction, symptomatic Chiari malformation or tethered cord.

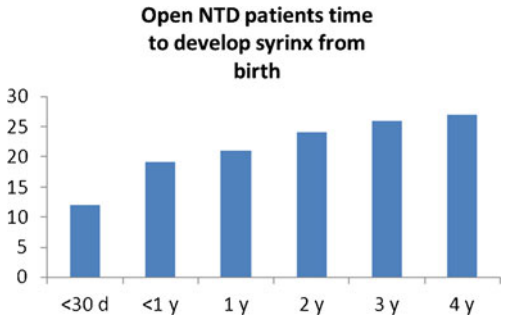

Figure 1 Time from birth that open neural tube defect (NTD) patients developed a syrinx.

Table 1 Comparison of open neural tube defect (NTD) patients that developed syrinxes and those that did not.

	Syrinx	No Syrinx
Number of patients with shunted hydrocephalus	25/27 (93%)	15/23 (65%)
Mean number of shunt revision procedures/patient	1.44 revisions/pt	1.13 revisions/pt
Number of patients with chiari decompressions	8/27 (30%)	0/23 (0%)
Number of patients with tethered cord releases	3/27 (11%)	0/23 (0%)

Poster #: SCI-008

Imaging Features of Atypical Intussusception in Children
Anjum Bandarkar, MD, *Radiology, Children's National Medical Center, Washington DC, DC, anjumnb@gmail.com;* Eglal Shalaby-Rana, Anna Blask

Purpose or Case Report: 1. To describe imaging features of atypical intussusception in children using multimodality imaging case-based approach.
2. To highlight various causes of secondary intussusception through surgical pathologic correlation.

Methods & Materials: After IRB approval, we retrospectively reviewed 11 cases of surgically proven intussusception that presented between 1/1/08 and 12/31/11 and that we termed atypical due to presence of one or more of the following - distal location of intussusception beyond splenic flexure, associated small bowel obstruction, or surgical discovery of a mass as the lead point. Their clinical presentation and imaging findings on radiographs, fluoroscopic enema and sonography were reviewed with an emphasis on sonograhic features to include - transverse and longitudinal dimensions of the intussusception, its location in abdomen, trapped fluid between the layers, doppler flow characteristics, peritoneal free fluid and presence of underlying mass. Correlation was made with surgical and pathologic findings.

Results: Ages ranged from 2 months (m) to 17 years (y), five patients fell in the typical age group (6 m–3y), two were younger (2 m, 4 m), four were older (10y,13y,13y,17y). Three cases had 1–2 days of symptoms, the remaining eight had been sick for >3 days. Four intussusceptions were located in the pelvis, seven were in RLQ. The mean transverse diameter of intussusception was 4.5 cm (range 3.3–5.5 cm) and mean length was 7.7 cm (range 6–10 cm). Three had trapped fluid in between layers of intussusception, six had free peritoneal fluid. Doppler showed preserved vascularity in all. Underlying mass was not identified prospectively in any of the cases. Overall, four patients went directly to surgery and seven went for fluoroscopic reduction of which, five failed reduction and two that were successfully reduced had multiple recurrences. Nine of 11 patients had underlying pathology including cecal hemangioma, hamartomatous polypoid lesion of ileum, ileal duplication cyst, Meckel diverticulum, internal hernia, lymphoma, myofibroblastic tumor and Crohn's disease.

Conclusions: 1. Atypical intussusception commonly presents in extremes of ages, with prolonged duration of symptoms.
Sonography is extremely helpful in characterising the intussusception but did not prospectively identify underlying pathology in any of our cases.
3. Unusually distal location of intussusception, a large mean transverse diameter, presence of peritoneal free fluid, failed fluoroscopic reduction and recurrence may all suggest an atypical intussusception.

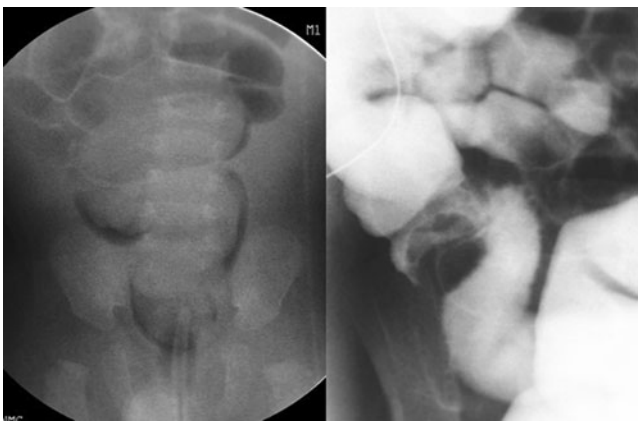

Poster #: SCI-009

Visualization of the pediatric appendix at 1.5 T
Page Wang, *University of Michigan, Ann Arbor, MI, pagew@umich.edu;* Ethan Smith, MD, Maria Ladino-Torres, Peter Strouse, Jonathan Dillman, MD

Purpose or Case Report: To determine how frequently the normal appendix is visualized on abdominopelvic MRI in pediatric patients.

Methods & Materials: A retrospective review of 48 normal pediatric magnetic resonance enterography exams at 1.5 T was performed (23 boys/25 girls; age: 4 months-16 years). Three fellowship-trained pediatric radiologists evaluated the following pulse sequences for appendix visualization: single-shot fast spin-echo (SSFSE), balanced steady-state free precession, T2-weighted fast spin-echo fat-saturated, and postcontrast 3D T1-weighted gradient recalled-echo (GRE) fat-saturated (with at least 2 weeks between review of each pulse sequence).

Results: The appendix was seen most frequently on SSFSE (72/144; 50%) for three readers; range: 18/48, 38% - 37/48, 77%; followed by postcontrast imaging (52/144; 36%) for three readers; range: 9/48, 19%–32/48, 67%. The mean anterior abdominal wall subcutaneous thickness in patients with appendix visualization on SSFSE is 1.7 cm (range: 0.3–5.5 cm), whereas the mean thickness in patients on which the appendix was not seen was 1.2 cm (range: 0.3–2.6 cm) ($p=0.01$). Patient age and gender was not associated with appendix visualization ($p>0.05$).

Conclusions: The normal appendix is more often seen at MRI in pediatric patients with increased abdominal wall subcutaneous fat. A combination of SSFSE and postcontrast T1-weighted GRE fat-saturated pulse sequences may be most appropriate for a rapid MRI appendicitis protocol at 1.5 T.

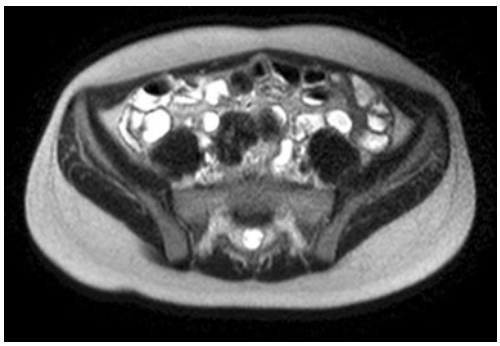

Poster #: SCI-010

Intussusception Revisited: Is Immediate On-Site Surgeon Availability at the Time of Reduction Necessary?

HaiThuy Nguyen, MD, *University of Texas Health Science Center at Houston, Houston, TX, haithuy.n.nguyen@uth.tmc.edu;* J. Kan, MD, R. Guillerman, Christopher Cassady

Purpose or Case Report: The ACR recommends that fluoroscopic-guided intussusception reduction be performed with a surgeon readily available. At many institutions, a surgeon may not be readily available at the time the reduction is attempted. The purpose of this study is to assess the need for immediate surgical availability at the time of radiologic intussusception reduction.

Methods & Materials: All fluoroscopic intussusception reductions at a children's hospital from 11/07 to 8/12 were reviewed to determine method (pneumatic vs. hydrostatic), outcome (successful vs. unsuccessful), and complications of attempted reduction; clinical status of the child, and the time interval between unsuccessful reduction and operative intervention.

Results: 433 intussusceptions(ave age:19 months, range:2–175 months) were referred for fluoroscopic reduction (79.2% pneumatic, 19.8% hydrostatic). 86.1%($n=373$) were successful, and 13.9%($N=60$) were unsuccessful(73.0%pneumatic; 27.0%fluid). Mean elapsed time between unsuccessful radiologic and operative reduction was 4.0 h(range 0.4–15.5 h). Five perforated(all pneumatic), representing 8.3%(5/60) of unsuccessful and 1.2%(5/433) of total reduction attempts. All perforations were successfully treated with percutaneous needle decompression by the radiologist. Mean elapsed time between perforation and operation was 1.3 h(range 0.4–1.6 h). Mean operative time was 163 min and mean hospital length of stay was 9 days for the perforated cases, and 111 min and 5 days, respectively, for the nonperforated cases requiring operative reduction. None of the perforations was complicated by peritonitis. Six patients became hemodynamically unstable during attempted reduction(4 perforations, 2 unsuccessful reductions without perforation), representing 10%(6/60) of unsuccessful and 1.4%(6/433) of total reduction attempts. Hemodynamic stability was restored in all cases by physician-directed resuscitation. Mean elapsed time between unsuccessful fluoroscopic-guided reduction and operative intervention in the six unstable cases was 2.2 h (range 0.4–6.3 h).

Conclusions: Complications requiring immediate surgical attention are rare (1.2%) in children undergoing radiologic intussusception reduction. On-site surgeon presence may not be necessary, provided that the radiologist is facile with percutaneous needle decompression of tension pneumoperitoneum and there is immediate physician availability to manage hemodynamic instability.

Poster #: SCI-011

Radiologic-Pathologic correlation of unusual pediatric hepatic tumors based on MR imaging features

Lamya Atweh, MD, *Radiology, Texas Children's Hospital, Houston, TX, laatweh@texasChildren's.org;* Rajesh

Krishnamurthy, MD, Sanjeev Vasudevan, Patrick Thompson, Dolores Lopez-Terrada, Prakash Masand, MD

Purpose or Case Report: We are increasingly seeing focal liver tumors in children imaged with dynamic contrast enhanced MRI, given the radiation risk associated with CT scanning. We attempt to show MRI features of some rare hepatic tumors, following pathologic confirmation.

Methods & Materials: After obtaining IRB approval, our radiology database was searched for atypical liver tumors from 2010 to date. 12 patients were identified. Scans were performed on a 1.5 T scanner and intravenous gadolinium administered. The MRI characteristics reviewed include T1 and T2 signal, presence of diffusion restriction, signal on in and opposed phase sequences and the pattern of enhancement. The α fetoprotein (AFP) levels and the pathologic diagnosis were noted from the patient charts.

Results: The ages of the patients ranged from 12 days to 21 years and included 6 male and 6 female pediatric patients. The lesions were classified as solid or cystic. Solid lesions are nodular regenerative hyperplasia (macroregenerative nodule) presenting as a solitary large mass, and in a patient post chemotherapy, solid variant of mesenchymal hamartoma, fibrolamellar hepatocellular carcinoma, liver adenomatosis, multifocal neuroblastoma metastases and primary liver angiosarcoma. The cystic masses are unilocular simple epithelial hepatic cyst, cystic hepatoblastoma, peliosis hepatis and undifferentiated embryonal sarcoma.

The AFP was elevated in the patient with cystic hepatoblastoma. The solid neoplasms have hypointense T1 and heterogeneous T2 signal with the nodular regenerative hyperplasia showing T1 and T2 isointense signal relative to the liver. The cystic tumors show fluid bright T2 signal and the presence of thick septations with nodular areas suggest malignancy. Extensive T1 bright signal within a multifocal cystic mass is seen in peliosis hepatis, due to presence of blood products within vascular lakes. On post contrast images the solid benign tumors show avid homogenous enhancement on arterial phase and persistent enhancement on delayed imaging seen only within nodular regenerative masses. The solid malignant tumors show intense diffusion restriction and heterogeneous enhancement with washout on the contrast kinetics.

Conclusions: Knowledge regarding the MR imaging features of these uncommon pediatric liver tumors is helpful in understanding the final pathologic diagnosis and a radiologic-pathologic correlation allows us to provide a relevant differential diagnosis especially since the use of MRI as a diagnostic tool is increasing in this era.

Poster #: SCI-012

Morbidity associated with delayed treatment of cholelithiasis in pediatric patients with sickle cell disease

Heather Imsande, MD, *Boston Medican Center, Boston, MA, heather.imsande@bmc.org*

Purpose or Case Report: The purpose of this case report and study is to demonstrate the morbidity associated with prolonging cholecystecomy in pediatric patients with sickle cell disease (SCD), abdominal pain, and cholelithiasis without imaging evidence of acute cholecystitis. The goal is also to determine cholelithiasis-related imaging findings of concern in this population, so that the radiologist can facilitate necessary intervention(s).

Cholelithiasis and choledocholithiasis are common complications of SCD. We introduce a case of a 19-year-old immigrant woman with SCD who presented to her first clinic visit at our institution with medical records stating a history of cholelithiasis. In the then asymptomatic patient, gallstones were documented with outpatient abdominal ultrasound. Within a year, during a 3-month period, the patient presented to the ED five separate times, and all but the 2nd visit were for abdominal pain. During this time, she had four hospital admissions, three outpatient clinic visits, and three abdominal ultrasounds. The 3rd ED visit led to an admission for gallstone pancreatitis, for which the patient had ERCP with distal CBD stone retrieval and sphincterotomy. The 5th ED presentation led to laparascopic cholecystectomy complicated by a bile leak. She subsequently underwent ERCP, laparotomy with intraoperative cholangiography, and cystic duct repair with hepaticojejunostomy.

In our IRB-approved retrospective chart review of 171 patients with SCD ages 0–21 during abdominal imaging studies performed between 1999 and 2011, 42 patients were found to have had a cholecystectomy. Thirty-three of the 42 patients had abdominal imaging studies at our institution prior to cholecystectomy. For these 33 patients, who include the woman above, the average number of abdominal ultrasounds prior to surgery was 2.6, ranging from 1 to 8.

In only two of the 33 cases, the initial abdominal ultrasound listed a gallbladder abnormality other than stones or sludge. Of the 85 ultrasounds performed on all 33 patients prior to cholecystectomy, only one was read as "acute cholecystitis." However, most of the patients had recurrent pain, and all were eventually treated for

symptomatic cholelithiasis and/or choledocholithiasis. For this study, we will determine and discuss the reported imaging findings that had the most impact on early or delayed intervention in our 33 patients.

Poster #: SCI-013

Portal vein Colour Doppler in the prediction of feed intolerance in neonates with antenatally detected absent/ reversed end diastolic flow (AREDF) in umbilical arteryAkshay Saxena, MD, *Department of Radio Diagnosis, Post Graduate Institute of Medical Education and Research, Chandigarh, India, fatakshay@yahoo.com;* Vineetha Raghu, Kushaljit Sodhi, Praveen Kumar, Vanita Jain, Niranjan Khandelwal

Purpose or Case Report: To evaluate whether serial measurements of portal vein diameter and colour Doppler parameters can predict feed intolerance in neonates with antenatally detected AREDF in the umbilical artery.

Methods & Materials: This prospective study was approved by our institute ethics committee. 35 neonates with antenatally detected AREDF in the umbilical artery were enrolled after obtaining informed written consent. Serial portal vein diameter measurements and portal vein colour Doppler examinations were performed at baseline and 15, 30, 45, and 60 min after administration of test feed (0.5 ml of expressed breast milk or formula feed). Doppler waveforms and indices, including peak systolic velocity (PSV), mean diastolic velocity (MDV), time average mean velocity (TAMV), pulsatility index (PI) and resistive index (RI), and the portal vein diameter were recorded. Doppler waveforms and indices, including peak systolic velocity (PSV), mean diastolic velocity (MDV), time average mean velocity (TAMV), pulsatility index (PI) and resistive index (RI), and the portal vein diameter were recorded. The neonates were followed by clinical examination to assess feed intolerance till he/she reached full feeds (150 ml/kg/day). Statisitical analysis was done to identify which paramaters can predict feed intolerance. p value<0.05 was considered statistically significant.

Results: During the follow up period 17 neonates tolerated the feed while 18 neonates developed feed intolerance. Baseline RI and PI were lower in babies who tolerated oral feed as compared to those who do not and this difference was statistically significant. Serial Doppler evaluation for portal vein flow and diameter after test feed were not useful in predicting feed intolerance.

Conclusions: Serial measurements of portal vein diameter and colour Doppler parameters are not useful in predicting feed intolerance in neonates with antenatally detected AREDF in the umbilical artery.

Poster #: SCI-014

Beware! Inguinolabial hernia containing reproductive organs in female children is not as rare as you think

Anjum Bandarkar, MD, *Radiology, Children's National Medical Center, Washington DC, DC, anjumnb@gmail.com;* Nabile Safdar, Eglal Shalaby-Rana

Purpose or Case Report: 1. Review differential diagnoses of groin swelling in girls <2 years of age.

2. Describe the sonographic appearance and the frequency of ovary, fallopian tube and uterus-containing inguinolabial hernias.

Methods & Materials: Using a radiology search engine, all female children <2 years who underwent sonography for groin swelling fromSeptember 2005 to May 2012 were retrospectively reviewed. 38 cases were identified. The clinical presentations, sonographic features and intraoperative findings were recorded.

Results: Of 38 patients with groin swelling, 31 (82%) had an inguinal hernia while 7 (18%) had other etiologies. Mean age of patients with inguinal hernia was 2 months (range 7 days–5 months) including ten premature infants while mean age in the other group was 16.5 months (range 5–24 months). The hernia sac contained ovary and/or fallopian tube in 26/31 patients (84%), nine of whom also had the uterus in the sac. In 4/31 cases, the male gonad (either atrophic testis or ovotestis) was present; these were later proven to have androgen insensitivity syndrome (AIS). Bowel was present in only 1/31 cases. The other etiologies in 7/38 patients were abscess ($n=3$), lymphadenopathy /cellulitis ($n=3$) and hydrocele of Canal of Nuck ($n=1$).

In patients with inguinal hernia, the ovary was seen as an oval structure with tiny intrinsic follicles, herniating through the fascial defect. When present, the uterus was identified as a homogeneously echogenic structure with central linear hyperechoic endometrium.

Correct sonographic diagnosis was made prospectively in 36/38 cases. The missed findings were identified retrospectively in two cases. Vascular compromise of the ovary was present in one case and was prospectively identified. All of the inguinal hernia cases were successfully repaired with favorable outcomes.

Conclusions: Inguinal hernia is the most common cause of groin swelling in young female infants, with premature infants comprising 1/3rd of the group. Ovary and/or fallopian tube and sometimes uterus are the most common contents of the hernia sac, with bowel rarely present. Infrequently, testis may be present in the hernia sac/labia, a clue to the diagnosis of AIS. Sonography easily and accurately depicts the contents of the hernia and may add

valuable information such as vascular compromise. It also helps to exclude other causes of inguinolabial swelling and should be included in the diagnostic and preoperative work-up of patients with groin swelling.

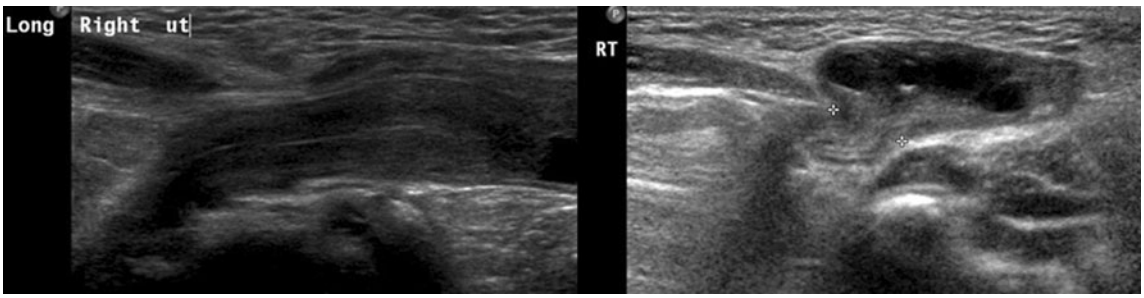

Poster #: SCI-015

The Claw Sign: Can It Determine The Organ of Origin of a Retroperitoneal Mass?

Cindy Miller, MD, **Gil Abramovici,** *Yale-New Haven Hospital, New Haven, CT, gil.abramovici@yale.edu*

Purpose or Case Report: The claw sign denotes a rim of normal appearing tissue surrounding a lesion. In the retroperitoneum, it has classically been taught that the presence of a claw sign allows for differentiation of a lesion of renal origin from a lesion of adrenal origin. The purpose of this exhibit is to demonstrate the appearance of a claw sign and to propose that in the case of neuroblastoma, an apparent claw sign may be present relatively frequently; therefore the presence of a claw sign in the retroperitoneum does not exclude an adrenal origin of a lesion.

Methods & Materials: ith the approval of our Hospital's Human Investigations Committee, the Section of Oncology in the Department of Pediatrics provided a list of all patients over the past 10 years with a diagnosis of neuroblastoma. From the original list of 98 patients, 66 were eliminated for the following reasons; no studies at all or no studies at the time of diagnosis (38); diagnosis other than that of neuroblastoma (15); site of tumor other than retroperitoneum (13). The lesions of the remaining 32 patients were assessed as to presence of a claw sign. Additionally, vascular encasement, size of lesion, and presence of calcification were also recorded.

Results: Approximately 46% of adrenal neuroblastomas demonstrated a possible or definite claw sign. Those which demonstrated a claw sign were on average considerably larger than those without (approximately 8.3 cm versus 4.1 cm). There was a relatively strong relationship between presence or absence of a claw sign and presence or absence of vascular encasement; of 15 with a claw, 11 demonstrated vascular encasement, and of 17 without a claw, ten did not demonstrate vascular encasement.

Conclusions: 1. Many adrenal neuroblastomas in our study population demonstrated a claw sign - a feature which had traditionally been assumed to exclude extrarenal sites of origin of retroperitoneal masses.

2. The presence of a claw sign does not necessarily connote a renal origin for a retroperitoneal mass.

3. Accurate diagnosis of retroperitoneal masses must take into consideration features including presence or absence of calcification as well as presence or absence of vascular encasement.

Poster #: SCI-016

Renal imaging abnormalities as a predictor of sickle cell nephropathy

Heather Imsande, MD, *Boston Medican Center, Boston, MA, heather.imsande@bmc.org*

Purpose or Case Report: The goal of this study is to determine whether commonly-seen renal imaging abnormalities in children with sickle cell disease correlate with significant microalbuminuria, and thus glomerular damage. If there is a positive correlation, the radiologist can alert the clinician regarding early glomerular injury, and thus facilitate early treatment.

Our retrospective study was approved by IRB, and informed consent requirements were waived. Sixty-one patients with sickle cell disease (HbSS, HbSC, HbSBo and HbSB+) ages 0–21 between 1999 and 2011 with abdominal imaging studies and microalbuminuria at our institution were included. Among the 61 patients, 167 abdominal imaging studies are available for review, including abdominal US, CT, and MRI, renal US, and MRCP.

Two pediatric radiologists will independently review the 167 studies to determine the renal imaging characteristics for our 61 patients, including renal size and echogenicity. These results will be compared with the children's prior microalbuminuria values, and corrected for variables such as serum ferritin, which corresponds with number of transfusions, to determine if there is positive correlation between renal imaging abnormalities and early renal dysfunction.

Poster #: SCI-017

An update on the utility of screening for malignancy in Beckwith-Wiedemann syndrome and idiopathic hemihypertrophy

Blake Niederhauser, Allison Clapp, Alan Hoffman, Jennifer McDonald, **Lyndsay Viers,** *Mayo Clinic Rochester, Rochester, MN, viers.lyndsay@mayo.edu*

Purpose or Case Report: To validate previous studies and provide an update to determine the effectiveness of screening retroperitoneal ultrasounds in patients with Beckwith-Wiedemann syndrome (BWS) and idiopathic hemihypertrophy (IHH) in identifying early-stage malignancy.

Methods & Materials: A search of the electronic medical record, departmental research databases, and the radiology information management system (RIMS) identified 176 patients under the age of 18 with BWS (42 patients) and IHH (152) presenting to a single academic facility from January 1, 1996 to December 31, 2011. The pathologic information database was additionally searched to identify all cases of pediatric Wilms tumor, hepatoblastoma, and adrenal cortical carcinoma. RIMS searches of indication key words such as "Wilms", "BWS", "hemihypertrophy", and "screening" identified all pediatric patients undergoing screening retroperitoneal ultrasounds. Screened and unscreened groups were compared with respect to disease stage.

Results: A total of 117 patients had undergone retroperitoneal ultrasound screening to rule out malignancy, 58 of which (49.6%) had BWS and/or IHH. The remaining 59 patients were eventually diagnosed with other conditions not warranting further screening. Twenty-eight pediatric Wilms tumors were identified over the study period including 7/176 with BWS/IHH. Three of these were identified by ultrasound screening programs (3/58, 5.2%) versus 4 in non-screening (4/118, 3.4%), $p=0.69$. All three screening patients had stage 1 disease, while of unscreened patients with BWS/IHH, 4/118 had Wilms tumors with stage 2, 4, 5, and unknown disease, respectively, a significant difference ($p=0.05$). No adrenocortical carcinoma or hepatoblastoma tumors were identified in BWH/IHH patients.

Conclusions: Half of patients undergoing screening do not have screening-indicated diseases. Screening retroperitoneal ultrasound for early detection of malignancy in BWS and IHH identifies earlier stage disease.

Poster #: SCI-018

Reduction of Dose Area Product in Pediatric Genitourinary Cases: An Effective and Sustained Departmental Initiative

Grace Guo, MD, *Medical Imaging, A.I. duPont Hospital for Children, Wilmington, DE, gguo@nemours.org;* Heidi Kecskemethy, BS, Leslie Grissom, MD

Purpose or Case Report: To monitor the effectiveness of staff education and incentive to decrease radiation exposure as measured by Dose Area Product (DAP) during voiding cystourethrography (VCUG) in children and evaluate the ability of the department to sustain the reduction.

Methods & Materials: A 1 year program consisting of awareness orientation, review of techniques for decreasing dose, incentive, and continuous monitoring with quarterly reporting of data was implemented. A second year of observation monitored effectiveness.

Reports of fluoroscopy cases detailing the procedure, Radiologist, patient age, and DAP were reviewed. Data were analyzed for eight successive quarters. Mean DAP level was calculated for age groups and Radiologists. Aggregate percent change and coefficient of variation was calculated quarterly and reviewed with Radiologists.

Results: Year 1: 806 cases were reviewed for ten Radiologists. The 0–18 year group mean DAP for the department decreased from 31.1 to 24.5 (21.4%); Radiologists' variation in dose decreased by 28.8%. DAP by age was consistently lowest for the youngest children and highest for the oldest children. Year 2: 780 cases were reviewed with continued reduction in DAP to19.6 (58.8%) and Radiologists' variation (32.2%) over baseline.

Conclusions: A one-year program featuring increased awareness, dose reduction techniques, and quarterly group/individual monitoring was effective in both reducing DAP levels and dose variation among Radiologists for pediatric genitourinary radiography procedures. This reduction was sustained for an additional year with continued improvement. This can serve

as a model to measure and encourage dose reduction for other studies within a Radiology Department.

Poster #: SCI-019

Identifying renal imaging biomarkers of mTOR inhibitor therapy for tuberous sclerosis complex

Srikala Narayanan, MD, *Division of Pediatric Imaging, Massachusetts General Hospital, Boston, MA, SNARAYANAN3@PARTNERS.ORG;* Michael Gee; Elahna Paul, MD, PhD; Elizabeth Thiele, MD, PhD

Purpose or Case Report: mTOR inhibition is a therapeutic strategy for tuberous sclerosis complex (TSC). The imaging appearance of TSC renal lesions undergoing mTOR inhibition has not been clearly defined. Purpose of this study is to identify imaging biomarkers of mTOR inhibition in TSC patients followed by serial cross-sectional (MRI or CT) exams before, during, and after treatment.

Methods & Materials: In this single institution IRB-approved and HIPAA-compliant study, retrospective review of imaging was conducted in 14 TSC patients who underwent treatment with an mTOR inhibitor (rapamycin, sirolimus, or everolimus). Imaging studies were performed at 6 or 12 month intervals. On initial imaging prior to mTOR inhibition, the dominant renal cyst and angiomyolipoma was identified. The volume of each dominant lesion was calculated using ellipsoid volume formula (0.52×(long axis diameter)×(short axis diameter)2). The dominant lesions were followed on subsequent imaging studies for changes in size, enhancement characteristics, and intralesional hemorrhage. Significant change in size was defined as >10% change in volume between two consecutive timepoints. The percentage of dominant lesions exhibiting change in these imaging features was calculated for pre-treatment, on treatment, and post-treatment timepoints.

Results: Of the 14 patients included in the study, 13 were followed by MRI and one by CT due to MR-incompatible hardware. For the dominant AML, the highest percentage of lesion shrinkage was observed on treatment (78%) compared with pre-treatment (30%) and post-treatment (33%). In contrast, a lower percentage of enlarging AMLs was observed on treatment (21%) compared with pre-treatment (44%) and post-treatment (91%). For the dominant renal cyst, 87% decreased in volume on treatment compared with 50% pre-treatment and 37% post-treatment. No cysts increased in size on treatment, compared with 50% pre-treatment and 75% post-treatment. In addition, 2 AMLs exhibited decreased enhancement on treatment, while 1 AML developed new hemorrhage on treatment. Neither of these were observed in any lesions in pre- or post-treatment periods.

Conclusions: This preliminary study of changes in imaging appearance of renal TSC lesions on mTOR inhibitor therapy suggests that decreased volume of dominant renal cyst or AML was predominantly observed during the on-treatment timepoints and may be an imaging biomarker of treatment effect. Changes in AML enhancement or hemorrhage were infrequently observed and not reliably associated with treatment.

Poster #: SCI-020

Percutaneous management of cervico-mediastinal lymphatic malformations associated with airway compromise

Rajan Patel, MD, *Department of Pediatric Radiology, Children's Medical Center, University of Texas Southwesten Medical Center, Dallas, TX, rajan_304@yahoo.com;* Nancy Rollins, MD

Purpose or Case Report: Trans-spatial lymphatic malformations associated with symptomatic airway compromise are challenging management problems due to high surgical morbidity. We report our experience with nonsurgical management of cervico-mediastinal lymphatic malformations associated with symptomatic airway compromise using sclerotherapy.

Methods & Materials: We performed an IRB-approved query of our PACS database for children with cervico-mediastinal lymphatic malformations associated with airway compromise who underwent sclerotherapy from 2007 to 2012 and reviewed imaging and medical records. Lesions were characterized on MRI as macrocystic, microcystic or mixed. We recorded type of sclerosing agent, number of sclerotherapies needed, response, complications from sclerotherapy, and surgical intervention if performed. Response was categorized by resolution of symptomatic airway compromise and when possible, follow-up MR imaging.

Results: We identified 17 patients ages 20 days to 5 years (mean=15 months). Indications for sclerotherapy included swelling of the soft tissues of the neck with torticollis and airway compromise; three patients also had superior vena cava compression syndrome. Sclerotherapy was done with doxycycline (concentration 25 mg/ml) in 11 patients, absolute alcohol in 1, and their combination in 5. Cysts were punctured using sonographic guidance. Number of treatments ranged from 1 to 10; mean was three treatments. Large cysts were drained of fluid or old blood and irrigated with the sclerosing agents after documenting absence of communication with regional veins. Total dosages of doxycycline ranged from 500 to 1500 mg and 5–15 cc absolute

alcohol per session which are higher than dosages used for sclerotherapy of venous malformations, without toxicity. Sixteen patients were extubated without surgical intervention. Sclerotherapy was ineffective in the microcystic components of the malformations and one patient underwent surgical debulking of a large microcystic component which was complicated by infection and persistent leakage of lymphatic fluid.

Conclusions: Cervico-mediastinal lymphatic malformations associated with airway compromise can be managed with sclerotherapy when macrocystic. Replacing the fluid contents of the cysts with the sclerosant exposes the endothelial lining of the cyst to undiluted sclerosing agent and accelerates involution.

Poster #: SCI-021

Imaging findings of central conducting lymphatics (CCL) using Dynamic Magnetic Resonance Lymphangiography (MRL)

Rajesh Krishnamurthy, MD, Alberto Hernandez, Serife Kavuk, **Aparna Annam,** *Texas Children's Hospital-Diagnostic Radiology, Houston, TX, axannam@texasChildren'shospital.org;* Sheena Pimpalwar, MD

Purpose or Case Report: Previous MR techniques for CCL using heavily T2 weighted sequences or digital contrast injection have limitations:inability to distinguish edema from small lymphatics, variable opacification of CCL,venous contamination, lack of functional or dynamic information like reflux or collateralization and artifacts related to breathing and peristalsis. Dynamic MRL provides rapid, selective opacification of the CCL with reliable visualization of thoracic duct(TD) and cisterna chyli(CC),dynamic imaging of lymphatic transit and lack of venous contamination. We describe our early experience in three patients

Methods & Materials: Three MRL's were performed after informed consent

Patient 1

13/F: Epidermal nevi, renal and splenic cysts, lytic bone lesions, interstitial lung disease, lung AVM's and recurrent chylopericardium. MRL to rule out TD obstruction

Patient 2

20/F: 11 years post Whipple's for pancreatic SPEN with chronic protein losing enteropathy imaged for mesenteric CLR

Patient 3

29/F: chronic lymphedema left leg, pelvic and retroperitoneal cysts,status post 20 surgical excisions of lymphatic cysts from left groin, skin grafting and radiotherapy to screen for CCL anomalies

Method

Under ultrasound guidance, 22/20 G angiocatheters were placed within the medulla of bilateral inguinal lymph nodes followed by intranodal injection of gadolinium and dynamic MR imaging with the following parameters: torso phased array coil with a large FOV to cover lower neck to inguinal region, single dose contrast diluted 1:1 with normal saline injected simultaneously into both inguinal nodes, dynamic 3D T1 FFE volumetric sequence repeated every 2 min until contrast noted in retroperitoneal lymphatics, then every minute to study transit to cisterna chyli and TD.

Results: Patient 1

CLR from the TD into dysplastic lymphatic channels in the mediastinum, pericardium, left lower lobe and left pleural cavity suggestive of lymphangiectasia. No delay in opacification of the central TD excluding obstruction. Patient managed with Denver shunt and Sirolimus therapy

Patient 2

Normal retroperitoneal lymphatics,CC,TD,no mesenteric CLR

Patient 3

Lymphatic outflow from right leg into large aneurysmal dysplastic lymphatic channels in the pelvis and retroperitoneum with poor visualization of TD. Extensive collateral lymphatic pathways in body wall. Further managed with lymphedema treatment and sclerotherapy

Conclusions: Imaging of the CCL with Dynamic MRL is a useful tool for evaluation of both anatomy and function and helps direct patient management

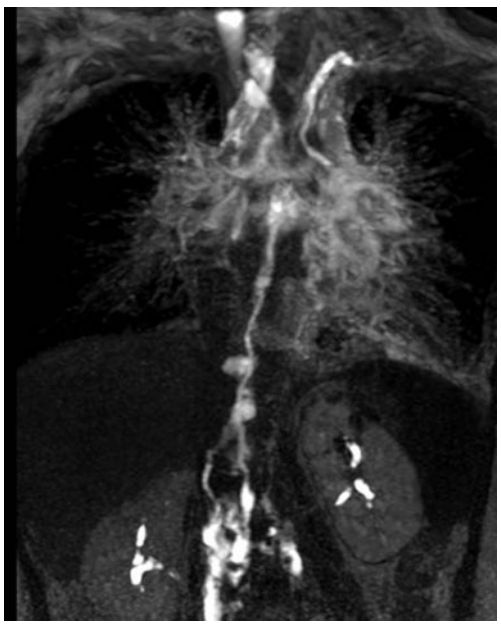

Poster #: SCI-022

Greater Saphenous Venous Access as an Alternative in Young Children

David Aria, MD, *Radiology, Phoenix Children's Hospital, Phoenix, AZ, daria@phoenixChildren's.com;* Seth Vatsky, Robin Kaye, Carrie Schaefer, Richard Towbin, MD

Purpose or Case Report: To demonstrate the utility and effectiveness in using the greater saphenous vein as a venous access site for the placement of peripherally inserted central catheters in young children.

Methods & Materials: This is a retrospective study from a large tertiary care children's hospital from November 2010 to August 2012. Peripheral insertion of central venous catheters using the greater saphenous vein was attempted in 86 children (54 male: 32 female) ranging in age from 3 days to 17 years (mean of 655 days). Indications for the study varied from congenital heart disease in 25 (29%), urinary tract infection in 24 (28%), access in 9 (10%), pneumonia in 7 (8%), meningitis in 4 (5%), TPN in 5 (6%), sepsis in 3 (4%), and other infections in 9 (10%). All procedures were performed by an attending or fellow pediatric interventional radiologist in an angiography suite. Utilizing ultrasound-guidance and/or clinical landmarks to obtain venous access, 3 or 4 Fr. catheters were placed in the greater saphenous vein at the level of the thigh or ankle. Ideal catheter tip position was considered to be in the inferior vena cava at the level of the diaphragm on frontal fluoroscopy. Immediate and short-term (30 days post-procedure) complications reviewed.

Results: Of the 86 patients in whom peripherally inserted central venous catheter placement via the greater saphenous vein was attempted, 67(78%) were successful. The mean weight of the 67 patients who underwent successful placement was 9.1 kg, with 51 (76%) weighing <10 kg. All 19 failures occurred in vessel diameters of ≤1.6 mm (mean of 1.2 mm) with inability to advance the wire/catheter centrally. The mean catheter length for thigh venous access was 29.6 cm. Ankle venous access was in a total of 31 patients all weighing less than 10 kg except for one patient weighing 11.7 kg with a mean catheter length of 32.6 cm. A total of 1060 catheter days were reviewed without reported complications except one catheter fracture that had to be removed/replaced.

Conclusions: In children with accessibility to the greater saphenous vein either by ultrasound guidance and/or clinical landmarks, the greater saphenous vein provides a suitable alternative for venous access, particularly in very young children (<10 kg) and in a select group of older children. Greater saphenous venous access is safe with a low rate of complications. In the lower extremities, greater saphenous venous puncture and access may be the preferred initial access site to preserve future femoral venous access.

Poster #: SCI-023

Minimal incremental value of frogleg lateral view of the pelvis in children with suspected DDH

Lauren Karbach, *Baylor College of Medicine, Houston, TX;* J. Kan, MD, William Phillips, Wei Zhang, Scott Rosenfeld

Purpose or Case Report: The ACR recommends AP radiographs only for screening developmental dysplasia of the hip (DDH) in children over 4 months with optional frog-leg lateral view if the AP view is abnormal. The ACR guidelines' references and our own literature review revealed no known studies comparing DDH screening efficacy with AP only versus AP and frogleg lateral radiographs. Furthermore, pediatric, orthopaedic, and radiology DDH literature vary in recommendations on the utility of single AP view versus AP and frog-leg lateral view. The purpose of this study is to evaluate the incremental value of the frog-leg lateral view after the AP view in screening for suspected DDH.

Methods & Materials: A case–control study was performed in children who had clinical follow-up after clinically indicated screening AP and frogleg lateral radiography for suspected DDH. Clinical follow-up was used as the reference standard. The study population was composed of 274 hips performed in 137 patients (mean age 9 months, range 1 month - 2 years and 9 months) with 233 (85%) that were normal, and 41 (15%) with DDH. Without knowledge of clinical follow-up and diagnosis, radiographs were reviewed by consensus by a fellowship trained pediatric orthopedist and CAQ pediatric radiologist. Both readers were unaware of the percentage of studies that were normal during review. Presence or absence of DDH was first screened using the AP view only. On a later date, presence or absence of DDH was screened using both the AP and frog-leg lateral view.

Results: Sensitivity and specificity for AP radiography was 0.93 and 0.94 respectively, Kappa=0.72. Sensitivity and specificity for AP and frogleg radiography was 1.00 and 0.95 respectively, Kappa=0.72. The P-values between AP and AP and frogleg for sensitivity was 0.24 while for

specificity was 0.83. A total of three false negative, and two false positive studies on review of AP views only were correctly reclassified after the addition of the frogleg lateral view.

Conclusions: There was no significant difference in screening efficacy for suspected DDH with AP versus AP and frogleg lateral pelvic radiography. The ACR recommendations for AP only radiographic screening for DDH should be adopted by pediatric and pediatric orthopaedic societies to minimize radiation exposure in children.

Table 1. Sensitivity, Specificity, Kappa and P value for AP only versus AP and frogleg lateral imaging in the diagnosis of DDH

	Sensitivity	Specificity	Kappa
AP only	0.93	0.94	0.72
AP and frogleg	1.00	0.95	0.72
P value	0.24	0.83	

Poster #: SCI-024

Effectiveness of screening DDH with and without acetabular angle measurements. Is gestalt diagnosis adequate?

Lauren Karbach, *Baylor College of Medicine, Houston, TX;* J. Kan, MD, William Phillips, Wei Zhang, Scott Rosenfeld

Purpose or Case Report: Gestalt diagnosis is a common practice amongst practitioners for screening pelvic radiography in children with suspected developmental dysplasia of the hip (DDH). Acetabular angles are not routinely performed particularly when a study appears unequivocally normal. The purpose of this study is to assess differences in screening efficacy comparing gestalt approach to interpretation and interpretation with routine acetabular angle measurements in DDH screening.

Methods & Materials: A case–control study was performed in children who had clinical follow-up after clinically indicated screening AP and frogleg lateral radiography for suspected DDH. Clinical follow-up was used as the reference standard. The study population was composed of 274 hips in 137 patients (mean age 9 months, range 1 month–2 years and 9 months) with 233 (85%) that were normal, and 41 (15%) with DDH. Without knowledge of clinical follow-up and diagnosis, radiographs were reviewed by consensus by a fellowship trained pediatric orthopedist and CAQ pediatric radiologist. Both readers were unaware of the percentage of studies that were normal during review. The images were reviewed for the presence or absence of DDH by gestalt screening without acetabular angle measurements. At a later date, radiographs were screened with acetabular angle measurements performed on every study.

Results: Gestalt screening sensitivity and specificity was 0.88 and 0.90 respectively, Kappa=0.70. When screening with routine measurement of acetabular angles, the sensitivity and specificity was 1.00 and 0.95 respectively, Kappa=0.72. For these two screening methods, the P-value for sensitivity was 0.06 and specificity was 0.03. For gestalt screening, there were five false negative and 13 false positive studies; which were correctly reclassified with the screening with routine use of acetabular angles. There were 11 false positive studies found for both gestalt screening and screening with routine acetabular angle measurements.

Conclusions: Gestalt screening for DDH has a significantly lower specificity when compared with screening with routine measurement of acetabular angles. Therefore, acetabular angle measurements should be routinely performed in children undergoing screening radiography for suspected hip dysplasia to improve diagnostic accuracy.

Table 1. Sensitivity, Specificity, Kappa values and P values for gestalt screening versus screening with routine acetabular angle measurements.

	Sensitivity (from consensus review)	Specificity (from consensus review)	Kappa
Gestalt	0.88	0.90	0.70
With measurements	1.00	0.95	0.72
P value	0.06	0.03	

Poster #: SCI-025

Evidence-Based Outcomes of Studies Addressing Diagnostic Accuracy of MRI of Juvenile Idiopathic Arthritis in the Axial Skeleton - A systematic review

Sohaib Munir, BHSc, *Queen's University, Kingston, ON, Canada;* Kedar Patil, Elka Miller, Marinka Twilt, Elizabeth Uleryk, Andrea Doria

Purpose or Case Report: Our objective was to evaluate the diagnostic accuracy of MRI for evaluation of axial (temporomandibular [TM], spinal and sacroiliac [SI]) joints in juvenile idiopathic arthritis (JIA) based on the level of evidence of relevant studies in order to make recommendations and identify gaps in literature. Overarching questions were: Can MRI detect early joint changes?; Can MRI detect intermediate joint changes?; Can MRI detect treatment effects on joint pathology?; Can early MRI findings predict future joint degeneration or functional status?; Is there an association between intermediate MRI findings and joint functional status?

Methods & Materials: Articles were screened using MEDLINE (1946-June 2012), EMBASE (1947-June 2012), DARE (2nd quarter 2012), and Cochrane Library (2nd quarter 2012). We assigned a semiquantitative score out of 25 to quality of reporting of studies, by using the Standards for Reporting of Diagnostic Accuracy (STARD) tool. Based on this score, studies were assigned a rating of "Good" (0.80–1.00), "Fair" (0.50–0.79), or "Poor" (0.00–0.49). Studies were also ranked based on their level of evidence (I–IV). Finally, grades of evidence were assigned to each overarching question according to the Canadian Task Force on Preventive Health Care guidelines.

Results: The literature search retrieved 1789 unique citations. On the basis of title and abstracts, 38 citations were selected. Upon full retrieval of articles and checking references for additional articles, 21 articles were chosen for review: 4/21 (19%) had a "Good" score, while 13/21 (62%) had a "Fair" score, and 4/21 (19%) had a "Poor" score. Included were studies in which validity (18/21 articles; 86%), responsiveness (6/21 articles; 29%), and reliability (4/21 articles; 19%) were assessed, some of which measured several clinical properties. 15/21 (71%) studies evaluated TM joints, 4/21 (19%) studies evaluated SI joints, and 2/21 (10%) studies evaluated spinal joints.

Conclusions: There is fair (grade B) strength of evidence that MRI is an accurate diagnostic method for evaluating early and intermediate changes of TM joints in JIA. There is insufficient data regarding the use of MRI in spinal joints (grade I) and SI joints (grade I). Further research is needed to determine the predictive value of early MRI findings in the axial skeleton (grade I), and correlation of MRI findings with functional clinical outcomes (grade I).

Poster #: SCI-026

Ultrasound and MRI of Growing Joints in Healthy Boys: Correlation with Ex-Vivo Phantom Measurements

Shyamkumar Keshava, Sridhar Gibikote, Arun Mohanta, Victor Blanchette, Alok Srivastava, **Andrea Doria,** *Christian Medical College, Vellore, India, andrea.doria@sickkids.ca*

Purpose or Case Report: Background: Defining normal cartilage and physiologic synovial fluid measurements in the immature skeleton at different ages enables differentiation of a normal joint from a joint with early changes. At present there is a lack of such knowledge both on ultrasound (US) and MRI.

Purposes: In-vivo: To establish normal measurements of soft tissue and osteocartilaginous components of knees and ankles in healthy boys.

Ex-vivo: To assess measurement variation in US and MR images as compared with corresponding phantom measurements (PM).

Methods & Materials: In-vivo: This prospective study was carried out at two centres (Toronto, Canada, and Vellore, India) upon ethics approval. Healthy boys in 3 age groups: 7–9; 10–14; and 15–18 years with no clinical evidence of joint abnormality were included. The subjects underwent clinical assessment (using the Hemophilia Health Joint Score), 1.5 Tesla MRI (extremity coils) and gray-scale US (12–17 MHz linear-array transducers) with standardized protocols. The images were read by four imaging experts from the two centres using standardized protocols. Measurements at predetermined sites on both MRI and US were recorded.

Ex-vivo: Agar phantoms of 3 different sizes ($\geq$1.5 cm; 1$\leq\times<$ 1.5 cm; <1 cm) were used as reference standards for US and MRI measurements (Fig.).

Results: In-vivo: The total number of boys was 42, mean age 12 years (standard deviation [SD]: 3.1). The joints studied were knees (20, 48%) and ankles (22, 52%). With an increase in age, there was a reduction in the thickness of measurable cartilage, as expected. Cartilage thickness measured on US was consistently less than what was measured on MRI ($P<0.05$) (Table). The synovium was not measurable in any of the joints. In knees, physiologic fluid was noted in 14 (70%) on MRI and 13 (65%) on US; in ankles, fluid was seen in 20 (91%) joints on MRI and in 7 (32%) on US. There were no hemosiderin or articular erosions detected in any of the healthy subjects.

Ex-vivo: For measurements ≥1.5 cm no significant differences were noted between US-PM and MRI-PM coefficients of variation (CV) ($p>0.05$). For measurements <1 cm, the CV of US-PM was 14% and of MRI-PM, 21%.

Conclusions: In this pilot study US and MRI of joints of healthy boys helped in establishing normative data for soft and osteochondral tissues according to age groups. For smaller structures, US provides less measurement variation than MRI, therefore compared with US, MRI may slightly overestimate measurements in growing joints as noted in this study.

Disclosure: Dr. Doria has indicated that Bayer Healthcare Canada provided a Research Grant.

Average cartilage thickness in mm is reported in the table below.

Joints: total 37	**7–9 years**	**10–14 years**	**15–18 years**			
MRI	**US**	**MRI**	**US**	**MRI**	**US**		
Knees	Number of joints 19	5	5	9	9	4	4
Cartilage thickness in mm	Mean±SD	4.50±0.30	3.78±0.52	2.45±0.46	1.72±0.51	1.99±0.23	1.17±0.18
Ankles	Number of joints 18	3	3	10	10	6	6
Cartilage thickness in mm	Mean±SD	1.7±0.03	1.36±0.26	1.27±0.28	1.08±0.42	1.10±0.26	0.68±0.20

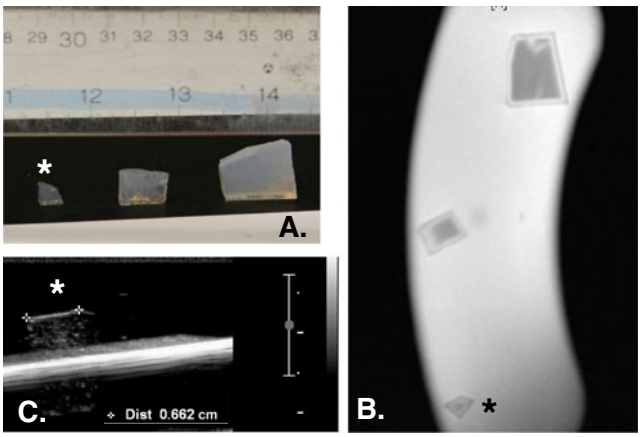

Fig. Different-sized agar phantoms: The smallest phantom (*) is shown as an ex-vivo specimen (A), on a coronal gradient-echo MR image (1.5 T scanner) (B) and on an axial ultrasound image (C).

Poster #: SCI-027

Evidence-Based Outcomes on Diagnostic Accuracy of Quantitative Ultrasound for Assessment of Pediatric Osteoporosis

Kuan Chung Wang, *The Hospital for Sick Children, Toronto, ON, Canada, kcwang0410@hotmail.com;* Kuan Chieh Wang, Afsaneh Amirabadi, Elizabeth Uleryk, Andrea Doria

Purpose or Case Report: To semi-quantitatively assess the diagnostic accuracy of Quantitative Ultrasound (QUS) for evaluating osteoporosis in pediatric patients according to the U.S. Preventive Services Task Force's recommendation guidelines.

Methods & Materials: Articles on diagnostic accuracy of QUS for assessing abnormal bone quality or quantity in patients of mean age ≤18 were screened and retrieved from the MEDLINE(1946-May 2012), EMBASE(1947-May 2012), and Cochrane Library(1988-May 2012) databases through the Ovid interface. After determining the eligibility of articles for inclusion three reviewers independently evaluated the quality of reporting and methodological quality with the Standards for Reporting of Diagnostic Accuracy (STARD) and the Quality Assessment of Diagnostic Accuracy Studies 2 (QUADAS-2) tools. For each individual study, the scores for STARD ≥15 corresponded to excellent, scores ≥10 and <15 corresponded to fair, and scores <10 corresponded to poor quality of reporting. For QUADAS-2, studies were rated as having adequate or inadequate methodological quality based on specific criteria for risk of bias and applicability. Evidences were aggregated, and descriptively analysed for QUS' construct and criterion validity, responsiveness, and reliability, according to the following questions: 1) Does QUS have the ability to detect or characterize bony trabeculae in osteoporotic children? 2) Is QUS responsive to detect changes in bone status following treatment aimed at improving bone quality? 3) Does QUS has the ability to predict future skeletal fractures?

Results: The literature search retrieved 203, 49 and 4 citations from MEDLINE,EMBASE and Cochrane databases, respectively. A total of 28 studies (1957 patients, 708 reported boys and 860 girls, reported age, 0–19 years) were selected for inclusion. With the STARD tool, the mean quality of reporting score was 'fair' =13.41 (out of 25). With the QUADAS-2 tool 11 out of 28 [39.29%] had 'adequate' research design quality. There was insufficient quality and quantity of studies to recommend for or against the use of QUS as a diagnostic tool for assessing pediatric osteoporosis (Grade C). Current gaps in the literature include: QUS' ability to accurately detect osteoporosis using calcaneal QUS and to detect interval changes pre-post treatment; and to predict future fracture or skeletal degeneration.

Conclusions: There is insufficient evidence that QUS is an accurate diagnostic tool for assessing pediatric osteoporosis and predicting an unfavourable outcome (fractures).

ANALYTIC FRAMEWORK FOR THE USE OF QUANTITATIVE ULTRASOUND AS A DIAGNOSTIC TOOL FOR DETECTING PEDIATRIC OSTEOPOROSIS

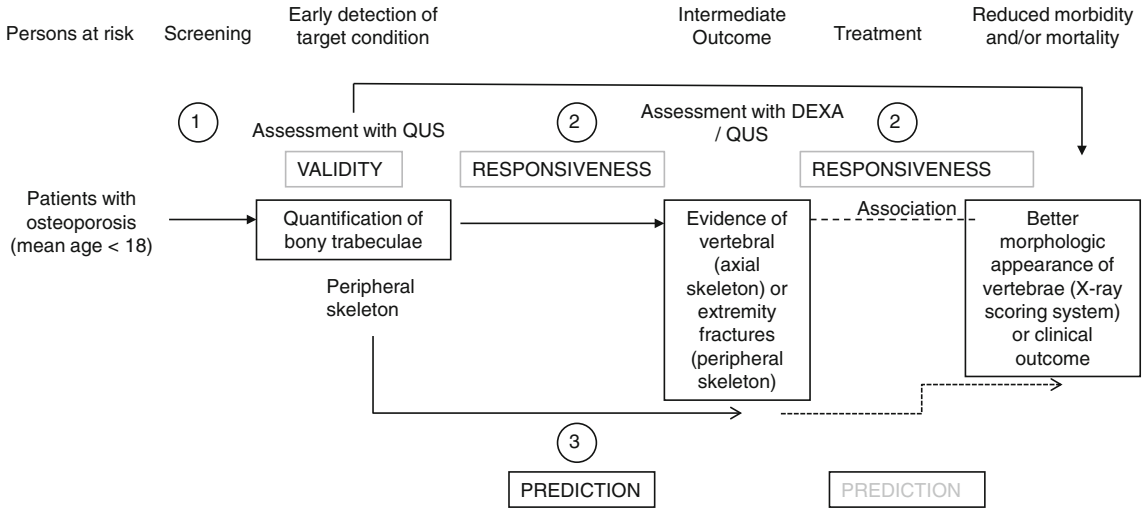

Poster #: SCI-028

Fish Tail Deformity: Trochlear Osteonecrosis- A Delayed Complication Of Distal Humeral Fractures

Srikala Narayanan, MD, *Division of Pediatric Imaging, Massachusetts General Hospital, Boston, MA, snarayanan3@partners.org;* Katherine Nimkin

Purpose or Case Report: Concavity in the central portion of the distal humerus, due to trochlear osteonecrosis, is referred to as fishtail deformity. This entity is an uncommon complication of distal humeral fractures in children. Our objective is to describe pathophysiology and imaging features of post-traumatic fishtail deformity.

Methods & Materials: Retrospective review from 2004 to 2012 using imaging database search engine revealed six cases of post-traumatic trochlear osteonecrosis and two cases of trochlear osteochondral defect (OCD).

Results: Six patients, aged 7–14 years (4 males, 2 females), presented with elbow pain and history of prior distal humeral fracture. Three of six children had limited range of motion. Four patients had prior grade 3 supracondylar fracture treated with closed reduction and percutaneous pinning, while the remaining two had medial and lateral condylar fractures treated with conservative casting.

All patients had radiographs, five had CT and two had MRI. Characteristic radiographic abnormality of a concave defect secondary to underdeveloped lateral trochlear ossification center was noted in all cases, confirmed on CT. Increased subchondral signal intensity within diminutive trochlea on MRI was consistent with AVN. Two cases, aged 11 and 14, with no history of prior fracture, showed a smaller, focal defect involving the lateral trochlea, compatible with OCD. Both had radiographs and CT, one had MRI.

Conclusions: Fishtail deformity of the distal humerus is a rare complication of distal humeral fracture in children. Precarious blood supply to the lateral trochlea and epiphyseal cartilage between the trochlea and capitellum

likely predisposes to this condition. Differential diagnosis, in the absence of prior fracture, includes trochlear OCD, idiopathic osteonecrosis (Hegemann's disease), epiphyseal dysplasia and chondroblastoma. This entity is infrequently reported in the radiology literature and is likely underreported. Awareness of the classic imaging features can result in earlier diagnosis and appropriate treatment.

Poster #: SCI-029

False Positive Shunt Discontinuity at Digital VP Shunt Survey Radiography

Lillian Lai, MD, *Radiology, University of Iowa Hospital and Clinics, Iowa City, IA, lillian-lai@uiowa.edu;* Mark Madsen, Edmund Franken, Yutaka Sato

Purpose or Case Report: To analyze cases of false positive shunt discontinuity at digital VP shunt survey radiography (DVPR) and to investigate its causes and solutions.

Methods & Materials: Periodic evaluation of ventricular peritoneal shunts is essential in the ongoing evaluation of patients with hydrocephalus at our institution. Such images have been recorded digitally for several years. Retrospective analysis of 224 consecutive DVPR studies obtained over a 6-month period was performed, with particular attention to positive shunt discontinuity. Our routine was 3 AP and 3 lateral views of the head/neck/chest/abdomen covering the course of the VP shunt, visualized on a PACS monitor capable of adjusting window level/width. We also performed a phantom study to test a hypothesis that apparent (false positive) discontinuity occurred in the neck images, where soft tissue was thinnest and x-ray attenuation the least.

Results: Apparent shunt tubing discontinuity in at least one view, usually the lateral head and neck, was found in 25 studies (11.2%) even after window-level/width adjustment at a viewing station. 9.4% of these were false positive findings while 1.8% represented true shunt discontinuity. None of the false positive cases were called true discontinuity because the orthogonal plane DVPR showed continuity. The average kV/mAs of false positive images (71.7/6.8) was higher compared to the other views (69.9/5.5), but only kV was statistically significantly different. Experimental results confirmed the hypothesis that apparent overexposure at standard kV/mAs settings occurred at the least attenuated region of the body. They also revealed that this problem could be eliminated by adjusting the latitude of the raw image to include extremes of the exposure intensity range.

Conclusions: One of the pitfalls of digital imaging technique is that false positive discontinuity in DVPR can be due to inadequate latitude adjustment of the initial image, resulting in saturation of the image at the thinnest, least attenuating body region. It can be corrected by properly adjusting the initial image's latitude. Because of the ability to adjust windowing on PACS, there is a tendency to take digital radiography results at face value. These results demonstrate that healthy skepticism is still needed to avoid overcalling shunt discontinuity in DVPR.

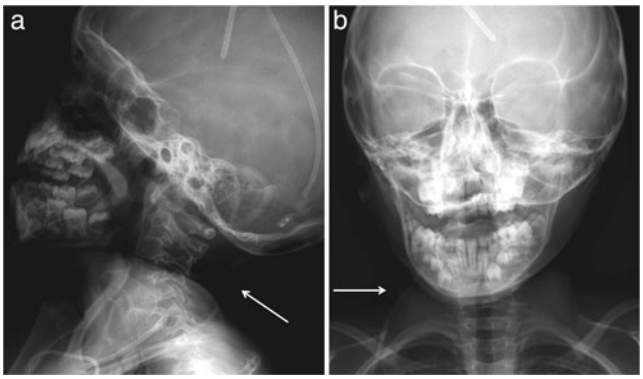

Figure 1: An example of a false positive VP shunt discontinuity, which is not seen on lateral view (a) but is on the AP view (b). The apparent break could not be resolved despite windowing on PACS.

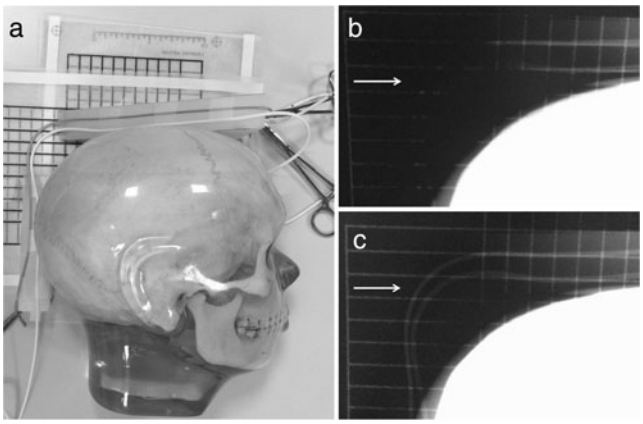

Figure 2: Experiment set up by placing shunt tubing over a plastic wedge with graded thickness next to a skull phantom (a). Image burnout occured in the thinnest part of the wedge where x-ray beam was least attenuated (b), but when latitude was increased, the shunt tubing could be seen (c).

Poster #: SCI-030

Evaluation of Optic Pathway Gliomas in patients with Neurofibromatosis Type I Under the Age of 4 Years

Usha Nagaraj, MD, *Diagnostic Imaging and Radiology, Children's National Medical Center, Washington, DC, usha.d.nagaraj@gmail.com;* Nadja Kadom, Shams Jubouri, Gilbert Vezina, Roger Packer, Maria Acosta

Purpose or Case Report: To evaluate the incidence and imaging characteristics of optic pathway glioma and to discuss the value of early screening MRI in patients with known NF1.

Methods & Materials: This is a single center, retrospective analysis of brain MRIs performed on children newly diagnosed with NF1 under the age of 4 years at our institution between January 1, 2000 and June 30, 2012. Patients were identified through a radiology search system [Montage Healthcare Solutions, Philadelphia, PA, USA] by time period, age (<4 years), NF1 diagnosis, study type and six referring clinicians specialized in the care of NF1 patients at our institution. All MRIs were reviewed by two board certified radiologists. Optic pathway gliomas were identified and characterized using multiple imaging parameters including bilaterality, location (single versus both optic nerves, intraorbital versus intracranial optic nerves, optic chiasm, optic tracts), and the presence and characteristics of non-optic pathway lesions. The number of affected patients that needed treatment (chemotherapy) was also recorded. Statistical analysis done with Stata v. 12.1.

Results: A total of 134 patients, 64 females (48%) and 70 males (52%), underwent MRI. Age distribution was 3% (n=4) less than 1 year, 49% (n=66) age 1–2 years, 20% (n=27) age 2–3 years, and 28% (n=37) age 3–4 years. In this cohort 27% (n=36) had an enhancing optic pathway lesion with mass effect on their first MRI and an additional 2% (n=2) were identified on subsequent screening MRI. There were fewer enhancing lesions outside the optic pathway, 5% were seen on the first and an additional 6% were seen on subsequent screening MRI. Treatment for optic pathway lesions was initiated for 34% (n=13/38) of patients.

Conclusions: Twenty-nine percent of patients with NF1 under the age of 4 years showed tumors in the optic pathway on MRI in our series, which is significantly higher than the previously reported incidence (15%). Though not all of our patients underwent treatment and the role of screening MRI in asymptomatic patients with NF1 is controversial, our data suggests that MRI may be valuable in early identification of patients at risk for progressive optic pathway lesions and compromise of visual function

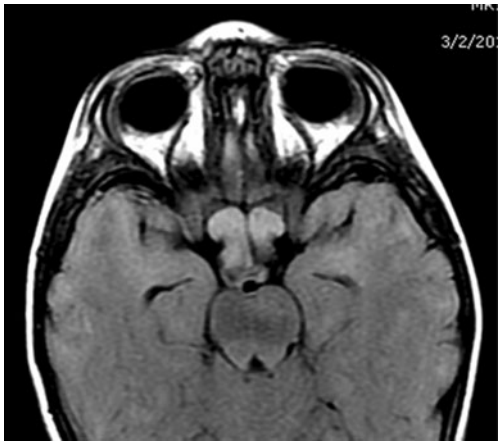

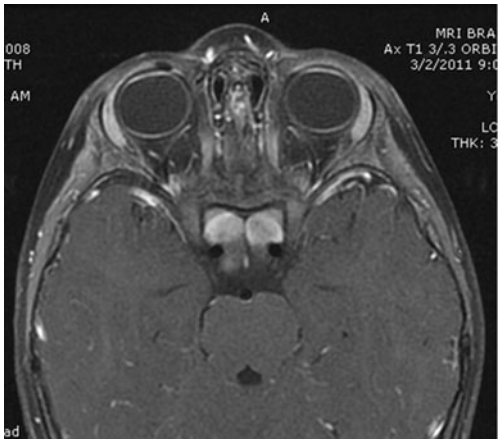

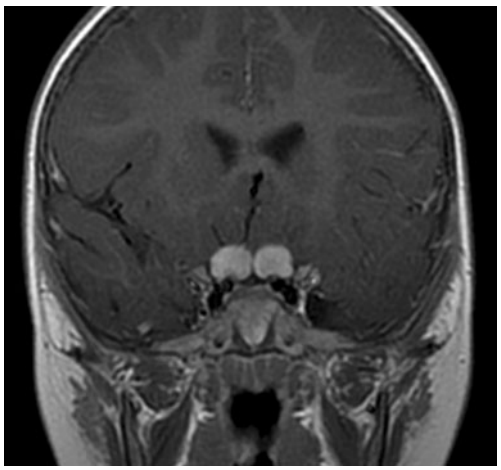

Poster #: SCI-031

Role of MRI in the Evaluation of Obstetrical Brachial Plexus Injury in Pediatric Patients

Marie-Claude Lefebvre, *Radiology, CHU Sainte Justine, Montreal, QC, Canada;* Ramy El Jalbout, MD, Josée Dubois, MD, MSc., Chantale Lapierre

Purpose or Case Report: To compare MRI of the brachial plexus and CT myelography in the detection of pseudomeningoceles in pediatric patients with brachial palsy. To study the effectivness of MRI in the pre surgical assessment of obstetrical brachial plexus injury.

Methods & Materials: Retrospective review was done of all the brachial plexus MRI studies performed between September 2002 and June 2012. Inclusion criteria included the cases performed for the assessment of obstetrical brachial plexopathy with concomitant CT myelography. The presence of a pseudomeningocele on an MRI consisted of a positive examination and in all cases a CT myelography was performed subsequently to the MRI. The study included 43 patients. Each examination consisted of mutiplanar T2 weighted sequences and 3D CISS. CT myelography consisted of intrathecal injection of contrast in the angio suite with subsequent axial CT cuts at the level of the cervical spine and upper-most thoracic spine.

Results: Of the 43 patients, 27 had anomalies detected on either MRI and or CT myelography. 215 nerve roots were studied of which 37 nerve roots were abnormal. Excluding the doubtful cases 1 pseudomeningocele seen on CT myelography was not detected on MRI and two pseudomeningoceles seen on MRI were not seen on CT myelography. This gives a sensitivity of MRI of 97.2% and a specificity of 98.8%. The NPV for MRI was 0.99. Keeping in mind that often more than one nerve root is affected per patient, this result translates into a sensitivity for MRI of 96.2% when considering the number of positive patients. The different sensitivity values are due to the fact that although MRI missed one positive patient, CT missed more nerve roots.

Conclusions: Brachial plexus MRI is a good first line modality of imaging for the preoperative assessment of pediatric patients with obstetrical brachial palsy. MRI is a safe, non invasive, radiation free and relatively sensitive modality to assist clinicians in the accurate detection of all the pseudomeningoceles and to guide them for the appropriate surgical approach. It has the additional advantage of assessing the associated muscle atrophy and bone changes.

Poster #: SCI-032

Chiari Type 1 malformations in Adolescent Sportspersons-Size Isn't Everything!

Marc Jordaan, MBChB, FRCR, *Radiology, Boston Children's Hospital, Boston, MA, marc.jordaan@Children's.harvard.edu;* William Meehan, Mark Proctor, Sanjay Prabhu

Purpose or Case Report: Diagnosis of a Chiari malformation in an individual is likely to result in the patient being advised against participation of contact sports. Aims of this study included-

1. To investigate whether additional features such as degree of crowding at the formen magnum, degree of CSF attenuation and the presence a cervical cord syrinx are strong indicators of clinical morbidity in pediatric sportspeople with "low-lying" tonsils.
2. To investigate whether Chiari Type 1 malformations are over-diagnosed in clinical practice and confirm whether objective criteria would help establish a firm diagnosis that correlated with clinical symptomatology and morbidity.

Methods & Materials: The study received IRB approval. Medical records, and brain and cervical MRI's of 29 pediatric sportspeople seen consecutively for a diagnosis of Chiari I malformation our Sports Medicine Clinic. Clinical symptoms detailed particulars of sport played (including type of sport, length of participation, and history of traumatic head injury) were evaluated. We correlated this with objective imaging parameters including degree of cerebellar descent, tonsillar morphology (rounded vs. pointed), degree of CSF attenuation, and the presence of crowding at the foramen magnum and cervical cord syrinx. For patients that underwent decompressive surgery, we assessed the clinical and radiologic parameters both before and after surgery.

Results: Of the 29 patients, we excluded four patients (3 because of lack of available imaging, and 1 because of presence of a large supratentorial glioma). Of the remaining 25, 12 were not surgically treated, while 13 underwent decompressive surgery. Three cases did not have evidence of Chiari malformation based on objective imaging criteria. We found that, for patients with higher degrees of foraminal crowding and CSF attenuation, cervical cord syrinx, and/or a skull base abnormality (e.g. retroverted dens and short clivus) had more significant clinical morbidity. Performance of these athletes on the field was more likely to be affected.

Conclusions: In patients with Chiari I malformations, tonsillar protrusion beyond the level of C1, degree of crowding and CSF

space attenuation, skull base abnormalities and cervical cord syrinx are indicators of significant clinical morbidity in pediatric sportspeople. Chiari malformations are frequently over-diagnosed based on size criteria alone, and additional prospective studies are required to reduce this trend in pediatric sportspeople.

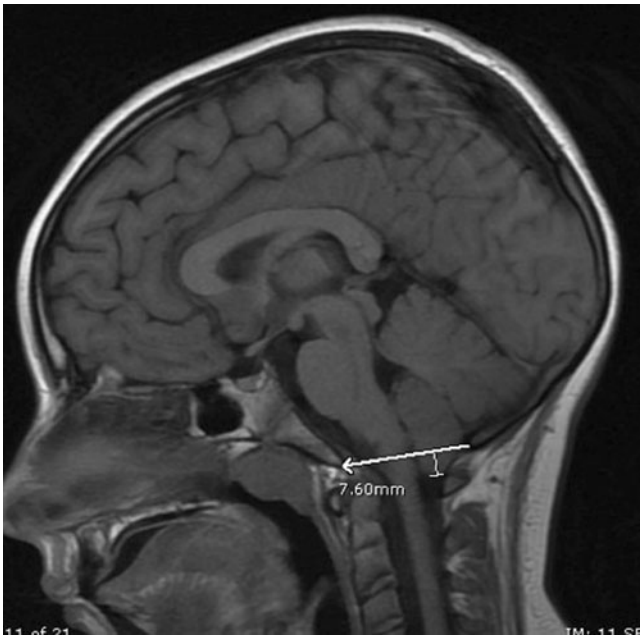

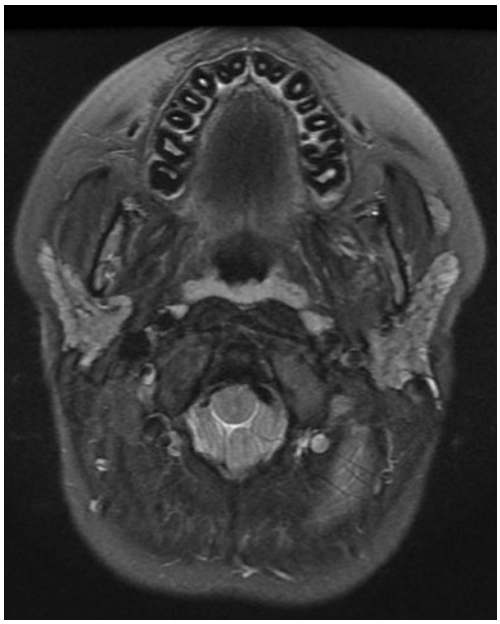

Poster #: SCI-033

Appendiceal 18F-FDG Uptake in Children: What's Normal?

Hamilton Reavey, MD, *Radiology, Emory University, Atlanta, GA, hfryer@emory.edu;* Adina Alazraki, Stephen Simoneaux

Purpose or Case Report: The biodistribution of 18F-FDG has been well described in both adults and children. However, many findings are limited to children and warrant understanding prior to interpretation. Active lymphoid tissue has increased FDG uptake when compared with inactive tissue. Since children have more active lymphoid tissue than adults, and because the appendix contains aggregated lymphoid tissue, we postulated that appendiceal uptake may be increased in pediatric patients. The purpose of our research is to determine the normal level of appendiceal uptake in children, not previously reported in the literature to date, in a series of consecutive FDG PET/CT scans performed in children for other indications.

Methods & Materials: With IRB approval, we retrospectively reviewed 54 consecutive whole-body pediatric 18FFDG PET/CT examinations obtained for various clinical indications. Scans on which the appendix could be visualized were objectively evaluated, and standardized uptake value (SUV) was determined. Maximum SUV of the appendix was compared to normal liver, and ratios were recorded. Pathology in the appendix was excluded.

Results: The scans of 54 patients, ages 1 month to 18 years (mean 12.5 years) were reviewed. Thirteen patients were excluded because of inability to visualize the appendix. Maximum appendiceal SUVs ranged from 0.7 to 4.3 with an appendix to liver background ratio ranging from 0.4 to 1.7 (mean 0.9).

Conclusions: 18F-FDG uptake in the appendix is typically not significantly higher than background 18F-FDG uptake, regardless of patient age. However, slight variations in appendiceal 18F-FDG uptake do occur, which should not be misinterpreted as pathologic.

Poster #: SCI-034

Fusion PET-MR: Correlation of contrast enhancement and 18-FDG-PET activity for the development of an integrated scanning protocol

VyThao Tran, *Pediatric Radiology, Stanford Lucile Packard Children's Hospital, Palo Alto, CA, vtran1012@gmail.com;* David Weinreb, Andrew Quon, Heike Daldrup-Link, Matthew Schmitz, Sandy Napel

Purpose or Case Report: MRI is the modality of choice for local staging of many pediatric malignancies and is often complemented by FDG-PET for whole body staging. We hypothesize that areas of increased metabolic activity seen on 18-FDG PET corroborate with areas of contrast enhancement on MR imaging hence obviating the need for administering contrast for PET-MR staging or restaging.

Methods & Materials: We retrospectively queried our PACS/RIS system for pediatric patients with an age of less than 18 years and a histologically confirmed solid malignancy, who had received both a PET and MRI within an interval of 3 weeks or less. Patients in remission and patients with brain tumors were excluded. A total of 35 children were identified with a variety of small round blue cell tumors. We manually fused PET and MR scans of these patients utilizing OsiRix software and determined by qualitative consensus amongst board certified radiologists and nuclear medicine physicians if areas of increased 18-FDG PET corroborated with areas of T1+contrast.

Results: 29/35 patients had regions of tumor that demonstrated avid contrast enhancement that correlated with regions of significant FDG avidity (83%). 6/35 patients had areas of contrast enhancement that was discordant with regions of FDG avidity (17%). Statistical evaluation will be performed utilizing a McNemar's test. False positives on MRI were seen in the setting of post treatment head and neck tumors including lymphoma and Ewings sarcoma. False negative with PET was seen in the setting of mild epidural disease spread from lymphoma, possibly due to lack of adequate resolution. Tumors with associated calcification demonstrated poor contrast enhancement and conspicuity on MRI, possibly related to the hypointense signal from the calcifications alone, but demonstrated hypermetabolic activity helping to discern active disease on fused PET-MR.

Conclusions: PET-MR as a combined imaging modality is highly effective for staging and restaging of pediatric malignancies. There is high concordance of increased 18-FDG avidity with areas of T1+contrast in abdominal tumors and soft tissue sarcomas. Thus, contrast administration may not be necessary and should be assessed on a case-by-case basis.

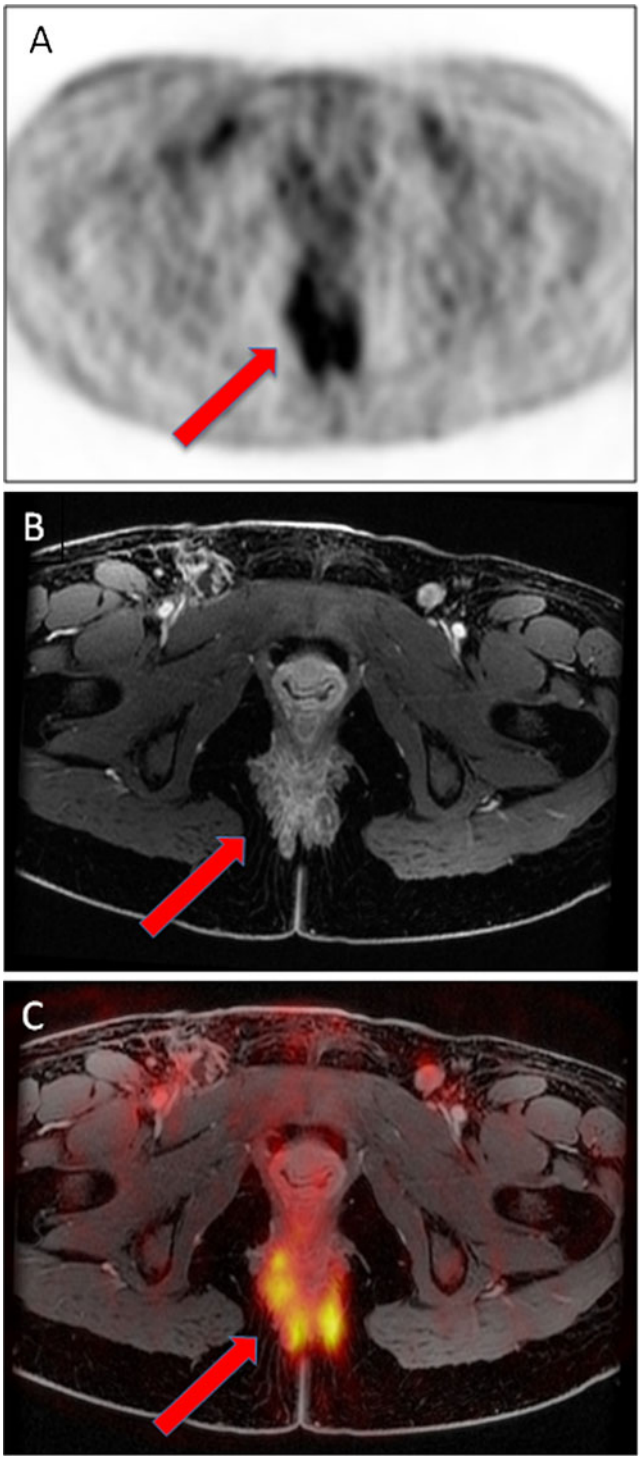

Figure 1: A) 18-FDG PET demonstrating increased metabolic activity in the posterior pelvis. B) MR Axial LAVA FLEX post contrast image demonstrating clear delineation of an enhancing mass in the ischio-rectal fat posterior to the rectum which represents extension in to the parametrium from a rhabdomyosarcoma of the vagina. C) Fused PET-MR demonstrating that the areas of enhancement correspond to areas of increased 18-FDG uptake.

Poster #: SCI-035

Clinical Presentation, Imaging Characteristics and Management of Parotid Hemangiomas

Fabiola Weber, MD, *Radiology, Boston Children's Hospital, Chestnut Hill, MA, fabiola.weber@gmail.com;* Gulraiz Chaudry, John Mulliken, Stephan Voss

Purpose or Case Report: Hemangioma is the most common tumor involving the parotid gland that presents in infancy. The predictable regression of parotid hemangiomas allows for conservative management in most patients. Incorrect diagnosis can potentially lead to unnecessary investigations and interventions. The purpose of this study was to identify the age of presentation of parotid hemangiomas, presenting signs/symptoms, imaging characteristics and appropriate management.

Methods & Materials: Our Vascular Anomalies Center database search yielded a total of 53 patients, with adequate imaging in 31. The medical records, photographs, and imaging were reviewed to ascertain demographic information, clinical presentation, physical appearance, imaging findings, and management.

Results: Of the 31 infants, 20 were female. All presented at or less than 4 months of age; and 32% presented at less than 4 weeks of age. Thirty-five percent of tumors were on the right side, 58% on the left, and 7% bilateral. The presenting signs/symptoms were: swelling (50%), palpable mass/lump (25%) and cutaneous vascular mark (25%). Forty-seven percent of the patients had no medical or surgical therapy, 43% received oral corticosteroid, 7% underwent pulsed dye laser, and 3% (1 patient) received interferon. One patient underwent partial resection due to an atypical clinical course.

The sonographic, CT and MRI studies all demonstrated a well defined homogeneous mass replacing most of the parotid gland. High internal vascularity was seen, with fast flow. The lesion was hyperintense on the T2 - weighted images and isointense to muscle on T1. There was intense homogeneous enhancement on both CT and MRI.

Conclusions: Typical age of presentation and clinical history are often sufficient to make an accurate diagnosis of parotid hemangioma. In deep lesions with normal overlying skin, the imaging appearance of these tumors is sufficiently characteristic to establish the diagnosis. Sonography with a high-frequency transducer is the ideal first line study. If a well defined, fast flow mass is seen in the parotid in this age group, serial ultrasonic studies may be the only investigation required. For cross sectional imaging, MRI provides more accurate characterization of the lesion and, if available, should be chosen rather than CT. For the problematic parotid hemangiomas, systemic corticosteroid or propranolol is the first line of treatment.

AUTHOR INDEX

KEYWORD INDEX